

Methods in
Molecular Biology 1641

Springer Protocols

Jean-Charles Gautier *Editor*

Drug Safety Evaluation

Methods and Protocols

Second Edition

 Humana Press

METHODS IN MOLECULAR BIOLOGY

Series Editor

John M. Walker

School of Life and Medical Sciences

University of Hertfordshire

Hatfield, Hertfordshire, AL10 9AB, UK

For further volumes:

<http://www.springer.com/series/7651>

Drug Safety Evaluation

Methods and Protocols

Second Edition

Edited by

Jean-Charles Gautier

Preclinical Safety, Sanofi, R&D, Vitry-sur-Seine, France

 **Humana Press**

Editor

Jean-Charles Gautier
Preclinical Safety
Sanofi, R&D
Vitry-sur-Seine, France

ISSN 1064-3745 ISSN 1940-6029 (electronic)
Methods in Molecular Biology
ISBN 978-1-4939-7170-1 ISBN 978-1-4939-7172-5 (eBook)
DOI 10.1007/978-1-4939-7172-5

Library of Congress Control Number: 2017944283

© Springer Science+Business Media LLC 2017

This work is subject to copyright. All rights are reserved by the Publisher, whether the whole or part of the material is concerned, specifically the rights of translation, reprinting, reuse of illustrations, recitation, broadcasting, reproduction on microfilms or in any other physical way, and transmission or information storage and retrieval, electronic adaptation, computer software, or by similar or dissimilar methodology now known or hereafter developed.

The use of general descriptive names, registered names, trademarks, service marks, etc. in this publication does not imply, even in the absence of a specific statement, that such names are exempt from the relevant protective laws and regulations and therefore free for general use.

The publisher, the authors and the editors are safe to assume that the advice and information in this book are believed to be true and accurate at the date of publication. Neither the publisher nor the authors or the editors give a warranty, express or implied, with respect to the material contained herein or for any errors or omissions that may have been made. The publisher remains neutral with regard to jurisdictional claims in published maps and institutional affiliations.

Printed on acid-free paper

This Humana Press imprint is published by Springer Nature
The registered company is Springer Science+Business Media LLC
The registered company address is: 233 Spring Street, New York, NY 10013, U.S.A.

Preface

Nonclinical drug safety evaluation is the assessment of the safety profile of therapeutic agents through the conduct of laboratory studies in *in vitro* systems and in animals. The main objectives of drug safety evaluation studies are to differentiate between new drug entities that are unacceptably toxic and those that are not, characterize the potential adverse effects of new drugs, determine animal dosage levels that do not cause toxicity, and estimate safe dosages to be used in clinical studies. Several types of studies are conducted in drug safety evaluation: acute to chronic general toxicity studies, reproductive toxicity studies, genotoxicity studies, carcinogenicity studies, safety pharmacology studies, and investigative toxicity studies.

The volume *Drug Safety Evaluation Methods and Protocols* was published as an earlier edition in the *Methods in Molecular Biology* series in 2011. In this second edition, some of the chapters from the previous edition have been updated to take into account the most recent advances in this field. In addition, several new chapters have been added to describe innovative tools and methods that have been developed and applied in the last 6 years to improve the safety evaluation of new drug candidates. Part I presents specific aspects related to the experimental design of toxicity studies conducted to support combination drugs in humans and pediatric indications. Part II focuses on Pathology with two chapters on detailed procedures of necropsy, tissue sampling, and processing for histopathological evaluation, and one chapter on the principles and methods of immunohistochemistry. A new chapter describes the applications of mass spectrometry imaging which are gaining more and more interest to detect and map compounds within tissue sections, thus providing useful information on drug distribution in relation to histopathological findings. Part III provides detailed protocols on Genetic Toxicology. A chapter describes the comet assay, a sensitive electrophoretic method for measuring DNA strand breaks at the level of single cells, together with the use of bacterial repair endonucleases to detect specific DNA lesions. Two new chapters describe recent advancements of the *Pig-a* mutation assay, which is anticipated to be a useful trans-species tool for evaluating the *in vivo* mutagenicity of chemicals and has been proposed as a new tool for preclinical safety assessment of regulated chemicals. Part IV provides methods on Safety Pharmacology, in which progress has been made to early evaluate the cardiotoxicity liability of new drug candidates. A new chapter describes how automatization procedures can be used to replace the resources and time-consuming manual patch-clamp approach for the hERG cardiac potassium channel. Another new chapter describes a method for measuring the contractility of induced human pluripotent stem cell derived cardiomyocytes using an impedance measurement system. Part V details methods on Investigative Toxicology aimed at better understanding mechanisms of toxicity and assessing potential translation to humans. Several chapters from the first edition have been updated on protocols and applications of nuclear magnetic resonance and mass spectrometry methods for metabolomics in several biological matrices, statistical analysis of real-time reverse transcription polymerase chain reaction (RT-PCR) which is a benchmark technology to detect and quantify mRNAs, and *in vitro* evaluation of mitochondrial respiration in cultured rat hepatocytes. A new chapter has been added on the early *in silico* evaluation of target safety, an approach which has now proven to be an invaluable resource

to support both drug discovery and development phases. Part VI is dedicated to screening assays for Developmental Toxicity. Two chapters provide detailed protocols of the Fetax assay and the Zebrafish model. Part VII encompasses methods to identify and characterize novel translational safety biomarkers to better monitor potential toxicity of drug candidates in both preclinical and clinical studies. One chapter provides protocols on the absolute quantification of protein safety biomarkers by mass spectrometry. Given that there is a growing interest to explore microRNAs as potential novel safety biomarkers in biofluids, several new chapters have been included to describe how next-generation sequencing, quantitative RT-PCR, and in situ hybridization technologies can be applied to investigate microRNAs for this purpose. A new chapter has also been added on the isolation and characterization of urine exosomes, which can potentially be used to detect nephrotoxicity.

I would like to thank all the contributing authors for providing state-of-the-art procedures, detailed protocols, and tips and tricks to avoid pitfalls. I am grateful to the series editor, John Walker, for inviting me to edit this second edition of the volume. The result is a compendium of analytical technologies, including some review chapters, with a focus on clarity and applicability in real life laboratory practice. The intended audience mainly consists of pharmaceutical scientists, toxicologists, biochemists, and molecular biologists, and anyone else with a specific interest for a method used in drug safety evaluation that could be used in other disciplines.

Vitry-sur-Seine, France

Jean-Charles Gautier

Contents

<i>Preface</i>	<i>v</i>
<i>Contributors</i>	<i>ix</i>
PART I GENERAL TOXICOLOGY	
1 Nonclinical Development of Combination Drugs	3
<i>Alberto Lodola</i>	
2 Juvenile Nonclinical Safety Studies in Support of Pediatric Drug Development	25
<i>Paul C. Barrow and Georg Schmitt</i>	
PART II PATHOLOGY	
3 Procedures of Necropsy and Tissue Sampling	71
<i>Laurence Fiette, Mohamed Slaoui, and Anne-Laure Bauchet</i>	
4 Tissue Sampling and Processing for Histopathology Evaluation	101
<i>Mohamed Slaoui, Anne-Laure Bauchet, and Laurence Fiette</i>	
5 Principles and Methods of Immunohistochemistry	115
<i>José A. Ramos-Vara</i>	
6 Applications of Mass Spectrometry Imaging for Safety Evaluation	129
<i>David Bonnel and Jonathan Stauber</i>	
PART III GENETIC TOXICOLOGY	
7 In Vivo Rat T-Lymphocyte <i>Pig-a</i> Assay: Detection and Expansion of Cells Deficient in the GPI-Anchored CD48 Surface Marker for Analysis of Mutation in the Endogenous <i>Pig-a</i> Gene	143
<i>Vasily N. Dobrovolsky, Javier Revollo, Dayton M. Petibone, and Robert H. Heflich</i>	
8 Detection of In Vivo Mutation in the <i>Pig-a</i> Gene of Mouse Bone Marrow Erythroids	161
<i>Takafumi Kimoto and Daishiro Miura</i>	
9 The Use of Bacterial Repair Endonucleases in the Comet Assay	173
<i>Andrew R. Collins</i>	
PART IV SAFETY PHARMACOLOGY	
10 Automated Patch-Clamp Methods for the hERG Cardiac Potassium Channel	187
<i>Sylvie Houtmann, Brigitte Schombert, Camille Sanson, Michel Partiseti, and G. Andrees Bohme</i>	
11 Impedance Measurement in Induced Pluripotent Stem Cell-Derived Cardiomyocytes	201
<i>Emma-Jane Poulton</i>	

PART V INVESTIGATIVE TOXICOLOGY

12	Target Safety Assessment: Strategies and Resources	213
	<i>Richard J. Brennan</i>	
13	NMR and MS Methods for Metabolomics.	229
	<i>Alexander Amberg, Björn Riefke, Götz Schlotterbeck, Alfred Ross, Hans Senn, Frank Dieterle, and Matthias Keck</i>	
14	Protocols and Applications of Cellular Metabolomics in Safety Studies Using Precision-Cut Tissue Slices and Carbon 13 NMR	259
	<i>Gabriel Baverel, Maha El Hage, and Guy Martin</i>	
15	Statistical Analysis of Quantitative RT-PCR Results	281
	<i>Richard Khan-Malek and Ying Wang</i>	
16	Evaluation of Mitochondrial Respiration in Cultured Rat Hepatocytes	297
	<i>Jean-Pierre Marchandean and Gilles Labbe</i>	

PART VI SCREENING ASSAYS FOR DEVELOPMENTAL TOXICITY

17	FETAX Assay for Evaluation of Developmental Toxicity	311
	<i>Isabelle Mouche, Laure Malésic, and Olivier Gillardeaux</i>	
18	Evaluation of Embryotoxicity Using the Zebrafish Model	325
	<i>Lisa Truong and Robert L. Tanguay</i>	

PART VII SAFETY BIOMARKERS

19	Absolute Quantification of Toxicological Biomarkers via Mass Spectrometry.	337
	<i>Thomas Y. K. Lau, Ben C. Collins, Peter Stone, Ning Tang, William M. Gallagher, and Stephen R. Pennington</i>	
20	Next-Generation Sequencing to Investigate Urinary microRNAs from <i>Macaca fascicularis</i> (Cynomolgus Monkey)	349
	<i>Yaligara Veeranagouda, Jean-François Léonard, Jean-Charles Gautier, and Eric Boitier</i>	
21	Quantitative RT-PCR for MicroRNAs in Biofluids	379
	<i>Michael Thorsen, Thorarinn Blondal, and Peter Mouritzen</i>	
22	Chromogenic In Situ Hybridization Methods for microRNA Biomarker Monitoring of Drug Safety and Efficacy	399
	<i>Barbara R. Gould, Tina Damgaard, and Boye Schnack Nielsen</i>	
23	Urine Exosome Isolation and Characterization	413
	<i>Jonathan M. Street, Erik H. Koritzinsky, Deonna M. Glispie, and Peter S.T. Yuen</i>	
	<i>Index</i>	425

Contributors

- ALEXANDER AMBERG • *Preclinical Safety, Sanofi R&D, Hattersheim, Germany*
- PAUL C. BARROW • *Roche Pharmaceutical Research and Early Development, Pharmaceutical Sciences, Roche Innovation Center Basel, F. Hoffmann-La Roche Ltd, Basel, Switzerland*
- ANNE-LAURE BAUCHET • *Translational Medicine and Early Development, Biomarkers and Clinical Bioanalyses, Sanofi R&D, Vitry-sur-Seine, France*
- GABRIEL BAVEREL • *Metabolys Inc., Lyon, France*
- THORARINN BLONDAL • *Exiqon A/S, Vedbæk, Denmark*
- G. ANDREES BOHME • *Integrated Drug Discovery, Sanofi R&D, Vitry-sur-Seine, France*
- ERIC BOITIER • *Translational Medicine and Early Development, Biomarkers and Clinical Bioanalyses—Genomics, Sanofi R&D, Vitry-sur-Seine, France*
- DAVID BONNEL • *ImaBiotech, Parc Eurasanté, Loos, France*
- RICHARD J. BRENNAN • *Sanofi, Waltham, MA, USA*
- BEN C. COLLINS • *Institute of Molecular Systems Biology, ETH Zürich, Switzerland*
- ANDREW R. COLLINS • *Department of Nutrition, University of Oslo, Oslo, Norway*
- TINA DAMGAARD • *Exiqon A/S, Vedbæk, Denmark*
- FRANK DIETERLE • *New Products and Medical, Near Patient Testing, Novartis, Basel, Switzerland*
- VASILY N. DOBROVOLSKY • *Division of Genetic and Molecular Toxicology, National Center for Toxicological Research, US Food and Drug Administration, Jefferson, AR, USA*
- LAURENCE FIETTE • *IMMR, Paris, France*
- WILLIAM M. GALLAGHER • *School of Biomolecular and Biomedical Science, UCD Conway Institute, University College Dublin, Dublin, Ireland*
- JEAN-CHARLES GAUTIER • *Preclinical Safety, Sanofi, R&D, Vitry-sur-Seine, France*
- OLIVIER GILLARDEAUX • *Paris, France*
- DEONNA M. GLISPIE • *Renal Diagnostics and Therapeutics Unit, NIDDK, National Institutes of Health, Bethesda, MD, USA*
- BARBARA R. GOULD • *Exiqon Inc., Woburn, MA, USA*
- MAHA EL HAGE • *Metabolys Inc., Lyon, France*
- ROBERT H. HEFLICH • *Division of Genetic and Molecular Toxicology, National Center for Toxicological Research, US Food and Drug Administration, Jefferson, AR, USA*
- SYLVIE HOUTMANN • *Integrated Drug Discovery, Sanofi R&D, Vitry-sur-Seine, France*
- MATTHIAS KECK • *Analytical Development 1, Bayer Pharma AG, Wuppertal 42096, Germany*
- RICHARD KHAN-MALEK • *Biostatistics and Programming, Sanofi US, Inc., Bridgewater, NJ, USA*
- TAKAFUMI KIMOTO • *Toxicology Research Department, Teijin Institute for Bio-medical Research, Teijin Pharma Limited, Hino, Tokyo, Japan*

- ERIK H. KORITZINSKY • *Renal Diagnostics and Therapeutics Unit, NIDDK, National Institutes of Health, Bethesda, MD, USA*
- GILLES LABBE • *Investigative Toxicology, Preclinical Safety, Sanofi R&D, Vitry-sur-Seine, France*
- THOMAS Y.K. LAU • *Pfizer Inc., Andover, MA, USA*
- JEAN-FRANÇOIS LÉONARD • *Translational Medicine and Early Development, Biomarkers and Clinical Bioanalyses—Genomics, Sanofi R&D, Vitry-sur-Seine, France*
- ALBERTO LODOLA • *ToxAdvantage, Noizay, France*
- LAURE MALÉSIC • *Paris, France*
- JEAN-PIERRE MARCHANDEAU • *Investigative Toxicology, Preclinical Safety, Sanofi R&D, Vitry-sur-Seine, France*
- GUY MARTIN • *Metabolys Inc., Lyon, France*
- DAISHIRO MIURA • *Toxicology Research Department, Teijin Institute for Bio-medical Research, Teijin Pharma Limited, Hino, Tokyo, Japan*
- ISABELLE MOUCHE • *GenEvolutioN, Rosny-sur-Seine, France*
- PETER MOURITZEN • *Exiqon A/S, Vedbæk, Denmark*
- BOYE SCHNACK NIELSEN • *Bioneer A/S, Hørsholm, Denmark*
- MICHEL PARTISETI • *Integrated Drug Discovery, Sanofi R&D, Vitry-sur-Seine, France*
- STEPHEN R. PENNINGTON • *UCD School of Medicine and Medical Science, UCD Conway Institute, Dublin, Ireland*
- DAYTON M. PETIBONE • *Division of Genetic and Molecular Toxicology, National Center for Toxicological Research, US Food and Drug Administration, Jefferson, AR, USA*
- EMMA-JANE POULTON • *Preclinical Safety, Sanofi, Framingham, MA, USA*
- JOSÉ A. RAMOS-VARA • *Department of Comparative Pathobiology, Purdue University, West Lafayette, IN, USA*
- JAVIER REVOLLO • *Division of Genetic and Molecular Toxicology, National Center for Toxicological Research, US Food and Drug Administration, Jefferson, AR, USA*
- BJÖRN RIEFKE • *Investigational Toxicology, Metabolic Profiling and Clinical Pathology, Bayer Pharma AG, Berlin, Germany*
- ALFRED ROSS • *Roche Pharmaceutical Research and Early Development, Pharmaceutical Sciences, Roche Innovation Center Basel, F. Hoffmann-La Roche Ltd, Basel, Switzerland*
- CAMILLE SANSON • *Integrated Drug Discovery, Sanofi R&D, Vitry-sur-Seine, France*
- GÖTZ SCHLOTTERBECK • *School of Life Sciences, Institute for Chemistry and Bioanalytics, University of Applied Sciences, Northwestern Switzerland, Muttenz, Switzerland*
- GEORG SCHMITT • *Roche Pharmaceutical Research and Early Development, Pharmaceutical Sciences, Roche Innovation Center Basel, F. Hoffmann-La Roche Ltd, Basel, Switzerland*
- BRIGITTE SCHOMBERT • *Integrated Drug Discovery, Sanofi R&D, Vitry-sur-Seine, France*
- HANS SENN • *Heythrop College UCL, Kensington Square, London, UK*
- MOHAMED SLAOUİ • *Preclinical Safety, Sanofi R&D, Vitry-sur-Seine, France*
- JONATHAN STAUBER • *ImaBiotech, Parc Eurasanté, Loos, France*
- PETER STONE • *Agilent Technologies, Santa Clara, CA, USA*
- JONATHAN M. STREET • *Renal Diagnostics and Therapeutics Unit, NIDDK, National Institutes of Health, Bethesda, MD, USA*

NING TANG • *Agilent Technologies, Santa Clara, CA, USA*

ROBERT L. TANGUAY • *Department of Environmental and Molecular Toxicology, Oregon State University, Corvallis, OR, USA; Sinnhuber Aquatic Research Laboratory, Oregon State University, Corvallis, OR, USA*

MICHAEL THORSEN • *Exiqon A/S, Vedbæk, Denmark*

LISA TRUONG • *Department of Environmental and Molecular Toxicology, Oregon State University, Corvallis, OR, USA; Sinnhuber Aquatic Research Laboratory, Oregon State University, Corvallis, OR, USA*

YALIGARA VEERANAGOUDA • *Molecular Biology & Genomics, Translational Science, Sanofi R&D, Chilly-Mazarin, France*

YING WANG • *Translational Medicine and Early Development, Sanofi US, Inc., Bridgewater, NJ, USA*

PETER S.T. YUEN • *Renal Diagnostics and Therapeutics Unit, NIDDK, National Institutes of Health, Bethesda, MD, USA*

Part I

General Toxicology

Chapter 1

Nonclinical Development of Combination Drugs

Alberto Lodola

Abstract

We define “combination drugs” as “fixed-dose combinations” (FDCs), that is, two or more drugs (marketed or not) combined in a single pill or two or more separate drugs packaged together. FDCs have been available commercially for many years but only relatively recently have nonclinical development guidelines been released by a number of regulatory authorities and the World Health Organization; as yet there are no ICH guidelines specific to combination drugs. In general however, the ICH guidelines for monotherapy development provide a framework for FDC development. Depending on the type of drug combination (marketed drug/market drug; marketed drug/NME and NME/NME) the scope and complexity of toxicity studies will vary greatly. In all cases however, a key issue is the potential for pharmacokinetic and/or toxicologic interaction between the components. For a marketed drug/market drug combination a detailed review of the nonclinical data available may suffice, particularly when the components have a history of coadministration at about the same dose and ratio as that of the proposed combination. For a marketed drug/NME combination, in addition to a review of the data for the marketed drug, a full ICH program of studies will be required for the NME, and a study of up to 90-day duration (in one species) for the combination. With an NME/NME combination each component will require a full ICH battery of studies and a combination study in one species. In all cases additional studies may be needed to address data gaps. Given the many novel and complex issues which arise when developing FDCs we recommend that, whenever possible, the nonclinical study strategy is discussed with the regulatory authorities.

Key words Combination drugs, Fixed-drug combinations, Regulatory guidelines, Nonclinical issues, Study design, Dose selection, Development strategies

1 Introduction

“Combination drugs” have been defined by a number of regulatory authorities (Table 1) [1–5]. Although descriptive detail and the presentation format differ from one authority to the other, overall there is agreement between authorities as to the nature of “combination drugs.” For clarity and to facilitate discussion we will simplify the definition to “fixed-dose combinations,” that is, two or more drugs (marketed or not) combined in a single pill or two or more separate drugs packaged together. These fixed-dose

Table 1
Definition of “combination” drugs by regulatory authorities

Food and Drug Administration [1]	European Medicines Agency [2]	Australian Therapeutic Goods Administration [3]	Canadian Agency for Drugs and Technologies in Health [4]	Indian Central Drugs Standard Control Organization [5]
Copackaged products (two or more separate drugs packaged together)	Products containing two or more active substances, which can be either well known or not yet authorized in the EU for the intended claim	Containing more than one active ingredient	Two or more drugs that have not been previously marketed in Canada in that combination. It may consist of: Two or more new drugs Two or more previously marketed drugs A combination of new drug(s) and previously marketed drug(s)	Not marketed in India and one or more active ingredient(s) is a new drug not approved in India: Category I: One of the ingredients of the combination is an investigational new drug Category II: One or more of the ingredients of the combination is a new drug not approved individually in the country; however the same is approved in other countries
Adjunctive therapy (when a second drug is used together with the drug for primary treatment)	The combination of active substances within a single pharmaceutical form of administration is a so-called fixed combination medicinal product	The active ingredients may be present as separate entities, a mixture, in a chemical combination which is intended to degrade into the active components in vivo		Not marketed in India but the active ingredients are approved/marketed individually and it is likely to have significant PK/PD interactions

<p>Fixed-dose combinations (two or more drugs combined in a single pill)</p> <p>A “combination pack” consists of more than one medicinal product, or more than one pharmaceutical form of the same medicinal product, presented under a single (invented) name and in a single product package (e.g., box, blister pack), where the individual products/forms are intended for simultaneous or sequential administration</p>	<p>The active ingredients may be: In the same dose form (e.g., a tablet) In separate dose forms packaged in a manner which indicates that they are to be taken together</p> <p>FDC: Marketed abroad</p>
	<p>FDC: Marketed in India but some changes are sought FDC: Only for convenience FDC: Subsequent approvals after the approval of primary applicant’s FDC</p>

combination drugs (FDCs) should not be confused with “combination products” defined in 21 CFR3.2(e) [6] as:

- Two or more regulated components (drug/device, biologic/device, drug/biologic, or drug/device/biologic) that are physically, chemically, or otherwise combined or mixed and produced as a single entity.
- Two or more separate products packaged together in a single package or as a unit (drug/device products, device/biological products, or biological/drug products).
- A drug, device, or biological product packaged separately that according to its investigational plan or proposed labeling is intended for use only with an approved individually specified drug, device, or biological product where both are required to achieve the intended use, indication, or effect and where upon approval of the proposed product the labeling of the approved product would need to be changed, e.g., to reflect a change in intended use, dosage form, strength, route of administration, or significant change in dose.
- Any investigational drug, device, or biological product packaged separately that according to its proposed labeling is for use only with another individually specified investigational drug, device, or biological product where both are required to achieve the intended use, indication, or effect.

A brief description of the development of “combination products” has been provided by Segal [7] and Portnoy and Koepke [8]. In this chapter we discuss the nonclinical development of FDCs. These drugs have been available in our pharmacies for many years; for example in 1975 in West Germany greater than two-thirds of the drugs on the official list were fixed combinations [9]. In 1982 it was reported that about half of all marketed drugs in the USA were fixed combinations [10]. Combination drugs are used in the treatment of a wide range of illnesses; see for example [11–16]. Their major disadvantage is that neither the dose nor the ratio of the individual components can be varied by the physician. However, for patients on multiple medication, a combination drug simplifies treatment and hence compliance; given that fewer pills are taken there may also be a cost advantage [17]. Combination therapy may also be more effective than monotherapy or have an improved safety profile. For example in stage I or II hypertension, monotherapy may only produce a modest effect on blood pressure while a combination drug can produce a more significant reduction given that each component blocks different effector pathways. Similarly, the incidence of peripheral edema, linked to the use of calcium channel antagonist therapy, is reduced when

coadministered with an ACE inhibitor [11]. Improved tolerance and/or efficacy have also been reported for FDCs, for example in the treatment of open-angle glaucoma or chronic obstructive pulmonary disease [18, 19].

In general therefore, while there is still some debate about the pros and cons of FDCs there has been a continuing steady flow of approvals for these drugs [20–22].

2 Regulatory Guidance

The “International Conference on Harmonisation of Technical Requirements for Registration of Pharmaceuticals for Human Use” (ICH) has defined the nonclinical data requirements for monotherapy development [23]. These requirements are an essential backcloth when assessing the nonclinical needs for FDC development.

2.1 Guidance for Monotherapy Development

Current guidance for monotherapy development is described in a range of guidelines [23] which are detailed in Table 2. In addition to data from these studies, “special studies,” developed in the light of the emerging nonclinical and clinical data, may also be needed to address specific issues. The relevance of these documents to FDC development is twofold. Firstly, for marketed drugs they are the reference against which the nonclinical data for the marketed drug, often produced pre-ICH, are judged. Secondly, they define the studies and data needed for the novel component of an FDC and guide the choice of studies with the combination.

2.2 Guidance for FDC Development

There are no ICH guidelines specific to FDCs; however there is reference to FDC development in the ICH M3(R2) guideline on nonclinical safety studies for the conduct of human clinical trials and marketing authorization for pharmaceuticals [24]; the key points from this guideline are summarized in Table 3. More recently ICH has amplified the M3(R2) guideline by releasing a Questions and Answers document [25] that discusses a number of nonclinical testing issues for “combination drug” development; some of the key issues raised and the response of ICH are summarized in Table 4.

Nationally based nonclinical guidelines for FDC development are available for some countries. The FDA guidance for the nonclinical development of FDCs [1] makes the following general point with respect to (drug) safety considerations: “If existing clinical and nonclinical safety data for each separate drug or biologic are sufficient to support the safety of the proposed new indication ... then a review of a range of safety factors (detailed in the text) should be undertaken...to determine whether further nonclinical

Table 2
List of current preclinical guidance documents available for the development of monotherapies [23]

ICH guideline	Topic
S1A	Need for carcinogenicity studies of pharmaceuticals
S1B	Testing for carcinogenicity of pharmaceuticals
S1C(R2)	Dose selection for carcinogenicity studies of pharmaceuticals
S2(R1)	Guidance on genotoxicity testing data interpretation for pharmaceuticals intended for human use
S3A	Note for guidance on toxicokinetics: the assessment of systemic exposure in toxicity studies
S3B	Pharmacokinetics: guidance for repeated-dose tissue distribution studies
ICH	Single-dose toxicity tests
S4	Duration of chronic toxicity testing in animals (rodent and nonrodent toxicity testing)
S5(R2)	Detection of toxicity to reproduction for medicinal products and toxicity to male fertility
S6(R1)	Preclinical safety evaluation of biotechnology-derived pharmaceuticals
S7A	Safety pharmacology studies for human pharmaceuticals
S7B	The nonclinical evaluation of the potential for delayed ventricular repolarization (QT interval prolongation) by human pharmaceuticals
S8	Immunotoxicity studies for human pharmaceuticals
M3(R2)	Guidance on nonclinical safety studies for the conduct of human clinical trials and marketing authorization for pharmaceuticals

studies are warranted.” More specifically the nonclinical requirements for three FDC scenarios are addressed [1]:

- Combinations of marketed drugs
- Combinations of marketed drugs and new molecular entities (NME)
- Combinations of NMEs

Data requirements from the FDA guideline are summarized in Table 5. In general for marketed drugs, and if the components have a history of concomitant use at about the projected ratio, little or no nonclinical work is needed for the FDC. For combinations involving NMEs, a full ICH package of studies is needed for the NME (*see* Subheading 2.1) and additional studies with the FDC are required (Table 5).

Additional discussion of the nonclinical development of FDCs is provided in the FDA’s Guidance for Industry: The codevelopment of two or more new investigational drugs for use in combination [26]. This guidance applies only to drugs and biological

Table 3

Summary of the key points relating to FDCs from the ICH M3 (R2) Guidance on nonclinical safety studies for the conduct of human clinical trials and marketing authorization for pharmaceuticals [24]

Type of FDC	Nonclinical requirements
Combinations which involve two late-stage entities	<ul style="list-style-type: none"> • <i>There is adequate clinical experience</i> with coadministration <ul style="list-style-type: none"> – Combination toxicity studies are not generally required unless there is significant toxicological concern (e.g., similar target organ toxicity) • <i>There is not adequate clinical experience</i> with coadministration <ul style="list-style-type: none"> – If there is no cause for toxicological concern nonclinical combination studies not generally required to support small-scale, short-duration clinical studies (e.g., Phase II studies of up to 3-month duration) – Nonclinical combination studies are recommended before large-scale or long-term combination trials, as well as for marketing
Two early-stage entities	<ul style="list-style-type: none"> • Nonclinical combination toxicity studies are recommended • If nonclinical development programs are being conducted on the individual entities the duration of the combination study should be equivalent to that of the clinical trial, up to a maximum duration of 90 days <ul style="list-style-type: none"> – A 90-day combination toxicity study would also support marketing – A combination toxicity study of shorter duration can also support marketing, depending on the duration of the intended clinical use • Combination genotoxicity, safety pharmacology, or carcinogenicity studies are not recommended to support clinical trials or marketing if the individual agents have been tested according to current standards • If women of child-bearing potential are to be treated with the FDC <ul style="list-style-type: none"> – Studies with the individual agent(s) have shown findings indicative of embryo-fetal risk, combination studies are not recommended: potential human developmental hazard has already been identified. – Studies have indicated that neither agent poses a potential human developmental risk, combination studies are not recommended unless concerns exist, based on the properties of individual components, that their combination could give rise to a hazard for humans. – If embryo-fetal studies of the drug combination are warranted, the study(ies) of the combination should be available to support the marketing application

products regulated by the Center for Drug Evaluation and Research. While there is only limited discussion of nonclinical issues, a number of key points emerge:

- With respect to nonclinical safety characterization of individual drugs or combination, reference is made to ICH guidelines for monotherapy (ICH M3(R2) and ICH S9).
- If it is not possible to characterize the safety of the individual new investigational drugs in humans then nonclinical studies of the combination should be undertaken to support initial dosing of the combination in humans. The nonclinical data for the combination should include pharmacokinetic (absorption,

Table 4

Summary of some key points from the ICH M3(R2) Implementation Working Group M3(R2) guideline: guidance on nonclinical safety studies for the conduct of human clinical trials and marketing authorization for pharmaceuticals questions and answers (R2) [25]

Issue	ICH response
Need for a combination toxicity study if two (or more) late-stage entities are combined but for one of them the human dosage/exposure will be higher than that already approved	<ul style="list-style-type: none"> • If there has been previous clinical experience with the two entities used together, a combination toxicity study is generally not recommended unless there is significant toxicological concern due to increased exposure
Description of “adequate clinical experience with coadministration” for combinations of late-stage products	<ul style="list-style-type: none"> • Adequate clinical experience is defined in ICH M3(R2) as data from Phase III clinical studies and/or postmarketing use <ul style="list-style-type: none"> – Adequate clinical experience can also be the result of common clinical practice with drug combinations
Selection of dosage, duration, and endpoint of a combination toxicity study	<ul style="list-style-type: none"> • Study should be equivalent to that of the clinical trial it is intended to support, up to a maximum of 90 days <ul style="list-style-type: none"> – A shorter duration can be used depending on the duration of clinical use – A toxicity study intended to address a particular toxicological concern should be of a duration that is appropriate to address the concern • Study endpoints should allow evaluation of additive and synergistic effects for known toxicities or predicted toxicities • Dosages should be appropriate to address any identified cause for concern or to provide exposure margins that are clinically relevant (e.g., when conducting a study with two early-stage agents)
FDC developed to reduce the side effect of one component	<ul style="list-style-type: none"> • If combination toxicity studies are warranted, they generally cannot be replaced by combination pharmacology studies except for anticancer pharmaceuticals <ul style="list-style-type: none"> – Toxicity endpoints are not usually adequately evaluated in the pharmacology studies
FDC under development for treatment of life-threatening or serious diseases	<ul style="list-style-type: none"> • Combination toxicity studies generally not warranted unless there is a specific cause for concern under clinically relevant conditions <ul style="list-style-type: none"> – Advanced cancer, tuberculosis, and HIV products • Combination toxicity studies are also not generally warranted for antiviral agents for treatment of hepatitis C • Other situations case by case
Combinations with at least one biotechnology-derived product	<ul style="list-style-type: none"> • Nonclinical combination study needs to be considered on a case-by-case basis

Table 5
Summary of the key points from the FDA guidance for industry

Study	Combination type		Comment
	MD/MB + NME	NME + NME	
Genetic toxicology	On the NME Combination	On the NME Combination	Not required for MD/MB if data consistent with modern requirements Generally not required
PK/ADME and toxicokinetics	On the NME	On the NME Combination	Per ICH-M3(R2) and/or ICH-S6 If same target organ/system
Safety pharmacology	On the NME Combination	On the NME Combination	Per ICH-M3(R2) and/or ICH-S6 If same target organ/system
General toxicology	On the NME Combination	On the NME Combination	Per ICH-M3(R2) and/or ICH-S6 Study of up to 90-day duration
Reproductive and development toxicology			
Fertility (study 1)	On the NME	On the NME	Per ICH-M3(R2)
Implantation/early development (study 2)	On the NME	On the NME	Per ICH-M3(R2)
Embryo-fetal development (study 3)	On the NME Combination	On the NME Combination	Per ICH-M3(R2) Unless the MD or NME is pregnancy category "D" or "X"
Carcinogenicity	On the NME	On the NME	Generally not needed for the combination if NMEs tested
Animal models of efficacy	Generally not needed	Generally not needed	
Further studies	As required to address data gaps/specific issues	As required to address data gaps/specific issues	

Nonclinical Safety Evaluation of Drug or Biologic Combinations [1] for combinations involving NMEs
MD marketed drugs, *MB* marketed biologics, *NME* new molecular entity

Table 6

Summary of preclinical data requirements from the FDA's Guidance for Industry: fixed-dose combinations, copackaged drug products, and single-entity versions of previously approved antiretrovirals for the treatment of HIV [27]

Requirement	Scenario 1	Scenario 2
FDC components	2 or 3 drugs which have been separately approved	
Data from human usage	Data available to show that components are safe and effective when used together	No support data for concomitant use
Type of FDA application	Stand-alone NDA Applicant/s own or have a right to reference underlying preclinical and safety and efficacy data	NDA
Preclinical data	No new preclinical data for the components or FDC	No new preclinical data for the components Safety data for the FDC either from studies or from the literature are required
Bioavailability	For the FDC to show that efficacious blood levels of each component are achieved	

NDA New Drug Application

distribution, metabolism, and excretion) and toxicokinetic data and appropriate biomarker/target interaction data.

- Sponsors are encouraged to communicate as early as possible (e.g., pre-IND meeting) with the appropriate CDER review division when considering codevelopment.

The FDA has also released specific guidelines for the development of FDCs for the treatment of HIV infections [27]. This wide-ranging document is focused on combinations developed using only marketed drugs. Two nonclinical FDC development scenarios of interest to us are presented and we have summarized the data requirements in Table 6.

Liminga and Silva Lima [28] have discussed the background to the European Medicines Agency (EMA) guidance documents on the nonclinical development of FDCs. The EMA guideline on the nonclinical development of FDCs [2] mirrors the FDA's guideline; the EMA presents three nonclinical development scenarios for FDCs:

- An FDC of compounds already approved as free combination therapy
- An FDC of approved compounds not approved as combination therapy

Table 7

Summary of the key points from the EMA's guideline on the nonclinical development of fixed combinations of medicinal products [2]

Combination type		
Compounds already approved as combination therapy	Compounds not approved as combination therapy	FDC containing one or more new active substances
<ul style="list-style-type: none"> • If there is sufficiently documented human experience of their individual and combined use, safety studies in animals are generally not required (CPMP/EWP/240/95) • With compounds from the same classes, as other compounds in well-established combinations and considerable clinical experience with no pharmacokinetic interactions identified, further nonclinical studies may not be needed • When the nonclinical data package does not fulfil the recommendations outlined on the draft Note for Guidance on the Non-Clinical Documentation of Medicinal Products for Mixed Marketing Applications (CPMP/SWP/799/95) nonclinical studies may be needed 	<ul style="list-style-type: none"> • Even if the safety of the individual substances has been adequately documented unexpected interactions may still need to be addressed (CPMP/EWP/240/95) • Studies with the FDC may be needed if: <ul style="list-style-type: none"> – Systemic exposure expected from FDC is not covered by the existing data – The compounds to be combined target the same organ system(s), or belong to a class of compounds associated with a specific type of toxicity • Special and/or mechanistic studies may be warranted (e.g., immunotoxicity or dependence), depending on the properties of the individual components in the combination 	<ul style="list-style-type: none"> • A complete nonclinical development program with the new active substance(s), with additional bridging studies with the combination <p>OR</p> <ul style="list-style-type: none"> • A nonclinical development program with the combination, together with a limited set of studies with the new active substance alone

- An FDC containing one or more new active substances (new active substance in combination with one or more approved/well-known compound or a combination of two or more new active substances)

The key elements of the EMA guideline are summarized in Table 7. Overall the position adopted by the EMA is consistent with that of the FDA, although the general nature of the guidance suggests to us a more flexible approach than that of the FDA.

The nonclinical requirements for FDC development in Japan [29] have been summarized by the Regulatory Information Task Force of the Japanese Pharmaceutical Manufacturers Association (JPMA). It is important to note that “new combination prescription drugs” refer to drugs with different active ingredients or combining ratios from those of combination drugs specified in the

Table 8
Data to be submitted with an Application for Approval to Manufacture/
Market Distribute a New Prescription Drug in Japan for a “new
combination prescription drugs” FDC for a new prescription-based
combination drug [29]

Data type	Study	Required	May be required
Pharmacological action	Tests to support efficacy	✓	
	Secondary pharmacology, safety pharmacology		✓
	Other pharmacology		✓
Pharmacokinetics	Absorption	✓	
	Distribution	✓	
	Metabolism	✓	
	Excretion	✓	
	Other pharmacokinetics		✓
Toxicity studies	Single-dose toxicity	✓	
	Repeated-dose toxicity	✓	
	Genotoxicity		
	Carcinogenicity		
	Reproductive toxicity		
	Local irritation		✓
	Other toxicity		

Japanese Pharmacopoeia or combination drugs that have already been approved for manufacture/marketing as prescription drugs. The nonclinical requirements for the development of “new combination prescription drugs” in Japan are summarized in Table 8.

Hunt [30] has discussed the Australian regulatory perspective on FDC development. With respect to regulatory guidance for the development of an FDC the Australian Therapeutic Goods Administration (TGA) has adopted a number of EMA guidelines. For nonclinical development of FDCs the EMAs “Guideline on the non-clinical development of fixed combinations of medicinal products” [2] has been adopted by the TGA.

No specific nonclinical guidelines relating to FDC development have been released by the Canadian authorities. However, the Canadian Therapeutic Products Directorate (TPD) in a guideline relating to hormone replacement therapy in menopause [31] makes reference to “fixed combinations.” The principal data requirements are for bioavailability, pharmacokinetics, pharmacodynamics, and metabolic studies in all species studied. It is accepted however that when there is substantial information already available for the monotherapies then there may only be a need for

“abridged toxicology,” that is, a reduced program of studies. Moreover, with the agreement of the Therapeutic Products Programme staff the need for toxicology testing will in certain cases be waived.

The Indian Central Drugs Standard Control Organization (CDSCO) have issued a draft guidance on FDCs [5] and we have summarized the nonclinical data requirements for nonclinical development in India in Table 9.

The World Health Organization’s (WHO) “Expert Committee On Specifications For Pharmaceutical Preparations” published guidelines for the registration of “combination medicinal products” [32]. This document is focused on the regulatory needs for the development and marketing of combination drugs to treat HIV infections, tuberculosis, and malaria. The information provided by the WHO is highly detailed describing preclinical, clinical, and marketing requirements for the specific indications listed above. They consider four scenarios:

1. A generic copy of an existing combination
2. The combination is composed of established monotherapies which have been used in combination
3. A combination composed of established monotherapies which have not previously been used in combination
4. The combination contains one or more NMEs

The data requirements for each scenario are summarized in Table 10. For scenarios 1 and 2, no additional experimental work is required relative to the individual monotherapies. While there is no specific description of the preclinical data which is required for Scenarios 3 and 4, it is made clear that the WHO guideline is not “stand-alone” and has to be used in conjunction with current national and ICH guidelines (*see* Subheadings 2.1 and 2.2).

Overall therefore, the regulatory guidelines from the FDA, EMA, TGA, TPD, CDSCO, and WHO are broadly aligned. Not surprisingly guidance for FDC development draws heavily on ICH guidelines (particularly the ICH M3(R2) guideline [24]) for monotherapy development.

3 Nonclinical Safety Issues for FDCs

The issues which underpin the need for the wide range of preclinical ICH studies associated with monotherapy development also apply for combination drug development. These issues have been discussed in detail elsewhere [33]. In addition, however, particular attention is focused on the potential for pharmacokinetic and/or toxicologic interaction when developing combination drugs.

Table 9
Summary of nonclinical data requirements described in the Indian CDSCO draft guidance on fixed-dose combinations [6]

	Not marketed in India: one or more active ingredient(s) is not approved in India			Not marketed in India: the active ingredients are approved/marketed individually and it is likely to have significant PK/PD interactions	
	Category I	Category II	Marketed abroad	Individual components used concomitantly	Individual components not used concomitantly
Follow-up and supplemental safety pharmacology studies	✓	✓	• No specific nonclinical data requirement	• No specific nonclinical data requirement	✓
Pharmacokinetics: ADME	✓	✓			
Acute toxicity data (LD 50)	✓	✓			✓
Systemic toxicity studies	✓	✓			
Subacute toxicity	✓	✓			✓ ^a
Male fertility study	✓	✓			
Female reproduction and developmental toxicity studies	✓	✓			
Local toxicity	✓	✓			
Allergenicity/hypersensitivity	✓	✓			
Genotoxicity	✓	✓			
Carcinogenicity	✓	✓			

ADME absorption, distribution, metabolism, excretion

Category I: One of the ingredients of the combination is an investigational new drug (IND)

Category II: One or more of the ingredients of the combination is a new drug not approved individually in the country; however the same is approved in other countries

^aFor injectable formulation

Table 10
Summary of nonclinical data requirements developed in the WHO Guidelines for registration of fixed-dose combination medicinal products [32]

Requirement	Scenario			
	1	2	3	4
Type of FDC	Generic copy	Approved components previously used in combination	Approved components not previously used in combination	Contains one or more NCEs
Analysis of literature	Not required		Required	
Bioavailability data	Not usually required		Sometimes required	Required
Pharmacology and Safety data	Not usually required		Sometimes required	Required

If we consider a two-drug combination containing components “A” and “B,” component A may affect the pharmacokinetic (PK) profile of component B (or *vice versa*). This can result in circulating levels of “B” being increased or decreased, altered tissue binding, and/or distribution or altered rates of metabolism and elimination. These changes in PK profile can result in reduction of the no observed effect level (NOEL) and no observed adverse effect levels (NOAEL), hence the safety margin (for specific toxicities) and the overall risk assessment of the combination relative to that of the individual components when used in monotherapy.

Similarly, a PK interaction can produce a pharmacodynamic effect; that is, component “A” increases or reduces the response of the organism to the pharmacological effects of component “B.” It should be noted that in some instances, this effect is the pharmacological basis for the combination: for example Kaletra, a combination of lopinavir and ritonavir used in the treatment of HIV infections. Ritonavir inhibits the metabolism of lopinavir, thus improving the PK profile of lopinavir, thus increasing its pharmacological effectiveness [34]. In other cases, both drug components could have a common target organ of toxicity; this could result in an aggravation of this toxicity with a potentially reduced safety margin and an altered risk assessment for the combination relative to that of its components.

4 Nonclinical Study Issues for FDCs

There are a number of tactical issues that need to be considered when developing combination drugs. Primarily these issues relate to the increased complication of defining the dose–response and the effects of component ratio changes on safety for a “chemical mixture.”

4.1 Dose Selection for Nonclinical Studies

Genotoxicity studies with the FDCs are usually not required. However, this is not the case for safety pharmacology, general toxicology, and developmental toxicology studies. In studies with an FDC, dose selection is complicated by the need to consider two factors. The first is the dose itself; this is made up of the dose of the individual components (A mg/kg and B mg/kg) and the combined dose (total (A + B) mg/kg). The second is the ratio of the components which will be used (i.e., 1:10 vs. 1:1 vs. 10:1 of A and B, respectively) at a given dose.

In safety pharmacology studies dose selection is not, in our view, problematic. In general the doses used are small multiples of the expected therapeutic dose, so it is unlikely that severe toxicity will occur with a combination [35]. Nevertheless, if there are fears about the severity of adverse effects the approach described below can be adopted.

In toxicity studies (general and reproductive) the high dose must produce toxicity or be a limit dose [24]. For studies with a combination of marketed compounds, to answer a specific question or resolve a specific issue, the dose and component ratio used in studies will most probably be defined by the data available. In this instance, the dose/ratio used may not need to produce adverse effects. For novel combinations or combinations involving one or more NMEs this is not the case. The high dose used will be expected to produce an adverse effect [1]. If for each component its toxic dose is used in the combination there is a strong possibility that the combined toxicity of the components will be excessive (compromising the relevance of the study) or lethal for the test animals (compromising the integrity of the study). In our view a more rational approach is to identify the high dose on the basis of the “total dose”; then as for monotherapy development, the mid and low doses can be set accordingly.

In the early stages of the development program, the ratio of components for optimal pharmacological/therapeutic effect is usually uncertain. However, preclinical studies must fully characterize the safety profile of the combination while providing flexibility in clinical studies to vary the total dose and component ratio. The “Factorial Study” described in the ICH-E12A guideline [36] is a good basis with which to address this issue. Since the optimal (pharmacological) ratio of the components is unclear in the early stages of development, a reference ratio can be set using the best estimate of a clinically relevant ratio (for example 1:1). This ratio can then be bracketed with ratios that favor one component and then the other (for example 10:1 and 1:10). In preclinical studies as the ratio is altered the *same* total dose is maintained. Thus a study with total doses of 100, 40, and 10 mg/kg and a reference component ratio of 1:1 could employ a dosing regimen as shown in Table 11. The choice of total dose must clearly be based on data from studies with the individual components (A and B) and possibly (small scale) preliminary studies with the combination.

Table 11
Possible dosing regimen for early studies in the development of a combination drug

Total dose (mg/kg)	Component	Component ratio (A:B)		
		10:1	1:1	1:10
Dose (mg/kg)				
10	A	9.1	5	0.9
	B	0.9	5	9.1
40	A	36.4	20	3.6
	B	3.6	20	36.4
100	A	90.9	50	9.1
	B	9.1	50	90.9

Based on the “Factorial Study” described in the Draft ICH-E12A “Consensus Principle” [36]

4.2 Species Selection for Combination Studies

For studies with a single NME or the marketed drug component, species selection should not be a major issue. It is likely that the rodent used will be the rat or mouse and the nonrodent will be the beagle dog, rabbit, and less often the nonhuman primate. For studies with a marketed drug, the species used will almost certainly be that used in the original study which generated the issue which needs to be investigated.

Species selection can become more problematic for studies with the combination however. The species used must be “the most appropriate species” and problems may be heightened if studies must also be conducted in a second species [1]. Problems are due principally to two factors:

- Poor toleration of one species to one component
- Different species being optimal from PK/ADME considerations for each component

If toleration is a problem and the use of an alternate species does not resolve the issue then the dose of the combination drug used should be lowered to ensure that the adverse events produced are acceptable [1]. If PK/ADME is an issue and changing dose levels of the combination and/or the test species does not produce PK/ADME profiles for each component which are broadly similar to that in humans the best compromise in terms of dose and species should be adopted.

In general, in cases where species selection is a major problem a pragmatic approach should be adopted. Where such cases arise, it is imperative that a clear set of arguments is developed, ideally

supported by experimental data, for the choice that is made. Given the uncertainty in such cases, whenever possible, it is advisable to discuss species selection with the regulatory authorities.

4.3 Study Structure

For monotherapies, preclinical studies usually follow a standard design. In general male and female animals are used with four dose levels; control, low, mid, and high dose. As shown in Table 11, with combination drugs the number of groups needed in a study is greatly increased. Even if individual components have been characterized in separate studies, studies with the combination should include groups treated with the highest dose of the single components. This insures that there is a bridge to studies with the individual components, and they are internal references for the source of any adverse events in the study.

A single study composed of all these groups would be of significant size and complexity. This is not to say that it is not feasible. However, at an early stage in the project it must be decided whether to conduct a single study or a set of overlapping studies. There is no right answer; the response is conditioned by the specific characteristics of the combination drug being developed and the emerging data. This problem of complexity primarily affects the early stages of the preclinical program at a time when the final clinical dose and component ratio are ill defined. As the program unfolds, preclinical studies can be simplified. Once the effective clinical dose and ratio of the combination have been defined, preclinical studies can be conducted at a single ratio.

5 Scenarios for the Preclinical Development of Combination Drugs

To facilitate discussion we will consider three main development scenarios, and while we will focus on a two-component combination the rationale we develop applies equally to combinations with greater numbers of components; only the complexity increases.

Overall, given the level of detail provided by the FDA's guidance [1], we recommend this as the base case for establishing a preclinical strategy for a combination drug; given the breadth and scope of this document it will, in our view, also be consistent with needs of the European and Japanese regulatory authorities. However, we recommend that, if possible, as soon in the development process as feasible the preclinical strategy is discussed with the regulatory authorities.

5.1 Combination of Established (Marketed) Drugs

The simplest case is for a combination of marketed drugs *with* a significant history of concomitant use of the components in humans at about the same ratio as that of the intended combination. In this instance, the first key step is a rigorous review of all the preclinical data available; this should include regulatory submission

documents and publications in the open literature and, ideally, original study reports. The objectives of this review are:

- To identify any issues with the quality of the data relative to modern (ICH) standards
- To determine the potential for interaction between the components and any actual or potential overlapping toxicities
- To identify any unresolved preclinical issues
- To review the safety assessment of the individual components and the combination to ensure that the safety margins for the components are acceptable (for both dose and duration of treatment)

If there are no significant issues or data gaps, this review should fulfil the preclinical needs for the combination. If data gaps are identified, then studies with the individual components and/or the combination may be needed; these studies would fall within the scope of the ICH studies for monotherapies or be specifically designed in the light of the data/issues.

For combinations of marketed drugs *with no* significant history of concomitant use in humans, the initial approach is identical to that described above. Additionally, data from a toxicity study of up to 3-month duration in one species will be required (depending on the duration of treatment in humans). Usually, unless one or both of the components has been assigned pregnancy category “D” or “X,” then an embryo-fetal development study (in one species) should also be conducted. However, depending on the target population and/or therapeutic indication it may not be necessary to conduct such a study; this underlines the importance of discussing key development issues with the regulatory authorities.

5.2 Combination of an Established Drug with an NME

The preclinical requirements for the marketed drug component have been described in Subheading 5.1. For the NME, a complete ICH program of studies is required to evaluate the safety profile of the new molecule (*see* Subheading 2.1). Additional preclinical studies will be required with the combination. As a minimum a study of up to 3-month duration will be required and depending on the developmental toxicity of each component possibly a developmental toxicity study. The value of an additional combination group(s) in the carcinogenicity study for the NME (using the most appropriate species) should be considered. If it is decided that carcinogenicity data on the combination are not required then a literature argument should be developed to justify this decision.

Finally, in the light of the emerging data additional studies may be needed to address data gaps or emerging safety issues. Designs for these studies could be based on standard ICH studies or may need to be developed specifically to address the question under investigation.

5.3 **Combination of NMEs**

In general, a choice has to be made between conducting preclinical studies only with the combination of the single components and the combination. The latter is probably the best option since this allows the components to be changed while retaining the ability to exploit the data generated for the other component/s. In addition, this also supports the option to develop one (or both) of the NMEs as a monotherapy or indeed its use in other combinations.

For each NME, a complete ICH program of studies is required to evaluate the safety profile of the new molecule (*see* Subheading 2.1). Additional preclinical studies will be required with the combination. As described above, as a minimum a study of up to 3-month duration will be required and depending on the developmental toxicity of each component possibly a developmental toxicity study. A choice must also be made between conducting a carcinogenicity study with the combination or additional combination group(s) in the carcinogenicity study for one NME component (using the most appropriate species). As in all the scenarios described, additional studies may be needed in the light of the emerging data.

5.4 **Conclusions**

FDCs have been available commercially for many years; recently nonclinical development guidelines for FDCs have been released by a number of regulatory authorities. However, the ICH guidelines for monotherapy development provide a framework for FDC development. Depending on the type of drug combination (marketed drug/market drug; marketed drug/NME; and NME/NME) the scope and complexity of toxicity studies vary greatly. In all cases however, a key issue is the potential for pharmacokinetic and/or toxicologic interaction between the components. For a marketed drug/market drug combination a detailed review of the nonclinical data available may suffice. For a marketed drug/NME combination, in addition to a review of the data for the marketed drug, a full ICH program of studies will be required for the NME, and a study of up to 90-day duration (in one species) for the combination. With an NME/NME combination each component will require a full ICH battery of studies and a combination study in one species. In all cases additional studies may be needed to address data gaps. Whenever possible, the nonclinical study strategy for FDC development should be discussed with the regulatory authorities.

References

1. FDA (2006) Nonclinical safety evaluation of drug or biologic combinations. <http://www.fda.gov/downloads/drugs/guidancecomplianceregulatoryinformation/guidances/ucm079243.pdf>
2. EMA (2008) Guideline on the non-clinical development of fixed combinations of medicinal products. http://www.ema.europa.eu/docs/en_GB/document_library/Scientific_guideline/2009/10/WC500003976.pdf
3. TGA (2014) Fixed combination prescription medicines. <https://www.tga.gov.au/combined-combination-prescription-medicines>

4. CADTH (2014) CADTH common drug review. Submission guidelines for the CADTH common drug review. https://www.cadth.ca/media/cdr/process/CDR_Submission_Guidelines.pdf
5. CDSCO (2010) Guidance for industry on fixed dose combinations (FDCs). <http://www.cdscn.in/writereaddata/FDC%20Guidelines%20-%20Revised1.pdf>
6. FDA (2015) <http://www.fda.gov/CombinationProducts/AboutCombinationProducts/ucm118332.htm>
7. Segal SA (1999) Device and biologic combination products. Understanding the evolving regulation. Medical Device and Diagnostic Industry. January. pp 180–184
8. Portnoy S, Koepke K (2005) Regulatory strategy. Preclinical testing of combination products. Medical Device and Diagnostic Industry. May. pp 152–157
9. Herxheimer H (1975) The danger of fixed drug combinations. *Int J Clin Pharmacol Biopharma* 12(1–2):70–73
10. Shenfield GM (1982) Fixed combination drug therapy. *Drugs*. 23(6):462–480
11. Sica DA (2002) Rationale for fixed-dose combinations in the treatment of hypertension: the cycle repeats. *Drugs* 62(3):443–462
12. Moulding T, Dutt AK, Reichman LB (1995) Fixed-dose combinations in antituberculous medications to prevent drug resistance. *Ann Intern Med* 122(12):955–956
13. Majori G (2004) Combined antimalarial therapy using artemisinin. *Parasitologia* 46(1–2):85–87
14. Fechtner RD, Realini T (2004) Fixed combinations of topical glaucoma medications. *Curr Opin Ophthalmol* 15(2):132–135
15. Prescott J, Manalo B (2011) Considerations for fixed-dose combination products in cardiometabolic disease. <http://www.pharmacytimes.com/publications/issue/2011/December2011/Considerations-for-FixedDose-Combination-Products-in-Cardiometabolic-Disease>
16. Kararli TT (2010) Fixed dose combination (fdc) products overview. http://www.pharmacircle.com/presentations/Fixed_Dose.pdf
17. Wertheimer A, Morrison A (2002) Combination drugs: innovation in pharmacotherapy. *P&T* 27(1):44–49
18. Hommer A (2011) Role of fixed combinations in the management of open-angle glaucoma. *Exp Rev Pharmacoecon Outcomes Res.* 11(1): 91–99
19. American Thoracic Society (2015) What kind of medications are there for COPD? <http://www.thoracic.org/copd-guidelines/for-patients/what-kind-of-medications-are-there-for-copd/what-are-combination-drugs.php>
20. Kararli TT, Sedo K, Bossart J (2014a) Fixed-dose combination products—a review (part 1—introduction). <http://www.drug-dev.com/Main/Back-Issues/FIXEDDOSE--COMBINATIONS-FixedDose-Combination-Produ-661.aspx>
21. Kararli TT, Sedo K, Bossart J (2014b) Fixed-dose combination products—a review (part 2—analysis). <http://www.drug-dev.com/Main/Back-Issues/FIXEDDOSE--COMBINATIONS-FixedDose-Combination-Produ-673.aspx>
22. Kararli TT, Sedo K, Bossart J (2014c) Fixed-dose combination products—what’s in the clinic? (part 3—pipeline). <http://www.drug-dev.com/Main/Back-Issues/FIXEDDOSE--COMBINATIONS-FixedDose-Combination-Produ-673.aspx>
23. ICH Guidelines (2007) <http://www.ich.org/home.html>
24. ICH (2009) Guidance on nonclinical safety studies for the conduct of human clinical trials and marketing authorization for pharmaceuticals M3(R2). http://www.ich.org/fileadmin/Public_Web_Site/ICH_Products/Guidelines/Multidisciplinary/M3_R2/Step4/M3_R2_Guideline.pdf
25. ICH (2012) M3(R2) Implementation Working Group M3(R2) guideline: guidance on nonclinical safety studies for the conduct of human clinical trials and marketing authorization for pharmaceuticals. Questions & answers (R2). http://www.ich.org/fileadmin/Public_Web_Site/ICH_Products/Guidelines/Multidisciplinary/M3_R2/Q_As/M3_R2_Q_A_R2_Step4.pdf
26. FDA (2013) Guidance for industry. Codevelopment of two or more new investigational drugs for use in combination. <http://www.fda.gov/downloads/Drugs/GuidanceComplianceRegulatoryInformation/Guidances/UCM236669.pdf>
27. FDA (2006) Fixed dose combinations, co-packaged drug products, and single-entity versions of previously approved antiretrovirals for the treatment of HIV. <http://www.fda.gov/downloads/Drugs/GuidanceComplianceRegulatoryInformation/Guidances/UCM079742.pdf>
28. Liminga U, Silva L (2003) Non-clinical development of fixed combinations. A European regulatory perspective. *Int J. Pharm Med* 18(3): 135–138
29. Japanese Pharmaceutical Association (2015) Pharmaceutical administration and regulations in Japan. <http://www.jpma.or.jp/english/parj/pdf/2015.pdf>

30. Hunt L (2003) Fixed-combination medicines: an Australian perspective. *WHO Drug Inform* 2:110–112
31. Therapeutic Products Directorate (2000) Guidelines for preparation of new drug submissions for products used for estrogen--progesterin replacement therapy in menopause (HRT). http://www.hc-sc.gc.ca/dhp-mps/prodpharma/applic-demanded/guide-ld/hrt-ths/hrt_ths-eng.php
32. WHO (2005) WHO Expert Committee on Specifications for Pharmaceutical Preparations Guidelines for registration of fixed-dose combination medicinal products Technical Report Series. WHO Tech Rep Ser 929: 93–142
33. Rogge MC, Taft DR (eds) (2005) Preclinical drug development. Taylor & Francis Group, Boca Raton, FL
34. CDER. Medical review for Kaletra. http://www.accessdata.fda.gov/drugsatfda_docs/nda/2002/21-251S003_Kaletra.cfm.
35. ICH (2000) Safety pharmacology studies for human pharmaceuticals S7A. http://www.ich.org/fileadmin/Public_Web_Site/ICH_Products/Guidelines/Safety/S7A/Step4/S7A_Guideline.pdf
36. FDA (2000) DRAFT ICH Consensus principle for clinical evaluation of new antihypertensive drugs E12A. http://www.ich.org/fileadmin/Public_Web_Site/ICH_Products/Guidelines/Efficacy/E12/Step4/E12_Guideline.pdf

Chapter 2

Juvenile Nonclinical Safety Studies in Support of Pediatric Drug Development

Paul C. Barrow and Georg Schmitt

Abstract

A pediatric assessment is now a required component of every drug marketing application in North America, Europe, and Japan, unless a waiver has been granted previously. Nonclinical juvenile toxicity studies are often required as part of this assessment. The protocols for juvenile toxicity studies are best devised in consultation with the regulatory authorities. It is important to submit the pediatric investigation plan (PIP) or pediatric study plan (PSP) early, in order not to delay the marketing authorization of the drug in adults. The choice of species and the design of juvenile toxicity studies are based on a series of complex considerations, including the therapeutic use of the drug, age at which children will be treated, duration of treatment, and potential age- or species-specific differences in efficacy, pharmacokinetics, or toxicity.

Key words Juvenile animals, Toxicology, Pediatric, Safety testing

1 Introduction

1.1 What Are Nonclinical Juvenile Animal Studies, When Are They Needed?

Safety studies may be performed in juvenile laboratory animals (usually rats) to help ensure the safety of children who will be given a new medicine.

- Juvenile animal studies are performed to fill important gaps in the knowledge between safety in the adult and safety in the child.
- In many cases, sufficient data are generated in clinical trials in adults and in the routine nonclinical safety studies in adult animals without the need for juvenile animal studies prior to the inclusion of children in clinical trials [2].
- In other cases, juvenile nonclinical studies are warranted to support the inclusion of children in clinical trials or to extend the marketing approval of an adult medicine for use in children.

To the children of the world: For their patience in waiting for the safe and effective medicines they deserve! John van den Ander [1].

This chapter discusses the rationale for juvenile safety studies, regulatory strategies for pediatric drug development, selection of model species, experimental design, and practical running of the experiments.

1.2 Definitions

- Juvenile: any immature organism from birth up to sexual maturity.
- Child: juvenile human, including neonate, infant, and adolescent (note that the International Council on Harmonisation (ICH) E11 guidance document [3] uses a more restricted definition: 2–11 years old).
- Pediatric-specific or pediatric-only: a therapeutic indication to treat a disease which only occurs in children, or has its onset in childhood.
- Pediatric-first: a pediatric drug development program in which all clinical trials will be conducted in children (as opposed to starting in healthy adult volunteers).
- First-in-pediatrics: first clinical trial in a pediatric population, whether or not clinical trials in adults have already been performed (not to be confused with above).
- Neonate: newborn baby up to 27 days of age, including pre-term neonates (<37 weeks' gestational age at birth), or newborn animal.

1.3 Children as a Unique Therapeutic Population

The efficacy and safety of an adult medicine may be very different in the child, infant, or baby. Several accidents have occurred when adult medicines have been used in the pediatric population [4].

Children as a population have been described as “therapeutic orphans” in view of the lack of information on safety, dosing, and efficacy of medicines for pediatric use. The term was coined in 1968 by Shirkey [5].

Before the passage of the Food and Drug Administration Modernization Act (FDAMA) in the USA in 1997, there was little inclination by the pharmaceutical industry to develop medicines for pediatric use, forcing pediatricians to prescribe adult drugs that had not been evaluated for safety in children [6].

- Before 1997, more than 80% of the drugs approved for adult use were being used in pediatrics, even though their safety and effectiveness had not been established in children. By 2015, that proportion had been reduced to about 50% [7]. Even so, up to 90% of drugs used to treat neonates and infants are still off-label [8].
- According to the American Academy of Pediatrics in 1995, the majority of marketed drugs were not labeled, or were insufficiently labeled, for use in pediatric patients [9].

- Some adult dosage forms are not adapted for use in children (e.g., tablets in neonates) necessitating ad hoc formulation [10].

This forced unregulated use of adult drugs and of adult dosage forms in children posed an obvious risk of adverse effects or of under- or overdosing.

As a result of the new legislation, labeling changes have been made to nearly 500 drugs studied in children under the Best Pharmaceuticals for Children Act (BPCA), but the vast majority of drugs still have insufficient labeling regarding their use in children [11]. The legislative changes favoring the development of better medicines for children in the USA and Europe are described in **Note 1**.

1.4 Safety Studies in Juvenile Animals: A Twenty-First-Century Development

Regulatory guidelines for safety studies in juvenile animals to support clinical trials in children are a recent development:

- The first regulatory guidance on juvenile animal studies was issued by the US Food and Drug Administration (FDA) in 2006 [17].
- Similar guidelines were issued by the European Medicines Agency (EMA) in 2008 [18] and by the Japanese Ministry of Health and Welfare in 2012 [19].
- Before 2006, juvenile animal models, while not mandatory, had nonetheless been frequently used by some companies to evaluate the safety of the few medicines that had been developed for pediatric use, e.g., [20].
- An international harmonized guideline on nonclinical juvenile studies is currently in preparation [21].

1.5 Clinical Trials in Children

The general principles of clinical trials in children are outlined in a harmonized tripartite guideline ICH E11 issued in 2000 and currently under revision [3]. Before this legislation came into effect, clinical trials in children were rare [6]. In 2014, 1599 pediatric studies were under way in the world according to the US National Institutes of Health [22] (*see Note 2* for more detail).

Generally, data from phase 2b/3 clinical trials in adults will be available before initiating clinical trials in children. This may not be true for pediatric-specific indications, however (see below). An earlier initiation of pediatric clinical trials may be justified for therapies to treat severe or life-threatening diseases which frequently affect children and for which there is no therapy available or all accepted therapies have failed.

The following nonclinical studies are usually available prior to initiation of pediatric clinical trials:

- Repeat-dose studies of appropriate duration in adult animals, usually in two species.
- Core safety pharmacology package in adult animals.

- Standard battery of genotoxicity tests (not performed for biopharmaceuticals).
- Reproductive toxicity studies may be important for the assessment of developmental toxicity or potential effects on the reproductive system, but are not critical to support initial and short clinical trials in young children.
- Carcinogenicity studies are only required if there is a particular concern and the proposed treatment duration exceeds 6 months.

Juvenile animal studies (JAS) are required only when the existing clinical and nonclinical data are insufficient to support the proposed clinical trial(s). The youngest age at which children will be treated and the proposed duration of treatment are important considerations.

- Generally, juvenile animal toxicity studies are not considered important for short-term pharmacokinetic (PK) studies (e.g., 1–3 doses) in pediatric populations.
- Juvenile animal toxicity studies are generally not required for drugs intended only for adolescents, since adequate data is often provided by the repeat-dose studies (see below).

Guidelines for the Ethical Conduct of Studies to Evaluate Drugs in Pediatric Populations have been issued by the American Academy of Pediatrics [23]:

- The conduct of clinical trials in children carries with it ethical obligations in addition to those that apply to clinical trials in adults.
- It is unethical to unnecessarily repeat clinical trials in children, so all pediatric trials must be registered before initiation (www.clinicaltrials.gov) and the results should be made public, even negative findings.
- In addition to the informed consent form signed by the parents or guardian, the internal review board must assure that the assent of the child has been sought where possible.

2 Pediatric Plans

The pediatric plan is termed the Pediatric Investigation Plan (PIP) in Europe and the Pediatric Study Plan (PSP) in the USA.

- The final agreed plan contains the full details and timing of the pediatric clinical trials, including details of the formulations to be used and any necessary JAS.
- The plan is legally binding and must be completed in its entirety.

- All modifications to the study designs or timing of the studies must be agreed with the authority in the form of an approved amendment.

Industry, academia, and regulatory authorities have worked closely since the inception of the pediatric initiative to develop the most appropriate approaches to providing nonclinical support for pediatric development [24]. For instance, monthly joint teleconferences are held between the FDA and the EMA pediatric committee (PDCO), with the Japanese Pharmaceuticals and Medical Devices Agency (PMDA) and Health Canada as regular observers [25].

Because of the differences in timing of submission of the pediatric plan, the initial pediatric consultation for global pharmaceutical companies is usually with the EMA.

2.1 Pediatric Investigation Plan Submission in Europe

- The application for a PIP, a waiver, or a deferral is submitted to the EMA during clinical phase 2 (proof of concept) at the latest.
 - An application during phase 3 or after initiation of pediatric clinical trials is unacceptable.
- The application is reviewed by the PDCO and discussed at four meetings on days 30, 60, 90, and 120.
 - The nonclinical working group (NcWG) reviews the non-clinical proposals before the day-60 meeting and may be involved in later discussions as necessary.
- The initial conclusions of the PDCO are issued after the day-60 meeting, along with any request for modification.
 - The clock is stopped until a reply is received from the applicant.
- The applicant's responses are reviewed by the PDCO on day 90.
- The final opinion is discussed and issued on day 120.
- A PIP compliance check is initiated by the applicant prior to filing.
 - All pre-filing studies or measures in the PIP must have been completed.
 - If the PIP contains postmarketing commitments (e.g., in case of a deferral), a partial compliance check is made to allow filing.
- The rewards or incentives under the pediatric regulation are only granted once full compliance has been demonstrated.

2.2 Pediatric Study Plan Submission in the USA

The FDA encourages discussion of pediatric plans as early as possible:

- For life-threatening illnesses by the end of phase 1.
- For nonlife-threatening illnesses, within 60 days of the end of phase 2 meeting and no later than 210 days before NDA filing.

The applicant seeks the opinion of the FDA in the form of a proposed pediatric study request (PPSR):

- The FDA reviews the PPSR and issues a written request (WR) that specifies the requirements for pediatric exclusivity and labeling.
- Most often the discussion over the pediatric development plan takes place at the end of phase 2 meeting.
- The pediatric plan should be agreed by the start of phase 3 trials, allowing all agreed studies to be completed before filing of the adult NDA.

Under Pediatric Research Equity Act (PREA), the FDA has the right to demand a pediatric plan for an existing drug.

2.3 Pediatric Drug Development Plan Submission in Japan

Since 2009, Japan started to catch up with the pediatric regulations of the USA and Europe.

- Submission of a pediatric drug development plan in Japan can result in an extension of the exclusivity period of an existing drug from 8 to 10 years, if the plan is accepted.
- The PMDA is responsible for the review and discussion of the plan, while the Ministry of Health, Labor, and Welfare (MHLW) has the final judgment on approval. Drugs such as fluvoxamine, paroxetine, and aripiprazole have been approved for pediatric use under this scheme [26].
- For well-known existing drugs, for which there is a depth of may be granted without further work (副知申請 or *Kouchi-shinsei* = known application) [25].
- The Japanese Children Trials Network (JCTN) was established in November 2010 and the Pediatric Working Group was established in 2011.
- The number of drugs approved by MHLW for pediatric indications has steadily increased over recent years, reaching 36 in 2013 (40% of approvals). In total, 177 pediatric drugs had been approved by 2013 [25].

2.4 Lessons Learned So Far

Information on opinions and decisions of the EMA PDCO on PIPs, including deferrals and waivers, can be found on the EMA website [27]. Information on the decisions of the FDA on PSPs is not readily accessible.

A report by the US Institute of Medicine (IOM) [28] commissioned by the FDA reached the following conclusions among others:

- Pediatric studies conducted under BPCA and PREA are yielding important information to guide clinical care for children. Information from pediatric studies sometimes supports and

sometimes runs counter to expectations about the efficacy, safety, and pharmacokinetics of a drug in children of different ages.

- Some studies requested under BPCA or required under PREA do not achieve their full potential. Reasons vary and may include the inability of sponsors to recruit sufficient numbers of children, the use of weak study designs and underpowered samples, the lack of dose-ranging studies to guide efficacy trials, and the omission of relevant study information from a product's labeling. FDA has taken steps to address many of these problems.
- More timely planning, initiation, and completion of pediatric studies would benefit children. European requirements for the submission of plans for pediatric studies apply at a stage of drug development that may be somewhat premature, whereas US requirements apply later than may be warranted. Delays in sponsor completion of required studies also warrant further attention.

The US IOM also made the following recommendations:

- Expand public access to information from pediatric studies conducted under BPCA and PREA.
- Improve the timeliness of certain pediatric studies.
- Address areas of limited pediatric investigation under BPCA and PREA, including neonatal studies and long-term safety studies.
- Increase the clarity and understanding of FDA judgments about pediatric studies.
- Continue to encourage pediatric studies of biologics.

In Europe, according to a recent analysis by Hurtt and Engel [29]:

- Out of 1028 PIPs with decisions from 2007 to 2013, 30% were granted a complete waiver from pediatric investigations.
 - This proportion, however, has steadily declined over the years, falling to 18% by 2013.
- Among the approved PIPs requiring pediatric investigation, 21% included a requirement for JAS.
 - This proportion has remained stable when the PIPs are ordered by the date of the original submission (and not the date of the most recent modification indicated on the EMA website).
- The actual proportion of PIPs that include JAS is actually higher than 21%, since the above figure does not include JAS that were already available at submission of the PIP.

A previous review by Baldrick [30] breaks down the approved PIPs by therapeutic indication.

Little information is available from non-ICH countries on the regulatory need for juvenile animal data. Most countries will follow ICH and FDA guidance or have released their own guidelines with similar content. In Russia, a pediatric protocol was first rejected with the feedback that “it is unethical to include children in the study if data on drug-related toxicity in sexually immature animals have not been reported”. The case was solved by the sponsor submitting a rationale for the absence of dedicated toxicity studies in juvenile animals (not published).

3 Unique Vulnerability of the Juvenile: Functional Immaturity

A thorough understanding of the changes that occur during development and maturation is necessary to adequately assess potential safety concerns of a new drug in children [31].

Many organs are not fully functional at birth and continue to mature during postnatal development.

- This functional immaturity may have complex and far-reaching consequences on the effects of drugs in children. For instance, the absorption of a drug following oral ingestion may differ between the child and adult due to differences in the permeability of the intestinal wall or due to differences in the pH of the gastrointestinal tract.
- The distribution of the drug following absorption or parenteral administration may then be influenced by differences in membrane permeability. The blood–brain barrier, for instance, is more permeable up to the age of about 6 months, which may result in adverse central nervous system (CNS) effects in infants with drugs that do not cross the blood–brain barrier in adults.
- The bioavailability and distribution of drugs may also be influenced by differences in the composition of body tissues and fluids between children and adults (e.g., water content of organs or the binding affinity of plasma proteins).
- Drugs are often metabolized more slowly or via different pathways in children due to a reduced enzyme activity related to immaturity of the liver.
- A drug may be eliminated more slowly from the circulation in the child due to the relative inefficiency of the immature kidney.
- The pharmacological efficacy of the drug may be enhanced or diminished due to differences in the relative numbers of receptors present in the target tissue of the immature organism compared with the adult.

3.1 Neonates

Neonates are a particularly vulnerable subpopulation. They possess unique disease states and susceptibilities and therefore require the most careful considerations of benefit-risk, feasibility, formulation development, and nonclinical support.

Preterm newborns represent a highly heterogeneous and rapidly developing population [3]:

- Neonates show a number of significant physiological differences compared with older pediatric age groups, such as reduced lung function.
- The rapid development of neonates results in extensive intra- and interindividual variability in both PK and pharmacodynamics (PD), making extrapolation of data from older children to neonates a huge challenge.

Examples of PK-related adverse events in neonates:

- Gray baby syndrome [32]: This rare and serious condition occurred following IV injection of chloramphenicol as an antimicrobial therapy. The newborn lacks the enzyme UDP-glucuronyl transferase and has insufficient renal capacity to excrete unconjugated chloramphenicol, leading to an accumulation of toxic metabolites.
- Gasping syndrome [33]: This occurred in babies following IV exposure to benzyl alcohol used as an antibacterial excipient in various drug formulations. The symptoms are caused by metabolic acidosis due to immaturity of the metabolizing pathway leading to benzoic acid accumulation.

Neonates are often viewed as the “last therapeutic orphans” [34]. Conditions affecting neonates may not occur in other pediatric age groups.

There is an urgent need for effective therapies to treat neonates for the following conditions [35]:

- Lung, brain, and gastrointestinal injury
- Perinatal infections
- Retinopathy of prematurity
- Sepsis
- Neonatal abstinence syndrome

Clinical therapy of neonates is typically short-term, aiming at safeguarding survival. There has been little opportunity to identify any long-term consequences of these therapies. Therefore, models (in silico, in vitro, and in vivo) to identify hazards in this vulnerable age group are urgently needed. Collaborative networks have been built to advance the understanding of neonates and thus improve their intensive care. For example, a first “Neonatal Scientific Workshop” was held by the US FDA in 2014 [35] and

a network on neonatal animal models was created in 2015 under the umbrella of the International Life Sciences Institute-Health and Environmental Sciences Institute (ILSI-HESI).

The Large White landrace pig has been used as a model of the preterm human neonate: the development of neonatal pigs delivered by cesarean section at various ages was successfully studied using standard neonatal care techniques [36].

3.2 PK/ADME

A major source of increased risk of adult medicines in pediatric applications is due to unexpected high exposure in the child resulting from functional immaturity of the drug metabolism, distribution, or elimination mechanisms.

- An industry survey commissioned ILSI-HESI and published in 2011 [37] reported that more than one-third (43/102) of juvenile animal studies found greater exposure in the juvenile than would be anticipated based on adult PK data. These differences are most notable in neonates.

For orally administered drugs:

- The drug may be more or less rapidly absorbed across the immature gastrointestinal mucosa than in the adult.
- The absorption characteristics of the drug may be influenced by the differences in pH between the juvenile and adult in the region of the digestive tract in which absorption takes place.
- The degree of hydrolysis of the drug may vary according to the functional maturity of the digestive enzymes.

Once in the systemic circulation:

- The bioavailability of the drug may be influenced by differences in the composition of the plasma proteins between the adult and the neonate.
- The volume of distribution is often greater in the neonate than in the adult, due to greater penetration of the drug into the brain. Greater brain penetration may also lead to unexpected central nervous system toxicities in the neonate [38].
- Reduced hepatic portal blood flow or reduced kidney filtration rate may lead to slower elimination in the juvenile than in the adult [39, 40].

3.3 Metabolism

Metabolism of a drug in the juvenile depends on the relative functional maturity of the enzymes responsible for its catabolism.

Such differences may be predicted by examining the ontogeny of the enzymes involved in the metabolism of the drug [41]. For example:

- CYP3A4 has low expression at birth in the human and only reaches 50% of adult levels by 12 months of age, after which

it becomes the prevalent cytochrome P450 (CYP) in the adult liver.

- Before this time, CYP3A7 is more prevalent [42].
- The predominant isoforms in adult rats are CYP2C11 (male) and CYP2C12 (female), which develop during weaning and reach adult levels by postnatal day (PND) 5 [43].

This type of knowledge is needed to understand differences in TK data between the adult and the juvenile in animals or humans.

Commercial PK modeling and simulation tools, such as SimCYP (Simcyp Ltd, <http://www.simcyp.com>) and GastroPlus (Simulations Plus, Inc, <http://www.simulations-plus.com/>), include modules for human adults and children [44], but as yet not for juvenile animals. These human physiologically based pharmacokinetic (PBPK) models are now being routinely applied to guide dose adjustment prior to pediatric PK studies. Such dose estimations have been accepted by health authorities for several recent projects [45, 46].

It is important to mention that more knowledge is needed on the ontogeny of many enzyme systems, particularly in extrahepatic tissues [31].

4 Preclinical Guidelines

The FDA, EMA, and Japanese MHLW have issued guidelines on juvenile animal studies [17–19]. The scope and content of the three documents are remarkably similar (except for the spelling of “pediatric” and “harmonization”): a comparison is given in Table 1. The new guidelines complemented the existing ICH guidelines for the reproductive toxicity testing of medicinal agents, which are currently under revision [47].

A harmonized ICH guideline on juvenile animal studies is currently under preparation [21].

Other subsidiary details included in the various guidance documents for JAS are as follows:

- The US and European guidances highlight effects on development of the nervous, renal, reproductive, immune, and pulmonary systems. The FDA text insists as well on the detection of potential effects on the development of the skeleton and gastrointestinal system.
- The European text is more detailed regarding the need and design of specific studies addressing potential neurotoxic, immunotoxic, or nephrotoxic effects.
- The US guidance provides examples of human-to-animal comparison of developmental periods and considerations for the use of juvenile animal data in risk management.

Table 1
Comparison of guidelines for Juvenile Animal Studies (JAS) between USA, Europe, and Japan

Content	USA	Europe	Japan
Scope	Describes when JAS are needed and when JAS are <i>not</i> needed	Describes situations when JAS are needed	Describes situations when JAS are needed
Number of species	1 usually sufficient	1 usually sufficient	1 usually sufficient
Recommended species	Rat (preferred) or dog	Rat (preferred) or dog	Rat only
Dosing duration	Cover developmental periods of interest	Based on human duration of treatment	May stop at the age of animals at the start of dosing in adult studies
Testing protocols	Endpoints and parameters listed	Endpoints and parameters listed	No specific guidance
Number of dose levels	3	3, 2 may be sufficient	Dose–response to be investigated, only high dose mentioned
High-dose selection	Should produce identifiable toxicity	Should produce some, but not marked, toxicity	Slight toxicity in juvenile, or dose at which toxicity was seen in adults
Low-dose selection	NOAEL ^a	NOAEL	NOAEL not essential

^aNo observed adverse effect level

- The US guidance indicates circumstances where juvenile animal studies would be neither informative nor necessary (*see Note 3*). The European document specifies circumstances when a case-by-case approach should be used.

The ICH M3 guideline on nonclinical safety studies for the conduct of human clinical trials for pharmaceuticals [2] states that general toxicity studies and genotoxicity tests should be completed before the initiation of clinical trials in children and that the reproductive toxicity studies may also provide useful information.

5 Submission Strategy: Instructions

Once a pediatric strategy has been outlined, the following steps may be followed:

5.1 Determine Any Remaining Data Needs

It may be helpful to perform limited preliminary juvenile animal studies to answer outstanding questions before submitting a pediatric dossier to the regulatory authority. Such preliminary studies could, for instance, provide the following information:

- Investigate sensitivity of animals of various ages.
- Compare the sensitivity of different potential species.
- Evaluate the feasibility of the route of administration, method of dosing, and formulation under the planned experimental conditions.
- Provide preliminary TK data.

5.2 Request a Waiver If a Pediatric Program Is Not Warranted

JAS are not necessary for drugs that have no therapeutic use in children (e.g., Alzheimer therapies). If a pediatric program is not warranted, seek the agreement of the FDA, or a formal waiver from the EMA, well before the time of submission of the adult dossier.

5.3 Consider Whether Juvenile Animal Studies Are Necessary in Support of the Proposed Clinical Program in Children

Example situations where JAS may serve no purpose:

- When sufficient human data are already available from off-label use of the drug in children: Note, however, that reliable data is rarely compiled for off-label drug use.
- For drugs only intended for older age groups (e.g., 10 years of age or older), sufficient safety information can usually be obtained from the safety studies in young adult animals, without the need for specific juvenile animal studies (*see Note 4*).
- A pre- and postnatal development (PPND) study, in which the lactating female rat is dosed, could result in sufficient exposure of the pups for a preweaning juvenile assessment if the drug is present at high concentrations in the milk and is readily absorbed by the pups (*see Subheading 11* below). Pup exposure via the milk would have to have been measured to justify this approach.
- For oncology indications with a very short life expectancy, the principal objective is to detect increased sensitivity of the juvenile and to contribute to the estimation of first doses in children. It may be possible to obtain this information from a proof-of-concept study in an animal disease model with additional endpoints. Otherwise, sufficient data may be obtained from a single-dose or short-term JAS [48].

Proportion of 97 approved or ongoing PIPs between Nov 2008 and May 2010 [49]:

- 41% with no juvenile studies.
- 33% with juvenile studies suggested by applicant.
- 26% with juvenile studies requested by EMA.

5.4 Consider If the Pediatric Assessment Can Be Deferred

The potential therapeutic benefit of the drug in children may be in doubt pending the initial results on efficacy and/or safety in the adult. In such cases, the FDA or the EMA should agree to defer the pediatric assessments until more data are available in adults. Again, the agreement of the agency should be sought well in advance.

Table 2
PIP decisions

Total published PIP decisions 2007–2013	1028	
Without complete waiver	722	
With juvenile animal studies	164	23%
With studies in two species ^a	8	5%
With single species identified ^b	134	
Rat	107	80%
Dog	11	8%
Mouse	8	6%
Nonhuman primate	4	3%
Pig	3	2%
Sheep	1	1%

Data compiled from Hurtt and Engel [29] and Baldrick [30]

^aExcluding preliminary or PK studies in a second species

^bNot all published PIP decisions specify the species used

5.5 One or Two Species?

According to the US, European, and Japanese guidance documents, JAS in a single species are generally sufficient to complete a New Drug Application (NDA) or a Marketing Authorization Application (MAA) submission. The published opinions of the EMA PDCO appear to be in accordance with this principle, with only 5% of the approved PIPs to date specifying pivotal juvenile studies in two species (*see* Table 2).

Two species may occasionally be preferable to investigate separate safety concerns that cannot be evaluated simultaneously in a single study. For instance, a juvenile dog study may be the most appropriate model system to assess a cardiovascular concern in the infant, while a rodent study is more effective and practical for the assessment of potential developmental consequences of long-term exposure.

For example, for a janus kinase inhibitor for use in juvenile idiopathic arthritis [50], following discussions between the applicant and the EMA, it was agreed to perform studies in both juvenile rats and juvenile primates. A primate study was needed to complement the rat study in which immune function could not be adequately assessed due to an oversensitivity of the rat to B-cell depletion.

Another circumstance in which JAS in two species are most often needed is for pediatric-specific indications, when no repeat-dose studies have been performed in adult animals (*see* below).

5.6 Interaction with the Regulatory Authorities

The PIP submitted to the EMA or a Proposed Pediatric Study Request (PPSR) submitted to the FDA should include all of the following nonclinical information:

- Outlines or protocols of the proposed JAS.
- The reasoning behind the proposed strategy, including the details of any discounted alternative strategies.
- All of the pertinent PD, TK, and toxicology data.
- A full discussion of the underlying safety issues.

The response from the agency may or may not be in agreement with the proposed strategy, but an open constructive discussion is possible.

The results of any requested JAS will be a requirement of the NDA or MAA submission for the adult (unless a deferral is granted).

6 Oncology and Treatments for Life-Threatening Juvenile Diseases

According to the current regulatory guidance documents [51], JAS are not required for life-threatening oncology indications. However, JAS are included in the pediatric development for one-third of new oncology drugs [52]. It appears that the regulators have a concern for long-term (late) effects if survival occurs [30].

7 Pediatric-Specific Indications

The clinical development of drugs intended specifically for pediatric use (i.e., “pediatric specific”) may start with clinical trials in healthy adult human volunteers, which is the most common approach, or may exceptionally proceed directly with trials in pediatric populations (i.e., “pediatric first”).

A pediatric-first clinical program may be supported by subchronic studies in a rodent and a nonrodent species, starting dosing in young animals at a developmental stage corresponding to the youngest intended pediatric population. It may be advisable to extend the treatment period past the usual 4 weeks for conventional studies to cover the developmental stages up to maturity.

Alternatively, the chronic studies (6 months in rodent and 9 or 12 months in nonrodent) may be performed in juvenile animals, which has the advantage of providing all of the repeat-dose data required up to marketing. However, because of the large investments and long timelines, it is usually more time effective to perform subchronic studies in juveniles first to allow a rapid start of the initial pediatric clinical trials.

For example, in 2013 the PDCO of EMA agreed to allow the start of clinical trials in children from 6 years of age with lisdexamfetamine for the treatment of attention-deficit hyperactivity disorder following an 8-week study in the juvenile rat and a 2-week dose range finding study in the juvenile dog [53].

8 Combination Pediatric Drug Therapies

JAS are not usually required for combination therapies (i.e., two or more drugs intended to be given simultaneously), provided that a pediatric dossier is available for each of the component drugs and covers the intended patient age range. JAS may be necessary, however, in the following circumstances:

- The component drugs have a similar mechanism of action.
- The component drugs have the same target organ(s) of toxicity.
- The PK characteristics of the component drugs may be altered when given in combination to the juvenile (e.g., by competing for limited metabolizing capacity).

A juvenile toxicity study was requested by the EMA PDCO in 2008 (but not the FDA) to test an antifungal combination therapy with anidulafungin and voriconazole with groups of rats given each drug alone or in combination [54]. Preclinical and clinical studies in adults had indicated the liver as a potential target organ of toxicity for both drugs. The two drugs, however, had not shown any adverse interactions in adults and both are metabolized and eliminated by separate pathways. The completed combination study did not reveal any novel or synergistic toxicities in the juvenile.

9 Excipients

The development of drug products for pediatric use often requires age-appropriate formulations which can be more complex and may involve a broader range of excipients than adult dosage forms. Excipients established for adult use are not always appropriate for use in children because they can affect children differently than adults [55]. These issues are covered in an EMA guideline on pharmaceutical development of medicines for pediatric use [56].

In the USA, use of age-appropriate formulations in pediatric assessments is stipulated in PREA, but no further specific guidance with respect to pediatric formulations is provided by the FDA. European regulations and expectations are more specific and detailed. An EMA reflection paper provides general guidance regarding pediatric formulation development [57]. The composition of the intended formulation(s) for clinical use has to be detailed in the PIP. Further regulation regarding pediatric formulations can be expected in the EU.

A comprehensive safety assessment of all excipients in pediatric formulations is essential. For this purpose, the following published data may be available:

- Adult human safety data.
 - And from pediatric use if available.
- Adult animal toxicology data.
 - And from juvenile animals if available.

The overall risk assessment needs to balance any perceived hazard from the excipients against benefit of the drug in treating the disease.

JAS are useful for the detection of juvenile-specific toxicities or increased sensitivity of juveniles to excipients and for establishing safe exposures in pediatric age groups. As for active ingredients, JAS should only be performed for excipients if they are likely to contribute valuable data for clinical risk assessment and labeling.

Whenever possible, the human pediatric dose formulation should be used in JAS, to avoid the need for separate animal studies to assess each excipient.

A European database called Safety and Toxicity of Excipients for Paediatrics (STEP) [58] is currently being populated with information from the following sources:

- Clinical data.
- Toxicity data.
- Regulatory references.
- Toxicology reviews.

10 Biopharmaceuticals

The same principles for pediatric testing are followed for biopharmaceuticals as for small-molecule drugs. The following general characteristics, however, often differ from conventional therapies:

- Limited species specificity (often with pharmacological activity only in primates).
- Increased liability for immunogenicity (leading to the production of antidrug antibodies).
- Parenteral administration (usually IV or SC).
- Long systemic half-life (particularly for monoclonal antibodies (mAbs)).
- Toxicity not associated with the intended pharmacological activity is relatively rare.

For the biologics tested in juvenile animals or in children to date, no major differences in PK between the juvenile and the adult have been identified [59]. This is unsurprising given the limited metabolism and uniform mode of elimination of engineered

proteins (i.e., catabolism and renal filtration). However, any significant differences in the abundance or affinity of the target during juvenile development could have consequences on elimination and hence PK of the mAb.

For mAbs which do not cross-react in lower species, the non-human primate (NHP) is used for the reproductive toxicity assessment. The enhanced PPND (ePPND) study is performed in the place of the embryo-fetal development and PPND studies in rodents and rabbits for small molecules [60]. IgGs readily cross the placenta in primates during late gestation, so the newborn monkey usually has high levels of maternally administered mAb at birth, which may persist for weeks or months. Thus, important information of potential effects of the mAb in the neonate can often be gleaned from the ePPND study. Consideration may also be given to the possibility of directly dosing offspring in the ePPND study to avoid the need for a stand-alone juvenile study.

Juvenile studies in NHPs should be avoided whenever possible, because of the practical and ethical concerns around the handling of baby monkeys, which can be stressful for the juvenile and mother. Also only a very limited number of juvenile NHPs can be included in each study due to the low availability of pregnant monkeys, poor reproductive performance of NHPs, and low numbers of offspring (one per pregnancy).

Even if a biopharmaceutical is pharmacologically active in rats or rabbits, it may be rapidly neutralized due to immunogenicity. The immune reaction may also confound the interpretation of the study results, for instance due to renal effects caused by the deposition of immune complexes. Possible strategies, such as the administration of a high loading dose followed by smaller maintenance doses, have been successfully used to minimize immunogenicity to biologics in rodents [61].

While homologous surrogate molecules do not test the actual clinical candidate and cannot be used for dose extrapolation [62], they can be useful to test hypothesized effects of the pharmacology of the drug on juvenile development [61].

Disadvantages of NHPs for JAS are as follows (taken from Morford et al. [59]):

- Challenge to procure adequate numbers of appropriately aged animals, of suitable gender mix.
- Youngest age typically available from vendors (approx. 12 months old) may not provide match to clinical pediatric age range.
- Not practical to test full span of postnatal development, for example until sexual maturity.
- Limited reference data for some parameters due to infrequent use for juvenile testing.

- Potential animal welfare issues associated with use of the model.
- Appropriate technical experience limited to a few laboratories.

In practice, the monkeys used for the repeat-dose studies are often relatively young (e.g., 2–3 years) and may provide information pertaining to the toxicity of the drug in the anticipated pediatric age group. In designing repeat-dose studies in NHPs, however, the need for juvenile data must often be weighed against the main objectives of the studies, such as a requirement to evaluate the effects on the mature reproductive organs.

11 Nonclinical Testing Strategy

11.1 *Considerations Influencing Study Design*

Each study is designed case by case, based upon the following considerations:

- Therapeutic use of drug and age groups.
- Timing and duration of treatment in children.
- Potential age- or species-specific differences in PK or toxicity.
- Interspecies differences in the timing of development.
- Known organ toxicity of the drug.
- Existing toxicity studies involving adolescent and young adults.

11.2 *Devising a Testing Strategy: Steps to Follow*

1. Seek to understand the potential consequences of the pharmacology of the drug on the developing juvenile. Information may be obtained from various sources:
 - Published literature.
 - Receptor distribution and tissue expression data in juvenile models.
 - Specific juvenile disease models at stages relevant for human pediatric age groups. For example, a B-cell progenitor kinase (bpc) mouse model was used at various juvenile stages to assess the potential effects of a drug candidate to treat autosomal recessive polycystic kidney disease [63].
2. Review the available human data (including pediatric data, if available) alongside the toxicology data in adult animals.
3. Identify the potential target organ(s) in children based on adult data and PD target.
4. Select an appropriate juvenile animal model that shows a similar pattern of postnatal development of the identified target organ(s). Preference should be given to the species previously used for the repeat-dose studies.

5. Perform preliminary studies to evaluate the tolerance of the drug in the juvenile under the anticipated conditions of the main study and also to generate any required data on PK and metabolism in the juvenile animal.
6. Adapt the treatment period in the main juvenile studies to encompass all of the relevant developmental stages of the animal with respect to the therapeutic use of the drug in children.
7. If necessary, adapt the dose levels during the course of the treatment period to account for maturation-related influences on PK and maintain the required level of exposure throughout all developmental stages.
8. Consider specific endpoints for inclusion in the study design in order to monitor the development and function and of the potential target organs. Consideration should also be given to monitoring potential concerns that cannot be effectively or ethically examined during the pediatric clinical trials.

As indicated above, a PPND study may provide sufficient pup exposure to evaluate the influence of the drug on preweaning development. In addition, it may be feasible to avoid a stand-alone juvenile study and to save animals by adapting the standard PPND study design to provide pups for direct dosing with the drug. This option is particularly valuable if the juvenile pups only need to be treated from weaning, since the excess pups are normally discarded in the PPND study at this age.

12 Comparative Organ Development: A Moving Target

A comparison of the ages of the different developmental stages of various species with respect to the human is given in Table 3. The value of this oversimplified summary is limited, however, since the timing of the treatment period and examinations in a juvenile study must be based on an in-depth consideration of the comparative timing of development of the potential target organs in the species in question (*see Note 5*).

If neonates are to be treated, consideration should be given to those organs which develop prenatally in some species and postnatally in others, such as the kidney. The nephrons are present at birth in humans, but only form postnatally in rats. Kidney dysmorphology can be induced in the neonatal rat by angiotensin-converting enzyme (ACE) inhibitors. Children are insensitive to this effect, but similar abnormalities are induced in human newborns following late gestational exposure of the mother to ACE inhibitors.

Only a very brief overview of the comparative development of selected organ systems is given below; the cited references should be consulted for more complete information.

Table 3
Age comparison between humans and various animal models

Species	Preterm	Newborn	Infant	Child	Adolescent
Human	–	0–28 days	1–23 months	2–12 years	12–16 years
Monkey	–	0–15 days	0.5–6 months	0.5–3 years	3–4 years
Dog	–	0–21 days	3–6 weeks	6–20 weeks	5–7 months
Pig/minipig	–	0–15 days	2–4 weeks	4–14 weeks	4–6 months
Rabbit	0–4 days	4–10 days	1.5–5 weeks	5–12 weeks	3–6 months
Rat	0–4 days	4–12 days	1.5–3 weeks	3–5 weeks	5–10 weeks
Mouse	0–4 days	0–10 days	1.5–3 weeks	3–5 weeks	5–7 weeks

Adapted from Barrow 2007 [98]

12.1 Heart

The postnatal morphological and functional development of the heart appears to be relatively similar across mammalian species [66].

12.2 Kidney

The anatomical and functional development of the kidney varies considerably between species [39]. Nephrogenesis is complete before birth in NHPs, monkeys, mice, and guinea pigs, but not in rats, dogs, pigs, and rabbits. Therefore, the mouse may be a better model than the rat for neonatal studies where kidney toxicity is a concern. Renal function is relatively easily monitored using routine clinical pathology determinations, though this is most easily accomplished after weaning when greater volumes of urine and plasma can be obtained. In addition to routine histopathology, morphometric examinations of the kidneys and adrenals may be useful.

12.3 Bone

Growth and development of the skeleton generally follow similar patterns in humans and the common animal species [71]. The period of fastest growth occurs before and shortly after weaning. In humans there is a second growth spurt at the start of puberty in girls and the end of puberty in boys. Growth measurements, such as tibia length, are routine endpoints in JAS. In vivo X-ray imaging and/or bone mineral density determinations (dual-energy X-ray absorptiometry) may be incorporated into JAS to assess specific concerns. Failing this, bones may be weighed and sampled at necropsy.

12.4 Gut

The gastrointestinal tract and digestive organs are structurally well developed at birth and generally show similar patterns of functional development across species. The development of the stomach is atypical in the rat compared with humans, pigs, and rabbits [40].

The small and large intestines are structurally and functionally immature at birth in rodents, pigs, and rabbits compared with humans, monkeys, and dogs.

12.5 Liver

Morphological maturation of the liver is complete in the human at about 5 years of age or in the rat at 4 weeks [40]. This occurs at only 1 week of age in the dog. The timing of functional development of the various liver enzymes may have a crucial influence on the metabolism and PK of the drug in children and juvenile animals.

12.6 Lung

Some structural development of the pulmonary tissue and airways occurs after birth. Alveolar development is mainly postnatal in the human, while the cynomolgus monkey has a full complement of alveoli at birth [72]. Even though cross-species comparative data are largely lacking, the rat and the dog are presumed to be the most relevant animal models of postnatal pulmonary development.

12.7 Reproductive System

Male reproductive development is largely comparable across species [68].

The landmarks of female reproductive development are more variable between species due to the different types of ovarian cycle [65].

Rodents, rabbits, and minipigs are the most practical species if a JAS is to include mating investigations, due to earlier sexual maturation than in dogs or NHPs.

12.8 Central Nervous System

While there is no animal species that provides a direct correlation to human neurological development, functional measures of CNS development are available in rats, NHPs, dogs, and minipigs [70]. NHPs are more mature at birth than humans and may therefore be less sensitive to effects on CNS development during the neonatal period. Generally, the rat is considered an acceptable model for most aspects of postnatal CNS development [69]. Postnatal synaptogenesis and synapse reorganization, however, are unique to human and NHPs.

12.9 Immune System

The immune system has a prolonged period of maturation in all species [67]. The developing immune system is particularly sensitive to the effects of several immunotoxicants [73]. The immune system is much more mature at birth in humans, monkeys, and dogs than in rodents. Toxic insult on the developing immune organs may induce latent defects which only become visible as impaired immune function later in life, as demonstrated with benzodiazepines [74].

13 Safety Pharmacology Investigations

Many of the known adverse effects of drugs in children could in principle be detected by safety pharmacology investigations in animals of an appropriate age, without the need for long complicated toxicology studies in juvenile animals. Indeed, of the four examples given in the FDA guidance where juvenile animals may have been useful in the prediction of age-related toxicity in children [17], three could be detected by conventional safety pharmacology investigations in juvenile animals:

- The vulnerability of human neonates to hexachlorophene neurotoxicity.
- The increased susceptibility of infants to verapamil-induced cardiovascular complications.
- An increased risk of convulsions in young children treated with theophylline.

So far, few methods have been adapted for use in juvenile animals, particularly in the neonate. Also the limited reference data available are hindered by a high individual variability in juveniles and between animals of different ages. Nonetheless, some physiological investigations may be accomplished in young animals. New instruments are being developed for this purpose and reference data are being generated, including the following:

- Electrocardiography (ECG) in juvenile dogs, minipigs, and monkeys [75–77].
- Assessment of CNS function [78].
- Lung function [79].
- ECG, respiratory parameters, and body temperature in neonatal rodents, e.g., PhysioPups®.
- Neonatal sensorimotor development in rodents using gait analysis, e.g., NeoGait®.
- Neonatal memory in rodents using a place preference test, e.g., MemoryPups®.

Findings in the adult toxicology study may trigger a request from regulators for physiological investigations in the juvenile (e.g., lung function monitoring triggered by dyspnea seen in adult rats).

14 Objectives of Juvenile Toxicity Studies

Regulatory juvenile toxicity studies are designed to detect two distinct types of hazard:

- Increased vulnerability of the immature organism to systemic toxicity of the drug.

- An adverse influence of the drug on the development or maturation of the organism, which may be manifest only at a later age or in adulthood.

Systemic toxicity in the juvenile can usually be detected at the end of the period of exposure, though a recovery period may be necessary to investigate the persistence of any induced lesions.

The detection of developmental toxicity, on the other hand, requires monitoring of the development of the animal at least during the critical periods of vulnerability or until the target organs reach maturity. Developmental insults may result in latent defects that are only manifest much later in development, thus necessitating an extended follow-up period in juvenile studies. Postnatal developmental insult frequently results in functional defects, which may only be manifest sometime after exposure.

JAS should also aim to provide information on the following:

- Pharmacodynamics or safety biomarkers for use in the clinic.
- Extrapolation of exposure levels to guide the selection of safe dose levels for use in pediatric clinical trials.
- Evaluation of the risk-benefit ratio in children.

15 Selection of Species

The choice of species to be used for the juvenile studies is influenced by the following factors:

- Data from adult toxicology studies.
- Pharmacokinetics of the drug in the adult versus the juvenile.
- Species differences in PK, PD, and metabolism.
- Physiological similarities to human.
- Developmental similarities to human (i.e., timing of organ development).
- Practical considerations.

15.1 Rodents

The rat is the most practical and most commonly used species for juvenile toxicology studies (*see Note 6*). It is also the most commonly used species for general and reproductive toxicology. The mouse is more difficult to handle because of its smaller size and greater activity, but is a feasible alternative to the rat.

The short, compressed life-span of rodents allows the evaluation of many life stages in a relatively short experiment (e.g., 3 months). The small size and low cost of rodents are also obvious advantages over larger species.

Rodents are comparably immature at birth: a rat pup of less than 9 days old is roughly equivalent to a preterm human neonate [80].

15.2 Nonrodents

The dog is currently the second most common species for juvenile studies. It is also the most used nonrodent species for pharmaceutical safety testing, so toxicology data are usually available in the adult dog prior to commencement of the juvenile studies.

The minipig is the most practical nonrodent species for juvenile studies and is the species of choice when the general toxicity studies have been performed in a nonrodent species other than the dog. All routes of administration are feasible in the juvenile minipig except inhalation [75].

Juvenile toxicity studies in monkeys are problematic, in part due to the poor availability of suitable animals and in part due to the technical complexities of handling baby monkeys and their mothers. Because of these limitations, and for ethical reasons, NHP studies should only be performed as a last resort. Nonetheless, juvenile studies in NHPs are sometimes unavoidable, particularly for biopharmaceuticals [59]. The cynomolgus is the predominant species, but juvenile studies are also feasible in the rhesus or marmoset. Extensive reference data on the growth and development of monkeys from birth are available, since they are routinely collected during ePPND studies [60].

The use of juvenile rabbits is limited to a single approved PIP, for which it was used for specific bone investigations in addition to similar studies in the rat [30]. The lack of popularity of the rabbit may be due to the common misconception that the young kits cannot be handled without provoking cannibalism or rejection by the mother [81]. Nonetheless, several laboratories have overcome these difficulties and have validated all of the techniques necessary for juvenile studies in the rabbit [82].

Juvenile studies have been successfully, but rarely, performed in other species, such as cats, sheep, and goats [30].

15.3 Genetically Modified Animal Models

Transgenic and knock-in or knockout animal models may gain importance in coming years. For example, a transgenic mouse has been developed with immunological tolerance to a broad range of human IgG1 mAbs [83].

16 Study Design

Each study is designed case by case, based on the following considerations:

- Therapeutic indication.
- Known pharmacology, therapeutic and secondary.
- Timing and duration of treatment in children.
- Potential age- or species-specific differences in PK, PD, or toxicity.

- Interspecies differences in the timing of development.
- Known toxicity of the drug in previous studies.

16.1 Postweaning Studies

The practical organization of juvenile studies in all species is considerably simpler if dosing can be commenced after weaning. The litter origin of the pups nonetheless needs to be taken into account in the allocation of pups to the treatment groups. Pups from the same litter should preferably be spread across all treatment groups, or failing this, randomized.

16.2 Dose-Level Selection

For pediatric-first indications, where JAS are intended to replace repeat-dose studies in adult animals, the low, mid, and high dose selection is similar to that for adult repeat-dose studies [2]:

- Some toxicity at the high-dose level is expected, in order to identify the target organs and the reversibility of any findings.
- For essentially nontoxic drugs, the high dose may be limited to that providing a 50-fold (for small molecules) or 10-fold (for biopharmaceuticals) margin of exposure relative to the clinical area under the curve (AUC) (unless C_{max} is more relevant). Otherwise, a limit dose of 1000 mg/kg/day or the maximum feasible dose may be applied, provided that this dose results in an exposure in excess of the anticipated therapeutic AUC.

When JAS are performed to address concern, in addition to existing adult repeat-dose studies, the following should be considered:

- The high dose should be selected in the lower range of already identified relevant toxicities in adults. As stated above, the current FDA guidance insists on an expectation of seeing frank toxicity at the high-dose level in a JAS, which is not stated in the European and Japanese guidelines.
- The low dose should be chosen to result in exposures at/or slightly above the therapeutic clinical exposure and to identify a no observed adverse effect level (NOAEL) when feasible.
- A mid dose is not necessarily required as long as the dose-response is adequately characterized with two dose levels (e.g., when differences in terms of dose/exposure between high- and low-dose levels are small).

It is advisable to perform tolerance and/or dose range finding studies in animals of the youngest age envisaged for the pivotal study, to confirm tolerability and adequate exposure (*see* Subheading 16.4).

When there are significant age-related differences in PK (e.g., increasing metabolizing enzyme activity with age) dose-level adjustments may be necessary to ensure adequate exposure over

the entire developmental phases of interest. Likewise, adjustments may be needed to counter gender differences in metabolism, which may develop during the course of the study.

16.3 Route of Administration

Generally, the intended human route of administration should be used for JAS. This may not always be feasible in the chosen species at the appropriate age. The following adaptations may be considered:

- Change in the method of administration, e.g., IV infusion in the place of bolus injection.
- Change of the route of administration for another route resulting in equivalent exposure: For example, the IV antifungal agent anidulafungin, was tested in juvenile rats by the subcutaneous route after it was shown to closely mimic the PK profile following IV infusion [54].
- Change in the formulation, e.g., suspension in carboxymethylcellulose, rather than capsule administration, for oral administration to neonatal dogs.

The practicability of the various routes of administration will depend upon the youngest age at which the animals will be dosed (*see* Subheading 16.7).

16.4 Preliminary and Dose Range Finding Studies

Dose range finding studies with limited numbers of animals are practically always necessary before starting a pivotal JAS. The dose levels used in the adult toxicology studies are often not good indicators of the tolerated dose levels in juveniles [84].

Data from dose range finding studies may also serve to inform discussions with health authorities after submission of the PIP or PSP.

16.5 Number of Animals and Group Sizes

There is no clear regulatory guidance on the number of animals required per dose group. As a general rule, the group sizes for juvenile studies are based on the requirements for other types of toxicology studies (i.e., general toxicology studies, neurotoxicity studies for JAS including behavioral tests, or reproductive toxicology studies for protocols with a mating phase).

Rodents and rabbits:

- Each subgroup should include at least ten males and ten females (i.e., the minimum numbers considered necessary in order to interpret the findings from behavioral tests and mating). Most rodent studies comprise at least two subgroups (see below), so at least 20 pups of each sex per group are allocated to the study.

Nonrodents:

- The usual group size for dog, NHP, and minipig studies is four males and four females per treatment group, plus an equivalent number for any recovery subgroups.

The use of multiple subgroups in rodents (e.g., TK, reversibility, behavioral testing, immune function) quite often leads to very large group sizes of 40 pups or more. There is an urgent need to develop and refine our methods to permit a reduction in the numbers of animals used for these studies.

Where historical control data is lacking or sparse, consideration may be given to increasing or doubling the size of the control group.

16.6 Entire-Litter or Split-Litter Design?

Two basic study designs may be used:

1. Split-litter design: Different pups within each litter are allocated to different experimental groups, such that each dam raises a mixture of treated and control pups (*see Note 7*).
2. Entire litter design: All of the pups in each litter are allocated to the same experimental group.

Before weaning, all of the pups in a litter are dependent on the health and behavior of their mother. The rate of growth of each pup, for instance, depends to a large degree on the quantity and quality of milk available to it. Any adverse influence on the health of the mother will impact on the development of all of the pups in her litter. In developmental toxicity studies, maternal influences are usually taken into account in the interpretation of the litter data by considering the litter rather than the individual pup as the basic sampling unit [85]. Therefore, in a pre- and postnatal development study, the sample size used for statistical analysis is equal to the number of litters per group (about 20), rather than the number of pups (about 240).

In JAS, because the pups are treated directly, the individual sampling unit is usually taken to be the individual pup, even for preweaning studies. The genetic similarity between biological siblings can be controlled by cross-fostering (*see below*). Nonetheless, the influence of maternal performance can seriously distort the developmental data acquired, particularly if all of the pups in each litter are allocated to the same treatment group. Maternal influences during the preweaning period have lasting influences on the pups after weaning (e.g., growth retardation). One way of controlling the maternal influence is to use a split-litter design, where each mother raises a mixture of pups from each treatment group, allowing a direct comparison between the treated and control pups within the same litter.

Advantages and disadvantages of split-litter design are the following:

- Comparison of treated and control pups within each litter, thus controlling for genotypic and maternal influences.
- Increased statistical power for low group sizes, since each pup may be taken as an individual experimental unit.

- Less risk of death due to treatment-related hypothermia, with the few affected high-dose pups for instance kept warm by their healthy littermates.
 - High risk of cross contamination between pups of the same litter (possibly via the milk following contamination of the mother).
 - Higher risk of dosing errors due to confusion of littermates.

Advantages and disadvantages of entire-litter design are the following:

- Little risk of cross contamination.
- Lower risk of treatment error due to confusion of littermates.
 - Increased risk of maternal toxicity at high-dose levels, due to the mother grooming greater numbers of treated pups.
 - Poor statistical power with smaller group sizes, since the litter has to be taken as the experimental unit: This problem is avoided in larger studies, where different pups from each litter are allocated to different subgroups.

In practice, the entire-litter design has become by far the most frequent option over recent years.

16.7 Age at Start of Dosing

The age at which dosing is commenced in a JAS should correspond to the youngest age at which children will be exposed, taking into account the relative age of development of each organ system of interest (see above).

Thanks to recent advances, most common routes of administration can now be accomplished in the commonly used species from a relatively young age, though considerably more technical proficiency and training are needed than for adult studies [86]:

1. Oral: Rodent pups are frequently dosed by the oral from 4 days of age. Dogs and minipigs may be orally dosed from 7 days of age, and rabbits from PND14.
2. IV: Bolus administration is possible via the tail vein or a cheek vein in rats and mice from 4 days of age. Dogs and NHPs may be injected from birth. IV administration is easier in the juvenile minipig than in the adult (via the precaval sinus): Implanted vascular access ports may also be used. Rabbits may be injected from 2 weeks of age. Continuous infusion via an indwelling catheter is possible in the rat from about 14 days of age or from about 8 weeks of age in dogs.
3. SC: Subcutaneous administration is feasible in all species from birth, either by injection or implantation of an osmotic minipump.

4. IM: Intramuscular administration to rodent pups is limited to very small volumes before weaning owing to the low muscle mass. Other species can be injected from birth.
5. Inhalation: Rodent litters may be exposed with the mother using whole-body exposure. Individual pups may be exposed from 4 days of age by nose-only exposure [79]. Dogs may be exposed via mouth breathing or nose only from 2 weeks of age using an adapted mask. Inhalation studies are not normally conducted in juvenile minipigs, NHPs, or rabbits.
6. Dermal application is problematic before weaning in all species because of the mother's compulsion to clean the offspring. A 6-h daily exposure is possible in rats if the pups are separated from the mother and kept warm following the dose application [87].

16.8 Duration of Treatment

The duration of exposure in the JAS should cover all critical periods of postnatal development which have not been evaluated in previous repeat-dose studies. Two options have been successfully followed:

1. Stop treatment shortly after the age at which dosing started in the chronic repeat-dose studies in the same species (provided that the adult studies covered all necessary juvenile endpoints (*see Note 4*)).
2. Continue dosing up to sexual maturity to be sure of detecting possible manifestations of developmental toxicity, which may not have been investigated in the general toxicity studies, e.g., effects on fertility.

16.9 Posttreatment Follow-Up or Reversibility Period

It is necessary to retain at least a proportion of the animals from rodent studies up to maturity to detect any latent defects, such as neurobehavioral defects or influences on reproductive development. This period also serves to investigate the reversibility of any induced lesions seen during the treatment period.

It is not usually feasible to retain juvenile NHPs up to sexual maturity (4–5 years). Likewise, juvenile dog and minipig studies are not generally prolonged up to sexual maturity (albeit feasible in the minipig, which reaches sexual maturity within 4–5 months).

16.10 Subgroups in Rodent Studies

Rodent studies usually comprise two or more subgroups of at least ten animals of each sex within each treatment group:

1. Subgroup 1: necropsied 1 day after the last dose (e.g., at 7 weeks of age).
2. Subgroup 2: retained after the end of the treatment period for further developmental and behavioral monitoring and mating at 12 weeks of age.

Table 4
Subsets in a complex rat juvenile animal studies with dosing on postnatal days 14–70, including bone and immune endpoints

Subset	N/group	Examinations	Age at termination
I	10M + 10F	Clinical pathology Functional neurobehavioral tests Organ weights Histopathology Bone mineral density	10 weeks
II	10M + 10F	Functional neurobehavioral tests Ophthalmoscopy Organ weights Histopathology	23 weeks (90-day recovery)
III	20M + 20F	Sexual maturation Long bone growth Functional neurobehavioral tests TK sampling, day 70 Reproductive performance Caesarian GD13—females Macroscopic necropsy—males Sperm evaluation	17 weeks
IV	6M + 6F	TK sampling	2 weeks
V	10M + 10F	Immune function (T-cell-dependent Ab response)	10 weeks
VI	10M + 10F	Functional neurobehavioral tests Immune function (T-cell-dependent Ab response)	23 weeks (90-day recovery)

3. Additional subgroups for additional examinations, e.g., functional immune testing.

An example of the subsets in a complex JAS is given in Table 4.

17 Study Performance

17.1 Animal Supply

1. Rodents: Many breeders will supply lactating rats or mice with litters soon after birth. Otherwise, it is also possible to order time-mated females and allow them to give birth at the testing facility. Large numbers of animals are required to give birth at the same time in order to provide enough pups for the purposes of a full juvenile study. The females may be mated in-house, but logistical challenges need to be overcome in order to provide the large numbers of animals that are required to give birth at the same time.

2. Nonrodents: It is not normally considered ethical to transport neonatal dogs, minipigs, or rabbits. It is therefore necessary to either order pregnant females or to mate the females in-house. As for rodents, it is important to ensure that a sufficient number of pups are born within a short period.

17.2 Cross Fostering

Cross fostering is used to optimize the number of pups available by exchanging pups between mothers to obtain litters of the required size. This is easily accomplished in rodents and minipigs, and is also possible in dogs.

All of the pups born over a period of about 24 h are pooled and then randomly redistributed with equal numbers of each sex in each litter. Ideally, steps should be taken to avoid any dam from raising its own pups, which could be a source of bias within the reconstituted litter.

17.3 Identification of Pups

Rodent pups are best identified by tattoo on the paws.

Dogs and minipigs may be tattooed on a pinna or implanted with a transponder. Rabbits are tattooed on a pinna.

17.4 Clinical Condition and Body Weight up to Weaning

All pups are examined frequently during the study in order to observe any clinical reactions to treatment.

- Rodent pups are weighed every 2 or 3 days.
- Dogs and minipigs are weighed at least twice per week.
- Juvenile NHPs are weighed weekly.

17.5 Monitoring of Prewaning Growth and Development

Rodents and rabbits: The growth and development of rodent pups are assessed by individual daily monitoring of developmental milestones and reflex testing using similar techniques as those routinely employed in developmental toxicity studies [88]. In addition, specific growth measures, such as manual external measurement of tibia length, are determined every 2 or 3 days.

- Dog: Growth measures, such as standing shoulder height and external tibia length, are recorded at least twice per week for each dog. The puppies are examined daily to determine the days of tooth eruption and eye opening. The auditory, fossorial, labial, and perineal reflexes may be evaluated at various ages. The days of acquired locomotion are noted, i.e., crawling, standing, walking, and running.
- NHP: Morphological measurements are made monthly, including head circumference, distance between the eyes, crown-rump length, tail length, chest circumference, length of limbs, and anogenital distance.
- Minipig: Growth measures, such as standing shoulder height and external tibia length, are recorded at least twice per week for each piglet. The piglets are examined daily to determine

the days of tooth eruption and eye opening. The papillary and auditory reflexes may be evaluated at various ages.

- Rabbit: Each rabbit kit is examined daily to determine the days of incisor eruption and eye opening. Tibia length is recorded twice per week. The surface righting, papillary, and auditory reflexes may be evaluated at various ages.

17.6 Blood Sampling for Toxicokinetics or Clinical Pathology

Rodents: Very low volumes of blood can be obtained from neonatal rodents. Microsampling techniques have recently been developed [89, 90] and should be used whenever possible to minimize the number of pups allocated to PK subgroups. At older ages, microsampling can be used to sample the main study animals and thus avoid the need for TK satellite animals.

- Dog: Blood may be withdrawn from a jugular vein of dogs under anesthesia from birth.
- NHP: Blood may be withdrawn from a limb vein under anesthesia from birth.
- Minipig: Blood may be withdrawn from the cranial vena cava of minipigs without anesthesia from birth [91]. This method becomes increasingly more difficult after a few weeks of age when the cranial aspect of the sternum ossifies.
- Rabbit: Blood sampling may be performed from an ear artery from about 2 weeks of age.

17.7 Prewaning Cardiovascular Examinations

Cardiovascular parameters may be determined in dogs, NHPs, and minipigs from 1 week of age.

A standard ECG trace is recorded with the neonate lightly restrained in a net hammock, allowing the determination of the heart rate. The ECG waveform is difficult to analyze before regularizing at around the age of weaning.

Blood pressure can be measured using a limb or tail cuff.

17.8 Weaning

Approximate age of weaning:

- Rodents: 3 weeks.
- Dog: 7 weeks.
- Cynomolgus monkey: 8 months.
- Minipig: 5 weeks.
- Rabbit: 5 weeks.

For studies in which dosing was started before weaning, the animals are rehoused following separation from the mother. The same treatment regime will normally be continued during the posttreatment period, though the dosing regimen may be adjusted to allow for age-dependent differences in PK or metabolism.

Group housing by sex, if possible, is preferred after weaning for juvenile animals of all commonly used species (*see Note 8*).

After weaning, the animals of all species are individually identified by tattoo on a pinna and/or tail or using an implanted transponder.

The routine examinations, as described for the preweaning phase, are continued after weaning. The frequency of body weights and growth measurements may be reduced to twice weekly in view of the slower rate of growth.

17.9 Specific Postweaning Examinations

The food consumption of each cage of animals is recorded.

Other postweaning examinations include the following:

- Vaginal opening in females.
- Balanopreputial separation in males.
- Clinical pathology (hematology, serum clinical chemistry, and coagulation): determined at intervals for nonrodents and at termination for rodents (*see Note 9*).
- ECG examinations are performed during the last week of the treatment period (and during the recovery period if applicable) in nonrodents. Electrocardiography may also be performed at intervals during the study to assess specific concerns (see also Subheading 13 above).

17.10 Neuro-behavioral Tests

Neurobehavioral tests are generally included in juvenile rodent studies (*see Note 10*). These tests are typically performed once during the treatment period (in the subgroup terminated at the end of dosing) and once after the end of the treatment period. The types of test requested include the following:

- Motor activity (total activity and stereotypy).
- Cognitive function using a complex maze test.
- Auditory startle reflex, including habituation and prepulse inhibition.

If required, similar tests can be performed in the juvenile mini-pig or NHP. Rudimentary tests of motor activity and cognitive function, such a hole-board (bucket) or maze test, have been proposed [94].

17.11 Mating and Fertility Assessment

17.11.1 Rodents

Rodents are paired at approximately 12 weeks of age.

- One male and one female from the same treatment group (avoiding siblings) are housed in the same cage until copulation occurs, as detected by the presence of sperm in a vaginal smear.
- The pregnant females are submitted to caesarean section at midpregnancy. The numbers of live and dead embryos in the uterus are counted.

17.11.2 Nonrodents

Mating assessments are rarely performed in nonrodent species. Nonetheless, a detailed histopathology evaluation of the reproductive organs can be expected to reveal any adverse effects of the drug on reproductive capacity (provided that the animals are sufficiently mature at the end of the study).

Copulation is very unpredictable in dogs and NHPs. Mating studies would be feasible, however, in minipigs or rabbits, which also have the advantage of reaching sexual maturity within 5 months.

17.12 Monitoring of Sexual Maturation

The attainment of male sexual maturity in rodents is best determined by balanopreputial separation. Testicular descent can be monitored in nonrodent species. Also sperm samples can be obtained from NHPs by electroejaculation to confirm the onset of spermatogenesis. Blood samples may also be taken for testosterone determination.

Female sexual maturation may be determined by the onset of estrous cycling in rodents or the onset of menses in NHPs. Hormone analyses may also be useful. Beckman and Feuston have published a cross-species comparison of landmarks in the development of the female reproductive system [65].

17.13 Necropsy and Histopathology

All animals (whether terminated at the end of the treatment period or at maturity) are submitted to routine necropsy. Organs are weighed, sampled, and examined microscopically using similar procedures as those in the general toxicity studies in the same species.

If neurohistopathology is to be performed, the recommendations of the Society of Toxicologic Pathology should be followed [95].

17.14 Nonroutine Endpoints After Weaning

Additional endpoints may be incorporated into the study design in order to evaluate the development and integrity of potential target organs, e.g.:

- Serum samples for hormone determinations.
- Skeletal examinations: periodic X-ray imaging or bone densitometry at termination.
- Periodic or terminal sperm analysis.

Immune evaluations (*see Note 11*):

- Immunoglobulin and cytokine serum determinations.
- Lymphocyte subset determinations.
- Primary antibody response to sheep red blood cells or keyhole limpet hemocyanin.

The objectives of immune evaluations within the context of juvenile studies are essentially limited to the detection of effects

leading to immune depression. There are no validated tests available at the present time for the evaluation of adverse effects resulting in immune stimulation, which may make the child more vulnerable to autoimmune disease or hypersensitivity [92, 97].

18 Timing of Juvenile Animal Studies in Relation to Pediatric Clinical Trials

In general, when warranted, JAS are required before children are exposed to clinical trials. There are, however, some discrepancies between the guidance documents of the various regions.

USA (FDA):

- If warranted, JAS should be conducted before starting long-term pediatric clinical trials.
 - Where pediatric clinical studies do not involve long-term exposure, it is not necessary to complete JAS before initiation of pediatric clinical trials. However, JAS may be required prior to short-term pediatric clinical trials when insufficient adult human data are available to identify potential hazards.
- Where the indication is for long-term use, but the clinical trials are short-term, the juvenile animal studies should be available before submission of the marketing application.

Europe (EMA):

- If warranted, JAS should preferably be available before starting pediatric clinical trials.
- Pharmacokinetic data from humans and animals (including juvenile animals if available) should also be evaluated before the proposed pediatric clinical trial(s).

The Japanese guideline reflects ICH M3(R2):

- If warranted, JAS should be conducted before starting pediatric clinical trials, however:
 - Generally, juvenile animal toxicity studies are not considered important for short-term PK studies (e.g., 1–3 doses) in pediatric populations.

19 Notes

1. The Food and Drug Administration Modernization Act (FDAMA) passed in the USA in 1997 offered an additional 6-month patent protection from generic competition on all juvenile and adult applications of a (nonbiologic) drug in return for the additional work to develop the product for pediatric use.

The Pediatric Rule issued in the USA the following year obliged pharmaceutical companies to assess the safety and effectiveness of all new drugs likely to be of therapeutic value in children (including biologics). Pediatric drug development in the USA is currently regulated under the Pediatric Research Equity Act (PREA) [12] and the Best Pharmaceuticals for Children Act (BPCA) [13]. The additional patient protection is prolonged to 2 years for pediatric orphan drug indications. Ten-year patient protection is granted for a new pediatric indication of a previously nonpatented drug. The incentives offered in the USA for the pediatric development of drugs were extended to biopharmaceuticals, with the passage of the Biologics Price Competition and Innovation Act of 2009 [14].

Similar legislation, with equivalent incentives (including biopharmaceuticals), became effective in Europe from 2007. The European pediatric regulation is comprised of EC Regulation No. 1901/2006 and amendment No 1902/2006 [15, 16].

2. Out of 1599 pediatric clinical trials under way in 2014, 965 were in the USA, 382 in Europe, 216 in Canada, and the rest scattered over the remaining continents [22]. Within Europe, the major countries were France (125), Italy (125), Germany (121), the United Kingdom (100), Spain (94), and Poland (85).
3. According to the US guidance, juvenile animal studies might not be necessary when (1) data from similar therapeutics in a class have identified a particular hazard and additional data are unlikely to change this perspective; (2) there are adequate clinical data and adverse events of concern have not been observed during clinical use; (3) target organ toxicity would not be expected to differ in sensitivity between adult and pediatric patients because the target organ of toxicity is functionally mature in the intended pediatric population and younger children with the functionally immature tissue are not expected to receive the drug. The EU guidance indicates that medicinal products under development for specific pediatric indications or in life-threatening or serious diseases without current effective therapies warrant a case-by-case approach. In some cases, some studies may then be adapted, deferred, or omitted.
4. In practice, the animals used for many subchronic and chronic studies are not sexually mature at the start of the study. It is quite usual, for instance, to commence a 3-month general toxicology study with rats of 6 weeks of age, roughly corresponding to the stage of development of a 10-year-old child.
5. The Development and Reproductive Toxicology (DART) Technical Committee of the International Life Sciences Institute-Health and Environmental Sciences Institute (ILSI-HESI) has issued a series of reviews on comparative organ

development for use in the design of juvenile studies [39, 40, 64–72].

6. The rat is by far the most common species for juvenile safety testing, accounting for 80% of the 134 approved PIPs to date that cite a single species [29]. The mouse is used in a further 6% of studies. The dog is the most used nonrodent species (8%), followed by the NHP (3%). Only three PIPs approved to date mention studies in the pig, which is surprising considering its practical and scientific attributes.
7. Also called “within-litter design” (all dosage groups equally represented in each litter) or “between-litter design” (all dosage groups in the litter).
8. Group housing is preferred for the housing of juvenile rats, mice, dogs, NHPs, minipigs, and rabbits, since social contact is necessary for normal neurobehavioral development. Aggressive behavior is rarely a problem between immature animals that have been housed together from weaning. Cage-mates should be of the same sex, of the same approximate postnatal age, and, if possible, derived from different litters.
9. Clinical pathology endpoints may be monitored as indicators of anticipated organ toxicity (e.g., liver hypertrophy or renal tubular dilatation). Other parameters, such as differential blood cell counts, are also used to monitor the postnatal development of the bone marrow or immune organs. In rodent studies, clinical pathology is often only included as an apical measure at the end of the study, due to the limited volume of blood that can be sampled from the young pups. A larger volume of blood can be withdrawn from puppies or piglets, allowing clinical pathology parameters to be monitored regularly throughout the study. Reference data for rats and dogs at various ages are available [80, 92].
10. Behavioral and cognitive tests are most often performed in rodents. A battery of tests is used to assess sensorimotor function, locomotor activity, reactivity, learning, and memory. The battery used in juvenile studies is usually based on that already in place for developmental toxicity studies. The most common tests include motor activity monitoring, open-field activity, learning and memory tasks in a water-filled maze, passive avoidance, performance on a rotating rod, grip strength, and startle habituation [93].
11. An initial screen for immune effects in a juvenile study may be limited to histopathological examination of the lymphoid organs/tissues (including organ weights) and routine clinical pathology. If necessary, functional tests are available for the detection of immune depression in juvenile rodents [92, 96].

References

- Mulberg AE, Silber SA, Van den Anker JN (2009) Pediatric drug development: concepts and applications. Wiley, Hoboken, NJ
- ICH (2009) Guideline M3(R2) on non-clinical safety studies for the conduct of human clinical trials and marketing authorisation for pharmaceuticals. http://www.ich.org/fileadmin/Public_Web_Site/ICH_Products/Guidelines/Multidisciplinary/M3_R2/Step4/M3_R2_Guideline.pdf. Accessed 17 Feb 2016
- ICH (2000) Harmonised Tripartite Guideline: Clinical investigation of medicinal products in the pediatric population E11. http://www.ich.org/fileadmin/Public_Web_Site/ICH_Products/Guidelines/Efficacy/E11/Step4/E11_Guideline.pdf. Accessed 14 Jan 2016
- FDA (2006) Guidance for industry: nonclinical safety evaluation of pediatric drug products. FDA, Silver Spring
- Shirkey H (1968) Editorial comment: therapeutic orphans. *J Pediatr* 72(1):119–120
- Choonara I (2000) Clinical trials of medicines in children: US experience shows how to ensure that treatment of children is evidence based. *Br Med J* 321(7269):1093
- FDA (2013) FDA Voice: FDA takes step to encourage pediatric drug studies. <http://blogs.fda.gov/fdavoices/index.php/tag/best-pharmaceuticals-for-children-act-bpca/>. Accessed 5 Aug 2015
- Allegaert K, van den Anker JN (2015) Adverse drug reactions in neonates and infants: a population-tailored approach is needed. *Br J Clin Pharmacol* 80(4):788–795
- American Academy of Pediatrics Committee on Drugs (1995) Guidelines for the ethical conduct of studies to evaluate drugs in pediatric populations. *Pediatrics* 95(2):286–294
- Nunn A, Richey R, Shah U, Barker C, Craig J, Peak M, Ford J, Turner M (2013) Estimating the requirement for manipulation of medicines to provide accurate doses for children. *Eur J Hosp Pharm Sci Pract* 20(1):3–7
- American Academy of Pediatrics Committee on Drugs (2014) Off-label use of drugs in children. *Pediatrics* 133(3):563–567
- 108th Congress S. (2003) 650 (108th): Pediatric research equity act. GovTrack.us. <https://www.govtrack.us/congress/bills/108/s650>. Accessed 9 Sep 2015
- FDA (2007) Food and drug administration amendments act. <http://www.fda.gov/RegulatoryInformation/Legislation/FederalFoodDrugandCosmeticActFDCAct/SignificantAmendmentsstotheFDCAct/FoodandDrugAdministrationAmendmentsActof2007/FullTextofFDAAALaw/default.htm>. Accessed 03 March 2015
- FDA (2011) Implementation of the biologics price competition and innovation act of 2009. <http://www.fda.gov/Drugs/GuidanceComplianceRegulatoryInformation/ucm215089.htm>. Accessed 16 Sep 2015
- European Union, Regulation (EC) No 1901/2006 of the European Parliament and of the Council of 12 December 2006 on medicinal products for paediatric use and amending Regulation (EEC) No 1768/92, Directive 2001/20/EC, Directive 2001/83/EC and Regulation (EC) No 726/2004. *Off J Eur Union* (2006). pp L378-1-19. 27 Dec 2006
- European Union, Regulation (EC) No 1902/2006 of the European Parliament and of the Council of 20 December 2006 amending Regulation 1901/2006 on medicinal products for paediatric use. *Off J Eur Union* (2006). pp L378-20-21. 27 Dec 2006
- FDA (2006) Non-clinical testing in juvenile animals on human pharmaceuticals for pediatric indications. <http://www.fda.gov/downloads/drugs/guidancecomplianceregulatoryinformation/guidances/ucm079247.pdf>. Accessed 14 Jan 2016
- EMA (2008) Guideline on the need for non-clinical testing in juvenile animals on human pharmaceuticals for paediatric indications. Ref. EMEA/CHMP/SWP/169215/2008. http://www.ema.europa.eu/docs/en_GB/document_library/Scientific_guideline/2009/09/WC500003305.pdf
- MHLW Japan (2012) Guideline on the non-clinical safety study in juvenile animals for pediatric drugs and questions and answers regarding guideline on the non-clinical safety study in juvenile animals for pediatric drugs
- Barrow P (1990) Oral dosing of neonatal rats. In: Barrow P (ed) *Technical procedures in reproduction toxicology*, vol 11. Laboratory Animal Handbooks Royal Society of Medicine, London, p 49
- ICH (2014) Final concept paper. S11: non-clinical safety testing in support of development of pediatric medicines. http://www.ich.org/fileadmin/Public_Web_Site/ICH_Products/Guidelines/Safety/S11/S11_Final_Concept_Paper_10_November_2014.pdf. Accessed 05 Aug 2015
- USNIH (2014) *ClinicalTrials.gov*. https://clinicaltrials.gov/ct2/results/map?term=pediatric&recr=Open&no_unk=Y. Accessed 17 Jan 2016

23. Shaddy RE, Denne SC (2010) The Committee on Drugs, Committee on Pediatric Research, Guidelines for the ethical conduct of studies to evaluate drugs in pediatric populations. *Pediatrics* 125(4):850–860
24. Cappon GD (2011) Nonclinical support of pediatric drug development in a global context: an industry perspective. *Birth Defects Res B Dev Reprod Toxicol* 92(4):269–272
25. Sakiyama M (2013) Current research situation and challenges of pediatric clinical studies in Japan (Presentation). <http://www.pmda.go.jp/files/000153085.pdf>. Accessed 18 Sep 2015
26. Ishikawa I (2013) PMDA's experiences and challenges in pediatric drug development (Presentation). <http://www.pmda.go.jp/files/000205934.pdf>. Accessed 18 Sep 2015
27. EMA (2015) Opinions and decisions on paediatric investigation plans. http://www.ema.europa.eu/ema/index.jsp?curl=pages/medicines/landing/pip_search.jsp&mid=WCOB01ac058001d129. Accessed 16 Sep 2015
28. Field M, Boat T (2012) Safe and effective medicines for children: pediatric studies conducted under the best pharmaceuticals for children act and the pediatric research equity act. The National Academies Press, Washington, DC
29. Hurtt ME, Engel S (2015) An update of juvenile animal studies in the European Union: What do the numbers say? *Reprod Toxicol* 56:105–108
30. Baldrick P (2013) The evolution of juvenile animal testing for small and large molecules. *Regul Toxicol Pharmacol* 67(2):125–135
31. Hines RN, Sargent D, Atrup H, Birnbaum LS, Brent RL, Doerrer NG, Cohen Hubal EA, Juberg DR, Laurent C, Luebke R, Olejniczak K, Portier CJ, Slikker W (2010) Approaches for assessing risks to sensitive populations: lessons learned from evaluating risks in the pediatric population. *Toxicol Sci* 113(1):4–26
32. Krasinski K, Perkin R, Rutledge J (1982) Gray baby syndrome revisited. *Clin Pediatr (Phila)* 21(9):571–572
33. Gershanik J, Boecler B, Ensley H, McCloskey S, George W (1982) The gasping syndrome and benzyl alcohol poisoning. *N Engl J Med* 307(22):1384–1388
34. Allegaert K, van den Anker J (2015) Neonatal drug therapy: The first frontier of therapeutics for children. *Clin Pharmacol Ther* 98(3):288–297
35. Offringa M, Davis JM, Turner MA, Ward R, Bax R, Maldonado S, Sinha V, McCune SK, Zajicek A, Benjamin DK (2015) Applying regulatory science to develop safe and effective medicines for neonates report of the US Food and drug administration first annual neonatal scientific workshop, October 28–29, 2014. *Therap Innov Regul Sci* 49(5):623–631
36. Eiby YA, Wright LL, Kalanjati VP, Miller SM, Bjorkman ST, Keates HL, Lumbers ER, Colditz PB, Lingwood BE (2013) A pig model of the preterm neonate: anthropometric and physiological characteristics. *PLoS One* 8(7):e68763
37. Bailey GP, Marien D (2011) The value of juvenile animal studies “What have we learned from preclinical juvenile toxicity studies? II”. *Birth Defects Res B Dev Reprod Toxicol* 92(4):273–291
38. Walzer M, Bekersky I, Wanaski S, Collins S, Jortner B, Patterson R, Garman R, Sagar S, Tolbert D (2011) Oral toxicity of vigabatrin in immature rats: Characterization of intramyelinic edema. *Neurotoxicology* 32(6):963–974
39. Zoetis T, Hurtt ME (2003) Species comparison of anatomical and functional renal development. *Birth Defects Res B Dev Reprod Toxicol* 68(2):111–120
40. Walthall K, Cappon GD, Hurtt ME, Zoetis T (2005) Postnatal development of the gastrointestinal system: a species comparison. *Birth Defects Res B Dev Reprod Toxicol* 74(2):132–156
41. Hines RN (2008) The ontogeny of drug metabolism enzymes and implications for adverse drug events. *Pharmacol Ther* 118(2):250–267
42. de Wildt SN, Kearns GL, Leeder JS, van den Anker JN (1999) Cytochrome P450 3A. *Clin Pharmacokinet* 37(6):485–505
43. Morgan E, MacGeoch C, Gustafsson J (1985) Hormonal and developmental regulation of expression of the hepatic microsomal steroid 16 alpha-hydroxylase cytochrome P-450 apoprotein in the rat. *J Biol Chem* 260(22):11895–11898
44. Johnson TN, Rostami-Hodjegan A (2011) Resurgence in the use of physiologically based pharmacokinetic models in pediatric clinical pharmacology: parallel shift in incorporating the knowledge of biological elements and increased applicability to drug development and clinical practice. *Pediatr Anesth* 21(3):291–301
45. Yang X, Morris SM, Gearhart JM, Ruark CD, Paule MG, Slikker W, Jr., Mattison DR, Vitiello B, Twaddle NC, Doerge DR, Young JF, Fisher JW (2014) Development of a physiologically based model to describe the pharmacokinetics of methylphenidate in juvenile and adult humans and nonhuman primates. *PLoS One* 9(9):e106101.

46. Parrott N, Davies B, Hoffmann G, Koerner A, Lave T, Prinssen E, Theogaraj E, Singer T (2011) Development of a physiologically based model for oseltamivir and simulation of pharmacokinetics in neonates and infants. *Clin Pharmacokinet* 50(9):613–623
47. ICH (2015) Harmonised tripartite guideline: detection of toxicity to reproduction for medicinal products & toxicity to male fertility S5(R2). http://www.ich.org/fileadmin/Public_Web_Site/ICH_Products/Guidelines/Safety/S5/Step4/S5_R2_Guideline.pdf. Accessed 1 April 2016
48. Silva-Lima B, Due Theilade-Thomsen M, Carleer J, Vidal JM, Tomasi P, Saint-Raymond A (2010) Juvenile animal studies for the development of paediatric medicines: a description and conclusions from a European Medicines Agency workshop on juvenile animal testing for nonclinical assessors. *Birth Defects Res B Dev Reprod Toxicol* 89(6):467–473
49. Carleer J, Karres J (2011) Juvenile animal studies and pediatric drug development: a European regulatory perspective. *Birth Defects Res B Dev Reprod Toxicol* 92(4):254–260
50. Leconte I, Bailey G, Davis-Bruno K, Hew KW, Kim J, Silva Lima B, Liminga U, Moffit J, De Schaepdrijver L, Schmitt G, Tassinari M, Thompson K, Hurtt M (2011) Value of juvenile animal studies. *Birth Defects Res B Dev Reprod Toxicol* 92(4):292–303
51. ICH (2010) Guidance for industry: S9 nonclinical evaluation for anticancer pharmaceuticals. <http://www.fda.gov/downloads/Drugs/.../Guidances/ucm085389.pdf>. Accessed 17 Feb 2016
52. Duarte DM (2015) Use of juvenile animal studies to support oncology medicine development in children. *Reprod Toxicol* 56:97–104
53. EMA (2013) European Medicines Agency decision (lisdexamfetamine). P/0321/2013. http://www.ema.europa.eu/docs/en_GB/document_library/PIP_decision/WC500160560.pdf. Accessed 30 Nov 2015
54. Cross DM, Chmielewski G, Lewis EM, Liu L, Modesitt MS, Ripp SL, Sawaryn CM, Bowman CJ (2012) Non-clinical safety assessment and toxicokinetics of voriconazole and anidulafungin in the juvenile rat: a combination study design in support of a Paediatric Investigation Plan. *Regul Toxicol Pharmacol* 63(1):29–39
55. Schmitt G (2015) Safety of excipients in pediatric formulations—a call for toxicity studies in juvenile animals? *Children* 2(2):191–197
56. EMA (2013) Guideline on pharmaceutical development of medicines for paediatric use. http://www.ema.europa.eu/docs/en_GB/document_library/Scientific_guideline/2013/07/WC500147002.pdf. Accessed 13 Aug 2015
57. EMA (2006) Reflection paper: formulations of choice for the paediatric population. http://www.ema.europa.eu/docs/en_GB/document_library/Scientific_guideline/2009/09/WC500003782.pdf. Accessed 30 Nov 2015
58. EuPFI (2015) STEP database. <http://pharmacypapp-a.ucl.ac.uk:8080/eupfi>. Accessed 13 Aug 2015
59. Morford LL, Bowman CJ, Blanset DL, Bøgh IB, Chellman GJ, Halpern WG, Weinbauer GF, Coogan TP (2011) Preclinical safety evaluations supporting pediatric drug development with biopharmaceuticals: strategy, challenges, current practices. *Birth Defects Res B Dev Reprod Toxicol* 92(4):359–380
60. Weinbauer GF, Luft J, Fuchs A (2013) The enhanced pre- and postnatal development study for monoclonal antibodies. *Methods Mol Biol* 947:185–200. [doi:10.1007/978-1-4939-9811-1_11](http://dx.doi.org/10.1007/978-1-4939-9811-1_11)
61. Sakurai T, Takai R, Buergin H, Shioda A, Sakamoto Y, Amano J, Grimm HP, Richter WF, Higuchi Y, Chiba S (2013) The effects of interleukin-6 signal blockade on immune system, reproductive and skeletal development in juvenile mice. *Birth Defects Res B Dev Reprod Toxicol* 98(2):170–182
62. ICH (2011) Harmonised tripartite guideline: preclinical safety evaluation of biotechnology-derived pharmaceuticals. S6(R1). http://www.ich.org/fileadmin/Public_Web_Site/ICH_Products/Guidelines/Safety/S6_R1/Step4/S6_R1_Guideline.pdf. Accessed 17 Feb 2016
63. Guay-Woodford LM, Bryda EC, Lindsay JR, Avner ED, Flaherty L (1996) The mouse bpk mutation, a model of autosomal recessive polycystic kidney disease (ARPKD) and jcpk: a phenotypically distinct PKD mutation, are allelic. *Pediatr Res* 39:361–361
64. Hurtt ME, Sandler JD (2003) Comparative organ system development: introduction. *Birth Defects Res B Dev Reprod Toxicol* 68(2): 85–85
65. Beckman DA, Feuston M (2003) Landmarks in the development of the female reproductive system. *Birth Defects Res B Dev Reprod Toxicol* 68(2):137–143
66. Hew KW, Keller KA (2003) Postnatal anatomical and functional development of the heart: a species comparison. *Birth Defects Res B Dev Reprod Toxicol* 68(4):309–320
67. Holsapple MP, West LJ, Landreth KS (2003) Species comparison of anatomical and functional immune system development. *Birth Defects Res B Dev Reprod Toxicol* 68(4): 321–334

68. Marty MS, Chapin RE, Parks LG, Thorsrud BA (2003) Development and maturation of the male reproductive system. *Birth Defects Res B Dev Reprod Toxicol* 68(2):125–136
69. Watson RE, DeSesso JM, Hurtt ME, Cappon GD (2006) Postnatal growth and morphological development of the brain: a species comparison. *Birth Defects Res B Dev Reprod Toxicol* 77(5):471–484
70. Wood SL, Beyer BK, Cappon GD (2003) Species comparison of postnatal CNS development: functional measures. *Birth Defects Res B Dev Reprod Toxicol* 68(5):391–407
71. Zoetis T, Tassinari MS, Bagi C, Walthall K, Hurtt ME (2003) Species comparison of postnatal bone growth and development. *Birth Defects Res B Dev Reprod Toxicol* 68(2):86–110
72. Zoetis T, Hurtt ME (2003) Species comparison of lung development. *Birth Defects Res B Dev Reprod Toxicol* 68(2):121–124
73. Landrigan PJ, Kimmel CA, Correa A, Eskenazi B (2004) Children's health and the environment: public health issues and challenges for risk assessment. *Environ Health Perspect* 112(2):257
74. Schlumpf M, Bütikofer E, Schreiber A, Parmar R, Ramseier H, Lichtensteiger W (1994) Delayed developmental immunotoxicity of prenatal benzodiazepines. *Toxicol In Vitro* 8(5):1061–1065
75. Barrow P (2012) Use of the swine pediatric model. In: Hoberman A, Lewis E (eds) *Pediatric nonclinical drug testing*. Wiley, Hoboken, NJ, pp 213–229. doi:10.1002/9781118168226.ch11
76. Robinson K, Smith SY, Viau A (2012) Dog juvenile toxicity. In: Hoberman A, Lewis E (eds) *Pediatric nonclinical drug testing: principles, requirements, and practices*. Wiley, Hoboken, NJ, pp 183–212
77. Weinbauer GF, Chellman GJ, Rasmussen AD, Vogelwedde E (2012) Use of primate pediatric model. In: Hoberman A, Lewis E (eds) *Pediatric nonclinical drug testing: principles, requirements, and practices*. Wiley, Hoboken, NJ, pp 255–279
78. Himmel HM (2008) Safety pharmacology assessment of central nervous system function in juvenile and adult rats: Effects of pharmacological reference compounds. *J Pharmacol Toxicol Methods* 58(2):129–146
79. Lewin G, Hoymann HG, Fuhst R, Berger-Preiss E, Pohlmann G, Buschmann J (2010) Assessment of pulmonary function and serum substance levels in newborn and juvenile rats. *Reprod Toxicol* 30(3):422–428
80. Beck MJ, Padgett EL, Bowman CJ, Wilson DT, Kaufman LE, Varsho BJ, Stump DG, Nemec MD, Holson JF (2006) Nonclinical juvenile toxicity testing. In: Hood RD (ed) *Developmental and reproductive toxicology: a practical approach*, 2nd edn. CRC, Boca Raton, pp 263–328
81. Parker RM (2014) Juvenile Toxicology. In: Derelanko MJ, Auletta CS (eds) *Handbook of toxicology*, 3rd edn. CRC, Boca Raton, pp 400–452
82. Barrow P, Allais L (2013) Developmental toxicity testing of vaccines. *Methods Mol Biol* 947:81–89
83. Bessa J, Boeckle S, Beck H, Buckel T, Schlicht S, Ebeling M, Kiialainen A, Koulov A, Boll B, Weiser T (2015) The immunogenicity of antibody aggregates in a novel transgenic mouse model. *Pharm Res*:1–16
84. Laffan S, Posobiec L (2012) Approaches to rat juvenile toxicity studies and case studies: a pharmaceutical perspective. In: Hoberman AM (ed) *Pediatric non-clinical drug testing Principles, requirements and practices*. Wiley, Hoboken, NJ, pp 281–301
85. Gad SC (1998) *Statistics and experimental design for toxicologists*, 3rd edn. CRC, Boca Raton
86. Zoetis T, Walls I (2003) A report of the ILSI risk science institute expert working group on direct dosing of pre-weaning mammals in toxicity testing. International Life Sciences Institute, Washington, DC
87. Hoberman AM, Barnett JF (2012) Juvenile toxicity study design for the rodent and rabbit. In: Hoberman A, Lewis E (eds) *Pediatric non-clinical drug testing: principles, requirements, and practices*. Wiley, Hoboken, NJ, pp 141–182
88. Barrow P (2000) Reproductive and developmental toxicology safety studies. In: Krinke GJ (ed) *The laboratory rat*. Academic, London, pp 199–225
89. Jonsson O, Villar RP, Nilsson LB, Norsten-Höög C, Brogren J, Eriksson M, Königsson K, Samuelsson A (2012) Capillary microsampling of 25 µl blood for the determination of toxicokinetic parameters in regulatory studies in animals. *Bioanalysis* 4(6):661–674
90. Nilsson LB, Ahnoff M, Jonsson O (2013) Capillary microsampling in the regulatory environment: Validation and use of bioanalytical capillary microsampling methods. *Bioanalysis* 5(6):731–738
91. NC3Rs Blood Sampling/Pig/Ear vein. <http://www.nc3rs.org.uk/pig-ear-vein-non-surgical>. Accessed 25 Aug 2015

92. Sewald K, Mueller M, Buschmann J, Hansen T, Lewin G (2015) Development of hematological and immunological characteristics in neonatal rats. *Reprod Toxicol* 56:109–117
93. Meyer J (1998) Behavioral assessment in developmental neurotoxicology: approaches involving unconditioned behaviors and pharmacologic challenges in rodents. In: Slikker W, Chang LW (eds) *Handbook of developmental neurotoxicology*. Academic, New York, pp 403–426
94. Haagenen AM, Grand N, Klastrup S, Skytte C, Sørensen DB (2013) Spatial discrimination and visual discrimination: two methods evaluating learning and memory in juvenile göttingen minipigs. *Behav Pharmacol* 24(3):172–179
95. Bolon B, Garman RH, Pardo ID, Jensen K, Sills RC, Roulois A, Radovsky A, Bradley A, Andrews-Jones L, Butt M (2013) STP position paper recommended practices for sampling and processing the nervous system (brain, spinal cord, nerve, and eye) during nonclinical general toxicity studies. *Toxicol Pathol* 41(7):1028–1048
96. Allais L, Condevaux F, Fant P, Barrow P (2009) Juvenile toxicity of cyclosporin in the rat. *Reprod Toxicol* 28(2):230–238
97. Barrow P, Ravel G (2005) Immune assessments in developmental and juvenile toxicology: practical considerations for the regulatory safety testing of pharmaceuticals. *Regul Toxicol Pharmacol* 43(1):35–44
98. Barrow P (2007) Toxicology testing for products intended for pediatric populations. *Nonclinical drug safety assessment: practical considerations for successful registration*. FDA News, Washington, DC, pp 411–440

Part II

Pathology

Chapter 3

Procedures of Necropsy and Tissue Sampling

Laurence Fiette, Mohamed Slaoui, and Anne-Laure Bauchet

Abstract

Necropsy is a major step of most studies using laboratory animals. During necropsy, tissue and organ noticeable grossly changes should be recorded and critical tissue samples may be stored for the subsequent evaluation. It is therefore important that the personnel in charge of this key experimental step to be adequately trained and aware of the study endpoints.

Key words Necropsy, Histology, Histopathology, Macroscopy, Sampling, Rodents, Mouse, Rat

1 Introduction

Necropsy is a *postmortem* procedure that consists of observation of macroscopic changes of tissue and organ in situ with bare eyes and of collection of key organs and tissue samples for further analyses.

Necropsy techniques have been developed to diagnose diseases in animals and are classically used in health status monitoring of domestic and laboratory animals. These *postmortem* procedures are also considered as an important step in biomedical research using laboratory animals and in particular in toxicity studies where histopathology is a major endpoint. In all cases, necropsy is the ultimate examination of the animal body. It allows detecting, describing, and reporting of gross findings that could be key to understand changes noted during the *in vivo* phase of an experiment. It is therefore important that the personnel in charge of the *postmortem* procedure have access to the animal history including clinical examination and behavioral changes that preceded necropsy as well as to the results of any imaging or laboratory investigations. On the other hand, the necropsy personnel should have access to the experiment study plan in order to harvest tissue samples important to meet the objectives of the study. Since necropsy can be performed only once, it is crucial to follow a precise procedure that allows identification of gross abnormalities and adequate sampling of organs.

The necropsy procedure consists of a series of systematic operations that allow examining all body organs and cavities without altering the characteristics of any tissue or organ of the animal. The collection of samples for histology or other complementary analyses also follows precise rules.

Histopathology is a major endpoint of many experiments. It is therefore crucial that tissues be sampled and preserved in a standardized manner especially when the microscopic findings need to be compared groupwise. The amount of tissue that needs to be sampled should be representative of the whole organ since the probability of detecting lesions is primarily dependent on the amount of the tissue examined. For large organs of the body, such as the lungs or the liver, it is therefore necessary to define the number of sections and specific areas to be sampled. The anatomic characteristics of each organ should be considered. For example, the kidney is composed of a cortex, a medulla, and a pelvis. Each of these anatomical regions has distinct histological characteristics that need to be evaluated as microscopic changes may reside only in one or more structures. For organs comprising a lumen or a cavity (such as intestines, urinary bladder, uterus, or heart), the amount and type of structures present on a transversal section may considerably vary and may subsequently compromise, and sometimes irreversibly hamper, adequate microscopic evaluation. Therefore, the plane of section should be considered and carefully standardized during sampling. For tissues with multiple or complex anatomical structures (like the brain or nasal cavity), it is advised to collect multiple sections in order to examine all structures of interest.

The probability of detecting lesions in the histological slide is also influenced by the technical procedures such as method of preservation and preparation. It is essential that the *postmortem* degradation process (otherwise termed as autolysis) be controlled. This is achieved by immersion of tissue samples in a fixative like formalin. Other fixation techniques are available and should be always considered depending on each experiment-specific endpoints.

The purpose of this chapter is to describe the different steps of the necropsy, and to give general guidelines for sampling procedures in rodents although these can be easily adapted to other laboratory animal species. As the knowledge of anatomy basics and species differences is required to perform a necropsy, basic anatomical description is also given. It is extremely useful to be aware of the subsequent histological processing of organs/tissues for histology in order to understand sampling and trimming rules. So this chapter is intimately linked to the next one in this book and dedicated to histopathology procedures.

Well-illustrated descriptions of necropsy protocols are available [1–5], some of them are online [6] and would complement this chapter. Handbooks on the anatomy of rodents are also useful [7, 8]. The reader is also strongly encouraged to refer to the three

publications from the RITA/NACAD group or website about organ sampling and trimming in rats and mice that give guidelines in a didactic manner, with excellent full-color macrophotographs and microphotographs from the corresponding hematoxylin and eosin (H&E)-stained slides [9–11].

2 Materials

1. Fume hood.
2. Rubber gloves (vinyl gloves in case of allergy to latex), protective clothing, eyeglasses, and mask.
3. Dissecting board preferentially in plastic that could be easily cleaned and if necessary autoclaved.
4. Small hair clipper.
5. Blunt-ended forceps: Serrated forceps should be avoided as they cause damage to tissues.
6. Small dissecting scissors, surgical scissors, and microsurgical (ophthalmologic type) scissors (these are very useful especially during extraction of the central nervous system).
7. Syringes (1, 5, 10 mL) and needles (a 21-gauge needle is suitable for infusion of the lung with fixative).
8. Scalpels (new blades and handle).
9. Plastic bags, paper towels.
10. Containers for histological specimens, cassettes, labels: All containers should be adequately identified prior to starting necropsy.
11. Specific containers for other specimens (bacteriology, virology, mycology, parasitology, chemistry) should be available.
12. Tubes for liquid samples.
13. Euthanasia solution or suitable source of CO₂ and container.
14. Fixative (usually 10% neutral buffered formalin): Unless otherwise specified, the fixative mentioned in the text will be 10% neutral buffered formalin. Ready-to-use 10% neutral buffered formalin is commercially available from major suppliers. However, this fixative can be easily prepared. A detailed procedure is described in Table 1. Caution should be taken as formalin is included in the list of human carcinogens. Different commercial alternatives are proposed but formalin still remains the standard for fixation in histopathology.
15. Decalcifying solution (in case bones should be examined): There are several decalcifying solutions. A 26% formic acid solution (TBD2® Shandon Lipshaw) is routinely used in histopathology laboratories.
16. Ethanol 95 and 70%.

Table 1**Protocol for preparation of formalin and modified Davidson's fixatives**

Protocol for preparation of formalin 10%, buffered	
– Formaldehyde (37–40%)	100 mL
– Distillated water	900 mL
– Monosodium phosphate anhydrous	4 g
– Disodium phosphate anhydrous	6.5 g
– Final solution 3.7–4% formaldehyde (To be used preferentially within 6 months after preparation. Keep at room temperature)	
Protocol for preparation of Paraformaldehyde 4%	
– Paraformaldehyde 4% (PFA 4%)	
– Paraformaldehyde (powder)	4 g
– Distillated water	80 mL
– Put 6 µL of sodium bicarbonate	
– Put 10 mL of PBS 10×	
– Filtrate on a paper	
– Add PBS to obtain	100 mL
– Adjust the pH to 7.2 à 7.4	
The solution should be heated to facilitate the dissolution of the PFA, but below 65 °C and in a fume hood	
– Store at 4 °C up to 24 h	
Can be also frozen in aliquots	
Protocol for preparation of modified Davidson's fixative	
– 30% of a 37–40% solution of formaldehyde	
– 15% Ethanol	
– 5% Glacial acetic acid	
– 50% Distilled H ₂ O	

17. Saline solution or phosphate-buffered solution (PBS).

18. Weighing scale.

19. Material to take photographs.

20. Metric scale.

21. Recording necropsy cards.

During necropsy, it is recommended to place the instruments in a stainless steel instrument holder with 70% ethanol. Used needles and scalpel should be placed in a special container for harmful material.

There are several hazards related to handling and dissection of laboratory animals during necropsy that should be considered. The chemical risk is one of them. For example, formalin causes eye, skin, nose, and respiratory tract irritation; it is also classified as a strong skin sensitizer and carcinogen in humans. Therefore formalin should not be handled without gloves or outside a fume hood [12, 13].

Laboratory rodents can spontaneously carry diseases that are transmissible to humans (also called zoonoses) [14]. Although laboratory rodents are usually tested for these agents, there is always a risk to contract one of these diseases. In addition, the allergic risk remains important especially for people with known animal allergies. Working with laboratory animals can lead to exposure to allergens via inhalation, and direct skin and eye contact with animal dander, hair, urine, serum, or saliva. It is therefore essential that all necropsy personnel use protective equipment [15, 16] and that cadavers and all waste be eliminated appropriately.

3 Methods

3.1 General Recommendations

3.1.1 Necropsy Protocol and Specimen Collection

It is strongly recommended to carefully read the experimental study plan or protocol. The list of organs that should be examined and sampled differs from one study to another depending on the aim and the duration of the study. The following procedure allows examining and collecting most tissues and organs in rodents with the main purpose of histopathology evaluation of tissue samples. It is very much inspired from necropsy performed in toxicological studies. The major steps are as follows:

- Examination of the live animal
- Euthanasia
- Exsanguination
- Opening of the abdominal cavity
- Opening of the thoracic cavity
- Opening of the skull
- Examination of muscles and skeleton

This protocol should be followed step by step. It is the most convenient way to remove, examine, and sample each organ or tissue. The sequence of necropsy can be adapted to each experiment. For example, if the brain is the main organ of interest, it can be sampled at the beginning of the necropsy.

Organs should always be immersed in the fixative as quickly as possible after sampling, macroscopic examination, and weighing. It is sometimes required to perform necropsy on animals found dead. Although variable degrees of autolysis will inevitably take

place, valuable information can be gained from collected tissues. Carcasses of found dead animals can be placed in a refrigerator (but should NEVER be frozen). Necropsies should be performed as soon as practicable (if possible within the same day).

3.1.2 Weighing of Organs

One important part of necropsy is to describe the size of organs. This requires that the dissector has in reference the normal size of the organ. Small variation in size can be challenging even for an experienced pathologist especially when organ sizes need to be compared among several individuals and groups. To accurately compare organ sizes, it is most helpful to record individual organ weights. These can be compared either as absolute organ weights or as ratios of organ weight to total body weight or to brain weight. Following the recommendations from the Society of Toxicologic Pathology (STP) [17] liver, kidneys, heart, brain, adrenal glands, testes, spleen, and thymus should be weighed routinely in all general toxicology studies with multidose administration in rodents (*see* Table 2). Thyroid and pituitary gland should be weighed in rats but not in mice as handling of these minute tissues may induce artifacts that can complicate microscopic assessment. Epididymides and prostate weighing is recommended in rat studies but only on a case-by-case basis in mouse as well as other organs including female reproductive organs in rodents. Organ weights are not recommended in carcinogenicity studies.

Table 2
List of organs for weighing

Rat	Mice
Liver	Liver
Kidney	Kidney
Heart	Heart
Adrenal glands	Adrenal glands
Brain	Brain
Testes	Testes
Prostate	Spleen
Epididymis	Thymus
Spleen	Thyroid/parathyroid
Thymus	Pituitary gland
Thyroid/parathyroid	
Pituitary gland	

Sellers, R., et al., in *Toxicologic Pathology* 35, 751–755 (2007)

In all cases, organs should be weighed free of surrounding fat and connective tissues. It is important to remove these tissues in a standardized manner and without inducing any damage or artifact to the tissue.

3.1.3 Organ Sampling for Histology

Most of the tissue samples from one animal will be directly immersed in a fixative container identified with the animal number. Small tissues can be kept in histology cassettes for fixation at the time of dissection. This will allow easy retrieval of samples for trimming. The same cassette, adequately identified, can be used for both paraffin embedding and paraffin block preparation. The number of cassettes and hence paraffin blocks can be considerably reduced by combining a few tissues and organs in one cassette. For example, several small and large intestine samples can be grouped [18, 19] (*see* Table 3).

3.1.4 Examination and Recording of Macroscopic Observations

The description of macroscopic findings should be sufficiently detailed to give a visual representation of gross changes. Therefore, all criteria should be used to describe the gross changes of an organ: location, appearance (color, shape, consistency), demarcation from surrounding tissues, number, distribution and severity, and size that should always be measured in two or three dimensions (cm, or mm), or in volume (mL). Taking pictures of lesions is a useful way to share data and experience on identification and description of macroscopic observations.

3.1.5 Orientation (Fig. 1)

It is critical for the necropsy personnel to use correct terms that define the orientation of an organ or a section:

1. Dorsal refers to the back of the animal whereas ventral refers to the abdomen.
2. Cranial refers to the skull, whereas caudal refers to the tail.
3. Rostral refers to the organs or structures situated toward the front of the head.
4. Lateral pertains to a side, medial is related to, situated in, or extending toward the middle, closer to the body's midline.
5. Proximal is located nearer to a point of reference; distal is located far from a point of reference (origin, point of attachment, or midline of the body).

The major planes of sections are defined as follows:

1. Median plane, passing longitudinally through the middle of the body from front to back, dividing it into right and left halves.
2. Frontal (coronal) planes, passing longitudinally through the body from side to side, perpendicular to the median plane, dividing the body into front and back parts.

Table 3**Example of blocking scheme**

Cassette	Tissues
1	Muscle: heart (bisected), skeletal (diaphragm, tongue, soleus) Thymus
2	Lung: entire (all lobes, formalin infused via trachea) Thyroid: with trachea (specimen immediately caudal to larynx, cross section)
3	Kidneys: right in cross section, left in longitudinal section Adrenal glands: separated from kidneys but in the same cassette
4	Submandibular and parotid salivary glands and lymph nodes
5	Stomach: glandular and nonglandular portions Duodenum: with pancreas Ileum: distal small intestine with lymphoid nodule if available Cecum: tip with lymphoid nodule if available Proximal colon: two sections Rectum/distal colon: between fecal balls
6	Lymph nodes: mesenteric chain and any enlarged lymph nodes
7	Liver: left lateral (largest) lobe (one section cut from hilus to periphery), median lobe (one section to include gallbladder) Spleen: one longitudinal section (half of spleen)
8	Female: ovaries, uterus (two to several cross sections), vagina/bladder/rectum (one to several cross sections) Male: testes and epididymides, seminal vesicles, and coagulating glands (cross sections or longitudinal sections depending on size), bladder/rectum/intervening prostate (one to several cross sections)
9	Skin: dorsal cervical specimen (one section parallel to hair growth), ventral inguinal specimen (one section parallel to hair growth, to include mammary and clitoral or preputial glands)
10	Decalcified hind limb: femur with knee and tibia with tarsus Decalcified sternum
11	Decalcified head One section to include ears (also includes, pituitary, cerebrum, hippocampus) One section to include eyes (also includes olfactory lobes, molar teeth) One section to include nose (includes olfactory and respiratory epithelium, maxillary incisor root) One section to include cerebellum
12	A, B, C, etc. Tissues with macroscopic observations

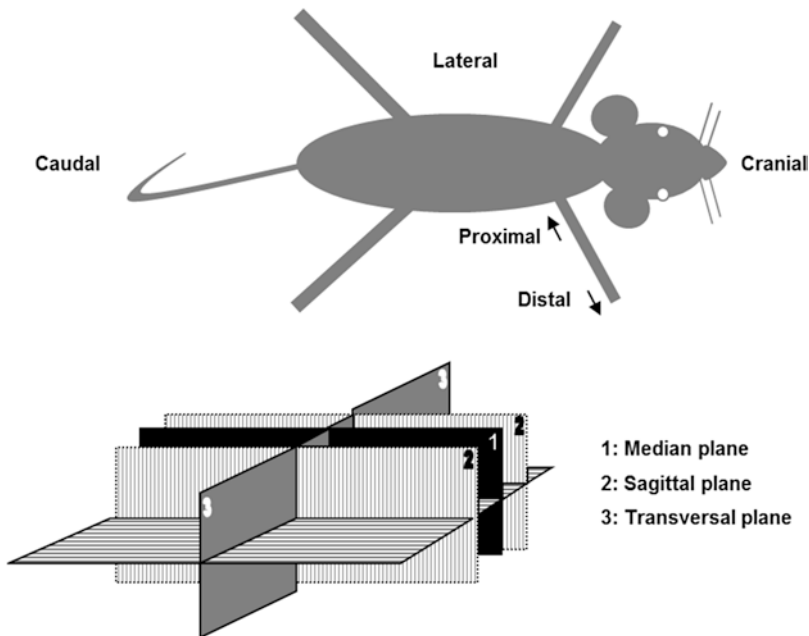


Fig. 1 Anatomical orientation descriptors usually used at necropsy

3. Sagittal planes are vertical planes passing through the body parallel to the median plane dividing the body into left and right portions.
4. Transverse plane (dorsoventral), passing horizontally through the body, perpendicular to the sagittal and frontal planes, and dividing the body into upper and lower portions.
5. Horizontal plane, passing through the body, perpendicular to both the frontal and median planes, dividing the body into upper and lower parts.
6. Vertical plane, perpendicular to a horizontal plane, dividing the body into left and right, or front and back portions.

3.2 Examination of the Live Animal

1. Observe the behavior of the animal.
2. Observe the fur and the skin to detect any changes.

3.3 External Examination

1. Weigh the animal. As indicated in Subheading 3.1.2, this will be useful to calculate organ weight-to-body weight ratios.
2. Examine the animal before proceeding to the necropsy.
3. Assess the general condition of the animal (emaciated, thin, adequate/good condition, obese).
4. Check and record any external lesions (skin lesions, fur loss or discoloration, and subcutaneous masses). Record sizes whenever possible and record their gross appearance and precise location.

5. Check and record the color changes of the skin and mucosae (gingival, genital mucosae, conjunctiva).
6. Examine the eyes, mouth, teeth, and nasal openings and record any abnormality.
7. Examine the anogenital region to look for signs of diarrhea, and rectal or vaginal prolapse, and record any abnormality.
8. Gently palpate the abdomen to reveal abdominal masses or presence of fluid.
9. If the abdomen is distended by fluid, take a sample with a sterile needle and syringe for further evaluation.
10. Palpate any mass, and record its consistency (soft, fluctuant, firm, or hard).

3.4 Euthanasia

Various methods of euthanasia are available for rodents. The selected method should induce death quickly with minimal animal pain or distress and should not interfere with the gross observation and microscopic evaluation of the tissues. Euthanasia protocols should be approved by the local ethical committee.

We describe in this chapter probably the most common euthanasia method which is commonly used in toxicological studies: exposure to carbon dioxide (CO₂). This method requires only a source of CO₂ and a polycarbonate box of a size that is well matched with the size of rodents. The euthanasia procedure is as follows:

1. Place a wet sponge in one of the corners of the box.
2. Place the lid with the CO₂ tube attachment on the box
3. Charge the chamber with CO₂ gas for 1–2 min.
4. Place animals in the box.
5. Turn gas on low so as not to frighten the animals.
6. Administer CO₂ until deep sedation is observed.
7. Death is induced by maximal exsanguination from the abdominal aorta performed quickly on sedated animal taken out of the box (this can be the time to collect for hematology, blood coagulation, and clinical chemistry parameters).
8. Check absence of respiration and heartbeat to verify death.

3.5 Incision of the Skin and Examination of the Subcutaneous Tissues/Organs

Skin, subcutaneous tissue, mammary glands, salivary glands, superficial cervical lymph nodes, extraorbital lacrimal gland, clitoral glands, preputial glands, penis, and prepuce.

3.5.1 *Incision of the Skin and Examination of the Subcutaneous Tissue*

1. Pin the animal on the dissection board, ventral side up and head in front of you. Remember that from this point, the left side of the animal is on your right side and *vice versa*.
2. Skin of the inguinal area at the site of mammary gland and skin sampling can be clipped to facilitate histological processing. Moisten the skin and hairs with 70% alcohol.
3. Incise the skin with a scalpel on the midline, from the mandibles to the pubis. In males, incision should end on both sides of the penis.
4. Reflect the skin on both sides of the incision.
5. Examine the skin and the subcutaneous tissue. Record any lesion; confirm skin changes observed in the previous step.

3.5.2 *Examination and Sampling of the Mammary Glands*

1. Examine the mammary glands: The mouse has five pairs of mammary glands (three thoracic and two abdominal) while the rats have six pairs (three thoracic and three abdominal). There are six or seven pairs in hamsters [20, 21]. In females, the mammary tissue extends from the salivary gland region to the base of the tail. When lactating, the mammary gland occupies almost all the abdominal and thoracic ventral subcutaneous area in the mouse and in the rat.
2. Harvest the mammary gland from the inguinal region where the mammary tissue is abundant in both rats and mice. Take a transverse section (1 cm × 3 cm) including the associated nipple and skin (*see Note 1*). This applies to males as well as to females as mammary gland is present in both genders.

3.5.3 *Examination and Sampling of the Superficial Lymph Nodes*

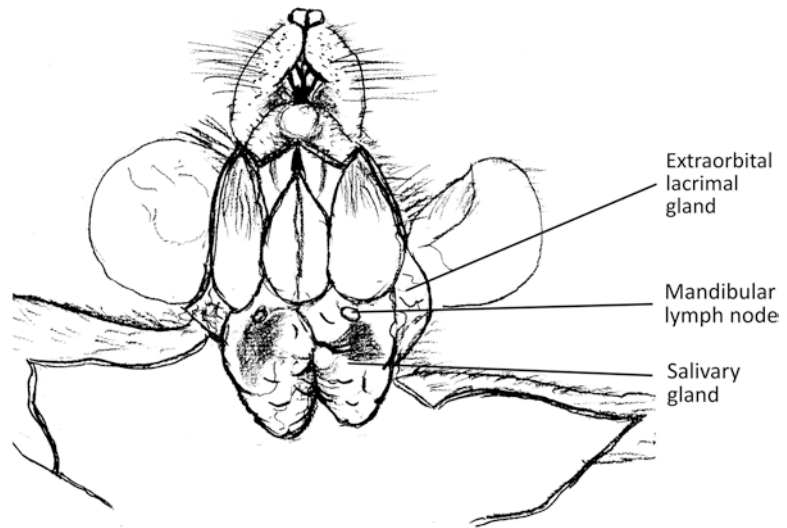
Examine the superficial lymph nodes. Under normal conditions, lymph nodes are grayish organs and bilateral and have the size and shape of a small pea. Major superficial lymph nodes, located in the subcutaneous area, are the cervical superficial/mandibular, axillary in the axillary fossa, brachial, inguinal, and popliteal lymph nodes. The peripheral lymph nodes that are most often examined are the mandibular, axillary, and/or popliteal lymph nodes (*see Note 2*). The location of these lymph nodes is detailed in Table 4 [22].

3.5.4 *Examination, Removal, and Sampling of Salivary Glands, Mandibular Lymph Nodes, Extraorbital Lacrimal Glands (Fig. 2), and Clitoral and Preputial Glands*

1. Examine the three pairs of salivary glands located on both sides in the cranioventral region of the neck: *mandibular glands*, *sublingual glands*, and *parotid glands* [23, 24]. The mandibular gland is the largest one, located in the ventral region of the neck. The sublingual glands are situated on the top of the former. Parotid glands are the most lateral ones; they extend to the base of the ears. Mandibular lymph nodes are located between sublingual and mandibular glands; they are collected with salivary glands.

Table 4**Nomenclature and location of major lymph nodes**

Lymph node		Location
Superficial	Mandibular	Rostromedial to the sublingual and mandibular salivary glands
	Axillary	Axillary fossa
	Brachial	Proximity to the angle of the capsula, upon the biceps, underneath the pectorals
	Inguinal	Adherent to the skin of the groin
	Popliteal	Between the adductor muscle and the semimembranosus muscle behind the knee
Deep	Deep cervical	Behind the salivary glands hidden in the connective tissue encircling the trachea
	Lumbar, caudal	Anterior to the bifurcation of the abdominal aorta
	Mediastinal	Posterior face of the thymus
	Mesenteric	Lengthened shape, with the mesentery, close to the ascending portion of the colon
	Pyloric (pancreatic)	Anterior end of the pancreas, near the pylorus
	Renal	Between the aorta and hilum of the kidneys
	Sacral Sciatic	Posterior to the bifurcation of the abdominal aorta Below the sciatic nerve on the back

**Fig. 2** Overview drawing of the ventral neck region

2. Collect salivary glands by gently grasping the tip of the closest salivary gland to the thorax with forceps. Then slowly pull toward cutting the surrounding tissues with scissors and immerse the salivary glands in fixative.
3. Examine the extraorbital lacrimal glands. These glands are located on the ventrolateral aspect of the head. They appear as flat, brown-grey glands next to the parotids.

4. Remove the extraorbital glands on both sides by gently grasping the tip of the gland with forceps, isolate the gland from its attachment in the eye socket using scissors, and immerse the two glands in fixative (*see Note 3*).
5. Examine the clitoral glands in females, or preputial glands in males. Clitoral/preputial glands are modified sebaceous glands that are included in the subcutaneous adipose tissue. They can be found cranial to the vulva in females, and lateral to the penis in males. Preputial glands are leaf shaped with a yellowish color and a soft consistency.
6. Remove the whole glands on both sides by gently grasping the tip with forceps to isolate them from the surrounding tissue. Immerse the clitoral/preputial glands in fixative.

3.5.5 Examination of the Penis

Examine the penis and the prepuce in males. These organs will be harvested with the remaining genital organs.

3.6 Opening of the Abdomen and Examination of Abdominal Organs

Peritoneum, spleen, mesenteric lymph nodes, pancreas, digestive tract, liver, adrenal glands, kidneys, and genital organs.

3.6.1 Opening of the Abdominal Cavity

1. Grasp the abdominal wall with forceps near the sternal xiphoid appendix and lift firmly.
2. Make a small incision to let air into the abdomen. This will allow abdominal viscera to be separated from the abdominal wall.
3. Cut the abdominal wall on the midline with scissors from the pelvis to the xiphoid appendix, avoiding cutting any of the abdominal organs that lie underneath.
4. Reflect the abdominal wall on the sides.
5. Examine the abdominal serous membrane (*peritoneum*) and look for the presence of abnormal contents such as serous fluid, blood, or fibrin as well as any adhesion between abdominal wall and abdominal organs.
6. Check the position of the different organs in situ.
7. Check the fat deposits and score the nutritional conditions (1. Obese, 2. Good nutritional condition, 3. Poor nutritional condition, 4. Bad nutritional condition, 5. Emaciation-absence of fat in the body deposits). The amount of fat depends on the age, gender, and strain of the animal: adults and aged animals tend to have more fat deposits in the abdominal cavity.

3.6.2 Removal, Examination, and Sampling of the Spleen

1. The spleen is situated in the left superior abdominal quadrant. To remove it, grasp the connective tissues and fat surrounding the spleen with the forceps. Cut them along the hilus of the spleen and cut the gastrosplenic ligament as well.

2. Examine the spleen. It is a lengthened, oval, slightly curve-shaped organ; has a dark-red color; and is soft in consistency with a thin transparent capsule [25]. It is attached to the stomach by the gastrosplenic ligament.
3. Should spleen be weighted, it should be carefully freed from all remnants of connective and adipose tissues, in particular along the hilus.
4. The entire spleen can be sampled and immersed in fixative although a 2 mm thick transverse middle section can be sufficient.
5. Alternatively, the spleen can be sampled at the same step as the pancreas.

3.6.3 Removal of the Digestive Tract and Mesenteric Lymph Nodes

Abdominal part of the esophagus, stomach, small intestine (duodenum, jejunum, ileum), large intestine (cecum, colon, rectum), and mesenteric lymph nodes

1. Dissect the anus free from the surrounding skin.
2. Insert the tip of heavy-duty scissors between the lower urinary tract and the ventral pelvis to cut the pelvic arch on both sides. Take off the resulting bone chip to facilitate the subsequent removal of the genital tract and rectum.
3. Hold the rectum with forceps, and lift it upwards.
4. Isolate the rectum from the vagina in females.
5. Gradually extract the intestines in a caudal-cranial direction while cutting the insertion of the mesentery as close to the intestines as possible.
6. Cut the esophagus just below the diaphragm in the abdomen leaving a small portion of esophagus connected to the stomach.
7. Isolate the whole digestive tract together with the pancreas.
8. Examine the deep abdominal lymph nodes [22, 26] (Table 4 for nomenclature and location) before unzipping the intestines. The mesenteric lymph nodes are usually the largest lymph nodes of the abdominal cavity. They drain the duodenum, ileum, cecum, and colon.
9. Starting at the rectum, progressively unzip the coiled intestines by pulling gently with scissors.

3.6.4 Examination and Sampling of the Pancreas

1. In rodents, the pancreas is very diffuse and completely enclosed in the mesentery. It is tan in color and therefore easily identifiable from the surrounding fat. It has one *left lobe* located close to the spleen in the great omentum, and one *right lobe* adjacent to the duodenum.
2. Lift up the pancreas and separate it from the intestines by cutting its insertion with scissors.

3. Isolate the spleen from the pancreas with the scissors.
4. Take a sample from the *left pancreatic lobe* to have the largest surface. The *right pancreatic lobe* will be sampled with the duodenum.

3.6.5 Examination and Sampling of the Stomach

1. In small rodents (mice, rats, hamsters, and gerbils), the stomach has two distinct regions: the proventricular or anterior region or forestomach with a white mucosa, and the glandular region which has a reddened and thicker wall [27, 28]. Both are clearly demarcated by a limiting ridge in these species but not in the guinea pigs.
2. Isolate the stomach from the esophagus and the intestines.
3. In mice, open the stomach along the greater curvature, mount on a plastic card, fix it with pins, and immerse it in the fixative. In rats open the stomach of the rat along or paramedian to the greater curvature. Remove the gastric content and, if necessary, clean carefully the mucosa with saline solution or fixative. Spread out the stomach and pin it on the cardboard. This procedure avoids folds in the mucosa and therefore is essential for the macroscopic orientation and allows reproducible microscopic evaluation of the height of gastric mucosa.

3.6.6 Examination and Sampling of the Intestines

1. The small intestine has three different regions: *duodenum*, which is very short (1 cm) in rodents, and *jejunum* and *ileum* that are not recognizable grossly. The large intestine is composed of the *cecum*, *colon*, and *rectum* (short segment in rodents, included in the pelvis) [29]. Lymphoid tissue associated with the small intestine (jejunum and ileum) is also called gut-associated lymphoid tissue (GALT) or Peyer's patches. These appear as slightly elevated lighter fields in the intestine's wall, and can be discernible as prominent areas when activated.
2. Separate carefully the intestines from the mesentery during necropsy (or after fixation).
3. Intestine examination should comprise at least the content, wall thickness, color, aspect of mucosa, or any noticeable lesion in each intestinal segment.
4. If the microscopic evaluation of the whole intestine and GALT on a single section is preferred, the so called Swiss roll method can be performed [30, 31] (*see Note 4*). Other techniques for evaluation of the intestine have also been recently described [32].
5. In toxicology studies, routine intestine samples for histopathology evaluation usually consist of one transverse section (2–3 mm thick) from each part of the bowel without opening it: duodenum (1 cm distal to the pyloric sphincter), jejunum (central section), ileum (1 cm proximal to cecum), cecum, colon (central section), and rectum (2 cm proximal to the anus). For small

intestines, it is also essential to sample the GALT. Standardized sampling procedure of the bowel segments is necessary to guarantee examination of each required segment.

6. It is also possible to sample and fix the entire intestine after cleaning with PBS by using a syringe introduced into the duodenum.
7. After sample collection for histopathology, the remaining intestine could be opened longitudinally and examined for abnormalities. To better examine the mucosa, a gentle rinse of the ingesta with saline solution may be necessary. This latter procedure is time consuming and should be considered on a case-by-case basis only.

3.6.7 Removal, Examination, and Sampling of the Liver

1. The liver has four lobes: *medial lobe*, *right medial lobe*, *right lateral lobe*, *caudate lobe*, plus a *papillary process* (see **Note 5**). There is no gallbladder in the rat. The liver is normally dark-reddish and has a hard but friable consistency. A thin transparent capsule covers the liver.
2. The liver is a fragile organ that should be handled with caution.
3. Remove the liver gently out the way with the forceps.
4. Grasp the xiphoid process firmly with the forceps.
5. Puncture the diaphragm with scissors and trim it completely away from the ribs.
6. Pull upward to create a negative pressure in the thorax.
7. Using the diaphragm as a handle, pull the liver out of the abdominal cavity. Separate the liver from the diaphragm by cutting the falciform and coronary ligaments that attach the liver to the diaphragm.
8. Before weighing the liver, remove all remnants of the diaphragm and ensure that the small lobes are present to weigh the entire organ.
9. Sampling of the liver (see **Note 6**): In the rat, take a piece from the left lateral lobe (transverse), and the right medial lobe (transverse); in the mouse from the left lateral lobe (transverse), and from the left and right medial lobe including gallbladder (longitudinal-vertical preferentially to keep the gallbladder with the liver). In both species, a transverse section from the caudate lobe is optional. Size of samples should be as large as possible as trimming will be performed after fixation to fit all pieces into one cassette. Immerse the two or three liver samples in the fixative. It is advised to keep the remaining liver tissue in fixative.

3.6.8 *Removal, Examination, and Sampling of the Kidneys, Ureters, and Adrenal Glands*

1. Remove the kidney and adrenals, grasp the caudal part of the ureter with forceps near its opening, and keep the adrenals attached to the kidneys. The adrenal glands and kidneys are located deep in the retroperitoneal space; they should be recognized as early as possible during the process.
2. Separate the adrenals from each kidney.
3. Examine each adrenal gland. These glands are small white structures within the perirenal fat. In male, adrenal glands tend to be large, often rose-colored, and translucent, while in females, they are smaller and, due to high lipid content, have an opaque pale color [23, 33, 34]. Adrenals have an external *cortex* and central *medulla*.
4. Check their shape, volume, as well as the presence of nodular formations.
5. Before weighing adrenal glands, remove carefully all remnants of fat and connective tissues. As for all paired organs, unless otherwise specified in the study plan, the weight of the pair is recorded.
6. Immerse the adrenal glands in the fixative. Due to their relatively small size in rodents, they will be embedded in toto.
7. Examine the kidneys. Kidneys are located on the dorsal wall of the abdominal cavity. They are bean-shaped pair organs, with a hilus in the concave margin from which main vessels, nerves, and ureters exit. Their color is brownish red and their consistency is firm. The right kidney is located more cranially and is usually larger and heavier than the left one [35, 36]. The kidneys are surrounded by a capsule, and have three different regions: *cortex*, *medulla*, and *papilla*.
8. Before weighing, kidneys must be freed of all remnants of connective and adipose tissues.
9. Kidneys can be immersion fixed in toto or after trimming (for example: take a longitudinal section from the left kidney and a transverse section from the right kidney).
10. Ureters can be sampled and because of their small size put in a cassette for fixation.

3.6.9 *Removal, Examination, and Sampling of the Urinary Bladder*

1. Examine the urinary bladder [11, 37].
2. The bladder can be freed of urine after incision of the wall and then sampled in toto. Alternatively, the bladder can be sampled after instillation of the fixative under a hood. In the mouse, instill the fixative (0.05 mL) through the bladder wall after ligation of the urethra with a ventral knot. In the rat, it is more convenient to instill the fixative (0.2 mL) with a needle inserted via the urethra. In both rats and mice, fixative instillation should not be performed when the bladder is distended with urine.

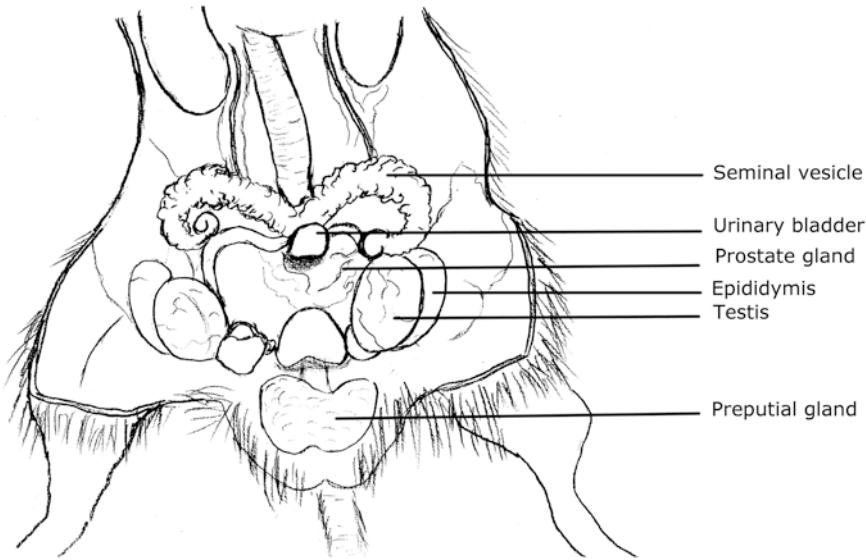


Fig. 3 Overview drawing of male genital organs

3. Then continue the fixation by immersion in a container of fixative or directly immerse the sampled bladder in the fixative.
4. It may be helpful also to mark the ventral side of the bladder with a stick of silver nitrate.

3.6.10 Removal, Examination, and Sampling of the Male Genital Organs (Fig. 3)

1. Remove the testes. They are oval-shaped paired organs, a few millimeters in diameter that lay inside the scrotum. They are covered by a smooth and transparent membrane (*tunica albuginea*). They are grayish-white with a soft elastic consistency. When the abdominal cavity is opened, testes are often found outside the scrotum, in an intra-abdominal position. Grasp them delicately by the inguinal fat pad and cut them away from the viscera. If the testes are still in the scrotum, open the scrotum and extract the testes with the epididymides by cutting the fibrous ligaments anchoring the tail of the epididymis to the scrotum. Cut the vas deferens.
2. Examine the testes [38–41]. Check the shape, volume, weight, consistency, and presence of tumor masses.
3. Weigh the testes individually or as a pair. Weigh the epididymis (in rats only) separately if needed. Before weighing of the testes and epididymis, all remnants of connective and adipose tissues should be removed.
4. Fix the testes and epididymis as a whole (*see Note 7*), without cutting the testes prior to fixation; otherwise they will rupture (*see Note 8*).
5. It is suggested to fix testes and epididymis in Davidson solution instead of formalin (Table 1).

6. Remove the male accessory glands: *seminal vesicles*, *coagulating glands* (dorsocranial lobe of the prostate), and *prostate* (two ventral lobes and two dorsolateral lobes). The dorsolateral and ventral lobes lie in a vertical axis above each other with urinary bladder and seminal vesicles in between.
7. Remove the group of adjacent organs consisting of prostate, urinary bladder, seminal vesicles, and coagulating glands.
8. Examine the male accessory glands [38, 39, 42, 43]. Check for any size or color changes or presence of nodular masses.
9. Before weighing the prostate (rats only), all remnants of connective and adipose tissues should be carefully removed.
10. Immerse these organs into the fixative in toto if weights are not required to be fixed to prevent leakage of the glandular secretions.
11. Remove the penis, prepuce, and urethra.

3.6.11 *Removal, Examination, and Sampling of the Genital Organs in Female (Fig. 4)*

1. Dissect the vulva and vagina free from the skin and cut the supporting ligaments of the vagina, uterus, and oviducts.
2. Cut the ligaments and isolate the ovaries with the oviduct and the whole genital tract.

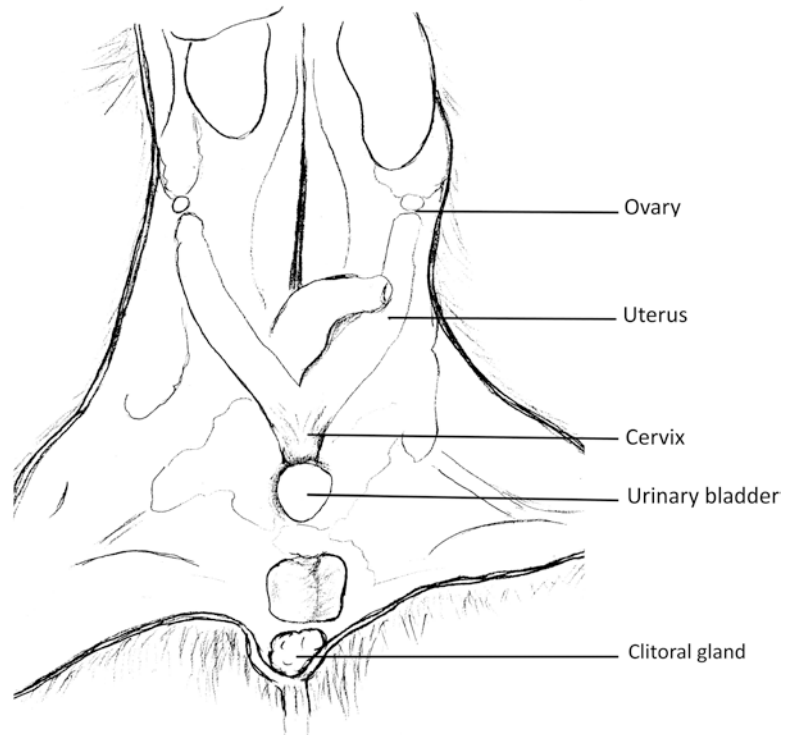


Fig. 4 Overview drawing of female genital organs

3. Examine the ovaries and oviducts. Ovaries are small oval red-dish organs found within the fat tissue caudally to the kidneys and attached to the inferior poles of the kidneys, and to the posterior wall of the abdomen by ligaments. Check the shape, volume, consistency, and presence of any gross lesions [23, 38, 44, 45].
4. If ovaries are to be weighed, isolate them from the oviducts before weighing.
5. Examine the uterus and vagina. Record any enlargement, fluid, or mass [24, 38, 44, 45].
6. If uterus has to be weighed, uterine horns and the cervix should be weighed together but separated from the vagina.
7. The *uterine body* (fused part of the uterus) and the vagina should be placed with their dorsal aspect on cardboard before fixation.

3.7 Opening of the Thorax and Examination of Thoracic Organs

Tongue, larynx, trachea, thymus, mediastinal lymph nodes, lungs, heart, and thyroid gland (with parathyroids).

3.7.1 Opening of the Thorax

1. Open the thorax by first lifting the sternal xiphoid process with forceps. Then cut the ribs starting from the xiphoid process and up to the first rib to remove the sternum and rib cage to reveal the thoracic organs.
2. The sternum is a convenient organ for bone marrow examination after decalcification. Take a piece containing 2–3 sternabrae and immerse this sample into fixative.
3. Examine the thoracic serous membrane (*pleura*) and occurrence of abnormal contents such as serous fluid, blood, fibrin, or adhesions between the organs.
4. Check the position of the different organs in situ.

3.7.2 Removal of the Tongue, Trachea, Esophagus, and Thoracic Organs

1. Cut the muscles of the lower jaw with a scalpel.
2. Cut the soft palate and pharynx.
3. Grasp the tip of the tongue with forceps and retract gently to remove the tongue, larynx, and trachea with esophagus from the head and neck.
4. Continue retracting to remove the heart and lungs from the thorax. Use scissors to perform a blunt dissection to free these tissues.
5. Cut the thoracic aorta and posterior vena cava at the level of the diaphragm.

3.7.3 Isolation, Examination, and Sampling of the Heart and Aorta

1. Isolate the heart from the lungs by delicately cutting the main vessels with scissors.
2. Examine the heart without opening the inner cavities (*atria* and *ventricles*) [23, 46, 47]. Before weighing the heart, all blood should be removed. In rodents, this can be easily achieved by placing the base of the heart over a piece of cleaning paper.
3. Immerse the heart in toto in the fixative.
4. Take a section from the *thoracic aorta* (in the middle of the last 1 cm caudal segment). This region is closely attached to dorsal vertebrae and can easily be removed.

3.7.4 Isolation, Examination, and Sampling of the Thymus

1. Isolate the thymus by gently grasping one of the two lobes in its inferior part and cut the ligament connecting it to the pericardium.
2. Examine the thymus [48]. In rodents the thymus is an oval-shaped lobulated organ with a whitish-translucent color. With age, the thymus shrinks but remains grossly visible.
3. Before weighing the thymus, all remnants of connective and adipose tissues should be carefully removed.

3.7.5 Examination and Sampling of the Tongue

1. Examine the tongue [27].
2. Make a transversal incision to sample half the tongue and immerse it in the fixative (*see Note 9*).

3.7.6 Examination and Sampling of the Thyroids, Parathyroids, Trachea, and Esophagus

1. Examine the thyroid gland. Thyroid gland has two small symmetric oval lobes, adherent to the lateral and dorsal surfaces of the trachea, and has a translucent, tan yellowish color. The parathyroids are located around or within the thyroids but are not visible grossly [49, 50], (*see Note 10*).
2. Take the *larynx* including *epiglottis*, *ventral pouch*, and *cricoid cartilage* (rats only) and immerse it in the fixative.
3. If the thyroid is weighed (rat only), carefully remove all remnants of connective and adipose tissues. Immerse the thyroids in the fixative. It is advised to weigh the thyroid gland after 1 or 2 min of fixation.
4. Take then a transverse sample section of trachea and esophagus. If the thyroids are not weighed, leave them on the trachea. Take a transverse section of the esophagus and trachea, including the thyroids and parathyroids. Tracheal content should be noted and reported.

3.7.7 Examination and Sampling of the Lungs

1. Examine the lungs [51, 52]. The rodent lungs have three right lobes (*right cranial lobe*, *right middle lobe*, *right caudal lobe*), an *accessory lobe*, and one *left lobe* (*see Note 11*).

2. The lung parenchyma has normally a smooth surface and a nice light pink color (but color depends on air and blood present if not inflated) and they have a spongy consistency. Examine all lung lobes and note any changes.
3. For optimal microscopic evaluation, instillation of the lung by the fixative is strongly recommended and should be performed under a hood. This can be performed easily through the trachea. A 21 g needle is placed on a 3 mL syringe filled with the fixative. The needle is introduced in the trachea at its open end. Clamp gently around the needle with forceps and inflate the lung by depressing the plunger of the syringe very slowly until excess fixative refluxes up the trachea. The lung with the trachea should be then immersed in the fixative. If the procedure is correctly executed, there is no need to place a ligature on the trachea (*see Note 12*). If lungs have to be weighted, lungs should be separated from the trachea, weight, and then instillation should be performed through main bronchi.

3.8 Head and Central Nervous System

Brain, cerebellum, spinal cord, pituitary gland, eyes, Harderian glands, nasal cavities, and Zymbal's gland.

The most optimal way to fix the central nervous system is intracardiac perfusion of fixative (*see Note 13*). However fixation of the nervous system by immersion allows acceptable preservation of tissues and is routinely performed in toxicity studies.

3.8.1 Removal of the Brain and Spinal Cord

1. Cut the skin over the head with a median-longitudinal incision from the nape to the snout.
2. Reflect the two edges of the skin and pull them to better observe the entire skull.
3. Remove any excess tissue or muscle from the cranium and neck.
4. Keeping the head firmly with large forceps, insert the tip of heavy-duty scissors in the left eye socket (avoid any damage to the eyeball) and cut the nasal bone transversely at the level of the nasal septum between the two orbital cavities. The used scissors for this operation should be exclusively dedicated to this step.
5. Then, with the ophthalmologic scissors, cut progressively the parietal, interparietal, and occipital bones in a craniocaudal direction on both sides in order to isolate a bone cap and reveal the brain. Be very careful to avoid damaging the brain beneath the skull bones during this operation.
6. Pull the skullcap caudally with forceps and take it away.
7. Use the small ophthalmologic scissors to cut the vertebrae. Start from the occipital bone level and then, with the tip of the scissors, alternate right- and left-side cuts of the vertebral bod-

ies to progressively remove the vertebral arches. In this way, the spinal cord will be uncovered in the vertebral canal.

8. Raise the brain by gently introducing forceps under the frontal lobe of the encephalon, and then cut intracranial vessels and nerves at the brain base.
9. Gently handle the brain between the thumb and forefinger and cut successively the spinal nerves coming from the ventral aspect of the spinal cord on each side of the brain, and hold the detached segment of the spinal cord. In the area of the *cauda equina* (where nerves are numerous), cut the spinal cord transversely (*see Note 14*).
10. Isolate the brain and the spinal cord by a scalpel frank transversal section at the junction between the medulla oblongata and the brain.

3.8.2 Examination of the Brain and Spinal Cord

1. Examine the encephalon (brain and cerebellum) [53, 54]. The encephalon is covered by the meninges: the *dura mater* is fibrous and in direct contact with the skull, the *pia mater* is highly vascularized and adheres intimately to the surface of the brain, and the *arachnoid* is a transparent membrane located between the *dura mater* and the *pia mater*, but too thin to be visualized grossly.
2. The brain has two *cerebral hemispheres*, separated by a longitudinal fissure. There are no cerebral circumvolutions in rodents that have a lissencephalic brain. Rodent brains have two large *olfactory bulbs* located in the front. The cerebellum shows thin convolutions and lays in the caudal part of the brain.
3. On the ventral part of the brain, the *optic chiasma*, *median eminence* (representing a part of the hypothalamus), *pons*, and *medulla oblongata* can be observed.
4. The brain is a very fragile tissue, especially if not fixed. It is therefore important not to handle this organ with the forceps but rather lift it carefully using the scalpel blade.
5. Before weighing the brain, carefully remove all remnants of connective tissue (*see Note 15*). To achieve accurate brain weights, the spinal cord should be cut off at a consistent level.
6. It is preferable that the brain (undetached from the cerebellum) be immersion fixed in toto. The brain is an anatomically complex tissue. Therefore, microscopic examination of the brain should be performed at standardized section levels: transverse section of the cerebrum at the optic chiasma, cerebrum at the base of the posterior hypothalamus, midcerebellum, and medulla oblongata [12]. Therefore the brain slices are routinely prepared after fixation.
7. Examine the *vertebral canal* on the cadaver.

8. Examine the spinal cord.
9. Take three transverse sections of the spinal cord for microscopic examination at the upper cervical, mid-thoracic, and lumbar levels. Put all three segments in a cassette and immerse in the fixative (*see Note 16*). As for the brain, spinal cord is a very fragile tissue and should not be handled with the forceps.

3.8.3 Examination, Removal, and Sampling of the Pituitary Gland

1. Examine the pituitary gland [23, 55]. The pituitary gland can be easily seen on the ventral aspect of the cranial cavity after the removal of the brain. It appears as a small spherical gland, covered by a thin layer of *dura mater* and located behind the optic chiasma in the *sella turcica*, a small depression of the sphenoid bone.
2. The fixation in situ of the gland is recommended before removal or weighing. Weighing after fixation provides accurate weight measurements and improves morphology. Fixation can be performed by a few drops of fixative on the ventral aspect of the cranial cavity or by immersion of the remaining skull in the fixative; the gland can be removed later [10] (*see Note 17*).
3. Weighing of the pituitary gland is not required in mice and usually performed after fixation.

3.8.4 Removal, Examination, and Sampling of the Eyes, Optic Nerve, Harderian Gland, and Lachrymal Glands (Internal/External)

1. Remove the eyes by sinking a pair of curved forceps behind the orbit. Gently grasp the optic nerve, and isolate the eye by pulling it outward and cutting its attachments to the socket (*see Note 18*).
2. Examine the eyes [56].
3. Immerse the eyes with the optic nerve in the fixative (*see Note 19*).
4. Examine the Harderian glands (or retro-orbital gland). The Harderian gland lies intraorbitally behind the eyes and embraces the back of the ocular globe. It is grey-colored gland under normal conditions, cone shaped in the rat, and horse-shoe shaped in the mouse.
5. Remove the Harderian glands and immerse them in the fixative.

3.8.5 Sampling of the Nasal Cavity and Zymbal's Glands

1. Remove the skin and muscles and immerse the head in the fixative if further histological examination of the nasal cavity and paranasal sinuses, nasal cavity, nasopharynx, and paranasal sinuses is needed [57, 58].
2. Zymbal's glands are modified sebaceous glands located at the base of the external ear in anterioventral position [59]. A section through the base of the skull after gentle decalcification will allow histological examination of these glands.

3.9 Muscles, Skeleton

Bone (femur, sternum), skeletal muscle (biceps femoris), peripheral nerve (sciatic nerve), bone marrow (femur, sternum)

1. Remove the skin from one of the hind legs.
2. Transversally cut the biceps femoris with a scalpel [11, 26, 60]. Gently grasp one edge with the forceps and immerse it into the fixative.
3. Take a sample of the sciatic nerve (1 cm long) [11] (*see Note 20*). Gently grasp one edge with forceps and fix it on a cardboard.
4. Remove the distal portion of one femur, the knee joint with the proximal portion of the adjacent tibia. This will allow microscopic examination of the bone, joint tissues, and bone marrow after decalcification [11, 61, 62]. For routine bone and bone marrow microscopic examination, a sternum section should be sampled (*see Note 21*).
5. Immerse the samples in the fixative.

4 Notes

1. A longitudinal section, vertical to the direction of the hair flow, can be taken to examine the skin and mammary glands; in this case the nipple is not included if the lymph node is enclosed.
2. In case of parenteral application, one lymph node draining the application site and another distant one could be collected.
3. The extraorbital glands can be removed and embedded together with the salivary glands.
4. Swiss roll technique: This technique allows examining the whole intestine and the gut-associated lymphatic tissue (GALT) on a single section. However, these transverse sections when they are made properly will often provide a better morphology. Strip the intestines off the mesentery, opened with a pair of scissors, and gently rinse the intestine to remove the content. Then recoil the intestine—except cecum—on cotton swabs and put in the fixative. After fixation, detach the spooled intestine and proceed to embedding. This procedure is not required in routine microscopic examination of the intestines. Bear in mind that with this technique, the intestinal mucosa and the lymph follicles will often be cut tangentially. Other techniques for intestine examination are also described [32].
5. Nomenclature of hepatic lobes can differ. We recommend the anatomical terms.
6. If major bile duct is required, take a section through the left lateral lobe of the liver.

7. Optionally epididymides can be isolated from the testes, fixed, and trimmed separately.
8. In short-term studies, fixation of the testes with modified Davidson's or Bouin's solutions is highly recommended to detect less extensive early and subtle changes [63].
9. The longitudinal vertical section of the tongue covers a large part of the dorsum including the dorsal prominence. The section also includes the lingual lesser salivary glands and should be slightly lateral to the median sulcus. A transverse section of the tongue is recommended if blood sampling from the tongue is performed.
10. There are variations in position and number of parathyroids in rodents. In the rat, there is one pair of parathyroids, with a variable position but usually on the anterior lateral aspect of the thyroid lobes. In the mouse, there are usually two parathyroids (sometimes more than two), situated bilaterally just under the capsule near the dorsolateral border of each thyroid lobe. They are rarely at the same level and may be deeply embedded in the thyroid tissue.
11. Nomenclature of lung lobes can differ. We have elected to use the anatomical terms that we recommend: right cranial, right middle, right caudal lobe, accessory lobe, and left lobe.
12. Alternative procedure for the lung in oral studies in the rat: right lobes embedded ventral surface down and in the mouse: whole lung embedded, ventral surface down.
13. The optimal way to fix the central nervous system is to perfuse it *in situ* while the animal is deeply anesthetized. The procedure is as follows: anesthetize the animal (for example with intraperitoneal injection of Nembutal working solution –1.6 mL stock solution with 8.4 mL PBS, 0.1 mL/10 g body weight, or use deep inhalational anesthesia like isoflurane). Then, pin the mouse on a dissection board ventral side up. Trim back the skin from the thorax to the mandible. Open the thorax following the necropsy protocol (herein described). If blood is needed, collect it by cardiac puncture at this time. With small scissors, cut the right auricle [64]. Blood will start to flow from the heart. Insert a 23-gauge needle within the left ventricle connected to either a syringe or a peristaltic pump. First perfuse about 15 mL of PBS with steady pressure, until the blood that comes out from the right auricle becomes clear. The liver (and other organs) would normally go pale very quickly. The lungs should not bulge; if they do, your syringe has perforated the interventricular septum. Then perfuse about 20–25 mL of formalin or 4% paraformaldehyde in the same way. If fixation is successful, the body will stiffen from the tip of the tail to the tip of the nose. Proceed as usual for tissue collection.

14. Alternatively remove the vertebral bodies with the spinal cord.
15. The utility of brain weight rests in the ability to calculate organ-to-brain weight ratios which is helpful when terminal body weights are affected or to normalize organ weight data.
16. In order to avoid artifact vacuolation in the white matter, do not store specimens from nervous tissue in alcohol.
17. The pituitary gland can be trimmed *in situ* as transverse section of skull. This procedure is not recommended.
18. Each eye can be removed from the socket together with the optic nerve and the Harderian gland after fixation of the head.
19. For long-term studies, formalin fixation of the eyes is generally sufficient. For other study types, fixation in Davidson's fixative is recommended to avoid detachment of the retina.
20. Alternatively the skeletal muscle and sciatic nerve can be sampled together. In this case, the gracilis, adductor, semimembranosus, and semitendinosus muscles are removed from the medial aspect of the thigh to get access to the sciatic nerve running along the medial surface of the biceps femoris muscle. After fixation, transverse and longitudinal sections are prepared.
21. The bone marrow is generally examined concurrently with the bone tissue after decalcification. On this specimen, it is possible to evaluate the cellularity, number of megakaryocytes, and stromal compartment. If evaluation of the iron content and more precise cytology are needed, examination of a bone marrow smear of a core sample from the femur may be useful. This method requires training to obtain satisfactory results. Prepare bone marrow smears as fresh as possible to avoid blood clotting. Cut off the proximal and distal epiphyses off with scissors. Then blew air from one end into the marrow cavity and collect the marrow cast onto a glass slide. The smear is prepared conventionally with a cover glass. A smear of adequate quality contains grossly visible particles. Alternatively, aspiration with a pipette containing anticoagulated serum or a small paintbrush or a cotton bud from the longitudinally opened femur can also be performed. (This procedure implies that the contralateral femur, knee joint, and proximal tibia should be sampled.)

References

1. Olds RJ, Olds JR (1979) A color atlas of the rat-dissection guide. Wolfe Medical Publications Ltd, London
2. Feldman DB, Seely JC (1988) Necropsy guide: rodents & the rabbit. CRC, Boca Raton
3. Walker WF Jr, Homberger DG (1998) Anatomy and dissection of the rat. W.H. Freeman and Company, New York
4. Bono CD, Elwell MR, Rogers K (2000) Necropsy techniques with standard collection and trimming of tissues. In: Krinke GJ (ed) The laboratory rat. Academic, San Diego, pp 569–600
5. Relyea MJ, Miller J, Boggess D, Sundberg JP (2000) Necropsy methods for laboratory mice: biological characterization of a new

- mutation. In: Sundberg JP (ed) *Systematic approach of Mouse mutations*. CRC, Boca Raton, pp 57–89
6. EULEP, European Late Effects Project. Covelli's necropsy protocol & pictures. http://eulep.pdn.cam.ac.uk/Necropsy_of_the_Mouse/printable.php
 7. Cook M (1965) *Anatomy of the laboratory mouse*, Academic (Web version). <http://www.informatics.jax.org/cookbook/>
 8. Krinke GJ (ed) (2000) *The laboratory rat*. Academic, San Diego
 9. Ruehl-Fehlert C, Kittel B, Morawietz G, Deslex P, Keenan C, Mahrt CR, Nolte T, Robinson M, Stuart BP, Deschl U (2003) Revised guides for organ sampling and trimming in rats and mice—part 1. *Exp Toxicol Pathol* 55:91–106
 10. Kittel B, Ruehl-Fehlert C, Morawietz G, Klapwijk J, Elwell MR, Lenz B, O'Sullivan G, Roth DR, Wadsworth PF (2004) Revised guides for organ sampling and trimming in rats and mice—part 2. *Exp Toxicol Pathol* 55:413–431
 11. Morawietz G, Ruehl-Fehlert C, Kittel B, Bube A, Keane K, Halm S, Heuser A, Hellmann J (2004) Revised guides for organ sampling and trimming in rats and mice—part 3. *Exp Toxicol Pathol* 55:433–449
 12. Formaldehyde: health-based recommended occupational exposure limit. Dutch Expert Committee on occupational standards (DECOS): Health Council of The Netherlands (Gezondheidsraad) vol. 02 osh (2003) 124
 13. Woods AE, Ellis RC (1994) *Laboratory histopathology, a complete reference*, vols I and II. Churchill Livingstone, Edinburgh
 14. Fox JG, Cohen BJ, Loew FM (eds) (1984) *Laboratory animal medicine*. Academic, Orlando
 15. Bush RK, Stave GM (2003) Laboratory animal allergy: an update. *ILAR J* 44(1):28–51
 16. Figler N (2004) Laboratory animal allergies: overview of causation and prevention. *Lab Anim* 33(10):25–27
 17. Sellers RS, Morton D, Michael B, Roome N, Johnson JK, Yano BL, Perry R, Schafer K (2007) Society of toxicologic pathology position paper: organ weight recommendations for toxicology studies. *Toxicol Pathol* 35(5):751–755
 18. Leblanc B (2000) Pathology and tissue sampling protocols for Rodent carcinogenicity studies, time for revision. *Toxicol Pathol* 28:628–633
 19. Bregman CL, Adler RR, Morton DG, Regan KS, Yano BL (2003) Recommended tissue list for histopathologic examination in repeat-dose toxicity and carcinogenicity studies: a proposal of the Society of Toxicologic Pathology (STP). *Toxicol Pathol* 31(2):252–253
 20. Russo IH, Tewari M, Russo J (1989) Morphology and development of the rat mammary gland. In: Jones TC, Mohr U, Hunt RD (eds) *Monographs on pathology of laboratory animals. Integument and mammary glands*. Springer, Berlin, pp 233–252
 21. Boorman GA, Wilson JT, Van Zwieten MJ, Wilson JT, Eustis SL (1990) Mammary gland. In: Boorman GA, Eustis SL, Elwell MR, Montgomery CA, MacKenzie WF (eds) *Pathology of the Fischer rat. Reference and atlas*. Academic, San Diego, pp 295–313
 22. Van den Broeck W, Derore A, Simoens P (2006) Anatomy and nomenclature of murine lymph nodes: descriptive study and nomenclature standardization in BALB/cAnNCrI mice. *J Immunol Methods* 312(1–2):12–19
 23. Hebel R, Stromberg MW (1986) *Anatomy and embryology of the laboratory rat*. BioMed Verlag, Worthsee
 24. Botts S, Jokinen M, Gaillard ET, Elwell MR, Mann PC (1999) Salivary, Harderian, and lacrimal glands. In: Maronpot RR (ed) *Pathology of the mouse*. Cache River Press, Boca Raton, pp 49–79
 25. Dijkstra CD, Veerman AJP (1990) Spleen. Structure and function. Normal anatomy, histology, ultrastructure, rat. In: Jones TC, Mohr U, Hunt RD, Ward JM, Burek JD (eds) *Monographs on pathology of laboratory animals. Hemopoietic system*. Springer, Berlin, pp 185–193
 26. Popesko P, Rajtova V, Horak J (1992) *A colour atlas of the anatomy of small laboratory animals. Vol 2. Rat, mouse, golden hamster*. Wolfe Publishing, Bratislava, p 89
 27. Brown HR, Hardisty JF (1990) Oral cavity, esophagus and stomach. In: Boorman GA, Eustis SL, Elwell MR, Montgomery CA, MacKenzie WF (eds) *Pathology of the Fischer rat. Reference and atlas*. Academic, San Diego, pp 9–30
 28. Matsukura N, Asano G (1997) Anatomy, histology, ultrastructure, stomach, rat. In: Jones TC, Popp JA, Mohr U (eds) *Monographs on pathology of laboratory animals. Digestive system*, 2nd edn. Springer, Berlin, pp 343–350
 29. Elwell MR, McConnell EE (1990) Small and large intestine. In: Boorman GA, Eustis SL, Elwell MR, Montgomery CA, MacKenzie WF (eds) *Pathology of the Fischer rat. Reference and atlas*. Academic, San Diego, pp 43–61
 30. Moolenbeek C, Ruitenber EJ (1981) The “Swiss roll”: a simple technique for histological

- studies of the Rodent intestine. *Lab Anim* 15:57–59
31. Soul NW (1987) Gut rolls: a better technique for GI tumor assessment. *Toxicol Pathol* 15:374
 32. Williams JM, Duckworth CA, Vowell K, Burkitt MD, Pritchard DM (2016) Intestinal preparation techniques for histological analysis in the mouse. *Curr Protoc Mouse Biol* 6:148–168
 33. Paget EG, Thomson R (1979) Standard operating procedures in pathology. MTP Press, Lancaster, pp 134–139
 34. Nyska A, Maronpot RR (1999) Adrenal Gland. In: Maronpot RR, Boorman GA, Gaul BW (eds) *Pathology of the mouse. Reference and atlas*. Cache River Press, Vienna, pp 509–536
 35. Liebelt AG (1998) Unique features of anatomy, histology and ultrastructure, kidney, mouse. In: Jones TC, Hard GC, Mohr U (eds) *Monographs on pathology of laboratory animals. Urinary system*, 2nd edn. Springer, Berlin, pp 37–57
 36. Khan KNM, Alden CL (2002) Kidney. In: Haschek WM, Rousseaux CG, Wallig MA (eds) *Handbook of toxicologic pathology*, vol. 2, 2nd edn. Academic, San Diego, pp 255–336
 37. Cohen SM, Wanibuchi H, Fukushima S (2002) Lower urinary tract. In: Haschek WM, Rousseaux CG, Wallig MA (eds) *Handbook of toxicologic pathology*, vol. 2, 2nd edn. Academic, San Diego, pp 337–362
 38. Ferm VH (1987) Embryology and comparative anatomy, Rodent reproductive tract. In: Jones TC, Mohr U, Hunt RD (eds) *Monographs on pathology of laboratory animals. Genital system*. Springer, Berlin, pp 3–7
 39. Creasy DM, Foster PMD (2001) Male reproductive system. In: Haschek WM, Rousseaux CG, Wallig MA (eds) *Handbook of toxicologic pathology*, vol. 2, 2nd edn. Academic, San Diego, pp 785–846
 40. Lanning LL, Creasy DM, Chapin RE, Mann PC, Barlow NJ, Regan KS, Goodman DG (2002) Recommended approaches for the evaluation of testicular and epididymal toxicity. *Toxicol Pathol* 30:507–520
 41. Boorman GA, Chapin RE, Mitsumori K (1990) Testis and epididymis. In: Boorman GA, Eustis SL, Elwell MR, Montgomery CA, MacKenzie WF (eds) *Pathology of the Fischer rat. Reference and atlas*. Academic, San Diego, pp 405–418
 42. Lee CH, Holland JM (1987) Anatomy, histology, and ultrastructure (correlation with function), prostate, rat. In: Jones TC, Mohr U, Hunt RD (eds) *Monographs on pathology of laboratory animals. Genital system*. Springer, Berlin, pp 239–251
 43. Boorman GA, Elwell MR, Mitsumori K (1990) Male accessory sex glands, penis, and scrotum. In: Boorman GA, Eustis SL, Elwell MR, Montgomery CA, MacKenzie WF (eds) *Pathology of the Fischer rat. Reference and atlas*. Academic, San Diego, pp 419–428
 44. Heindel JJ, Chapin RE (eds) (1993) *Methods in reproductive toxicology: female reproductive toxicology*, vol 3B. Academic, Orlando
 45. Yuan YD, Foley GL (2002) Female reproductive system. In: Haschek WM, Rousseaux CG, Wallig MA (eds) *Handbook of toxicologic pathology*, vol. 2, 2nd edn. Academic, San Diego, pp 847–894
 46. Piper RC (1981) Morphological evaluation of the heart in toxicologic studies. In: Balazs T (ed) *Cardiac toxicology*, vol 3. CRC, Boca Raton, pp 111–136
 47. Van Vleet JF, Ferrans VJ, Herman E (2002) Cardiovascular and skeletal muscle system. In: Haschek WM, Rousseaux CG, Wallig MA (eds) *Handbook of toxicologic pathology*, vol 2, 2nd edn. Academic, San Diego, pp 363–455
 48. Dijkstra CD, Sminia T (1990) Thymus. Structure and function. Normal anatomy, histology, immunohistology, ultrastructure, rat. In: Jones TC, Mohr U, Hunt RD, Ward JM, Burek JD (eds) *Monographs on pathology of laboratory animals. Hemopoietic system*. Springer, Berlin, pp 249–256
 49. Kittel B, Ernst H, Kamino K (1996) Anatomy, histology and ultrastructure, parathyroid, mouse. In: Jones TC, Capen CC, Mohr U (eds) *Monographs on pathology of laboratory animals. Endocrine system*, 2nd edn. Springer, Berlin, pp 328–329
 50. Kittel B, Ernst H, Kamino K (1996) Anatomy, histology and ultrastructure, parathyroid, rat. In: Jones TC, Capen CC, Mohr U (eds) *Monographs on pathology of laboratory animals. Endocrine system*, 2nd edn. Springer, Berlin, pp 330–332
 51. Gopinath C, Prentice DE, Lewis DJ (1987) The respiratory system. In: *Atlas of experimental toxicological pathology*. MTP Press, Lancaster, pp 22–42
 52. Plopper CG (1996) Structure and function of the lung. In: Jones TC, Dungworth DL, Mohr U (eds) *Monographs on pathology of laboratory animals. Respiratory system*, 2nd edn. Springer, Berlin, pp 135–150
 53. Cassella JP, Hay J, Lawson SJ (1997) The rat nervous system. Wiley, Chichester
 54. Dorman DC, Brennehan KA, Bolon B (2002) Nervous system. In: Haschek WM, Rousseaux

- CG, Wallig MA (eds) Handbook of toxicologic pathology, vol 2, 2nd edn. Academic, San Diego, pp 509–537
55. Mahler JF, Elwell MR (1999) Pituitary Gland. In: Maronpot RR, Boorman GA, Gaul BW (eds) Pathology of the mouse. Reference and atlas. Cache River Press, Vienna, pp 491–507
56. Whiteley HE, Peiffer RL (2002) The eye. In: Haschek WM, Rousseaux CG, Wallig MA (eds) Handbook of toxicologic pathology, vol 2, 2nd edn. Academic, San Diego, pp 539–584
57. Popp JA, Monteiro-Riviere NA (1985) Macroscopic, microscopic, and ultrastructural anatomy of the nasal cavity, rat. In: Jones TC, Dungworth DL, Mohr U (eds) Monographs on pathology of laboratory animals. Respiratory system, 2nd edn. Springer, Berlin, pp 3–10
58. Boorman GA, Morgan KT, Uriah LC (1990) Nose, larynx and trachea. In: Boorman GA, Eustis SL, Elwell MR, Montgomery CA, MacKenzie WF (eds) Pathology of the Fischer rat. Reference and atlas. Academic, San Diego, pp 315–337
59. Copeland-Haines D, Eustis SL (1990) Specialized sebaceous glands. In: Boorman GA, Eustis SL, Elwell MR, Montgomery CA, MacKenzie WF (eds) Pathology of the Fischer rat. Reference and atlas. Academic, San Diego, pp 279–294
60. MCGavin MD (1991) Procedures for morphological studies of skeletal muscle, rat, mouse, and hamster. In: Jones TC, Mohr U, Hunt RD (eds) Monographs on pathology of laboratory animals. Cardiovascular and musculoskeletal systems. Springer, Berlin, pp 101–108
61. Valli VE, Villeneuve DC, Reed B et al (1990) Evaluation of blood and bone marrow, rat. In: Jones TC, Mohr U, Hunt RD, Ward JM, Burek JD (eds) Monographs on pathology of laboratory animals. Hemopoietic system. Springer, Berlin, pp 9–26
62. Woodard JC, Burkhardt JE, Lee W (2002) Bones and joints. In: Haschek WM, Rousseaux CG, Wallig MA (eds) Handbook of toxicologic pathology, vol 2, 2nd edn. Academic, San Diego, pp 457–508
63. Latendresse JR, Warbritton AR, Jonassen H, Creasy DM (2002) Fixation of testes and eyes using a modified Davidson's fluid: comparison with Bouin's fluid and conventional Davidson's fluid. *Toxicol Pathol* 30:524–533
64. Hoff J (2000) Methods of blood collection. *J Lab Anim* 29(10):47–53

Chapter 4

Tissue Sampling and Processing for Histopathology Evaluation

Mohamed Slaoui, Anne-Laure Bauchet, and Laurence Fiette

Abstract

Histological procedures aim at providing good-quality sections that can be used for a light microscopic evaluation of tissue. These are applicable to identify either spontaneous or diseases-induced changes. Routinely, tissues are fixed with neutral formalin 10%, embedded in paraffin, and manually sectioned with a microtome to obtain 4–5 μm thick paraffin sections. Dewaxed sections are then stained with HE&S (hematoxylin-eosin and saffron) or can be used for other purposes (special stains, immunohistochemistry, in situ hybridization, etc.). During this processing, many steps and procedures are critical to ensure standard and interpretable sections. This chapter provides key recommendations to efficiently achieve this objective.

Key words Histology, Embedding, Sectioning, Staining, Histological slides, Anatomic pathology, Microscopy, Necropsy

1 Introduction

Histopathology is the study of diseased tissue under the microscope. It is an important investigative medical tool that is based on the study of human or animal histology (also called microscopic anatomy). It is performed by examining a thin tissue section under light microscope. Histotechnique consists of a number of procedures that allow visualization of tissue and cell microscopic features and recognize specific microscopic structural changes of diseases.

Observation of tissues under a light microscope is an old concern for science and medicine. The earliest evidence of magnifying glass forming a magnified image dates back to 1021 when the physicist Ibn al-Haytham (965–1039) published the “Book of Optics.” The name “microscope” was crafted by the German botanist Johann Faber (1574–1629). The original light microscope used by Anton Van Leeuwenhoek’s (1632–1723) was a small, single convex lens mounted on a plate. Nowadays sophisticated light

microscopes use multiple lenses and are widely used in research and in diagnostic.

Most histology techniques were described in the nineteenth century. They mostly use physicochemical reactions with tissue components that allow preservation, cutting, or staining of tissues. It was only in the 1970s that the processing of tissue became partially automated, but some critical steps like embedding and sectioning are still performed manually. These steps are delicate and time and resource intensive.

Histopathology evaluation basically compares diseased or experimentally altered tissues with matching samples from healthy or control counterparts. Therefore, rigorous standardization of every histology process is very important (i.e., specimen sampling, trimming, embedding, sectioning, staining).

The purpose of this chapter is to describe routine histological processing steps used for histopathological evaluation and, in particular, paraffin embedding, sectioning, and staining. Several other techniques are available and could be performed on tissues for specific purposes (special stains, immunohistochemistry, in situ hybridization, etc.) [1, 2]. Tissues can also be frozen or embedded in plastic, but these latter techniques are beyond the scope of this chapter.

2 Materials

2.1 Fixation

1. Fixative solution (usually commercially available formalin).
2. Phosphate buffer.
3. Rubber or gloves (*see Note 1*).
4. Protective clothing.
5. Eyeglasses and mask.
6. Fume hood.
7. Containers with appropriate lids (volume is commensurate with sample size; large-neck plastic containers are preferable).
8. Labels and permanent ink.

2.2 Trimming

1. Fume hood.
2. Rubber or gloves (*see Note 1*).
3. Protective clothing.
4. Eyeglasses and mask.
5. Dissecting board (plastic boards are preferred as they can be easily cleaned and autoclaved).
6. Blunt-ended forceps (serrated forceps may damage small animal tissues).

7. Scalpel blades and handle.
8. Plastic bags, paper towels.
9. Containers for histological specimens, cassettes, and permanent labels. Containers and cassettes should be correctly labeled before starting tissue trimming.

2.3 Pre-embedding

1. Disposable plastic cassettes for histology (with appropriate lids). For small samples, disposable plastic cassettes for histology with subdivision (Microsette®).
2. Foam pads (31 × 25 × 3 mm) can be used to immobilize tissue samples inside the cassettes.
3. Commercial absolute ethyl alcohol and 96% ethanol solution.
4. 90 and 70% ethanol solutions.
5. Paraffin solvent/clearing agent: xylene or substitute (e.g., Histosol®, Neoclear®).
6. Paraffin wax for histology, melting point 56–57 °C (as an example: Paraplast® Tissue Embedding Media).
7. Automated vacuum tissue processor.

2.4 Embedding

1. Tissue embedding station (a machine that integrates melted paraffin dispensers, heated and cooled plates).
2. Paraffin wax for histology, melting point 56–57 °C (e.g., Paraplast® Tissue Embedding Media).
3. Histology stainless steel embedding molds or disposable plastic base molds. These are available in different sizes (10 × 10 × 5 mm; 15 × 15 × 5 mm; 24 × 24 × 5 mm; 24 × 30 × 5 mm).
4. Small forceps.

2.5 Sectioning

1. Rotary microtome.
2. Tissue water bath with a thermometer: Alternatively a thermostatic warm plate can be used.
3. Disposable microtome blades (for routine paraffin sections use wedge-shaped blades).
4. Sharps container to discard used blades.
5. Fine paintbrushes to remove paraffin debris.
6. Forceps to handle the ribbons of paraffin sections.
7. Clean standard 75 × 25 mm microscope glass slides (other dimension microscope glass slides are commercially available).
8. Laboratory oven (set at 37 °C).
9. Coated glass slides (e.g., Superfrost® or Superfrost Plus®): This is especially recommended when slides are used for immunohistochemistry.

10. 0.1% Gelatin in water (1 g of gelatin in 1 L of distilled water): This should not be used with Superfrost® or Superfrost Plus® slides and should be reserved for immunohistochemistry sections.
11. Cut-resistant gloves.

2.6 Staining and Cover Slipping

1. Harris hematoxylin (commercial solution, ready to use).
2. Eosin Y solution.
3. Hydrochloric acid 37%.
4. Absolute ethanol.
5. Ethanol 96%.
6. Clearing agent (xylene or substitute, e.g., Histosol®, Neoclear®).
7. Staining dishes and Coplin jars suitable for staining.
8. Permanent mounting medium (e.g., Eukitt®).
9. Glass cover slips (25 × 60 mm).
10. Filter paper.
11. Ethanol solutions:
 - (a) Add 12.5 mL of water to 1 L of commercial 96% ethanol to obtain 95% ethanol.
 - (b) Add 408 mL of water to 1 L of commercial 96% ethanol to obtain 70% ethanol.

2.7 Storage of Paraffin Blocks and Slides

1. Paraffin block storage cabinets.
2. Histological slide storage cabinets.

3 Methods

3.1 Fixation

Autolysis is a combination of postmortem changes due to rupture of cell homeostasis that leads to uncontrolled water and electrolytes dynamics in and out of the cell and of alteration of enzymatic activity. These changes are favorable conditions for bacterial and fungal growth and ultimately result in complete destruction of tissue structures. To halt autolysis, tissues should be preserved in an appropriate fixative.

The process of autolysis virtually begins immediately after death. Therefore, rapid and adequate fixation after sampling is essential. This can be achieved by immersion of the tissue sample in an adequate volume of fixative solution. There are several methods of fixation including aldehydes, mercurial, alcohols, oxidizing agents, and picric acid derivatives [3] and more recently Paxgene fixative that allows better preservation of RNA if concomitant genomic analysis is required. Tissue immersion in aldehyde

(formaldehyde, paraformaldehyde, or glutaraldehyde) is the most frequently used fixation method in biomedical research. Formalin (formaldehyde) is commercially available as ready-to-use 4 or 10% neutral phosphate-buffered solutions (*see Note 2*). It is generally accepted that a volume ratio of tissue to fixative of at least 1:10 is necessary for optimal fixation. Small tissue samples are usually fixed at room temperature after 12–48 h. Larger specimen may require more fixation time as formalin slowly penetrates tissues (*see Note 3*). The duration of fixation depends also on the type of fixative: paraformaldehyde and glutaraldehyde require more time for tissue penetration. For these fixatives, a better fixation is achieved with small tissue samples kept at 4 °C.

1. Place the fixative container under a fume hood.
2. Plunge tissue samples in the fixative solution.
3. Stir gently the fixative container for a few seconds to make sure that the tissue sample does not stick to the container surface.
4. Replace cap over the container after each tissue (one container can be used for several tissue samples).
5. Add identification label on each container.

3.2 *Trimming*

After fixation, tissue samples need to be properly trimmed in order to reach the adequate size and tissue orientation. This step is also important to reach a sample size compatible with subsequent histology procedures like embedding and sectioning.

Hard tissues (like bones and teeth) must be decalcified prior to trimming.

Under a fume hood, tissues and organs are trimmed to small pieces and placed into cassettes.

The readers are highly recommended to use the excellent comprehensive papers from the RITA group [4–6] or to use the Web version [7]. Specific methods have been proposed for many organs: gut [8, 9], heart [10], male reproductive system [11–13], female reproductive system [14], or muscle [15].

3.3 *Preinclusion*

The goal of this step is to infiltrate tissue samples with paraffin and replace water content of tissue by this wax material. Paraffin is used as a supporting material prior to sectioning. Histology-grade paraffin wax has a melting point at around 56 or 57 °C, a temperature that does not alter the structures and key morphologic characteristics of tissues, thus allowing adequate microscopic evaluation by the pathologist. At room temperature, paraffin wax offers enough rigidity to allow very thin sections just a few micrometers thick (usually 4 or 5 µm).

Pre-embedding is a sequential process that consists of dehydration of tissues in increased concentrations of alcohol solutions, and then gradual replacement of alcohol by a paraffin solvent. Xylene

(or its substitutes, e.g., Histosol[®], Neoclear[®], HistoClear[®]) has the advantage to be miscible in both alcohol and paraffin. As a result, the tissue sample is dehydrated and fully infiltrated by paraffin. This step is generally automated using a variety of vacuum processors (*see Note 4*).

When using a tissue processor, the following steps should be followed:

1. Check that the baskets are clean and free of wax.
2. Do not pack the tissues too tightly to allow fluid exchange and circulation.
3. Check that the processor is free of spilt fluids and wax.
4. Check that fluid levels are above specimen containers.
5. Select the appropriate protocol and check the clock.
6. Dehydrate in a graded series of ethanol:
 - (a) Wash in 70% ethanol for 1 h.
 - (b) Wash in 95% ethanol for 1 h (two times).
 - (c) Wash in 100% ethanol for 1 h (two times).
7. Clear with a paraffin solvent (xylene) for 1 h (two times).
8. Infiltrate with paraffin for 1 h (two times).
9. Tissue samples are retrieved at the end of the processing program (automates are usually run overnight in order to start the embedding process the next morning).

The following is a list of rescue procedures that can be helpful to consider in case the pre-embedding procedure is not completed normally:

1. Recovery of tissues that have air-dried because of mechanical or electrical failure of the processor:
 - (a) Rehydrate the tissue in Sandison's solution (absolute alcohol 30 mL, formaldehyde 37% 0.5 mL, sodium carbonate 0.2 g water up to 100 mL) or Van Cleve & Ross' solution (trisodium phosphate 0.25 g in 100 mL of water).
 - (b) Immerse the tissues in one of these two solutions for 24–72 h (actually most of the tissues rehydrate and soften within 4–6 h).
 - (c) Process to dehydration and pre-embedding as usual, starting in 70% ethanol.
2. Recovery of tissues accidentally returned to fixative following wax infiltration. Discard all contaminated fluids:
 - (a) Rinse in ethanol 70% followed by ethanol 95%.
 - (b) Rinse in absolute ethanol (two to three times).

- (c) Rinse in xylene (or substitute).
 - (d) Carry out the paraffin infiltration three times, 30–60 min each.
3. Recovery of tissues accidentally returned to ethanol 70% following wax infiltration:
- (a) Discard all contaminated fluids.
 - (b) Rinse in ethanol 95%.
 - (c) Rinse in absolute ethanol (two changes).
 - (d) Rinse in xylene (or substitute).
 - (e) Carry out the paraffin infiltration two to three times, 30–60 min each.

The same steps can be used for manual tissue processing. Melt the paraffin in an oven at 60 °C in glass containers. Immerse the specimens into the melted paraffin.

3.4 Embedding

Once tissue samples are infiltrated by paraffin, they are removed from the cassettes, carefully positioned inside a base mold.

This step is critical as correct orientation of the tissue is essential for accurate microscopic evaluation. The mold is filled with melted paraffin and then immediately placed on a cooling surface. In order to trace each tissue specimen, the cassette with permanent tissue and study identification is placed on top of the base mold and incorporated in the paraffin block before cooling. In this manner, the cassette will be used as a base of the paraffin block for microtome sectioning (once the base mold is removed) (*see Note 5*).

1. Check that the different compartments of the station have the appropriate temperature. Paraffin should be liquid in the paraffin reservoir, work surface should be warm, and cool plate should be cold. Stainless steel molds should be kept warm.
2. Remove the cassettes from the last tissue processor bath (normally melted paraffin) and transfer to the warm compartment of the embedding station.
3. Transfer one cassette onto the hot plate.
4. Snap off the cassette lid and discard it.
5. Select a mold of the appropriate size. The specimen must not come into contact with the edge of the mold.
6. Transfer the mold onto the hot plate.
7. Pour melted paraffin from the paraffin dispenser.
8. Transfer the paraffin-infiltrated tissues into the mold.
9. Using heated forceps, orientate the tissue inside the mold to obtain the desired position in relation with the cutting axis, the specimen surface in contact with the base of the mold being the one that will be on the slide after sectioning.

10. Center the specimen in the mold ensuring that paraffin entirely surrounds the edge of the tissue.
11. Carefully transfer the mold onto the cool plate. Allow a few seconds to paraffin to turn white (this means that paraffin returned to solid phase). During cooling, the paraffin will shrink (up to 15% of its initial volume); this compression will be fully recovered later after sectioning.
12. Make sure that the specimen does not move during this step and still keeps its desired orientation. If not, put the mold back onto the warm work surface until the whole paraffin liquefies and then start again from **step 9**.
Immediately place the base of the original cassette on top of the mold. Incorporation of the cassette in the paraffin block before cooling allows tracing the specimen identification and uses the cassette as a holder during sectioning.
13. Carefully fill the mold with paraffin to above the upper edge of the cassette.
14. Carefully transfer the mold and cassette onto the cool plate and allow time (at least 15 min) until the paraffin has hardened.
15. Snap off the mold.
16. Bring the paraffin blocks together.
17. Store the paraffin blocks at room temperature until sectioning.

3.5 Sectioning

The objective of this step is to cut 4–5 μm thick sections from paraffin blocks. This is achieved using precision knives (microtomes). In order to obtain constant high quality and extremely thin tissue sections, disposable blades should be used and changed after a limited number of blocks or when damaged by small pieces of bone within the tissue for example.

The paraffin block is mounted on the microtome holder. Sections are cut as a ribbon and are floated on a water bath maintained at 45 °C to stretch the paraffin section. A standard microscope glass slide is placed under the selected tissue section and removed from the water bath. Tissue sections are then allowed to dry, preferably in a thermostatic laboratory oven at 37 °C.

Tissue sectioning and floating steps are delicate operations that should be performed by trained personnel wearing cut-resistant gloves.

1. Heat the tissue water bath to 45 °C and fill it with water. In order to avoid microorganism growth, the bath should be carefully cleaned every day and the water flotation bath discarded.
2. Put the paraffin blocks on a cold surface (e.g., refrigerated cold plate or ice) to harden the cut surface. Avoid prolonged cooling and very cold surfaces as they may lead to cracking in the block surface.

3. Install a disposable blade in the microtome.
4. Set angle between the blade edge bevel and the block to 2–5° (clearance angle). A correct angle should be set to avoid compression in cut sections and to reduce friction as the knife passes through the block. Angles in the above-mentioned range are recommended for paraffin sections, but the exact angle is generally found by trial and error.
5. Lock the blade in place.
6. Lock the microtome hand-wheel.
7. Trim the edges of one block with a sharp razor blade so that the upper and lower edges of the block are parallel to the edges of the knife. Otherwise a ribbon cannot be cut. Keep 2–3 mm of paraffin wax around the tissue.
8. Fit the cassette paraffin block onto the cassette holder of the microtome. Orientate the block so that its greater axis is perpendicular to the edge of the knife, and also that the edge offers the least resistance (e.g., the smallest edge will be cut first).
9. Unlock the hand-wheel.
10. Advance the block until it is in contact with the edge of the knife. Paraffin block edges must be parallel to the knife. If not, adjust the block orientation.
11. Set the section thickness around 15 μm .
12. Coarse cut (trim) the block at 15 μm until the whole surface of the embedded tissue can be cut.
13. Lock the microtome hand-wheel.
14. Return the trimmed block to cold plate for 1–2 min.
15. Set the section thickness to 4–5 μm .
16. Remove wax debris from the knife with alcohol. Avoid use of xylene to clean the paraffin debris as it often leaves an oily remnant on the knife and following sections will stick (not mentioning the xylene hazards for the operator).
17. Move to an unused area on the blade or install a new disposable blade.
18. Install the cassette paraffin block onto the cassette holder again.
19. Cut a series of paraffin sections. If sectioning is doing well, you will obtain a ribbon of serial sections.
20. Gently breathe upon the sections to eliminate static electricity, flatten the sections, and facilitate the removal of the ribbon from the blade.
21. Separate the ribbon (including 4–5 sections) from the knife edge with a paintbrush.
22. Transfer the piece of ribbon onto a glass slide coated with a drop of gelatin-water, or to the surface of the water bath.

23. Gently separate the floating sections on the water bath with pressure from the tips of forceps.
24. Collect sections on a clean glass slides. Hold the slide vertically beneath the section and lift carefully the slide up to enable tissue adherence.
25. Label slides with a histo-pen or pencil. Avoid pens with nonalcohol-resistant ink (ballpoint or felt-tipped pens).
26. Allow the slides to dry horizontally on a warm plate for 10 min to ensure that the section firmly adheres to the glass slide. Alternatively slides can be dried vertically in an oven for 20 min at 37 °C.
27. Transfer the slides (vertically placed) to a laboratory oven overnight at 37 °C.
28. Store the slides in dry boxes at room temperature. For immunohistochemistry, slides should be stored at 4 °C to minimize antigen loss.
29. Empty the water bath and wipe it with a damp cloth at the end of each day.

3.6 Staining and Mounting

Unstained paraffin sections offer very low contrast and therefore cannot be evaluated microscopically in routine histopathology. It is necessary to apply coloring reagents (mostly chemicals) to stain tissue structures. There are many histochemistry staining techniques that can be applied to examine specific tissues or cell structures. As most of these dyes are water soluble, tissue sections should be rehydrated to remove paraffin (using xylene, alcohol solutions ending in water). Hematoxylin and eosin (H&E) is the routine staining used to study histopathology changes in tissues and organs from animals in toxicity studies. Hematoxylin is a basic dye that has affinity for acid (basophilic) structures of the cell (mostly nucleic acids of the cell nucleus) and eosin is an acidic dye that binds to cytoplasmic (acidophilic or eosinophilic) structures of the cell. As a result, H&E stains nuclei in blue and cytoplasm in orange-red. A variant to this staining method is the hematoxylin-eosin and Saffron (HE&S) stain. As compared to the H&E method, HE&S stains collagen in a yellow-orange allowing a better highlight of interstitial connective tissue or fibrosis (*see Note 6*).

The following protocol describes manual H&E staining technique. It is suitable for small series of slides. This operation is usually automated in drug safety evaluation studies to allow high-throughput staining of slides.

1. Prepare the Harris hematoxylin working solution. Filter the commercial solution through filter paper to remove the metallic precipitant that forms in the solution upon standing.

2. Prepare 0.1% aqueous eosin Y working solution. Dissolve 1 g of eosin Y in 1 L of deionized water. Add four drops of HCl to obtain a pH between 4 and 5.
3. Add a thymol crystal to prevent mold growth.
4. Label and date the solutions. Aqueous eosin solution is stable at room temperature for at least 2 months.
5. Prepare the differentiation solution (acid alcohol). Add 1 mL of 37% HCl to 100 mL of 70% ethanol.
6. Dewax the paraffin sections in xylene 2 × 5 min each.
7. Rehydrate in 100% ethanol 2 × 5 min each.
8. Rehydrate in 95% ethanol 2 × 5 min each.
9. Wash in running tap water for 3 min.
10. Stain for 3–5 min in Harris hematoxylin.
11. Wash in running tap water for 3 min.
12. Decolorize briefly in acid alcohol for 2 s.
13. Wash and blue the sections in running tap water for 3 min.
14. Stain for 2–5 min in 0.1% aqueous eosin Y.
15. Rinse in tap water for 30 s.
16. Dehydrate in 95% ethanol two times for 2 min each.
17. Dehydrate in 100% ethanol two times for 2 min each.
18. Clear sections in clearing agent two times for 2 min each.
19. The slides may remain in clean clearing agent until cover slipping.
20. The nuclei will be stained in blue, and the cytoplasm and other tissue components in pink orange. Decreased staining intensity of the sections (after approximately 500 slides) indicates that the staining solutions should be renewed.

After staining, a very thin glass (or cover slip) should be placed over the tissue section in order to protect it and to enhance the optical evaluation of the tissue. This also allows tissue section storage for several years. Cover slipping process consists of gluing the cover slip glass over the tissue section on the microscope slide glass. The mounting medium is usually insoluble in water. Therefore, the tissue should be dehydrated again using solutions of increasing concentrations of alcohol and xylene.

The following protocol describes manual cover slip mounting technique. It is suitable for small series of slides.

1. Wipe the surface under the slide while keeping the tissue section covered with the clearing agent.
2. Apply two or three drops of the mounting medium (e.g., Eukitt®).

3. Place a cover slip on the slide and avoid the formation of bubbles. Press gently with forceps to remove any bubble.
4. Dry the slides overnight at room temperature on a flat surface within the fume hood.

To allow high-throughput slide preparation, this operation is usually automated in drug safety evaluation studies. These automated machines are commercially available from many suppliers.

3.7 Storage of Paraffin Blocks and Slides

1. After sectioning, store paraffin block at room temperature.
2. Store stained slides in appropriate boxes (avoid prolonged exposure to light).

4 Notes

1. Vinyl gloves are preferable as latex gloves may be allergenic.
2. Formaldehyde is an eye, nose, respiratory tract, and skin irritant. It is a strong skin sensitizer and can cause cancer in humans [16]. Therefore, it should not be handled without gloves, or outside a fume hood. As a result, a variety of alternative fixatives, mostly compound fixatives containing chemicals with differing fixation characteristics, have been investigated [17]. However, as of today, there is no unique formalin successor.
3. The best fixation is achieved by intracardial perfusion of the body with formaldehyde, paraformaldehyde, or glutaraldehyde. However, this technique needs specific training and is time consuming. It is therefore only used on a case-by-case basis.
4. The following is a nonexhaustive list of hazards associated with some of the above-mentioned chemicals used during pre-embedding [16]:
 - **Absolute ethanol** is inflammable, and irritant to the eye. It should never be handled close to a naked flame or heat. The vapor is heavier than air and can travel a considerable distance to a source of ignition.
 - **Paraffin** is not hazardous for health when pure, but wax additives can be potential carcinogen as, e.g., dimethyl sulfoxide (DMSO). Molten wax should not be inhaled, as it produces small lipid droplets that can lead to lipid pneumonia. Prefer paraffin wax without DMSO.
 - **Xylene** is an aromatic compound that contains benzene. It is moderately inflammable, a mild eye and mucous membrane irritant, and a primary skin irritant that may causes dermatitis. It might cause central nervous system depression.

Overexposure can lead to respiratory failure. Avoid contact with skin. Xylene substitutes are preferred, but if hazards of xylene are well documented, its substitutes have not been so thoroughly evaluated.

5. Alternative techniques of paraffin embedding exist; they use plastic or resin polymers that should be considered when paraffin embedding is not appropriate (i.e., methyl methacrylate to section nondecalcified bone, Epon to obtain very thin sections in the range of 1 μm or for electron microscopy). These embedding media require specific reagents and equipment. These techniques will not be described in this chapter as they are not used in routine histology in the context of drug safety evaluation.
6. The following is a nonexhaustive list of hazards associated with some of the chemicals used during staining/cover slip mounting [16]:
 - **Harris hematoxylin:** Irritant to eyes, skin, and mucous membranes. Toxic by inhalation and ingestion. Handle with care.
 - **Eosin Y:** Bromofluorescein dye and other dyes of this group are highly toxic. They are skin and eye irritant and reported as being carcinogens.
 - **Mounting medium:** This is usually xylene or a xylene-based solvent. See xylene.

References

1. Paget EG, Thompson R (1979) Standard operating procedures. In: Pathology. MTP Press, Lancaster, pp 134–139
2. Makki JS (2016) Diagnostic implication and clinical relevance of ancillary techniques in clinical pathology practice. *Clin Med Insights Pathol* 9:5–11
3. Leong AS-Y (1994) Fixation and fixatives. In: Woods AE, Ellis RC (eds) *Laboratory histopathology, a complete reference, vol 1*. Churchill Livingstone, New York, pp 4.1-1–4.2-26
4. Ruehl-Fehlert C, Kittel B, Morawietz G, Deslex P, Keenan C, Mahrt CR, Nolte T, Robinson M, Stuart BP, Deschl U (2003) Revised guides for organ sampling and trimming in rats and mice—part 1. *Exp Toxicol Pathol* 55:91–106
5. Kittel B, Ruehl-Fehlert C, Morawietz G, Klapwijk J, Elwell MR, Lenz B, O’Sullivan MG, Roth DR, Wadsworth PF (2004) Revised guides for organ sampling and trimming in rats and mice—part 2. *Exp Toxicol Pathol* 55:413–431
6. Morawietz G, Ruehl-Fehlert C, Kittel B, Bube A, Keane K, Halm S, Heuser A, Hellman J (2004) Revised guides for organ sampling and trimming in rats and mice—part 3. *Exp Toxicol Pathol* 55:433–449
7. Revised guides for organ sampling and trimming in rats and mice (2003) <http://reni.item.fraunhofer.de/reni/trimming/>
8. Soul NW (1987) Gut rolls: a better technique for GI tumor assessment. *Toxicol Pathol* 15:374
9. Moolenbeek C, Ruitenber EJ (1981) The “Swiss roll”: a simple technique for histological studies of the rodent intestine. *Lab Anim* 15:57–59
10. Piper RC (1981) Morphological evaluation of the heart in toxicologic studies. In: Balazs T (ed) *Cardiac toxicology, vol 3*. CRC, Boca Raton, pp 111–136
11. Latendresse JR, Warbriation AR, Jonassen H, Creasy DM (2002) Fixation of testes and eyes using a modified Davidson’s fluid: comparison

- with Bouin's fluid and conventional Davidson's fluid. *Toxicol Pathol* 30:524–533
12. Lanning LL, Creasy DM, Chapin RE, Mann PC, Barlow NJ, Regan KS, Goodman DG (2002) Recommended approaches for the evaluation of testicular and epididymal toxicity. *Toxicol Pathol* 30:507–520
 13. Creasy DM, Foster PMD (2002) Male reproductive system. In: Haschek WM, Rousseaux CG, Wallig MA (eds) *Handbook of toxicologic pathology*, vol 2. Academic, San Diego, pp 785–846
 14. Heindel JJ, Chapin RE (1993) Female reproductive toxicology. In: Heindel JJ, Chapin RE (eds) *Methods in reproductive toxicology*, vol 3B. Academic, Orlando
 15. McGavin MD (1991) Procedures for morphological studies of skeletal muscle, rat, mouse, and hamster. In: Jones TC, Mohr U, Hunt RD (eds) *Cardiovascular and musculoskeletal systems, monographs on pathology of laboratory animals*. Springer, New York, pp 101–108
 16. <http://www2.hazard.com/msds/index.php> (safety data)
 17. Titford M, Horenstein M (2005) Histomorphologic assessment of formalin substitute fixatives for diagnostic surgical pathology. *Arch Pathol Lab Med* 129(4):502–506

Chapter 5

Principles and Methods of Immunohistochemistry

José A. Ramos-Vara

Abstract

Immunohistochemical techniques detect antigens in tissue sections by means of immunological and chemical reactions. This technique is highly sensitive and specific and can detect a wide variety of antigens in multiple animal species. This chapter reviews common immunohistochemical methods used in the characterization of normal and pathologic tissue and the reagents used. Pretreatments such as blocking steps for endogenous activities and antigen retrieval are included. Standard procedures on formalin-fixed, paraffin-embedded tissues as well as method standardization for new antibodies and troubleshooting are emphasized.

Key words Antigen retrieval, Detection methods, Fixation, Immunohistochemistry, Standardization, Troubleshooting

1 Introduction

Immunohistochemistry (IHC) is the detection of antigens in tissue sections by means of specific antibodies. The unique advantage of IHC over other protein detection methods is the ability to correlate the presence of an antigen with its location in a tissue or cell. This is very important for the study of cell function in normal and pathological tissues. Since its introduction six decades ago, IHC has been applied extensively to multiple areas of biology including cell function and characterization of lesions [1]. As its name indicates, IHC bridges three major disciplines: immunology, histology, and chemistry. This chapter focuses on materials and methods used in immunohistochemistry. In addition, a strategy for standardization of immunohistochemical tests and troubleshooting in immunohistochemistry is discussed.

2 Materials

2.1 Buffers, Diluents, and Antigen Retrieval Solutions

1. Rinse buffer: Corresponds to Tris buffer normal saline (TBS) (0.05 M, 0.15 M NaCl, 0.05% Tween 20, pH 7.6). Use TBS concentrate $\times 20$ (Biocare, Concord, CA) and mix 50 mL of concentrate buffer and 950 mL of distilled water (working buffer) (*see* **Notes 1** and **2**).
2. Antibody diluent, Renoir Red (Biocare).
3. Background reducing solution: Background Punisher (Biocare).
4. Target retrieval solution, Diva Decloaker, concentrate $\times 10$, Tris, pH 6 (Biocare): Add 900 mL of distilled water to 100 mL of target retrieval solution to prepare a working dilution.
5. Target retrieval solution, EDTA Decloaker, concentrate $\times 5$, pH 8.5 (Biocare). To prepare a working dilution, add 800 mL of distilled water to 200 mL target retrieval solution.
6. Target retrieval solution, Borg Decloaker, Tris, pH 9.5 (Biocare), ready to use (*see* **Note 3**).
7. Proteinase K (Dako).

2.2 Substrates, Chromogens, and Counterstain Solutions

1. Peroxidase chromogen kit, Betazoid DAB (Biocare): This substrate is intended for peroxidase-based immunohistochemical methods (*see* **Notes 4** and **5**).
2. Bajoran, purple chromogen kit for peroxidase (Biocare).
3. Mayer's Hematoxylin from Dako (*see* **Note 6**).

2.3 Endogenous Activity-Blocking Solutions

1. Peroxidase blocking reagent, Peroxidized 1 (Biocare) (*see* **Notes 7** and **8**).
2. Protein block, serum free from Biocare (Background Sniper) (*see* **Note 9**).
3. Biotin blocking system from Biocare (*see* **Note 10**).

2.4 Silanized Slides (Dako)

Use silanized (positive-charged) slides to avoid tissue detachment.

3 Methods

3.1 Tissue Fixation and Processing

Tissue fixation will depend in some ways on the type of antigen to be detected (e.g., some antigens will become undetectable following fixation in formaldehyde and tissues have to be frozen or fixed in a different fixative). Regardless of the antigen examined, collect and process samples before tissues undergo autolysis. Formaldehyde is the gold standard fixative for routine histology and immunohistochemistry. Formalin fixation is a progressive

time- and temperature-dependent process. Overfixation has been considered deleterious for antigen detection. However, current antigen retrieval methods (*see* Subheading 3.2) are able to retrieve antigenic loss due to fixation, and overfixation is not a critical issue for many antigens. There is no universal optimal standard fixation time. Minimal fixation of 12–24 h is recommended (*see* **Note 11**).

1. Samples need to be <4 mm thick.
2. Immerse immediately the sample to be fixed in 10% neutral buffered formalin for 1–2 days.
3. Trim samples.
4. Embed samples in paraffin.
5. Cut 3–5 μm thick sections with a microtome.
6. Place sections on silanized slides (*see* **Note 12**).
7. Dry sections in a 55–60 °C oven for 30–60 min (*see* **Note 13**).
8. Stain the sections after deparaffinizing.

3.2 Antigen Retrieval Methods

Fixation with cross-linking agents modifies the tertiary and quaternary structure of many antigens making them undetectable by antibodies. Antigen retrieval (AR) methods are intended to retrieve the loss of antigenicity, theoretically returning proteins to their prefixation conformation. Approximately 85% of antigens fixed in formalin require some type of AR to optimize the immunoreactions [2]. The need for AR depends not only on the antigen examined but also on the antibody used.

3.2.1 Detergents in Antigen Retrieval

Detergents solubilize membrane proteins by mimicking the lipid-bilayer environment, forming mixed micelles consisting of lipids and detergents and detergent micelles containing proteins (usually one protein molecule per micelle). The more common detergents used in IHC are of nonionic type (e.g., Triton R-X 100, Tween 20, saponin, BRIJR, and Nonidet P40). These are usually added to rinsing buffers (e.g., 0.05% for Tween 20).

3.2.2 Enzymatic Antigen Retrieval

Protease-induced epitope retrieval (PIER) was the most commonly used antigen retrieval method before the advent of heat-based antigen retrieval methods. Many enzymes have been used for this purpose with the most common being proteinase K because it is active at room temperature (*see* **Note 14**). The mechanism of PIER is most likely digestion of protein cross-linkages introduced during formalin fixation, but this cleavage is nonspecific and some antigens may be negatively affected by this treatment. The effect of PIER depends on the concentration and type of enzyme, incubation parameters (time, temperature, and pH), as well as duration of fixation. The enzyme digestion time is inversely related to the fixation time.

3.2.3 Heat-Induced Epitope Retrieval (HIER)

HIER is based on a concept developed by Fraenkel-Conrat and collaborators who documented that the chemical reactions between proteins and formalin may be reversed, at least in part, by high temperature or strong alkaline hydrolysis [3]. The mechanism involved in HIER is unknown but its final effect is to revert some of the conformational changes produced during fixation. The degree of fixation can dramatically modify the response of antigens to antigen retrieval. Unfixed proteins are denatured at temperatures of 70–90 °C, whereas such proteins do not exhibit denaturation at the same temperatures when they have been fixed in formaldehyde. Caution must be taken when testing new antibodies using different AR protocols. The possibility of unexpected immunostaining should always be considered when using HIER, particularly with buffers at low pH. Regardless of the HIER method used, do not let the slides dry out at any time after being dewaxed and re-hydrated.

HIER in a Microwave Oven

1. Using a microwave with revolving plate, timer, and choice of watt settings, heat 500 mL of target retrieval solution (either citrate pH 6.2 or EDTA pH 8.5 or Tris pH 9.5) in a plastic jar that will hold the slides and a plastic beaker with 200 mL of water for 2 min at 750 W. At the end of this time, remove the beaker of water.
2. Immerse the dewaxed slides completely in the warm buffer. Cover the container loosely with its lid.
3. Microwave at 750 W for 5 min (the solution needs to boil).
4. Check the level of the solution and fill to the original volume with the warm water.
5. Repeat **steps 3** and **4** for the required length of time (usually 15–20 min).
6. Remove the container from the microwave oven and place it in cold tap water for 15 min.
7. Rinse the slides in distilled water and transfer to rinse buffer.

HIER in a Pressure Cooker

1. Plug in the unit and place the pan into the decloaker's body.
2. Fill the pan of the decloaker (Biocare Medical) with 500 mL of deionized water and turn the unit on.
3. Place slides into Tissue Tek™ containers filled with 250 mL of target retrieval solution (either citrate pH 6.2 or EDTA pH 8.5 or Tris pH 9.5). Alternatively, plastic Coplin jars may be used filled with 50 mL of target retrieval solution.
4. Place containers with slides into the center of pan.
5. Place the heat shield in the center of the pan.
6. Place the monitor steam strip on top of the staining dish, put the lid on, and secure.
7. Put the weight on the vent nozzle.

8. Push the display set and check each of the displayed parameters.
9. Set the SP1 function (heating time) between 30 s and 5 min, depending on the antigen.
10. Push the display set button to SP1 and push start.
11. When the timer goes off, push the start/stop button.
12. When the temperature reaches 90 °C, the timer will sound off again.
13. Push the start/stop button to end the program. The pressure should read 0.
14. Open the lid and let the slides cool for several minutes.
15. Remove slide container and slowly rinse the slides in running tap water.
16. Transfer slides to rinse buffer.

HIER in a Steamer (See Note 15)

1. Fill the bottom of steam container with deionized water.
2. Place Tissue Tek™ containers filled with 250 mL of retrieval buffer into steamer basket. Alternatively, plastic Coplin jars may be used filled with 50 mL of target retrieval solution (either citrate pH 6.0 or EDTA pH 8.5 or Tris pH 9.5).
3. Turn steamer on and preheat the AR buffer in the Tissue Tek™ containers/Coplin jars. Place thermometer through steam holes in the lid of the steamer suspended in the AR buffer. Bring the buffer up to 95 °C.
4. When the temperature reads 95 °C, quickly place the slides in the AR buffer (avoid touching it with bare hands) and increase the temperature of the buffer back to 95 °C.
5. Steam for 20 min or the required time for antigen retrieval only after the temperature reaches 95 °C.
6. Remove the beaker with the slides from the steamer and let it cool at room temperature for 20 min.
7. Wash in tap water for 10 min.
8. Put the slides in rinse buffer and continue with immunohistochemical staining.

3.3 Immunoenzyme Techniques

The final aim of any immunohistochemical method is to detect the maximum amount of antigen with the least possible background (maximum signal-to-noise ratio). As a rule, with some exceptions, the more complex the technique, the more sensitive it is. The choice of method will depend on the amount of antigen present, level of sensitivity required, and technical capabilities of the laboratory. There are numerous commercially available detection kits. The methods included in this chapter use some of these commercial kits in an automatic stainer, but manual staining following these procedures is also possible. The number of steps that can be done in the automatic stainer depends on the model, ranging from

full automation starting with dewaxing through counterstain. Some devices are also able to do reagent incubations at different temperatures.

3.3.1 Direct Methods

1. Dewax sections in three changes of xylene or substitute, 5 min each.
2. Hydrate sections using 100% ethanol (two changes, 5 min each) and 95% ethanol (three changes, 2 min each). Rinse slides in water to adequately remove alcohol.
3. HIER or antigen retrieval with enzymes at 37 °C (if enzyme incubation is done at RT, do this treatment after **step 6**), if needed (*see Note 3*).
4. Place the slides in rinse buffer for 5 min and transfer to the autostainer.
5. Block endogenous peroxidase with peroxidase and alkaline phosphatase-blocking reagent and block endogenous biotin with biotin-blocking system.
6. Rinse in buffer.
7. Antigen retrieval with proteinase K at RT (if needed), 5 min.
8. Incubate sections with serum-free nonspecific binding blocking solution for 10–20 min.
9. WITHOUT rinsing, blow (blot if done manually) the fluid off the slide.
10. Incubate with primary labeled antibody for 30 min (*see Note 16*).
11. Rinse with rinsing buffer three times.
12. Incubate sections in the DAB solution for 5–10 min.
13. Rinse sections in distilled water.
14. Counterstain with Mayer's hematoxylin.
15. Rinse sections in distilled water. Blue sections using diluted ammonium hydroxide solution.
16. Dehydrate using 95% ethanol (two changes, 3–5 min), 100% ethanol (two changes, 3–5 min), and xylene or substitute (three changes, 3–5 min).
17. Mount in synthetic mounting medium.

3.3.2 Indirect Methods

Two-Step Method

1. Follow **steps 1–11** as in Subheading **3.3.1**.
2. Incubate with labeled secondary antibody for 30 min.
3. Follow **steps 11–17** as in Subheading **3.3.1**.

Polymer-Based Immunoenzyme Method

This method is more sensitive than the indirect method. It is based on the capability of binding many molecules of label (e.g., peroxidase) to an inert backbone of polymer (e.g., dextran) to which molecules of immunoglobulin (e.g., goat anti-rabbit

immunoglobulins) recognizing the primary antibody (in this case, rabbit immunoglobulins) are also bound. Another advantage of this method is the lack of avidin or biotin molecules involved in the reaction and therefore the lack of endogenous avidin-biotin activity (EABA) background. A second generation of polymer-based immunoenzyme methods uses a second (link) unlabeled antibody between the primary and the polymer incubations. This method is more sensitive than the one-step polymer-based method.

1. Follow **steps 1–11** as in Subheading **3.3.1**.
2. Incubate with polymer-immunoglobulin-enzyme complex for 30 min.
3. Follow **steps 11–17** as in Subheading **3.3.1**.

3.3.3 Multiple-Step Methods

Multiple-step methods are more laborious than indirect methods but usually are more sensitive. Most commonly used multiple-step methods are based on the high affinity of avidin (glycoprotein found in egg white) or streptavidin (glycoprotein from *Streptomyces avidinii*) for biotin (glycoprotein present in egg yolk). Streptavidin produces less background due to its lack of oligosaccharide residues and its neutral isoelectric point. Avidin-biotin methods are highly sensitive and are still widely used IHC methods.

Streptavidin-Biotin Complex (ABC) Method

1. Follow **steps 1–11** as in Subheading **3.3.1**.
2. Incubate with biotinylated secondary antibody for 30 min.
3. Rinse with rinsing buffer three times.
4. Incubate with tertiary reagent (preformed avidin/streptavidin-peroxidase complex) for 30 min.
5. Follow **steps 11–17** as in Subheading **3.3.1**.

Tyramide-Based Methods

Tyramide-based methods amplify the immune reaction 100- to 1000-fold when compared with a conventional ABC method. Also the dilution of the primary antibody can be increased several hundred-fold. These methods are based on the deposition of molecules of labeled (biotin, fluorescein) tyramide followed by a secondary reaction with peroxidase conjugated to streptavidin- or peroxidase-conjugated antityramide.

1. Follow **steps 1–11** as in Subheading **3.3.1**.
2. Incubate with $F(ab')_2$ biotinylated secondary antibody (avidin-biotin method) or peroxidase-IgG secondary antibody (fluorescein method), 15 min.
3. Rinse with rinsing buffer three times.
4. Incubate with primary peroxidase-streptavidin-biotin complex (avidin-biotin method) or fluorescein-tyramide amplification reagent (fluorescein method), 15 min.
5. Rinse with rinsing buffer three times.

6. Incubate with biotinyl-tyramide amplification reagent, (avidin-biotin method), 15 min, or anti-fluorescein-peroxidase (fluorescein method), 15 min.
7. Rinse with rinsing buffer three times.
8. Incubate with peroxidase-streptavidin complex (avidin-biotin method), 15 min.
9. Follow **steps 11–17** as in Subheading **3.3.1**. For fluorescein method, follow **steps 12–17** as in Subheading **3.3.1**.

3.3.4 Immunohistochemical Detection of Multiple Antigens

Currently, there are detection kits that allow the detection of at least two antigens using two different enzymes as labels (e.g., peroxidase and alkaline phosphatase). These detection kits are highly effective but also very expensive. The key issue in multiple detection of antigens is their location (different or same tissues, cells, or cellular compartments). A careful selection of the chromogen for each antigen is also necessary to achieve the best distinction between antigens. Examples of enzyme-substrate combinations in double immunostaining are included in Vector Laboratories catalog (<http://vectorlabs.com/products/enzyme-substrates.html?SID=d00812c9d3fb4bf0b5b09df158f4342a>). The chance of good visualization of both antigens is reduced if they are anatomically close to each other (e.g., both antigens are within the nucleus of the same cell type). Double immunodetection is also complicated by the variety of AR methods used for different antigens. In other words, an AR necessary for one antigen might have deleterious effects for the second antigen to be detected. For a comprehensive review of multiple immunostaining, read van der Loos' monograph [4] on multiple immunoenzymatic staining. The method included can be used for primary antibodies from same or different species.

Sequential Double-Immunoenzymatic Staining Using Primary Antibodies from Same or Different Species (Modified from van der Loos [4] (See Note 17)

1. Follow **steps 1–11** as in Subheading **3.3.1**.
2. Incubate with polymer ENVISION™/peroxidase reagent, 30 min (*see Note 18*).
3. Rinse with rinsing buffer three times.
4. Develop peroxidase activity with DAB-chromogen reagent, 5 min.
5. Elution step with DAKO double-staining block or alternatively, 5 min. boiling in citrate pH 6.0.
6. Rinse with rinsing buffer three times.
7. Incubate sections with nonspecific binding blocking solution for 10 min.
8. WITHOUT rinsing, blow (blot, if done manually) the fluid off the slide.
9. Incubate with second primary unlabeled antibody, 30–90 min.

10. Rinse with rinsing buffer three times.
11. Incubate with ENVISION™/alkaline phosphatase reagent, 30 min.
12. Rinse with rinsing buffer three times.
13. Develop alkaline phosphatase activity with Fast Red, 5–30 min.
14. Rinse with distilled water.
15. Light counterstain with Mayer's hematoxylin.
16. Mount in aqueous mounting medium.

3.4 Standardization of a New Immunohistochemical Test

The standardization of a new IHC test is a challenging process in which many factors affect the outcome. Most commercial antibodies have been tested in human tissues and rarely in other species. Information from the manufacturer of the antibody is essential to determine the suitability of the antibody for a particular species as well as the IHC detection of a particular antigen in frozen sections and/or by western blot. However, many times this information is unavailable, and the researcher needs to develop a standard protocol to test new antibodies. The following protocol assumes that tissues have been fixed in formalin and embedded in paraffin.

1. Select the tissue that is most likely to be used as a positive control. Ideally, it should have areas known to lack the antigen of interest.
2. Processing (e.g., fixation, embedding) of the control tissue should be done in the same manner as for test tissues. Control tissue should be from the same species as test tissues (an additional control tissue from a species known to react with that antibody, if available, is also recommended).
3. Prepare dilutions of the primary antibody (usually 4 twofold dilutions will suffice).
4. Prepare three sets of slides: one without AR; another with enzymatic AR (e.g., proteinase K); the third set of slides with heat-induced epitope retrieval (HIER) with citrate buffer at pH 6.0.
5. Run the IHC test following a standard procedure. Incubation of the primary antibody (time, temperature) will depend on the antigen in question. Default incubation time, 30–60 min.
6. After the IHC test is done, examine the slides to determine staining quality (*see Note 19*).

3.5 Troubleshooting

3.5.1 Excessive Background Staining

1. Prestaining Problems
 - (a) Inadequate fixation, necrosis, and autolysis.
 - (b) Tissue sections allowed to dry out. Reduce incubation time; incubate in a humidified chamber.

- (c) Sections not completely deparaffinized. Use fresh dewaxing solutions.
 - (d) Slide adhesive inappropriate or too thick. Use adhesives specific for IHC or positive-charged slides.
 - (e) Tissue section too thick. Prepare thinner sections.
 - (f) Inappropriate antigen retrieval used. Reevaluate antigen retrieval conditions.
 - (g) Incubation temperature too high. Reduce temperature.
2. Blocking Problems
- (a) Endogenous enzyme activity not suppressed. Increase concentration of blocking agent.
 - (b) Inadequate protein blocking. Use a different blocking agent.
 - (c) Inadequate blocking of endogenous avidin-binding activity. Use an avidin-biotin-blocking step or use a nonavidin-biotin detection method.
 - (d) Inadequate blocking of endogenous biotin. Use an avidin-biotin-blocking step or a nonavidin-biotin detection method.
 - (e) Blocking serum from improper species. Use blocking serum from same species as the link (secondary) antibody.
3. Primary Antibody Problems
- (a) Primary antibody too concentrated. Retitrate the primary antibody.
 - (b) Primary antibody incubation time too long. Reduce incubation time.
 - (c) Primary antibody is from a similar or an identical species as the test tissue (mouse on mouse, rat on mouse, etc.). Use specific protocols (e.g., MOM or ARK commercial kits) or additional blocking steps.
 - (d) Inadequate buffer washes (inappropriate buffer ion concentration). Modify ionic strength of the buffer solution.
4. Secondary Antibody Problems
- (a) Secondary antibody and label concentration too high.
 - (b) Secondary antibody and label incubation time too long.
 - (c) Buffer washes insufficient.
 - (d) Secondary antibody recognizes endogenous (tissue) immunoglobulins.
5. Chromogen and Counterstain Problems
- (a) Chromogen concentration too high. Reduce concentration of chromogen.
 - (b) Chromogen allowed to react too long. Reduce incubation time with chromogen.

- (c) Buffer washes insufficient. Prolong buffer washes.
- (d) Counterstain obscures the IHC reaction. Use a different counterstain that does not interfere with immunohistochemical staining.

3.5.2 Inadequate or No Staining of the Test Slide and Adequate Staining of the Positive Control Slide

1. The antigen in question is not present in the test tissue.
2. The antigen is present in the test tissue, but in a concentration below the method's detection limits. Consider using an amplification procedure, or increasing the primary antibody concentration, incubation time, or temperature, or a combination thereof.
3. The test tissue is over- or under-fixed. Modify antigen retrieval protocol.
4. The test tissue is from a different species than the control tissue and has different reactivity with the primary antibody. Validate the IHC test with same species control and test tissues.

3.5.3 Weak or No Staining of Positive Control and Weak or No Staining of Test Slides

1. All slides from some of the primary antibodies used in the run are affected. Check for inadequacy of the primary antibody, method incompatibility, primary and link antibody incompatibility, or inadequate antigen retrieval.
2. The whole run is affected. Check assay log and adequacy of reagent volumes and sequence of reagent delivery to the slide. Determine whether reagents were delivered to all slides (e.g., buffer, chromogen).
3. If it is hit and miss throughout the run, consider technical problems or problems with the tissues. Check for inadequate sequence of reagents, unbalanced autostainer, and inadequate drop zone.

3.5.4 No Staining of Positive Control Slide and Adequate Staining of the Test Slide

1. Technical error in the staining or handling of the positive control slide: The log or check list should be reviewed; if everything is in order, the assay should be repeated. For control blocks for infectious diseases, the antigen to be tested may not be present through the entire block.
2. Tissue section aging [5–7]: This is probably the result of tissue photooxidation and dehydration during prolonged storage of tissue control sections [8]. Test the tissue control section with a known positive case by IHC or test a freshly cut tissue control section.

4 Notes

1. The average shelf life of TBS working solution at room temperature is 4 days and at 4 °C is 7 days.
2. Do not add sodium azide as a preservative to enzyme-labeled reagents because it inhibits enzyme activity.

3. When using heat-induced epitope retrieval (antigen retrieval), use the target retrieval solution more appropriate to detect that particular antigen of the three included in Subheading 2. Several antigen retrieval methods may need to be tested to achieve optimal immunohistochemical reaction.
4. The incubation time depends on the amount of antigen. Longer incubation times tend to increase background.
5. Disposal of DAB: DAB is considered toxic or potentially carcinogenic, so proper disposal is necessary. Each institution has its own regulations. Contact your waste hazard office. In general, to inactivate DAB, add several drops of household bleach or sodium hypochlorite. The solution will turn black (due to oxidation of DAB) and can be washed down the sink with plenty of water. An FDA-approved alternative method consists of preparing a solution containing 15 mL of concentrated sulfuric acid added slowly to 85 mL of water. Add 4 g of potassium permanganate. Add this solution to the used DAB and leave overnight. Neutralize with sodium hydroxide, and then discard.
6. It is critical to use a counterstain that is compatible with the color produced by the histochemical reaction. In this chapter we use hematoxylin as a counterstain for a histochemical reaction producing a brown or red color. However, other combinations of chromogen-counterstain are available. For a list of compatibility between counterstains and chromogens, look at the Vector Laboratories catalog or at <http://vectorlabs.com/products/immunohistochemistry/counterstains.html>.
7. Pretreatment of the sections for antigen retrieval can be done before or after the endogenous peroxidase blocking step.
8. For some antigens, particularly those in the cytoplasmic membrane, this treatment is deleterious and should be done after the incubation with the primary antibody.
9. Alternatively, a solution of bovine serum albumin (BSA) or normal serum can be used.
10. This solution should be added immediately before the incubation with the biotinylated antibody. This solution is only needed when endogenous biotin background is likely to occur [9].
11. Other fixatives: Many of the formalin substitutes are coagulating fixatives that precipitate proteins by breaking hydrogen bonds in the absence of protein cross-linking. The typical noncross-linking fixative is ethanol. Other fixatives used in IHC are glyoxal (dialdehyde), a mixture of glyoxal and alcohol, 4% paraformaldehyde (PFA), and zinc formalin. A trial-and-error approach starting with the recommendations on the manufacturer's antibody specification sheet should be used.

12. Other slide adhesives can be used (e.g., poly-L-lysine). There are commercially available glass slides for immunohistochemistry.
13. Drying paraffin sections at higher temperatures may destroy antigenicity [10].
14. Other enzymes (trypsin, pronase, pepsin) may be used, although their activity may not be optimal at room temperature. The optimal working temperature of most of these enzymes is 37 °C, but similar enzymatic activity can be achieved with longer incubation times at room temperature, which facilitates their use in automated systems.
15. When using a steamer for HIER, buildup of mineral salts may progressively cover the heating device, reducing the temperature output. Check periodically the heating device and remove the salt buildup with an appropriate solution (vinegar or commercial solution).
16. All antibody incubations are at room temperature. However, incubation duration and incubation temperature (e.g., 37 °C, 4 °C) can be modified as necessary.
17. This method is laborious and needs an elution or a blocking step between the primary and second immune reactions. There are commercially available kits based on polymer-based technology (e.g., PROMARK™, MACH4™, ENVISION™). The concentrations of the primary antibodies should be at least double concentrated to those used in separate IHC methods. For sequential double immunostaining it is recommended that peroxidase activity using DAB as chromogen is developed first [11]. It is critical to choose the right color combination, which will depend greatly on the amount of antigen and its location in the tissue section. The counterstain should not mask the color of the immune reaction.
18. A different polymer can be used. Minor technique adjustments may be needed.
19. If specific staining is achieved, the concentration of the primary antibody, incubation times, and incubation temperature, as well as antigen retrieval procedures, may need to be optimized to obtain the best signal-to-noise ratio. If there is no staining, the concentration of the primary antibody, incubation and temperature time (including overnight or longer incubation at 4 °C), and antigen retrieval procedures (use of other enzymes or buffers at different pH) may need to be modified. Keep in mind that the detection of the antigen may not be possible due to fixation, animal species' lack of cross-reactivity of primary antibody, and lack or low amount of the epitope recognized by the antibody.

References

1. Ramos-Vara JA, Kiupel M, Baszler T, Bliven L, Brodersen B, Chelack B, Czub S, Del Piero F, Dial S, Ehrhart EJ, Graham T, Manning L, Paulsen D, Valli VE, West K (2008) Suggested guidelines for immunohistochemical techniques in veterinary diagnostic laboratories. *J Vet Diagn Investig* 20:393–413
2. Ramos-Vara JA, Beissenherz ME (2000) Optimization of immunohistochemical methods using two different antigen retrieval methods on formalin-fixed, paraffin-embedded tissues: experience with 63 markers. *J Vet Diagn Investig* 12:307–311
3. Ramos-Vara JA, Miller MA (2014) When tissue antigens and antibodies get along: Revisiting the technical aspects of immunohistochemistry, the red, brown, and blue technique. *Vet Pathol* 51:42–87
4. Van der Loos CM (1999) Immunoenzyme multiple staining methods. Bios Scientific Publishers, Oxford, UK
5. Ramos-Vara JA, Webster JD, DuSold D, Miller MA (2014) Immunohistochemical evaluation of the effects of paraffin section storage on biomarker stability. *Vet Pathol* 51:102–109
6. Fergenbaum JH, Gracia-Closas M, Hewitt SM, Lissowska J, Sakoda LC, Sherman ME (2004) Loss of antigenicity in stored sections of breast cancer tissue microarrays. *Cancer Epidemiol Biomarkers Prev* 13:667–672
7. Mirlacher M, Kasper M, Storz M, Knecht Y, Durmuller U, Simon R, Mihatsch MJ, Sauter G (2004) Influence of slide aging on results of translational research studies using immunohistochemistry. *Mod Pathol* 17:1414–1420
8. Blind C, Koepenik A, Pacyna-Gengelbach M, Fernahl G, Deutschmann N, Dietel M, Krenn V, Petersen I (2008) Antigenicity testing by immunohistochemistry after tissue oxidation. *J Clin Pathol* 61:79–83
9. Wood GS, Warnke R (1981) Suppression of endogenous avidin-binding activity in tissues and its relevance to biotin-avidin detection systems. *J Histochem Cytochem* 29:1196–1204
10. Henwood AF (2005) Effect of slide drying at 80°C on immunohistochemistry. *J Histotechnol* 28:45–46
11. Malik NJ, Daymon ME (1982) Improved double immunoenzyme labeling using alkaline phosphatase and horseradish peroxidase. *J Clin Pathol* 35:1092–1094

Applications of Mass Spectrometry Imaging for Safety Evaluation

David Bonnel and Jonathan Stauber

Abstract

Mass spectrometry imaging (MSI) was first derived from techniques used in physics, which were then incorporated into chemistry followed by application in biology. Developed over 50 years ago, and with different principles to detect and map compounds on a sample surface, MSI supports modern biology questions by detecting biological compounds within tissue sections. MALDI (matrix-assisted laser desorption/ionization) imaging trend analysis in this field shows an important increase in the number of publications since 2005, especially with the development of the MALDI imaging technique and its applications in biomarker discovery and drug distribution. With recent improvements of statistical tools, absolute and relative quantification protocols, as well as quality and reproducibility evaluations, MALDI imaging has become one of the most reliable MSI techniques to support drug discovery and development phases. MSI allows to potentially address important questions in drug development such as “What is the localization of the drug and its metabolites in the tissues?”, “What is the pharmacological effect of the drug in this particular region of interest?”, or “Is the drug and its metabolites related to an atypical finding?” However, prior to addressing these questions using MSI techniques, expertise needs to be developed to become proficient at histological procedures (tissue preparation with frozen or fixed tissues), analytical chemistry, matrix application, instrumentation, informatics, and mathematics for data analysis and interpretation.

Key words MALDI, Mass spectrometry imaging (MSI), Label-free, Staining, Tissue distribution

1 Introduction

MALDI (matrix-assisted laser desorption ionization) imaging, a label-free technique developed in 1997 by Caprioli [1], is a powerful tool today, especially when combined with the classical staining approaches performed by a pathologist. After two decades of development, this technique allows an analyst to obtain distribution information of targeted molecules in a tissue section [2–20]. Described as a molecular histology technique, MALDI imaging uses a laser to ionize and detect molecules from the tissue surface. At each laser shot position, a spectrum is recorded with the molecular composition and then an image is created with the molecules of interest. MALDI imaging is a label-free technique which can

distinguish parent drug, metabolites, and biomarkers (lipids, proteins, and endogenous metabolites) with a resolution to 5–20 μm (with commercial mass spectrometers). It can usually detect more than a thousand compounds from a tissue surface for most abundant or most “ionizable” compounds. With such capabilities, MALDI imaging has been used in a wide range of applications in life sciences and pharmaceutical industry. The technique provides a great tool to investigate the role of targeted molecules or identify nontargeted molecules. For example, it is possible to evaluate the distribution and quantification of a drug and its metabolites together with endogenous molecules which can potentially be used as biomarkers in a single experiment. MSI experiments allow combining the pharmacokinetics and pharmacodynamics information of the drug at a cellular level, bridging early stage DMPK to late stage development [21]. In another example, lesions (observed by pathologist) can be analyzed to identify the composition of the lesions and to characterize the compounds which could be responsible for the toxicity. Castellino et al. [22] perfectly illustrate this application of using MALDI imaging in a toxicological study.

In addition, the development of quantification within MALDI imaging [23–26] has added an important benefit to the technique. The ability to perform quantitation of a label-free targeted molecule (drug and/or related metabolites), per histological structure, is an added value compared to the classical approaches such as Liquid Chromatography coupled to Mass Spectrometry (LC/MS) and Quantitative Whole Body Autoradiography (QWBA) [27]. We present here the detailed protocols that permit to detect, identify, and investigate the role of drugs with MALDI imaging in support of safety evaluation.

2 Materials

2.1 Biological Tissues

Several types of tissue preparations can be used for the MSI investigation: fixed, fixed and frozen, fixed and paraffin embedded, and fresh frozen. We recommend using the snap-frozen fresh tissues without fixation (*see Note 1*). Frozen tissues are stored at $-80\text{ }^{\circ}\text{C}$ until analysis.

2.2 Sample Preparation and Sectioning Process

1. Reagents: isopentane (HPLC grade), liquid nitrogen, dry ice, and aluminum foil.
2. Cryomicrotome HM560 (Thermo Scientific Microm).

2.3 Matrix Deposition

1. Matrix reagent: 2,5-dihydroxybenzoic acid (2,5-DHB), hydroxycinnamic acid (CHCA), 9-aminoacridine (9-AA).

2. Reagents: trifluoroacetic acid (TFA), methanol (HPLC Grade), and HPLC grade water (H₂O).
3. Optimal Cutting Temperature (OCT) polymer (Fisher Scientific, Illkirch, France).

2.4 Matrix Deposition Instruments

1. Different matrix deposition systems are available such as SunCollect System (SunChrom, Friedrichsdorf, Germany), ImagePrep (Bruker Daltonics, Bremen, Germany), TM-sprayer (HTX, Chapel Hill, USA), iMLayer (Shimadzu, Japan).

2.5 MALDI-MS Instruments

1. MALDI source combined with high resolution instruments is preferred (Solarix MALDI-FTICR 7.0 T Mass Spectrometer (Bruker Daltonics, MA)) equipped with a Smartbeam II laser used at a repetition rate of 1 kHz.

2.6 Staining and Image Acquisition

1. Reagents: Hematoxylin, Tap water, Eosin, Ethanol (70%, 90%, 100%).
2. Antibodies: Anti-Phospholipid phosphatase 3 (LPP3/PPAP2B, Novus Biologicals), Rabbit polyclonal, heating retrieval pH: 6, 1:50 diluted in Da Vinci Green solution. Detection system was through horseradish peroxidase followed by Warp Red (red chromogen).
3. Instrument: Panoramic SCAN II (3DHitech, Budapest, Hungary).

2.7 Data Analysis

Multiple software platforms are available for overlaying MS images with histological images such as Fleximaging, Tissueview, HD Imaging, and Quantinetix. The software Multimaging has also been developed for the overlay of high resolution images without data reduction between different commercial solutions (Aperio, Histotech, Hamamatsu) and Mass Spectrometry images.

3 Methods

3.1 Snap Frozen Procedure

One method is to use isopentane chilled in liquid nitrogen (*see Note 2*).

1. Place a small stainless steel bowl (or Pyrex or polypropylene beaker) in the bottom of a styrofoam container and fill the space around the bowl with liquid nitrogen.
2. Add isopentane (2-methyl butane) in the bowl (work in a fume hood).
3. The isopentane will start to become opaque as it nears freezing. Take the isopentane out of the liquid nitrogen and freeze the specimen as described below. Chill the isopentane again as necessary for subsequent tissues.

4. Place crushed ice in an ice pan.
5. Cut tissue from each anatomic site to the appropriate size or isolate the targeted organ.
6. Place aluminum foils on crushed ice (the foils need to be “cold”).
7. Place isolated segments of tissue onto aluminum foils on crushed ice if the tissues are not snap frozen immediately (*see* **Notes 3** and **4**).
8. Snap-freeze the tissue directly in the isopentane (*see* **Notes 5–8**):
 - (a) Small tissue: 1 min (skin biopsy, tumor xenograft, cartilage chip).
 - (b) Medium tissue: 3 min (rat brain, rat kidney, rat liver).
 - (c) Large tissue: 10 min (mouse or rat whole body).
9. Place tissue into a separate sterile labeled tube or container previously cooled at -80°C , or on dry ice, or at least on crushed ice (*see* **Note 9**). The integrity of the tissue has to be preserved for the histological analysis.
10. Store the tissue at -80°C until shipment in dry ice or until analysis.

3.2 Quality Control Preparation

1. A quality control is prepared with a frozen control tissue.
2. Weigh the control tissue.
3. Homogenize the control tissue with a specific blender.
4. Add a known concentration of a standard molecule in the tissue homogenate (*see* **Note 10**). The final concentration of the standard in the tissue can be calculated in gram per gram (g/g) of tissue.
5. Mix vigorously in order to obtain a homogenous distribution of the standard in the tissue homogenate.
6. Apply the snap frozen procedure described previously on the tissue homogenate placed in a plastic tube.
7. Unmold the spiked tissue from the tube.
8. Store the tissue at -80°C until shipment in dry ice or until analysis.

3.3 Frozen Tissue Sectioning

1. Select the appropriate temperatures for the cryostat chamber and for the blade according to the manufacturer recommendations (*see* **Notes 11** and **12**).
2. Place the biological tissues, the quality control tissue, and the slides in the cryostat chamber 10 min before starting.
3. Stick the frozen tissue onto the cryomicrotome support with OCT. Do not fully submerge the tissue with OCT in order to minimize the molecular potential interferences.
4. Prepare 8–10 μm thick sections for an isolated tissue or 20 μm for a whole body in the cryostat (*see* **Note 13**).

5. Place your thumb on the back of the slide to warm the area where the section will be deposited. Then put the slide in contact with the tissue section.
6. Keep the slide with the tissue section adhered in the cryostat chamber at the appropriate temperature.
7. Apply the same procedure on the quality control tissue and add one section on the slide. A section of the quality control is added on each slide prepared during the study.
8. If some additional analyses have to be performed on the tissues, they can be stored at $-80\text{ }^{\circ}\text{C}$ until the next analysis (*see Note 14*). It is crucial to apply the same conditions of storage to all samples in order to properly compare each tissue sample on a study by MALDI imaging.
9. Air dry the tissue sections on the slide in the cryostat chamber at the appropriate temperature for approximately 30 min after preparation.
10. The slides can then be stored at $-80\text{ }^{\circ}\text{C}$ in a dedicated box until analysis. If they are not analyzed immediately (*see Note 15*).
11. Place the slide in a desiccator for at least 15 min at room temperature.

3.4 Standard Deposition

We recommend adding at least three quality control standard spots per slide at a low, medium, and high concentration. If quantification of the targeted molecule is required, points on the dilutions series can be used as the quality control standard spots (*see Note 16*).

1. Add a position mark on the back of the slide for the droplet deposition.
2. Add $1\text{ }\mu\text{L}$ of the standard on a mark.
3. Place the slide in a desiccator for 15 min at room temperature. The standard spots must be perfectly dried.
4. Depending on the MS instrument used for the MALDI imaging acquisition, some teach marks may be required. In this case, the teach mark can be performed with a Tipp-Ex pen.

3.5 MALDI Matrix Spray

The use of an automatic robot to spray the MALDI matrix is important for some reproducibility considerations. The same matrix preparation and the same spray must be used for the comparison of several slides during a project.

Several MALDI matrices are commercially available. The most appropriate matrix is selected based on the targeted molecule class and its mode of ionization.

1. Acquire an optical image of the slide with the tissue sections, the quality control section, the quality control standard spots, and the teach marks.

2. If available, add a known concentration (between 0.1 and 10 μM) of an isotope labeled compound (internal standard) in the MALDI matrix solution (*see Note 17*).
3. The right concentration of internal standard should be close to the concentration of the standard within the tissue. To assess this parameter, we recommend testing different concentrations first to obtain an intensity ratio between the internal standard and the standard equal to 1. This means the concentrations of both molecules are similar.
4. As there are several instruments dedicated to the MALDI matrix spray, we suggest following the manufacturer recommendations for the spray parameters.
5. Spray homogeneously the MALDI matrix on the slide.

3.6 MALDI Imaging Acquisition

1. Use the added marks on the slide to perfectly teach the instrument.
2. Standardize an analytical method for the entire study. Refer to the quality control signal in order to evaluate the analytical deviation prior to start of the acquisition.
3. Perfectly calibrate the instrument based on a reference list (standard and/or matrix peaks).
4. Define the region of acquisitions (*see Note 18*):
 - (a) Treated tissue(s).
 - (b) Control tissue(s).
 - (c) Matrix area.
 - (d) Quality control tissue.
 - (e) Dilution series or quality control standard spots.
5. Select the spatial resolution in accordance with the size of the targeted histological structure.
6. Check if your software will be able to load the generated data set at the end of the acquisition (*see Note 19*).
7. Launch the acquisition.

3.7 Hematoxylin and Eosin Staining

1. Remove the MALDI matrix sprayed on the slide with a methanol bath. If the tissue section was damaged during the MALDI imaging acquisition, an adjacent tissue section can be used for the Hematoxylin and Eosin staining process.
2. Perform the following baths:
 - (a) Hematoxylin; 3'.
 - (b) 2 \times Tap water; 2'.
 - (c) Eosin; 5''.
 - (d) Ethanol 70%; 30''.

- (e) Ethanol 90%; 30".
 - (f) Ethanol 100%; 30".
3. Generate an optical image of the stained section with a microscope or with a HD scanner (*see Note 20*).

3.8 Data Analysis

1. Load the MALDI imaging data set and the optical image into a dedicated software.
2. Use software that allows obtaining a perfect overlay between the IHC pictures and the molecular distributions as illustrated with Lysophosphatidic Acid (LPA 18:0) and a phospholipid phosphatase 3 enzyme (LPP3/PPAP2B) in the human carotid section in Fig. 1. Or in another example, software allows the

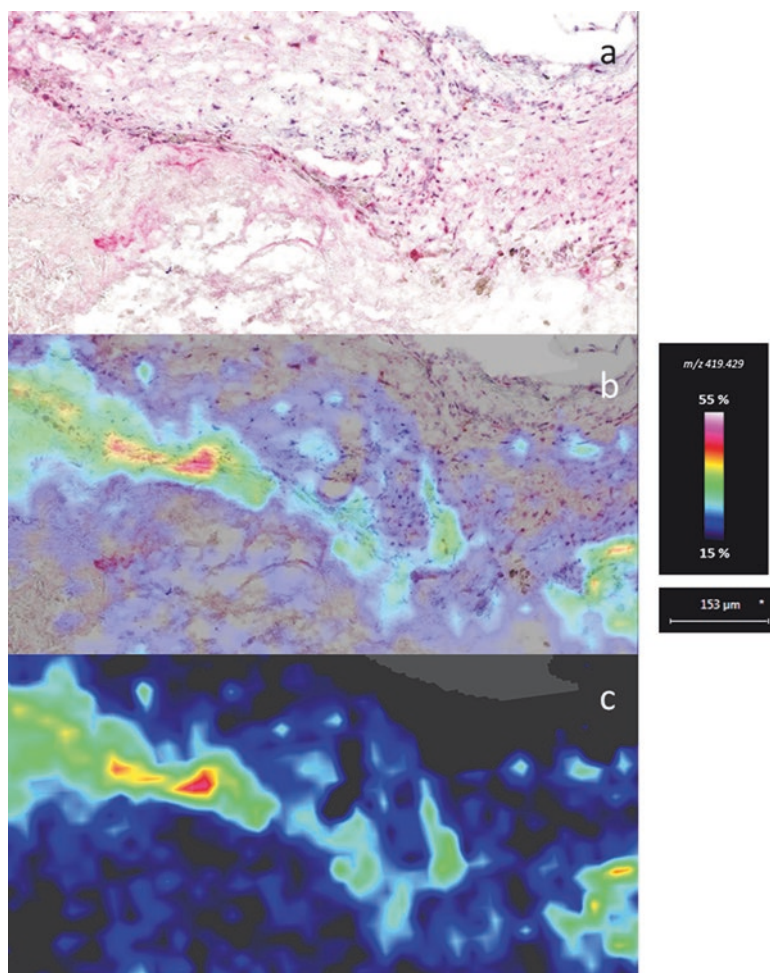


Fig. 1 Illustration of the 7T-MALDI-FTICR imaging at 20 μm and Immunohistochemistry (IHC) staining compared in the Multimaging software. (a) IHC picture of a human carotid section stained to visualize LPP3/PPAP2B enzyme. (b) Molecular distribution of a Lysophosphatidic Acid (LPA 18:0) at m/z 219.429. (c) Overlay of the IHC image with the LPA distribution in Multimaging software

overlay of H&E picture with an endogenous compound (phosphatidylcholine, PC) in Pelvis, Cortex, and Medulla of a mouse kidney in Fig. 2 (*see Note 21*).

3. Select the m/z of the targeted molecules (drug and/or related metabolites) and confirm the correlation between the molecular distribution and atypical findings.

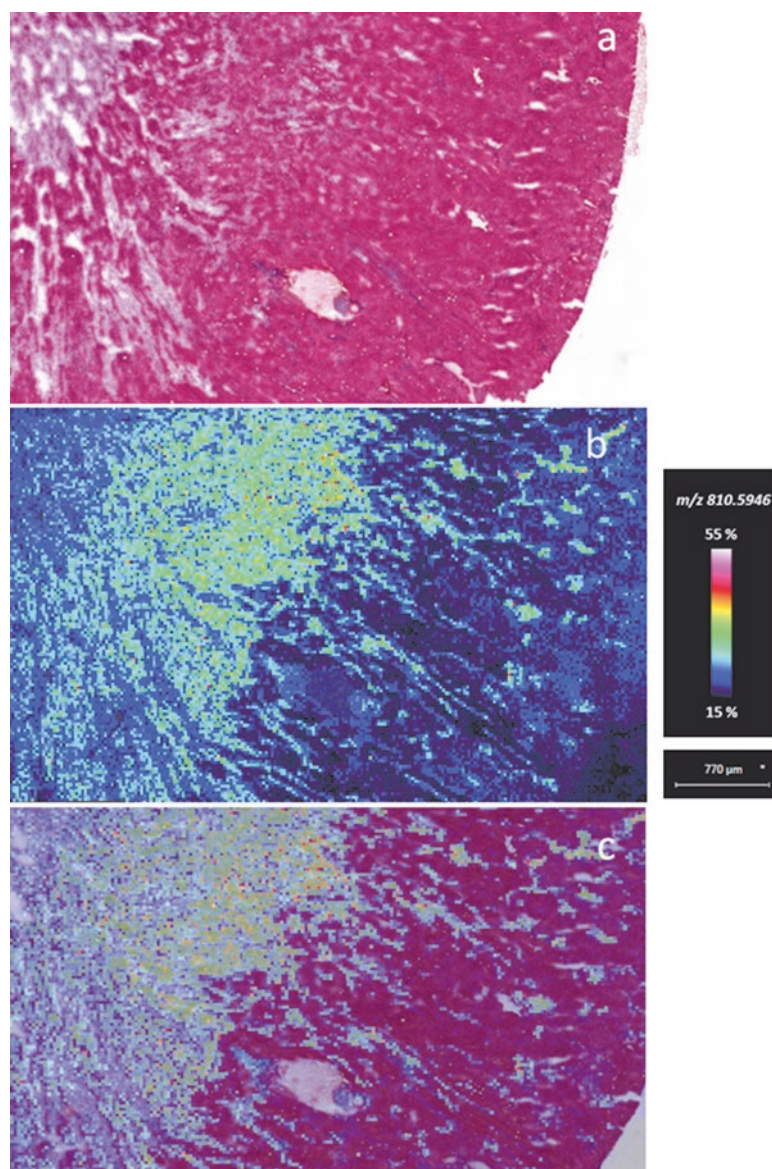


Fig. 2 Illustration of the 7T-MALDI-FTICR imaging at 20 μm and H&E staining compared in the Multimaging software. (a) H&E picture of a mouse kidney section from the pelvis to the cortex. (b) Molecular distribution of an endogenous lipid (m/z 810.5946) obtained by MALDI imaging. (c) Overlay of the H&E image with the endogenous molecule distribution in Multimaging software

4. If needed, use dedicated software like Quantinetix to perform the quantification based on the dilution series and the normalized signal of the drug with its isotope labeled form (added in the MALDI matrix).

4 Notes

1. Concerning the sample preparation, classical Fixation using Formaldehyde is possible but may delocalize the small and hydrophilic molecules making the interpretation difficult. For larger molecules such as proteins, fixation does not affect the localization but creates methylene bonds between proteins [28, 29], making the tool less sensitive, and reduces the chance to identify those molecules. So, we recommend using frozen procedure to guarantee good localization of the endogenous or exogenous compounds.
2. It has been observed that some free amino acids or nucleotides degrade, even after a few hours under -80°C freezer conditions. We recommend testing the stability of the molecules of interest prior to performing a larger study.
3. Ensure that the resected tissue never desiccates or is contaminated by surrounding tissue samples. Use clean scalpels and forceps between procedures to avoid cross contamination between samples.
4. Do not use any embedding solution (OCT, etc...). Indeed the embedding media could interfere in the molecular mass range of interest during the MSI analysis. We recommend performing the first tissue section without any embedding media. If the quality of the sections is not acceptable, the use of an embedding solution can be then evaluated (OCT, carboxymethylcellulose, etc...).
5. The snap frozen procedure could be performed in liquid nitrogen-cooled isopentane (as described in the protocol) but also in dry ice-cooled isopentane.
6. If there is any doubt about the potential solubility of the targeted molecules in the isopentane, then we recommend freezing the samples directly in the liquid nitrogen; except for whole body carcasses which must be frozen in a dry ice-cooled isopentane or hexane bath.
7. The isopentane bath prevents tissue fracturing during the freezing and sectioning process.
8. The freezing time described in the protocol is crucial. Indeed an “over-freezing” of the sample will automatically lead to fracture of the tissue during the cryosectioning process.

9. All the containers or aluminum foils must be cooled prior to being in contact with the frozen samples. This step allows maintaining the tissue histological integrity. Indeed one of the common mistakes during the sample preparation is to use a container at room temperature. The tissue will then take the shape of the container.
10. The quality control tissue can be prepared with the compound of interest for the study if its stability is well known.
11. We recommend lowering the temperature of the cryostat to $-30\text{ }^{\circ}\text{C}$ or lower if some biological fluids have to be sectioned. For example, the aqueous and vitreous humors of the eye can easily contaminate the surrounded tissues during the sectioning process if they are not perfectly frozen.
12. The tissue and its sections must never be placed at room temperature during the sectioning process. Only the frozen condition can guarantee the quality of the molecular analyses if no fixation was used [30].
13. In case of high concentrations of certain molecules in tissues, delocalization may occur during the cryosectioning and contaminate the surrounding area. In that case, we recommend using the direction of cut to avoid contamination of area of interest or to duplicate the analysis with different orientations of sectioning.
14. It is strongly recommended to minimize freezing ($-80\text{ }^{\circ}\text{C}$)—thawing ($-20\text{ }^{\circ}\text{C}$) cycle on a tissue during a study.
15. The annotations can be added to the back of the slides during the sectioning process. The ink of the pen can interfere with mass spectrometry.
16. The dilution series can be deposited directly on the slide or on some control tissue sections. We recommend using the control tissue sections if the dosed sample is an isolated organ. For a whole body investigation, the dilution series can be deposited directly on the slide.
17. The ratio between the signal of the targeted compound in the dosed tissue and the signal of the isotope labeled compound sprayed with the MALDI matrix should be as close to 1 in order to minimize tissue suppression (biological matrix affects the ionization of the standards).
18. A minimum of two negative controls are crucial for a MALDI imaging acquisition: the MALDI matrix alone and a control (wild-type or untreated or vehicle) tissue. If a signal is detected in these negative controls at the same m/z as the targeted exogenous molecules, the MSI data set must be rejected.
19. The use of the Fourier Transform Ion Cyclotron Resonance (FTICR) analyzer has led to a considerable increase of the data

set size (5–6 Gb). The use of the big data architecture for the data analysis is now a well-defined necessity (e.g., Multimaging software).

20. The staining method described is for a hematoxylin-eosin staining protocol. Presently, this is the most common staining procedure combined with the MSI. However, all types of staining procedures can be used and correlated with the molecular distribution.
21. During a safety evaluation, the quality of the overlay (Fig. 2c) between the Hematoxylin and Eosin picture (Fig. 2a) and the molecular distribution of an endogenous ion detected in the selected mass range (Fig. 2b) can be used to confirm the quality of the superposition. This step allows validating the distribution of the targeted molecules (drug and/or related metabolites) in the identified histological structures and/or lesions.

Acknowledgments

The authors would like to thank Juliette Masure for the technical support and Stefan Linehan for his comments that greatly improved the manuscript.

References

1. Caprioli R, Farmer T, Gile J (1997) Molecular imaging of biological samples: localization of peptides and proteins using MALDI-TOF MS. *Anal Chem* 69(23):4751–4760
2. Stoeckli M, Chaurand P, Hallahan DE, Caprioli RM (2001) Imaging mass spectrometry: a new technology for the analysis of protein expression in mammalian tissues. *Nat Med* 7(4):493–496
3. Chaurand P, Schwartz SA, Caprioli RM (2002) Imaging mass spectrometry: a new tool to investigate the spatial organization of peptides and proteins in mammalian tissue sections. *Curr Opin Chem Biol* 6(5):676–681
4. Chaurand P, Cornett DS, Caprioli RM (2006) Molecular imaging of thin mammalian tissue sections by mass spectrometry. *Curr Opin Biotechnol* 17(4):431–436
5. Lemaire R, Menguellet SA, Stauber J, Marchaudon V, Lucot JP, Collinet P, Farine MO, Vinatier D, Day R, Ducoroy P, Salzet M, Fournier I (2007) Specific MALDI imaging and profiling for biomarker hunting and validation: fragment of the 11S proteasome activator complex, Reg alpha fragment, is a new potential ovary cancer biomarker. *J Proteome Res* 6(11):4127–4134
6. Stoeckli M, Staab D, Schweitzer A (2007) Compound and metabolite distribution measured by MALDI mass spectrometric imaging in whole-body tissue sections. *Int J Mass Spectrom* 260(2–3):195–202
7. Cornett D, Frappier S, Caprioli R (2008) MALDI-FTICR imaging mass spectrometry of drugs and metabolites in tissue. *Anal Chem* 80(14):5648–5653
8. Groseclose MR, Massion PP, Chaurand P, Caprioli RM (2008) High-throughput proteomic analysis of formalin-fixed paraffin-embedded tissue microarrays using MALDI imaging mass spectrometry. *Proteomics* 8(18):3715–3724
9. Franck J, Arafah K, Elayed M, Bonnel D, Vergara D, Jacquet A, Vinatier D, Wisztorski M, Day R, Fournier I, Salzet M (2009) MALDI imaging mass spectrometry: state of the art technology in clinical proteomics. *Mol Cell Proteomics* 8(9):2023–2033
10. Grey AC, Chaurand P, Caprioli RM, Schey KL (2009) MALDI imaging mass spectrometry of integral membrane proteins from ocular lens and retinal tissue. *J Proteome Res* 8(7):3278–3283

11. Solon EG, Schweitzer A, Stoeckli M, Prideaux B (2010) Autoradiography, MALDI-MS, and SIMS-MS imaging in pharmaceutical discovery and development. *AAPS J* 12(1):11–26
12. Bonnel D, Legouffe R, Willand N, Baulard A, Hamm G, Deprez B, Stauber J (2011) MALDI imaging techniques dedicated to drug-distribution studies. *Bioanalysis* 3(12):1399–1406
13. Bonnel D, Longuespee R, Franck J, Roudbaraki M, Gosset P, Day R, Salzet M, Fournier I (2011) Multivariate analyses for biomarkers hunting and validation through on-tissue bottom-up or in-source decay in MALDI-MSI: application to prostate cancer. *Anal Bioanal Chem* 401(1):149–165
14. Seeley EH, Caprioli RM (2011) MALDI imaging mass spectrometry of human tissue: method challenges and clinical perspectives. *Trends Biotechnol* 29(3):136–143
15. Brignole-Baudouin F, Desbenoit N, Hamm G, Liang H, Both J-P, Brunelle A, Fournier I, Guerineau V, Legouffe R, Stauber J, Touboul D, Wisztorski M, Salzet M, Laprevote O, Baudouin C (2012) A new safety concern for glaucoma treatment demonstrated by mass spectrometry imaging of benzalkonium chloride distribution in the eye, an Experimental Study in Rabbits. *PLoS One* 7(11):e50180
16. Kreye F, Hamm G, Karrout Y, Legouffe R, Bonnel D, Siepmann F, Siepmann J (2012) MALDI-TOF MS imaging of controlled release implants. *J Control Release* 161(1):98–108
17. Prideaux B, Stoeckli M (2012) Mass spectrometry imaging for drug distribution studies. *J Proteome* 75(16):4999–5013
18. Navis AC, Niclou SP, Fack F, Stieber D, van Lith S, Verrijp K, Wright A, Stauber J, Tops B, Otte-Holler I, Wevers RA, van Rooij A, Pusch S, von Deimling A, Tigchelaar W, van Noorden CJ, Wesseling P, Leenders WP (2013) Increased mitochondrial activity in a novel IDH1-R132H mutant human oligodendroglioma xenograft model: in situ detection of 2-HG and alpha-KG. *Acta Neuropathol Commun* 1:18
19. Anderson DG, Ablonczy Z, Koutalos Y, Spraggins J, Crouch R, Caprioli R, Schey K (2014) High resolution MALDI imaging mass spectrometry of retinal tissue lipids. *J Am Soc Mass Spectrom* 25(8):1394–1403
20. Miyamoto S, Hsu C-C, Hamm G, Darshi M, Diamond-Stanic M, Declèves A-E, Slater L, Pennathur S, Stauber J, Dorrestein PC, Sharma K (2016) Mass spectrometry imaging reveals elevated glomerular ATP/AMP in diabetes/obesity and identifies sphingomyelin as a possible mediator. *EBioMedicine* 7:121–134
21. Sun N, Fernandez IE, Wei M, Wu Y, Aichler M, Eickelberg O, Walch A (2016) Pharmacokinetic and pharmacometabolomic study of pirfenidone in normal mouse tissues using high mass resolution MALDI-FTICR-mass spectrometry imaging. *Histochem Cell Biol* 145(2):201–211
22. Groseclose MR, Laffan SB, Frazier KS, Hughes-Earle A, Castellino S (2015) Imaging MS in toxicology: an investigation of juvenile rat nephrotoxicity associated with dabrafenib administration. *J Am Soc Mass Spectrom* 26:887–898
23. Hamm G, Bonnel D, Legouffe R, Pamelard F, Delbos J-M, Bouzom F, Stauber J (2012) Quantitative mass spectrometry imaging of propranolol and olanzapine using tissue extinction calculation as normalization factor. *J Proteome* 75(16):4952–4961
24. Pirman DA, Reich RF, Kiss A, Heeren RMA, Yost RA (2012) Quantitative MALDI tandem mass spectrometric imaging of cocaine from brain tissue with a deuterated internal standard. *Anal Chem* 85(2):1081–1089
25. Groseclose MR, Castellino S (2013) A mimetic tissue model for the quantification of drug distributions by MALDI imaging mass spectrometry. *Anal Chem* 85(21):10099–10106
26. Chumbley CW, Reyzer ML, Allen JL, Marriner GA, Via LE, Barry CE 3rd, Caprioli RM (2016) Absolute quantitative MALDI imaging mass spectrometry: a case of rifampicin in liver tissues. *Anal Chem* 88(4):2392–2398
27. Stauber J (2013) Quantitation by MS imaging: needs and challenges in pharmaceuticals. *Bioanalysis* 4(17):2095–2098
28. Lemaire R, Desmons A, Tabet JC, Day R, Salzet M, Fournier I (2007) Direct analysis and MALDI imaging of formalin-fixed, paraffin-embedded tissue sections. *J Proteome Res* 6(4):1295–1305
29. Stauber J, Lemaire R, Franck J, Bonnel D, Croix D, Day R, Wisztorski M, Fournier I, Salzet M (2008) MALDI imaging of formalin-fixed paraffin-embedded tissues: application to model animals of Parkinson disease for biomarker hunting. *J Proteome Res* 7(3):969–978
30. Goodwin RJA, Iverson SL, Andren PE (2012) The significance of ambient-temperature on pharmaceutical and endogenous compound abundance and distribution in tissues sections when analyzed by matrix-assisted laser desorption/ionization mass spectrometry imaging. *Rapid Commun Mass Spect* 26(5):494–498

Part III

Genetic Toxicology

In Vivo Rat T-Lymphocyte *Pig-a* Assay: Detection and Expansion of Cells Deficient in the GPI-Anchored CD48 Surface Marker for Analysis of Mutation in the Endogenous *Pig-a* Gene

Vasily N. Dobrovolsky, Javier Revollo, Dayton M. Petibone, and Robert H. Heflich

Abstract

The *Pig-a* assay is being developed as an in vivo gene mutation assay for regulatory safety assessments. The assay is based on detecting mutation in the endogenous *Pig-a* gene of treated rats by using flow cytometry to measure changes in cell surface markers of peripheral blood cells. Here we present a methodology for demonstrating that phenotypically mutant rat T-cells identified by flow cytometry contain mutations in the *Pig-a* gene, an important step for validating the assay. In our approach, the mutant phenotype T-cells are sorted into individual wells of 96-well plates and expanded into clones. Subsequent sequencing of genomic DNA from the expanded clones confirms that the *Pig-a* assay detects exactly what it claims to detect—cells with mutations in the endogenous *Pig-a* gene. In addition, determining the spectra of *Pig-a* mutations provides information for better understanding the mutational mechanism of compounds of interest. Our methodology of combining phenotypic antibody labeling, magnetic enrichment, sorting, and single-cell clonal expansion can be used in genotoxicity/mutagenicity studies and in other general immunotoxicology research requiring identification, isolation, and expansion of extremely rare subpopulations of T-cells.

Key words Glycosyl phosphatidylinositol, Phosphatidylinositol glycan class A gene, Flow cytometry, Sorting, Antibody

1 Introduction

Many (if not all) eukaryotic cells have a system for tethering specific proteins to the exterior surface of their cytoplasmic membrane using glycosyl phosphatidylinositol (GPI) [1]. In mammals, the GPI biosynthesis pathway involves approximately 30 genes, and it is evolutionally conserved [2, 3]. All of the genes involved in the pathway are autosomal (present in two functional copies of the

This chapter reflects the views of the authors and should not be construed to represent FDA's views or policies.

cellular genome) except for the phosphatidylinositol glycan class A gene (*PIG-A* in humans; *Pig-a* in animals). The X-linked *Pig-a* gene is present in a single functional copy: in males there is one physical copy of the gene, and in females one of the two available copies is on the transcriptionally inactive X-chromosome. The *Pig-a* enzyme is involved in the first step of GPI synthesis. In theory, a single inactivating mutation in the functional *Pig-a* gene can disrupt GPI synthesis and cause a deficiency in the GPI-anchored markers at the surface of the cell.

In humans, mutation in the *PIG-A* gene is associated with a rare acquired genetic disorder, paroxysmal nocturnal hemoglobinuria (PNH) [4–6]. As an extension of the PNH diagnostic procedure, methods were developed for monitoring somatic mutation in humans with *PIG-A* serving as a reporter gene [7–10]. These methods were later adapted for measuring gene mutation in laboratory animals [11–13]. In these models, mutation is measured in the endogenous *Pig-a* gene of peripheral blood cells by labeling the cells with fluorescent antibodies against a ubiquitously expressed GPI-anchored marker (e.g., CD48; see Fig. 1). Consequently, *Pig-a* wild-type cells having a normal GPI-anchored marker phenotype will be fluorescent, while *Pig-a* mutant cells, in which GPI synthesis is disrupted and the protein marker is not expressed at the surface, will not fluoresce. The nonfluorescent *Pig-a* mutant cells can be efficiently quantified by flow cytometry.

This approach to measuring *Pig-a* mutation works exceptionally well for detecting mutation in rodents treated with prototypical mutagens [14, 15]. As a result, the rat red blood cell-based *Pig-a* assay has been proposed as a tool for preclinical safety assessment of regulated chemicals (e.g., human drugs) [16, 17]. The development of an appropriate guideline for performing the *Pig-a* assay and interpreting its results is an ongoing project under the auspices of the Organisation for Economic Co-operation and Development.

An important step in the development of the guideline is to prove unambiguously that the assay detects what it claims to detect; namely, that the marker-deficient phenotype detected by flow

Fig. 1 (continued) T-cells will react with both fluorescent anti CD48 antibodies and fluorescent anti CD3 antibodies, and fluoresce in the PE and APC emission spectra. An inactivating mutation in the single functional copy of the *Pig-a* gene disrupts GPI synthesis and alters the cellular phenotype to being deficient in CD48 surface marker expression. *Pig-a* mutant T-cells will not react with anti CD48 antibody (and will not fluoresce in the PE emission spectrum), but they will react with anti CD3 (and fluoresce in the APC emission spectrum). In order to increase the efficiency of sorting mutant phenotype CD3-positive/CD48-negative cells, the complex mixture of labeled spleen-derived MNCs is depleted of the majority of CD48-positive cells using magnetic anti PE particles. PE-labeled CD48-positive cells will react with anti PE magnetic particles. These CD48-positive cells will be retained by a powerful magnet, while CD48-negative cells (including the CD48-deficient *Pig-a* mutant T-cells) will pass through the magnetic field and will be collected for further processing and sorting

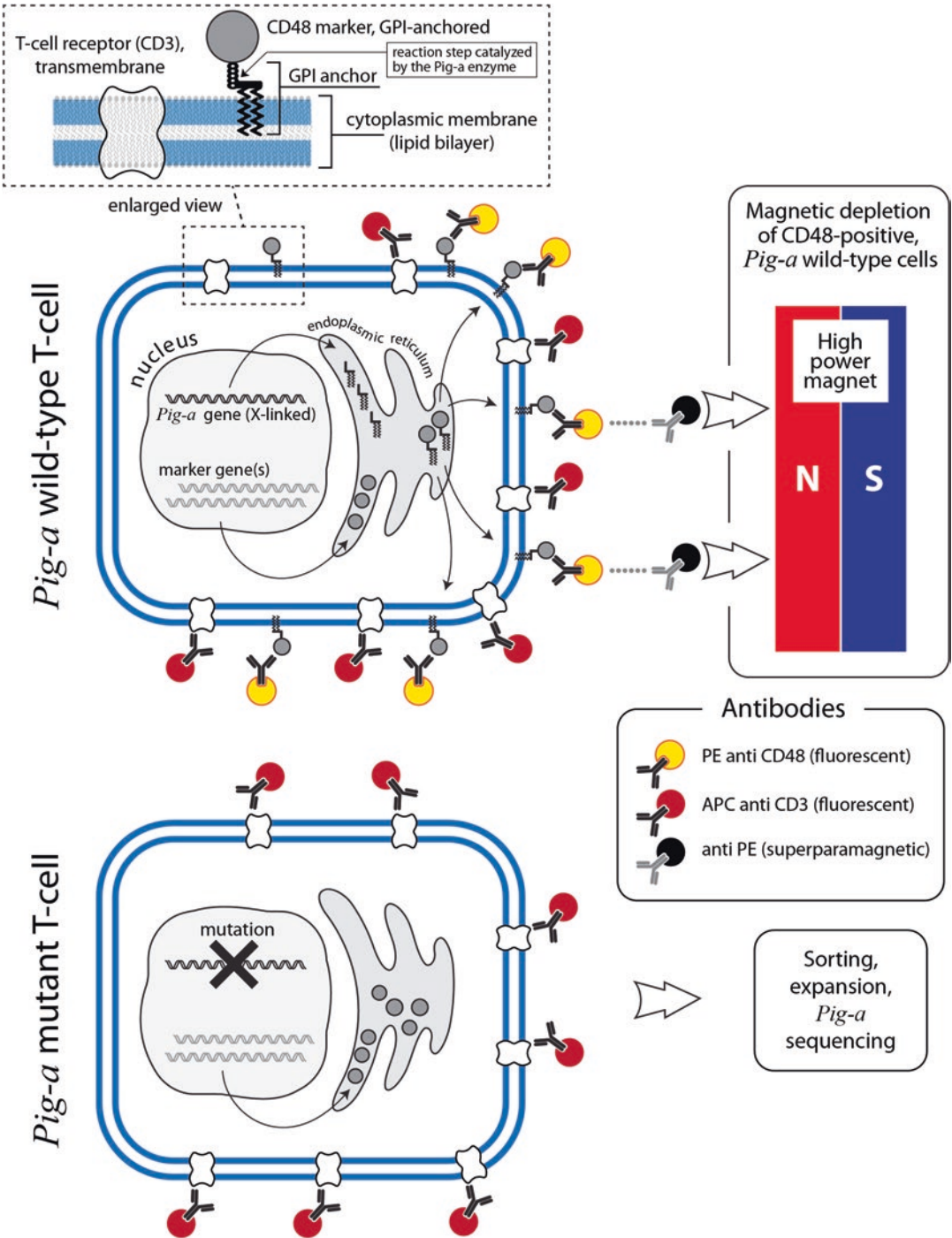


Fig. 1 The principle of the T-cell *Pig-a* assay. In wild-type cells, GPI anchors are assembled on the membrane of endoplasmic reticulum, initially at its cytoplasmic leaf, then at the luminal leaf. GPI synthesis is described elsewhere [2, 3]. Independently synthesized protein markers (e.g., CD48, CD59) are enzymatically attached to the membrane-bound GPI anchors in the lumen of endoplasmic reticulum; the GPI-anchored markers then are exported to the exterior surface of the cytoplasmic membrane. Pan-leukocyte GPI-anchored CD48, ubiquitously present on T-lymphocytes, is used in the version of the *Pig-a* assay described here. *Pig-a* wild-type

cytometry in the *Pig-a* assay is equivalent to mutation in the *Pig-a* gene. This proof is necessary because, at least hypothetically, marker deficiency can be caused by events other than mutation in the *Pig-a* gene (e.g., by mutation(s) or epigenetic silencing of other genes in the GPI synthesis pathway, and/or the gene(s) encoding the surface marker measured in the assay, to mention just a few). Here we present a methodology for establishing the linkage between a deficiency in the GPI-anchored CD48 surface marker and mutation in the *Pig-a* gene at the level of individual rat spleen lymphocytes. Because the frequencies of mutant cells induced even by very powerful mutagens are still extremely low by flow cytometry standards, simple sorting of such rare events is inefficient. In order to overcome this inefficiency, we have selectively depleted spleen cell samples for *Pig-a* wild-type cells. In this approach, magnetic particles that target GPI-anchored CD48 on the surface of the wild-type cells retain most wild-type cells with a powerful magnet, allowing the mutant cells to be isolated as an enriched population suitable for single-cell sorting and molecular characterization. Another important element of our approach is the use of specially formulated growth medium that promotes the clonal expansion of individual T-cells. With the flow gating strategy, and the sorting and clonal expansion techniques that we have developed, we were able to show that phenotypically mutant cells contain *Pig-a* mutations. Also we were able to demonstrate the expected spectra of *Pig-a* mutation in rats treated with *N*-ethyl-*N*-nitrosourea [18] and 7,12-dimethyl benz[*a*]anthracene [19], indicating that the mutations were induced de novo by these genotoxic carcinogens.

The general approach to labeling, magnetic enrichment, and sorting of mutant rat T-cells could be applied to mouse spleen samples or human peripheral blood—as the appropriate species-specific antibodies are commercially available. Finally, a similar approach with magnetic depletion/enrichment could be employed for analysis of *Pig-a* mutation in erythroid cells of bone marrow, thus linking flow cytometry-identified mutant phenotype of peripheral red blood cells (RBCs) to *Pig-a* mutant genotype of precursor cells.

2 Materials

2.1 Major Equipment

1. FACSaria I cell sorter (BD Biosciences; Milpitas CA) running FACSDiva software and equipped with a 70 μm sorting nozzle; 488 nm (blue) and 635 nm (red) excitation lasers; photomultiplier tubes (PMTs) equipped with a 585/42 nm filter for detecting blue laser-induced PE fluorescence, a 695/40 nm filter (for detecting blue laser-induced 7AAD fluorescence); a 488/10 filter (for measuring side light scatter off the blue laser); a PMT with a 660/20 nm filter (for measuring red laser-induced APC fluorescence); and a detector for measuring

forward scatter. The standard FACS Aria I configuration suggested by the manufacturer is sufficient.

2. Biological safety cabinet (BSC).
3. Benchtop centrifuges (e.g., Eppendorf 5810R and 5430; Hauppauge NJ) with bucket rotors for 50- and 15-mL tubes, and fixed angle rotor for 1.5-mL tubes.
4. Cell counter, e.g., Z1 particle counter (Beckman Coulter; Indianapolis IN).
5. QuadroMACS magnet with stand (Miltenyi Biotec; San Diego CA).
6. Humidified CO₂ cell culture incubator.

2.2 Reagents and Consumables

1. RPMI 1640 medium.
2. Ca²⁺- Mg²⁺-free Dulbecco's phosphate buffered saline (PBS).
3. Fetal bovine serum (FBS): divide into 30–40-mL aliquots in 50-mL tubes, heat inactivate for 30 min at 56 °C, and store at –20 °C.
4. Lympholyte[®]-R (Cedarlane; Burlington NC).
5. 10× RBC lysis buffer (BioLegend; San Diego CA).
6. 0.2 mg/mL PE anti-rat CD48 antibody, clone OX-47 (BioLegend; available as custom order).
7. 0.2 mg/mL APC anti-rat TCRαβ antibody (anti-rat CD3), clone R73 (BioLegend).
8. Anti-PE magnetic microbeads (Miltenyi Biotec).
9. 7AAD viability stain (BD Biosciences).
10. RNeasy (Plus) mini kit (QIAGEN; Valencia, CA).
11. HotStarTaq DNA Polymerase kit (QIAGEN).
12. Mixture of deoxynucleoside triphosphates containing 2.5 mM dATP, 2.5 mM dCTP, 2.5 mM dGTP, and 2.5 mM dTTP (dNTP mixture for PCR).
13. HL-1™ medium (Lonza; Walkersville, MD).
14. Rat T-STIM medium (BD Biosciences).
15. 1 M HEPES, pH from 7.2 to 7.5.
16. 200 mM L-glutamine.
17. 100× MEM non-essential amino acids solution (Gibco; Grand Island, NY).
18. 100 mM sodium pyruvate.
19. Penicillin-Streptomycin solution containing 10,000 U/mL of penicillin G sodium and 10,000 µg/mL of streptomycin sulfate.
20. 55 mM 2-mercaptoethanol (βME) in PBS.

21. 10,000 U/mL mouse interleukin-2 (Roche; Indianapolis IN).
22. Ionomycin (Sigma-Aldrich; St. Louis, MO): prepare 1 mg/mL stock in DMSO, dispense into 250- μ L aliquots, and store at -80°C .
23. Phorbol myristate acetate (PMA; Sigma-Aldrich): prepare 400 $\mu\text{g}/\text{mL}$ stock in DMSO, dispense into 50- μ L aliquots, and store at -80°C .
24. Using reagents mentioned above prepare 200 mL of the rat T-lymphocyte growth medium (sufficient for filling ten 96-well plates): combine 99.6 mL of RPMI 1640, 40 mL of HL-1, 26 mL of heat-inactivated FBS, 20 mL of rat T-STIM, 5 mL of 1 M HEPES, 5 mL of 200 mM L-glutamine, 2 mL of MEM non-essential amino acids solution, 2 mL of 100 mM sodium pyruvate, 0.4 mL of Penicillin-Streptomycin solution, 0.2 mL of 55 mM β ME, 0.2 mL of mouse interleukin-2, 50 μL of ionomycin stock, and 5 μL of PMA stock. Sterilize through 0.2 μm filter and store at 4°C . Use within 2 weeks.
25. Scissors, forceps, and sterile razor blades for excision and processing of spleens.
26. 100-mm tissue culture plates: 12-well (flat bottom) and 96-well (round bottom) tissue culture plates.
27. 10-mL syringes with serrated plunger butts (individually packaged).
28. 5/8-in 25 Ga hypodermic needles.
29. 70- μm cell strainers and 5-mL flow tubes with 35- μm cell strainer caps (BD Falcon, Bedford, MA).
30. LS MACS separation columns (Miltenyi Biotec).
31. Cytometer setup and tracking (CS&T) microbeads and Accudrop microbeads (BD Biosciences).
32. Primers for amplification and sequencing.

External (e) primers:

2Fe, GGCCACACAGCACATTCTTA.

2Re, GAGGCTGGGAATGCTGAGTT.

3Fe, GCCTGCAAGAGAAAGGAAATGT.

3Re, CAGTGCCTGTTAGAACCTGTATC.

4Fe, TGCCAATGATGATTTTCCTGT.

4Re, CCTGACCCCCAGAAGAGTTT.

Internal (i) primers:

2Fi, GGCAGCATTTATAGCCGCTT.

2Ri, TGAGTTCAAGGTCGGTGTGA.

3Fi, AGGAAATGTGCAGGGAAAGC.

3Ri, TGTTGTA CTTGGGAGCCGAT.

4Fi, GCATTTGGTATGTTGGCTGTT.

4Ri, GTTTCCAGGATGTGGGATCA.

Additional primers for sequencing:

2F, CGATAATCCATTCCCACAGTT.

1R, GACTGTCTGAAGCCCCATTG.

All primer sequences are given in 5' → 3' orientation. Make 100 μ M stock solution for each individual primer. In addition, make the following six stocks of e- and i-primer pairs: 2Fe and 2Re, 3Fe and 3Re, 4Fe and 4Re, 2Fi and 2Ri, 3Fi and 3Ri, 4Fi and 4Ri, containing each primer at concentrations of 10 μ M.

3 Methods

3.1 Spleen Cell Recovery and Purification

1. In advance, prepare sufficient PBS containing 2% heat-inactivated FBS (PBS/FBS) to conduct the procedures that follow (80 mL per animal to be processed).
2. Dispense 3 mL of RPMI 1640 into 50-mL tubes, one tube per animal.
3. Fill a 250-mL glass beaker with 70% ethanol for sterilizing instruments (scissors, forceps, and razor blades) between the samples.
4. Prefill 15-mL tubes with 3 mL of room temperature Lympholyte-R (one tube for each piece of spleen processed; at least four tubes per animal).
5. In an animal procedure room, euthanize one or two rats at a time using a procedure approved by your Institutional Animal Care and Use Committee. Place the animal on its right side on an absorbent towel; spray 70% ethanol copiously on the exposed left side; lift the skin with sterile forceps and make a small transverse incision (without cutting through the abdomen) approximately 1 cm below the rib cage and extend the incision 1.5 cm in the posterior and anterior directions, separating the skin from the abdominal wall. Using another set of forceps and scissors, lift the abdominal wall, make an incision into the abdomen, and extend the opening to a total length of 2–3 cm. Find the elongated dark purple-colored spleen; holding the side of the spleen with blunt-end forceps, gently pull the spleen out of the body cavity while trimming the surrounding tissue with sharp scissors. Place the recovered spleen in a 50-mL tube containing 3 mL of RPMI 1640. Place the tube on ice until ready for the next step. Sterilize the surgical instruments in a beaker with 70% ethanol before starting surgery on

the next rat. Bring the spleens to a tissue culture laboratory for further processing.

6. Working in a BSC, pour the spleen from the 50-mL tube into a 100-mm Petri dish. Hold the spleen to the bottom of the dish with sterile forceps and, using a sterile razor blade, cut the spleen into four to six 5–7-mm pieces. Transfer the individual pieces of spleen into wells of a 12-well tissue culture plate pre-filled with 3 mL RPMI 1640 per well. Process at least four pieces of spleen from each animal.
7. Separate the barrel and plunger of one 10-mL syringe; discard the barrel. Using the serrated butt-end of the plunger as a pestle, release the cells by gently crushing pieces of spleen with squeeze and twist motions. All spleen pieces from the same animals can be processed with the same plunger.
8. Fit a 25 Ga needle onto a new 10-mL syringe and slowly aspirate the released spleen cells from a well of the 12-well plate (avoid tissue debris that can clog the needle). For density gradient separation of mononuclear cells (MNCs), slowly discharge the cell suspension from the syringe (through the needle) against the wall into a tube containing Lympholyte-R, layering the cells on top of the Lympholyte-R without mixing.
9. Centrifuge the tubes for 20 min at room temperature at $1500 \times g$. MNCs form a distinct layer at the interface between the Lympholyte-R and RPMI 1640. Using a 5-mL pipet, transfer just the MNC fraction in a volume of 1.5–2.5 mL into a 50-mL tube. Combine all the MNCs isolated from the same animal into one 50-mL tube.
10. Top off the tube with RPMI 1640, invert the tube several times, and centrifuge at room temperature for 10 min at $800 \times g$. Meanwhile prepare $1 \times$ RBC lysis buffer by diluting the $10 \times$ concentrate with water; keep on ice.
11. Aspirate the supernatant from the 50-mL tube and resuspend the pellet in 5 mL of ice-cold $1 \times$ RBC lysis buffer. Lyse the residual RBCs by incubating the tube on ice for 5 min with occasional gentle mixing. Wash off the lysis buffer two times: add 30 mL of PBS/FBS, invert the tube several times, centrifuge the tube for 5 min at $340 \times g$, remove the supernatant, and resuspend the pellet in 10 mL of PBS/FBS; repeat centrifugation for 5 min at $340 \times g$. Next, remove the supernatant and resuspend the pellet in 2 mL of PBS/FBS per 1 mm thickness of the pellet (depending on the initial size of the spleen, 1.5–3 mL of PBS/FBS should be sufficient).
12. Filter the purified cells into a fresh 50-mL tube through a 70- μ m cell strainer fitted to the tube. Using a small aliquot of cells determine the cell concentration on a Z1 counter. Adjust the concentration of the cell suspension to $20\text{--}40 \times 10^6$ cell/

mL with PBS/FBS. At this point, check the appearance of the cell suspension under a microscope. The sample should appear as a suspension of spherical cells.

3.2 Cell Labeling

1. Prepare the following antibody-labeled samples in 1.5-mL Eppendorf tubes: a mutant-mimic sample containing 100 μ L of PBS/FBS, 3 μ L of APC anti-rat CD3, and 100 μ L of cells from Subheading 3.1, **step 12** (preferably cells derived from a vehicle-control animal); and standard 2-antibody-labeled experimental samples (one for each experimental animal) containing 100 μ L of PBS/FBS, 3 μ L of APC anti-rat CD3, 3 μ L of PE anti-rat CD48, and 100 μ L of cells from Subheading 3.1, **step 12** (*see Note 1*).
2. Incubate the mutant-mimic and the experimental samples on ice in the dark for 30 min. After incubation, centrifuge for 3 min at $300 \times g$ at room temperature, resuspend the pellets in 500 μ L of PBS/FBS, add 20 μ L of 7AAD to each, mix, and filter each sample into 5-mL BD Falcon flow tubes equipped with cell strainer caps. Keep the samples on ice until ready for flow cytometry; these samples will be used for setting up the flow gating and determining the frequencies of CD48-deficient T-cells in all experimental animals (which include vehicle-control and mutagen-treated animals).

3.3 Setting Up FACSria Flow Cytometer/Sorter

1. Install a 70 μ m nozzle into the cytometer (*see Note 2*); choose the 70 psi/70 μ m configurations. Perform the required fluidics startup, start and stabilize the stream, and perform the Cytometer Setup and Tracking (CS&T) routine with calibration beads. The suggested initial cytometer settings for spleen cell sample acquisitions are provided in Table 1, although the actual voltages for each PMT may vary substantially from instrument to instrument (less so for day-to-day use on the same instrument).
2. If mutant sorting will be performed on the same day, optimize the side stream and homing for the sorting device (i.e., 96-well plate), and determine the value for the sorting drop delay using Accudrop beads and the manufacturer's suggested procedure.

3.4 Gating Strategy

1. Load an experimental two-antibody-labeled sample with cells from a control (untreated) animal onto the FACSria, and begin data acquisition; adjust the flow rate to 2000–3000 events per second.
2. Create the following four cytograms/histograms (as a, b, c, and d shown in Fig. 2): FSC (horizontal) versus SSC (vertical); 7AAD versus SSC; APC histogram and APC versus PE. Use bi-exponential scaling for the 7AAD, APC, and PE parameters. Let all cytograms show all events. Open the population hierarchy view.

Table 1
Suggested initial settings for FACSaria I

Parameter	Type	Voltage	Log	Collected on PMT equipped with bandpass filter
FSC	A	55	Off	Dedicated detector (no filter)
SSC	A	346	Off	488/10 on blue octagon
PE	A	427	On	582/42 on blue octagon
7AAD	A	531	On	695/40 on blue octagon
APC	A	592	On	660/20 on red trigon
Threshold operator		OR		
Threshold parameter		Threshold		
FSC		5000		

With these parameters, the fluorophores employed and the gating strategy, fluorescence compensation is not required

3. On the APC histogram, there should be two peaks similar to those in Fig. 2c (the right peak may be lower than the left peak); adjust the voltage on the APC PMT to place the two peaks horizontally into positions similar to Fig. 2c. Make an interval gate broadly covering the right peak, and assign a color (e.g., red) to events associated with this interval gate; red-colored events should appear on the FSC versus SSC cytogram. Adjust the voltages on the FSC and SSC detectors to fit the red-colored events approximately in the bottom middle area of the cytogram and the overall cell population as shown in Fig. 2a (see Note 3). Make an elongated gate on the FSC versus SSC cytogram covering the nucleus of the colored population; this gate should be very similar to the red-colored gate in Fig. 2a. Name this gate “Lymphocytes”, assign a color to events in this gate other than black or white. Now the interval gate on the APC histogram can be deleted.
4. Let the 7AAD versus SSC cytogram show events from the “Lymphocytes” gate only. On this cytogram, create an interval gate like in Fig. 2b, excluding highly 7AAD-positive events (damaged or dead cells with compromised membrane). Call this gate “Viable”, and assign a color to it.
5. Let the APC histogram show the events from the “Viable” gate only. Now, the peaks on this histogram should be of similar height. Make a tight interval gate around the right peak (just like in Fig. 2c); name it “TCR positive”, and assign a color to it. This peak will contain CD3-positive T-cells.

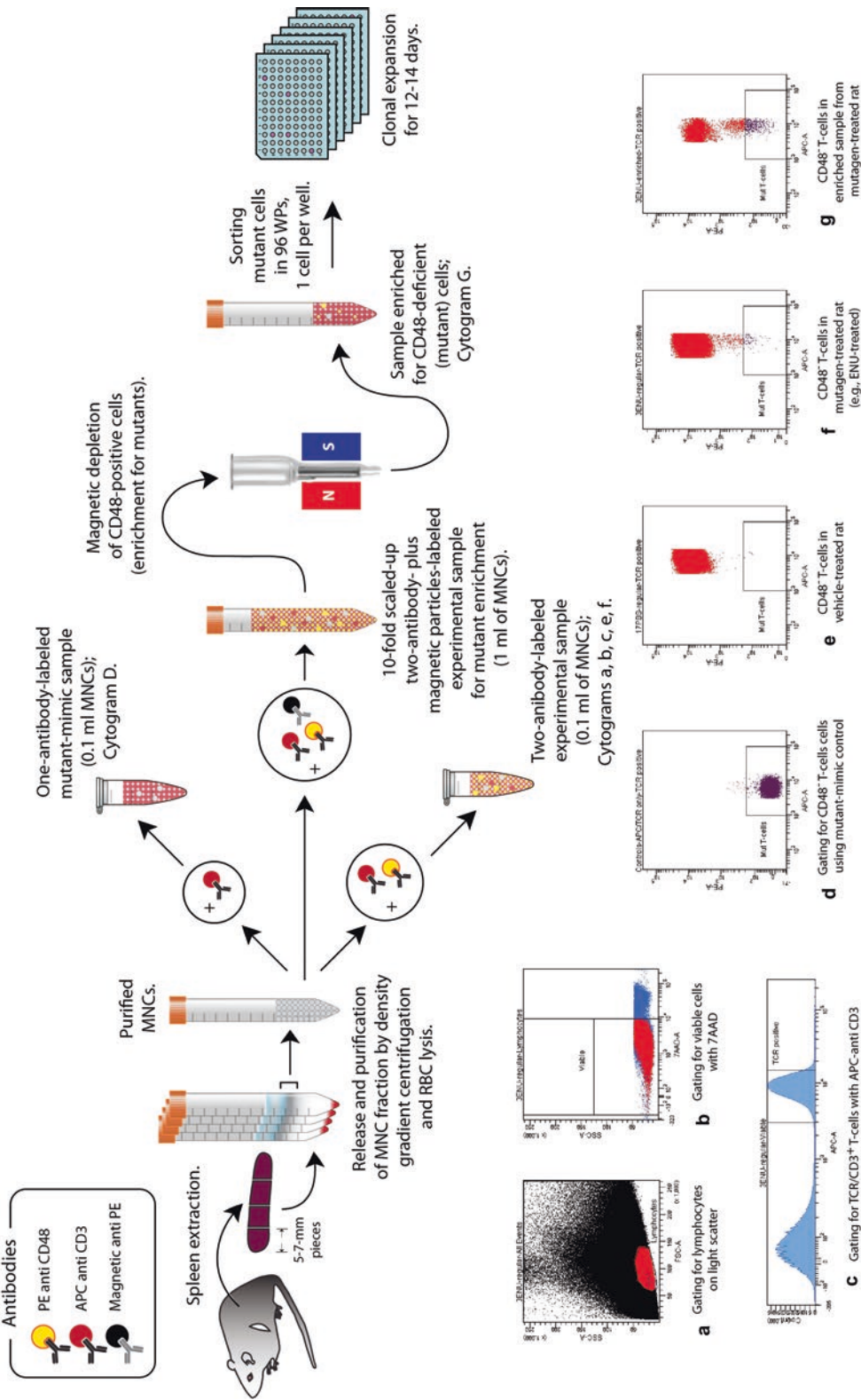


Fig. 2 Steps involved in performing the T-cell *Pig-a* assay: labeling, gating strategy, and representative cytograms. Consult the text for specific details relevant to each step. **(a)** Gating for lymphocytes on light scatter. **(b)** Gating for viable cells with 7AAD. **(c)** Gating for TCR/CD3+ T-cells with APC anti CD3. **(d)** Gating for CD48+ T-cells using mutant-mimic control. **(e)** CD48+ T-cells in vehicle-treated rat. **(f)** CD48+ T-cells in mutagen-treated rat (e.g., ENU-treated). **(g)** CD48+ T-cells in enriched sample from mutagen-treated rat

6. Let the APC versus PE cytogram show the events from the “TCR positive” gate. During acquisition using a sample from an untreated (vehicle-control) rat, the events in this cytogram should appear similar to Fig. 2e: overwhelmingly positive for PE fluorescence (i.e., positive for surface expression of GPI-anchored CD48) with practically no events in the lower portion of the cytogram. Adjust the voltage on the PE PMT to place the main population in an area similar to what is shown in Fig. 2c (in the top half of the cytogram). Remove the experimental standard-labeled sample from the cytometer.
7. Place the mutant-mimic sample on the cytometer. Cells in this sample are not labeled with PE anti CD48, and T-cells will appear as CD48-deficient mutants. Start acquisition; in the APC versus PE cytogram the events should appear as a tight population at the bottom of the cytogram. Make a rectangular gate around this population (just like in Fig. 2d), extending it well into negative values on the Y-axis (below the horizontal axis). Name the gate “Mut T-cells” and assign it a color identifier. This gate will denote the place where CD48-deficient, presumed *Pig-a* mutant, T-cells will appear in experimental samples labeled with two fluorescent antibodies (with APC anti CD3 and PE anti CD48).
8. Acquire and record a file containing 50,000 cells from the “TCR positive” gate. Remove the mutant-mimic sample from the flow cytometer. Run a tube with 2 mL PBS/FBS (without cells) for 2–3 min in order to wash the sampling line of any leftover cells from the mutant-mimic sample.
9. Re-analyze (re-acquire) and record the standard-labeled experimental sample from the untreated control animal using the gating strategy established above. This time acquire and record a file containing 1,000,000 events from the “TCR positive” gate (or as many events as the sample allows until running empty). During recording, the flow rate can be increased to 10,000–15,000 events per second to speed up the overall process. If everything was labeled and setup correctly, the resulting cytogram should show most events in the upper part with only a handful (or no) events falling into the “Mut T-cells” gate (as in Fig. 2e). The frequency of CD48-deficient, potentially *Pig-a* mutant, cells in this sample will be the ratio of the number of events in the “Mut T-cells” gate to the number of events in the “TCR positive” gate.
10. Using the same gating strategy, acquire a large number of events (ideally, close to 1,000,000 events) from the “TCR positive” gate for all the 2-antibody-labeled experimental samples that were prepared (*see Note 4*); calculate the frequency of CD48-deficient mutant T-cells for each sample. For animals

treated with powerful mutagens, such as *N*-ethyl-*N*-nitrosourea (ENU) or 7,12-dimethyl benz[*a*]anthracene (DMBA), the fraction of events falling into the “Mut T-cell” gate should be visibly increased (like in Fig. 2f).

3.5 Magnetic Enrichment for CD48-Deficient Mutant Cells

1. Working in a BSC, prepare a tenfold-scaled-up two-antibody-labeled experimental sample for each animal: combine 1 mL PBS/FBS, 30 μ L of PE anti CD48, 30 μ L APC anti-rat CD3, and 1 mL of purified spleen cells from Subheading 3.1, step 12 in a 15-mL tube. Incubate the tubes in the dark on ice. After a 30-min incubation, add 10 mL of PBS/FBS, invert the tubes a few times, and centrifuge for 5 min at $340 \times g$. Resuspend the pellets in 500 μ L of PBS/FBS.
2. Add 50 μ L of magnetic anti PE beads to the labeled cells, and mix by pipetting. Next, incubate the cells in the dark on ice for 20 min; then add 10 mL PBS/FBS, centrifuge for 5 min at $340 \times g$, and resuspend the pellets in 2 mL of PBS/FBS.
3. Mount LS magnetic columns on a QuadroMACS magnet; pre-wet the columns with 3 mL of PBS/FBS; let the liquid flow through the column by gravity, and discard the flow-through. Load the entire 2 mL of antibody- and magnetic particles-labeled sample onto the column, and collect the flow-through into a fresh 15-mL tube. After the whole volume of cell suspension has entered the column, add an additional 5 mL of PBS/FBS to the top of the column and continue collecting the flow-through.
4. Centrifuge the collected eluate for 5 min at $340 \times g$, and carefully aspirate the supernatant without disturbing the now significantly smaller (and sometimes hardly visible) cell pellet. Gently resuspend the cells in 1 mL of PBS/FBS, add 40 μ L of 7AAD, and filter the cells into a 5-mL flow tube through the 35- μ m cell strainer top; keep on ice. The mutant-enriched sample is ready for sorting.

3.6 Sorting and Expanding Mutant Cells

1. Working in a BSC, dispense 200 μ L of the lymphocyte growth medium into each well of round bottom 96-well plates. Prepare one plate for each untreated (vehicle-control) animal and 3–6 plates for each animal treated with mutagens.
2. Remove the lid off a prefilled 96-well plate and place the plate onto the sliding access stage of the sorter. In the sort layout of the FACSDiva software, select all 96 wells and set sorting for 1 cell per well from the “Mut T-cells” gate; choose the “single-cell sorting” purity mode.
3. Load the enriched sample (from Subheading 3.5, step 4) on the cytometer, start acquisition, and adjust the flow rate to achieve a throughput of less than 1500 events/s. The overall

pattern of events appearing in real-time cytograms will be similar to the unenriched standard-labeled experimental samples, but with the number of events falling into the “Mut T-cells” gate being noticeably higher.

4. Start the sort; simultaneously record the data for up to 200,000 events from the “TCR positive” gate. The resulting cytograms for the enriched samples from animals treated with powerful mutagens should appear as in Fig. 2g, with a noticeable relative increase in the events in the “Mut T-cells” gate and a relative decrease of the wild-type CD48-positive events.
5. After the first plate is filled up with sorted cells, the sorting will stop and the access stage will extend for removal of the plate. Cover the filled-up plate with the lid, and put it into a 37 °C humidified CO₂ incubator. Place a fresh 96-well plate with growth medium on the flow cytometer access stage and resume sorting. Continue sorting until the desired number of 96-well plates is collected or until the enriched sample is exhausted (*see Note 5*).
6. After 10–12 days of incubation, inspect the plates using an inverted tissue culture microscope (*see Note 6*).
7. The expanded clones now are ready for molecular analysis of mutation in the *Pig-a* gene. Alternatively, the clones may be frozen and stored at –80 °C for analysis in the future (*see Note 7*).
8. Freezing clones: resuspend the clone by pipetting the medium in the well up and down (avoid forming foam); transfer the resuspended cells into a 1.5-mL Eppendorf tube prefilled with 0.5 mL of PBS (without FBS). Centrifuge the tube for 3 min at 1000 × *g*, aspirate the supernatant (for large clones the cell pellet may be visible at the bottom of the tube), and quickly freeze the tube with the cells at –80 °C.

3.7 Amplification of Genomic *Pig-a* Fragments for Sequencing

1. For simultaneous isolation of RNA and DNA from medium and large clones (containing 200 or more cells), follow the RNeasy (Plus) mini kit instructions for extraction of RNA from animal cells (*see Note 8*). Do not use the DNase digestion step. Start with the lysis of cells (cell pellets) in 350 µL of RTL buffer by pipetting; and in the final step, elute the nucleic acids in 30 µL of water.
2. Perform the first round amplification of *Pig-a* exons using QIAGEN’s HotStarTaq polymerase kit (*see Fig. 3* for position of primers relative to the rat genomic *Pig-a* gene). Amplify each fragment separately using an appropriate pair of e-primers in the following reaction mix: 2 µL of 10× PCR buffer (from the QIAGEN’s HotStarTaq kit), 2 µL of dNTP mixture, 2 µL of e-primer pair stock, 11.8 µL of water, 2 µL of nucleic acids isolated from a clone, and 0.2 µL of HotStarTaq polymerase.



Fig. 3 Primers employed for amplification and sequencing of *Pig-a* gene fragments (shown relative to genomic DNA). Numbered boxes represent exons of the rat *Pig-a* gene. The white background inside exons indicates the open reading frame (which starts in exon 2)

Run temperature profile 95 °C × 15 min + (95 °C × 1 min + 57 °C × 1 min + 72 °C × 2 min 30 s) × 40 + 4 °C soak.

3. Analyze 3 μL of reactions on a 1% agarose gel; target fragment sizes are from ~1.5 to ~1.7 kb. If the bands are sufficiently bright and clean, then the amplified fragments can be purified for sequencing.
4. If the e-primer reactions produce only weak bands, then the first round PCR products can be diluted 1:100 in water and nested fragments can be amplified in a second-round PCR with i-pairs of primers and 2 μL of the dilution. Amplify each nested fragment separately using the appropriate pair of i-primers in the following reaction mix: 2 μL of 10× PCR buffer (from QIAGEN's HotStarTaq kit), 2 μL of dNTP mixture, 2 μL of i-primer pair stock, 11.8 μL of water, 2 μL of the 1:100 dilution of the first round PCR product, and 0.2 μL of HotStarTaq polymerase. Run temperature profile 95 °C × 15 min + (95 °C × 1 min + 57 °C × 1 min + 72 °C × 2 min 30s) × 30 + 4 °C soak.
5. Analyze 3 μL of the reactions on a 1% agarose gel; purify the amplified fragments for sequencing. Perform the sequencing using your favorite protocol and instrumentation.
6. For identifying mutations, compare the sequences from mutant cells to the reference sequences available at NCBI website. The rat genomic *Pig-a* sequence can be found at www.ncbi.nlm.nih.gov/gene/?term=363464, and the rat *Pig-a* cDNA sequence containing the complete open reading frame can be found at http://www.ncbi.nlm.nih.gov/nuccore/XM_343783.3?report=genbank.

4 Notes

1. Antibody labeling is a critical step in performing *Pig-a* assays: it is essential that the cells are added last into a homogeneous solution containing antibodies and mixed well by pipetting (not vortexing). Make sure that all cells are exposed to antibodies and not even a tiny fraction of cells remains unlabeled (e.g., sitting on the wall or on the lid of the tube).

2. Flow sorters are sophisticated, expensive, and delicate instruments. It is recommended that the following steps are performed with help from an experienced FACS Aria/FACSDiva operator.
3. During acquisition the cytograms will appear less “dense” than shown in Fig. 2, as images for real-time cytograms usually refresh following every 500–1000 processed events (cells). The cytograms in Fig. 2 show final results for the acquisition of up to 1,000,000 or more events.
4. With consistent labeling and appropriate cytometer maintenance, the voltages and gating for sample acquisition and analysis will not drift from day to day. Once successfully established, the same voltage settings and gating strategy can be used as a template for processing samples on the same cytometer on different experimental days.
5. It is possible that our approach for mutant sorting can be employed for the direct sequencing of the *Pig-a* gene from a single cell. Examples of sequencing using single-cell templates are available in literature; however, the published methods are not as robust as analyses conducted with expanded clones.
6. When the sorting has been successful, cell clones should be observed in 30–50% wells. The degree of individual clonal expansion will be variable: some clones may expand exceptionally well and contain hundreds (perhaps, even thousands) of cells; these might be visible even with the unaided eye. Other clones may expand poorly to just a few cells or maybe a few dozen cells. Some wells may appear to be empty, or contain only a single cell. Very small clones may be difficult to find under the microscope. The plates may remain in the incubator for a few more days of clonal growth, but culturing beyond day 14 usually does not improve the yield of cells.
7. Choosing the clones for molecular analysis may depend upon the sensitivity of the available amplification and sequencing techniques. After 2 weeks of incubation, very small (weakly expanded) clones may contain only dead cells, so the genetic material in these cells may be unsuitable for amplification. On the other hand, if a clone (even a small-size clone consisting of fewer than 100 cells) appears healthy, e.g., having three-dimensional and elongated (dividing) cells on the periphery, then such a clone may be amenable to preservation and sequencing.
8. Both the mRNA and genomic DNA of clones derived from male rats may be analyzed for mutations in the *Pig-a* gene. Sequencing *Pig-a* genomic DNA may be advantageous as it can identify mutations in nontranscribed sequences (e.g., mutations affecting splice sites); also, DNA is easier to work with than

mRNA. DNA is more stable than RNA, and the reverse transcription step is not required for DNA analysis. The overall protocol for detecting, sorting, and expansion of CD48-deficient T-cells was optimized for male rats. A similar protocol can be used for sorting and expansion of mutant phenotype cells from female rats. However, genomic DNA sequencing would not be recommended for analysis of mutant clones derived from females. Female T-cells have two copies of the genomic *Pig-a* gene—mutation in the copy residing on the transcriptionally active X-chromosome can confer the CD48-deficient phenotype. But at the same time, the second copy of the *Pig-a* gene residing on the transcriptionally silent X-chromosome will have wild-type sequence, and it will obscure the mutant allele in sequencing. Thus, analysis of cDNA from females will provide more unambiguous sequencing results. Various protocols and kits for the extraction of mRNA and genomic DNA from small cell samples are commercially available. When DNase digestion is not used, we found that nucleic acids extracted using QIAGEN's RNeasy (Plus) mini kit from fresh or frozen T-cell clones (consisting of more than ~200 cells) contain sufficient genomic DNA for amplification and subsequent sequencing of exons of the *Pig-a* gene.

References

1. Tiede A, Bastisch I, Schubert J, Orlean P, Schmidt RE (1999) Biosynthesis of glycosylphosphatidylinositols in mammals and unicellular microbes. *Biol Chem* 380:503–523
2. Kinoshita T, Fujita M, Maeda Y (2008) Biosynthesis, remodelling and functions of mammalian GPI-anchored proteins: recent progress. *J Biochem* 144:287–294
3. Kinoshita T, Inoue N (2000) Dissecting and manipulating the pathway for glycosylphosphatidylinositol-anchor biosynthesis. *Curr Opin Chem Biol* 4:632–638
4. Tomita M (1999) Biochemical background of paroxysmal nocturnal hemoglobinuria. *Biochim Biophys Acta* 1455:269–286
5. Inoue N, Murakami Y, Kinoshita T (2003) Molecular genetics of paroxysmal nocturnal hemoglobinuria. *Int J Hematol* 77:107–112
6. Bessler M, Mason PJ, Hillmen P, Miyata T, Yamada N, Takeda J, Luzzatto L, Kinoshita T (1994) Paroxysmal nocturnal haemoglobinuria (PNH) is caused by somatic mutations in the *PIG-A* gene. *EMBO J* 13:110–117
7. Araten DJ, Nafa K, Pakdeesuwan K, Luzzatto L (1999) Clonal populations of hematopoietic cells with paroxysmal nocturnal hemoglobinuria genotype and phenotype are present in normal individuals. *Proc Natl Acad Sci U S A* 96:5209–5214
8. Dobrovolsky VN, Elespuru RK, Bigger CA, Robison TW, Heflich RH (2011) Monitoring humans for somatic mutation in the endogenous *PIG-A* gene using red blood cells. *Environ Mol Mutagen* 52:784–794
9. Dertinger SD, Avlasevich SL, Bemis JC, Chen Y, MacGregor JT (2015) Human erythrocyte *PIG-A* assay: an easily monitored index of gene mutation requiring low volume blood samples. *Environ Mol Mutagen* 56:366–377
10. Rondelli T, Berardi M, Peruzzi B, Boni L, Caporale R, Dolara P, Notaro R, Luzzatto L (2013) The frequency of granulocytes with spontaneous somatic mutations: a wide distribution in a normal human population. *PLoS One* 8:e54046
11. Miura D, Dobrovolsky VN, Kasahara Y, Katsuura Y, Heflich RH (2008) Development of an in vivo gene mutation assay using the endogenous *Pig-A* gene: I. Flow cytometric detection of CD59-negative peripheral red blood cells and CD48-negative spleen T-cells from the rat. *Environ Mol Mutagen* 49:614–621
12. Phonethpswath S, Bryce SM, Bemis JC, Dertinger SD (2008) Erythrocyte-based *Pig-a*

- gene mutation assay: demonstration of cross-species potential. *Mutat Res* 657:122–126
13. Dobrovolsky VN, Shaddock JG, Mittelstaedt RA, Manjanatha MG, Miura D, Uchikawa M, Mattison DR, Morris SM (2009) Evaluation of *Macaca mulatta* as a model for genotoxicity studies. *Mutat Res* 673:21–28
 14. Phonethepswath S, Franklin D, Torous DK, Bryce SM, Bemis JC, Raja S, Avlasevich S, Weller P, Hyrien O, Palis J et al (2010) *Pig-a* mutation: kinetics in rat erythrocytes following exposure to five prototypical mutagens. *Toxicol Sci* 114:59–70
 15. Dertinger SD, Bryce SM, Phonethepswath S, Avlasevich SL (2011) When pigs fly: immunomagnetic separation facilitates rapid determination of *Pig-a* mutant frequency by flow cytometric analysis. *Mutat Res* 721:163–170
 16. Gollapudi BB, Lynch AM, Heflich RH, Dertinger SD, Dobrovolsky VN, Froetschl R, Horibata K, Kenyon MO, Kimoto T, Lovell DP, Stankowski LF, White PA, Witt KL, Tanir JY (2015) The in vivo *Pig-a* assay: a report of the International Workshop on Genotoxicity Testing (IWGT) Workgroup. *Mutat Res* 783:23–35
 17. Dobrovolsky VN, Miura D, Heflich RH, Dertinger SD (2010) The in vivo *Pig-a* gene mutation assay, a potential tool for regulatory safety assessment. *Environ Mol Mutagen* 51:825–835
 18. Revollo J, Pearce MG, Petibone DM, Mittelstaedt RA, Dobrovolsky VN (2015) Confirmation of *Pig-a* mutation in flow cytometry-identified CD48-deficient T-lymphocytes from F344 rats. *Mutagenesis* 30:315–324
 19. Dobrovolsky VN, Revollo J, Pearce MG, Pacheco-Martinez MM, Lin H (2015) CD48-deficient T-lymphocytes from DMBA-treated rats have de novo mutations in the endogenous *Pig-a* gene. *Environ Mol Mutagen* 56:674–683

Detection of In Vivo Mutation in the *Pig-a* Gene of Mouse Bone Marrow Erythroids

Takafumi Kimoto and Daishiro Miura

Abstract

Detection of in vivo mutation is important for evaluating the health risks associated with chemicals. The *Pig-a* in vivo gene mutation assay has been developed over the last decade for this purpose. Most approaches for the assay, however, measure cells with a *Pig-a* mutant phenotype in erythrocytes from the peripheral blood, with the mutations causing the phenotype being difficult to determine directly. This chapter describes a procedure for detecting mutations in the *Pig-a* gene of phenotypically mutant mouse bone marrow erythroids, the precursors of peripheral blood erythrocytes. The strategy for molecular analysis of *Pig-a* gene mutation includes enrichment of GPI-anchor deficient cells with a cell sorter followed by a cloning and sequencing of *Pig-a* cDNAs.

Key words CD24, GPI-anchor, Flow cytometry, Sorting, Cloning

1 Introduction

The in vivo mutation assay using the *Pig-a* gene as an endogenous reporter of somatic cell mutation is a promising tool for evaluating the mutagenicity of chemicals [1–4]. The *Pig-a* gene (which stands for phosphatidylinositol glycan class A gene) codes for an enzyme that is involved in an early step of glycosyl phosphatidylinositol (GPI) anchor synthesis. In mammalian cells, the *Pig-a* gene is located on the X-chromosome, while all other genes required for GPI synthesis (e.g., *Pig-b*, *Pig-c*, and approximately 20 other genes) are autosomal, present in two functional copies. For almost any gene, being on the X-chromosome enables single mutations to produce an altered cell phenotype, which for *Pig-a* means that a single inactivating mutation in the single functional copy of the gene can abolish GPI synthesis, resulting in deficiency of GPI-anchored protein markers (e.g., CD59 or CD24) on the surface of the mutant cell. The *Pig-a* mutation assay is anticipated to be a useful trans-species tool for evaluating the in vivo mutagenicity of

chemicals because GPI anchor biosynthesis and the *Pig-a* gene location are highly conserved in mammalian species [1–5].

Currently there are two distinct approaches for detecting and quantifying *Pig-a* mutant cells. One is using flow cytometric (FCM) analysis to discriminate GPI-deficient mutant cells from wild-type cells by employing fluorescently conjugated antibodies against GPI-anchored protein markers. Flow cytometric analysis is a relatively high-throughput approach that facilitates measuring mutant frequencies in cells from peripheral blood (mainly erythrocytes) or (rarely) from other hematopoietic organs [6, 7]. An alternative approach to detect *Pig-a* mutant cells is limiting-dilution culturing of cells capable of clonal growth (i.e., T-lymphocytes) using selection by proaerolysin (ProAER). ProAER is a bacterial enterotoxin (produced by a Gram-negative *Aeromonas hydrophila*) that binds to GPI anchors present on the surface of wild-type cells and induces apoptosis. *Pig-a* mutant cells are not affected by ProAER and can grow in its presence [7, 8]. Molecular analysis of *Pig-a* mutants has been developed for rat T-lymphocytes expanded under ProAER selection in cell culture and for mutant mouse bone marrow erythroids identified and sorted by flow cytometry [8, 9].

In this chapter, we describe a procedure for the molecular analysis of *Pig-a* mutants in mouse bone marrow erythroids. As a first step, a five color flow cytometric analysis of *Pig-a* gene mutation is conducted using four fluorescently conjugated antibodies (specific for CD24, CD45, CD71, and TER-119) and a fluorescent nucleic acid viability stain (7-AAD). GPI anchor deficient erythroids identified by the flow analysis as CD24-negative cells are collected by cell sorting. The cell pool is lysed and *Pig-a* cDNAs synthesized by reverse transcription of RNA from the mutants. *Pig-a* cDNAs are then PCR amplified, ligated into plasmid vectors, and transformed into bacterial hosts for subsequent selection with ampicillin. Plasmid DNA is purified from individual ampicillin-resistant colonies and the cloned *Pig-a* cDNAs are analyzed by DNA sequencing.

2 Materials

2.1 Flow Cytometric *Pig-a* Assay for Mouse Bone Marrow Erythroids

1. FACSARIA I flow cytometer, equipped with a 70 μm sorting nozzle, 488 nm (blue) and 635 nm (red) excitation lasers (BD Biosciences, Tokyo Japan) or an equivalent cell sorter by another manufacturer.
2. Consumables for operating FACSARIA (e.g., FACSSheath fluid).
3. Fetal Bovine Serum (FBS) (heat inactivated for 30 min at 65 $^{\circ}\text{C}$).

4. Phosphate Buffered Saline without magnesium and calcium (PBS).
5. Staining Buffer (PBS + 2% FBS).
6. Inverted microscope.
7. Multi-chamber counting hemocytometer slides.
8. 1.5-mL microcentrifuge tubes.
9. Benchtop centrifuge for 1.5-mL tubes.
10. Liquid aspirator.
11. 10-, 20-, 100-, 200-, and 1000- μ L micropipettes and matching tips.
12. 5-mL round bottom polystyrene tubes with 35- μ m mesh cell strainer cap (Corning, Tokyo Japan).
13. Antibodies and reagents for cell labeling and analysis (all from BD Biosciences): anti-mouse CD24 antibody (clone M1/69, FITC-conjugated), anti-mouse CD71 antibody (clone C2, PE-conjugated), anti-mouse CD45 antibody (clone 30-F11, APC-conjugated), anti-mouse TER-119 antibody (clone TER-119, PE-Cy7-conjugated), mouse BD Fc Block (anti-mouse CD16/CD32, unconjugated), BD Via-Probe (7-AAD).

2.2 Amplification of *Pig-a* cDNA from Sorted Cells Deficient in GPI-Anchored Marker

1. SuperScript III First-Strand Synthesis System for RT-PCR (Thermo Fisher Scientific, Kanagawa Japan).
2. Bovine Serum Albumin (BSA).
3. DEPC-treated water.
4. SUPERase-In RNase inhibitor (20 U/ μ L) (Thermo Fisher Scientific).
5. Dry ice.
6. 0.2-mL PCR tubes.
7. 96-well plate cold rack for PCR tubes.
8. Thermal cycler (e.g., GeneAmp PCR System 9700 thermocycler, Applied Biosystems, Foster City, CA).
9. RNaseOut (40 U/ μ L) (Thermo Fisher Scientific).

2.3 Molecular Analysis of *Pig-a* cDNA

1. PrimeSTAR Max DNA polymerase kit containing 2 \times Premix solution (Takara Bio, Shiga, Japan).
2. Primers for amplification and sequencing of *Pig-a* cDNA shown in 5' \rightarrow 3' sequence format. All primers are at concentration of 3 μ M.
 mPigA-F1 (first round PCR) GACTGGAGGGTGACAGAAGACACA.
 mPigA-R1 (first round PCR) TACTTGGTGTATGCCAGCGATGAT.
 MpigAW1-F (nested PCR) TGGCTTGCTCTGAGAACTGA.

MpigAW2-R (nested PCR) GGAGCAAACCTCCTTTC
AAATGC.

mPigA-Seq1F (sequencing) TGC GTGAACCACTCA
GCAT.

mPigA-Seq2F (sequencing) CGATAATCCATTCCCACA
GTTC.

mPigA-Seq3F (sequencing) AAGGGACTGATTTGCTTA
GTGGT.

mPigA-Seq4F (sequencing) TTTGTGTGACGGTCTGGA
AAAA.

T7 Primer (sequencing) GTAATACGACTCACTATAGGGC.

T3 Primer (sequencing) AATTAACCCTCACTAAAGGGA.

3. DNase-free water.
4. Agarose (electrophoresis-grade).
5. Horizontal gel electrophoresis apparatus and power supply.
6. QIAquick Gel Extraction kit (QIAGEN, Tokyo Japan).
7. TArget Clone -Plus- (TOYOBO, Osaka Japan).
8. Competent Quick DH5 α (TOYOBO).
9. Fast-Media Amp Agar X-Gal (InVivoGen, San Diego, CA).
10. Water bath.
11. Insert Check-Ready-*Blue* (TOYOBO).
12. Orbital incubator shaker (e.g., BR-40LF, TAITEC, Saitama, Japan).
13. QIAprep Spin Miniprep kit (QIAGEN).

3 Methods

3.1 *Pig-a* Assay in Mouse Bone Marrow Erythroids (See Note 1)

3.1.1 Staining Bone Marrow Cells with Fluorescent Antibodies

1. Collect bone marrow cells from mouse femurs by flushing with 1 mL of 100% FBS. Centrifuge the samples at $420 \times g$ for 5 min at room temperature, aspirate the supernatants, and resuspend the cell pellets in 1 mL of staining buffer.
2. Remove debris from the samples by filtering cell suspensions through 35- μ m cell strainer cap into 5-mL round bottom polystyrene Falcon tubes (*see Note 2*).
Dilute 10 μ L of the filtrated suspension into 990 μ L of PBS for determining concentration of nucleated cells in the sample. Inject appropriate volume of the diluted sample into the counting chamber of hemocytometer slide, and then, on an inverted microscope, count the number of nuclear cells.
3. Based on the determined cell concentrations, dilute the samples to final $1\text{--}2 \times 10^7$ cells/mL; and then dispense the cells in 100- μ L aliquots into microcentrifuge tubes. As many tubes with 100- μ L aliquots should be prepared from each mouse sample as possible (e.g., ten tubes with 100- μ L aliquots of

2×10^7 cells/mL would be appropriate for each mouse treated with a genotoxic compound).

4. Add to the dispensed aliquots 1 μ g of mouse BD Fc Block to reduce subsequent nonspecific labeling with fluorescent antibodies, mix the contents by gently tapping the bottom of microcentrifuge tubes and then incubate the tubes for 5 min at 4 °C.
5. Add to the aliquoted cells in microcentrifuge tubes 1 μ g of each of the following four fluorescent antibodies: anti-mouse CD24 antibody, anti-mouse CD45 antibody, anti-mouse TER-119 antibody, and anti-mouse CD71 antibody. The rationale for the use of these antibodies is to detect CD45-negative, TER-119-positive, and CD71-positive cells which are defined as erythroids (*see* Subheading 3.1.2, step 4). Mix the labeling samples by gentle pipetting. These samples will be subsequently used for sorting *Pig-a* mutant erythroids.
6. Prepare four additional FCM compensation control samples each consisting of 100 μ L of cells (preferably derived from untreated mice) stained with Fc Block and with only one fluorescent antibody (four tubes for four different antibodies). These will be used for determining values for fluorescence compensation.
7. Also, prepare a mutant-mimic control sample consisting of 100 μ L of cells stained with Fc Block, anti CD45, anti CD71, and anti TER-119 (i.e., all antibodies, but anti CD24). This will be used for determining the gate for CD24-deficient *Pig-a* mutant cells.
8. After incubation for 30 min at 4 °C in the dark, centrifuge the tubes with antibody-stained cells at $420 \times g$ for 5 min at room temperature. Aspirate the supernatants from all tubes. Resuspend the single antibody-stained FCM compensation controls and mutant-mimic control in 0.5 mL of staining buffer. For sorting samples, add 1.0 mL of staining buffer to the first tube with cells stained with all four fluorescent antibodies, resuspend the pellet and transfer the entire contents to the next tube with the pellet of four antibody-labeled cells. Resuspend the cells and transfer the whole contents into the next tube. Repeat the process for the rest of the available tubes to concentrate the cells for sorting in a single tube.
9. Filter the labeled cell samples (the sorting samples and controls) through 35- μ m cell strainer caps into 5-mL Falcon tubes (*see* Note 2). Keep the cells on ice in the dark until ready for analysis/sorting.
10. Just prior to analysis or sorting, add 20 μ L of BD Via-Probe to the cells. After a few minutes incubation on ice, process the samples on the cell sorter.

3.1.2 Analysis of GPI-
Anchored Protein
Expression with Flow
Cytometry

1. For both analysis and sorting, start FACSaria cell sorter according to the operating manual. Check performance of the instruments as recommended by the manufacturer (*see Note 3*).
2. As the first step in designing the gating strategy, adjust fluorescence compensation according to the instrument manual using FCM control samples, cells stained with single fluorescent antibodies. Figure 1 shows typical cytograms for detecting *Pig-a* mutant erythroid cells deficient for GPI-anchored protein CD24.
3. First, the cells are gated by light scatter (Fig. 1a). Then dead cells stained with Via-Probe are excluded from the analysis (Fig. 1b).
4. Next, viable cells are analyzed for surface expression of CD45 and CD71 (Fig. 1c). Actively proliferating erythroblasts are positive for CD71 and negative for CD45. These are gated for further analysis of TER-119 expression for excluding contaminating nonerythroid cells (Fig. 1d).
5. Finally, approximately 300,000 TER-119-positive erythroids are analyzed for the presence of GPI-anchored protein CD24 on their surface (*see Note 4*). Figure 1e and 1f show typical

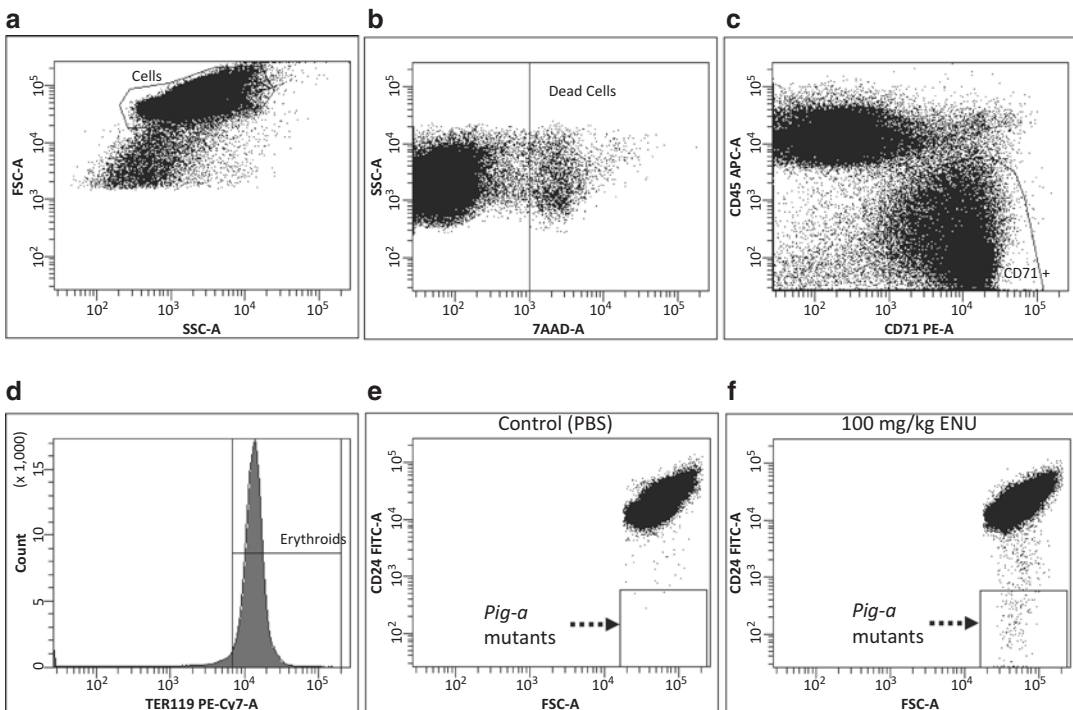


Fig. 1 Typical flow cytograms for *Pig-a* assay in mouse bone marrow erythroids. Description for each cytogram is given in the text. (a) Gating cells, (b) Excluding dead cells, (c) Gating CD71⁺ cells, (d) Gating TER119⁺ erythroids, (e) CD24 expression analysis of control (PBS), (f) CD24 expression analysis of 100 mg/kg ENU

cytograms for CD24 expression analysis of bone marrow cells derived from mice treated with PBS (negative control) and mice treated with a single dose of 100 mg/kg of *N*-ethyl-*N*-nitrosourea (ENU) as measured on days 7–28 after the treatment. The frequencies of CD24-negative cells for each animal are calculated using the following formula:

$$\frac{[\text{Number of cells in the “}Pig-a\text{ mutants” gate}]}{([\text{Number of cells in the “Erythroids” gate}] \div 10^6)}.$$

3.2 Sorting Cells Deficient in GPI-Anchored Protein CD24, and Synthesizing *Pig-a* cDNA from the Sorted Cells

3.2.1 Sorting CD24-Negative *Pig-a* Mutant Erythroids

1. Prior to start of sorting, thaw the tubes with 10 mM dNTPs and Oligo(dT) from the SuperScript III First-Strand Synthesis System for RT-PCR on ice. Keep other reagents of the System at -20°C .
2. Prepare 100 ng/ μL solution of BSA. Dissolve 0.5–1.0 mg of BSA in 5–10 mL of DEPC-treated water.
3. Take SUPERase-In (20 U/ μL) from -20°C freezer and store on ice. Mix in 0.2-mL PCR tubes: 6 μL of DEPC-treated water, 1 μL of 10 mM dNTPs, 1 μL of Oligo(dT), 1 μL of SUPERase-In, and 1 μL of BSA solution (*see Note 5*).
4. Store all tubes in a cold 96-well tube rack. The rack with tubes should be kept on dry ice in a styrofoam box.
5. The settings for sorting (e.g., side stream, drop delay, sorting device homing) should be adjusted according to the manufacturer’s instructions. For FACSaria sorters running FACSDiva software, sheath pressure should be set to 35 psi, a 70- μm nozzle should be used, and the sorting precision mode should be set to “purity” (*see Note 6*).
6. Install a 0.2-mL PCR tube containing 10 μL of mixed reagents (from Subheading 3.2.1, step 4) on the collection device of the instrument. Load a sample labeled with all antibodies, begin data acquisition and sorting. Once up to 100 CD24-negative erythroid cells are sorted, stop the sort, remove the tube with the sorted cells from the collecting device and immediately place it back into dry ice-cold 96-well tube rack.
7. Install another 0.2-mL tube from the cold rack onto the collecting device, resume sorting of CD24-negative erythroids as in the previous step. Continue sorting until all tubes prepared in Subheading 3.2.1, step 3, are used or the cell sample is exhausted. Collect a tube with a few hundred CD24-positive erythroids (or bulk bone marrow cells) as positive control for RT-PCR and sequence analysis, if necessary.

3.2.2 *Pig-a* cDNA Synthesis

1. Transfer the components of the SuperScript III First-Strand Synthesis System for RT-PCR (10 \times RT buffer, 25 mM MgCl_2 , 0.1 M DTT, and SuperScript III RT 200 U/ μL) and the tube with RNaseOUT (40 U/ μL) from -20°C freezer to ice.

2. Lyse cells from Subheading 3.2.1, step 7: incubate tubes with sorted cells at 65 °C for 5 min in a thermal cycler, and then move the tubes onto ice until the next step.
3. Prepare reverse transcription master mix in a volume sufficient to process all tubes with lysed cells from Subheading 3.2.2, step 2. The following reagents are required for processing one tube: 2 µL of 10 × RT buffer, 4 µL of 25 mM MgCl₂, 2 µL of 0.1 M DTT, 1 µL of RNaseOUT, and 1 µL of SuperScript III RT.
4. Dispense the reverse transcription master mix in 10-µL aliquots into the tubes containing cell lysates. Mix the contents of the tubes gently.
5. Transfer tubes to the thermal cycler and start the reverse transcription temperature profile: 50 °C × 50 min + 85 °C × 5 min + 4 °C soak.
6. After the reverse transcription step, degrade the remaining RNA in the samples by adding 1 µL of RNaseH in the kit to the tubes and incubating the tubes for 20 min at 37 °C (*see Note 7*).

3.3 Molecular Analysis of *Pig-a* cDNA

3.3.1 Amplification of *Pig-a* cDNA

1. Dispense 12.5 µL of 2 × Premix solution from the PrimeSTAR Max DNA polymerase kit into new 0.2-mL PCR tubes, one tube for each sample to be processed.
2. Add up to 7.5 µL of synthesized cDNA from Subheading 3.2.2, step 6, to the PCR tubes and mix the contents gently.
3. Prepare a primer mix with 2.5 µL of forward primer (mPigA-F1) and 2.5 µL of reverse primer (mPigA-R1) per each sample to be processed. Dispense 5 µL of the primer mix into the PCR tubes with cDNA in Premix solution. The strategy for amplification and sequencing of *Pig-a* cDNA is shown in Fig. 2.
4. Adjust the final volume in the tubes to 25 µL with DNase-free water.
5. Perform the first round of PCR on a thermocycler using the following temperature profile: (98 °C × 10 s + 55 °C × 5 s + 72 °C × 30 s) × 30 + 4 °C soak.
6. Amplify the *Pig-a* cDNA template synthesized in the first round of PCR using nested PCR. Dispense 12.5 µL of 2 × Premix solution into new 0.2-mL PCR tubes, add 2 µL of amplified cDNA from Subheading 3.3.1, step 5, and mix the contents gently.
7. Prepare a primer mix with 2.5 µL of forward primer (MpigAW1-F) and 2.5 µL of reverse primer (MpigAW2-R) per each sample to be analyzed. Dispense 5 µL of the primer mix into each tube.

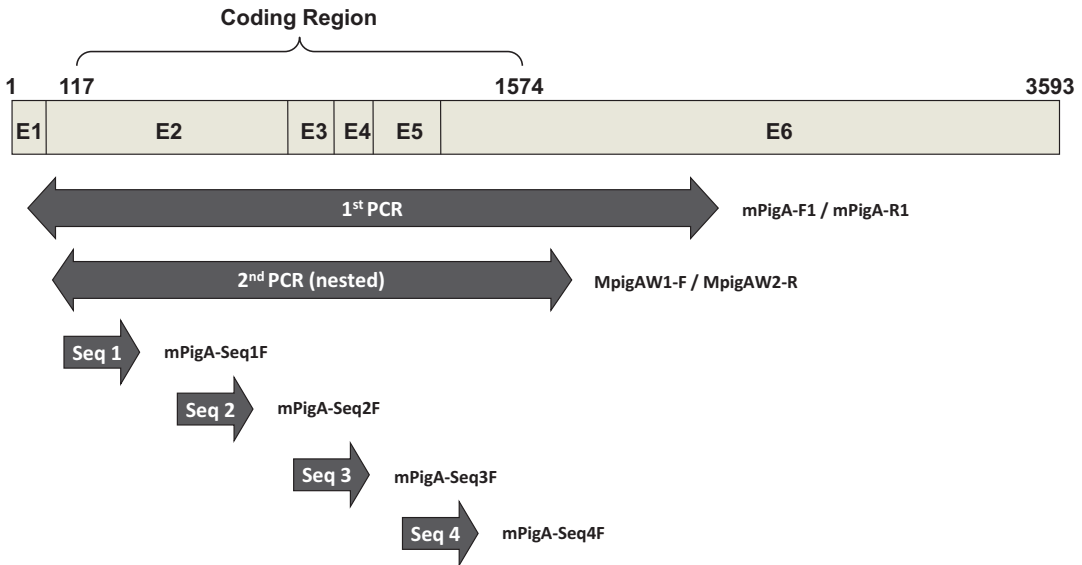


Fig. 2 Schematic representation of mouse *Pig-a* cDNA (GenBank accession number NM_011081) showing primers used for amplification and sequencing. E1 through E6 are exons; exon 1 of the *Pig-a* gene is not translated. The combination of mPigA-F1 and mPigA-R1 is for first PCR to cover the coding region. The nested primer pair MpigAW1-F/MpigAW2-R is for second PCR to amplify the coding region. Seq1, seq2, seq3, and seq4 indicate the relative positions of primers mPigA-Seq1F, mPigA-Seq2F, mPigA-Seq3F, and mPigA-Seq4F

8. Adjust the final volume to 25 μL with 5.5 μL of DNase-free water.
9. Process on a thermal cycler using the temperature profile: (98 $^{\circ}\text{C} \times 10 \text{ s} + 55 \text{ }^{\circ}\text{C} \times 5 \text{ s} + 72 \text{ }^{\circ}\text{C} \times 10 \text{ s}) \times 35 + 4 \text{ }^{\circ}\text{C}$ soak.
10. Mix the whole 25 μL of the amplified nested *Pig-a* cDNA product with 5 μL of $6 \times$ gel loading dye and process on 1, 1.5, or 2% agarose gel. Add DNA stain (ethidium bromide or SYBRgreen) to the running buffer. The size of the nested PCR product is in the range from 1000 to 1600 bp. Photograph the resulting gel using documentation system and UV light transilluminator.
11. Using razor blades, cut out all potential *Pig-a* cDNA bands from the gel and purify them with QIAquick Gel Extraction Kit according to the manufacturer's instructions.
12. Determine DNA concentrations of each PCR product and dilute them with DNase-free water to 52.3 ng/ μL .
13. Mix 5 μL of adjusted amplified cDNA sample with 5 μL of $2 \times$ Premix solution; store the mixture at $-20 \text{ }^{\circ}\text{C}$ until ready for ligation into pTA2 vector.

3.3.2 Cloning and Molecular Analysis of the Amplified *Pig-a* cDNA (See Note 8)

1. Before ligation, mix 9 μL of amplified *Pig-a* cDNAs from the previous step with 1 μL of $10 \times$ A-attachment Mix from TArget Clone -Plus- and then incubate on thermal cycler at 60 $^{\circ}\text{C}$ for 10 min. Store samples at 4 $^{\circ}\text{C}$ until ready for the next step.

2. Ligate amplified *Pig-a* cDNAs with A-overhangs into pTA2 vector in the following mixture: 5 μ L of 2 \times ligation buffer, 1 μ L of pTA2 vector, 1 μ L of T4 DNA ligase, 3 μ L of amplified cDNA from Subheading 3.3.2, step 2. Incubate at 24 $^{\circ}$ C for 30 min, or at 4 $^{\circ}$ C for 12 to 18 h. Store the ligated samples at 4 $^{\circ}$ C until ready to use for transfection.
3. For transfection, prepare the appropriate number of LB soft agar plates with Fast-Media Amp Agar X-Gal which contains 100 μ g/mL of ampicillin, 100 μ g/mL of IPTG, and 100 μ g/mL of X-Gal. Mix 2 μ L of ligated sample from the previous step with 100 μ L of Competent Quick DH5 α and then place the mixture on ice for at least 5 min.
4. Incubate the transformation samples in water bath at 42 $^{\circ}$ C for 30 s for heat shock and then chill them on ice.
5. Pour each transformation mixture onto a separate LB agar plate and spread it uniformly with a spreader. Invert the plate and incubate at 37 $^{\circ}$ C for 8–16 h. Store the remainder of the ligated samples at –20 $^{\circ}$ C.
6. Select several white colonies and check for the presence of *Pig-a* cDNA inserts by colony-direct PCR. Use primers provided in the Insert Check-Ready-*Blue* kit and follow the procedure described in the manual. Amplify the inserts using the following temperature profile: 94 $^{\circ}$ C \times 4 min + (94 $^{\circ}$ C \times 30 s + 55 $^{\circ}$ C \times 5 s + 72 $^{\circ}$ C \times 1 min) \times 30 + 4 $^{\circ}$ C soak.
7. Check PCR products by agarose gel electrophoresis. DNA bands that are less than 200 bp are not specific to *Pig-a*; colonies producing such bands can be discarded. Choose colonies that produce appropriately sized DNA fragments (for *Pig-a*, usually more than 1000 bp); inoculate the colonies into 3 mL of LB medium containing 100 μ g/mL ampicillin. Incubate at 37 $^{\circ}$ C for 15 h. Extract and purify plasmids from minipreps using QIAprep Spin Miniprep kit. Determine DNA concentration in each sample and dilute it to appropriate concentration for sequencing analysis (*see* Note 9).
8. Perform sequencing reactions and identify the potential mutation in the *Pig-a* cDNA using your favorite sequencing protocol, instrumentation, and software. Recommended primers for sequencing are listed in Subheading 2.3, step 2. For complete coverage of amplified *Pig-a* cDNA in Sanger method, it is recommended to use all six sequencing primers. Mutations in individual clones should be identified by comparing their sequences to the reference wild-type *Pig-a* cDNA sequence (GenBank accession number NM_011081).

4 Notes

1. For procedures starting from Subheading 3.1, samples should be protected from light as much as possible to preserve the integrity of fluorescent antibodies.
2. A Pasteur pipette is preferred for this process. Discharge the cell suspension from the pipette held at a right angle to the cell strainer.
3. Flow cytometers are delicate, complicated, and expensive instruments. It is recommended that all steps from adjusting fluorescence measurement to designing analysis strategy and sorting be performed with help from an experienced operator.
4. The gate for detecting and enumerating CD24-negative cells, the “*Pig-a* mutants” gate in Fig. 1e, is determined by processing the mutant-mimic control sample. The shape and the size of the “*Pig-a* mutants” gate should be adjusted to include more than 99% of CD45-negative, CD71-positive, TER-119-positive viable erythroid cells that are negative for FITC fluorescence (as they were not stained with FITC-conjugated anti CD24).
5. At least ten tubes should be prepared for each sorted sample.
6. For sorting into 0.2-mL PCR tubes using a FACSAria sorter, use 96-well plate as a collection device (rather than two- or four-way device), which allows both sorting into multi-well plates and tubes installed in multi-well racks. See manufacturer’s instruction manual in case of using 96-well plate.
7. At this point, it might be possible to store the samples at -20 or -80 °C. Nevertheless, we usually proceed immediately to cDNA amplification step to assure sample stability.
8. It is necessary to use cloning since the amplified *Pig-a* cDNA was produced from bulk-sorted mutant cells. Ligation of *Pig-a* cDNA into pTA2 vector and transfection of plasmids into Competent Quick DH5 α are basically conducted according to the manufacturer’s instruction manual.
9. If a white colony does not produce the anticipated DNA band in the insert check PCR, use an alternative PCR method with PrimeSTAR Max polymerase and primers that were employed for amplification of *Pig-a* cDNA. Dispense 12.5 μ L of 2 \times Premix solution into new 0.2-mL PCR tubes; then add 2.5 μ L of forward primer (mPigA-F1) and 2.5 μ L of reverse primer (mPigA-R1). Adjust the final volume with DNase-free water to 25 μ L. Pick the colony with the tip of a micropipette and transfer it to a PCR tube: gently shake. Continue with the PCR protocol described in Subheading 3.3.1, **step 9**.

Acknowledgments

The authors would like to thank Ms. Kumiko Suzuki-Okada and Xiao Mei Kobayashi for their cooperation and technical assistance with all the experiments.

References

1. Dobrovolsky VN, Miura D, Heflich RH, Dertinger SD (2010) The *in vivo* *Pig-a* gene mutation assay, a potential tool for regulatory safety assessment. *Environ Mol Mutagen* 51:825–835
2. Gollapudi BB, Lynch AM, Heflich RH, Dertinger SD, Dobrovolsky VN, Froetschl R, Horibata K, Kenyon MO, Kimoto T, Lovell DP, Stankowski LF Jr, White PA, Witt KL, Tanir JY (2015) The *in vivo* *Pig-a* assay: a report of the international workshop on genotoxicity testing (IWGT) workgroup. *Mutat Res* 783:23–35
3. Heflich RH, Dobrovolsky VN, Dertinger SD (2015) Continued progress in developing the *Pig-a* gene mutation assay. *Mutagenesis* 30:313–314
4. Miura D (2014) The *in vivo* *Pig-a* gene mutation assay. *Genes Environ* 36:169–173
5. Phonethepswath S, Bryce SM, Bemis JC, Dertinger SD (2008) Erythrocyte-based *Pig-a* gene mutation assay: demonstration of cross-species potential. *Mutat Res* 657:122–126
6. Miura D, Dobrovolsky VN, Kasahara Y, Katsuura Y, Heflich RH (2008) Development of an *in vivo* gene mutation assay using the endogenous *Pig-a* gene: I. Flow cytometric detection of CD59-negative peripheral red blood cells and CD48-negative spleen T-cells from the rat. *Environ Mol Mutagen* 49:614–621
7. Bryce SM, Bemis JC, Dertinger SD (2008) *In vivo* mutation assay based on the endogenous *Pig-a* locus. *Environ Mol Mutagen* 49:256–264
8. Miura D, Dobrovolsky VN, Mittelstaedt RA, Kasahara Y, Katsuura Y, Heflich RH (2008) Development of an *in vivo* gene mutation assay using the endogenous *pig-a* gene: II. Selection of *Pig-a* mutant rat spleen T-cells with proaerolysin and sequencing *Pig-a* cDNA from the mutants. *Environ Mol Mutagen* 49:622–630
9. Kimoto T, Suzuki K, Kobayashi XM, Dobrovolsky VN, Heflich RH, Miura D, Kasahara Y (2011) Manifestation of *Pig-a* mutant bone marrow erythrocytes and peripheral blood erythrocytes in mice treated with *N*-ethyl-*N*-nitrosourea: direct sequencing of *Pig-a* cDNA from bone marrow cells negative for GPI-anchored protein expression. *Mutat Res* 723:36–42

The Use of Bacterial Repair Endonucleases in the Comet Assay

Andrew R. Collins

Abstract

The comet assay is a sensitive electrophoretic method for measuring DNA breaks at the level of single cells, used widely in genotoxicity experiments, in biomonitoring, and in fundamental research. Its sensitivity and range of application are increased by the incorporation of an extra step, after lysis of agarose-embedded cells, in which the DNA is digested with lesion-specific endonucleases (DNA repair enzymes of bacterial or phage origin). Enzymes with specificity for oxidized purines, oxidized pyrimidines, alkylated bases, UV-induced cyclobutane pyrimidine dimers, and misincorporated uracil have been employed. The additional enzyme-sensitive sites, over and above the strand breaks detected in the standard comet assay, give a quantitative estimate of the number of specific lesions present in the cells.

Key words Comet assay, DNA damage, Altered bases, Electrophoresis, Repair endonucleases

1 Introduction

The comet assay (single cell gel electrophoresis) is widely used in genetic toxicology for measuring DNA damage in the form of strand breaks (SBs). It can be applied to cells from animal tissues after *in vivo* testing, or to cultured cells used in *in vitro* experiments. Cells are embedded in agarose on a microscope slide, and lysed with 2.5 M NaCl and non-ionic detergent; this removes membranes and soluble cell components, including most of the histones, leaving the DNA still attached to the nuclear matrix in a structure known as a nucleoid. Although the nucleosomes (around which the DNA is wound in the living cell) are disrupted by removal of histones, the turns of the DNA around the histone-nucleosome core are retained in the form of (negative) supercoils. The DNA is not free to rotate, being constrained as a series of loops attached at their bases to the matrix.

After lysis, the gel-embedded nucleoids are incubated in an alkaline solution and then electrophoresed at high pH. DNA is attracted to the anode, but little migration occurs unless breaks are

present in the DNA. A single break in a DNA loop relaxes supercoiling in the loop and it is then free to extend. After electrophoresis, gels are neutralized and “comets” visualized by fluorescence microscopy with a suitable stain. The relative intensity of fluorescence in the comet tail, reflecting the number of relaxed DNA loops, is thus a quantitative measure of DNA break frequency.

SBs are just one form of DNA damage. Most chemical genotoxic agents induce other kinds of damage, such as small base changes (oxidation or alkylation), base loss, cross-links, or addition of large chemical groups (bulky adducts). Enzymes with specific endonucleolytic activity against some of these DNA lesions have been employed in conjunction with the comet assay to enhance its sensitivity and selectivity. The gels containing nucleoids are incubated with enzyme following the lysis step, in parallel with control gels incubated with enzyme buffer alone. Thus endonuclease III or Nth (EC 4.2.99.18) is used to detect oxidized pyrimidines [1]; formamidopyrimidine DNA glycosylase (Fpg; EC 3.2.2.23) recognizes oxidized guanines [2]; and 3-methyladenine DNA glycosylase or AlkA (EC 3.2.2.21) has activity against alkylated bases [3]. T4 endonuclease V, also known as DenV endonuclease V (EC 3.1.25.1), repairs UV-damaged DNA, and has been used to detect cyclobutane pyrimidine dimers in the comet assay [4]. Uracil DNA glycosylase (Udg; EC 3.2.2.3) detects uracil that has been misincorporated in DNA [5]. UvrABC, which recognizes bulky adducts, unfortunately has not yet been used successfully in the comet assay. Net enzyme-sensitive sites are calculated by subtracting the comet score for the enzyme buffer control from the comet score for digestion with enzyme.

The first application of a repair endonuclease was in a nutritional intervention study [6]. Endonuclease III was used to measure the level of oxidized pyrimidines in peripheral blood mononuclear cells (“lymphocytes”) taken from volunteers before and after a 20-week supplementation with a mixture of antioxidants. A substantial decrease in oxidized bases was seen in those taking supplements compared with a placebo group. Since then the assay has been widely used as a biomonitoring tool. The other main application is in genotoxicity testing. Fpg is particularly useful as it enhances the ability of the comet assay to detect various kinds of lesion [7]. Figure 1 illustrates the ability of Fpg to reveal enzyme-sensitive sites in the DNA from cells treated with several (though not all) test chemicals with known mutagenic activity. Recently, Fpg has been included in tests for the genotoxic effects of nanomaterials—presumably detecting the oxidation damage that frequently accompanies exposure of cells to nanomaterials [8].

This chapter describes the use of specific endonucleolytic enzymes in this way. A general knowledge of the comet assay is assumed or the reader is referred to a review article such as [9].

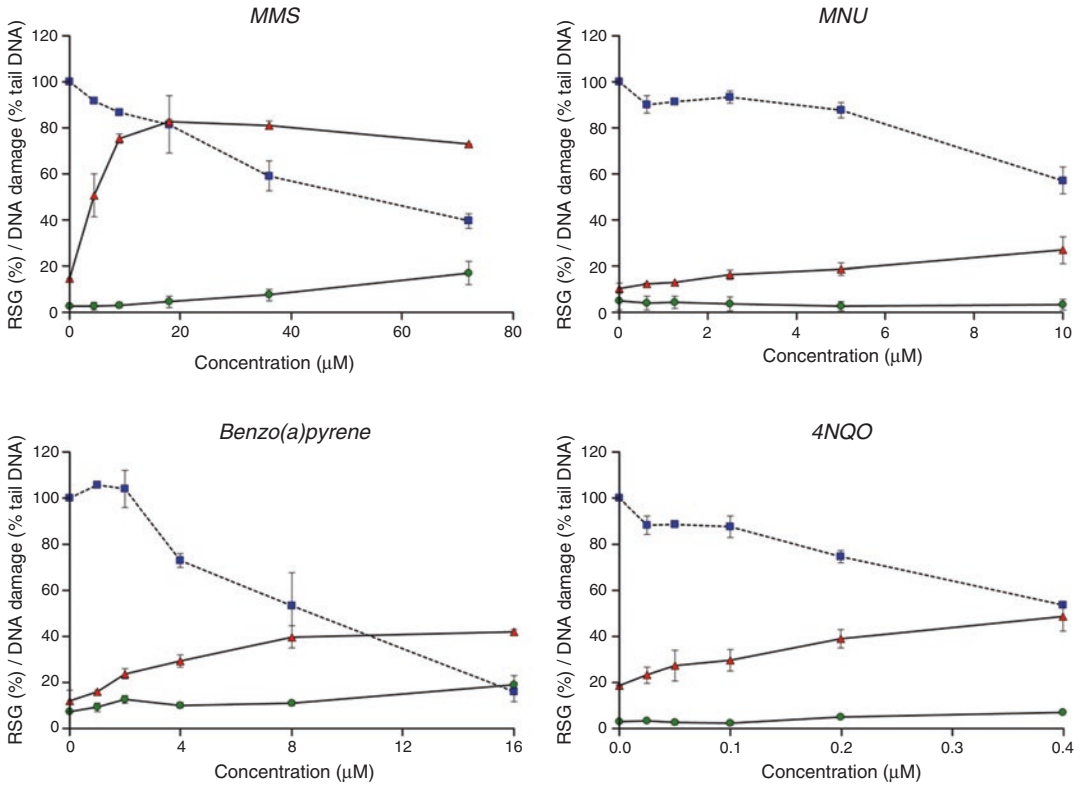


Fig. 1 Detecting effects of known genotoxic chemicals on TK6 lymphoblastoid cells over a range of concentrations with the comet assay. *Square* symbols and broken line represent cytotoxicity (Relative Suspension Growth at 48 h). DNA SBs and Fpg-sensitive sites, as indicated by % tail DNA in the comet assay, are shown as *circles* and *triangles*, respectively. Data are mean values from two experiments, and the *bars* indicate the range of values. MMS, methylmethanesulfonate; MNU, methylnitrosourea; 4NQO, 4-nitroquinoline 1-oxide (reprinted from reference [7], by permission of Oxford University Press)

However, sufficient information is included to enable the assay for specific DNA damage to be set up without prior comet assay experience.

2 Materials

2.1 Equipment

Standard comet assay equipment (electrophoresis tank, power supply, fluorescence microscope).

Staining jars, vertical or horizontal (depending on how many slides are to be incubated).

Enzyme incubation box: this can be a plastic food-storage box with lid, with water in the bottom to maintain humidity, and a platform above the water for the slides to be placed on. The box should be kept at 37 °C (prewarmed so that the enzyme reaction is optimal).

2.2 Solutions

Prepare solutions from appropriate stocks, such as 0.5 M Na₂EDTA, 1 M Tris, 10 M NaOH, 1 M KCl, etc. Keep solutions at 4 °C. It is also useful to keep a stock of distilled water at 4 °C for rapid preparation of cold solutions.

1. Lysis solution: 2.5 M NaCl, 0.1 M EDTA, 10 mM Tris. Prepare 1 l. Set pH to 10 with either solid NaOH, or preferably concentrated (10 M) NaOH solution. Add 35 mL of NaOH straight away to ensure that EDTA dissolves, and then add dropwise to pH 10. Add 1 mL Triton X-100 per 100 mL immediately before use.
2. Enzyme reaction buffer (*see Notes 1 and 2*): 40 mM HEPES, 0.1 M KCl, 0.5 mM EDTA, 0.2 mg/mL bovine serum albumin, pH 8.0 with KOH. This buffer can be made as 10× stock, adjusted to pH 8.0, and frozen at −20 °C.
3. Electrophoresis solution: 0.3 M NaOH, 1 mM EDTA.
4. Neutralizing buffer: Phosphate buffered saline (PBS) (*see Note 3*).
5. 4′6-diamidine-2-phenylindol dihydrochloride (DAPI) 1 µg/mL in distilled H₂O (stored at −20 °C).
6. Agarose: Normal melting point, electrophoresis grade, and low melting point (LMP) (necessary for embedding cells at 37 °C).
7. Enzymes: the repair enzymes endonuclease III, Fpg (*see Note 4*), T4 endonuclease V, AlkA, and UDG may be obtained commercially in purified form, in which case the supplier’s instructions for use should be followed. An alternative source is the various researchers who produce their own enzyme from bacteria containing over-producing plasmids. Crude extract is generally satisfactory; because the enzyme represents such a high proportion of the protein in the extract, there is unlikely to be significant nonspecific nuclease activity.

The final working dilution of the enzyme will vary from batch to batch (*see Note 5*). To illustrate the best way to handle the enzymes (avoiding repeated freezing and thawing, and minimizing wastage), we refer here to Fpg as an example, with a recommended final dilution of 3000×. On receipt, the enzyme (which should have been frozen in transit) should be dispensed into small aliquots (say, 5 µL) and stored at −80 °C (this minimizes repeated freezing and thawing). Take one of these aliquots and dilute to 0.5 mL using the regular enzyme reaction buffer—with the addition of 10% glycerol. Dispense this into 10 µL aliquots (label as “100× diluted”) and freeze at −80 °C. For use, dilute one of these 10 µL aliquots to 300 µL with buffer (no glycerol) and keep on ice until you add it to the gels: do not refreeze this working solution.

3 Methods

3.1 Preparing Agarose

1. Normal melting point agarose is used for precoating slides. Prepare a 1% solution in water, heating in a microwave oven to near-boiling point, shaking occasionally; the agarose should form a transparent gel. It can then be cooled, stored at 4 °C, and melted in the microwave oven whenever needed for precoating slides.
2. Low melting point agarose is used for the gel containing cells. Prepare a 1% solution in PBS, dissolving the agarose by heating, as above. Make no more than 10 or 20 mL (enough for several experiments). If a larger quantity is made, and repeatedly melted, evaporation occurs and the concentration is then significantly higher than 1%.

3.2 Slide Preparation

Early versions of the comet assay used fully frosted slides, which give good anchorage for agarose, but can only be used a few times before agarose layers begin to detach. The use of ordinary clear glass slides with frosted end, precoated with agarose, is now recommended. The use of plain slides (as well as being cheaper) has the advantage that, if slides are dried down after electrophoresis for storage and later examination, the comets (now very close to the glass surface) do not suffer from the high background of reflection from the frosted surface. Another advantage is that the comets, after drying, are in the same plane, obviating the need for constant refocusing.

1. Dip each slide in a beaker of melted 1% standard agarose in H₂O.
2. Drain off excess agarose, wiping the back clean with tissue.
3. Leave the slides, coated side up, on a clean surface at 37 °C overnight to dry.
4. Mark one corner of the frosted end to indicate which side of the slide is coated.
5. Slides can then be returned to a slide box for storage at room temperature until needed.

(The slides for precoating should be grease-free; clean if necessary by soaking in alcohol and then wiping dry with a clean tissue.)

It is increasingly common to use a high-throughput version of the comet assay, with 12 mini-gels on one slide (or 96 mini-gels on a plastic film). A chamber device clamped onto the slide isolates each mini-gel in a well, in which incubation with enzyme can be carried out [10].

3.3 Embedding Cells in Agarose

1. Suspend cells in PBS at approximately 10^6 per mL.
2. For each slide, take an aliquot of 40 μL in a microcentrifuge tube.
3. Quickly add 140 μL of 1% LMP agarose in PBS at 37 °C and mix by tapping the tube and then pipetting once up and down.
4. Using a 70 μL pipettor, quickly place two separate drops on one slide, and cover each with an 18 \times 18 mm cover slip. Work quickly as the agarose sets quickly at room temperature!
5. Leave the slides on a cold metal plate at 4 °C for 5 min. Cells maintain metabolic activity even after embedding, and can be treated in the gel with DNA-damaging agents, and then incubated in medium to monitor DNA repair [11] (*see Note 6*).

3.4 Lysis

1. Add 1 mL Triton X-100 to 100 mL of lysis solution (4 °C). Use a pipettor tip with the end cut off, as Triton is viscous.
2. Mix thoroughly.
3. Remove cover slips from slides and place in this solution in a staining jar.
4. Leave at 4 °C for 1 h (*see Note 6*).

3.5 Enzyme Incubation

1. Prepare 300 mL of enzyme reaction buffer. Put aside a few mL for enzyme dilutions.
2. Wash slides in three changes of this buffer (4 °C) in a staining jar, for 5 min each in order to equilibrate with enzyme buffer.
3. Dilute an aliquot of enzyme with enzyme buffer. The final dilution of the working solution will vary from batch to batch.
4. Remove slides from last wash, and dab off excess liquid with tissue.
5. Place 50 μL of enzyme solution (or buffer alone, as control) onto each gel, and cover with 22 \times 22 mm cover slip. As an alternative, you can cover the gels with thin plastic film cut to size (*see Note 7*).
6. Put slides into moist box (to prevent desiccation) and incubate at 37 °C for 45 min.

3.6 Alkaline Treatment and Electrophoresis

1. Ensure that electrophoresis solution is cold before use, e.g., by pouring into the electrophoresis tank in the cold room an hour or so before it is needed.
2. Gently place slides (minus cover slips) on platform in tank, forming 1 or 2 complete rows (gaps should be filled with blank slides). Gels must be (just) covered.
3. Leave for 40 min.
4. For most tanks (i.e., of standard size), run at 25 V (constant voltage setting) for 30 min (*see Note 8*). If there is too much

electrolyte covering the slides, the current may be so high that it exceeds the maximum—so set this at a high level. If necessary, i.e., if 25 V is not reached, remove some solution. Normally the current is around 300 mA but this is not critical.

3.7 Neutralization and Staining

1. Wash 5 min with neutralizing buffer in staining jar at 4 °C, followed by 5 min in water; then dry (room temperature) for storage (or proceed to stain immediately).
2. Stain with 4'-6-diamidino-2-phenylindol dihydrochloride (DAPI): place 20 μ L of a 1 μ g/mL solution of DAPI in distilled H₂O (stored at -20 °C) onto each slide and cover with a 22 \times 22 mm cover slip.
3. Keep slides in a dark, moist chamber until they are viewed. They may be left overnight before viewing, either stained or unstained (however, if stained, some fluorescence is lost) (*see Note 9*).

3.8 Image Analysis and Calculation

1. Image analysis. Generally, 50 or 100 comets are analyzed per gel. There are numerous commercially available comet image analysis software packages, linked to a CCD (charge-coupled device) camera, or visual scoring can be used. Visual scoring depends on sorting comets into one of 5 classes with “values” from 0, no visible tail, to 4, almost all DNA in tail, and adding the individual values for 100 comets to give a score of between 0 and 400 arbitrary units. The computer-based systems offer a selection of parameters, some more useful than others. Comet tail length is only useful at very low damage levels; once the tail is established its length hardly changes as the damage level increases (as expected if the tail is a collection of relaxed DNA loops). % Tail DNA is the most useful parameter, being proportional to DNA break frequency over a relatively wide range of damage levels before saturation is reached. Tail moment combines tail length and intensity (% tail DNA), and is unaccountably popular. It does not show a linear relation to break frequency, since it includes the tail length factor which saturates at low dose. Furthermore, it deprives us of valuable information: it has no generally recognized units, and so there is no way of visualizing a comet of a particular tail moment value. In contrast, given a value of % tail DNA, it is immediately clear what kind of comet is being described.
2. Calculation. The control gels (no enzyme treatment) provide an estimate of the background level of SBs (strictly speaking, strand breaks plus alkali-labile sites) in the DNA. The enzyme-treated gels reveal strand breaks plus base damage (SBs + BD). Assuming a linear dose response, whether working in % DNA in tail or in arbitrary units, subtraction of (SBs) from (SBs + BD)

gives net enzyme-sensitive sites as a measure of damaged bases (*see Note 10*).

3. Calibration. Ionizing radiation produces SBs in DNA with known efficiency. If the breaks introduced in cells by different doses of X-rays are detected with the comet assay, a standard curve can be drawn, with break frequency expressed as Gray equivalents, or as breaks per unit length of DNA [12].

3.9 Storage and Re-examination

1. Place slides in a warm oven, or leave on bench, until the gel has dried.
2. Slides can then be stored at room temperature.
3. For re-examination, stain as above.

3.10 Quality Control

1. Reference standards: It is important to include cells containing DNA damage as a positive control in experiments to assess genotoxicity. When the lesion-specific enzymes are being used in the comet assay, the reference cells should be treated with an appropriate agent, i.e., an alkylating agent for AlkA, UV(C) for T4 endonuclease V, a reactive oxygen generating agent for Fpg or endonuclease III. H₂O₂ is often used, but as it produces many SBs as well as oxidized bases, it is important to incubate the cells to allow repair of these breaks (*see Note 5*).

When measuring DNA damage in human lymphocytes, as part of a population study, standard samples of lymphocytes should be included in every batch of samples. The standard lymphocytes are prepared from 50 mL of blood from one or more donors; after isolation the lymphocytes are pooled, counted, and aliquoted at about 10⁶ per mL in ice-cold freezing medium (cell culture medium, e.g., MEM or RPMI, with 10% fetal calf serum and 10% DMSO), each tube containing enough cells for several gels. Freeze slowly to -80 °C and store until needed. Results from the standard lymphocytes should not show variation from experiment to experiment; if they do, there is a problem with the procedure which should be sorted out. If the variation is large, then the samples may need to be re-analyzed.

2. Visual scoring and image analysis: If using visual scoring, each operator should ideally be “calibrated” against the computer image analysis system at regular intervals. This simply involves scoring comets on a slide showing a range of damage levels, visually (classes 0–4) and then by computer image analysis (% DNA in tail), until there are 20 of each class. For all class 0 comets, calculate the mean % DNA in tail, and similarly for all comets of the other classes. Then plot *mean % DNA in tail* against *comet class*. The resulting line is unlikely to be perfectly straight, but should show a near-linear relationship. More important than

the exact relationship is the point that individual operators should be trained (if necessary) to give a similar “calibration curve” when plotted in this way.

3.11 Interpretation of Results

In comet assay experiments with enzymes, there should always be a “buffer control,” incubated alongside the enzyme-treated gels but without enzyme. After alkaline treatment and electrophoresis, this gives the level of SBs plus alkali-labile sites. Subtracting the buffer control value from the value obtained with enzyme gives “net enzyme-sensitive sites” (but *see* **Note 10**), and this is the preferred way to express results—rather than the combined total of SBs plus enzyme-sensitive sites.

Careful use of lesion-specific endonucleases in the comet assay can give valuable information about the different kinds of DNA damage that may be present, either as “natural” background, or induced by a particular genotoxic agent. However, it is important to be aware that the enzyme specificities are not absolute. Fpg-sensitive sites are often equated with 8-oxoguanine [13], but Fpg also recognizes purine breakdown products, formamidopyrimidines (fapy). Speit et al. [14] reported the recognition by Fpg of alkylation damage. Endonuclease III recognizes a range of oxidized pyrimidines. AlkA has as its main substrate 3-methyladenine, but will also attack other alkylated bases and even, at high enough concentration, undamaged DNA [15]. In addition, many of the enzymes have a hydrolytic activity against AP sites (apurinic/aprimidinic sites), which occur in DNA spontaneously. This should not be a problem, since AP sites are alkali-labile, and therefore should appear as SBs and be included in the enzyme buffer control score—but it has not been definitively established that the comet assay conditions are sufficiently alkaline to break all AP sites.

4 Notes

1. The HEPES buffer is used for Fpg, endonuclease III, AlkA, and T4 endonuclease V. The recommended buffer for Udg is: 60 mM Tris-HCl, 1 mM EDTA, pH 8.0.
2. The buffer in which the enzyme is prepared and stored normally contains β -mercaptoethanol or dithiothreitol to preserve the enzyme. However, inclusion of sulfhydryl reagents in the reaction buffer significantly increases background DNA breakage. It is therefore recommended to omit this reagent from the reaction buffer.
3. Three washes in 0.4 M neutral Tris buffer were originally recommended for neutralizing gels after electrophoresis. One wash in standard, cheaper buffer such as phosphate-buffered saline (PBS) is adequate. Even water will bring the pH down

to a level at which DNA no longer unwinds, which is all that is required.

4. The mammalian analog of Fpg, Ogg1, has been used in the comet assay [16]. It has a rather narrower specificity, detecting 8-oxoguanine and methyl fapy guanine, but is as yet not routinely used.
5. Suppliers of enzyme will normally recommend a working concentration and incubation time. However, you are recommended to carry out a titration experiment, varying both incubation period and enzyme concentration, to be sure that damage detection is optimized. To do this, cells containing the specific damage are required. HeLa cells (or another common transformed cell line) can be treated with H_2O_2 , and incubated for 1 h so that virtually all SBs are repaired, leaving oxidized bases, which are much more slowly repaired by the cell (*see* Fig. 2). Incubation of cells with a photosensitiser, Ro19-8022 (supplied by F. Hoffmann-La Roche), followed by irradiation with visible light, induces 8-oxoguanine and provides a good substrate for titrating Fpg. Alkylation damage can be induced

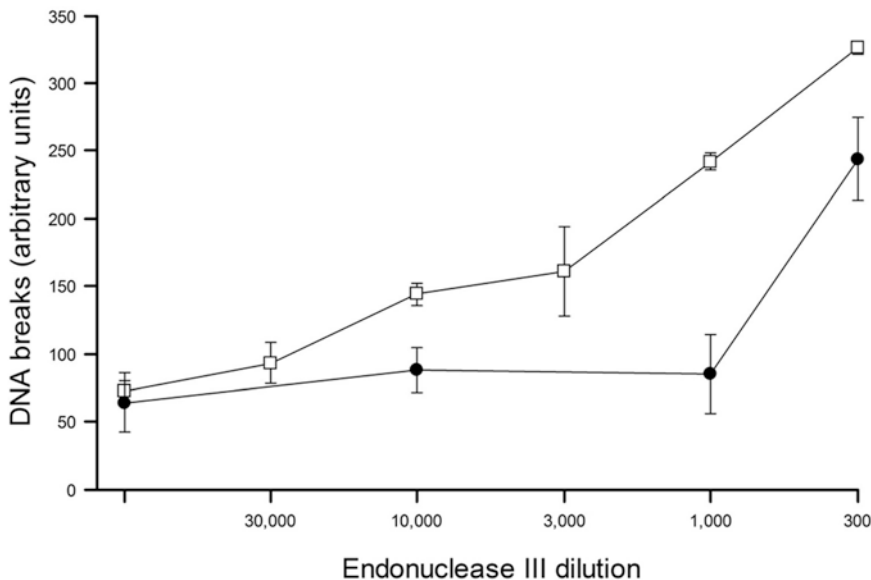


Fig. 2 Titration of endonuclease III. HeLa cells were incubated with 0.6 mM H_2O_2 for 5 min on ice, to induce strand breaks and oxidized bases. During subsequent incubation at 37 °C for 45 min, the strand breaks were repaired, leaving oxidized bases. Slides were prepared for the comet assay, and after lysis, gels were incubated with endonuclease III at different dilutions from the stock (and without enzyme—data on far left), and breaks measured by visual scoring (range 0–400). *Solid symbols (filled circle)*: control cells, not treated with H_2O_2 . *Open symbols (open square)*: after H_2O_2 and incubation. *Bars* indicate range, in duplicate experiments. At high enzyme concentrations, nonspecific DNA breakage occurs (as is seen from the steep rise in breaks in the DNA from the untreated cells). The working range of the endonuclease III is therefore a dilution of 10,000- to 3000-fold

by treating cells with methylmethanesulfonate. UV(C) irradiation induces cyclobutane pyrimidine dimers that can be used to titrate UV endonuclease.

6. Sometimes cells are treated with a genotoxic chemical after embedding in the gel. If this is the case, it is advisable to dip the slides in water before lysis, and to keep treated and control slides in separate lysis vessels to avoid cross-contamination.
7. If dealing with a large number of slides, carry out this step (addition of enzyme) with the slides on a cold plate before transferring to the moist box, to ensure that they all have the same period of incubation at 37 °C.
8. It is the voltage drop across the gels that causes the movement of DNA into the tail. The current is not critical [12].
9. Propidium iodide (2.5 µg/mL), Hoechst 33,258 (0.5 µg/mL), ethidium bromide (20 µg/mL), or SybrGold (10–25,000 diluted with respect to manufacturer's stock) is often used in place of DAPI for the visualization of comet DNA.
10. Subtraction of the comet score for enzyme buffer control from the score for enzyme digestion gives an accurate estimate of net enzyme-sensitive sites—if the response curve for the relative tail intensity against DNA break frequency is linear. This is the case at relatively low damage levels, but at higher levels the assay tends toward saturation and the curve is distinctly non-linear. In that case it is necessary to calibrate the assay, for example using ionizing radiation as a standard DNA-damaging agent, so that results can be expressed as, e.g., Gray equivalents, or DNA breaks per 10⁹ daltons (since the DNA breakage efficiency of radiation is known).

Acknowledgments

I thank Katja Lange and Anna Tirado for excellent technical support.

References

1. Collins AR, Duthie SJ, Dobson VL (1993) Direct enzymic detection of endogenous oxidative base damage in human lymphocyte DNA. *Carcinogenesis* 14:1733–1735
2. Dusinska M, Collins A (1996) Detection of oxidised purines and UV-induced photoproducts in DNA of single cells, by inclusion of lesion-specific enzymes in the comet assay. *Altern Lab Anim* 24:405–411
3. Collins AR, Dusinska M, Horska A (2001) Detection of alkylation damage in human lymphocyte DNA with the comet assay. *Acta Biochim Pol* 48:611–614
4. Collins AR, Mitchell DL, Zunino A, de Wit J, Busch D (1997) UV-sensitive rodent mutant cell lines of complementation groups 6 and 8 differ phenotypically from their human counterparts. *Environ Mol Mutagen* 29:152–160

5. Duthie SJ, McMillan P (1997) Uracil misincorporation in human DNA detected using single cell gel electrophoresis. *Carcinogenesis* 18:1709–1714
6. Duthie SJ, Ma A, Ross MA, Collins AR (1996) Antioxidant supplementation decreases oxidative DNA damage in human lymphocytes. *Cancer Res* 56:1291–1295
7. Azqueta A, Arbillaga L, Lopez de Cerain A, Collins A (2013) Enhancing the sensitivity of the comet assay as a genotoxicity test, by combining it with bacterial repair enzyme FPG. *Mutagenesis* 28:271–277
8. Huk A, Izak-Nau E, El Yamani N, Uggerud H, Vadset M, Zasonska B, Duschl A, Dusinska M (2015) Impact of nanosilver on various DNA lesions and HPRT gene mutations – effects of charge and surface coating. *Part Fibre Toxicol* 12:25
9. Azqueta A, Collins AR (2013) The essential comet assay: a comprehensive guide to measuring DNA damage and repair. *Arch Toxicol* 87:949–968
10. Shaposhnikov S, Azqueta A, Henriksson S, Meier S, Gaivão I, Huskisson NH, Smart A, Brunborg G, Nilsson M, Collins AR (2010) Twelve-gel slide format optimised for comet assay and fluorescent *in situ* hybridisation. *Toxicol Lett* 195:31–34
11. Collins AR, Horvathova E (2001) Oxidative DNA damage, antioxidants and DNA repair; applications of the comet assay. *Biochem Soc Trans* 29:337–341
12. Collins AR, Azqueta A, Brunborg G et al (2008) The comet assay: topical issues. *Mutagenesis* 23:143–151
13. Collins AR, Cadet J, Moller L, Poulsen HE, Vina J (2004) Are we sure we know how to measure 8-oxo-7,8-dihydroguanine in DNA from human cells? *Arch Biochem Biophys* 423:57–65
14. Speit G, Schütz P, Bonzheim I, Trenz K, Hoffmann H (2004) Sensitivity of the protein towards alkylation damage in the comet assay. *Toxicol Lett* 146:151–158
15. Berdal KG, Johansen RF, Seeberg E (1998) Release of normal bases from intact DNA by a native DNA repair enzyme. *EMBO J* 17:363–367
16. Smith CC, O'Donovan MR, Martin EA (2006) hOGG1 recognizes oxidative damage using the comet assay with greater specificity than FPG or ENDOIII. *Mutagenesis* 21(3):185–190

Part IV

Safety Pharmacology

Automated Patch-Clamp Methods for the hERG Cardiac Potassium Channel

Sylvie Houtmann, Brigitte Schombert, Camille Sanson, Michel Partiseti, and G. Andrees Bohme

Abstract

The *human Ether- α -go-go* Related Gene (hERG) product has been identified as a central ion channel underlying both familial forms of elongated QT interval on the electrocardiogram and drug-induced elongation of the same QT segment. Indeed, reduced function of this potassium channel involved in the repolarization of the cardiac action potential can produce a type of life-threatening cardiac ventricular arrhythmias called *Torsades de Pointes* (TdP). Therefore, hERG inhibitory activity of newly synthesized molecules is a relevant structure-activity metric for compound prioritization and optimization in medicinal chemistry phases of drug discovery. Electrophysiology remains the gold standard for the functional assessment of ion channel pharmacology. The recent years have witnessed automatization and parallelization of the manual patch-clamp technique, allowing higher throughput screening on recombinant hERG channels. However, the multi-well plate format of automatized patch-clamp does not allow visual detection of potential micro-precipitation of poorly soluble compounds. In this chapter we describe bench procedures for the culture and preparation of hERG-expressing CHO cells for recording on an automated patch-clamp workstation. We also show that the sensitivity of the assay can be improved by adding a surfactant to the extracellular medium.

Key words Torsade de Pointes, Drug-induced QT prolongation, Cardiosafety screening, Electrophysiology

1 Introduction

Electrical activity in cardiac tissue orchestrates heart rate and synchronizes cardiac muscle contraction to allow efficient blood supply to the body. Ion channels are the molecular entities controlling generation and conduction of electrical activity in the cardiac tissue through fast depolarization and repolarization of the cellular membrane potential. These activities involve essentially inward and outward movements of Na⁺, K⁺, or Ca²⁺ ions down their respective electrochemical gradient through multiple ion channels to which they are specifically permeable.

Inherited dysfunctions of cardiac ion channels (also known as cardiac channelopathies) have established a translational path between gain-of-function or loss-of-function mutations in the sequence of proteins forming the ion channel pore (or their accessory regulatory or trafficking proteins) and an increased risk of cardiac sudden death. These mutations influence the action potential duration and its correlate at the surface electrocardiogram, the length of the QT segment. Notably, an increase in the QT length can produce *Torsades de Pointes* (TdP), a type of ventricular tachycardia that can evolve into ventricular fibrillation and end up in fatal cardiac arrest in the absence of appropriate medical intervention [1].

Several drugs of diverse chemical structure belonging to different pharmacological classes have been withdrawn from the market or were burdened with safety warnings because of their elongating effect on the QT segment and the associated torsadogenic risk. Most of these drugs have in common the property to inhibit the repolarizing current mediated by the K⁺ channel encoded by the *human Ether-a-go-go Related Gene* (hERG). Regulatory bodies have recommended since 2005 that pharmacological activity at hERG channels be part of the preclinical safety package of new drugs, and that in-depth cardiac safety assessment be performed during thorough QT studies at early clinical stages. Although it is known that other repolarizing or depolarizing cardiac ion channels can contribute to, or sometimes compensate for their torsadogenic potential, screening of new chemical entities at recombinant hERG channels remains a mainstay of early safety assessment during pharmaceutical research and development [2].

Patch-clamp electrophysiology is the method of choice for the functional assessment of ion channel pharmacology. In recent years, progress has been made to automatize and parallelize the resources and time-consuming manual patch-clamp approach using computer-controlled robotized platforms allowing higher throughput screening with recombinant ion channels [3]. By virtue of the development of planar electrodes engineered in the bottom of multi-well plates associated with sophisticated microfluidics, it has become possible to reasonably reproduce the experimental quality standards prevailing in manual patch-clamp (gigaohm seal, low access resistance, capacity compensation), although at the expense of individual control over the selection of the cells which are to be used for the recordings. Moreover, the multi-well plate format does not allow visual detection of potential micro-precipitation of poorly soluble discovery compounds upon the dilution in the aqueous saline recording media of concentrated stock solutions of the compounds in commonly used organic solvents such as DMSO. While the former limitation can be compensated for by using homogeneous cell lines expressing high levels of the channel of choice and known for their patch-clamp friendliness and good vitality such as

CHO or HEK cells, the latter issue can lead to underestimation of drug activity and hence to false negatives in high-throughput cardiosafety liability assessment at early discovery stages. The addition of a surfactant to the final aqueous samples applied to the cells may help maintain lipophilic drugs in solution by kinetically slowing their potential precipitation.

The present chapter details bench procedures for the culture and preparation of CHO cells expressing hERG for automated patch-clamp recording on a QPatch HTX station. The purpose of this paper is neither to duplicate technical or software documentation of the instrument nor to detail the implementation of the workflow beyond its general principles. The interested reader is referred to the documentation accompanying the QPatch HTX, as well as to relevant reviews (e.g., [4]). We will focus here on a practical recipe for cell preparation, buffer composition, and compound handling for early evaluation of cardiosafety liability in drug discovery.

2 Materials

2.1 Cell Cultures

1. Chinese hamster ovary cells constitutively expressing hERG (CHO hERG Duo[®], B'SYS GmbH, Switzerland).
2. Serum-supplemented growth medium: to 500 mL DMEM/F-12 growth medium, add aseptically in a laminar air-flow cell culture hood 55 mL fetal bovine serum, 1 mL Geneticin solution at 50 mg/mL, 1 mL Hygromycin B solution at 45–60 mg/mL, and 5.5 mL L-Alanyl-L-Glutamine dipeptide solution at 200 mM. Keep this medium stored at 4 °C for no longer than 2 weeks.
3. Polypropylene 15 and 50 mL centrifugation tubes.
4. Disposable 1, 2, 5, 10, and 50 mL plastic pipettes with electric pipetting device.
5. Standard single-channel adjustable pipettes.
6. T-75 and T-175 polystyrene cell culture flasks.

2.2 Preparation of Cells for Recording

1. Dulbecco's phosphate-buffered saline (PBS) without Ca²⁺ and Mg²⁺.
2. Trypsin (5 g/L) – EDTA(2 g/L) solution.
3. Cell sustainment medium: in a 50 mL centrifuge tube, prepare 25 mL of cell sustainment medium by adding 0.625 mL 1 M HEPES solution, 0.25 mL penicillin-streptomycin solution at 10,000 Units/mL, and 200 µL soybean trypsin inhibitor solution at 0.5% (w/v) to 25 mL of warm Ex-Cell[®] Animal-component free CHO medium (Sigma-Aldrich).

2.3 Preparation of Compounds for Pharmacological Testing

1. Dimethyl-sulfoxide (DMSO) (*see Note 1*).
2. Standard 96-well polypropylene microtiter plates.
3. Pluronic F-68, 10% (w/v) solution (e.g., from Gibco, Cat. N° 24,040-032) (*see Note 2*).
4. Eight-channel 30–300 μL and 0.5–10 μL multi-pipettes.
5. Plastic reservoir boats.

2.4 Recording Buffers and Standard

The extracellular and intracellular solutions should be prepared extemporaneously from concentrated stock solutions stored at 4 °C (*see Note 3*).

1. The extracellular buffer contains 150 mM NaCl, 4 mM KCl, 2 mM CaCl_2 , 1 mM MgCl_2 , 10 mM HEPES, and 10 mM Glucose. It is usually prepared in a 1 L measuring cylinder by adding to approximately 800 mL pure H_2O , 150 mL 1 M NaCl, 4 mL 1 M KCl, 2 mL 1 M CaCl_2 , 1 mL 1 M MgCl_2 , and 10 mL 1 M HEPES. Add a magnetic rod and adjust pH to 7.4 with concentrated NaOH (5 M). Remove magnetic rod, complete to final volume with H_2O , and filter through a 0.22 μm disposable filtration unit. Store this buffer in the receiver bottle at 4 °C for up to 1 month. On the day of the experimentation, fill a 50 mL centrifuge tube with 49.5 mL buffer and add 0.5 mL of a 1 M glucose solution aliquot freshly thawed in a warm water bath. Osmolarity measured with a recently calibrated vapor pressure osmometer should be above 300 mOsmol.
2. The intracellular medium contains 120 mM KCl, 10 mM EGTA, 5 mM CaCl_2 , 2 mM MgCl_2 , 10 mM HEPES, and 4 mM MgATP. For convenience, this medium is dispensed in 13.5 mL aliquots in 15 mL screw-caped centrifugation tubes stored frozen at -20 °C. Upon preparation of a new batch of intracellular medium, one fresh sample is validated in an electrophysiology experiment before freezing the rest. To prepare 0.5 L of intracellular buffer, add to about 350 mL pure H_2O in a 500 mL measuring cylinder, 60 mL 1 M KCl, 62.5 mL 0.08 M/0.25 M EGTA/KOH, 2.5 mL 1 M CaCl_2 , 1 mL 1 M MgCl_2 , and 5 mL 1 M HEPES. Add a magnetic rod and adjust pH to 7.2 with concentrated KOH (5 M). Remove magnetic rod, complete to final volume with H_2O , and filter through a 0.22 μm disposable filtration unit. On the day of recording, thaw a frozen 13.5 mL tube and add a 1.5 mL aliquot of a 40 mM MgATP stock solution (*see Note 4*). To ease gigaseal formation, adjust the osmotic pressures of the intracellular solution with concentrated KCl (1 M) to either iso-osmotic or slightly (10–20 mOsmol) hypo-osmotic with respect to the extracellular buffer.
3. Positive control (full block) stock: dissolve 6.6 mg terfenadine citrate (internal synthesis) in a final volume of 1 mL DMSO.

Dispense in 0.02 mL aliquots and keep frozen at -20°C . On the day of experimentation, dilute 10 μL in 10 mL extracellular buffer.

2.5 Equipment

1. Automated patch-clamp workstation (QPatch HTX[®]) and consumables (QPlates[®]) (Sophion/Biolin Scientific, Ballerup, Denmark).
2. Heated circulating water bath (37°C).
3. Cell culture incubator (37°C , 5% CO_2 atmosphere, 90% relative humidity).
4. Automated cell viability analyzer (Vi-Cell[®], Beckman-Coulter).
5. Vapor pressure osmometer (Vapro[®], Wescor).
6. Live cell imaging system (Incucyte[®], Essen Bioscience).

3 Methods

The QPatch system associates two robotized arms and an electrophysiological measurement interface. One arm is equipped with eight pipettes allowing precision distribution of micro-volumes of cell suspensions or drug solutions. The other arm comprises a mechanical gripper enabling the displacement of microtiter plates and other movable parts between parking and operating slots on the work area. These components are gathered in the upper part of the workstation within a transparent protection cabinet. The electrophysiological interface is composed of 48 patch-clamp amplifiers and analogic/digital converters controlled by a built-in PC-type computer located in the lower chassis of the station. This interface allows the acquisition and processing of membrane currents from multiple recording sites in parallel. Each site comprises a micro-perforated planar patch-clamp silicon chip engineered at the bottom of a recording chamber. Forty-eight such recording sites are fitted in a disposable multi-well type plate called a QPlate. There are two types of QPlates depending on whether each planar patch-clamp chip is endowed with a single hole or with ten holes, the latter allowing currents recorded from parallel cells to be summed. Each recording site within a QPlate is equipped with microfluidic pipes allowing the supply of intracellular and extracellular solutions on either side of the micro-perforated chip. During an experimental session, the individual recording sites are submitted to calibrated pulses of positive or negative pressure once an airtight gasket is placed over the QPlate by the robot gripper arm. The pipette arm ensures the dispensation of the buffers, as well as the distribution of cell suspensions. The pressure pulses are alternated following a software-defined sequence so as to force the solutions through the microfluidic pipes and to drive the cells

towards the basal chip perforations. Once contact is established with their membrane and gigaohm sealing is obtained, the cell membranes are ruptured to gain whole-cell access for patch-clamp recording, thereby recapitulating the cardinal features of manual patch-clamp.

3.1 Cell Cultures

CHO cells expressing hERG cDNA following dual transfection with two vectors are grown under the permanent pressure of Hygromycin and Geneticin according to the specifications of the manufacturer. For routine screening, the CHO hERG Duo cells give the best results when grown in T-175 flasks containing 25–30 mL of serum-supplemented growth medium. Fresh cells between passages 15 and 45 yield reliable currents for pharmacology. Experiments can also be conducted directly with frozen cells although with a slightly lower success rate. The following steps detail the regeneration of CHO hERG Duo cultures from frozen vials and the maintenance of viable colonies.

1. Equip a centrifuge with rotors for 50 mL tubes and place a bottle of growth medium in a heated circulating water bath at 37 °C.
2. Take a frozen vial from the liquid nitrogen tank and place it in a warm bath (*see Note 5*).
3. Pick the vial before its content is totally thawed to avoid over-exposing the cells to potentially cytotoxic concentrations of 10% DMSO contained in the freezing medium.
4. Decontaminate the vial with ethanol. Under the culture hood, add drop-wise 2 mL warm growth medium with a 1 mL single-channel pipette. Gently work the cell suspension through the tip to dislodge cell clumps, and transfer into 20 mL warm growth medium in a centrifuge tube.
5. Spin at *ca* 200 × *g* for 3 min at room temperature (*see Note 6*).
6. Remove the freezing medium by carefully aspirating the supernatant, then resuspend the cell pellet in 10 mL warm growth medium.
7. Sample 1 mL of the suspension in a trypan blue-exclusion image-analysis cell counting station. Viability should be at least 80% to ensure proper regeneration of a vigorous colony.
8. Transfer the cell suspension into a small T-75 culture flask and place in a 90% humidified, 37 °C/5% CO₂ incubator.
9. Monitor adherence and growth of the CHO hERG Duo cells on a daily basis under the microscope.
10. For maintenance purposes, routinely passage the cells twice a week using trypsin-EDTA as a detaching agent once the cells have reached about 80% confluence (*see Note 7*). This is typically achieved by seeding 1 × 10⁶ cells into a T-175 flask containing

25–30 mL serum-supplemented growth medium. Lower seeding densities (0.7×10^6 cells) and/or larger flasks (T-225) can be adopted to cover prolonged bank holidays.

3.2 Cell Preparation for Recording

The seeding density required to obtain an optimal amount of cells depends on the planned experimental schedule. Typically, seeding 2×10^6 cells in a T-175 flask yields enough cells after 3 days in culture to complete 2–3 multi-hole jobs. Seed 1.2×10^6 for recordings planned 4 days later. Once harvested, cells for QPatch recordings need to be washed to remove debris, and then resuspended in serum-free sustainment medium to avoid the formation of cell clumps. The latter contains soybean trypsin inhibitor to terminate the action of the detaching agent, as well as HEPES and penicillin-streptomycin to sustain the cells outside the incubator. Viability greater than 95% is required for optimal hERG current recording quality.

1. Take a T-175 flask containing the cultured cells from the incubator. Ensure that the cells have reached 80% confluence by observing under the microscope or, better, using a live cell imaging system.
2. Under the hood, remove the old growth medium by aspiration and add 5–10 mL PBS to flush remaining fetal bovine serum and cell debris. Avoid squirting the PBS against the flask wall where the cells adhere.
3. Remove PBS, add 3 mL Trypsin-EDTA, and roll it over the cell monolayer to form a thin, uniform film. Close the flask and place it briefly (about 3 min) in the incubator. Gently tap the culture flask to help detach the cells without stressing them. Check under a microscope for the characteristic round shape of floating CHO cells.
4. Spread 20 mL of serum-supplemented growth medium against the wall to detach remaining adherent cells. The serum will start to halt the action of trypsin. Decant in an angle of the flask, aspirate, and flush the medium steadily 5–10 times through a pipette to homogenize. Collect the cell suspension in a 50 mL centrifuge tube.
5. Centrifuge 3 min at *ca* $200 \times g$, eliminate the supernatant, and resuspend the pellet in 26 mL Ex-Cell® Animal-component free CHO medium.
6. Count cells on a 1 mL-sample in the Vi-Cell. Note density, viability, and average diameter on the lab notepad. Centrifuge 3 min at *ca* $200 \times g$ and add to the pellet a volume of sustainment medium calculated to reach the desired cell density. The latter depends on the type of recording planned: target a density of 5×10^6 cells/mL for a single-hole QPlate and 8×10^6 cells/mL for a multi-hole QPlate.

7. Transfer 1 mL of the CHO hERG Duo cell suspension into a disposable Eppendorf vial placed directly in the mini-centrifuge of the QPatch station (*see Note 8*).

3.3 Test Compounds Preparation

Compounds for screening are usually delivered by compound management under small volumes (e.g., 30 μL) of concentrated (10 mM) stock solutions in 100% DMSO. The samples are delivered frozen in aluminum foil-sealed 96-well microtiter plate. From these stocks, we typically prepare a 6-point concentration range in two steps. A series of intermediate working solutions is prepared first, starting from the initial 10 mM DMSO stocks by serial 1:3 dilutions in 100% DMSO. Then, the targeted final concentration range is obtained by one-step 1:333 dilutions of the intermediate working solutions into extracellular media containing 0.06% pluronic F-68. The procedure below describes the preparation of a standard concentration range used for blind compound screening (i.e., 0.12, 0.37, 1.1, 3.3, 10, and 30 μM). This range needs to be shifted to lower concentrations to adjust for hERG reference inhibitors of known potency.

1. Take a frozen sealed microtiter plate containing 10 mM DMSO stocks for, e.g., eight compounds from the freezer and place it over a warm water bath (*see Note 9*).
2. Take an empty V-bottom standard 96-well microtiter plate and dispense 6 μL of fresh DMSO into all eight wells of columns 1–5 using an eight-channel multi-pipette. Leave column 6 empty.
3. With the multi-pipette, aspirate 3 μL from the thawed 10 mM DMSO stocks of the eight compounds. Then, dip the eight tips into the DMSO-containing wells of column 5 and mix thoroughly by steadily in- and out-pipetting several times.
4. Repeat this 1:3 dilution step between column 5 and column 4 by aspirating 3 μL from column 5, dipping the tips into the DMSO-containing wells of column 4, and mixing again several times.
5. Continue likewise for columns 3, 2, and 1 so as to obtain, horizontally and for each compound, a series of five working concentrations in pure DMSO (i.e., from left to right: 0.041, 0.123, 0.37, 1.1, and 3.3 mM) over half of the microtiter plate.
6. In another plate, dispense twice in each well of columns 1 to 6 a volume of 166 μL extracellular medium supplemented with 0.06% Pluronic F68 (total 332 μL , *see Note 10*).
7. Aspirate 1 μL in the wells of each of the 5 columns of the first microtiter plate, dip into the wells of the same column of the second microtiter plate, and mix thoroughly by in- and out-pipetting. Make sure the tips are plunging in the tiny concentrated volumes when you aspirate from the wells of the first microtiter plate.

8. Once these 1:333 dilution steps are completed for all 5 columns, aspirate 1 μL from the initial 10 mM stock plate to dilute into wells of column 6 in the second microtiter plate so as to finally obtain, horizontally and for each compound, the targeted range of six final concentrations in extracellular medium (i.e., from left to right: 0.12, 0.37, 0.11, 0.33, 10, and 30 μM) containing 0.06% Pluronic F68 and 0.3% residual DMSO.
9. Remove 60 μL from each of the wells to lower the volume.

3.4 Workflow and Evaluation of Reference hERG Inhibitors

The QPatch station is driven by a dedicated software combining logical blocks pertaining to the way the whole cell shall be obtained, the nature of the voltage steps that should be applied to activate the channels under examination, and what shall be the sequence of drug delivery to the cells. This software also encompasses electrophysiological signal processing tools (e.g., leak subtraction, resistance compensation), offline data handling (e.g., current amplitude normalization, run-down compensation), and pharmacometric routines (sigmoidal curve-fitting for IC_{50} calculations). The experimenter sets the parameters of the individual blocks and links them along with the identifications of the compounds under investigation into a sequence of tasks ready to be run (i.e., a “Job”). A prepared job can be run once the experimenter has positioned the biological material, the recording media, a microtiter plate containing the compounds at the final concentrations to be screened, and a disposable QPlate on the predefined locations in the station cabinet. Once launched, the procedure runs unattended according to the predefined workflow until the desired number of repetition of the concentration range has been achieved for each compound in the microtiter plate.

The biophysical properties of recombinant hERG channels recorded by patch-clamp are characterized by the large tail current elicited upon repolarization on which the pharmacological properties of inhibitory drugs are most sensitively assessed. To maximize this current, a two-step voltage command is employed, involving first a depolarization step from a negative -80 mV holding potential to a positive potential of $+20$ mV to activate the current. Prolonging this first voltage step for several seconds provides ample time for inhibitory drugs to bind the channel protein if it should happen. The second step consists in a repolarization from $+20$ to -50 mV. This triggers a large outward current surge due to a very rapid recovery from the inactivated state. Figure 1 shows the characteristic hERG waveform elicited by application of this two-step voltage protocol.

Half-maximal inhibitory concentrations (IC_{50}) are determined from a series of six concentrations applied to the cells in ascending order by the pipetting arm of the robot. The sequence starts once

the break-in into the cells is detected by the abrupt change in capacitance at the level of the recording chips. First, two or three applications of vehicle are executed, during each of which the cells are exposed to a small volume (e.g., 5 μL) of extracellular medium containing 0.3% DMSO and 0.06% Pluronic F68. During this baseline period, the cells stabilize and the size of the tail current is compared to settings predefined by the experimenter. The pipetting events can optionally be repeated in order to ensure appropriate impregnation of the cells. Moreover, for the handling of poorly soluble compounds, an improvement has been introduced in the latest release of the software which consists in the possibility to remix the drug solutions by working them in and out the pipette tips several times shortly before application to the cells. The voltage protocol pattern is repeated every 15 s throughout vehicle and drug application periods. At the end of the application of the six concentrations of a given compound, each recording site receives a maximally active concentration of a reference hERG inhibitor as a full-block positive control. Offline analysis of the data is performed after completion of each job. Recordings are retained only if the positive control induced a complete current blockade. Sigmoidal curve-fitting is performed on the concentration-response data normalized with respect to baseline using a classical four-parameter logistic equation with the top and the bottom usually fixed at 100 and 0%, and the Hill slope (nH) left as variable (Fig. 1). IC_{50} values determined on automated patch-clamp stations are usually slightly higher compared to data generated by manual patch-clamp (Table 1). However, the variation rarely exceeds one order of magnitude, and the systematic use of a dose-response approach ensures efficient flagging of most of the potentially arrhythmogenic compounds at early discovery stages.

4 Notes

1. DMSO is a highly hygroscopic solvent. It is advisable to frequently renew the DMSO containers since compound solubility may be decreased by the uptake of atmospheric humidity. Smaller 5–10 mL containers of DMSO, or larger bottles kept dry over molecular sieves desiccants are available from various vendors.
2. Pluronic[®] (registered trademarks of BASF) are water-soluble non-ionic surfactants (also known generically as poloxamers) consisting in copolymers associating hydrophobic poly(propylene oxide) and hydrophilic poly(ethylene oxide) blocks. We routinely add Pluronic F68 in an attempt to slow micro-precipitation of poorly water-soluble compounds upon dilution from concentrated DMSO stock solutions into aqueous saline recording

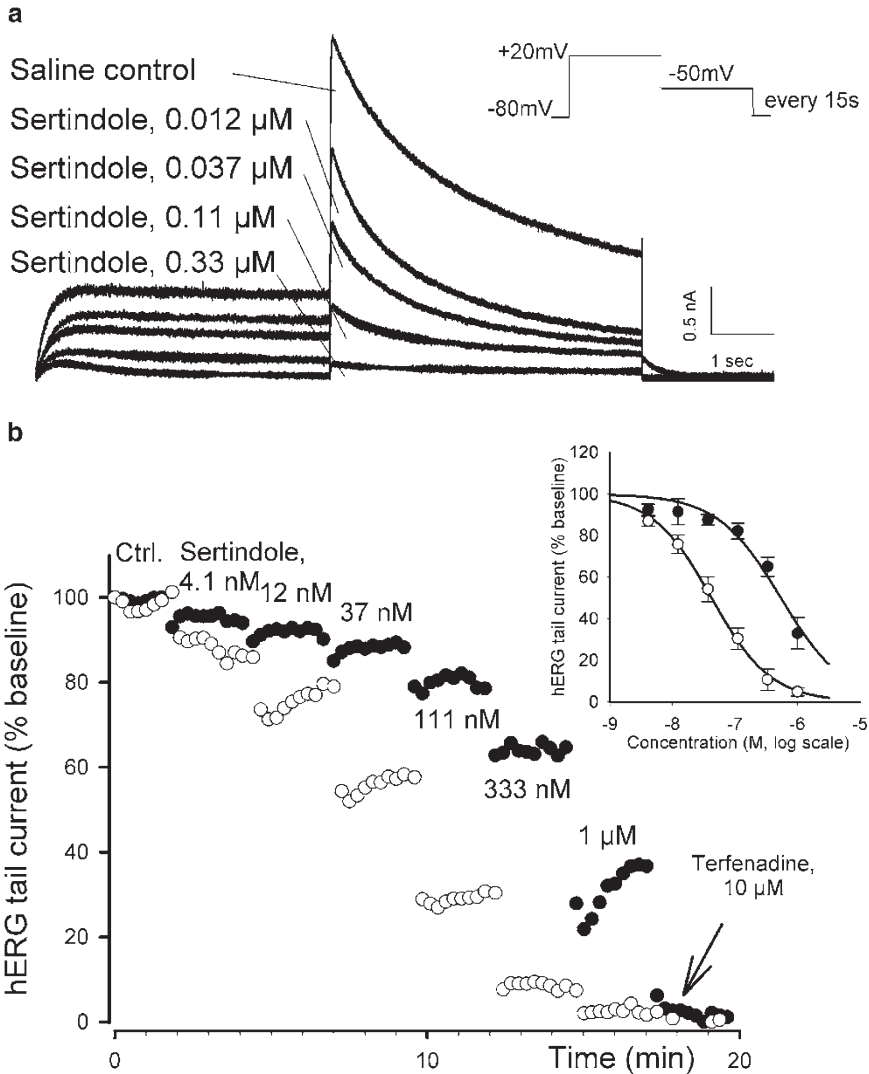


Fig. 1 Inhibition of hERG currents by the antipsychotic sertindole. Graph (a) shows a series of superposed representative current traces from whole-cell recordings of hERG cells in the absence or presence of the indicated concentration of sertindole. Upper right inset depicts the voltage protocol applied to trigger the hERG tail current. Graph in (b) shows time course of normalized hERG tail current amplitude in response to cumulative applications of six concentrations of sertindole prepared by dissolution of concentrated stocks in DMSO into extracellular recording medium either in the absence (*filled symbols*) or presence (*open symbols*) of 0.06% Pluronic® F-68. Inset illustrates sigmoidal concentration-response fitting of mean data collected from $n = 6$ to 7 recordings in the absence or presence of the surfactant, respectively. Note the >tenfold increase in the potency of sertindole. Error bars represent S.D.

media at neutral pH and room temperature. PF68 has no effect on hERG current when added to the cells in concentrations up to 0.5% (w/v).

- Use only $\geq 99.9\%$ analytical grade salts and ultra-pure water obtained by de-ionization and reverse osmosis (e.g., MilliQ®, Millipore) since metal traces can affect ion channel function.

Table 1
Evaluation of reference hERG inhibitors from various therapeutic classes and diverse chemical families

Therapeutic class	Drug	hERG IC ₅₀ (Mean ± SD, μM) by automated patch-clamp	Literature data (μM) from manual patch-clamp experiments
Antipsychotic	Chlorpromazine	2.8 ± 0.4 (<i>n</i> = 7)	1.2 [5]
	Pimozide	0.06 ± 0.04 (<i>n</i> = 8)	0.017 [6]
	Sertindole	0.043 ± 0.009 (<i>n</i> = 6)	0.011 [5]
Antihistamine	Terfenadine	0.06 ± 0.019 (<i>n</i> = 4)	0.019 [5]
	Loratadine	13 ± 1.3 (<i>n</i> = 4)	3.9 [7]
Antiarrhythmic	Bepriidil	0.27 ± 0.02 (<i>n</i> = 3)	0.15 [5]
	Dofetilide	0.045 ± 0.013 (<i>n</i> = 4)	0.012 [8]
Antibiotic	Moxifloxacin	45 ± 11 (<i>n</i> = 4)	93 [5]
Prokinetic	Cisapride	0.063 ± 0.017 (<i>n</i> = 3)	0.012 [5]

Data are half-maximal inhibitory concentrations (IC₅₀) determined either by automated or manual patch-clamp. Numbers in brackets indicate replicate determinations

Keep all stocks in glass or plastic bottles no longer than 6 months and at 4 °C to limit evaporation.

4. Some investigators use Na₂ATP but the free acid has affinity for Mg²⁺ and can decrease the seal quality. Adjust weight calculations according to Mg content of MgATP batch as needed.
5. Use security equipment (mask, gloves, protective clothing) for the safe handling of liquid nitrogen. Usually about one million CHO hERG Duo cells are banked in 1 mL cryopreservation medium.
6. Take this moment to note passage number, date of congelation, and number of cells contained in the vial just defrosted on the lab notepad.
7. Do not let the cells overgrow while passaging them as this is suspected to irreversibly degrade the quality of the hERG currents.
8. It is possible to program an automated transfer of the cells from a cell hotel located on the robot work area, but manual resuspension and transfer to the microcentrifuge affords better results and consumes less cells. Moreover, keeping the cells in serum-free sustainment medium in the refrigerator until being processed in the next job provides better recordings.
9. It is recommendable not to submit small volumes of concentrated DMSO solution to repeated freeze-thaw cycles since this tends to cause precipitation of poorly soluble compounds.

Use of glass-coated plates may be advised for particularly hydrophobic compounds.

10. This volume is slightly above the total well volume of a V-bottom standard microtiter plate and the liquid forms a convex meniscus. A volume of 60 μL is removed from each well at the end of the dilution process to prevent spillover during maneuvers of the microtiter plate by the robot.

Acknowledgments

The authors would like to thank David Rampe and Terence Appelqvist for their critical review of the manuscript.

References

1. Roden DM (2016) Predicting drug-induced QT prolongation and torsades de pointes. *J Physiol* 594:2459–2468
2. Rampe D, Brown AM (2013) A history of the role of the hERG channel in cardiac risk assessment. *J Pharmacol Toxicol Methods* 68:136–122
3. Terstappen GC, Roncarati R, Dunlop J, Peri R (2010) Screening technologies for ion channel drug discovery. *Future Med Chem* 2: 715–730
4. Mathes C (2006) QPatch: the past, present and future of automated patch clamp. *Expert Opin Ther Targets* 10:319–327
5. Crumb WJ Jr, Vicente J, Johannesen L, Strauss DG (2016) An evaluation of 30 clinical drugs against the comprehensive in vitro proarrhythmia assay (CiPA) proposed ion channel panel. *J Pharmacol Toxicol Meth* 81:251–262
6. Pearlstein R, Vaz R, Rampe D (2003) Understanding the structure-activity relationship of the human Ether-a-go-go-Related Gene cardiac K^+ channel. A model for bad behavior. *J Med Chem* 46:2017–2022
7. Kirsch GE, Trepakova ES, Brimecombe JC, Sidach SS, Erikson HD, Kochan MC, Shyjka LM, Lacerda AE, Brown AM (2004) Variability in the measurement of hERG potassium channel inhibition: effects of temperature and stimulus pattern. *J Pharmacol Toxicol Methods* 50:93–101
8. Snyders DJ, Chaudhary A (1996) High affinity open channel block by dofetilide of hERG expressed in a human cell line. *Mol Pharmacol* 49:949–955

Impedance Measurement in Induced Pluripotent Stem Cell-Derived Cardiomyocytes

Emma-Jane Poulton

Abstract

Impedance-based measurement is a useful tool for assessing the contractility of plated cardiomyocytes in the context of early preclinical cardiosafety assessment. Induced pluripotent stem cell-derived cardiomyocytes (iPSCs) can be used for this purpose as these cells display similar electrochemical properties to primary cardiomyocytes and beat reliably and in synchronicity in culture. Here we describe a method for measuring the contractility of iPSCs using the xCELLigence RTCA impedance measurement system.

Key words iPSC cardiomyocytes, iCells cardiomyocytes, Contractility measurement, Impedance, Cardiosafety

1 Introduction

Cardiosafety is of major concern during the drug development process, with more than a third of drug withdrawals attributed to cardiotoxicity [1, 2]. It is now routine to screen compounds for their ability to inhibit the human *ether-a-go-go*, hERG, channel, typically using the patch-clamp technique with mammalian cell lines stably expressing the channel, although binding and fluorescence assays may also be used [3, 4]. There are also assays that use whole-cell systems, screening for pro-arrhythmic effects by examining action potential duration in whole-animal hearts or Purkinje fibers, as well as in vivo studies using telemetered animals [4, 5].

The development of human induced pluripotent stem cell-derived cardiomyocytes (hiPSCs) has provided an additional tool for the development of in vitro cardiosafety assays. It is possible to obtain primary cardiomyocytes from rodents and humans, but low yields, technical challenges, and differences from in vivo cardiomyocytes have precluded wide adoption [6]. HiPSCs have been shown to possess similar electrophysiological properties to primary human cardiomyocytes. HiPSCs can be more than 98% cardiomyocytes, though with a mix of atrial, nodal, and ventricular-like action

potentials. They can be cultured successfully for over 2 weeks and begin to beat spontaneously and in synchrony [7].

A number of different technologies have been leveraged to study these cells, including microelectrode array, calcium flux assays, and electrical impedance measurement [8–10]. In electrical impedance measurement, cells are plated on gold-plated microelectrode arrays and a low voltage (less than 20 mV) is applied; the electric current created between the electrodes is modulated by the number of cells on the electrode, as well as the morphology and strength of attachment of those cells. Cardiomyocyte contraction creates changes in cell morphology, which can be monitored using impedance [11, 12].

Impedance measurement allows for real-time monitoring of beating cardiomyocytes in a label-free manner. In order to measure these morphological changes the instrument used must be capable of acquiring data at a rate that can resolve the morphological changes caused by cardiomyocyte beating. The real-time cell analysis (RTCA) cardio impedance measurement system from xCELLigence is able to acquire data at a 12.9-ms resolution, thus allowing for this measurement in real time. Data is reported in Cell Index (CI) values, an arbitrary number that is a reflection of cell number, attachment, and morphology. CI can be used to assess both contractility and overall effects on the cardiomyocytes [12]. A number of different publications have used impedance measurement in conjunction with iPSC-derived cardiomyocytes for preclinical safety assessment [8, 11–14]. This chapter describes the procedure for performing impedance measurement on iCells, an hiPSC-derived cell line, using the xCELLigence RTCA Cardio instrument.

2 Materials

Materials should be stored as indicated. Cell culture materials should be stored according to the manufacturer's instructions.

1. Fibronectin solution: Dilute sterile fibronectin (Roche, Basel, Switzerland) with sterile water to a concentration of 1 mg/mL. Freeze in 100 μ L aliquots (*see Note 1*).
2. iCells: hiPSC-derived cardiomyocyte cell line from Cellular Dynamics Inc., Madison, WI (*see Note 2*). Store in liquid nitrogen until ready to use.
3. Cardiomyocyte maintenance media (CMM) (Cellular Dynamics Inc., Madison WI) (*see Note 3*).
4. Cardiomyocyte plating media (CPM) (Cellular Dynamics Inc., Madison WI).
5. xCELLigence Real-Time Cell Analysis (RTCA) Cardio Analyzer (ACEA Biosciences, San Diego, CA).

6. Cardio software version 1.0. (ACEA Biosciences, San Diego, CA).
7. E-Plate cardio 96: 96-Well microtiter plates with gold micro-electrode (ACEA Biosciences, San Diego, CA).
8. Cell culture incubator capable of maintaining a temperature of 37 °C and a CO₂ concentration of 5%.
9. Biosafety cabinet for cell culture.
10. Water bath.
11. Multichannel pipet.
12. Filter-sterilized PBS.

3 Methods

All cell culture work should be performed in a biosafety cabinet to maintain sterility. Use disposable sterile pipette tips and tubes.

3.1 Cell Culture

3.1.1 Coat E-Plate Cardio 96 Plates

1. Prepare fibronectin-coating solution by mixing 100 µL fibronectin with 10 mL filter-sterilized PBS.
2. Pipette 50–100 µL fibronectin mixture into each well of the 96-well E-plate.
3. Seal plates with parafilm.
4. Place at 4 °C overnight (*see Note 4*).

3.1.2 Perform Background Read

1. Remove fibronectin-coated E-plate from storage at 4 °C.
2. Aspirate fibronectin mixture from each well using a multichannel pipette.
3. Pipette 100 µL CMM into each well of the E-plate.
4. Allow E-plate to equilibrate in the 37 °C incubator for 5 min.
5. Place E-plate in RTCA and perform background read(s) (*see Notes 5 and 6*).

3.1.3 Thaw and Plate the iCells (hiPSC Cardiomyocytes)

1. Bring CPM to room temperature.
2. Transfer cells from liquid nitrogen to dry ice for transport.
3. Thaw for 4 min in a 37 °C water bath.
4. Hold vial(s) stationary in water bath during thaw.
5. Decant cells into a sterile 50 mL tube, and dilute with 3–5 mL CPM per vial of cells (*see Note 7*).
6. Count and plate 30,000 cells per well in 100 µL plating media (*see Note 8*).
7. Gently tap the sides of the E-plate and allow to rest in biosafety cabinet for 30 min prior to placing into incubator.

3.1.4 Change the CPM to CMM After 48 h

1. Warm the aliquot of CMM in a 37 °C water bath.
2. Pause the RTCA Cardio Analyzer and remove E-plate to bio-safety cabinet.
3. Aspirate CPM from each well using a multichannel pipette and replace with 100 µL warmed CMM.
4. Repeat this process to change media every 48–72 h (*see Note 9*).

3.2 Compound Treatment

1. Check the beating pattern of the cells periodically with the RTCA Cardio Analyzer. The beating pattern should stabilize prior to compound treatment. With iCell cardiomyocytes this typically occurs 7 days after plating (*see Note 10*). Prior to compound treatment monitor beating every 2–10 min for at least 30 min to confirm that beating pattern is stable (*see Note 11*, Fig. 1).
2. Once beating is stable plates can be treated with compounds of interest. Dissolve compounds in appropriate solvent to create stock solution. Stock concentration should be 1000× final dosing concentration. Add 1.1 µL stock solution to 100 µL CPM. Then add 10 µL of this dosing media to the 100 µL media in the E-plate (*see Note 12*).
3. Begin recording immediately. Monitor beating more often during the first hour of treatment to examine transient effects; beating can be monitored less frequently for duration of experiment (*see Note 13*).
4. When the experiment is complete remove the plate from the instrument and discard in accordance with waste disposal regulations. Save the experimental data.

3.3 Data Analysis

1. Analyze data using the cardio software version 1.0. Select a normalized time from the beating patterns measured shortly before compound treatment (*see Note 14*).
2. Calculate normalized beating rate and normalized amplitude. Examine traces manually for irregular beating (*see Note 15*).

4 Notes

1. Avoid repeated freeze–thaw cycles with diluted fibronectin; freeze in aliquots appropriate to make enough coating solution for one E-plate.
2. Other manufacturers also produce iPSC-derived cardiomyocytes from both human and other species. Adjust cell culture materials and culturing methods to those adapted to the cardiomyocytes being used.

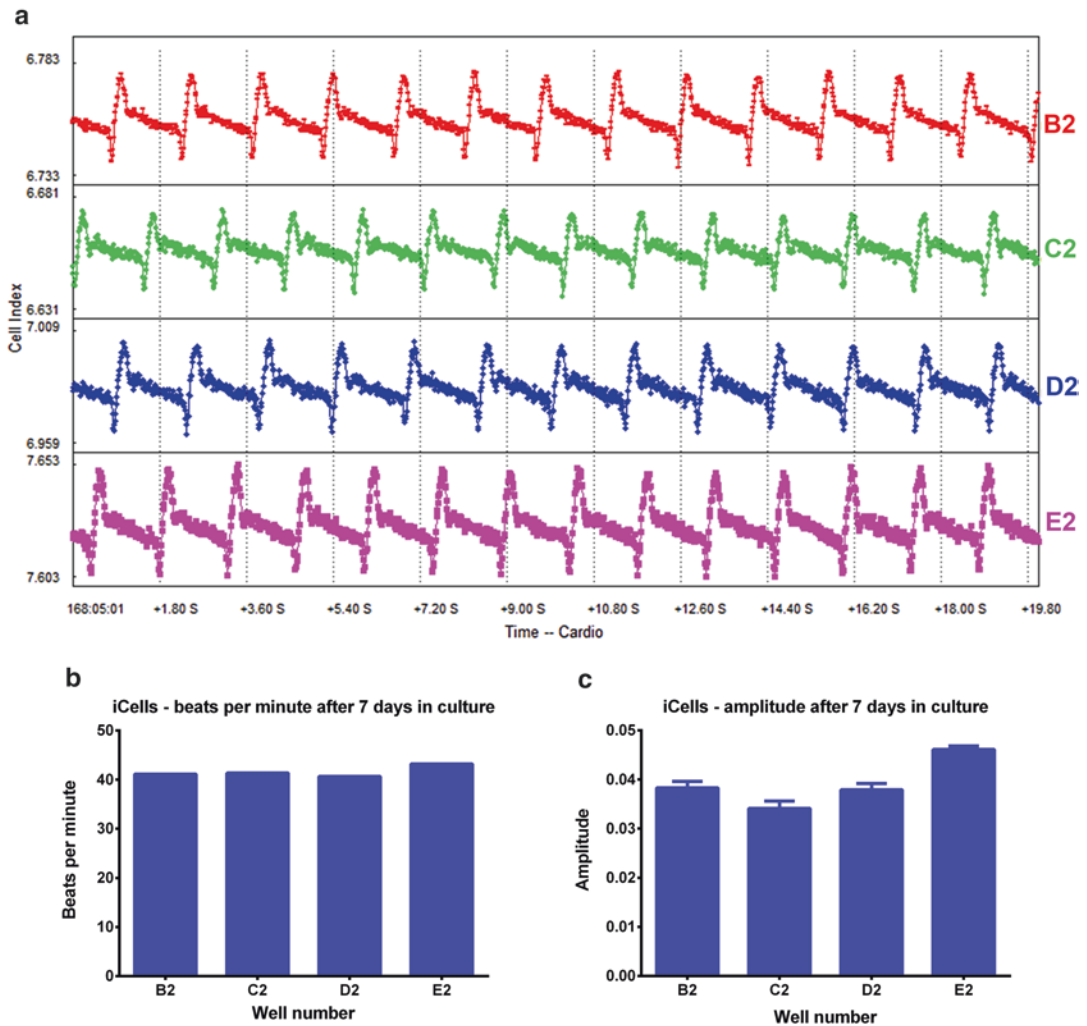


Fig. 1 (a) Beating pattern of iCells after 7 days in culture at threshold 12, data represent 4 individual wells (wells B2, C2, D2, E2). (b) Beating rate of iCells after 7 days in culture. (c) Amplitude of iCells after 7 days in culture

- Due to risk of contamination use sterile reservoirs and aliquot CMM into single-use aliquots. Aliquots of CMM can be thawed at 4 °C up to 4 days before use. Do not refreeze. Do not reuse the same aliquot of media.
- Fibronectin-coated plates can be left at 4 °C for up to 2 weeks.
- Background read should be performed in the same E-plate that will be used for the experiment. If this is not feasible another clean E-plate may be substituted.

6. Prior to performing the background read a schedule should be defined in the schedule tab. This should be designed to suit the needs of the experiment and can be modified prior to starting the plate read. The beating pattern of the cells prior to the start of the experiment can be monitored infrequently until the correct beating pattern is established.
7. Thawed cardiomyocytes are susceptible to osmotic shock. To prevent cellular damage add media slowly, beginning in a drop-wise fashion. Several vials of cells may be thawed simultaneously; media may be added faster as volume increases. Cells should be mixed by tube inversion and very gentle pipetting.
8. Edge effects from plating the cells make the wells lining the outer rim of the 96-well plate more prone to failure; it is recommended that only the inner 60 wells are plated. 100 μ l media should be placed in edge wells in order to maintain a consistent environment.
9. The beating pattern of the cells will begin to change if the media is not changed after more than 48 h. The cells should recover their normal beating pattern once the media is changed, but this can take a few hours. Due to this effect it is recommended that the media be changed the day before compound treatment. If media needs to be changed on the day of compound treatment ensure that sufficient time is allowed for restoration of stable beating pattern.
10. iCells should develop a steady and stable beating pattern after 2–3 days; by day 7 the beating pattern should have shifted from a beating pattern with only down strokes (noted by a diamond in the xCELLigence software) and moved to a pattern with both up and down stroke (noted by a square in the xCELLigence software) and the beating should be regular (*see* Fig. 1). iPSC cardiomyocytes from other sources may require different amounts of time in culture and developed sustained beating with a different pattern. It is recommended that each different line of iPSC-derived cardiomyocyte is studied before use so that the lab may understand typical beating patterns for each cell line. Cardiomyocytes from other species and cardiomyocytes derived from patient cell lines may also be used, as long as they beat in synchronicity.
11. Criteria for acceptable beating parameters should be established for every cell type used. Both beating rate and amplitude should be assessed. Amplitude will vary with cell plating density. For iCells at the suggested density, beat rate in our lab stabilizes between 35 and 50 beats per min (BPM) with an amplitude above 0.25. Wells which fail to meet these criteria

can be excluded from analysis. These criteria may differ for different iPSC-derived cardiomyocytes; establish these parameters before working with the cells.

12. Care should be taken to minimize the time cells remain outside of incubator as changes in temperature can affect the beating pattern. Either use a warming tool which will maintain the plate at 37 °C or take care to treat the cells rapidly. If DMSO is used as the solvent final concentrations should be no more than 0.1%. The effects of other solvents on cardiomyocyte beating patterns should be determined prior to their use. Less than 10% new media should be added to avoid affecting the beating pattern. Even with these precautions the beating pattern may take 5–10 min to stabilize.
13. The timing of beating pattern measurement will depend on the intention of the experiment. Beating should be measured more often immediately following treatment in order to ensure that acute effects are observed. A typical 24-h experiment may measure beating every minute for the first hour, every 5 min for the next 2 h, and then every hour until the experiment concludes. Since beating may take a few minutes to stabilize after compound addition, ensure that controls have restored normal beating patterns at the first time point used for analysis.
14. Setting threshold is important in measurement of beat rate and amplitude. Setting the threshold too low can result in overcounting of peaks. Setting the threshold too high can result in missing irregular beats of smaller magnitude. In order to minimize this problem, beat rate and amplitude can be measured at a high threshold, and irregular beats should be determined with the threshold reduced (*see* Fig. 2). Manual examination of the traces should be done to confirm that irregular beats are present.
15. If impedance is to be measured over longer periods of time (>1 h) it is recommended to calculate the normalized beat rate and amplitude over time. Compounds can cause delayed effects, or cause the cells to stop beating after short-term treatment with resumption of normal beating occurring later during the incubation. Total impedance values over time can also be followed to reveal doses cytotoxic to the cardiomyocytes. A supplemental biochemical assay, such as an ATP assay, can be performed when the experiment is terminated, to confirm measurement of cytotoxicity.

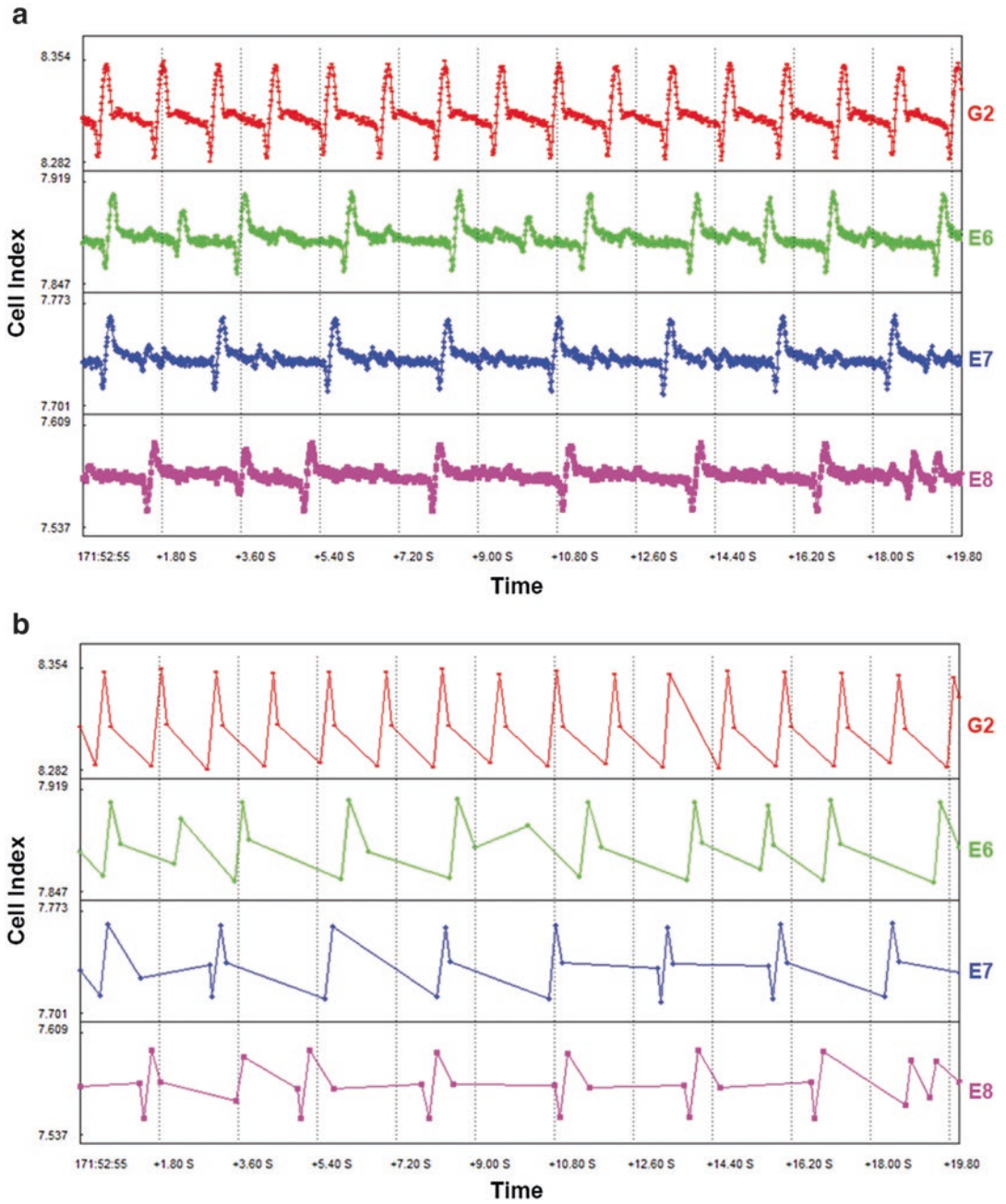


Fig. 2 (a) Beating pattern of iCells after 30 min of DMSO (top line for well G2) or cisapride treatment (0.125 μM) (wells E6, E7, E8) recorded at a high threshold of 12. Note small irregular beats in all cisapride-treated wells. (b) Beating pattern after 30 min of DMSO (top line for well G2) or cisapride treatment (0.125 μM) (wells E6, E7, E8) at a low threshold of 1. Irregular beats are still visible in wells E6 and E8

References

1. Shah RR (2005) Drugs, QT interval prolongation and ICH E14: the need to get it right. *Drug Saf* 28(2):115–125
2. Stevens JL, Baker TK (2009) The future of drug safety testing: expanding the view and narrowing the focus. *Drug Discov Today* 14(3–4):162–167
3. Brown AM (2005) HERG block, QT liability and sudden cardiac death. *Novartis Found Symp* 266:118–131; discussion 131–135, 155–158
4. Fermi B, Fossa AA (2003) The impact of drug-induced QT interval prolongation on drug discovery and development. *Nat Rev Drug Discov* 2(6):439–447
5. Valentin JP, Bialecki R, Ewart L, Hammond T, Leishmann D, Lindgren S, Martinez V, Pollard C, Redfern W, Wallis R (2009) A framework to assess the translation of safety pharmacology data to humans. *J Pharmacol Toxicol Methods* 60(2):152–158
6. Denning C, Anderson D (2008) Cardiomyocytes from human embryonic stem cells as predictors of cardiotoxicity. *Drug Discov Today: Ther Strateg* 5(4):223–232
7. Ma J, Guo L, Fiene SJ, Anson BD, Thomson JA, Kamp TJ, Kolaja KL, Swanson BJ, January CT (2011) High purity human-induced pluripotent stem cell-derived cardiomyocytes: electrophysiological properties of action potentials and ionic currents. *Am J Physiol Heart Circ Physiol* 301(5):H2006–H2017
8. Nguemo F, Saric T, Pfannkuche K, Watzele M, Reppel M, Hescheler J (2012) In vitro model for assessing arrhythmogenic properties of drugs based on high-resolution impedance measurements. *Cell Physiol Biochem* 29(5–6): 819–832
9. Harris K, Aylott M, Cui Y, Louttit JB, McMahon NC, Sridhar A (2013) Comparison of electrophysiological data from human-induced pluripotent stem cell-derived cardiomyocytes to functional preclinical safety assays. *Toxicol Sci* 134(2):412–426
10. Huebsch N, Loskill P, Mandegar MA, Marks NC, Sheehan AS, Ma Z, Mathur A, Nguyen TN, Yoo JC, Judge LM, Spencer CI, Chukka AC, Russell CR, So PL, Conklin BR, Healy KE (2014) Automated video-based analysis of contractility and calcium flux in human-induced pluripotent stem cell-derived cardiomyocytes cultured over different spatial scales. *Tissue Eng Part C Methods* 21(5):467–479
11. Peters MF, Lamore SD, Guo L, Scott CW, Kolaja KL (2014) Human stem cell-derived cardiomyocytes in cellular impedance assays: bringing cardiotoxicity screening to the front line. *Cardiovasc Toxicol* 15(2):127–139
12. Xi B, Wang T, Li N, Ouyang W, Zhang W, Wu J, Xu X, Wang X, Abassi YA (2011) Functional cardiotoxicity profiling and screening using the xCELLigence RTCA cardio system. *J Assoc Lab Autom* 16(6):415–421
13. Guo L, Abrams RMC, Babiarz JE, Cohen JD, Kameoka S, Sanders MJ, Chiao E, Kolaja KL (2011) Estimating the risk of drug-induced proarrhythmia using human induced pluripotent stem cell-derived cardiomyocytes. *Toxicol Sci* 123(1):281–289
14. Abassi YA, Xi B, Li N, Ouyang W, Seiler A, Watzele M, Kettenhofen R, Bohlen H, Ehlich A, Kolosov E, Wang X, Xu X (2012) Dynamic monitoring of beating periodicity of stem cell-derived cardiomyocytes as a predictive tool for preclinical safety assessment. *Br J Pharmacol* 165(5):1424–1441

Part V

Investigative Toxicology

Target Safety Assessment: Strategies and Resources

Richard J. Brennan

Abstract

An in-depth evaluation of target safety is an invaluable resource throughout drug discovery and development. The goal of a target safety evaluation is to identify potential unintended adverse consequences of target modulation, and to propose a risk evaluation and mitigation strategy to shepherd compounds through the discovery and development pipeline, to confirm and characterize unavoidable on-target toxicities in a timely manner to assist in early program advancement decisions, and to anticipate, monitor, and manage potential clinical adverse events. The role of an experienced discovery toxicologist in synthesizing the available information into an actionable set of recommendations for a safety evaluation strategy is critical to its successful application in early discovery programs. This chapter presents a summary of some of the information types and sources that should be investigated, and approaches that can be taken to generate an early assessment of potential safety liabilities.

Key words Drug target, In silico, Safety assessment

1 Introduction

Modern approaches to drug discovery and development increasingly demand a comprehensive understanding of the biological functions of the proposed target and its relationship to the projected indications. From the perspective of the project team toxicologist, understanding target function must go beyond “normal” biology and disease relationship, and take into account possible unintended adverse consequences of target engagement by whatever modality is chosen.

A recent review of the attrition of drug candidates from the discovery and development programs (up to phase II) of four major pharmaceutical companies between 2000 and 2010 shows that slightly more than half of attrition was due to preclinical (~40%) or clinical (~11%) toxicity [1]. Toxicity can arise due to the chemical nature of the agent, its pharmacokinetics or metabolism, off-target (secondary) pharmacology, immune-mediated hypersensitivity, or idiosyncratic effects [2]. On-target adverse events, however, are also major contributors to attrition and problems in clinical

development and application. Unanticipated on-target cardiovascular toxicity of the selective cyclooxygenase 2 inhibitors rofecoxib (Vioxx) and valdecoxib (Bextra) led to their withdrawal from the market in 2004 and 2005, respectively [3, 4]. On-target adverse effects have also been troublesome in recent years in the clinical development and application of kinase inhibitors. Adverse events of kinase inhibition have ranged from the manageable (e.g., skin rash arising from EGFR inhibition) to the potentially severe or life-threatening (hypertension following VEGFR inhibition) [5–7].

Ideally, a comprehensive synthesis of the biological pathways and processes that the target is involved in, and their relationship to critical functions, would be generated early in a drug discovery project as part of the target validation and nomination process, and adverse consequences arising from exaggerated pharmacology, or from interference with pathways additional to those modulating the disease state, anticipated and managed. In reality, the full spectrum of biological properties is seldom known, particularly for newly identified targets, and the toxicologist must assemble what knowledge can be gleaned and make a best estimate as to the potential adverse effects based on the available information and their own knowledge and experience.

The toxicologist additionally must consider differences in the target across the model species typically employed in safety assessment of new pharmaceuticals to that in humans. This will include, in addition to the physical similarity of the target (typically comparing both gene and protein sequences), consideration of target expression and distribution differences, and possible differences in biological function between species.

Relevant information is gathered from a variety of sources, including Internet websites, scientific literature, public and commercial databases (Table 1), and proprietary internal knowledge, perhaps from previous projects against the target or other targets in the same pathway or protein family. Each evaluation will be somewhat different in its specific content depending on the particular target, proposed indications, target population, planned modality, and amount of existing knowledge available for the target. Further, each company will have different requirements for the format, presentation, and storage of the report. A typical target safety package is, however, likely to consider at least the following types of information:

- The physiological role of the target.
- Similarity in gene and protein sequence between humans and preclinical model species.
- Tissue distribution and expression.
- Biological interactions and pathways.
- Disease or pathology association.

Table 1
Sources of and access to information relevant to early target safety assessment

Information included^a	Source	Owner	Access	Data licensing
General information on gene and protein	www.ncbi.nlm.nih.gov/gene	National Center for Biotechnology Information	Public	Public domain
Gene function	http://www.geneontology.org	GO Consortium	Public	Creative Commons Attribution 4.0 Unported License
	https://www.wikipedia.org/	Wikimedia Foundation	Public	Creative Commons Attribution-ShareAlike 3.0 Unported License
Gene and protein sequence comparisons	https://www.ncbi.nlm.nih.gov/homologene	National Center for Biotechnology Information	Public	Public domain
Gene and protein expression	http://biogps.org	The Scripps Research Institute	Public	Dependent on source
	http://www.proteinatlas.org	The Swedish Human Protein Atlas project	Public	Creative Commons Attribution-NonCommercial-NoDerivatives 4.0 International License
	https://basespace.illumina.com	Illumina	Mixed	Commercial

(continued)

Table 1 (continued)

Information included^a	Source	Owner	Access	Data licensing
Biological interactions and pathways	http://reactome.org	Reactome Team (Ontario Institute for Cancer Research, European Bioinformatics Institute, New York University Medical Center)	Public	Creative Commons Attribution 4.0 International License
	http://ctdbase.org	North Carolina State University	Public	Any reproduction or use for commercial purpose is prohibited without the prior express written permission of the MDI Biological Laboratory and NC State University
Gene-disease and gene-toxicity associations	http://www.pathwaycommons.org	University of Toronto, Dana-Farber Cancer Institute, Harvard Medical School, Oregon Health and Science University	Public	Dependent on source
	https://apps.ingenuity.com	Qiagen	Commercial	Commercial
	https://portal.genego.com	Clarivate Analytics	Commercial	Commercial
	http://www.omim.org	Johns Hopkins University	Public	Public domain
	https://apps.ingenuity.com	Qiagen	Commercial	Commercial
	https://portal.genego.com	Clarivate Analytics	Commercial	Commercial
	http://ctdbase.org	North Carolina State University	Public	Any reproduction or use for commercial purpose is prohibited without the prior express written permission of the MDI Biological Laboratory and NC State University

Knockout and transgenic model phenotypes	http://www.informatics.jax.org	The Jackson Laboratory	Public	Any reproduction or use for commercial purpose is prohibited without the prior express written permission of the Jackson Laboratory
Competitive information	https://clinicaltrials.gov http://ipsience.thomsonreuters.com/product/integrity http://lifesciences.thomsonreuters.com/products/cortellis	U.S. National Institutes of Health Clarivate Analytics Clarivate Analytics	Public Commercial Commercial	Public domain Commercial Commercial

^aMost resources collate information from multiple sources. The primary sources described in the text are presented

- Phenotypes of target knockout or transgenic models.
- Preclinical or clinical findings with competitor drugs.
- Summary and recommendations.

This information is typically gathered and assembled into a reference document or presentation for the discovery project team (*see Note 1*). While time consuming if done manually, the search, retrieval, and presentation of the information from the multitude of sources is not in itself inherently difficult. Indeed, IT departments at some major pharmaceutical companies have developed “target dashboard” information aggregation portals that automatically collate and present pertinent information from several sources (*see Note 2*), although these often are intended for target validation from an indication perspective and may exclude essential safety information sources. An understanding of the best sources of these data, their strengths and limitations, and the specific pieces of information most useful and relevant to the safety assessment is however of great value. The following sections hopefully provide a basic introduction to these aspects and provide a primer to the generation of a target safety assessment.

2 Physiological Role of the Target (See Note 3)

The starting point for a target safety assessment should be a basic understanding of the biological role of the target. The National Center for Biotechnology Information’s (NCBI) Gene database (www.ncbi.nlm.nih.gov/gene) [8] integrates gene-specific information from multiple data sources, and provides a brief synopsis of protein function on the gene report page, accessible via a simple gene symbol or name search (Fig. 1). NCBI Gene also collates

Full Report ▾ Send to ▾ Hide sidebar >>

PTGS2 prostaglandin-endoperoxide synthase 2 [*Homo sapiens* (human)]

Gene ID: 5743, updated on 25-Sep-2016

Summary

Official Symbol PTGS2 provided by HGNC

Official Full Name prostaglandin-endoperoxide synthase 2 provided by HGNC

Primary source HGNC:HGNC:9605

See related Ensembl: ENSG00000073756 HPRD:02599, MIM:600262, Vega: OTTHUMG00000035473

Gene type protein coding

RefSeq status REVIEWED

Organism [Homo sapiens](#)

Lineage Eukaryota; Metazoa; Chordata; Craniata; Vertebrata; Euteleostomi; Mammalia; Eutheria; Euarchontoglires; Primates; Haplorhini; Catarrhini; Homnidae; Homo

Also known as COX2; COX-2; PHS-2; PGG/HS; PGHS-2; hCox-2; GRIPGHS

Summary Prostaglandin-endoperoxide synthase (PTGS), also known as cyclooxygenase, is the key enzyme in prostaglandin biosynthesis, and acts both as a dioxigenase and as a peroxidase. There are two isozymes of PTGS: a constitutive PTGS1 and an inducible PTGS2, which differ in their regulation of expression and tissue distribution. This gene encodes the inducible isozyme. It is regulated by specific stimulatory events, suggesting that it is responsible for the prostanooid biosynthesis involved in inflammation and mitogenesis. [provided by RefSeq, Feb 2009]

Orthologs [mouse](#) [all](#)

Table of contents

- Summary
- Genomic context
- Genomic regions, transcripts, and products
- Bibliography
- Phenotypes
- Variation
- HIV-1 interactions
- Pathways from BioSystems
- Interactions
- General gene information
 - Markers, Homology, Gene Ontology
- General protein information
- NCBI Reference Sequences (RefSeq)
- Related sequences
- Additional links

Fig. 1 Screenshot of the Report page for human prostaglandin-endoperoxide synthase 2 from NCBI Gene (<https://www.ncbi.nlm.nih.gov/gene/5743>). Retrieved on 07/24/2016

information and provides links to other sources of useful information, including sequences, gene variants, genome-wide association study findings, links to biological pathways from KEGG (<http://www.kegg.jp>) and Reactome (<http://reactome.org/>), and “GenRIFs” which are investigator-submitted concise phrases describing a function or functions of a gene product, and are linked to the original publication.

Gene Ontology annotations also provide insight into target biology. The Gene Ontology (GO) project (<http://www.geneontology.org/>) is a large consortium of research groups who develop and use ontologies to provide biologically meaningful annotation of genes and their products [9]. Target functions are classified in three related categories: cellular component (where in the cell the protein is found), molecular function (the jobs that it does or the “abilities” that it has), and biological process (a recognized series of events or molecular functions) [10]. Conveniently, GO annotations are also available from NCBI Gene.

An increasingly valuable source of information on gene and protein function is the online crowd-sourced knowledge commons Wikipedia (<https://www.wikipedia.org/>). Particularly for well-studied targets, a wealth of information on target structure, function, pathways, and even clinical relevance may be available. As always with online sources, original references should be reviewed when information might be critical to the assessment.

A careful review of the current scientific literature relating to the target will round out functional awareness with newly published findings and any relevant obscure or esoteric findings not captured by other information-gathering sources. A variety of search strategies employing target name or ID with terms relating to function, toxicity, or adverse effects may be needed. Often, applying similar searches in broader Internet search engine such as Google (<https://www.google.com/>) will further reveal useful published information in nonindexed sources such as white papers or symposium presentations.

3 Similarity in Gene and Protein Sequence Between Humans and Preclinical Model Species

Surrogate animal species remain fundamental to preclinical evaluation of pharmaceutical safety. Given this necessity, it is important to evaluate whether the reported homolog to the target in the various species used is sufficiently similar in structure and function to that in humans. Gene and protein sequences can be readily retrieved and compared at the NCBI HomoloGene database (<https://www.ncbi.nlm.nih.gov/homologene>). A table comparing both gene and protein sequence similarity across several species, including rat, mouse, dog, and nonhuman primate, can be generated using the “Show Pairwise Alignment Scores” link on the

Pairwise Alignment Scores

Species	Gene	Symbol	Identity (%)	
			Protein	DNA
H.sapiens		PTGS2		
vs. P.troglodytes		PTGS2	99.7	99.6
vs. M.mulatta		PTGS2	98.2	97.8
vs. C.lupus		PTGS2	90.1	88.4
vs. B.taurus		PTGS2	89.0	87.7
vs. M.musculus		Ptgs2	87.1	84.9
vs. R.norvegicus		Ptgs2	86.6	84.1
vs. G.gallus		PTGS2	82.7	78.2
vs. X.tropicalis		ptgs2	75.9	71.2
vs. D.rerio		ptgs2b	75.3	70.9

Fig. 2 Pairwise alignment scores for human prostaglandin-endoperoxide synthase 2 against homologs in other species from NCBI HomoloGene (https://www.ncbi.nlm.nih.gov/homologene?cmd=Retrieve&dopt=AlignmentScores&list_uids=31000) (see **Note 4**). Retrieved on 07/24/2016

gene information page accessed via a search for gene or protein name or id (Fig. 2).

While a reasonable level of sequence similarity can give an initial indication that a chosen model species is likely to be appropriate, confirmation of candidate drug activity against the target in the chosen toxicology species is prudent, particularly when a highly specific modality such as a monoclonal antibody is to be developed. In the case of low target similarity, or lack of a suitable orthologue in a model species, use of that species as a primary safety model may be precluded, or the development of a substantially equivalent pharmacological surrogate drug necessitated.

4 Tissue Distribution and Expression

A good understanding of where the target is expressed in the body is an important consideration for a safety assessment. A high expression level in a particular organ, tissue, or cell type might for example indicate an increased likelihood of adverse effects in that region, particularly if the target is known to have an important function in that tissue or cell type. Particular attention might be directed to these areas in exploratory safety studies, especially if the cell type or tissue is not commonly evaluated in early studies. Similarly, if a target is expressed significantly in CNS and is being considered for a non-neurological indication, the toxicologist might encourage the discovery team to favor candidates with low blood–brain barrier penetration to avoid any potential neurotoxicity issues.

Information on the level of expression of human genes across tissue is available from a variety of sources. BioGPS (<http://biogps.org>) [11] is a publically accessible database that, among other information, provides a gene expression chart with detailed expression information across multiple tissue and cell types. Comparison of expression in mouse and rat is also possible in BioGPS, although the specific tissues and level of granularity vary across the species. BaseSpace Correlation Engine (Previously NextBio, <https://basespace.illumina.com/>) is a commercial tool that provides a Body Atlas of collated expression data for a particular human gene across multiple tissues and cell types. Data derived from either microarray experiments or RNA-Seq can be queried. Body Atlas also has expression data for mouse genes covering several common laboratory strains. More detailed information on expression in other model species may be available from species-specific resources, for example rat (<http://pgx.fudan.edu.cn/rat-bodymap/>) or dog (<https://ccrod.cancer.gov/confluence/Display/CCRCOPWeb/Canine+Normal+Tissue+Database>).

While gene expression data are useful and readily available, expression of functional protein is usually of greater interest. The Human Protein Atlas (<http://www.proteinatlas.org>) integrates RNA and protein expression data over most of the human protein-coding genes, with access to the primary data for both RNA and protein on an individual gene level [12] (Fig. 3) (*see Note 5*).

5 Biological Interactions and Pathways

There are a number of public databases that collate information on biological molecular interactions (protein–protein, compound–protein, transcription factor–gene, etc.) and pathways, including Reactome (<http://reactome.org>) [13], Kyoto Encyclopedia of Genes and Genomes [14], and The Comparative Toxicogenomics Database (<http://ctdbase.org/>) [15]. Pathway Commons (<http://www.pathwaycommons.org>) provides a collection of publicly available pathway data from multiple organisms and a Web-based interface enabling the user to browse and search pathways from multiple sources [16].

Commercial network and pathway analysis packages such as Ingenuity Pathway Analysis (Qiagen, <https://apps.ingenuity.com>) and MetaCore (Clarivate Analytics, <https://portal.genego.com/>) provide a “one-stop-shop” portal for information on genes, proteins, networks, and pathways, with powerful search, analysis, and visualization tools, comprehensive collections of prebuilt networks and canonical pathways maps, and tools for directed reconstruction of biological networks from high-quality internal databases of biological interactions (Fig. 4).

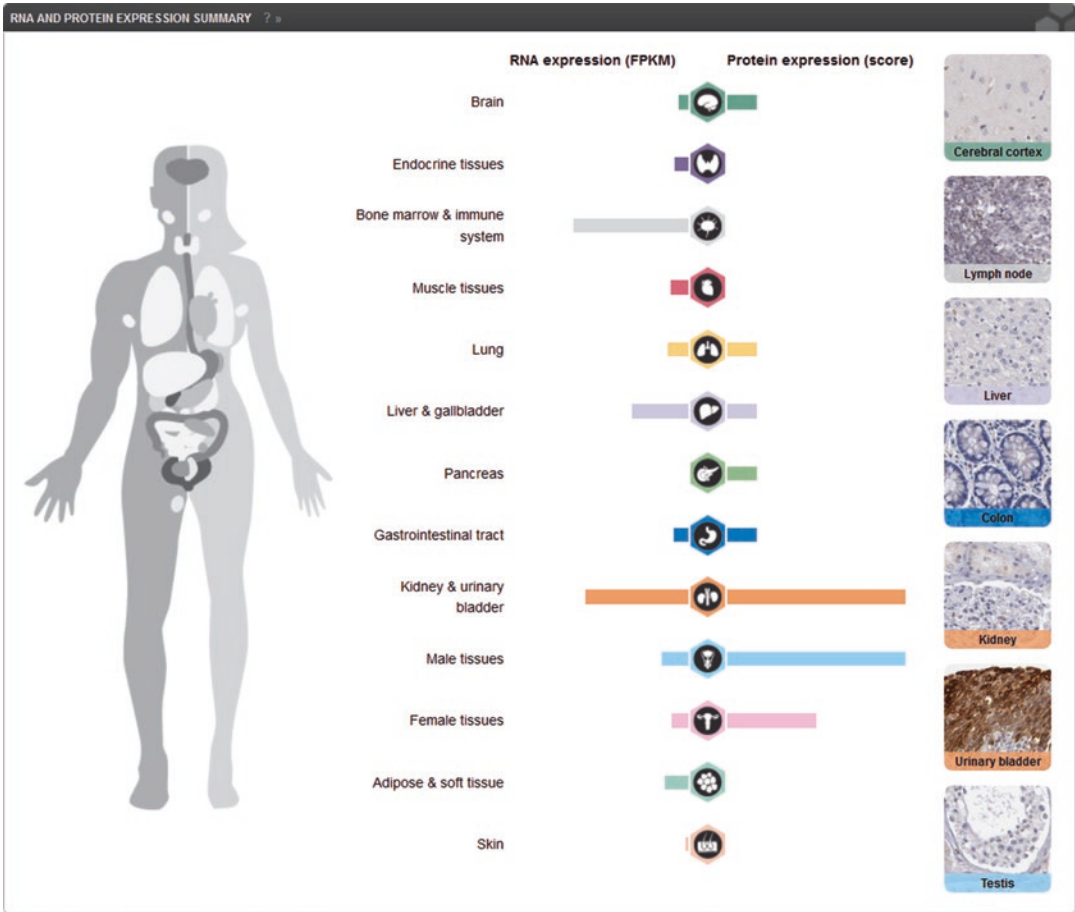


Fig. 3 mRNA and protein expression summary for human prostaglandin-endoperoxide synthase 2 from Human Protein Atlas (<http://www.proteinatlas.org/ENSG00000073756-PTGS2/tissue>) (see Note 5). High-level systems can be expanded to show more detailed tissue distributions. Retrieved on 07/24/2016

Information gathered from these sources may include not only known protein complexes, pathways, and signaling networks that the target participates in, but also a more holistic view of the biological neighborhood of the target, particularly with respect to which functions downstream of the target are likely to be affected by changes in its activity. In many cases, pathways may be annotated with their relationship to biological phenotypes, diseases, or pathological outcomes. Pathways and biological interactions can provide clues to potential adverse outcomes. With additional network analysis such as directed network reconstruction and causal network reasoning [17] the investigation may be further expanded to hypothesize specific mechanisms by which those outcomes are likely to arise, and suggest potential tractable biomarkers of toxicity pathway perturbation.

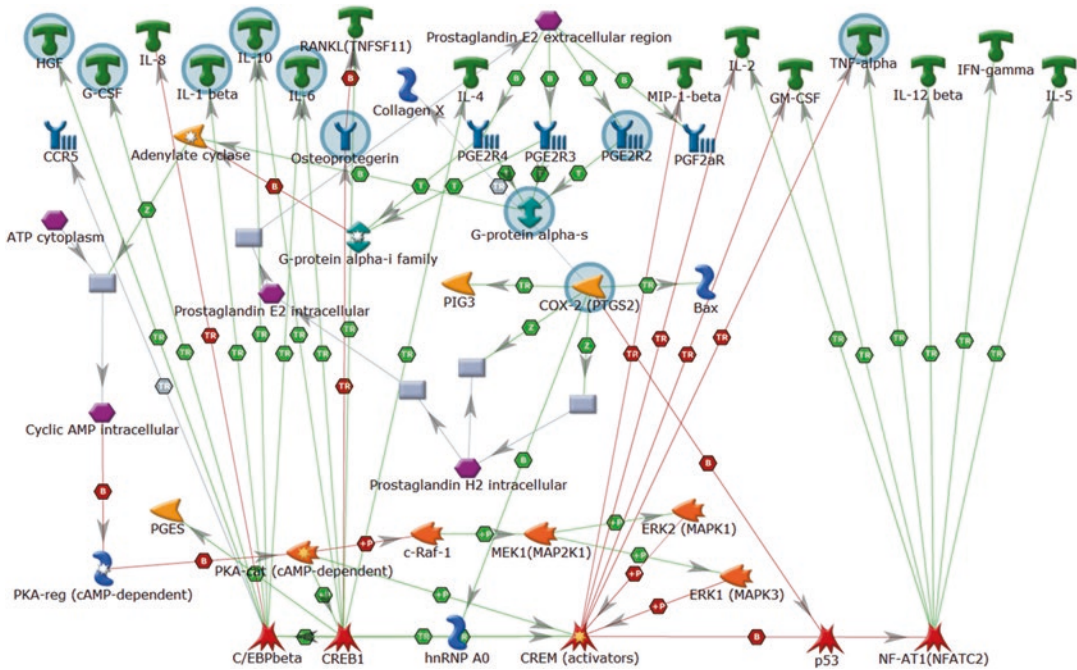


Fig. 4 Downstream signaling network of prostaglandin-endoperoxide synthase 2 (MetaCore). *Colored shapes* represent different classes of proteins. *Purple hexagons* represent small molecules. *Grey rectangles* represent catalytic functions. Objects are connected by *directional arrows* with a *central hexagon* indicating the mechanism and the color representing the effect (*red*—negative, *green*—positive) of the interaction. Full legend available at https://ftp.genego.com/files/MC_legend.pdf. Objects highlighted with a *blue-grey circle* are annotated in the MetaCore database having a disease association to thrombosis

6 Disease or Pathology Association

Known associations of the target to a disease or pathological phenotype can be very useful clues to the potential adverse effects of target modulation. Gene–disease and gene–toxicity relationships are captured in both Ingenuity Pathway Analysis and MetaCore. Usefully, this allows their consideration in network building and analysis (Fig. 4). BaseSpace Correlation Engine also includes Disease Atlas, comprising gene–disease association data from mutations, SNPs, epigenetic data, and expression alterations. Publically accessible sources of similar information include Reactome, KEGG, and The Comparative Toxicogenomics Database.

Especially informative are causal associations to human diseases arising from gene mutations or sequence variants with loss- or gain-of-function consequences. The Online Mendelian Inheritance in Man database (<http://www.omim.org/>) [18] is an excellent public source of such information, additionally providing a detailed summary of gene function (particularly as it relates to clinical phenotypes), and of clinically relevant observations in animal models.

7 Phenotypes of Target Knockout or Transgenic Models

Also highly informative are the phenotypes of animal models where the function of the target gene has been modified. Typically these data will be from knockout mice (*see* **Note 6**), but overexpression or reduced expression models, as well as knock-in mutation and other types of models, can also be informative.

The primary source for this information is the Jackson Lab Mouse Genome Database (<http://www.informatics.jax.org/>) [19]. Mouse genetic models for a target gene can be queried by the gene name or symbol using the “Phenotypes, Alleles & Disease Models Search” tool. This query returns a table of available in vivo and in vitro models along with their category (knockout, reporter gene, conditional, etc.) and a summary of abnormal phenotypes seen with the system. Details on phenotypes observed, organized by the physiological system or process affected, can be accessed via the link to each individual model. Links to the supporting scientific publications are provided for additional detail.

8 Preclinical or Clinical Findings with Competitor Drugs

In the competitive reality of modern drug discovery it is highly unlikely that one pharmaceutical company will have an intellectual monopoly on a given target. It is more common that several companies will be working on projects to address the same target, for the same or different indications, and often at approximately the same level of progress. Companies in the discovery and preclinical development phases however are highly protective of their sensitive information and it can be very difficult to find information on the progress and bottlenecks of other programs against a target. Even when development has been stopped the underlying reasons are seldom published in the scientific literature. Some information may be presented at scientific conferences and high-level information on the progress of a pipeline is often reported at investor meetings and the like. This can be hard to track down and assimilate however.

More information on clinical stage development projects is typically available, and when clinical trials have been run and completed, the outcomes, including information on adverse events, should eventually be published, although it can take several months or years for these data to be released. Perhaps however the project team is working on a target that has previously seen compounds in clinical trials against a different indication. It is also possible that drugs against a target that is in the same functional pathway and expected to have the same biological effect have been developed previously (for example the target is a ligand, and drugs targeting

its receptor have previously been in clinical trials). Any available safety data from clinical stage programs is, of course, of great value to assessing the potential liabilities (or safety) of a target.

Clinical trial outcome data, including adverse events, is available, for trials that have posted results, at the public website <https://clinicaltrials.gov/>. The website is notoriously difficult to navigate, and outcomes data, particularly for clinical trials less than a few years past completion, is sparse. Useful information can sometimes be found with iterative searching, patience, and persistence however.

Several commercial sources of competitive information are available that gather and organize competitive pharmaceutical information from multiple sources including patents, investor presentations, press releases, financial disclosures, and posters and platform presentations at scientific meetings. Integrity (Clarivate Analytics, <http://ipscience.thomsonreuters.com/product/integrity>) is a chemistry and pharmacology-centric database with detailed data on targets, pathways, chemical structure, and activity for current and closed pharmaceutical research and development programs. Information on the highest phase of development reached, whether the program is still active, and the last reported change in status can also be found. Cortellis (Clarivate Analytics, <http://lifesciences.thomsonreuters.com/products/cortellis>) is a competitive intelligence platform with available detailed data on clinical trials for drugs, biologics, and devices, covering trial designs, endpoints, combination therapies, location, recruitment, scheduling, and adverse events.

9 Summary and Recommendations

The most critical and expert-driven section of the target safety assessment is the final summary and recommendations. Here the toxicologist must ingest and synthesize all of the information coming from many disparate sources and give their best judgment as to the potential liabilities of target engagement. These liabilities must be then considered in the light of other factors such as the severity and reversibility of the potential toxicities, the indication, its severity and the concomitant tolerance for side effects, the target patient population (juvenile, child-bearing potential, etc.) and likely treatment scenario (short-term or chronic dosing, anticipated co-medications), as well as the competitive landscape. A plan must then be formulated to chaperone the project through its early phases, accelerating investigative or mechanistic studies where necessary to evaluate critical risks, or perhaps performing a pivotal safety study at an earlier stage of development. Nonstandard assays, novel safety biomarkers, or surrogate species may need to be considered and implemented.

This analysis requires an expert understanding of discovery toxicology, but also a solid grounding in molecular and systems biology, comparative physiology, mechanistic toxicology, and clinical safety. Toxicology colleagues with different expertise and backgrounds can of course be called upon to assist with areas of unfamiliarity or where expert input relating to specific subclass of toxicology such as reproductive and developmental, or systems toxicology, is required, but the role of the project toxicologist, who is most familiar with the program, the indication, and the target, is key to successful development and implementation of the recommendations.

In recent years, a number of service providers have begun to offer target safety assessments on a fee-for-service basis. This can be a welcome assistance to resource and time-constrained toxicology teams. It is the author's opinion however that close communication and feedback between the provider and the project toxicologist are still necessary in order to come up with the best risk summary and evaluation/mitigation strategy.

Finally, the target safety assessment should be considered a living document. New safety-relevant information will be generated internally, if not externally, during the course of the project, and the report must be updated at regular intervals to remain current. Many of the sources of information cited are able to provide periodic updates based on the availability of new information matching one or more key words, or in particular domains for example. A review and update of the report should be considered at least for the various stage gates of a discovery and development program, such as lead optimization and candidate nomination. In our experience, the availability of a target safety assessment and a plan of action based on its findings has been successful in providing timely data for predicted liabilities that has had a direct impact on project progression decisions.

10 Notes

1. This chapter focuses on safety assessment of a single specific protein target. It may be prudent in some cases to include safety evaluation for additional or alternative targets. This may be appropriate when the intended target is a member of a closely related protein family or group of isoforms for example, and it is anticipated that specificity for the intended target may be difficult to achieve. In this case a review of the related targets may be required to identify potential adverse effects of interaction with those similar targets, and to direct screening and lead prioritization efforts to avoid secondary targets with critical liabilities. In other cases, limited information may be available on the intended target; however another target in the same specific biological pathway (such as a ligand and its receptor for

example) may be better annotated or have been the subject of previous drug discovery and development efforts. A review of the pathway-related target might provide insights into the effect of pathway perturbation. At later stages of a discovery project, when a lead candidate has been nominated and its off-target activities have been evaluated, a safety evaluation for any secondary targets that are likely to be impacted at clinically relevant exposures to the candidate may be required.

2. A recent industry-academic partnership has led to the development of the Open Targets platform (<https://targetvalidation.org/>). Open Targets is a publically accessible information aggregation and visualization website that includes many of the data types and sources mentioned in this chapter.
3. A discovery project toxicologist will likely be supporting multiple research projects, and the generation of a comprehensive safety assessment, even with ready access to the necessary information, is time consuming. It is therefore reasonable to expect that prior to commencing the safety assessment, an in-depth assessment and validation of the target with respect to the indication have been performed by the research project team. This should include detailed background information on the target biology, as well as its disease association (why it is considered a target), and may also include other relevant information such as the availability, nature, and phenotype of animal models of the disease, or previous clinical experience with the target. These can be reviewed by the toxicologist and included as appropriate in the safety evaluation and report, saving significant time.
4. Although *Canis lupus* (grey wolf) is indicated, the alignment provided is, in fact, for *Canis familiaris* (dog). Alignments for *Macaca mulatta* (rhesus macaque) are provided by default in this automatically generated table; alignments for the more commonly used *Macaca fascicularis* (Cynomolgus monkey), along with other toxicologically relevant species like *Sus scrofa* (pig) and *Oryctolagus cuniculus* (European rabbit), are also accessible via the UniGene links on the NCBI HomoloGene gene information page for the target.
5. Protein expression data reliability is dependent on the sensitivity and specificity of the antibodies used. The quality of antibodies used in the Human Protein Atlas is monitored through a number of different quality assurance steps, and a high-level reliability score given for each protein quantified. Note that mRNA and protein expression in a particular tissue may not correlate and, indeed, there may be variations between different sources of gene expression data due to differences in technology used, experimental procedures, or sources of tissue. Where an accurate evaluation of expression in a particular tissue is critical, it may be advisable to confirm this independently.

6. Care must be taken when inferring potential effects of pharmaceutical intervention by comparison to knockout models (particularly homozygous loss-of-function mutations). Functional studies in knockout animals in which a signaling pathway element is absent during gestation due to ablation or mutation of its gene may lead to different effects than inhibition of the normal pathway in adults. Absence of a nonessential function during development can lead to compensatory changes in gene expression and pathway function [20].

References

1. Waring MJ, Arrowsmith J, Leach AR et al (2015) An analysis of the attrition of drug candidates from four major pharmaceutical companies. *Nat Rev Drug Discov* 14(7):475–486
2. Guengerich FP (2011) Mechanisms of drug toxicity and relevance to pharmaceutical development. *Drug Metab Pharmacokinet* 26(1):3–14
3. Dogné JM, Hanson J, Supuran C, Pratico D (2006) Coxibs and cardiovascular side-effects: from light to shadow. *Curr Pharm Des* 12(8):971–975
4. Sun SX, Lee KY, Bertram CT, Goldstein JL (2007) Withdrawal of COX-2 selective inhibitors rofecoxib and valdecoxib: impact on NSAID and gastroprotective drug prescribing and utilization. *Curr Med Res Opin* 23(8):1859–1866
5. Liu S, Kurzrock R (2014) Toxicity of targeted therapy: implications for response and impact of genetic polymorphisms. *Cancer Treat Rev* 40(7):883–891
6. Liu S, Kurzrock R (2015) Understanding toxicities of targeted agents: implications for anti-tumor activity and management. *Semin Oncol* 42(6):863–875
7. Small HY, Montezano AC, Rios FJ, Savoia C, Touyz RM (2014) Hypertension due to anti-angiogenic cancer therapy with vascular endothelial growth factor inhibitors: understanding and managing a new syndrome. *Can J Cardiol* 30(5):534–543
8. Brown GR, Hem V, Katz KS et al (2015) Gene: a gene-centered information resource at NCBI. *Nucleic Acids Res* 43(Database issue):D36–D42
9. Gene Ontology Consortium (2008) The Gene Ontology project in 2008. *Nucleic Acids Res* 36(Database issue):D440–D444
10. du Plessis L, Škunca N, Dessimoz C (2011) The what, where, how and why of gene ontology—a primer for bioinformaticians. *Brief Bioinform* 12(6):723–735
11. Wu C, Orozco C, Boyer J et al (2009) BioGPS: an extensible and customizable portal for querying and organizing gene annotation resources. *Genome Biol* 10(11):R130
12. Fagerberg L, Hallström BM, Oksvold P et al (2013) Analysis of the human tissue-specific expression by genome-wide integration of transcriptomics and antibody-based proteomics. *Mol Cell Proteomics* 13(2):397–406
13. Croft D, Mundo AF, Haw R et al (2014) The Reactome pathway knowledgebase. *Nucleic Acids Res* 42(Database issue):D472–D477
14. Kanehisa M, Goto S, Furumichi M, Tanabe M, Hirakawa M (2010) KEGG for representation and analysis of molecular networks involving diseases and drugs. *Nucleic Acids Res* 38(Database issue):D355–D360
15. Grondin CJ, Davis AP, Wieggers TC et al (2016) Advancing exposure science through chemical data curation and integration in the Comparative Toxicogenomics Database. *Environ Health Perspect* 124(10):1592–1599
16. Cerami EG, Gross BE, Demir E et al (2011) Pathway commons, a web resource for biological pathway data. *Nucleic Acids Res* 39(Database issue):D685–D690
17. Catlett NL, Bargnesi AJ, Ungerer S et al (2013) Reverse causal reasoning: applying qualitative causal knowledge to the interpretation of high-throughput data. *BMC Bioinformatics* 14:340
18. Amberger JS, Bocchini CA, Schiettecatte F, Scott AF, Hamosh A (2015) OMIM.org: Online Mendelian Inheritance in Man (OMIM®), an online catalog of human genes and genetic disorders. *Nucleic Acids Res* 43(Database issue):D789–D798
19. Eppig JT, Richardson JE, Kadin JA et al (2015) Mouse Genome Database: from sequence to phenotypes and disease models. *Genesis* 53(8):458–473
20. Rossi A, Kontarakis Z, Gerri C et al (2015) Genetic compensation induced by deleterious mutations but not gene knockdowns. *Nature* 524(7564):230–233

Chapter 13

NMR and MS Methods for Metabolomics

Alexander Amberg, Björn Riefke, Götz Schlotterbeck, Alfred Ross,
Hans Senn, Frank Dieterle, and Matthias Keck

Abstract

Metabolomics, also often referred as “metabolic profiling,” is the systematic profiling of metabolites in biofluids or tissues of organisms and their temporal changes. In the last decade, metabolomics has become more and more popular in drug development, molecular medicine, and other biotechnology fields, since it profiles directly the phenotype and changes thereof in contrast to other “-omics” technologies. The increasing popularity of metabolomics has been possible only due to the enormous development in the technology and bioinformatics fields. In particular, the analytical technologies supporting metabolomics, i.e., NMR, UPLC-MS, and GC-MS, have evolved into sensitive and highly reproducible platforms allowing the determination of hundreds of metabolites in parallel. This chapter describes the best practices of metabolomics as seen today. All important steps of metabolic profiling in drug development and molecular medicine are described in great detail, starting from sample preparation to determining the measurement details of all analytical platforms, and finally to discussing the corresponding specific steps of data analysis.

Key words Metabolomics, Metabolic profiling, NMR, UPLC-MS, GC-MS

1 Introduction

In this chapter, the principles of metabolomics, the associated technologies, and the best practices to apply these technologies are introduced. Besides the term metabolomics, metabonomics and metabolic profiling are often found in literature. The reason is a historical parallel evolution of the concept of metabolite profiling of plants mainly based on chromatographic technologies creating the term “metabolomics” and of metabolic profiling in preclinical and clinical applications primarily based on nuclear magnetic resonance spectroscopy (NMR) forming the associated term “metabonomics.” After the foundation of the Metabolomics Society and the increasing use of MS-based techniques the term metabolomics is nowadays used. The term “metabolic profiling” is used interchangeably.

But what is metabolomics precisely? The most cited definition of metabolomics/metabonomics was published in 1999 as

“the quantitative measurement of the dynamic multiparametric response of living systems to pathophysiological stimuli or genetic modification” [1]. In other words, metabolomics is the systematic profiling of metabolites in biofluids or tissues of organisms and their temporal changes caused by different factors such as drug treatment, environmental influences, nutrition, lifestyle, genetic effects, or diseases. Hereby, single endogenous metabolites but also patterns of endogenous metabolites can be of interest. The total number of different metabolites in an organism (the so-called metabolome) is not known. Estimates based on known pathways range from several hundreds to several thousands. Yet, recently it has been shown that more endogenous metabolites exist than the number of metabolites covered by presently known pathways [2]. Additionally, the swapping of metabolites between human or mammalian metabolism and the organisms in the gut microbiome increases the network of relevant reactions by a staggering amount. In the human metabolome database (HMDB) around 42,000 metabolites are listed. Adding the number of lipid variations in the order of 100,000, the lower limit of expected endogenous and exogenous metabolites is around 150,000. From this vast amount of metabolites, only 1500 may be identified from global profiling, 200–500 from targeted profiling, and fewer are routinely subject to quantitative analysis [3]. Biochemically, metabolomics is the ultimate endpoint measurement of biological events linking genotype to phenotype but also capturing the influence of nutrition, environmental influences, response to pharmaceuticals, and many more. The importance of metabolomics for assessing health and the influence of therapies are also expressed in terms of biological timing and biological probabilities: Genetics and genomics capture events which might happen, proteomics captures events which are happening, and metabolomics captures events which have happened.

This close reflection of the phenotype may be the reason why metabolomics has even more evolved and has reached an ever-increasing number of applications in life sciences, mostly in mammalian and clinical-related research since the first edition of this chapter in 2011 [4]. This was also enabled by further improvements in MS technologies, metabolite annotation workflows, as well as protocols for quality controls and subsequent data analysis. Additionally the introduction of MS-based kits during the last 2–3 years which analyze a targeted number of 20–1184 different metabolites covering interesting biomolecules in a quantitative way in combination with low sample volume needed and easier to use workflows brought a new dimension in data accuracy, data quality, and sample turnover into the field. For example, the targeted kits from Biocrates Life Science AG cover from 17 to 188 different metabolites including steroids, bile acids, amino acids, biogenic amines, and lipids. Also, for lipidomics as a part of metabolomics,

Sciex provides a new kit for the quantification of 1184 different lipids (Lipidyzer Platform, Sciex).

This targeted metabolomics approach is quite similar to the well-established measurements of small molecules in body fluids established and accepted in clinical biochemistry, also evident by the fact that 95% of all diagnostic clinical assays test for small molecules [5]. The Majority of these tests analyze single metabolites in a targeted way and are based on typical technologies common in clinical chemistry which are completely different from the nontargeted technologies to measure and quantify numerous metabolites simultaneously. Metabolomics technology is based on two main analytical platforms: nuclear magnetic resonance spectroscopy (NMR spectroscopy) and mass spectrometry (MS), whereby the latter is typically coupled with chromatographic separation technologies. In the field of drug development, four technologies are widely used: NMR, the combination of liquid chromatography with mass spectrometry (LC-MS), its evolution called ultraperformance liquid chromatography coupled to mass spectrometry (UPLC-MS), and gas chromatography coupled to mass spectrometry (GC-MS). Hereby, the different technologies do not compete, but complement each other in terms of metabolites being covered by the different technologies. Additionally, numerous examples exist to analyze the different metabolomics platforms together or combined with other omics technologies. The analytical platforms generate hundreds to thousands of data points, which render multivariate data analysis methods indispensable to reduce the amount of data and to simplify complexity.

In the next section, methods for the appropriate sampling of biofluids and sample preparation steps are discussed in detail. Afterwards, the application of the different technologies is described with the focus on best practices. Particularities of data analysis, appropriate software, and databases are also presented.

2 Sampling

In principle ^1H -NMR or LC-MS-based metabolomics analysis can be applied on a large variety of body fluids like blood serum or plasma, urine, cerebrospinal fluid, saliva, synovial fluid, amniotic fluid, ascites, and all types of tissue extracts (e.g., tumors, brain, muscle) as well as in cell culture [6]. Most important for studies in animals and humans are sampling of blood serum or plasma and also urine as these samples are easy to obtain and are often drawn in parallel to clinical chemistry sampling during a human study or pre-clinical experiment with animals. As mechanistic work in tissues or cell cultures using metabolomics techniques has gained increasing interest we will describe sampling techniques for blood, urine, tissues, and cell cultures in the following sections.

2.1 Human Sampling

In contrast to experiments with animals using inbred strains with homogenous genetic background, age distribution, controlled food and water supply, and living conditions (caging, standardized day–night cycles) [7, 8], the situation we face working in the clinical environment is the opposite. All the above-mentioned variables have influence on the metabolomics result and influence on the scatter of the effects to be measured [9, 10]. In human studies, some of the variables can be controlled for a certain time [11–13], but this will not be possible for a larger clinical study or trial for ethical reasons. In order to minimize variability, the sampling time and conditions should be standardized as much as possible.

Ideally blood serum samples should be taken in the early morning hours in an empty stomach state (fasted). For NMR and LC-MS methods, an aliquot of 200 μL of serum or plasma is sufficient, which means that 500 μL of whole blood has to be drawn. For NMR sampling the syringe equipment should not contain gel enhancer to avoid contamination of the sample or other additives like EDTA or citrate which would result in additional signals in the ^1H -NMR spectrum. Allow serum samples for NMR to clot for 30 min at room temperature or on ice and then centrifuge for 15 min at $1500 \times g$. In contrast to NMR the optimal matrix for MS-based profiling is K-EDTA plasma. After centrifugation the supernatant will be transferred to a sample tube (e.g., NUNC cryovials, Eppendorf Safe-Lock tubes) and will be stored below -80°C . Prepare all the necessary aliquots for different type of measurements (NMR, LC-MS, clinical chemistry, other biomarkers) before freezing to avoid thawing–freezing cycles of the samples. Samples should always be taken from single individuals separately; pooling of individual samples should be avoided [14, 15].

Human urine samples should be taken in the morning hours in a clean and dry container using midstream urine. Human urine can be kept at room temperature for 24 h without significant changes in metabolite composition. However, if the circumstances allow relatively fast cooling and freezing of the sample under standardized conditions it is better. Samples could be stored below -20°C or lower for long-term storage up to 3 months [16]. A minimum volume of 500 μL of urine sample should be used for NMR and LC-MS analysis each, allowing different extraction procedures as well as repetitions as for the later method.

2.2 Animal Sampling

Handling and sampling of laboratory animals have to be performed by especially trained and experienced personnel in compliance with the existing guidelines for good practice of laboratory animals [17–19] and in compliance with the respective regulations in the countries of the European Union which may differ for special sampling techniques and the local ethics committees.

Blood samples can be drawn from the smaller rodents (mice and rats) in conscious or, more common, anesthetized state,

depending on the established techniques and experiences of the respective laboratory. For nonrodents (dogs, minipigs, nonhuman primates) blood sampling in conscious animals is the common standard. An overview is given in [20].

Blood sampling for metabolomics is ideally performed in parallel to sampling for clinical pathology testing, which offers the opportunity of correlation analysis of metabolite profiles to classical endpoints. In order to obtain time profiles of the response, multiple sampling of single animals could be considered. In this case, the maximal extractable blood volume per time point is not to be exceeded in compliance with the good practice guide [21], and not to influence and stress the experimental system by exaggerated blood sampling. This is especially important in smaller animals like rats and critical in mice. Sample volumes are discussed in the section for human sampling above.

For noninvasive urine collection, the experimental animals, mice and rats or nonrodents, have to be transferred in metabolic cages and kept during a longer time interval, normally 24 h or 16–18 h. The design of the metabolic cages should allow separate collection of feces and urine to avoid contamination [22]. The metabolic response during this longer time interval reflects activity and resting phases of the animals. When the amount of urinary excretion is known to be sufficient, sampling can be fragmented in smaller intervals, e.g., 0–8, 8–16, 16–24, and 24–32 h, to study acute and late effects with higher time resolution and sensitivity [23]. During the sampling interval, urine should be collected in a clean container and kept at low temperatures between 0 and 4 °C by a cooling bath or ice container for example. To prevent metabolite degradation, addition of NaN_3 (sodium azide) is recommended [14].

In case of the larger nonrodent animals, it may be possible, depending on the construction of the metabolic cages, that urine is contaminated with feces or the animal has not urinated. In this case, urine collection via a catheterization from the bladder can be considered to get a clean and defined urine sample.

2.3 Cell Culture and Tissue Sampling

For the extraction of metabolites and sample preparation for ^1H -NMR spectroscopy the protocol from Ellis et al. [24] was adapted for T47D breast cancer cells [25]. In brief, the cell culture media of each wells of a 12-well plate was removed quickly and the cells were washed twice with ice-cold PBS. For quenching, 1 mL of ice-cold methanol was added to each well, scrapped, and transferred to an Eppendorf tube. Each well was washed again with 1 mL of ice-cold methanol and the two samples pooled. The pooled quenched methanol sample was dried over a flow of nitrogen at room temperature and stored at -80 °C until subsequent extraction. In principle this protocol can be used for MS-based metabolomics as well. Protocols

for tissue sampling for MS-based targeted metabolomics are described in [26].

3 Sample Preparation/Reagents

In contrast to other analytical techniques or clinical chemistry methods, metabolite profiling of biofluids by NMR requires in general no sophisticated sample preparation procedures [27]. In most cases adding of H₂O/D₂O or buffer to account for pH variation or to reduce viscosity is sufficient as sample preparation before the NMR measurement [28]. This means that potential source of variance due to sample extraction procedures is absent.

For NMR, the common sample preparation protocol for urine samples includes pH adjustment with phosphate buffer:

1. Mix two parts of urine with one part of 0.2 M phosphate buffer (pH 7.4) containing 1 mM TSP (sodium trimethylsilyl[2,2,3,3-²H₄]propionate), 3 mM sodium azide, and 15% D₂O.
2. Centrifuge at 4 °C for 10 min at >10,000 × *g*.

Dilution with saline is applied for plasma or serum:

1. Mix one part of plasma or serum with one part of 0.9% NaCl in 10% D₂O.
2. Centrifuge at 4 °C for 10 min at >10,000 × *g*.

For LC-MS investigations of the low-molecular plasma or serum metabolome, it is of key importance to selectively remove proteins before analysis without affecting the low-molecular-weight metabolome. Blood plasma and serum are indeed complex mixtures containing a wide variety of chemically diverse high- and low-molecular-weight components. This is mandatory to reduce signal suppression of low-abundance compounds and to avoid protein precipitation under reversed-phase (RP) liquid chromatography (LC) conditions. Several procedures for deproteinization exist, such as extraction of low-molecular-weight compound by organic solvents, acids, or denaturation of proteins by heat [29–31]. With regard to reproducibility, number of metabolic features detected, and robustness, extraction by methanol proved to be the best method. A common extraction method is as follows:

1. Mix one part of plasma or serum with four parts of methanol and incubate for at least 20 min at –20 °C.
2. Centrifuge at 4 °C for 10 min at >10,000 × *g*.
3. Evaporate supernatant to dryness.
4. Resuspend in one part of chromatographic starting conditions, e.g., acetonitrile/0.1% formic acid 5/95 (v/v).

For LC-MS metabolic profiling, urine is a challenging matrix. Especially the high salt content, complex composition, and varying dilution of urine oppose its advantage of easy and noninvasive collection to special analytical requirements. To overcome these problems, urine samples are normally desalted before LC-MS analysis by solid-phase extraction [32] or column switching procedures [33]. High-resolution chromatographic separation techniques such as rapid resolution (RR)-LC or ultrahigh-pressure liquid chromatography (UHPLC) are applied. In some cases small injection volumes of neat urine were used with UHPLC-MS analysis [34]. Regarding the targeted kits from Biocrates only 10 μL of plasma, serum, or urine samples is used except for the steroid kit. For tissue samples an extraction volume ranging from 3 to 12 $\mu\text{L}/\text{mg}$ tissue is recommended. From these extracts only 10 μL will be used for the kit.

4 NMR Methods

The theory of NMR is highly developed and the dynamics of nuclear spin systems is fully understood [35, 36]. For the acquisition of a NMR spectrum a liquid or a semisolid tissue sample is placed in a static magnetic field. After irradiation with high-frequency pulses (pulse sequences) the response of the NMR sample is detected by an induced current. The highest field strengths available in 2008's NMR spectrometers is 21 T corresponding to 900 MHz ^1H (proton) frequency. Most applications in metabolic profiling are using 600 MHz instruments.

The amplitude response of a NMR spectrometer is perfectly linear to the concentration of the sample which allows easy quantification of compound concentrations for metabolic profiling applications. All steps involved in the acquisition and processing of NMR data, including preparation and exchange of samples, can be performed fully automated for hundreds of samples without the need for manual interference. A state-of-the-art hardware setup is shown in Fig. 1.

The sensitivity of NMR spectrometers depends, besides the magnetic field strength and the nucleus detected, primarily on the inherent sensitivity of the detection device (probe head). Probe heads tailored for highest sensitivity in dependence on sample concentration and amount are available with different coil sizes, ranging from 10 mm down to 1 mm in diameter. Cryogenically cooled probe heads operated with 5 or 3 mm NMR tubes which enhance the signal-to-noise by a factor of approximately 4 compared to conventional room-temperature probes present an attractive compromise—flow-through inserts are available nowadays. It must be noted that a fourfold increase of sensitivity reduces experimental time 16-fold [37].

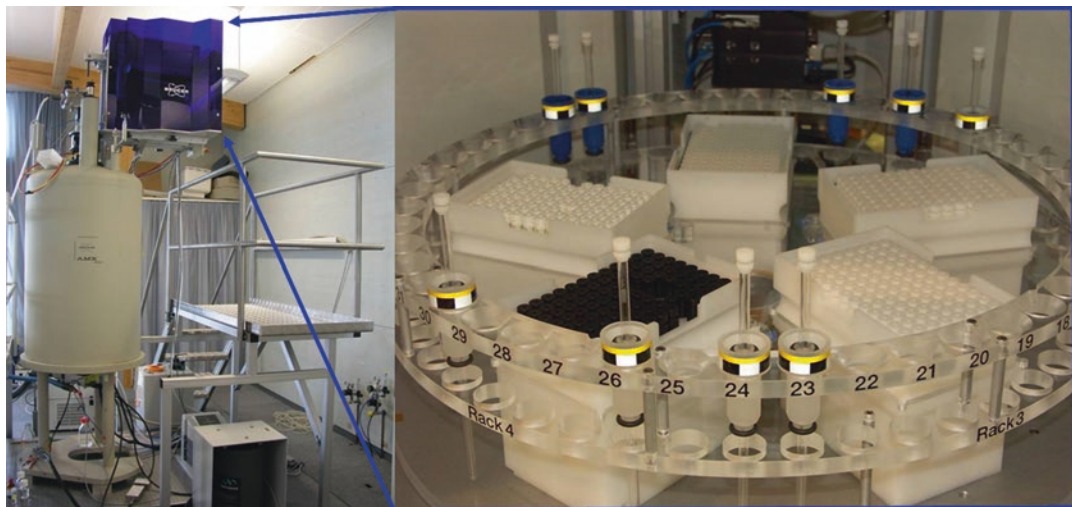


Fig. 1 A sample changing robot (Sample Jet, Bruker Fällanden Switzerland) allows fast sequential single-tube submission under temperature-controlled conditions. The system can thus efficiently handle up to 480 samples

The interlaboratory comparability of NMR data was tested for a set of samples shipped to different laboratories. Data were acquired with NMR spectrometers of different manufacturers. Compared to any other analytical technique NMR shows an impressive analytical reproducibility and repeatability reflecting itself in a coefficient of variation of 2% for a study invoking a large set of spectra [28]. Thus the observed variances in NMR spectra of a biological study are highly dominated by biological effects.

NMR offers a wealth of experimental techniques tailored for extraction of structural, chemical-kinetic, structural-dynamic, and other information especially in multidimensional applications.

Compared to more elaborate applications of NMR, pulse sequences applied in metabolomics require a relatively low level of sophistication. The application of NMR for biological samples is faced with the problem of water suppression as the metabolites are present in μM or lower concentration in the presence of water at 55 M concentration. This problem is solved by several water suppression techniques [38]. The method of water suppression has to be considered when combined data set [39] from different laboratories are analyzed.

In the following solvent suppression techniques, NMR experiments and data processing procedures which are employed in metabolic profiling widely are briefly reviewed. For applications of HR-MAS NMR for tissue samples and rarely used heteronuclear techniques, the reader is referred to the literature [40–45]. NMR experimental parameters as used in our laboratory are provided in Table 1.

Table 1
Parameters of NMR experiments as used in our laboratory for application to biological samples

Description	Number of scans (NS)	Inter-scan delay ($d1$) (s)	Time domain (TD)	Spectral width (SW)	Processing size (SI)	Window function	window function (parameters)
Noesy 1d with sign-alternating gradient prior of first pulse, presat [50 Hz] for $d1$ and during 100-ms mixing time no gradient during mixing time	32	2	32k	20 ppm	64k	Exponential	lb 1
Gradient dqf-cosy, presat [50 Hz] during $d1$	>32	1	4k 256	20 ppm 20 ppm	4k 1k	Squared sine	ssb 3
TOCSY, MLEV-17 mixing time of 80 ms, presat [50 Hz] during $d1$	>32	1	4k 300	20 ppm 20 ppm	4k 512	Squared sine	ssb 2.5
Jres, presat [50 Hz] during $d1$	>8	1	16k 64	20 ppm 40 Hz	16k 256	Exponential sine	lb 1 ssb 0

If two rows are given in a cell the first and second rows provide values for f_2 and f_1 , respectively

4.1 1D ¹H-Spectroscopy

Most applications of NMR for metabolomics rely on one-dimensional (1D) NMR experiments based on the ¹H nucleus which offers highest detection sensitivity. Typical 1D NMR spectra of serum, urine, and CSF are shown in Fig. 2. Spectra of these biofluids can be measured with sufficient signal-to-noise (S/N) within a few minutes per sample.

The most widespread solvent suppression technique in use is presaturation [46] applied in a NMR pulse method known as noesy-presat [47]. Due to the excellent chemical shift selectivity and baseline properties, the method allows for reliable quantification of signals resonating close to water, e.g., the anomeric proton of glucose. As a drawback, signals of hydrogen atoms interacting with water by chemical exchange (e.g., OH, NH, NH₂) show reduced signal intensities. This is for example seen for urea in urine, which cannot be quantified if water presaturation is applied.

Alternatively the WET [48] sequence is used for water suppression. Here, effects due to analyte–water interaction are less serious. The drawback of the method is a reduced performance with respect to chemical shift selectivity. WET allows for accurate absolute value quantification.

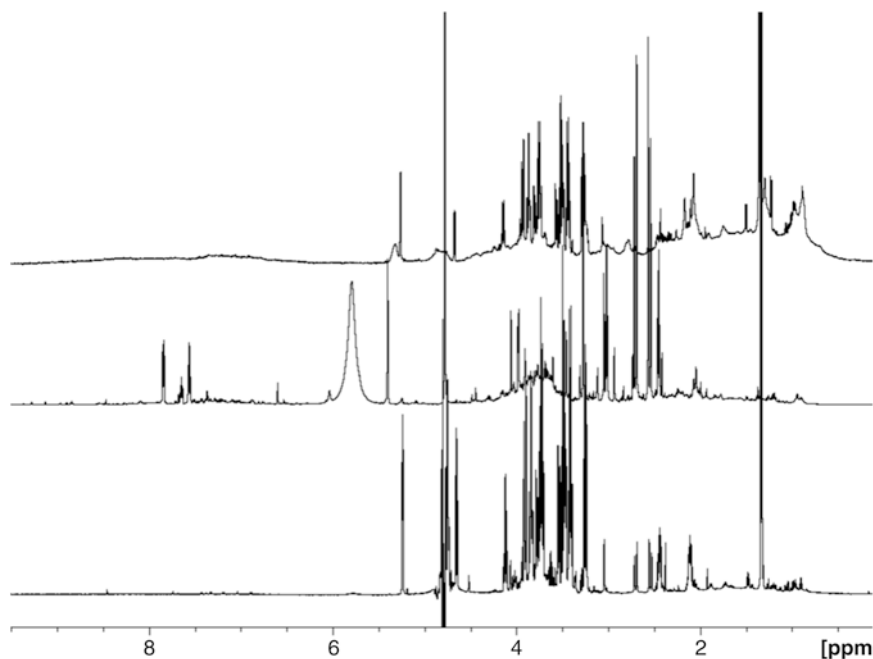


Fig. 2 1D ^1H NMR spectra of serum, urine, and CSF of rat (top to bottom). Very different spectral signatures of the body fluids are clearly visible. The serum spectrum is dominated by broad signal background due to high-molecular-weight proteins and lipoproteins. The most prominent signal of urine, the urea signal, around 5.9 ppm, whereas the CSF spectrum is characterized by high glucose (3–4 ppm) and lactate (1.2 ppm) content

4.2 Editing Techniques

NMR signals of rigid, high-molecular-weight molecules experience fast decay due to relaxation. This property is exploited in metabolomics for selective removal of signals of proteins and lipoproteins. These large biomolecules are found at high concentration in blood serum, plasma [49, 50], or tissue samples. Complementary information focusing on high-molecular-weight compounds can be obtained by removal of signals from small molecules employing diffusion editing methods [51–53]. Applications in metabolomics research with biofluids and tissues can be found in the literature [54, 55].

4.3 2D-NMR

The use of two-dimensional (2D) NMR in metabolomics is limited to small-sample arrays as the measuring time is up to several hours per sample. Nevertheless, examples can be found in the literature [56]. The 2D techniques unfold their full power if an unknown structure of a newly found biomarker has to be elucidated in a biological sample [57]. All 2D experiments applied so far depend on the detection of highly sensitive hydrogen nuclei.

In *J-resolved spectroscopy*, the J-coupling information is separated into a second dimension orthogonal to the chemical shift axes in the spectrum. This technique was applied to body fluids including urine [58], CSF [59], seminal fluid [60], and blood plasma [61].

From the J-resolved spectrum, a so-called chemical shift spectrum of reduced complexity can be extracted, which can be used for simplified quantification by use of a spectral reference database [62].

In *correlation* (COSY) and *total correlation* (TOCSY) spectroscopy [63], a correlation signal is obtained if two spins belong to a homonuclear J-coupling network [64–66]. Metabolomics applications for liquids are described in [67]. A combination of total correlation spectroscopy with diffusion editing has also been reported [68].

4.4 NMR Raw Data Processing

Fourier transformation (FT) of the NMR signal (FID) leads to the NMR spectrum. Prior to FT, data are multiplied by a window function [69, 70] to achieve an ideal compromise between high spectral resolution and signal-to-noise ratio in the spectrum. Often-used window functions in metabolomics involve exponentially decaying functions adding 1 Hz of additional line width to the data, and squared cosine-shaped windows for multidimensional data. After FT, the spectra have to be phased and baseline corrected by subtraction of a tailored polynom. Parameters of phase and baseline correction have to be determined for each individual spectrum manually, as reliable automation is missing for these procedures. The whole process is summarized in Fig. 3.

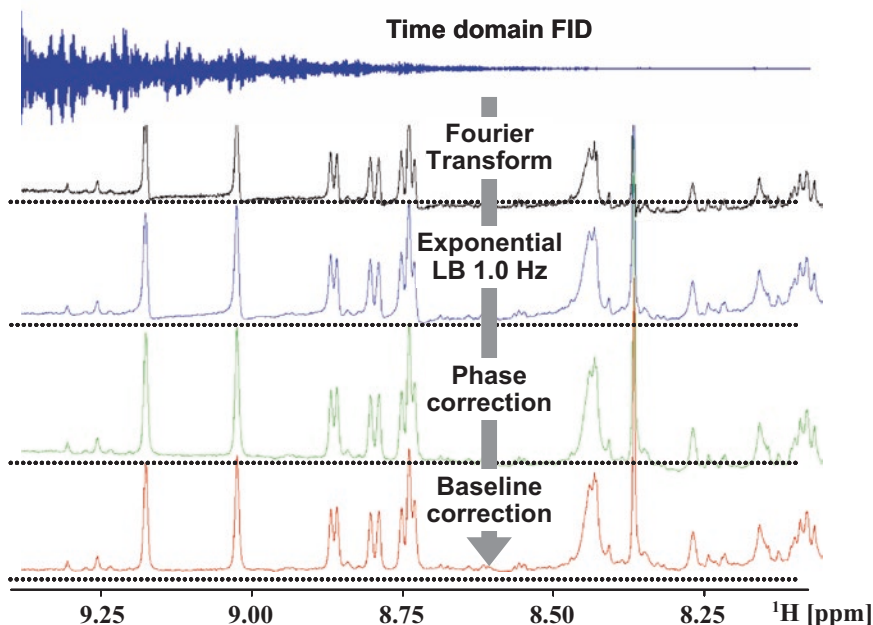


Fig. 3 Processing of a time-domain NMR signal (*blue at the top*). The frequency domain result after Fourier transformation (FT) of this signal is shown in *black* with low signal-to-noise ratio, baseline-offset, and dispersive contribution. Application of an exponential window function of 1 Hz LB prior to FT results in the *blue trace* with substantially improved signal-to-noise. Other artifacts remain. A spectrum suited for metabolomics interpretation is obtained after phase (*green trace*) and baseline correction. The last two steps have to be inspected visually

4.5 Data Preprocessing

Data preprocessing technologies in metabolomics based on NMR aim at reducing variances and influences, which could interfere with data analysis or which are not of interest. These variances can be attributed to NMR-specific effects (e.g., incorrect phases of the spectra, or shifting baselines), biological specific effects (e.g., different dilutions or different salt concentrations of biofluids), or combined effects such as shifting peaks in the spectra. Preprocessing of NMR in the context of metabolomics involves typically three steps, which are described in more detail in the following section.

4.5.1 Excluding Spectral Regions

The first step of NMR data preprocessing is the exclusion of spectral regions, which contain nonreproducible information, or which are dominated by drug metabolites, which are not of interest for metabolomics. In particular, the following exclusion steps are performed:

1. Usually, the spectrum outside the window of 0.2–10 ppm is excluded, since the corresponding regions are not populated by resonances of endogenous metabolites and the regions are sensitive for spectral artifacts such as incorrect phasing.
2. The water region between 4.6 and 5.0 ppm is removed, given that this region highly dominates the spectrum despite special water suppression techniques, which also add to the variance of the remaining water peaks.
3. In the case of urine, the signal of urea, which is directly located next to the water signal, is the most dominating peak besides that of water, as urea is the most concentrated metabolite in water. Since the protons of urea exchange with water, the signal is not quantitative and interferes with typical data analysis methods unless it is excluded. Therefore, common practice is the exclusion of the complete region between 4.50 and 5.98 ppm for urine as matrix. It needs to be taken into account that by this procedure some peaks of metabolites of interest are excluded (e.g., α -anomeric proton of glucose at 5.24 ppm).
4. The exclusion of regions covered by drug metabolites is a study- and drug-specific process. Typically, drug metabolites can be best identified in spectra of urine collected directly after the administration of drugs (e.g., 0–8 h post-dosing). To ensure compatibility of spectra between studies, these regions are often not excluded, but replaced by representative spectra of normal subjects.

4.5.2 Peak Shifts, Binning of Spectra, and Peak Alignments

Peaks, which are not exactly localized but shift from spectrum to spectrum, are one of the major obstacles of the automated data analysis and peak assignments for spectra of biofluids. The matrix of biofluids, and in particular of urine, varies highly and this influences the local environment of protons and consequently the localization of their peaks. Hereby many parameters play a role,

such as changes of the pH, varying salt concentrations, overall dilution of the biofluid, relative concentration changes of specific metabolites and ions, and many more. A particular problem is that not all peaks are affected and different peaks are affected to a different extent. As a consequence the automated assignment of shifting peaks to particular metabolites is difficult. Overlaid peak shifts and intensity changes of peaks (due to changes of metabolite concentrations) result in distorted shapes of peaks in loading plots of data decomposition methods (such as PCA) and cause other artifacts. Consequently, a reduction of peak shifts by specific sample preparation methods and *in silico* is highly beneficial for data analysis and interpretation. Three different mathematical methods are discussed in the following:

1. Equidistant binning: The most popular methods of reducing the influence of shifting peaks are the so-called binning or bucketing methods. Hereby, the spectra are integrated within small spectral regions, which are called “bins” or “buckets.” As long as the peaks shift only within the borders of the corresponding bins, subsequent data analysis procedures are not affected. The de facto standard of ^1H -NMR metabolomics is an equidistant binning of 0.04 ppm. This means that the spectrum is split into evenly spaced integral regions with a spectral width of 0.04 ppm. In addition it is common practice to sum up bins covering the citrate doublets (two bins each) into two super-bins. Although the binned spectra are a lot more suitable for multivariate data analysis methods to identify significantly changed spectral regions, the low resolution does not allow an interpretation of single peaks anymore. Consequently, the nonbinned spectra are still needed for a manual interpretation and assignment of peaks to metabolites.
2. Nonequidistant binning: To prevent that peaks are cut by the boundaries of bins, binning methods have been proposed, which use a nonequidistant spacing of the peaks. For example one approach starts with a bin size of 0.04 ppm and allows an adjustment of the borders by looking for minima of a sum of spectra or a skyline projection of spectra [71]. An unequal bin width has also fundamental influence on the subsequent data analysis, as data points belonging to bins of different width influence subsequent data analysis to a different extent. On one side, this can be advantageous if data analysis focuses on changes of metabolite concentrations directly, as in an ideal case the integral below each bin corresponds directly to the peak of a metabolite. On the other side, the binned spectrum does not correspond directly to the nonbinned spectrum in data analysis. A scaling of each bin by dividing by the corresponding bin width can account for this fact.

3. Peak alignment: The alignment of peaks is an alternative to reducing the spectrum to account for peak shifts. Hereby, the spectrum is segmented and the segments are shifted, stretched, and shrunk to maximize the correlation between the segments and a target spectrum. Overlaps are deleted and gaps are interpolated [72]. In another approach, peaks are identified by looking at shapes and peaks are shifted to a certain average frequency [73]. Although for both methods promising first results have been demonstrated, they have not reached a broad application in scientific community until now.

Although binning and peak alignment methods are beneficial for an automated data analysis, the resulting reduced spectra—especially in the case of binning—suffer from a high loss of information. Changes of low-concentrated metabolites might be hidden in the binned spectrum due to changes of metabolites, which have peaks in the same spectral region. As a consequence, recent developments have focused on analyzing spectra at full resolution using spectroscopic correlation methods (STOCSY) or orthogonal projection to latent structures (O-PLS) [74, 75]. In any case, a manual inspection of the high-resolution spectra is indispensable to validate if observed differences are artifacts and to find subtle differences in spectra, which analyses of low-resolution spectra or automated analyses might have missed.

4.5.3 Normalization of Spectra

A crucial step in data preprocessing, in particular for the quantitative analysis, is the normalization of spectra. Normalization is performed to account for variations in the overall concentration of samples. Especially when urine is analyzed, it is highly important to normalize, since the overall concentration of samples can highly vary. Urine samples of human and animals typically vary with a dilution factor of 4–5, but in the case of disease, food deprivation, or drug treatment (e.g., diuretics such as furosemide), the dilution factor can easily exceed a factor of 10 between normal subjects and affected subjects. Further factors, which can influence the dilution of samples, are sample preparation steps such as the addition of buffer. Also changes of the receiver gain or recording spectra with different numbers of scans, or comparing spectra recorded on different devices, render normalization indispensable.

In contrast to changes of the overall concentration of samples, metabolic responses and changes typically influence only a limited number of metabolites. These metabolic changes are visible as specific relative concentration changes of the corresponding metabolites versus the concentrations of the remaining majority of metabolites, whose concentrations represent the overall concentration of the sample. Hereby, the specific metabolic changes, which are usually of interest in a metabolomic analysis, overlay the overall changes due to different dilutions of samples, and might be obscured therefore. Normalization procedures compensate for the

changes of the overall concentration of samples and only specific changes of metabolites should be reflected comparing different normalized spectra in the ideal case. Hereby, all normalization methods scale complete spectra in a way that these spectra correspond to the same overall concentration of the samples, whereby the scaling factor of each spectrum corresponds to the dilution factor of the corresponding sample. Different normalization methods are used in the field of metabolomics: creatinine normalization, integral normalization, and quotient normalization. All normalization steps are usually applied after preprocessing steps mentioned before such as excluding spectral regions and binning spectra.

Creatinine Normalization

The creatinine normalization was the first normalization applied to metabolomics [76]. It originates from clinical chemistry, where it is common practice to normalize urinary parameters to the concentration of urinary creatinine [77, 78]. The assumption behind is a constant production of creatinine in the body and its constant excretion into urine. Therefore, the concentration of creatinine in urine is assumed to be representative for the overall concentration of the urine. In case of metabolomics, the creatinine normalization can be performed as follows:

1. Determine the integral below the creatinine peaks at 3.05 and 4.05 ppm.
2. Divide each point of the spectrum or, alternatively, each bin of the binned spectrum by the creatinine integral value.

Yet, the practical application of the creatinine normalization is faced by several problems. First of all, metabolites, which have peaks overlapping with the peaks of creatinine (e.g., creatinine at 3.04 ppm), could interfere with the determination of the concentration of creatinine. Also the peak of creatinine at 4.05 is prone to shifts due to changes of pH of the sample rendering a peak picking procedure necessary to determine the integral of the creatinine peak. The most problematic challenge is a biological factor: It has been shown in several studies that the excretion of creatinine into urine can be modulated as metabolic response or due to nephrotoxicity [79]. In that case, the creatinine normalization is worthless. As a consequence, the creatinine normalization was very soon replaced by the integral normalization in the field of metabolomics.

Integral Normalization

The integral normalization has been the standard normalization method in NMR metabolomics spectroscopy for the last two decades [80–82]. The primary assumption behind the integral normalization is that the integral of a spectrum is primarily a function of the total concentration of the corresponding sample, as the integral of a spectrum is a function of the concentrations of all NMR-visible metabolites of a sample. The impact of specific changes on single metabolites on the total integral of the spectrum

is assumed to be nonsignificant compared to the impact of changes on the overall concentration of samples. The different steps of the integral normalization are as follows:

1. Calculate the total integral of the complete spectrum.
2. Divide each data point of a full-resolution spectrum or each bin of a binned spectrum by the total spectrum.
3. Multiply each data point of a full-resolution spectrum or each bin of a binned spectrum by 100. This step is not needed, but it is a convention to use a total integral of 100 for each spectrum.

Though being the de facto standard, the integral normalization is faced by producing artifacts if the above-mentioned assumptions are not valid, for example when changes of single metabolites dominate the overall picture of the spectrum.

Quotient Normalization

Quotient normalization has been recently introduced to overcome some of the limitations of the integral normalization [83]. If the integral of the spectrum is dominated not by the overall concentration of the sample, but by the concentration of a single metabolite, the variation of this metabolite highly interferes with the calculated normalization factor. It has been observed in metabolomics studies that in the case of diseases or in the case of drug-induced kidney injury, single metabolites can be excreted at very high concentrations. An example is glucosuria, where the peaks of glucose account for a very high proportion (50–90%) of the total integral of the spectrum. In that case the integral normalization incorrectly down-scales such a spectrum with a factor corresponding to the proportion of glucose in the sample.

Similar to the integral normalization, the quotient normalization also assumes that the dilution of samples affects all metabolites, whereas metabolic responses only affect a limited number of metabolites. In contrast to the integral normalization, not a total integral is used as normalization factor, but a most probable concentration quotient between a spectrum and a reference spectrum is calculated as normalization factor. This most probable quotient is derived from the distribution of the quotients of each bin/data point of a spectrum divided by the corresponding bins/data points of a reference spectrum. The most probable quotient can be estimated in several ways, but the median quotient has been proven to be a very robust method. For the calculation of the quotients, a reference spectrum is needed. This could be a single spectrum of the study, a reference spectrum from a database, or a calculated median or mean spectrum of a set of spectra or all spectra from the corresponding study. Several simulations have demonstrated that taking a median spectrum of control animals or control subjects is the most robust approach. It is also recommended to perform an integral normalization before applying the quotient normalization to scale the spectra of different studies to the same absolute

magnitude. The single steps of the quotient normalization can be summarized as follows:

1. Perform an integral normalization of all spectra.
2. Calculate a reference spectrum as median spectrum of all control subjects (each data point/bin is the median value of the data points of the spectra of all control subjects).
3. Calculate the quotients of all data points/bins of the test spectrum with corresponding data points/bins of the reference spectrum.
4. Calculate the median of the quotients.
5. Divide all data points/bins of the test spectrum by this median.

The quotient normalization can be applied to binned spectra or to full-resolution spectra. When applying the method to full-resolution spectra, only data points in spectral regions which do not contain any peaks of metabolites should be excluded when calculating the most probable quotient (**steps 3 and 4**). These data points contain only noise and consequently are not subject to the effect of dilution. If more than 25–40% of the data points contain only noise, the most probable dilution factor might be influenced by the noise. This situation, which is rather improbable for complex spectra of urine or blood but can occur in the case of plant extracts, can be prevented by defining a minimum average signal intensity of the data points used for the calculation **steps 3 and 4**.

Besides this caveat, it has been shown that thanks to its robustness, the quotient normalization is superior to the integral normalization, especially when strong metabolomics responses are observed.

5 Chromatographic Methods

5.1 LC-MS

LC coupled with electrospray ionization mass spectrometry (ESI-MS) is the most common MS-based method for metabolomics investigations. Other ionization strategies for LC coupled to MS, like nanospray ESI, atmospheric pressure chemical ionization (APCI), and atmospheric pressure photoionization (APPI) [84], are less frequently used for nontargeted analyses of biofluids. Robust high-resolution separation methods like high-performance liquid chromatography (HPLC), RR-LC, or UPLC are able to reduce the complexity of biofluid samples significantly, and thus are ideal methods to be coupled to MS, especially with ESI interfaces, to investigate biological samples. Separation of hundreds to thousands of endogenous metabolites present in biofluids by high-resolution LC reduces the degree of coelution to a great extent. Thus the major drawback of ESI, ion suppression, is significantly decreased whereas sensitivity and reproducibility are improved

[85]. Other approaches like hydrophilic liquid interaction chromatography (HILIC) were recently applied in metabolomics studies as a complementary tool to study polar metabolites [86]. However, until now HILIC has not reached the level of reliability, stability, and reproducibility of HPLC or UPLC methods.

A generic LC method [87] for biofluid metabolomic investigations comprises:

1. 2.1 mm internal diameter RP HPLC column, normally packed with C₁₈ material, maintained at 40 °C
2. Gradient elution with acetonitrile/0.1% formic acid starting from 5 to 90% organic phase within 10–60 min and with flow rates between 250 and 400 µL/min
3. Injections of 5–10 µL extract/desalted sample

The most common mass analyzers for metabolomics studies are quadrupole and time-of-flight (TOF)-based analyzers and hybrids thereof [88, 89]. In addition, also ion traps, Fourier transform (FT), and Orbitrap instruments were used. Quadrupole mass spectrometers are robust and flexible, and have a high linear dynamic range, but are limited in full-scan data acquisition due to long duty cycles. Benefits of ion trap instruments are their capability to perform progressive fragmentation steps (MSⁿ), compact size, and fast full scanning but at low resolution. Linear ion trap quadrupole hybrid instruments (Q TRAP or QqLIT) combine the MSⁿ capabilities of ion trap instruments with the neutral loss and precursor ion scan capabilities of triple-quadrupole instruments. Therefore, the shortcomings of both approaches are overcome. TOF instruments excel in fast scanning capabilities, wide mass range, and high resolution. Quadrupole TOF (Q-TOF) hybrid instruments combine the stability and robustness of the quadrupole analyzer with TOF features and allow for MS-MS experiments.

Nontargeted metabolite profiling approaches require a sensitive full-scan mode and exact masses. Therefore Q-TOF instruments or linear ion trap FT-MS instruments are advantageous. In contrast, for targeted analysis of selected metabolites triple-quadrupole instruments and Q TRAP instruments with their capability for multiple reaction monitoring are frequently used.

5.2 GC-MS

A prerequisite of GC/MS analysis is to obtain volatile compounds. But the physicochemical properties of endogenous metabolites in metabolomics analysis are highly variable in complex biological matrices, e.g., (plant) tissue extracts, urine, and blood. Therefore, extraction that maximizes the number and amounts of metabolites combined with derivatization that transforms polar compounds (e.g., sugars, amino acids, organic acids) into volatile compounds is necessary before GC/MS analysis.

There are many methods of extraction and derivatization available. Most are based on the extraction of Bligh and Dyer's [90–92] with little

variations and optimization combined with two-stage derivatization methods [31, 93, 94]. In the first methoxymation step, aldehyde and keto groups are converted into oximes using hydroxamines or alkoxyamines to reduce the number of tautomeric forms (due to the limited rotation along the C=N bond). The second silylation step then derivatizes polar functional groups (e.g., -OH, -SH, -NH) into trimethylsilyl groups (TMS ethers, TMS sulfides, TMS amines) resulting in more volatile compounds. A typical method includes the following steps:

1. The sample (plants, organs, tissue, blood, urine, cell culture) of 100–200 mg is homogenized with a mixture of hydrophilic and lipophilic solvents, e.g., with 800 μL of a mixture of methanol/water/chloroform (750/250/200 v/v/v).
2. After extraction, the samples are centrifuged at $18,000 \times g$ for 10 min. The supernatant containing the aqueous phase (methanol and water) is then separated from the lipophilic phase (chloroform).
3. 180 μL of the aqueous extract is evaporated to dryness. The residue is then methoxymated with 30 μL of 20 mg/mL methoxyamine in pyridine for 17 h and silylated with 30 μL of MSTFA for 1 h.
4. 1 μL of each extract is analyzed by GC/MS using standard conditions [40] (e.g., 20 m \times 180 μm DB5-MS with 0.18 μm film, flow 1 mL/min, temperature gradient from 70 to 320 $^{\circ}\text{C}$ increasing by 15 $^{\circ}\text{C}/\text{min}$).

5.3 Data Preprocessing

The extraction of relevant information and denoising from full-scan metabolic profiles is an important step when analyzing LC-MS data from complex samples such as serum, plasma, or urine. It is a prerequisite for statistical analysis to apply data alignment procedures and to reduce variance between samples that is not attributed to true differences. For GC-MS and especially LC-MS, nonlinear shifts in retention time, peak overlap, and m/z shifts are the major source of such variances. In general, three preprocessing strategies are followed for LC-MS data sets: (1) alignment of spectra along the chromatographic and spectral axis, (2) reduction of dimensionality by binning or bucketing procedures, and (3) automatic detection and quantification of significant peaks. Several commercial and open-source routines for automatic alignment, denoising, deconvolution, and extraction of peaks have been published and are reviewed by Katajamaa et al. [95].

6 Challenges and Opportunities of Data Analysis of Metabolomics Datasets

For the data analysis of spectra recorded with NMR and LC-MS spectrometers, a plurality of methods have been proposed. Most of the methods come from the informatics discipline of pattern

recognition and the chemometrics discipline of multivariate data analysis. Among the various methods, principal component analysis (PCA) and projection to latent structures (PLS) play the predominant role, especially as these methods are implemented in a plurality of commercial and free data analysis software. Other less often used analysis methods comprise k-nearest neighbors (KNN), hierarchical cluster analysis (HCA), batch-PLS, orthogonal signal correction (OSC) combined with PCA, and different implementations of neural networks. In most cases, these methods are prone to shifts of peaks. Therefore these data analysis methods have been applied to reduced spectra (binned spectra) in most cases. The consequences are that small metabolic changes are often overlooked due to two factors. The first factor is the reduction of spectra. As a consequence, strong changes of low-concentrated metabolites can be masked by slight changes of highly concentrated metabolites if these metabolites have adjacent or overlapping peaks (*see* Subheading 4.5.2 for more details). The second factor can be attributed to the multivariate projection methods/data composition methods themselves (e.g., PCA and PLS). These methods look for the strongest variations in the data and rotate the new coordinate system in a way that the first new coordinates (components) are dominated by these variations. As a consequence, more subtle but important changes are represented by higher components often neglected by the data miner, or are distributed over several components not visible to the data miner any more. Experienced data miners circumvent this situation by a rather tedious manual approach of analyzing the data:

1. A multivariate analysis of the complete data set is performed.
2. The most important changes in the multivariate model are identified and the metabolites behind the corresponding peaks are assigned to the peaks. This assignment often raises the need to go back to the original high-resolution spectra to confirm the tentative assignment of peaks to metabolites.
3. The data points/bins of these identified metabolites are removed from the data set and the multivariate analysis is repeated.
4. **Steps 1–3** are repeated until only noise is identified as most significant variance in the multivariate model.

Recently introduced new methods for analyzing metabolomics data render these tedious data analyses unnecessary, as these methods can be applied to full-resolution spectra, such as O-PLS [74], or statistical correlation methods such as the statistical total correlation spectroscopy (STOCSY) [75]. These new methods (especially the correlation methods) also identify small but significant changes and significant changes of low-concentrated metabolites in the presence of changes of high-concentrated metabolites. STOCSY is based on the computation of correlation statistics between all data points in a set of complex mixture spectra. In this

way, the connectivities of signals from molecules, which vary in concentration between samples, are visible in two-dimensional plots similar to spectra of two-dimensional NMR methods. STOCSY has been applied to correlate not only spectra NMR spectroscopy, but also spectra of LC-NMR [96] and virtually coupling spectra of NMR and UPLC-MS recorded for the same samples (in the latter case, the name statistical heterospectroscopy SHY was used). Especially in the case of SHY, attention has to be paid to the fact that only metabolites will be identified, which are detected by both methods or which are correlated with metabolites detected by the other method. Therefore, when using these recent offsprings of metabolomics data analysis a careful manual inspection of the high-resolution spectra is highly advised.

Another source of discussion is the scaling of spectra. Scaling of spectra means that each data point/bin is divided by its total variance (univariate scaling) or by the square root of its variance (Pareto scaling) calculated along the complete data set. Scaling of spectra has been primarily used with data decomposition/projection methods such as PCA and PLS. In this context, scaling renders the influence of each bin/data point on the multivariate model equally important. Therefore, the above-described dominance of highly concentrated metabolites on projection methods is diminished. Yet, scaling spectra has also a number of disadvantages:

1. Scaled spectra are highly distorted and do not reflect the concentration–intensity relationship. Therefore, it is not visible in these spectra if changes of peaks correspond to strong or weak changes of the corresponding metabolite. These spectra are not usable for a quantification of metabolites.
2. Scaling also modulates noise. Areas of spectra, which are dominated by noise, can be rendered artificially important.

Therefore, scaling of spectra might only be advisable for subsequent analyses by projection/data analysis methods such as PCA and PLS. The same holds true for centering spectra. Hereby, the average of the bin/data point calculated for the complete study is subtracted from the corresponding bin/data point of each spectrum ending up in an average intensity of zero of each bin over the complete data set. This helps in the context of data decomposition/projection methods to reduce the number of components needed by a factor of 1. However, these centered spectra are distorted and cannot be used for a direct quantification of the metabolites behind the peaks. A further disadvantage is the fact that the physical constraint of non-negativity of the signal is removed, which is often used by certain data analysis procedures, including three-dimensional data decomposition methods and peak fitting algorithms. As a summary, it can be said that centering and scaling should be only used if absolutely necessary for data analysis. The results of these analyses should be inspected manually with care.

7 NMR Metabolite Assignment and Databases

The assignment of metabolites in the high-resolution ^1H -NMR spectra is the fundamental basis for the correct biological interpretation of metabolomics data. Metabolite assignment can be performed on the relevant peaks or bins in the spectra or binned data sets responsible for differences between groups of interest derived from multivariate analysis. This step requires to go back to the high-resolution spectra and to compare the signals in the respective chemical shift areas with spectra of the corresponding biofluid from reference examples in the literature [97]. Naturally, this work should be performed by an experienced NMR spectroscopist. As this manual assignment of metabolites in each spectrum of a study is a tedious and time-consuming process, especially when up to hundreds of spectra in a study have to be analyzed, easier and less time-consuming assignment technologies were highly needed. This “must have” need of the community was taken up by solution providers in NMR spectroscopy by developing metabolite databases during the last years with reference spectra of relevant metabolites at different pH and connection to biological information databases. Currently, there are three software modules available, which differ in size, number, and type of metabolites, as well as mode of assignment: Bio-Rad Laboratories KnowItAll, Bruker Biospin Metabolic Profiler, Chenomx NMR Suite.

8 Chromatographic Metabolite Assignment and Databases

For the biological interpretation, the assignment of unknown metabolites is an important step in metabolomics analysis. There are different noncommercial and commercial databases, software, and websites available of metabolites with information such as MS, MS/MS spectra, chromatographic information, and other meta-data, and the number of databases and compounds is still growing. Weckwerth et al. published a list of some of these databases [98], which are also summarized in Table 2.

9 Commercial CROs

Currently, several contract research organizations (CROs) offer commercial services in the field of metabolic profiling. Most of the CROs summarized in Table 3 have a strong focus on MS-based metabolic profiling. Complementary NMR information is only available for some providers.

Table 2
Noncommercial and commercial databases, software, and websites for assignment of unknown metabolites

Name	Publisher	Homepage	Application
KEGG: Kyoto Encyclopedia of Genes and Genomes	Kanehisa Laboratories in the Bioinformatics Center of Kyoto University and the Human Genome Center of the University of Tokyo.	http://www.genome.jp/kegg/	Database of biological systems (genes, proteins, metabolites, pathways)
Human Metabolome Database	Genome Alberta and Genome Canada (not-for-profit organization)	http://www.hmdb.ca/	Database with chemical, clinical, and molecular/biochemistry data
METLIN: Scripps Center for Mass Spectrometry	Siuzdak and Abagyan Groups and Center for Mass Spectrometry at The Scripps Research Institute	http://metlin.scripps.edu/	Repository for mass spectral metabolite data
Madison Metabolomics Consortium Database	National Magnetic Resonance Facility at Madison	http://mmcd.nmrfam.wisc.edu/	Database with NMR and MS data
CHEBI (Chemical Entities of Biological Interest)	European Bioinformatic Institute (EBI)	http://www.ebi.ac.uk/chebi/	Database dictionary of small chemical compounds
Automated Mass US National Institute of Standards (AMDIS)	US National Institute of Standards and Technology	http://chemdata.nist.gov/mass-spc/amdis/	GC mass spectral library
AnalyzerPro	MatrixAnalyzer Spectralworks	www.spectralworks.com	High-throughput LC-MS and GC-MS data processing engine
Component Detection Algorithm (CODA)	ACD Labs	www.acdlabs.com	Prediction of mass spectral, fragmentation for LC, simulation of LC and GC chromatograms
MassFrontier	Thermo Electron	http://www.highchem.com/	Management, interpretation, and evaluation of mass spectra
MetAlign	Plant Research International PRI	http://www.metalign.nl/UK/	Analysis, alignment, and comparison of GC-MS or LC-MS datasets

(continued)

Table 2
(continued)

Name	Publisher	Homepage	Application
CSBDB	Max Planck Institute of Plant Physiology	http://csbdb.mpimp-golm.mpg.de/	Access to public mass spectra libraries and metabolite profiling experiments
ArMet	University of Wales, Aberystwyth	http://www.armet.org/	Framework for the description of plant metabolomics experiments
MeT-RO	UK Centre for Plant and Microbial Metabolomic Analysis	http://www.metabolomics.bbsrc.ac.uk/MeT-RO.htm	Primary and secondary metabolite profiling approach
Lipidmaps	LIPID MAPS, University of California, San Diego	http://www.lipidmaps.org/	Database for lipids, protocols, pathways, structures, MS spectra

Table 3
CROs offering expertise and services for metabolic profiling (metabolomics) and/or data evaluation

Company name		
Amphioxus Cell Technologies 11222 Richmond Ave., Suite 180 Houston, TX USA, 77082-2646 Phone: 281-679-7900 www.amphioxus.com	Keio University ^a Institute for Advanced Biosciences Tsuruoka City, Yamagata, Japan Phone: +81 235 29 0534 Officetck.keio.ac.jp www.iab.keio.ac.jp	Metabolon, Inc. ^a 800 Capitola Drive, Suite 1 Durham, NC USA, 27713 Phone: 919-572-1711 www.metabolon.com
Avestha Gengraine Technologies Pvt. Ltd. International Technology Park Ltd., Whitefield Road Bangalore, India, 560066 Phone: 91-80-2841-1665 www.avesthagen.com	Kiadis Zerninkepark 6-8 Groningen Netherlands, 9747 AN Phone: 31-0-50-547-42-70 www.kiadis.com	Phenomenome Discoveries Inc. ^a 204-407 Downey Road Saskatoon, Saskatchewan Canada, S7N 4L8 Phone: 306-244-8233 www.phenomenome.com
BIOCRATES Life Sciences GmbH ^a Innrain 66/2 Innsbruck Austria, 6020 Phone: 43-512-57-98-23 www.biocrates.at	Lipomics ^a 3410 Industrial Boulevard, Suite 103 West Sacramento, CA 95691 USA Phone: +1 916 669 0475 www.lipomics.com	Quest Pharmaceutical Services 3 Innovation Way, Suite 240 Newark, DE USA, 19711 Phone: 302-369-5601 www.questpharm.com

(continued)

Table 3
(continued)

Company name		
BG Medicine (partnering with TNO Pharma) ^a 40 Bear Hill Road Waltham, MA 02451 USA Phone: +1 781 890 1199 www.bg-medicine.com	Linden Bioscience 35A Cabot Road Woburn, MA USA, 01801 Phone: 781-933-2769 www.lindenbioscience.com	Sidmap 2990 S. Sepulveda Blvd. #300B Los Angeles, CA USA, 90064 Phone: 310-478-1424 www.sidmap.com
Cantata Pharmaceuticals, Inc. (Private) 300 Technology Square, 5th Floor Cambridge, MA USA, 02139 Phone: 617-225-9009 www.cantatapharm.com	METabolic Explorer Biopole Clermont-Limagne Saint-Beauzire France, 63360 Phone: 33-473-334300 www.metabolic-explorer.com	SurroMed, Inc. 1430 O Brien Drive Menlo Park, CA USA, 94025-1435 Phone: 650-470-2300 www.surromed.com
CHENOMX Inc. ^a 10050 112 Street Edmonton, Alberta Canada, T5K 2J1 Phone: 780-432-0033 www.chenomx.com	Metabometrix Ltd. RSM, Prince Consort Road London UK, SW7 2BP Phone: 44-0-20-7594-6595 www.metabometrix.com	Shimadzu Biotech 7102 Riverwood Drive Columbia, MA USA, 21046 Phone: 925-417-2097 www.shimadzu-biotech.net
CombiSep Inc. 2711 South Loop Drive, Suite 4200 Ames, IA USA, 50010 Phone: 1-888-822-7949 www.combisep.com	Minkon Biotechnology 15875 Gaither Drive Gaithersburg, MD USA, 20877 Phone: 240-683-5851 www.minkon.com	Target Discovery, Inc. 4030 Fabian Way Palo Alto, CA USA, 94303 Phone: 1-650-812-8100 www.targetdiscovery.com
ESA, Inc. 22 Alpha Road Chelmsford, MA USA, 01824 Phone: 978-250-7000 www.esainc.com	Metabolomic Discoveries Am Mühlenberg 11, 14476 Potsdam Germany +49 0331 95143881 www.metabolomicdiscoveries.com	TNO Pharma (partner of BG-Medicine) ^a PO Box 6064 Delft Netherlands, 2600 JA Phone: 31-15-269-69-00 www.tno.nl/kwaliteit_van_leven/index.xml
Metanomics Health GmbH Tegeler Weg 33 10589 Berlin Germany Phone: +49 30 34807-400 Fax: +49 30 34807-401 Email: info@metanomics-health.com		

The list was compiled from publicly available information and from the author's scientific network

^aCompanies which have previously been collaborating with the authors

References

- Nicholson JK, Lindon JC, Holmes E (1999) "Metabonomics": understanding the metabolic responses of living systems to pathophysiological stimuli via multivariate statistical analysis of biological NMR spectroscopic data. *Xenobiotica* 29:1181–1189
- Dieterle F, Schlotterbeck G, Binder M, Ross A, Suter L, Senn H (2007) Application of metabolomics in a comparative profiling study reveals N-Acetylfelinine excretion as a biomarker for inhibition of the Farnesyl pathway by bisphosphonates. *Chem Res Toxicol* 20:1291–1299
- Markley JL, Brüschweiler R, Edison AS, Eghbalian HR, Powers R, Raftery D, Wishart DS (2017) The future of NMR-based metabolomics. *Curr Opin Biotechnol* 43:34–40
- Dieterle F, Riefke B, Schlotterbeck G, Ross A, Senn H, Amberg A (2011) NMR and MS methods for metabolomics. *Methods Mol Biol* 691:385–415
- Wishart DS (2007) Proteomics and the human metabolome project. *Expert Rev Proteomics* 4:333–335
- Bollard ME, Holmes E, Lindon JC, Mitchell SC, Branstetter D, Zhang W, Nicholson JK (2001) Investigations into biochemical changes due to diurnal variation and estrus cycle in female rats using high resolution ^1H NMR spectroscopy of urine and pattern recognition. *Anal Biochem* 295:194–202
- Bell JD, Sadler PJ, Morris VC, Levander OA (1991) Effect of aging and diet on proton NMR spectra of rat urine. *Magn Reson Med* 17:414–422
- Phipps AN, Steward J, Wright B, Wilson ID (1998) Effect on diet on urinary excretion of hippuric acid and other dietary-derived aromatics in the rat. A complex interaction between diet, gut microflora and substrate specificity. *Xenobiotica* 28:527–537
- Bollard ME, Stanley EG, Lindon JC, Nicholson JK, Holmes E (2005) NMR-based metabolomic approaches for evaluating physiological influences on biofluid composition. *NMR Biomed* 18:143–162
- Griffin JL, Walker LA, Garrod S, Holmes E, Shore RF, Nicholson JK (2000) NMR spectroscopy based metabolomic studies on the comparative biochemistry of the kidney and urine of the blank vole (*Clethrionomys glareolus*), wood mouse (*Apodemus sylvaticus*), white toothed shrew (*Crocidura suaveolens*), and the laboratory rat. *Comp Biochem Physiol* 127:357–367
- Van Dorsten FA, Daykin CA, Mulder TPJ, Duynhoven JPM (2006) Metabonomic approach to determine metabolic differences between green tea and black tea consumption. *J Agric Food Chem* 54:6929–6938
- Stella C, Beckwith-hall B, Cloarec O, Lindon JC, Powell J, van der Ouderaa F, Bingham S, Cross AJ, Nicholson JK (2006) Susceptibility of human metabolic phenotype to dietary modulation. *J Proteome Res* 5:2780–2788
- Solanky KS, Bailey NJC, Beckwith-Hall B, Davies A, Bingham S, Holmes E, Nicholson JK, Cassidy A (2003) Application of biofluid ^1H nuclear resonance-based metabolomic technique for the analysis of biochemical effects of dietary isoflavones on human plasma profiles. *Anal Biochem* 323:197–204
- Beckonert O, Keun HC, Ebbels TMD, Bundy J, Holmes E, Lindon JC, Nicholson JK (2006) Metabolic profiling and metabolomics procedures for NMR spectroscopy of urine, plasma and serum and tissue extracts. *Nat Protoc* 2(11):2692–2703
- Teahan O, Gamble S, Holmes E, Waxman J, Nicholson JK, Bevan C, Keun HC (2006) Impact of analytical bias in metabolomic studies of human blood serum and plasma. *Anal Chem* 78(13):4307–4318
- Maher AD, Zirah SF, Holmes E, Nicholson JK (2007) Experimental and analytical variation in human urine in ^1H NMR spectroscopy-based metabolic phenotyping studies. *Anal Chem* 79(14):5204–5211
- European Convention for the Protection of Vertebrate Animals Used for Experimental and Other Scientific Purposes Strasbourg, 18.III.1986 Text amended according to the provisions of the Protocol (ETS No. 170) as of its entry into force on 2 December 2005
- EEC Directive. Council Directive of November 24, 1986 on the approximation of laws, regulations and administrative provisions of the Member States regarding the protection of animals used for experimental and other scientific purposes 86/609/EEC. Official Journal of the European Community No. L 358 of 18 December 1986
- Good Laboratory Practice Regulations for Nonclinical Laboratory Studies of the United States Food and Drug Administration (21 CFR Part 58)
- Morton DB, Abbot D, Barclay R, Close BS, Ewbank R, Gask D, Heath M, Mattic S, Poole T, Seamer J, Southee J, Thompson A, Trussell B, West C, Jennings M (1993) Removal of blood from laboratory mammals and birds. *Lab Anim* 27:1–22
- Diehl K-H, Hull R, Morton D, Pfister R, Rabemampianina Y, Smith D, Vidal J-M, van den Vorstenbosch C (2001) A good practice

- guide to the administration of substances and removal of blood, including routes and volumes. *J Appl Toxicol* 21:15–23
22. Robertson DG, Reily MD, Lindon JC, Holmes E, Nicholson JK (2002) Metabonomic technology as a tool for rapid throughput in vivo toxicity screening. In: van den Heuvel JP, Perdew GH, Mattes WB, Greenlee WF (eds) *Comprehensive toxicology*, vol 14. Elsevier, Amsterdam, pp 583–610
 23. Nicholls A, Nicholson JK, Haselden JN, Waterfield CJ (2000) A metabonomics approach to the investigation of drug-induced phospholipidosis: an NMR spectroscopy and pattern recognition study. *Biomarkers* 5(6):410–423
 24. Ellis JK, Athersuch TJ, Cavill R, Radford R, Slattery C, Jennings P, McMorrow T, Ryan MP, Ebbels TM, Keun HC (2011) Metabolic response to low-level toxicant exposure in a novel renal tubule epithelial cell system. *Mol BioSyst* 7(1):247–257
 25. Wenzel C, Riefke B, Gruendemann S, Krebs A, Christian S, Prinz F, Osterland M, Golfier S, Råse S, Ansari N, Esner M, Bickle M, Pampaloni F, Mattheyer C, Stelzer EH, Parczyk K, Prectl S, Steigemann P (2014) 3D high-content screening for the identification of compounds that target cells in dormant tumor spheroid regions. *Exp Cell Res* 323(1):131–143
 26. Römisch-Margl W, Prehn C, Bogumil R, Röhring C, Suhre K, Adamski J (2012) Procedure for tissue sample preparation and metabolite extraction for high-throughput targeted metabolomics. *Metabolomics* 8:133
 27. Lindon JC, Nicholson JK, Holmes E, Everett JER (2000) Metabonomics: metabolic processes studied by NMR spectroscopy of biofluids. *Concepts Magn Reson* 12:289–320
 28. Keun HC, Ebbels TMD, Antti H, Bollard ME, Beckonert O, Schlotterbeck G, Senn H, Niederhauser U, Holmes E, Lindon JC, Nicholson JK (2002) Analytical reproducibility in ^1H NMR-based metabonomic urinalysis. *Chem Res Toxicol* 15:1380–1386
 29. Want EJ, O'Maille G, Smith CA, Brandon TR, Uritboonthai W, Qin C, Trauger SA, Siuzdak G (2006) Solvent-dependent metabolite distribution, clustering, and protein extraction for serum profiling with mass spectrometry. *Anal Chem* 78:743–752
 30. Boernsen KO, Gatzek S, Imbert G (2005) Controlled protein precipitation in combination with chip-based nanospray infusion mass spectrometry. An approach for metabolomics profiling of plasma. *Anal Chem* 77:7255–7264
 31. A J, Trygg J, Gullberg J, Johansson AI, Jonsson P, Antti H, Marklund SL, Moritz T (2005) Extraction and GC/MS analysis of the human blood plasma Metabolome. *Anal Chem* 77:8086–8094
 32. Wagner S, Scholz K, Sieber M, Kellert M, Voelkel W (2007) Tools in metabolomics: an integrated validation approach for LC-MS metabolic profiling of mercapturic acid in human urine. *Anal Chem* 79:2918–2926
 33. Waybright TJ, Van QN, Muschik GM, Conrads TP, Veenstra TD, Issaq HJ (2006) LC-MS in metabonomics: optimization of experimental conditions for the analysis of metabolites in human urine. *J Liq Chromatogr Relat Technol* 29:2475–2497
 34. Wilson ID, Plumb R, Granger J, Major H, Williams R, Lenz EM (2005) HPLC-MS-based methods for the study of metabolomics. *J Chromatogr B* 817:67–76
 35. Ernst RR, Bodenhausen G, Wokaun A (1990) Principles of nuclear magnetic resonance in one and two dimensions. Oxford University Press, Oxford
 36. Goldman M (1991) Quantum description of high-resolution NMR in liquids. Oxford University Press, Oxford
 37. Kovacs H, Moskau D, Spraul M (2005) Cryogenically cooled probes – a leap in NMR technology. *Prog Nucl Magn Reson Spectrosc* 46:131–155
 38. Prince WS (1999) Water signal suppression in NMR spectroscopy. *Annu Rep NMR Spectrosc* 38:289–354
 39. Potts BC, Deese AJ, Stevens GJ, Reily MD, Robertson DG, Theiss J (2001) NMR of biofluids and pattern recognition: assessing the impact of NMR parameters on the principal component analysis of urine from rat and mouse. *J Pharm Biomed Anal* 26:463–476
 40. Schlotterbeck G, Ross A, Dieterle F, Senn H (2006) Metabolic profiling technologies for biomarker discovery in biomedicine and drug development. *Pharmacogenomics* 7:1055–1075
 41. Ross A, Schlotterbeck G, Dieterle F, Senn H (2007) NMR spectroscopy techniques for application in metabonomics. In: Lindon JC, Nicholson JK, Holmes E (eds) *The handbook of metabonomics and metabolomics*. Elsevier, Amsterdam, pp 55–112
 42. Chen JH, Singer S (2007) High-resolution magic angle spinning NMR spectroscopy. In: Lindon JC, Nicholson JK, Holmes E

- (eds) The handbook of metabonomics and metabolomics. Elsevier, Amsterdam, pp 113–148
43. Keun HC, Beckonert O, Griffin JL, Richter C, Moskau D, Lindon JC, Nicholson JK (2002) Cryogenic probe ^{13}C NMR spectroscopy of urine for metabonomic studies. *Anal Chem* 74:4588–4593
 44. Boros LG, Brackett DJ, Harrigan GG (2003) Metabolic biomarker and kinase drug target discovery in cancer using stable isotope-based dynamic metabolic profiling (SIDMAP). *Curr Cancer Drug Targets* 3:445–453
 45. Ben-Yoseph O, Badar-Goffer RS, Morris PG, Bachelard HS (1993) Glycerol 3-phosphate and lactate as indicators of the cerebral cytoplasmic redox state in severe and mild hypoxia respectively: a ^{13}C - and ^{31}P -NMR study. *Biochem J* 291:915–919
 46. Hoult DI (1976) Solvent peak saturation with single phase and quadrature Fourier transformation. *J Magn Reson* 21:337–347
 47. Kumar A, Ernst RR, Wüthrich K (1980) A two-dimensional nuclear Overhauser enhancement (2D NOE) experiment for the elucidation of complete proton-proton cross-relaxation networks in biological macromolecules. *Biochem Biophys Res Commun* 95:1–6
 48. Ogg RJ, Kingsley PB, Taylor JS (1994) WET, a T_1 - and B_1 -insensitive water-suppression method for in vivo localized ^1H NMR spectroscopy. *J Magn Reson* 104B:1–10
 49. Lenz EM, Bright J, Wilson ID, Morgan SR, Nash AFP (2003) A ^1H NMR-based metabonomic study of urine and plasma samples obtained from healthy human subjects. *J Pharm Biomed Anal* 33:1103–1115
 50. Meiboom S, Gill D (1958) Effects of diffusion on free precession in nuclear magnetic resonance experiments. *Rev Sci Instrum* 29:688–691
 51. Gibbs SJ, Johnson CS Jr (1991) A PFG NMR experiment for accurate diffusion and flow studies in the presence of eddy currents. *J Magn Reson* 93:395–402
 52. Wider G, Dötsch V, Wüthrich K (1994) Self-compensating pulsed magnetic-field gradients for short recovery times. *J Magn Reson* 108A:255–258
 53. Morris KF, Johnson CS Jr (1992) Diffusion-ordered two-dimensional nuclear magnetic resonance spectroscopy. *J Am Chem Soc* 114:3139–3141
 54. Griffin JL, Williams HJ, Sang E, Nicholson JK (2001) Abnormal lipid profile of dystrophic cardiac tissue as demonstrated by one- and two-dimensional magic-angle spinning ^1H NMR spectroscopy. *Magn Reson Med* 46:249–255
 55. Garrod S, Humpfer E, Spraul M et al (1999) High-resolution magic angle spinning ^1H NMR spectroscopic studies on intact rat renal cortex and medulla. *Magn Reson Med* 41:1108–1118
 56. Dumas ME, Canlet C, André F, Vercauteren J, Paris A (2002) Metabonomic assessment of physiological disruptions using ^1H - ^{13}C HMBC-NMR spectroscopy combined with pattern recognition procedures performed on filtered variables. *Anal Chem* 74:2261–2273
 57. Günther H (1992) NMR spectroscopy. Wiley, New York
 58. Holmes E, Foxall PJD, Spraul M, Farrant RD, Nicholson JK, Lindon JC (1997) 750 MHz ^1H NMR spectroscopy characterization of the complex metabolic pattern of urine from patients with inborn errors of metabolism: 2-hydroxyglutaric aciduria and maple syrup urine disease. *J Pharm Biomed Anal* 15:1647–1659
 59. Sweatman BC, Farrant RD, Holmes E, Ghauri FY, Nicholson JK, Lindon JC (1993) 600 MHz ^1H -NMR spectroscopy of human cerebrospinal fluid: effects of sample manipulation and assignment of resonances. *J Pharm Biomed Anal* 11:651–664
 60. Lynch MJ, Masters J, Pryor JP, Lindon JC, Spraul M, Foxall PJD, Nicholson JK (1994) Ultra high field NMR spectroscopic studies on human seminal fluid, seminal vesicle and prostatic secretions. *J Pharm Biomed Anal* 12:19–25
 61. Nicholson JK, Foxall PJD (1996) 750 MHz ^1H and ^1H - ^{13}C NMR spectroscopy of human blood plasma. *Anal Chem* 67:793–811
 62. Viant MR (2003) Improved methods for the acquisition and interpretation of NMR metabolomic data. *Biochem Biophys Res Commun* 310:943–948
 63. Bax A, Davis DG (1985) MLEV-17-based two-dimensional homonuclear magnetization transfer spectroscopy. *J Magn Reson* 65:355–360
 64. Bax A, Freeman R (1981) Investigation of complex networks of spin-spin coupling by two-dimensional NMR. *J Magn Reson* 44:542–561
 65. Derome A, Williamson M (1990) Rapid-pulsing artifacts in double-quantum-filtered COSY. *J Magn Reson* 88:177–185
 66. Ancian B, Bourgeois I, Dauphin JF, Shaw AA (1997) Artifact-free pure absorption PFG-enhanced DQF-COSY spectra including a gradient pulse in the evolution period. *J Magn Reson* 125A:348–354
 67. Nicholls AW, Holmes E, Lindon JC et al (2001) Metabonomic investigations into hydrazine toxicity in the rat. *Chem Res Toxicol* 14:975–987

68. Liu M, Nicholson JK, Lindon JC (1996) High-resolution diffusion and relaxation edited one- and two-dimensional ^1H NMR spectroscopy of biological fluids. *Anal Chem* 68:3370–3376
69. Hoch JC, Stern AS (1997) *NMR data processing*. Wiley, New York
70. Traficante DD, Rajabzadeh M (2000) Optimum window function for sensitivity enhancement of NMR signals. *Concepts Magn Reson* 12:83–101
71. Lefebvre B, Golotvin S, Schoenbachler L, Beger R, Price P, Megyesi J, Safirstein R (2004) Intelligent bucketing for metabolomics – Part I, Poster. <http://www.acdlabs.com/download/publ/2004/enc04/intelbucket.pdf>
72. Forshed J, Schuppe-Koistinen I, Jacobsson SP (2003) *Anal Chim Acta* 487:189
73. Stoyanova R, Nicholls AW, Nicholson JK, Lindon JC, Brown TR (2004) Automatic alignment of individual peaks in large high-resolution spectral data sets. *J Magn Reson* 170:329–335
74. Cloarec O, Dumas ME, Trygg J, Craig A, Barton RH, Lindon JC, Nicholson JK, Holmes E (2005) Evaluation of the orthogonal projection on latent structure model limitations caused by chemical shift variability and improved visualization of biomarker changes in ^1H NMR spectroscopic metabolomic studies. *Anal Chem* 77:517–526
75. Cloarec O, Dumas ME, Craig A, Barton RH, Trygg J, Hudson J, Blancher C, Gauguier D, Lindon JC, Holmes E, Nicholson J (2005) Statistical total correlation spectroscopy: an exploratory approach for latent biomarker identification from metabolic ^1H NMR data sets. *Anal Chem* 77:1282–1289
76. Holmes E, Foxall PJD, Nicholson JK, Neild GH, Brown SM, Beddell CR, Sweatman BC, Rahr E, Lindon JC, Spraul M, Neidig P (1994) Automatic data reduction and pattern recognition methods for analysis of ^1H nuclear magnetic resonance spectra of human urine from normal and pathological states. *Anal Biochem* 220:284–296
77. Fauler G, Leis HJ, Huber E, Schellauf C, Kerbl R, Urban C, Gleispach H (1994) Determination of homovanillic acid and vanillylmandelic acid in neuroblastoma screening by stable isotope dilution GC-MS. *J Mass Spectrom* 32:507–514
78. Encyclopedia.com. Creatinine. <http://www.encyclopedia.com/doc/1O39-creatinine.html>
79. Shockcor JP, Holmes E (2002) Metabolomic applications in toxicity screening and disease diagnosis. *Curr Top Med Chem* 2:35–51
80. Antti H, Bollard ME, Ebbels T, Keun H, Lindon JC, Nicholson JK, Holmes E (2002) Batch statistical processing of ^1H NMR-derived urinary spectral data. *J Chemometr* 16:461–468
81. Keun HC, Ebbels TMD, Antti H, Bollard ME, Beckonert O, Holmes E, Lindon JC, Nicholson JK (2003) Improved analysis of multivariate data by variable stability scaling: application to NMR-based metabolic profiling. *Anal Chim Acta* 490:265–276
82. Brindle JT, Nicholson JK, Schofield PM, Grainger DJ, Holmes E (2003) Application of chemometrics to ^1H NMR spectroscopic data to investigate a relationship between human serum metabolic profiles and hypertension. *Analyst* 128:32–36
83. Dieterle F, Ross A, Schlotterbeck G, Senn H (2006) Probabilistic quotient normalization as robust method to account for dilution of complex biological mixtures. Application in ^1H NMR metabolomics. *Anal Chem* 78:4281–4290
84. Wang G, Hsieh Y, Korfmacher WA (2005) Comparison of atmospheric pressure chemical ionization, electrospray ionization, and atmospheric pressure photoionization for the determination of cyclosporin A in rat plasma. *Anal Chem* 77:541–548
85. Want EJ, Nordström A, Morita H, Siuzdak G (2007) From exogenous to endogenous: the inevitable imprint of mass spectrometry in metabolomics. *J Proteome Res* 6:459–468
86. Idborg H, Zamani L, Edlund PO, Schuppe-Koistinen I, Jacobsson SP (2005) Metabolic fingerprinting of rat urine by LC/MS Part I. Analysis by hydrophilic interaction liquid chromatography–electrospray ionization mass spectrometry. *J Chromatogr B* 828:9–13
87. Pham-Tuan H, Kaskavelis L, Daykin CA, Janssen HG (2003) Method development in high-performance liquid chromatography for high-throughput profiling and metabolomic studies of biofluid samples. *J Chromatogr B* 789:283–301
88. Dunn W, Ellis DI (2005) Metabolomics: current analytical platforms and methodologies. *Trends Anal Chem* 24(4):285–294
89. Ackermann BL, Hale JE, Duffin KL (2006) The role of mass spectrometry in biomarker discovery and measurement. *Curr Drug Metab* 7:525–539
90. Bligh EG, Dyer WJ (1959) A rapid method of total lipid extraction and purification. *Can J Biochem Physiol* 37:911–917
91. Peña-Alvarez A, Díaz L, Medina A, Labastida C, Capella S, Vera LE (2004) Characterization of three *Agave* species by gas chromatography and solid-phase microextraction-gas chromatography-mass spectrometry. *J Chromatogr A* 1027:131–136
92. Le Belle JE, Harris NG, Williams SR, Bhakoo KK (2002) A comparison of cell and tissue extraction techniques using high-resolution ^1H -NMR spectroscopy. *NMR Biomed* 15:37–44

93. Gullberg J, Jonsson P, Nordström A, Sjöström M, Moritz T (2004) Design of experiments: an efficient strategy to identify factors influencing extraction and derivatization of *Arabidopsis thaliana* samples in metabolomics studies with gas chromatography/mass spectrometry. *Anal Biochem* 331:283–295
94. Schröder NW, Schombel U, Heine H, Göbel UB, Zähringer U, Schumann RR (2003) Acylated cholesteryl galactoside as a novel immunogenic motif in *Borrelia burgdorferi sensu stricto*. *J Biol Chem* 278:33645–33653
95. Katajamaa M, Oresic M (2007) Data processing for mass spectrometry-based metabolomics. *J Chromatogr A* 1158:318–328
96. Cloarec O, Campbell A, Tseng LH, Braumann U, Spraul M, Scarfe G, Weaver R, Nicholson JK (2007) Virtual chromatographic resolution enhancement in cryoflow LC-NMR experiments via statistical total correlation spectroscopy. *Anal Chem* 79:3304–3311
97. Lindon JC, Nicholson JK (1999) NMR spectroscopy of biofluids. In: Webb GA (ed) *Annual reports in NMR spectroscopy*, vol 38. Academic Press, London, pp 2–78
98. Weckwerth W, Morgenthal K (2005) Metabolomics: from pattern recognition to biological interpretation. *Drug Discov Today* 10:1551–1558

Protocols and Applications of Cellular Metabolomics in Safety Studies Using Precision-Cut Tissue Slices and Carbon 13 NMR

Gabriel Baverel, Maha El Hage, and Guy Martin

Abstract

Numerous xenobiotics are toxic to human and animal cells by interacting with their metabolism, but the precise metabolic step affected and the biochemical mechanism behind such a toxicity remain often unknown. In an attempt to reduce the ignorance in this field, we have developed a new approach called cellular metabolomics. This approach, developed *in vitro*, provides a panoramic view not only of the pathways involved in the metabolism of physiological substrates of any normal or pathological human or animal cell but also of the beneficial and adverse effects of xenobiotics on these metabolic pathways. Unlike many cell lines, precision-cut tissue slices, for which there is a renewed interest, remain metabolically differentiated for at least 24–48 h and allow to study the effect of xenobiotics during short-term and long-term incubations. Cellular metabolomics (or metabolic flux analysis), which combines enzymatic and carbon 13 NMR measurements with mathematical modeling of metabolic pathways, is illustrated in this brief chapter for studying the effect of insulin on glucose metabolism in rat liver precision-cut slices and of valproate on glutamine metabolism in human renal cortical precision-cut slices. The use of very small amounts of test compounds allows to predict their toxic effect and eventually their beneficial effects very early in the research and development processes. Cellular metabolomics is complementary to other omics approaches, but, unlike them, provides functional, mechanistic, and dynamic pieces of information by measuring enzymatic fluxes.

Key words Toxicology, Liver, Kidney, Cellular metabolomics, Carbon 13 NMR

1 Introduction

Tissue slices, used since the 1920s [1], have proved to be a very useful *in vitro* tool to identify most of the cellular metabolic pathways. With the availability of collagenase in the 1970s [2], they have been progressively replaced by cells isolated from a great variety of tissues. Thanks to technical improvements that made possible to prepare automatically thinner slices [3], there has been a renewed interest in the use of precision-cut tissue slices starting about 30 years ago particularly for pharmaco-toxicology studies

[4–6]. The latter model presents a number of advantages over other cellular models used *in vitro*: maintenance of the *in vivo* tissue architecture, of the heterogeneity of cell populations, and of cell–cell and cell–matrix interactions; use of the same cellular model for short-term (for up to some hours) and long-term (for at least up to 48 h) incubations; possibility of histological studies, and preservation of differentiated metabolic functions.

Numerous xenobiotics are toxic to various tissues and cells because they interact negatively with cellular energy metabolism but, under most cases, the precise adverse mechanism involved remains unknown. This is why it is desirable to understand the precise biochemical step(s) altered and responsible for these toxic effects. For this, the development of methods allowing to provide a panoramic view of cellular metabolic pathways is needed.

Because this has been comprehensively covered by other authors [7–12], the objectives of this chapter are not to explain in detail how to prepare and incubate precision-cut tissue slices and how this experimental model can be used for toxicology and drug metabolism studies. Rather, we wish to illustrate our experience with the use of precision-cut liver and kidney slices in combination with what we call “cellular metabolomics” to understand how hepatotoxic and nephrotoxic drugs may interfere with cellular metabolic pathways. Indeed, traditional metabolomics, which uses either the mass spectrometry (MS) or the nuclear magnetic resonance spectrometry (MRS) techniques, is a large-scale method that allows to identify and quantify metabolites present in body fluids (mainly urine and plasma) [13]; metabolomics is of great diagnostic and prognostic values, but rarely allows to identify the mechanisms behind the biomarkers identified. This is why we have developed a cellular metabolomic approach which combines the use of enzymatic and carbon 13 MRS measurements with mathematical modeling of metabolic pathways. This new approach provides a panoramic view not only of all the pathways involved in the metabolism of any given substrate in any human or animal cell type *in vitro* but also of the beneficial and adverse effects of xenobiotics on these metabolic pathways. For this, only small amounts of test compounds are needed, which explains why it is possible to predict both the beneficial and toxic effects of these compounds at a very early stage of the research and development processes.

2 Materials

2.1 Reagents and Incubation Media

1. Enzymes, coenzymes, and L-lactate were supplied by Roche Molecular Biochemicals (Meylan, France). L-Glutamine, D-glucose, and valproate were obtained from Sigma Chemicals (St Louis, MO, USA). L-[3-¹³C]glutamine, [2-¹³C]glycine, deuterated water, and D-[2-¹³C]glucose were obtained from Euriso-Top (St. Aubin, France). These ¹³C-labeled compounds had a 99% isotopic abundance.

2. Krebs-Henseleit buffer (*see Note 1* for the composition of this buffer).
3. William's Medium E was obtained from Invitrogen (Cergy-Pontoise, France; *see Note 2* for the composition of this medium).

2.2 Liver and Kidney-Cortex Samples

1. Fresh human normal kidney cortex was obtained from the uninvolved pole of kidneys removed for neoplasm from 18-h-fasted patients.
2. Fed or 48-h-fasted male Wistar rats (250–300 g) were obtained from Charles River (Saint Germain sur l'Arbresle, France) and anesthetized with sodium pentobarbital (35 mg/kg body weight, i.p.). The portal vein was catheterized and the inferior vena cava was severed; then, ice-cold well-oxygenated Krebs-Henseleit buffer was infused for 3 min before removal of the liver and the kidneys. The kidneys were sagittally opened and the medulla discarded.

2.3 Preparation of Precision-Cut Liver and Renal Cortical Slices and Incubations

1. Tissue coring tool (Alabama R&D, Alabama, USA).
2. Krumdieck tissue slicer (Alabama R&D, Alabama, USA).
3. Teflon rollers (Vitron Inc., Tucson, Arizona, USA).
4. HClO₄.

2.4 ¹³C-NMR

1. Bruker AM-500 WB spectrometer.

3 Methods

This section describes the preparation of precision-cut liver and renal cortical slices, incubation procedures, metabolic characterization of precision-cut liver and kidney slices, and applications of cellular metabolomics to safety problems.

3.1 Preparation of Precision-Cut Liver and Renal Cortical Slices

1. Cylindrical cores of 5 or 8 mm diameter were prepared from renal cortical or liver sections with a tissue coring tool from the kidneys and the liver, respectively.
2. The cores were maintained in oxygenated (5% CO₂–95% O₂) ice-cold Krebs Henseleit buffer and transferred to a Krumdieck tissue slicer filled with oxygenated ice-cold Krebs-Henseleit buffer and set to produce slices of 200–250 μm thickness.

3.2 Incubation Procedures

1. Short-term incubations were performed for up to 4 h at 37 °C in 2 or 4 mL of Krebs-Henseleit medium in a shaking water bath in 25 mL stoppered Erlenmeyer flasks with an atmosphere of 5% CO₂–95% O₂. Slices were incubated with either unlabeled or ¹³C-labeled substrate (glutamine, glucose, lactate, ala-

nine, etc.) in the absence and the presence of the effector (agonist or antagonist) of interest (*see* **Notes 1** and **3**).

2. When “long-term” incubations were performed, the slices were floated on to Teflon rollers which were carefully loaded into scintillation vials containing 2 mL of William’s Medium E supplemented with the unlabeled or ¹³C-labeled substrate of interest in the absence and presence of the effector. Vials were closed with a cap that had a central hole and placed horizontally on a vial rotator in a humidified incubator and set at 37 °C and gassed with 40% O₂–5% CO₂–55% N₂ (*see* **Notes 2–4**). Then, the slices were incubated either between 0 and 24 h or between 24 and 48 h after a prior 24-h incubation period.
3. Incubations were terminated by removing the slices and adding HClO₄ [2% (v/v) final concentration] to the incubation medium. In the flasks in which lactate dehydrogenase (LDH) activity was measured, slices were used for intracellular LDH activity measurement and the medium was collected for extracellular LDH measurement before HClO₄ addition. In all experiments, zero-time flasks were prepared with slices by adding HClO₄ before the slices. In all experiments, each experimental condition was performed at least in duplicate.

3.3 ATP and Protein Content

1. After the incubation, two slices were homogenized in 0.2 mL of cold 7% (v/v) HClO₄ using an Ultraturrax homogenizer at 9500 rpm, and after centrifugation of the homogenate for 5 min at 3000 × *g*, the supernatant was neutralized with 20% KOH before ATP measurement. The slice ATP content was quantified using the method of Lamprecht and Trautschold [14].
2. Pellets were solubilized in 0.5 M NaOH for protein determination. Total protein was determined according to the method of Lowry et al. [15] using bovine serum albumin as internal standard.

3.4 LDH Release

At the end of the incubation period, the slices were removed, frozen in liquid nitrogen, and thawed three times to release intracellular LDH. Enzyme leakage, a marker of the integrity of the cellular plasma membrane, was determined in the incubation medium and compared with total LDH activity (extracellular and intracellular LDH). LDH activity was determined using the method described by Bergmeyer and Bernt [16].

3.5 Metabolite Assays

After removing the denaturated protein by centrifugation (3000 × *g* for 5 min), the supernatant was neutralized with 20% KOH and used for metabolite determinations. Glutamine, glutamate, ammonia, urea, alanine, glucose, aspartate, pyruvate, lactate, glycogen, triglycerides, acetoacetate, and β-hydroxybutyrate were measured by enzymatic methods described previously [17, 18].

3.6 ¹³C-NMR Techniques

1. Data were recorded at 125.75 MHz on a Bruker AM-500 WB spectrometer using a 5 mm broadband probe thermostated at 8 °C. Magnet homogeneity was adjusted using the deuterium lock signal. Supernatants containing the ¹³C-labeled substrates were lyophilized. The lyophilized material was redissolved in deuterated water containing [2-¹³C]glycine as internal standard and centrifuged (5000 × *g* at 4 °C for 5 min).
2. To obtain quantitative results, special care was taken for data acquisition. Acquisition parameters were as follows: spectral width, 25,000 Hz; tilt angle, 90 °C; data size, 32k; repetition time, 50 s; number of scans, 420. We used a standard (WALTZ 16) pulse sequence for inverse-gated proton decoupling [19]. We did not use the NOESY during proton decoupling to avoid the use of the corresponding correction factors. A 1 Hz line broadening was applied prior to Fourier transformation. Peak areas were determined by Lorentzian fitting. Chemical shifts were expressed as ppm with respect to tetramethylsilane. Assignments were made by comparing the chemical shifts obtained with those given in the literature [20, 21].

3.7 Calculations and Statistical Analysis

1. Net substrate utilization and product formation were calculated as the difference between the total flask contents at the start (zero-time flasks or rollers) and after the period of incubation.
2. When [¹³C]glutamine or [¹³C]glucose was the substrate, the transfer of the ¹³C of glutamine or glucose to a given position in a given metabolite was calculated using the formula $(L_m - l_m)/(E_s - e_s)$; L_m is the amount of ¹³C measured in the corresponding NMR resonance, l_m the natural ¹³C abundance (1.1%) multiplied by the amount of metabolite assayed enzymatically, E_s the ¹³C abundance of the ¹³C of glutamine or glucose, and e_s the ¹³C natural abundance. Note that $(E_s - e_s)$ is the specific enrichment of the corresponding species.
3. When absolute fluxes through metabolic pathways were calculated, they were obtained by replacing the parameters of the equations developed in the mathematical models of substrate metabolism by the enzymatic and ¹³C NMR values measured. The models were developed in-house as described in several publications from this laboratory [22–25].
4. Values presented as means ± SEM are expressed in μmol of substrate removed or metabolite produced $(\text{gram of protein})^{-1} (\text{incubation time})^{-1}$. Comparison of two groups was made by the paired Student's *t* test. $P < 0.05$ was considered to be statistically significant.

3.8 Metabolic Characterization of Precision-Cut Liver and Kidney Slices

Figure 1 is a general scheme of the renal metabolism of lactate and glutamine carbons. Lactate is converted into pyruvate by lactate dehydrogenase. Then, pyruvate (1) can be converted into alanine by cytosolic or mitochondrial alanine aminotransferase except in the rat kidney in which this enzyme is present at a very low activity, (2) can enter the gluconeogenic pathway thanks to the action of the key-gluconeogenic enzymes (pyruvate carboxylase, phosphoenolpyruvate carboxykinase, fructose 1,6-bisphosphatase, and glucose 6-phosphatase), or (3) can be converted into acetyl-CoA which binds to oxaloacetate to form citrate which is further metabolized in the tricarboxylic acid cycle. Note that, in the presence of ammonia, α -ketoglutarate can be partly converted into glutamate and glutamine thanks to the glutamate dehydrogenase and glutamine synthetase reactions. Note also that, in slices from the liver of fed animals, glycogen is degraded and is partly converted into glucose, pyruvate, and lactate; this does not occur in slices from the kidney of fed rats because the kidney does not accumulate glycogen.

Both in the liver and the kidney, the metabolism of glutamine (Fig. 1) is initiated by glutaminase which forms glutamate and ammonia. In the rat kidney, glutamate is converted into α -ketoglutarate by glutamate dehydrogenase which also gives ammonia. By contrast, in the rat liver, glutamate is converted into α -ketoglutarate by aspartate aminotransferase which also forms aspartate; then, the latter aspartate and the ammonia released by glutaminase provide the two nitrogens needed to synthesize urea via the urea cycle. The α -ketoglutarate formed both in the liver and

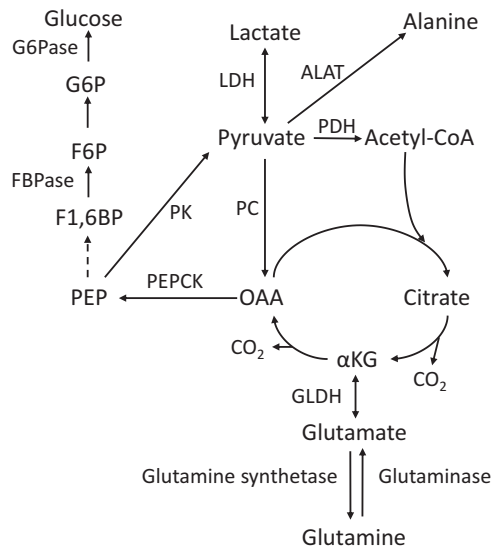


Fig. 1 Scheme of hepatic and renal metabolism of lactate and glutamine in the rat. α KG α -ketoglutarate, LDH lactate dehydrogenase, PDH pyruvate dehydrogenase, PC pyruvate carboxylase, PEPCCK phosphoenolpyruvate carboxykinase, F1,6BP fructose 1,6-bisphosphatase, G6Pase glucose 6-phosphatase, GLDH glutamate dehydrogenase, ALAT alanine aminotransferase

the kidney can be either converted into glucose by the gluconeogenic pathway or completely oxidized to CO₂ as a result of the conversion of phosphoenolpyruvate into pyruvate by pyruvate kinase and the subsequent operation of pyruvate dehydrogenase and the tricarboxylic acid cycle.

Tables 1, 2, and 3 show the results of enzymatic measurements of the removal of physiological substrates (lactate, glutamine, and

Table 1
Metabolism of 5 mM L-lactate in precision-cut slices from the renal cortex and liver of fed or 48-h-fasted Wistar rats

Tissue	Nutritional state	Number of experiments (<i>n</i>)	Incubation (h)	Metabolite removal (–) or production		
				Lactate	Pyruvate	Glucose
Kidney	Fed	3	4	–1751 ± 348	147 ± 56	168 ± 31
Kidney	Fasted	3	4	–1698 ± 223	90 ± 15	308 ± 34
Kidney	Fasted	4	24	–7091 ± 1100	–	563 ± 87
Liver	Fed	4	4	–764 ± 231	311 ± 48	1451 ± 194
Liver	Fasted	4	4	–1379 ± 82	54 ± 7	592 ± 106
Liver	Fasted	4	24	–3299 ± 139	–26 ± 6	1470 ± 83

Values, expressed in μmol (g protein)^{–1} (incubation time)^{–1}, are means ± SEM for *n* (3 or 4) experiments. In the experiments with liver slices from fed rats incubated for 4 h, lactate removal was a net removal because lactic acid (like pyruvic acid) was concomitantly produced from glycogen. In experiments with liver slices from fasted rats incubated for 24 h, alanine removal (–424 ± 47) also occurred. Incubations for 4 h were performed in Krebs-Henseleit buffer and those for 24 h in William’s Medium E without glucose

Table 2
Metabolism of 5 mM L-glutamine in precision-cut slices from the renal cortex and liver of fed or 48-h-fasted Wistar rats

Tissue	Nutritional state	Number of experiments (<i>n</i>)	Incubation (h)	Metabolite removal (–) or production		
				Glutamine	Glutamate	Glucose
Kidney	Fed	3	4	–2299 ± 258	671 ± 99	140 ± 21
Kidney	Fasted	3	4	–1453 ± 92	626 ± 44	178 ± 103
Kidney	Fasted	4	24	–4259 ± 309	681 ± 70	298 ± 48
Liver	Fasted	4	4	–827 ± 66	65 ± 10	426 ± 33
Liver	Fasted	4	24	–2634 ± 334	28 ± 14	1318 ± 141

Values, expressed in μmol (g protein)^{–1} (incubation time)^{–1}, are means ± SEM for *n* (3 or 4) experiments. In the experiments with slices from fasted rats incubated for 24 h, alanine removal (–370 ± 44) and pyruvate removal (–48 ± 5) also occurred. Incubations for 4 h were performed in Krebs-Henseleit buffer and those for 24 h in William’s Medium E without glucose

Table 3
Metabolism of D-glucose in precision-cut slices from the renal cortex and liver of fed Wistar rats

Tissue	Nutritional state	Number of experiments (<i>n</i>)	[Glucose] (mM)	Incubation (h)	Metabolite removal (–) or production			
					Glucose	Pyruvate	Lactate	Glycogen
Kidney	Fed	4	5	4	–411 ± 121	24 ± 6	94 ± 34	–
Kidney	Fed	4	5	24	–2996 ± 270	–82 ± 24	242 ± 53	–
Kidney	Fed	4	10	24	–3413 ± 534	–80 ± 6	236 ± 50	–
Liver	Fed	5	5.5	24	1761 ± 106	–36 ± 9	396 ± 62	–3791 ± 366
Liver	Fed	5	11	24	562 ± 142	3 ± 14	710 ± 90	–3780 ± 367

Values, expressed in $\mu\text{mol (g protein)}^{-1} (\text{incubation time})^{-1}$, are means \pm SEM for *n* (4 or 5) experiments. In the experiments with liver slices in the presence of 5.5 and 11 mM glucose as substrate, alanine removal (–253 \pm 23 and –148 \pm 34, respectively) also occurred. Glycogen removal is expressed in glucosyl units

glucose) and of the production of metabolites by precision-cut liver and kidney slices from fed or fasted rats. Such preliminary measurements are required before performing experiments with ^{13}C -labeled substrates to make sure that substrate removal, and therefore product formation, is sufficiently high to obtain reliably quantifiable resonances in ^{13}C NMR spectra and, therefore, to allow the application of our cellular metabolomic approach.

Table 1 shows that precision-cut kidney and liver slices from fed and fasted rats removed lactate and synthesized glucose at high rates although these rates substantially decreased during 24 h of incubation. Carbon balance calculations indicate that, irrespective of the experimental condition, a large fraction of the lactate removed by kidney slices was completely oxidized to CO_2 . By contrast, in liver slices from fasted rats, the lactate removed was almost completely converted into glucose leaving little room for lactate complete oxidation. It is important to emphasize that, in liver slices from fed rats, a large fraction of the glucose produced arose from the degradation of glycogen which also gave lactate. A cellular metabolomic approach using ^{13}C -lactate allows to differentiate the glucose arising from lactate from that synthesized from glycogen; this approach also allows to determine the ^{13}C -lactate removal and therefore the lactic acid synthesized from glycogen. Concomitantly, it is possible to evaluate the lactate oxidized in mitochondria. Thus, any xenobiotic interaction with all the pathways of lactate and glycogen metabolism in the liver (glycogen synthesis and glycogenolysis, glycolysis, lactic acid formation, lactate removal, lactate gluconeogenesis, glycogen, and lactate oxidation in mitochondria) can be assessed concomitantly.

Table 2 shows that precision-cut kidney and liver slices from fasted rats also removed glutamine and synthesized glucose at high rates but again these rates greatly declined during 24 h of incubation. As observed with lactate as substrate, carbon balance calculations reveal that, in kidney slices, most of the glutamine carbon removed was completely oxidized to CO_2 with a small fraction converted into glucose. By contrast, in liver slices from fasted rats, glucose explained virtually all the glutamine removed both after 4 and 24 h of incubation. It is important to note that, in our hands, the rates of removal of 5 mM glutamine and of glutamine gluconeogenesis in precision-cut liver slices from fasted rats and incubated for 4 h were approximately the same as those measured in isolated hepatocytes from fasted rats incubated for 1 h (*see ref. 26 and Table 2*). Similar rates of glutamine removal were also observed in precision-cut kidney slices incubated for 4 h and isolated proximal tubules from fed rats incubated for 1 h but the rate of glutamine gluconeogenesis was lower in slices than in isolated tubules (for comparison, *see ref. 27 and Table 2*).

Figure 2 is a general scheme of the metabolism of glucose. In the liver and kidney, glucose can be both removed and metabolized, or synthesized and released. During a short fast, the glucose

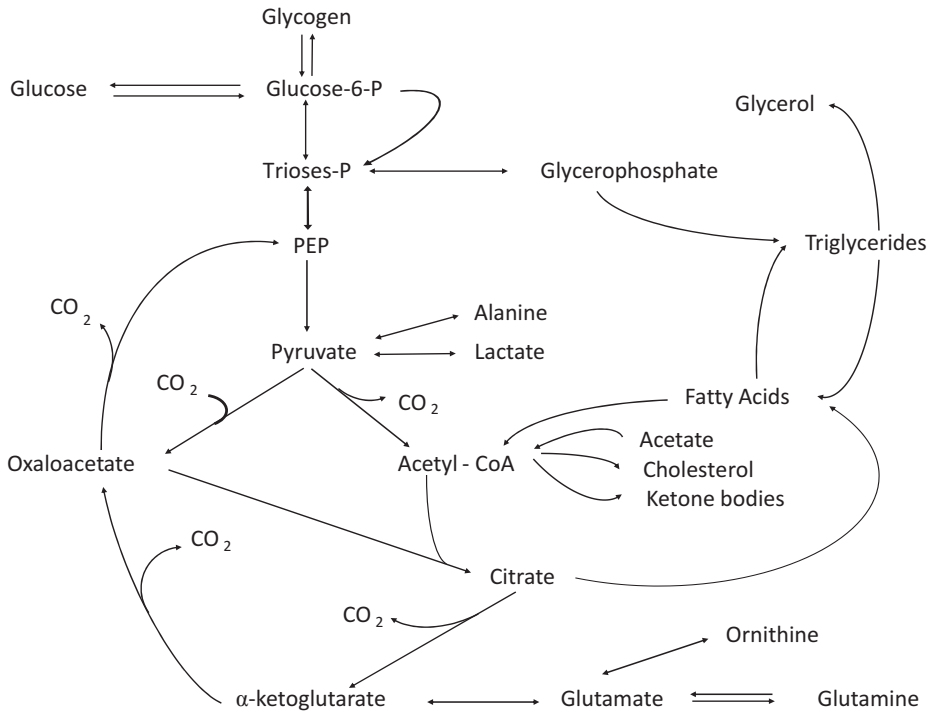


Fig. 2 General scheme of glucose metabolism. *PEP* phosphoenolpyruvate

released by the liver arises both from glycogenolysis and gluconeogenesis (from lactate, alanine, glutamine, and glycerol) whereas the glucose released by the kidney arises only from gluconeogenesis. After a prolonged fast (longer than 24 h), the glucose released by the liver and kidney is formed only by the gluconeogenic pathway. The liver, but not the kidney, has the capacity to synthesize, store, and degrade substantial amounts of glycogen. When glycogen is degraded, it is converted into glucose, lactic acid, and CO_2 in the mitochondria. The pentose phosphate pathway provides NADPH for fatty acid synthesis in the liver and the reduced form of glutathione in the kidney which, unlike the liver, is not able to synthesize fatty acids. Both the liver and kidney can synthesize and degrade triglycerides, the fatty acids needed to synthesize renal triglycerides being taken up from the circulating blood by the kidney. Numerous mitochondria, present in both the renal cortex and liver, can oxidize glucose to CO_2 ; glycogen can also be oxidized to CO_2 in liver mitochondria. Fatty acids taken up from the circulating blood can be oxidized to CO_2 both in the liver and the renal cortex, or can be converted into ketone bodies only in liver mitochondria.

Table 3 shows the characteristics of glucose metabolism in kidney and liver slices from fed rats. Kidney slices removed glucose at high rates both during 4 and 24 h and this rate did not diminish during 24 h of incubation. The elevation of glucose concentration

from 5 to 10 mM did not increase the rate of glucose removal during 24 h of incubation. Under all experimental conditions, the glucose removed was almost completely oxidized to CO₂ in the mitochondria as revealed by carbon balance calculations. In the presence of 5.5 and 11 mM glucose, liver slices from fed rats did not remove but rather produced glucose in net amounts because the large amounts of glucose formed as a result of the degradation of glycogen masked the glucose removal. Under these conditions, the use of ¹³C-glucose allowed to not only determine (data not shown) the removal of glucose but also differentiate the lactic acid formed from glucose on the one hand and, on the other hand, the lactic acid formed from glycogen; it also allowed to determine the CO₂ produced from glucose in mitochondria, and the glycogen and triglycerides synthesized from glucose.

3.9 Effect of Insulin on ¹³C-Glucose Metabolism in Precision-Cut Rat Liver Slices

Hyperglycemia, the hallmark of type 1 and type 2 diabetes, results from the deficit of insulin secretion and/or action. This leads to a deficit of hepatic glucose removal and an excess of hepatic glucose production. The following example illustrates how cellular metabolomics can be applied not only to safety but also to efficacy problems related to the effect of insulin on the hepatic metabolism of glucose. Table 4 shows the results of enzymatic measurements when 11 mM [2-¹³C]glucose was used as substrate in the absence and presence of 100 nM insulin.

Table 4 shows that, in liver slices incubated between 24 and 48 h, insulin converted a net glucose production into a net glucose removal. Insulin inhibited the net degradation of glycogen and the small accumulation of ammonia, and stimulated alanine removal. Insulin also converted the net degradation of triglycerides into a net production. The other parameters measured (glutamate and glutamine accumulation, ureagenesis, and ketogenesis) remained unaltered by insulin.

Figure 3 shows a typical carbon 13 NMR spectrum of a perchloric extract of the incubation medium after incubation with 11 mM [2-¹³C]glucose. In this spectrum, it can be seen that, after incubation, glucose carbons other than the C-2 became labeled which means that glucose resynthesis occurred thanks to the glucose 6-phosphatase reaction.

Figures 4 and 5 show typical carbon 13 NMR spectra of the glycogen and triglycerides extracted from the slices incubated under the same condition. It can be seen that all significant peaks could be assigned and corresponded to carbons of the products determined enzymatically. From these spectra, it was possible to calculate the amounts of labeled products after correction for the 1.1% ¹³C natural abundance.

As shown in Table 5, the results of these calculations indicate that, under the experimental conditions used, 100 nM insulin stimulated glucose removal without altering the resynthesis of

Table 4
Effect of insulin on the metabolism of [2-¹³C]glucose in Wistar rat liver slices incubated between 24 and 48 h (enzymatic data)

Experimental condition	Metabolite removal (-) or production											
	Glucose	Glycogen	Lactate	Pyruvate	Alanine	Glutamate	Glutamine	Aceto- acetate	β-OH- butyrate	Triglyce- rides	Urea	Ammonia
11 mM [2- ¹³ C] glucose	245 ±344	-193 ±49	968 ±69	52 ±22	-388 ±29	123 ±7	229 ±38	213 ±30	156 ±25	-35 ±10	653 ±34	40 ±3
11 mM [2- ¹³ C] glucose + 100 nM insulin	-725 ±472*	52 ±79*	941 ±74	47 ±22	-450 ±36*	125 ±9	203 ±34	170 ±24	121 ±17	17 ±10*	572 ±46	19 ±3*

The slices were incubated in William's Medium E for 24 h prior to these experiments. Values, expressed in μmol (g protein)⁻¹ 24 h⁻¹, are means ± SEM for five experiments.

* $P < 0.05$

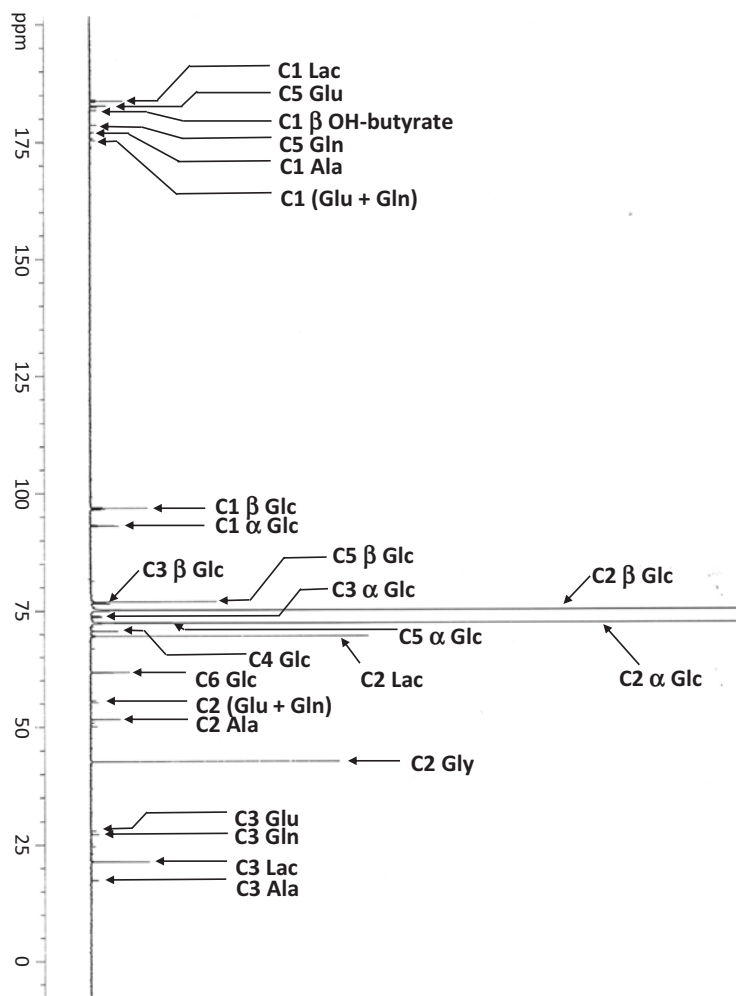


Fig. 3 Carbon 13 NMR spectrum of the medium incubated with liver slices between 24 and 48 h. [2- ^{13}C]glycine was used as internal standard

^{13}C -glucose or stimulating the production of lactic acid and triglycerides; insulin also stimulated the synthesis of ^{13}C -glycogen. In agreement with the absence of change in the production of CO_2 by liver mitochondria, there was no alteration of the β -hydroxybutyrate/acetoacetate or of the lactate/pyruvate ratios indicating that insulin did not modify the mitochondrial and cytosolic redox potentials, respectively.

It is easy to anticipate that this approach is applicable to assess early not only the efficacy and safety of any antidiabetic drug or drug candidate but also the hepatic safety of any xenobiotic (drug, chemical, environmental contaminant) that might stimulate lactic acid production (risk of lactic acidosis) or triglyceride accumulation (risk of steatosis) or inhibit mitochondrial functions (tricarboxylic acid cycle, respiratory chain, β -oxidation) (risk of energy restriction, ATP fall, and necrosis).

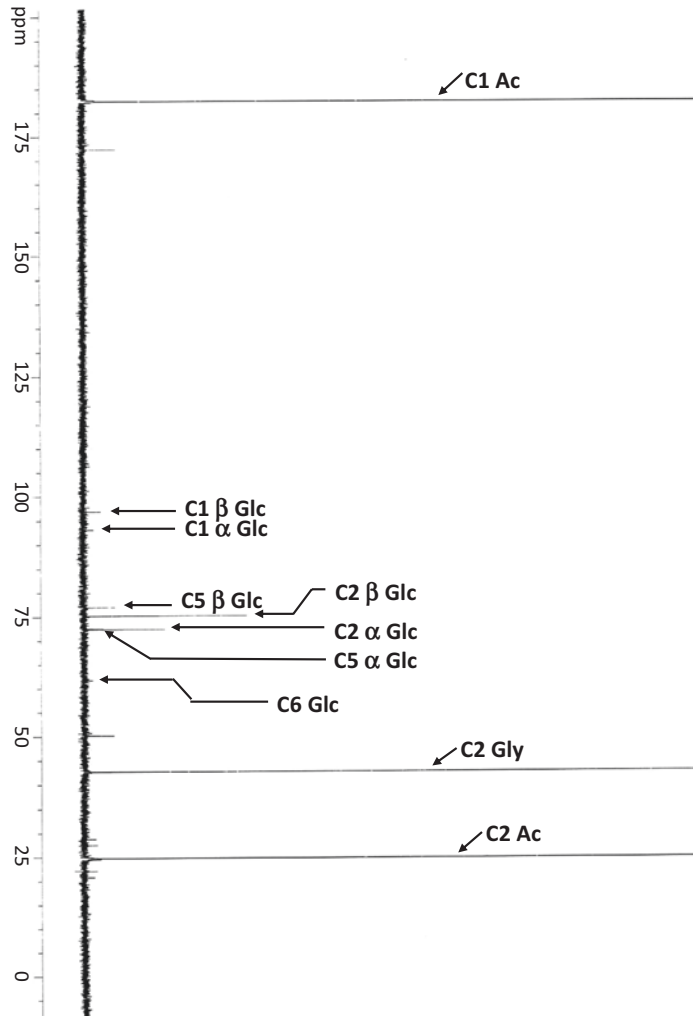


Fig. 4 Carbon 13 NMR spectrum of the glucose derived from glycogen accumulated in liver slices. $[2-^{13}\text{C}]$ glycine was used as internal standard

3.10 Effect of Valproate on ^{13}C -Glutamine Metabolism in Human Renal Cortical Precision-Cut Slices

Sodium valproate (*n*-dipropylacetic acid, sodium salt), a branched-chain fatty acid, is a widely used and very effective antiepileptic drug in adult and children [28]. Drug administration often induces a moderate hyperammonemia especially when other anticonvulsants are taken in addition to valproate [29]. Since this hyperammonemia is in some rare cases accompanied by clinical manifestations of liver dysfunction or of encephalopathy [30], it was of clinical importance to identify the origin of the valproate-induced elevation of blood ammonia levels.

Measurements on human and rat kidney *in vivo* have shown that valproate increases glutamine uptake and ammonia release [31–33].

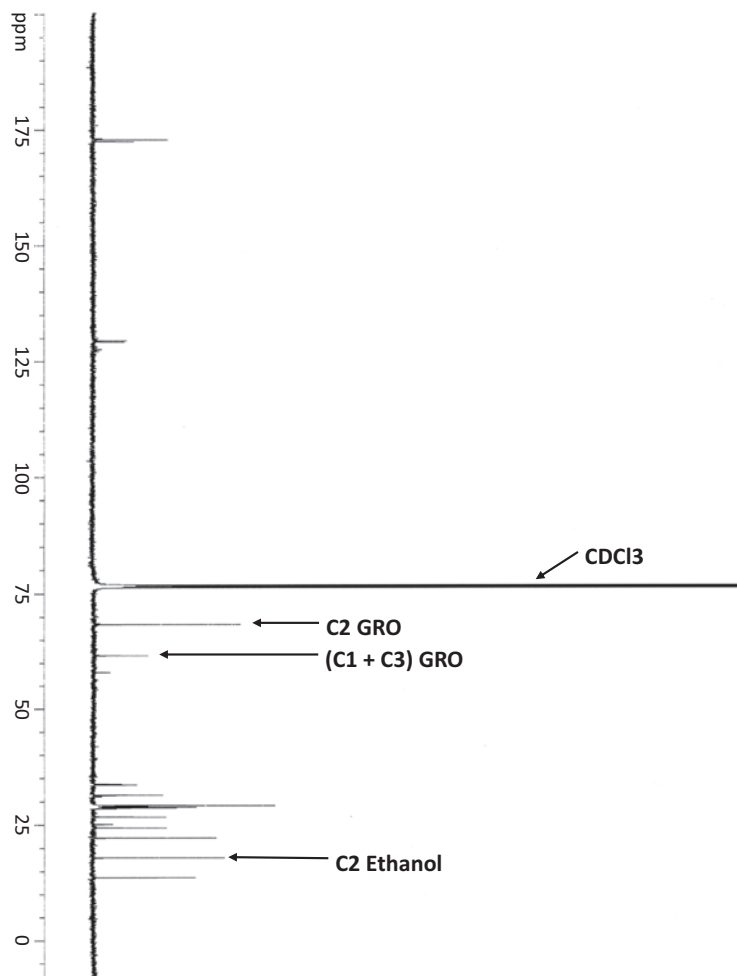


Fig. 5 Carbon 13 NMR spectrum of the triglycerides accumulated in liver slices. $[2-^{13}\text{C}]$ ethanol was used as internal standard. The resonances surrounding that of ethanol correspond to the fatty acid carbons of triglycerides

In order to examine the possible mechanisms by which valproate stimulates the renal production of ammonia in the human kidney, we have employed our cellular metabolomic approach in which we have incubated human renal cortical precision-cut slices for 4 h in Krebs-Henseleit buffer containing 2 mM $[1-^{13}\text{C}]$ - and $[3-^{13}\text{C}]$ glutamine in the absence and presence of 1 mM valproate. The methods employed are described in detail in a recent publication from this laboratory which shows the typical carbon 13 NMR spectra obtained [34]. Valproate did not increase the release of LDH from the human renal cortical slices used.

Figure 6 shows a panoramic view of the metabolism of glutamine obtained thanks to the application of our cellular metabolomic approach in a representative experiment in which it was possible to measure flux through pyruvate dehydrogenase. Values are fluxes

Table 5
Effect of insulin on the metabolism of [2-¹³C]glucose in Wistar rat liver slices incubated between 24 and 48 h (¹³C NMR data)

Experimental condition	Metabolite removal (–) or production									
	2- ¹³ C-glucose	¹³ C-glucose	2- ¹³ C-glycogen	¹³ C-lactate	¹³ C-alanine	¹³ C-glutamate	¹³ C-glutamine	¹³ C-β-OH-butyrate	¹³ C-triglycerides	¹³ CO ₂
11 mM [2- ¹³ C] glucose	-2096 ±305	270 ±47	15 ±4	179 ±14	37 ±6	37 ±4	29 ±6	3 ±1	113 ±48	1373 ±195
11 mM [2- ¹³ C] glucose + 100 nM insulin	-2279 ±189*	320 ±41	37 ±6*	197 ±19	39 ±6	55 ±7	33 ±6	4 ±1	140 ±59	1399 ±90

Values, expressed in μmol of carbon 13 (g protein)⁻¹ 24 h⁻¹, are means ± SEM for five experiments. *P < 0.05. The corresponding enzymatic results are presented in Table 4. The ¹³C-pyruvate and ¹³C-acetoacetate, which are destroyed during the lyophilization procedure, were calculated from the ¹³C-lactate and ¹³C-β-OH-butyrate, respectively. They were taken into account to calculate the production of ¹³CO₂.

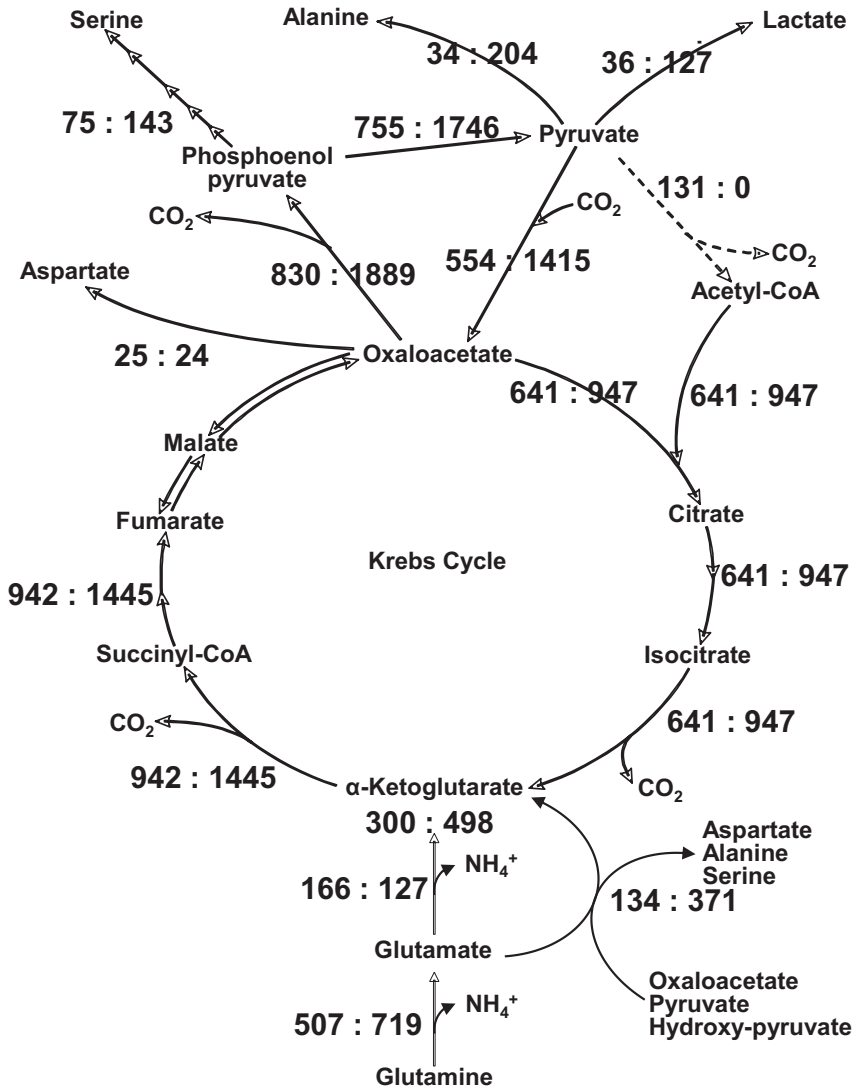


Fig. 6 Fluxes through the pathways of glutamine metabolism in human precision-cut renal cortical slices in the absence (*left*) and presence (*right*) of 1 mM valproate. Values are expressed in μmol/g tissue dry weight per 4 h

through the metabolic steps of glutamine metabolism in the absence (*left*) and presence (*right*) of 1 mM valproate. It can be seen that out of two ammoniagenic steps catalyzed by glutaminase and glutamate dehydrogenase, flux through the first but not through the second step was stimulated by valproate. Thus, it appears that glutaminase but not glutamate dehydrogenase is the target of valproate. In this experiment, the glutamate synthesized in greater amount by glutaminase was converted into α-ketoglutarate at increased rates not by a stimulation of flux through glutamate dehydrogenase but rather by a stimulation of fluxes through alanine aminotransferase and phosphoserine aminotransferase. Flux

through the tricarboxylic acid cycle (Krebs cycle) could also be measured revealing that flux from α -ketoglutarate to oxaloacetate was greatly stimulated. It should also be underlined that the cellular metabolomic approach revealed that glutamine metabolism is much more complex than previously thought. Indeed, it involves the futile cycle “oxaloacetate-phosphoenolpyruvate-pyruvate-oxaloacetate” catalyzed by phosphoenolpyruvate carboxykinase, pyruvate kinase, and pyruvate carboxylase; it is of interest that this cycle was greatly stimulated by valproate. It should also be emphasized that valproate completely inhibited flux through pyruvate dehydrogenase; this explains why valproate increased the production of lactate and alanine as a result of an increased availability of pyruvate. The latter inhibition is in line with our demonstration that valproate is metabolized by renal cells and accumulates as valproyl-coenzyme A that leads to a depletion of cellular levels of coenzyme A, a substrate of the pyruvate dehydrogenase reaction [35, 36].

This example clearly shows that cellular metabolomics allowed to better understand the mechanism of the hyperammonemic effect of valproate and represents a screening method for other valproate-related antiepileptics. Again, it is easy to understand that this approach can be used for detecting, understanding, and, if possible, preventing the nephrotoxicity of any xenobiotic (drug, drug candidate, chemical, metal).

4 Notes

1. The composition of Krebs-Henseleit buffer, that was gassed with 5% CO₂–95% O₂ for 20 min prior to utilization, was 118 mM NaCl, 4.7 mM KCl, 1.2 mM MgSO₄, 1.2 mM KH₂PO₄, 25 mM NaHCO₃, and 2.5 mM CaCl₂.
2. The composition of this medium was L-alanine 90 mg/L, L-arginine 50 mg/L, L-asparagine H₂O 20 mg/L, L-aspartic acid 20 mg/L, L-cysteine 30 mg/L, L-cystine 40 mg/L, L-glutamic acid 50 mg/L, glycine 50 mg/L, L-histidine 15 mg/L, L-isoleucine 15 mg/L, L-leucine 75 mg/L, L-lysine HCl 87.5 mg/L, L-methionine 15 mg/L, L-phenylalanine 25 mg/L, L-proline 30 mg/L, L-serine 10 mg/L, L-threonine 40 mg/L, L-tryptophan 10 mg/L, L-tyrosine 35 mg/L, L-valine 50 mg/L, D-glucose 2000 mg/L, ascorbic acid 2 mg/L, vitamin B12 (cobalamin) 0.2 mg/L, biotin 0.5 mg/L, choline chloride 1.5 mg/L, ergocalciferol 0.1 mg/L, folic acid 1 mg/L, L-inositol 2 mg/L, menadione sulfate 0.01 mg/L, pyridoxal hydrochloride (vitamin B6) 1 mg/L, riboflavin 0.1 mg/L, glutathione 0.05 mg/L, methyl linoleate 0.03 mg/L, phenol red 10 mg/L, sodium pyruvate 25 mg/L,

CaCl₂·2H₂O 264 mg/L, CuSO₄·5H₂O 0.0001 mg/L, Fe(NO₃)₃·9H₂O 0.001 mg/L, KCl 400 mg/L, MgSO₄·7H₂O 200 mg/L, MnCl₂·4H₂O 0.0001 mg/L, NaCl 6800 mg/L, NaHCO₃ 2200 mg/L, NaH₂PO₄·2H₂O 158 mg/L, and ZnSO₄·7H₂O 0.0002 mg/L.

3. Composition of the incubation media: We found useless to add fetal or newborn bovine serum to the Krebs-Henseleit medium or to the William's Medium E; this did not change the metabolism of the substrates used. Similarly, the addition of glutamax (the dipeptide alanylglutamine) did not improve the viability of the slices. In addition, both in liver and kidney slices, this dipeptide was rapidly hydrolyzed leading to the release and subsequent utilization of alanine and glutamine by the liver slices and of glutamine by the kidney slices. Therefore, the utilization of both alanine and glutamine was hardly evaluated with precision.
4. Oxygenation conditions: We found that 40% oxygen in the gas phase was sufficient to provide adequate amounts of oxygen to the slices during the 24–48-h incubation periods. When compared with the presence of 20% oxygen, this greatly decreased the lactic acid production from glucose but did not change the other characteristics of glucose metabolism. This allowed a good preservation of the slices whose metabolic functions were not improved with higher (up to 70%) oxygen percentages in the gas phase.

Acknowledgements

The authors would like to thank Claudie Pinteur, Rémi Nazaret, and Lara Koneckny for technical assistance as well as Claire Morel for secretarial assistance. This work was supported by grants from the European Commission [project numbers: BIO4-CT97-2145 (Euroslic) and STREP 032731 (CellNanoTox)], and from INSERM.

References

1. Warburg O (1923) Versuche an uberlebendem Carcinomgewebe. *Biochem Z* 142:317–333
2. Berry MN, Friend DS (1969) High-yield preparation of isolated rat liver parenchymal cells: a biochemical and fine structural study. *J Cell Biol* 43:506–520
3. Krumdieck CL, dos Santos JE, Ho KJ (1980) A new instrument for the rapid preparation of tissue slices. *Anal Biochem* 104:118–123
4. Hirsch GH (1976) Differential effects of nephrotoxic agents on renal transport and metabolism by use of in vitro techniques. *Environ Health Perspect* 15:89–99
5. Bach P, Lock E (1985) The use of renal tissue slices, perfusion and infusion techniques to assess nephrotoxicity related changes. In: Bach PH, Lock EA (eds) *Nephrotoxicity assessment and pathogenesis*, Monographs of applied toxicology, vol 1. Wiley, New York, pp 505–518

6. Berndt WO (1987) Renal slices and perfusion. In: Bach PH, Lock EA (eds) *Nephrotoxicity: the experimental and clinical situation*. Springer, Dordrecht, pp 301–316
7. Bach PH, Vickers AEM, Fisher R et al (1996) The use of tissue slices for pharmacotoxicology studies. *ATLA* 24:893–923
8. Parrish AR, Gandolfi AJ, Brendel K (1995) Precision-cut tissue slices: applications in pharmacology and toxicology. *Life Sci* 57:1887–1901
9. Lerche-Langrand C, Toutain HJ (2000) Precision-cut liver slices: characteristics and use for in vitro pharmaco-toxicology. *Toxicology* 153:221–253
10. Vickers AE, Fisher RL (2004) Organ slices for the evaluation of human drug toxicity. *Chem Biol Interact* 150:87–96
11. Vickers AE, Fisher RL (2005) Precision-cut organ slices to investigate target organ injury. *Expert Opin Drug Metab Toxicol* 1:687–699
12. De Graaf IAM, Groothuis GMM, Olinga P (2007) Precision-cut tissue slices as a tool to predict metabolism of novel drugs. *Expert Opin Drug Metab Toxicol* 3:879–898
13. Nicholson JK, Lindon JC, Holmes E (1999) ‘Metabonomics’: understanding the metabolic responses of living systems to pathophysiological stimuli via multivariate statistical analysis of biological NMR spectroscopic data. *Xenobiotica* 29:1181–1189
14. Lamprecht W, Trautchild I (1974) Adenosine-5'-triphosphate. Determination with hexokinase and glucose-6-phosphate dehydrogenase. In: Bergmeyer H (ed) *Methods of enzymatic analysis*, vol 4. Academic Press, New York, pp 2101–2110
15. Lowry OH, Rosebrough NJ, Farr AL, Randall RJ (1951) Protein measurement with the Folin phenol reagent. *J Biol Chem* 193:265–275
16. Bergmeyer HU, Bernt E (1974) Lactate dehydrogenase: UV assay with pyruvate and NADH. In: Bergmeyer H (ed) *Methods of enzymatic analysis*, vol 2. Academic Press, New York, pp 574–579
17. Baverel G, Bonnard M, D'Armagnac de Castanet E, Pellet M (1978) Lactate and pyruvate metabolism in isolated renal tubules of normal dogs. *Kidney Int* 14:567–575
18. Baverel G, Lund P (1979) A role for bicarbonate in the regulation of mammalian glutamine metabolism. *Biochem J* 184:599–606
19. Shaka AJ, Keeler J, Frenkiel T, Freeman R (1983) An improved sequence for broadband decoupling: Waltz 16. *J Magn Reson* 52:335–338
20. Howarth OW, Lilley DMJ (1978) Carbon-13-NMR of peptides and proteins. *Prog Nucl Magn Reson Spectrosc* 12:1–40
21. Canioni P, Alger JR, Shulman RG (1983) Natural abundance carbon-13 nuclear magnetic resonance spectroscopy of liver and adipose tissue of the living rat. *Biochemistry* 22:4974–4480
22. Martin G, Chauvin MF, Dugelay S, Baverel G (1994) Non-steady state model applicable to NMR studies for calculating flux rates in glycolysis, gluconeogenesis, and citric acid cycle. *J Biol Chem* 269:26034–26039
23. Martin G, Chauvin MF, Baverel G (1997) Model applicable to NMR studies for calculating flux rates in five cycles involved in glutamate metabolism. *J Biol Chem* 272:4717–4728
24. Dugelay S, Chauvin MF, Megnin-Chanet F et al (1999) Acetate stimulates flux through the tricarboxylic acid cycle in rabbit renal proximal tubules synthesizing glutamine from alanine: a ¹³C NMR study. *Biochem J* 342:555–566
25. Conjard A, Dugelay S, Chauvin MF, Durozard D, Baverel G, Martin G (2002) The anaplerotic substrate alanine stimulates acetate incorporation into glutamate and glutamine in rabbit kidney tubules. A ¹³C NMR study. *J Biol Chem* 277:29444–29454
26. Vincent N, Martin G, Baverel G (1992) Glycine, a new regulator of glutamine metabolism in isolated rat-liver cells. *Biochim Biophys Acta* 1175:13–20
27. Vercoutere B, Durozard D, Baverel G, Martin G (2004) Complexity of glutamine metabolism in kidney tubules from fed and fasted rats. *Biochem J* 378:485–495
28. Simon D, Penry JK (1975) Sodium di-N-propylacetate (DPA) in the treatment of epilepsy. A review. *Epilepsia* 16:549–573
29. Coulter DL, Allen RJ (1980) Secondary hyperammonaemia: a possible mechanism for valproate encephalopathy. *Lancet* 1:1310–1311
30. Powell-Jackson PR, Tredger JM, Williams R (1984) Hepatotoxicity to sodium valproate: a review. *Gut* 25:673–681
31. Warter JM, Marescaux C, Chabrier G, Rumbach L, Micheletti B, Imler M (1984) Renal glutamine metabolism in man during treatment with sodium valproate. *Rev Neurol (Paris)* 140:370–371
32. Ferrier B, Martin M, Baverel G (1988) Valproate-induced stimulation of renal ammonia production and excretion in the rat. *J Clin Chem Clin Biochem* 26:65–67
33. Elhamri M, Ferrier B, Martin M, Baverel G (1993) Effect of valproate, sodium 2-propyl-4-pentenoate and sodium 2-propyl-2-pentenoate on renal substrate uptake and ammoniogenesis in the rat. *J Pharmacol Exp Ther* 266:89–96

34. Vittorelli A, Gauthier C, Michoudet C, Martin G, Baverel G (2005) Characteristics of glutamine metabolism in human precision-cut kidney slices: a ^{13}C -NMR study. *Biochem J* 387:825–834
35. Durozard D, Baverel G (1987) Gas chromatographic method for the measurement of sodium valproate utilization by kidney tubules. *J Chromatogr* 414:460–464
36. Durozard D, Martin G, Baverel G (1991) Valproate-induced alterations of coenzyme A and coenzyme A ester concentrations in human kidney tubules metabolizing glutamine. *Contrib Nephrol* 92:103–108

Statistical Analysis of Quantitative RT-PCR Results

Richard Khan-Malek and Ying Wang

Abstract

Quantitative real-time reverse transcription polymerase chain reaction (RT-PCR) represents a benchmark technology in the detection and quantification of mRNA. Yet, accurate results cannot be realized without proper statistical analysis of RT-PCR data. Here we examine some of the issues concerning RT-PCR experiments that would benefit from rigorous statistical treatment including normalization, quantification, efficiency estimation, and sample size calculations. Examples are used to illustrate the methods.

Key words RT-PCR, Relative quantification, Statistical analysis

1 Introduction

Quantitative real-time reverse transcription polymerase chain reaction (RT-PCR) has become one of the most widely used approaches in the detection and quantification of mRNA [1]. Due to its high sensitivity, reproducibility, and wide dynamic range, RT-PCR is considered by many to be the “gold standard” for gene expression studies and it is commonly used for the validation of results from microarray experiments [2].

Both absolute quantification and relative quantification can be achieved in RT-PCR [3]. Absolute quantification determines precise copy numbers based on the construction of a standard curve with known copy numbers or concentrations. In relative quantification, gene expression is measured against a calibrator sample and expressed as an n -fold difference relative to the calibrator. In this chapter, we focus on relative quantification.

While there is an abundance of papers that discuss statistical analysis techniques for microarray data, there are notably less that present statistical methods for RT-PCR experiments. In this entry we examine key elements of RT-PCR data analysis that would benefit from rigorous statistical treatment, including selection of endogenous control genes, analysis of relative gene expression,

efficiency estimation, and sample size calculations. In each section an example is presented along with computational details. SAS [4] program code is provided for all of the examples.

2 Normalization

In a relative quantification RT-PCR experiment, a popular normalization method is to normalize the expression of a target gene against an endogenous control, or so-called housekeeping gene [5]. A fundamental assumption in the use of housekeeping genes is that the expression level of the gene remains constant across different experimental conditions. Selecting a candidate housekeeping gene from the literature might not satisfy this assumption, resulting in biased relative expression of the target genes and erroneous conclusions [6]. Therefore, we recommend that selection of a housekeeping gene be included as part of the experimental protocol.

Various methods for selecting a suitable housekeeping gene have been described in the literature. Vandesompele et al. [7] defined a gene-stability parameter M as the average pairwise variation of a particular gene with all other control genes. Genes with small values of M are considered to be the most stable. Pfaffl et al. [8] proposed calculating the pairwise correlation of all pairs of candidate genes. The highly correlated genes are combined into an index. Subsequently, the pairwise correlation between each gene and the index is calculated. Genes that correlate well with the index are considered suitable housekeeping genes. In accordance with methods described by Abruzzo et al. [9], Andersen et al. [10], and Szabo et al. [11], we illustrate the use of statistical modeling, along with *analysis of variance* (ANOVA), to select a housekeeping gene. ANOVA is a technique of partitioning the variability in a set of data into component parts.

Let Y_{ij} represent the threshold cycle (Ct) observed on the j th animal of the i th dose group. The observed response can be modeled as

$$Y_{ij} = \mu_i + e_{ij} \quad (1)$$

where μ_i denotes the mean of the i th treatment (dose group) and e_{ij} is the residual error.

An ANOVA table for the fixed-effects one-way model given in Eq. 1 is presented in Table 1 [12].

The ANOVA table for a one-way model partitions the total variance into two parts, between groups, due to *treatment* differences, and within groups, due to *error*, i.e.,

$$SS_{\text{TOTAL}} = SS_{\text{TREATMENT}} + SS_{\text{ERROR}}$$

Table 1
ANOVA table for fixed-effects one-way model

Source	Sum of squares	df	Mean square	F
Treatment (between)	$SS_{\text{TREATMENT}}$	$a - 1$	MST	MST/MSE
Error (within)	SS_{ERROR}	$N - a$	MSE	
Total	SS_{TOTAL}	$N - 1$		

a No. of treatments, N No. of animals

where $SS_{\text{TREATMENT}}$ is called the sum of squares due to treatments and SS_{ERROR} is called the sum of squares due to error. To make the sources of variability comparable, we divide each by their respective degrees of freedom (df) to obtain mean squares. The ratio of the mean squares yields an F -statistic, i.e., $F = \text{MST}/\text{MSE}$. Values of the F -statistic close to 1 indicate that the two sources of variability, between treatment and within treatment, are approximately equal.

A housekeeping gene that remains constant across different experimental conditions, or treatments, will have a small F -statistic compared to other genes. Thus, we define an optimum housekeeping gene based on a nonsignificant ($p > 0.05$), minimum F -statistic. If none of the genes yield a nonsignificant F -statistic, we advise that none is suitable for use as a housekeeping gene. In this case, other normalization methods, e.g., mean normalization [13], should be used instead.

Example. The ANOVA table for the HK001 data from Table 2 is given in Table 3, using the model given in Eq. 1.

Note that the F -statistic is 3.74. The F -statistics for both HK001 and HK002 are given in Table 4.

The minimum F -statistic is given by HK002, so this would be our choice for an optimum housekeeping gene. Alternately, one can use the geometric mean of several optimum genes as suggested by Vandesompele et al. [7].

A SAS program to select an optimum housekeeping gene based on a minimum F -statistic is provided in Appendix 1.

3 Statistical Analysis of Relative Quantification Data

Relative quantification of RT-PCR data is based on the expression ratio of a target gene versus a reference (housekeeping) gene. In this section we present two mathematical models used for the relative quantification of RT-PCR data, the $\Delta\Delta\text{Ct}$ model and the efficiency-corrected model. We then discuss the use of statistical modeling techniques to analyze the relative quantification data.

Table 2
Ct values for two potential reference genes, HK001 and HK002

Animal	Dose group	HK001	HK002
1	A	20.30	19.68
2	A	20.57	19.69
3	A	20.54	19.80
4	A	20.20	19.95
5	A	20.20	19.93
6	B	20.57	19.97
7	B	20.95	19.93
8	B	20.78	20.02
9	B	20.88	20.27
10	B	20.87	19.93
11	C	20.80	19.88
12	C	20.83	19.90
13	C	19.97	19.91
14	C	19.92	19.98
15	C	20.33	20.57
16	D	19.70	19.68
17	D	19.72	19.95
18	D	19.47	19.85
19	D	20.58	20.27
20	D	20.57	20.08
21	E	20.41	20.07
22	E	20.58	20.10
23	E	20.85	20.07
24	E	20.48	20.10
25	E	20.30	20.25

The $\Delta\Delta C_t$ model [5] assumes that the amplification efficiency for both the target and reference genes is 2 (indicating double the amount of PCR product in each cycle), and is given by the formula

$$\text{Ratio} = 2^{-\Delta\Delta C_t} \quad (2)$$

Table 3
ANOVA table for HK001 data

Source	Sum of squares	df	Mean square	<i>F</i>
Dose group (between)	1.6919	4	0.4230	3.74
Error (within)	2.2633	20	0.1132	
Total	3.9552	24		

Table 4
F-statistics for HK001 and HK002 data

Gene	<i>F</i> -statistic
HK001	3.74
HK002	1.88

where $\Delta\Delta Ct = \Delta Ct_{\text{TREATED}} - \Delta Ct_{\text{CONTROL}}$, $\Delta Ct_{\text{TREATED}}$ is the Ct difference of a reference and target gene for a treated sample (i.e., $\Delta Ct_{\text{TREATED}} = Ct_{\text{TARGET}} - Ct_{\text{REF}}$), and $\Delta Ct_{\text{CONTROL}}$ is the Ct difference of a reference and target gene for a control sample (i.e., $\Delta Ct_{\text{CONTROL}} = Ct_{\text{TARGET}} - Ct_{\text{REF}}$).

The efficiency-corrected model [14], which is a more general form of the $\Delta\Delta Ct$ model, is given by

$$\text{Ratio} = \frac{(E_{\text{TARGET}})^{\Delta Ct_{\text{TARGET}}}}{(E_{\text{REF}})^{\Delta Ct_{\text{REF}}}} \quad (3)$$

where E_{TARGET} is the target amplification efficiency, E_{REF} is the reference amplification efficiency, $\Delta Ct_{\text{TARGET}}$ is the Ct difference of a treated and control sample for the target gene (i.e., $\Delta Ct_{\text{TARGET}} = Ct_{\text{CONTROL}} - Ct_{\text{TREATED}}$), and ΔCt_{REF} is the Ct difference of a treated and control sample for the reference gene (i.e., $\Delta Ct_{\text{REF}} = Ct_{\text{CONTROL}} - Ct_{\text{TREATED}}$). The assessment of PCR efficiency is discussed in the next section.

One of the “early” references on the statistical analysis of relative expression data was Pfaffl et al. [15]. They introduced a software tool (REST[®]) which used the efficiency-corrected model to compute relative expression results; the expression results were then tested for significance using a randomization test. Fu et al. [16] proposed calculating the relative expression, $\Delta\Delta Ct$, using a generalized estimation equations (GEE) model. Following Yuan et al. [17], we discuss the use of analysis of variance (ANOVA) using the $\Delta\Delta Ct$ approach.

Table 5
Estimates of $\Delta\Delta Ct$ and fold change

Gene	$\Delta\Delta Ct$	SE	Ratio
TG001	-0.573	0.441	1.49
TG002	-2.508*	0.794	5.69

*Statistically significant with $p \leq 0.05$

Consider a simple experiment the objective of which is to determine the gene expression across a single factor, treatment. First, ΔCt values are calculated by subtracting the Ct value of the reference gene for a given sample (or the mean value for a given sample, if mean normalization is used instead) from the Ct value of the target gene for the given sample. Let Y_{ij} represent the ΔCt value observed on the j th animal and i th treatment (control or treated). The observed response can be modeled as

$$Y_{ij} = \mu_i + e_{ij} \tag{4}$$

where μ_i denotes the mean of the i th treatment and e_{ij} is the residual error. $\Delta\Delta Ct$ is given by the difference in treatment means.

Example. Table 5 provides estimates of the $\Delta\Delta Ct$ and its standard error for the data is given in Table 6, using the model given in Eq. 4. Technical replicates within animal (biological replicates) were averaged to increase precision. Target genes were normalized to the reference gene HK002. A significant treatment effect is indicated by $p \leq 0.05$.

A SAS program to perform $\Delta\Delta Ct$ analysis using ANOVA methodology is provided in Appendix 2.

For an amplification efficiency of less than 2, the efficiency-corrected model can be used, but to facilitate the statistical analysis we must first rewrite Eq. 3. Given that for all positive values of x , if $x = a^y$, then $y = \log_a(x)$, we proceed as follows:

$$\text{Ratio} = \frac{(E_{\text{TARGET}})^{\Delta Ct_{\text{TARGET}}}}{(E_{\text{REF}})^{\Delta Ct_{\text{REF}}}} = \frac{2^{EA_{\text{TARGET}}(\Delta Ct_{\text{TARGET}})}}{2^{EA_{\text{REF}}(\Delta Ct_{\text{REF}})}} = 2^{EA_{\text{TARGET}}(\Delta Ct_{\text{TARGET}}) - EA_{\text{REF}}(\Delta Ct_{\text{REF}})} \tag{5}$$

where we define EA as the ‘‘efficiency adjustment’’ given by $EA = \log_2(\text{efficiency})$.

Example. Let’s revisit the data given in Table 6 using Eq. 5 assuming that the efficiency of the reference gene (HK002) was only 1.85. For an efficiency of 1.85, the $EA = \log_2(1.85) = 0.8875$ (note: for efficiencies of 2, the $EA = 1$). Using TG001 as the target gene, the fold change is

$$\text{Ratio} = \frac{2^{1(0.375)}}{2^{0.8875(-0.1983)}} = \frac{2^{(0.375)}}{2^{(-0.176)}} = 2^{(0.551)} = 1.465.$$

Table 6
Ct values for two target genes (TG001 and TG002) and reference gene (HK002)

Animal	Treatment	TG001	TG002	HK002
1	Control	23.22	29.08	19.68
1	Control	23.34	29.04	19.69
1	Control	23.12	29.39	19.80
2	Control	24.06	28.23	19.95
2	Control	24.15	28.01	19.93
2	Control	24.15	28.12	19.97
3	Control	23.18	28.79	19.93
3	Control	23.13	28.43	20.02
3	Control	23.10	28.49	20.27
4	Control	24.78	31.37	19.93
4	Control	24.45	30.74	19.88
4	Control	24.67	31.09	19.90
5	Treated	23.11	27.11	20.61
5	Treated	22.99	27.24	19.98
5	Treated	23.10	27.37	20.57
6	Treated	22.77	25.52	19.68
6	Treated	22.99	25.72	19.95
6	Treated	23.06	25.52	19.85
7	Treated	23.73	27.43	20.27
7	Treated	24.01	26.73	20.08
7	Treated	23.80	26.65	20.07
8	Treated	23.73	27.96	20.10
8	Treated	23.83	27.84	20.07
8	Treated	23.73	27.98	20.10

4 Amplification Efficiency

If the assumptions behind the $\Delta\Delta C_t$ method are not valid, the efficiency-corrected model can be employed instead, in which case estimates of the amplification efficiencies are needed for the reference gene and any gene of interest (GOI). Common approaches used to assess PCR efficiency are the relative standard curve method as well as methods based on amplification kinetics.

The relative standard curve method requires running serial dilutions of cDNA for the reference gene and each GOI. Ct is then plotted against base 10 logarithm of cDNA and the PCR efficiency is calculated according to the relationship $E = 10^{(-1/\text{slope})}$ [14, 18].

There are a variety of methods based on amplification kinetics. A number of authors have suggested fitting a linear model to the log-linear portion of an amplification curve as a means of estimating efficiency [19, 20]. Others have suggested fitting multiple models to the exponential portion of the amplification curve [21, 22] or modeling the amplification curve using sigmoidal or other models [23–25]. Here we present the linear model method and the method of Khan-Malek.

The linear model method fits a linear regression line to the points in the log-linear (base 10 logarithm) phase of the PCR amplification curve. The PCR efficiency is calculated according to the relationship $E = 10^{(\text{slope})}$. Figure 1 illustrates the linear model method using three points around the midpoint of the log-linear phase.

For these data the fitted linear model yielded a $R^2 > 0.99$ and slope of 0.285 giving an efficiency estimate of $E = 10^{(0.285)} = 1.93$.

Instead of modeling the raw amplification curve, Khan-Malek fits a four-parameter logistic model of the form

$$f(x) = a + \frac{b}{1 + \exp(c - x) / d} \quad (6)$$

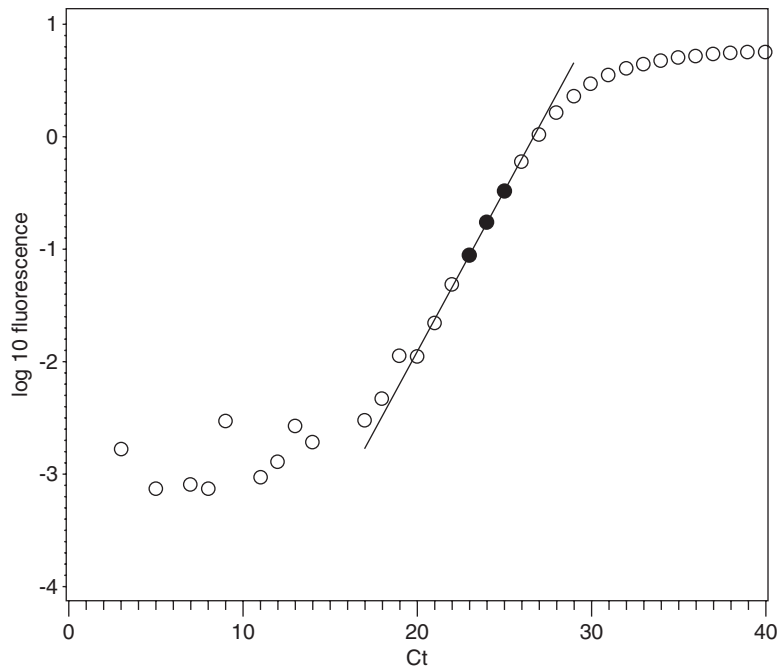


Fig. 1 Illustration of fitting a linear model to the log-linear portion of an amplification curve

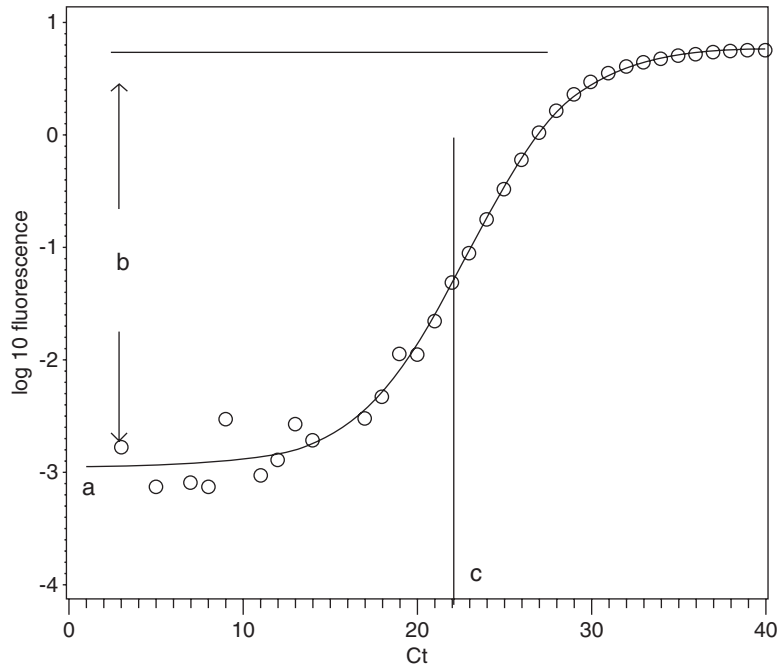


Fig. 2 Illustration of fitting a four-parameter logistic model to the log10 transformed fluorescence curve

to the log 10 transformed amplification curve. Here $f(x)$ is the observed log 10 fluorescence at cycle x , a is the lower asymptote, b is the difference between the lower and upper asymptote, c is a location parameter halfway between a and b , and d is a parameter relating to the slope; c , as a rule, falls in the middle of the log-linear phase (see Fig. 2).

The parameters of the model given in Eq. 6 are solved using nonlinear regression. Substituting the parameter estimates into the first derivative of Eq. 6 at $x = c$ gives the slope of the tangent line of the function at c . The benefits of this approach are twofold: first, the resulting efficiencies can be directly compared with “true PCR efficiency” although efficiencies can sometimes exceed the theoretical maximum of 2, depending on model fit; second, this approach is easily programmable and can be used for high-throughput screening with minimum user input. If the log10 transformed amplification curve lacks sufficient points in the lower and/or upper plateaus to permit modeling, the linear model method is recommended.

Example. Table 7 gives the parameter estimates of the four-parameter logistic model, fit to the data in Fig. 2.

If we substitute these estimates into the first derivative of Eq. 6, given by

$$f'(x) = (b / d) \frac{\exp(c - x) / d}{1 + 2 \exp(c - x) / d + \exp 2(c - x) / d} \quad (7)$$

Table 7
Parameter estimates of four-parameter logistic model

Parameter	Estimate
a	-2.9516
b	3.7290
c	22.8162
d	3.0980

and solve for $x = 22.8162$, it yields a slope of 0.3009 giving an efficiency estimate of $E = 10^{(0.3009)} = 1.99$.

A SAS program to perform the four-parameter logistic model fit is provided in Appendix 3.

5 Power and Sample Size

Statistically speaking, *power* is the probability of rejecting the null hypothesis (H_0) when the alternative hypothesis (H_1) is valid. In other words, it is the probability of detecting a difference or treatment effect if one truly exists. Power is dependent on the sample size, significance criterion (α -level), effect size, and sample standard deviation. Accordingly, prospective sample size calculations are important in the planning of an experiment as insufficient power may render any conclusions from an experiment as useless.

For simple comparative experiments comparing two treatment groups, power can be estimated using a two-sample *t*-test assuming normal populations and equal variances. In Fig. 3, the normal curve on the left represents a sampling distribution of no treatment effect ($H_0: \mu_1 - \mu_2 = 0$) whereas the normal curve on the right represents an alternate sampling distribution of an effect ($H_1: \mu_1 - \mu_2 = \delta$). The critical value c determines the point where H_0 is rejected. The power of the test is the area under the alternative curve beyond c . Notice that moving the alternative curve to the right increases the distance between the null and alternative hypothesis and thus increases the power.

Example. Suppose the objective is to determine the number of animals needed to achieve a power of at least 0.80 to detect a group mean difference of say $\delta = 1.0$ between treated and control Ct values. Based on historical data, you hypothesize that the common group standard deviation is between 0.40 and 0.50. The results for these parameters are given in Table 8 for an α -level of 0.05 (two-tailed).

A SAS program to perform the sample size calculations is provided in Appendix 4.

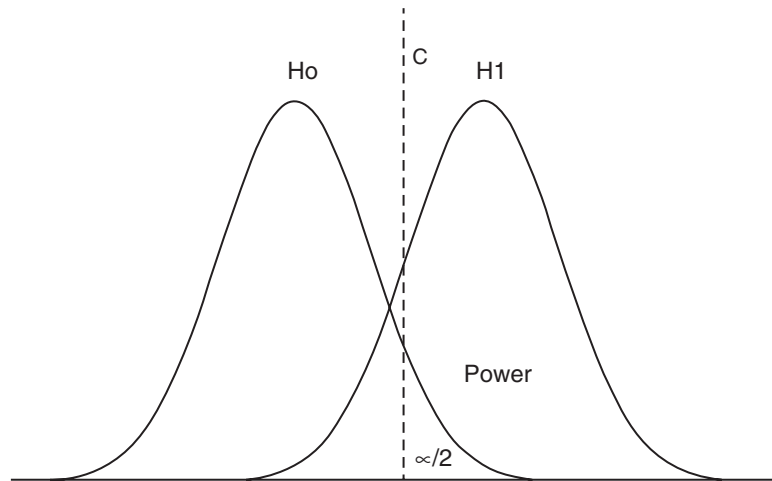


Fig. 3 Illustration of the two-sample *t*-test (two-tailed) with equal variances under the null and alternative hypotheses

Table 8
Sample size analysis

δ	SD	<i>n</i> (per group)
1.0	0.40	4
1.0	0.45	5
1.0	0.50	6

Appendix 1

SAS code to select an optimum housekeeping gene based on a minimum *F*-statistic.

```
data table2;
input ain dose$ gene$ Ct;
cards;
1 A HK001 20.30
2 A HK001 20.57
3 A HK001 20.54
4 A HK001 20.20
5 A HK001 20.20
.
Some data omitted for brevity
.
```

```

23 E HK002 20.07
24 E HK002 20.10
25 E HK002 20.25
;
proc sort;
  by gene;
  run;
ods listing close;
ods output OverallANOVA=ANOVA;
proc glm;
  by gene;
  class dose;
  model Ct=dose;
  run;
ods listing;
data ANOVA; set ANOVA;
  if Source="Model";
proc print;
  var gene FValue;
  run;

```

Appendix 2

SAS code to perform the relative quantification analysis using ANOVA methodology.

```

data table5;
input Animal Treatment $ TG001 TG002 HK002;
cards;
1 Control 23.22 29.08 19.68
1 Control 23.34 29.04 19.69
1 Control 23.12 29.39 19.80
2 Control 24.06 28.23 19.95
2 Control 24.15 28.01 19.93
2 Control 24.15 28.12 19.97
.
Some data omitted for brevity
.
7 Treated 23.73 27.43 20.27
7 Treated 24.01 26.73 20.08

```

```

7 Treated 23.80 26.65 20.07
8 Treated 23.73 27.96 20.10
8 Treated 23.83 27.84 20.07
8 Treated 23.73 27.98 20.10
;
proc summary nway;      *~~~ Take mean of
technical replicates ~~~*;
  class Animal Treatment;
  var TG001 TG002 HK002;
  output out=mean(drop=_type_ _freq_) mean=;
run;
data mean; set mean;
  deltaCt_TG001=TG001-HK002;
  deltaCt_TG002=TG002-HK002;
run;
*%let var=deltaCt_TG001;
%let var=deltaCt_TG002;
ods listing closed;
proc mixed data=mean;
  class treatment;
  model &var=treatment;
  estimate "&var" treatment -1 1 / e;
  ods output estimates=estimates;
run;
ods listing;
data estimates; set estimates;
  FoldChange=2**-(estimate);
proc print; run;

```

Appendix 3

SAS code to perform the four parameter logistic model fit.

```

data raw_curve;
input x FL;
cards;
1 -0.00576
2 -0.00568
3 0.00166
.

```

```

        Some data omitted for brevity
        .
        48 5.91043
        49 5.95599
        50 5.90091
        ;
        data log_curve; set raw_curve;
            logFL=log10(FL);      * <==== notice
log10 ;
        ods listing close;
        proc nlin method=newton;
            parms a=-10 to 0 by 1
                b=0 to 5 by 1
                c=25 to 30 by 1
                d=1 to 3 by 1;
            model logFL = a + b / (1+exp((c-x)/d));
            ods output parameterestimates=pe(keep=parameter estimate);
            output out=out p=p;
            run;
        ods listing;
        proc transpose data=pe
out=est(rename=(coll1=a coll2=b coll3=c coll4=d));
            var estimate;
            run;
        data est; set est;
            x=c;
            slope=(b/d)*exp((c-x)/d)/((1+2*exp((c-x)/d))+exp(2*(c-x)/d));
            E=10**slope;
            run;
        proc print data=est;
            run;

```

Appendix 4

SAS code to perform the sample size calculations.

```

proc power;
    twosamplemeans
    meandiff = 1

```



```

stddev = 0.40 0.45 0.50
power = 0.8
npergroup =.;
run;

```

References

- Walker NJ (2002) Tech.Sight. A technique whose time has come. *Science* 296:557–579
- Wang Y, Barbacioru C, Hyland F, Xiao W, Hunkapiller KL, Blake J, Chan F, Gonzalez C, Zhang L, Samaha R (2006) Large scale real-time PCR validation on gene expression measurements from two commercial long-oligonucleotide microarrays. *BMC Genomics* 7:59
- Wong ML, Medrano JF (2005) Real-time PCR for mRNA quantitation. *BioTechniques* 39:75–85
- SAS Institute Inc (2004) SAS/STAT® 9.1 user's guide. SAS Institute Inc, Cary, NC
- Livak KJ, Schmittgen TD (2001) Analysis of relative gene expression data using real-time quantitative PCR and the $2^{-\Delta\Delta CT}$ method. *Methods* 25:402–408
- Huggett J, Dheda K, Bustin S, Zumla A (2005) Real-time RT-PCR normalisation; strategies and considerations. *Genes Immun* 6(4): 279–284
- Vandesompele J, De Preter K, Pattyn F, Poppe B, Van Roy N, De Paepe A, Speleman F (2002) Accurate normalization of real-time quantitative RT-PCR data by geometric averaging of multiple internal control genes. *Genome Biol* 3(7):RESEARCH0034
- Pfaffl MW, Tichopad A, Prgomet C, Neuvians TP (2004) Determination of stable housekeeping genes, differentially regulated target genes and sample integrity: bestKeeper-Excel-based tool using pair-wise correlations. *Biotechnol Lett* 26:509–515
- Abruzzo LV, Lee KY, Fuller A, Silverman A, Keating MJ, Medeiros LJ, Coombes KR (2005) Validation of oligonucleotide microarray data using microfluidic low-density arrays: a new statistical method to normalize real-time RT-PCR data. *BioTechniques* 38:785–792
- Andersen CL, Jensen JL, Orntoft TF (2004) Normalization of real-time quantitative reverse transcription-PCR data: a model-based variance estimation approach to identify genes suited for normalization, applied to bladder and colon cancer data sets. *Cancer Res* 64:5245–5250
- Szabo A, Perou CM, Karaca M, Perreard L, Quackenbush JF, Bernard PS (2004) Statistical modeling for selecting housekeeper genes. *Genome Biol* 5:R59
- Dean A, Voss D (1999) Design and analysis of experiments. Springer, New York
- Mestdagh P, Van Vlierberghe P, De Weer A, Muth D, Westermann F, Speleman F, Vandesompele J (2009) A novel and universal method for microRNA RT-qPCR data normalization. *Genome Biol* 10:64–74. doi:10.1186/gb-2009-10-6-r64
- Pfaffl MW (2001) A new mathematical model for relative quantification in real-time RT-PCR. *Nucleic Acids Res* 29(9):e45
- Pfaffl MW, Horgan GW, Dempfle L (2002) Relative expression software tool (REST©) for group-wise comparison and statistical analysis of relative expression results in real-time PCR. *Nucleic Acids Res* 30:e36
- Fu WJ, Hu J, Spencer T, Carroll R, Wu G (2006) Statistical models in assessing fold change of gene expression in real-time RT-PCR experiments. *Comput Biol Chem* 30:21–26
- Yuan JS, Reed A, Chen F, Stewart CN (2006) Statistical analysis of real-time PCR data. *BMC Bioinf* 7:85
- Applied Biosystems (2006) Amplification Efficiency of TaqMan® Gene Expression Assays: Application Note
- Peirson SN, Butler JN, Foster RG (2003) Experimental validation of novel and conventional approaches to quantitative real-time PCR data analysis. *Nucleic Acids Res* 31:e73
- Ramakers C, Ruijter JM, Deprez RH, Moorman AF (2003) Assumption-free analysis of quantitative real-time polymerase chain reaction (PCR) data. *Neurosci Lett* 339(1):62–66
- Tichopad A, Dilger M, Schwarz G, Pfaffl MW (2003) Standardized determination of real-time PCR efficiency from a single reaction setup. *Nucleic Acids Res* 31:e122
- Zhao S, Fernald D (2005) Comprehensive algorithm for quantitative real-time polymerase chain reaction. *J Comput Biol* 12(8): 1047–1064

23. Liu W, Saint D (2002) Validation of a quantitative method for real time PCR kinetics. *Biochem Biophys Res Commun* 294(2): 347–353
24. Tichopad A, Dzidic A, Pfaffl MW (2002) Improving quantitative real-time RT-PCR reproducibility by boosting primer-linked amplification efficiency. *Biotechnol Lett* 24(24):2053–2056
25. Rutledge RG (2004) Sigmoidal curve-fitting redefines quantitative real-time PCR with the prospective of developing automated high-throughput applications. *Nucleic Acids Res* 32(22):e178

Evaluation of Mitochondrial Respiration in Cultured Rat Hepatocytes

Jean-Pierre Marchandeu and Gilles Labbe

Abstract

Mitochondrial dysfunction is a major mechanism whereby drugs can induce liver injury and other serious side effects, such as lactic acidosis and rhabdomyolysis, in some patients. Several *in vitro* and *in vivo* investigations can be performed in order to determine if drugs can disturb mitochondrial fatty acid oxidation (FAO) and the oxidative phosphorylation (OXPHOS) process, deplete hepatic mitochondrial DNA (mtDNA), or trigger the opening of the mitochondrial permeability transition pore (MPT). Among these investigations, mitochondrial respiration is a relatively easy test to measure the potential toxicity of a drug. The use of cells instead of isolated mitochondria allows one to test the toxic effect of a parent compound and its metabolites. The use of rat hepatocytes can detect drugs involved in drug-induced liver injuries (DILI). The method consists in measuring oxygen consumption by using a Clark electrode in a chamber containing a suspension of hepatocytes preincubated with drug.

Key words Mitochondrial respiration, Oxygen consumption, Clark electrode, Respirometer, Primary rat hepatocytes

1 Introduction

Drug-induced liver injury (DILI) is a major issue for pharmaceutical companies, as it is considered one of the frequent causes for the failure of a drug during the premarketing phase and for the withdrawal of a marketed medicine.

Although drugs can cause hepatotoxicity through different mechanisms [1], mitochondrial dysfunction is one such major mechanism of DILI [2]. By hampering mitochondrial energy production and/or releasing mitochondrial pro-apoptotic proteins into the cytoplasm, drugs can trigger necrosis or apoptosis of hepatocytes, thus causing “cytolytic” hepatitis, which can evolve toward liver failure. Drug-induced mitochondrial dysfunction can also lead to steatosis and steatohepatitis, which can sometimes progress to cirrhosis [2–4]. In addition, drug-induced mitochondrial dysfunction can also trigger diverse extrahepatic or

general manifestations, such as hyperlactatemia, lactic acidosis, myopathy, rhabdomyolysis, pancreatitis, peripheral neuropathy, or lipoatrophy [5–7]. Thus, because of its potential severity for patients, drug-induced mitochondrial dysfunction should be detected during the preclinical safety studies.

Mitochondria are able to oxidize many metabolites including fatty acids, pyruvate (generated from glycolysis), and several amino acids such as valine, leucine, and methionine [3, 8, 9]. During the fasting state, fatty acid oxidation (FAO) in the liver is incomplete; the acetyl-CoA that is generated is not oxidized in the liver, but condenses into ketone bodies (mainly acetoacetate and β -hydroxybutyrate), which are released into the plasma for subsequent oxidation in extrahepatic tissues. In the kidney, heart, and brain, the ketone bodies are then cleaved into acetyl-CoA, which is oxidized through the tricarboxylic acid cycle [3, 8].

The intramitochondrial oxidation of fatty acids, pyruvate, and amino acids generates reducing “equivalents” (FADH_2 and NADH), which must be reoxidized by the mitochondrial respiratory chain (MRC) in order to regenerate the FAD and NAD^+ that are needed for the oxidative processes such as FAO, pyruvate dehydrogenation, and activity of the tricarboxylic acid cycle. In addition to regenerating FAD and NAD^+ , the MRC also creates a large electrochemical gradient across the inner mitochondrial membrane, the so-called mitochondrial transmembrane potential, or $\Delta\psi_m$. Indeed, the transfer of electrons along the different components of the MRC (for instance, complexes I, III, and IV when electrons come from NADH) is associated with the ejection of protons from the mitochondrial matrix to the intermembrane space, thus raising the $\Delta\psi_m$. The $\Delta\psi_m$ serves as a reservoir of potential energy. When cells need energy, the rise in ADP levels within the mitochondria induces the reentry of protons into the mitochondrial matrix through the membrane-spanning F_0 portion of the ATP synthase complex (also referred to as the complex V of the MRC). This reentry of protons partially dissipates the $\Delta\psi_m$, thus liberating energy, which is used by the F_1 portion of ATP synthase to phosphorylate ADP into ATP. Concomitantly, the transient decrease in $\Delta\psi_m$ unleashes the flow of electrons in the respiratory chain and increases mitochondrial respiration to restore the $\Delta\psi_m$. Hence, there is a tight coupling within the mitochondria between ATP consumption, mitochondrial respiration, and ATP synthesis [5, 9]. A major dysfunction of this oxidative phosphorylation (OXPHOS) process can hinder cell metabolism and cellular function in the liver and elsewhere [2, 10].

Several *in vitro* assays can be used in order to detect drug-induced mitochondrial dysfunction either on hepatic cells or on isolated liver mitochondria. The mitochondrial respiration method will be described using primary rat hepatocyte cultures.

2 Materials

2.1 Anesthetic Used

Ketamine/xylazine mixture: Imalgene 1000/Rompun 2%™, 1.25/0.25 mL/kg, respectively, intraperitoneally.

2.2 Cell Preparation and Cell Culture

1. Culture medium (William's E with Glutamax, Invitrogen Life Science).
2. Fetal calf serum (Invitrogen Life Science).
3. Perfusion medium (Invitrogen Life Science).
4. Digestion medium (Invitrogen Life Science).
5. Wash medium (Invitrogen Life Science).
6. Insulin/transferrin/selenium (ITS) (Invitrogen Life Science) is stored at +4 °C.
7. Penicillin/streptomycin mixture (10,000 units/mL of penicillin and 10,000 µg/mL of streptomycin, Sigma) is stored in aliquot fractions of 10 mL at -20 °C.
8. Dexamethasone (Sigma) aliquots of 5 mL (1 µg/mL) are stored at -20 °C.
9. Phosphate-buffered saline (PBS) (Invitrogen Life Science).
10. Six-well plates coated with collagen I cellware (Biocoat cell environments, Becton Dickinson).

2.3 Respiration System

1. Oxytherm respirometer (Hansatek).
2. Clark electrodes.
3. Computer (HP Personal Computer).
4. Oxygraph Plus software (Hansatek).

2.4 Hepatocyte Viability, Cell Count

1. Inverted microscope (Axiovert 40C, Karl Zeiss).
2. Trypan blue (VWR).
3. Malassez hematimeter.

2.5 Cytotoxicity Study

1. LDH-cytotoxicity assay Kit II, lactate dehydrogenase (Biovision®, Roche).
2. CellTiter-Glo® Luminescent Cell Viability Assay (Promega).
Materials to be supplied by the user:
 - (a) Opaque-walled multiwell plates adequate for cell culture.
 - (b) Multichannel pipette or automated pipetting station for delivery of reagent.
 - (c) Device (plate shaker) for mixing multiwell plates.
 - (d) Luminometer.
3. Spectramax M5 spectrophotometer (Molecular Devices).

2.6 Trypsinization

1. Trypsin 25% EDTA 1X (Gibco).
2. Deionized water.

2.7 Experiment Solutions

1. Attachment medium: To William's E Glutamax, add fetal calf serum (final concentration 5%), penicillin/streptomycin (final concentration 100 UI/mL and 100 µg/mL, respectively), dexamethasone (final concentration 1% in PBS), and ITS (5 mL of the commercial solution 100×).
2. Culture medium: To William's E Glutamax, add penicillin/streptomycin (final concentration 100 UI/mL and 100 µg/mL, respectively), dexamethasone (final concentration 1% in PBS), and ITS (5 mL of the commercial solution 100X).
3. Respiration medium:
Mix 85.58 g of sucrose, 0.27 g of KH_2PO_4 , 2.38 g of HEPES, and 0.19 g of EGTA in 800 mL deionized water. Adjust to pH 7.4 with 1 N NaOH. Complete to 1000 mL with deionized water. Slowly add 0.7 g of BSA while stirring gently to avoid foam [11]. Store at +4 °C.

3 Methods**3.1 Cell Preparation (Protocol Is Approved by Local Ethical Committee)**

1. An adult male Sprague-Dawley rat (200–300 g) is anesthetized with a mixture of ketamine/xylazine.
2. Abdomen is washed with 70% ethanol.
3. When the animal is anesthetized, a ventral midline incision is made from xiphisternum to pubic bone, and hepatic portal vein and vena cava inferior are exposed.
4. A loose ligature is placed around the portal vein. Vena cava inferior is clamped. Portal vein is catheterized and ligature is tightened.
5. The catheter is then attached to the perfusion tubing containing perfusion medium. Vena cava superior is cut.
6. The liver is perfused with 100 mL of perfusion medium at a flow rate of 20 mL/min.
7. Liver is then perfused with 200–500 mL of perfusion medium containing collagenase until it is considered to be sufficiently digested.
8. After dissection, the liver is transferred into a sterile dish containing 30 mL of digestion medium prewarmed at 37 °C. The digested liver is gently teased with a sterile fork to dissociate cells from connective tissue.
9. The cell suspension is filled up to 50 mL with wash medium at +4 °C and is filtered through a 60 µm nylon sterilized filter.

10. The cell suspension is then centrifuged for 5 min at $50 \times g$.
11. The supernatant is aspirated, 25 mL of wash medium at $+4^\circ\text{C}$ is added, and the cell suspension is centrifuged for 5 min at $50 \times g$. This procedure is repeated twice.
12. After the last washing step, the wash medium is replaced by attachment medium at 37°C (from 10 to 20 mL, depending on the pellet size).
13. Viability is determined with trypan blue exclusion using Malassez hematimeter.

3.2 Cell Culture

1. Rat hepatocytes are seeded and incubated for 24 h for attachment in collagen-coated, 6-well plates in a humidified atmosphere containing 5% CO_2 and 95% air at 37°C . Cell density at the time of seeding is 1.5 million cells per well containing 1.5 mL of culture medium.
2. After the attachment period, the culture medium is removed and replaced by the treatment medium containing control articles or different concentrations of test articles.
3. The hepatocytes are then incubated for 24 h in a humidified atmosphere containing 5% CO_2 and 95% air at 37°C .

3.3 Cytotoxicity Study

1. LDH-Cytotoxicity Assay Kit II
Cell death or cytotoxicity is classically evaluated by the quantification of plasma membrane damage. Lactate dehydrogenase (LDH) is a stable enzyme, present in all cell types, and rapidly released into the cell culture medium upon damage of the plasma membrane. LDH Cytotoxicity Assay Kit II utilizes the advanced WST reagent for a fast and more sensitive detection of LDH released from damaged cells. The assay utilizes an enzymatic coupling reaction: LDH oxidizes lactate to generate NADH, which then reacts with WST to generate yellow color. The intensity of the generated color correlates directly with the number of cells lysed. Since WST is brighter, less amount of culture medium is required for the assay, and thus the background from serum and culture medium is significantly reduced. Using the LDH assay, cells can be cultured in regular 10% serum containing medium. There is no requirement for reducing serum or special medium. In addition, since the WST is more stable, the reaction can be read multiple times, and can also be stopped at any time point during the reaction. LDH activity can be easily quantified by spectrophotometer or plate reader at OD450 nm [12].

(a) Prepare the working solutions before start:

- Reconstitute the WST Substrate Mix in 1 mL ddH₂O for 10 min and mix thoroughly. The solution is stable for 2 months at 4°C .

- Preparation of LDH Reaction Mix: For 100 assays, mix 200 μL of WST Substrate Mix with 10.0 mL of LDH Assay Buffer. The LDH Reaction Mix should be stable for several weeks at 4 $^{\circ}\text{C}$.
- (b) Collect cells and wash once with fresh regular culture medium, and then seed 100 μL cells (with $2\text{--}10 \times 10^4$ cells) in a 96-well plate as follows:
- Background Control:* 100 μL culture medium per well in triplicates with no cells. The background control will measure reagents and LDH background from culture medium serum. The background value has to be subtracted from all other values.
- Low Control:* 100 μL cells in triplicate wells.
- High Control:* 100 μL cells in triplicates; add 10 μL cell lysis solution in each well, and mix. To adjust the increase of medium volume, 11 μL of the medium may be used in LDH activity assay at **step 4**.
- Test Sample:* 100 μL cells in triplicates; add test substances in each well, and mix.
- (c) Incubate cells in an incubator (5% CO_2 , 90% humidity, 37 $^{\circ}\text{C}$) for the appropriate time of treatment determined for test substance. Gently shake the plate at the end of the incubation to ensure that LDH is evenly distributed in the culture medium.
- (d) Centrifuge cells at $600 \times g$ for 10 min to precipitate the cells.
- (e) Transfer the clear medium solution (10 μL /well) into an optically clear 96-well plate.
- (f) Add 100 μL LDH Reaction Mix to each well, mix, and incubate for 30 min at room temperature.
- (g) Measure the absorbance of all controls and samples with a plate reader equipped with 450 nm (440–490 nm) filter. The reference wavelength should be 650 nm.
- (h) Calculation of the Percentage Cytotoxicity:

$$\text{Cytotoxicity (\%)} = \frac{(\text{Test sample} - \text{low control})}{(\text{high control} - \text{low control})} \times 100.$$

2. CellTiter-Glo[®] Luminescent Cell Viability Assay

The CellTiter-Glo[®] Luminescent Cell Viability Assay is a homogeneous method for determining the number of viable cells in culture based on quantitation of the ATP present, which signals the presence of metabolically active cells. The homogeneous assay procedure involves addition of a single reagent (CellTiter-Glo[®] Reagent) directly to cells cultured in serum-supplemented

medium. Cell washing, removal of medium, or multiple pipetting steps are not required. The homogeneous “add-mix-measure” format results in cell lysis and generation of a luminescent signal proportional to the amount of ATP present. The amount of ATP is directly proportional to the number of cells present in culture. The CellTiter-Glo® Assay relies on the properties of a proprietary thermostable luciferase (Ultra-Glo™ Recombinant Luciferase), which generates a stable “glow-type” luminescent signal and improves performance across a wide range of assay conditions [13].

(a) Reagent Preparation

1. Thaw the CellTiter-Glo® Buffer and equilibrate to room temperature prior to use.
2. Equilibrate the lyophilized CellTiter-Glo® Substrate to room temperature prior to use.
3. Transfer the appropriate volume (10 mL for the A size or 100 mL for the B size) of CellTiter-Glo® Buffer into the amber bottle containing CellTiter-Glo® Substrate to reconstitute the lyophilized enzyme/substrate mixture. This forms the CellTiter-Glo® Reagent.
4. Mix by gently vortexing, swirling, or inverting the contents to obtain a homogeneous solution. The CellTiter-Glo® Substrate should be added into solution easily in less than 1 min.

(b) At the end of the incubation period equilibrate the plate and its contents to room temperature for approximately 30 min.

(c) Add a volume of CellTiter-Glo® Reagent equal to the volume of cell culture medium present in each well (e.g., add 100 μ L of reagent to 100 μ L of medium containing cells for a 96-well plate).

(d) Mix contents for 2 min on an orbital shaker to induce cell lysis.

(e) Allow the plate to incubate at room temperature for 10 min to stabilize luminescent signal.

(f) Record luminescence (*see Note 1*).

3.4 Trypsinization

1. At the end of the incubation period with the test articles, treatment medium is removed and replaced with 1 mL of PBS prewarmed at 37 °C.
2. The plate is slightly shaken.
3. PBS is removed and replaced with 0.5 mL of trypsin solution prewarmed at 37 °C diluted to 1:2 (v/v) in PBS.
4. The plate is incubated for 8 min in humidified atmosphere containing 5% CO₂ and 95% air at 37 °C (*see Note 2*).

5. The trypsinization is stopped by rapid addition of 1 mL/well of treatment medium completed with 20% of FCS.
6. The plate is slightly shaken.
7. After several “backward and forward” motions into a pipette (from 5 to 10 times), the cell suspension is delivered into a conical vial.
8. An aliquot of 20 μL is mixed with 20 μL of trypan blue solution diluted 1:4 (v/v) in culture medium.
9. Viable cells are counted into Malassez hematimeter for at least 3 lines out of 10 (*see Note 3*).
10. N (number of alive cells/mL) = X (number of alive cells/number of counted lines) \times 10 (total number of lines) \times 2 (dilution factor) \times 1000 (hematimeter volume).
11. N' (total number of alive cells) = $N \times V$ (tube volume).
12. During the cell count step, cells are centrifuged for 5 min at $50 \times g$ at room temperature.

3.5 Respiration

3.5.1 Clark Electrode

The oxygen electrode is a specialized form of electrochemical cell which consists of two electrodes immersed in an electrolyte solution. Typically, a 50% saturated solution of KCl is used in oxygen electrode systems. Application of a polarizing voltage of 700 mV ionized the electrolyte and initiated current flow via a series of electrochemical reactions. Oxygen is “consumed” during the electrochemistry; thus the magnitude of the current flow is related to the oxygen concentration of the surrounding media. This type of electrode sensor was first developed by Clark in 1956 to measure oxygen in blood samples. As a result it is often referred to as the Clark electrode.

3.5.2 Electrode Preparation

Before use, the electrode disc needs to be prepared in such a way that an electrolyte bridge is formed between the anode and cathode in order for current to flow in the presence of oxygen. The disc also requires a protective membrane which prevents any deposits from the reaction mixture from settling on the cathode yet allowing oxygen to diffuse freely so as not to jeopardize the response time of the disc.

There are four preparation stages:

1. Place a small drop of electrolyte on top of the dome of the electrode disc.
2. Place a 1.5 cm^2 paper spacer over the electrolyte ensuring that at least one corner of the spacer is in the electrode well to act as a wick. Cover this with a similar sized piece of polytetrafluoroethylene (PTFE) membrane.

3. Place the small electrode disc O-ring over the end of the applicator tool. Hold the applicator vertically over the dome and slide the applicator shaft down to push the O-ring over the dome.
4. Check that the membrane preparation is smooth and that there are no trapped air bubbles. Top the reservoir well up with several drops of electrolyte.

3.5.3 System Calibration

Before any measurements could take place, the electrode disc must be calibrated so that the electrical signal received from the disc is presented as actual calibrated units (nmol/mL). Calibrating the disc for liquid-phase measurements involves a two-step procedure in which the signal from the oxygen electrode is referenced to two known oxygen concentrations. The two calibration steps are:

1. Air line.
2. Zero oxygen line.

3.5.4 Performing a Liquid-Phase Calibration

1. Connect the electrode disc to the rear of the control unit.
2. Place approximately 2 mL of air-saturated, deionized water into the reaction vessel. Air-saturated water is obtained by vigorously shaking a small quantity of deionized water (approximately 50 mL) in a large conical flask (approximately 1 L).
3. Connect the Peltier electrode chamber to the rear of the Oxytherm control unit and ensure that the sample and electrode disc equilibrate to the temperature required by the assay before starting calibration.
4. After setting temperature, atmosphere pressure, and stirring speed, the system starts recording the “air line” level corresponding to 100% of dissolved oxygen. After the signal plateau is reached the system proceeds to the “zero oxygen phase.” The “zero oxygen phase” can be achieved in three different ways:
 - (a) Addition of sodium dithionite, a strong oxygen-reducing agent, in the reaction chamber: However, care must be taken to remove all traces of dithionite from the chamber before continuing the experiment.
 - (b) Bubbling carefully nitrogen into the reaction chamber in order to displace oxygen.
 - (c) Bubbling carefully argon into the reaction chamber in order to displace oxygen: Argon is more efficient than nitrogen for establishing the “zero oxygen line.”

Calibration must be done every day of experimentation and for every electrode preparation (the calibration is valid for 24 h).

5. Remove the medium from the reaction chamber and replace it with deionized water. The water should be stirred under the air at 37 °C in the reaction chamber during 10–15 min (*see Note 4*).

6. Close the reaction chamber and record the level of oxygen in the water. The normal values are from 200 to 250 nmol/mL of oxygen.

3.5.5 Hepatocyte Respiration Measurement

1. Remove the medium used to stop the trypsinization process and replace it by the respiration medium (*see Note 5*).
2. Adjust the volume for having always the same number of alive cells (e.g., 3 million cells in 1.9 mL, working volume in the reaction chamber).
3. Remove water from the respirometer reaction chamber and replace it by the previous hepatocyte suspension.
4. Close the chamber.
5. Start recording.

In these conditions the oxygen concentration decreases as a function of time. After 10–15 min, the recording is stopped (*see Note 6*). The speed of oxygen consumption is calculated by determining the slope of the recording curve (Fig. 1). The speed is expressed in nmol oxygen/min/mL. This speed should be expressed in nmol oxygen/min/mL/million of viable cells to avoid variations depending on the number of cells into the chamber.

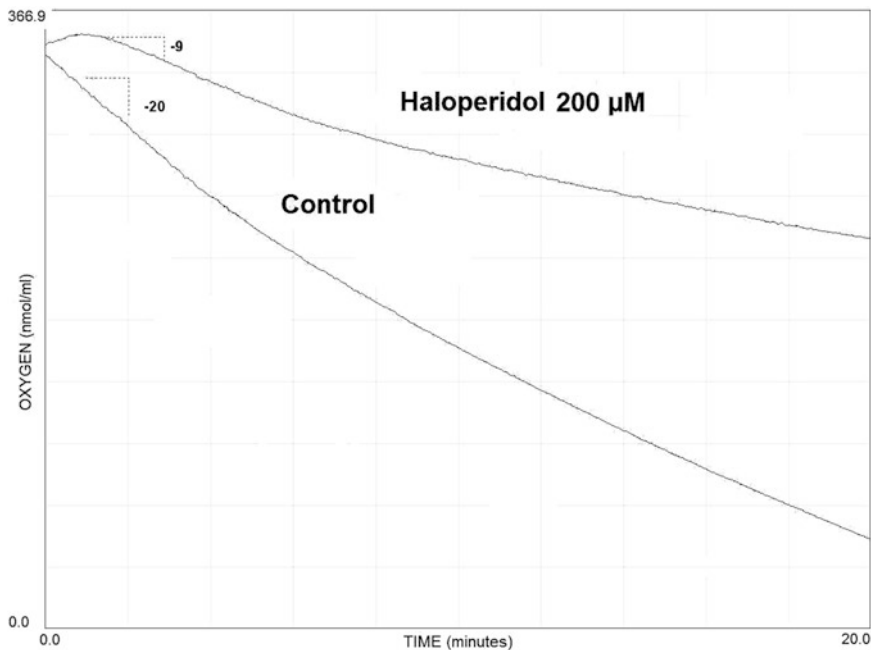


Fig. 1 Oxygen consumption in primary rat hepatocyte culture from control and haloperidol-treated cells. Hepatocytes are incubated for 24 h in the presence of haloperidol at a concentration of 200 μM or DMSO. The representation is a screenshot from the recording software. The slope calculation represents the rate of oxygen consumption expressed as nmol/mL/min. The rate of oxygen consumption is 20 nmol/mL/min for the control and 9 nmol/mL/min for the treated hepatocytes

4 Notes

1. For the measure of ATP endpoint in cytotoxicity study using luminometry instrument settings depend on the manufacturer. An integration time of 0.25–1 s/well should serve as a guideline.
2. The trypsinization step is a critical step as it leads to a great deal of cell destruction. The time of incubation with trypsin needs to be precisely respected. This time leads to a maximum of cell death of 50%.
3. The viable cell count is a mandatory critical step. A minimum range of viable cells is necessary to have a good signal in the respirometer; it should at least be in the range of 1.5–3 million of cells per measurement in the reaction chamber. A constant number of viable cells in the reaction chamber is important in order to compare the rates of oxygen consumption between samples.
4. An easiest way to saturate water with air is to shake deionized water at 37 °C into a bottle (50 mL in a bottle of 1 L) and to pipette an aliquot into the reaction chamber.
5. The same interval of time must be respected between the counting after trypsinization and the beginning of oxygen consumption recording for every sample of a same experiment.
6. It is important to keep in mind that this protocol of respiration in hepatocytes measures the spontaneous respiration as the consequence of the presence of the endogenous substrates and stimulated by the basic ATP consumption [11].

Acknowledgments

The authors would like to thank Delphine Hoët for her expertise and her support in hepatocyte culture.

References

1. Lee WM (2003) Drug-induced hepatotoxicity. *N Engl J Med* 349:474–485
2. Pessayre D, Fromenty B, Mansouri A, Berson A (2007) Hepatotoxicity due to mitochondrial injury. In: Kaplowitz N, DeLeve LD (eds) *Drug-induced liver disease*, 2nd edn. Informa Healthcare, New York, USA, pp 49–84
3. Fromenty B, Pessayre D (1995) Inhibition of mitochondrial beta-oxidation as a mechanism of hepatotoxicity. *Pharmacol Ther* 67: 101–154
4. Pessayre D, Mansouri A, Haouzi D, Fromenty B (1999) Hepatotoxicity due to mitochondrial dysfunction. *Cell Biol Toxicol* 15:367–373
5. Igoudjil A, Begriche K, Pessayre D, Fromenty B (2006) Mitochondrial, metabolic and genotoxic effects of antiretroviral nucleoside reverse-transcriptase inhibitors. *Curr Med Chem: Anti-Infect Agents* 5:273–292
6. Dykens JA, Will Y (2007) The significance of mitochondrial toxicity testing in drug development. *Drug Discov Today* 12:777–785

7. Scatena R, Bottoni P, Botta G, Martorana GE, Giardina B (2007) The role of mitochondria in pharmacotoxicology: a reevaluation of an old, newly emerging topic. *Am J Physiol Cell Physiol* 293:C12–C21
8. Salway JG (1994) *Metabolism at a glance*, 1st edn. Blackwell Scientific Publications, London, UK
9. Pessayre D, Fromenty B (2005) NASH: a mitochondrial disease. *J Hepatol* 42:928–940
10. Navarro A, Boveris A (2007) The mitochondrial energy transduction system and the aging process. *Am J Physiol Cell Physiol* 292:C670–C686
11. Berson A, Renault S, Letteron P, Robin MA, Fromenty B, Fau D, Le Bot MA, Riche C, Durand-Schneider AM, Feldmann G, Pessayre D (1996) Uncoupling of rat and human mitochondria: a possible explanation for tacrine-induced liver dysfunction. *Gastroenterology* 110:1878–1890
12. Korzeniewski C, Callewaert DM (1983) An enzyme-release assay for natural cytotoxicity. *J Immunol Methods* 64:313–320
13. Crouch SPM, Kozlowski R, Slater KJ, Fletcher J (1993) The use of ATP bioluminescence as a measure of cell proliferation and cytotoxicity. *J Immunol Methods* 160:81–88

Part VI

Screening Assays for Developmental Toxicity

Chapter 17

FETAX Assay for Evaluation of Developmental Toxicity

Isabelle Mouche, Laure Malésic, and Olivier Gillardeaux

Abstract

The frog embryo teratogenesis assay *Xenopus* (FETAX) test is a development toxicity screening test. Due to the small amount of compound needed and the capability to study organogenesis in a short period of time (96 h), FETAX test constitutes an efficient development toxicity alert test when performed early in drug safety development. The test is conducted on fertilized *Xenopus laevis* mid-blastula-stage eggs over the organogenesis period. Compound teratogenic potential is determined after analysis of the mortality and malformation observations on larvae. In parallel, FETAX test provides also information concerning embryotoxic effect based on larva length.

Key words Embryo, FETAX, *Xenopus laevis*, Development, Toxicity, Teratogenesis, Teratogen

1 Introduction

Developmental toxicity represents an important issue for drug development in pharmaceutical companies. A teratogenic potential found prior to preclinical trials is a major benefit to initiate earlier appropriate *in vivo* studies to confirm or not the alert. However, in early development stage, the number of compounds to be tested is large and their available quantities are generally low. Regarding these requirements, frog embryo teratogenesis assay *Xenopus* (FETAX) is adapted to evaluate developmental toxicity potential using small drug quantities compared to *in vivo* studies. Furthermore, the main organogenesis nearly completed in a short time (96 h) constitutes a second advantage of FETAX test to obtain rapid development toxicity assessment compared to *in vivo* studies more time consuming, even taking into account that FETAX assay should often be performed twice to conclude it positive or negative. An interlaboratory validation study based on the standard guide [1, 2] from the American Society for Testing and Materials (ASTM) showed advantages and difficulties to perform FETAX test. Herein the method described is the FETAX method used as a routine test, in the lab, for several years, after an in-house validation

period performed according to the ASTM standard guide 1439-98 [1]. The test was used to study around 400 test articles where 60 of them were also evaluated in mammalian embryotoxicity studies. According to these data the predictivity of the FETAX assay is 81% [3]. An update of the standard guide, ASTM E1439-12 has been published in 2012 [4]. The experimental conditions described herein are also in accordance with the ASTM E1439-12 guide, in particular regarding temperature conditions and the design of the test. However it is recommended to refer to this ASTM E1439-12 guide, before implementing FETAX assay. FETAX test is introduced as a developmental toxicity screening assay in this chapter, but it may be used as a mechanistic model to investigate developmental gene expression [5] which will not be discussed herein. Indeed transcriptomic articles showed a great conservation of genes expressed in oocytes between *Xenopus laevis* and mouse [6]. In that way FETAX could be a tool for both developmental toxicity screening and development mechanistic model.

2 Materials

2.1 *Xenopus laevis* and Facilities

1. Eighteen-month- to 3-year-old male and female *Xenopus laevis* frogs are purchased from the European Xenopus Resource Centre (EXRC, Portsmouth, UK) or Centre de Ressources Biologiques (CRB, Rennes, France) (*see Note 1*). The main problem one can face with *Xenopus laevis* is the pathology called red leg disease (*see Note 2*).
2. *Xenopus laevis* are housed in Xenopus aquatic housing self-contained system (AQUANEERING, San Diego, USA) with 16- or 50-L tanks (*see Note 3*) maintained in a semidarkness environment at $20\text{ }^{\circ}\text{C} \pm 2\text{ }^{\circ}\text{C}$.
3. Tanks have to be filled with chloride ion-free water obtained by filtration on $5\text{ }\mu\text{m}$ activated carbon cartridge (Millipore) (*see Note 4*).
4. Frozen stored mud worms are delivered to *Xenopus* twice a week.

2.2 Fertilization of Eggs

1. The human chorionic gonadotrophin (hCG) lyophilisat of 5000 IU (Sigma ref CG5) is dissolved with 5 mL sterile water to get a $1\text{ IU}/\mu\text{L}$ hCG solution. The solution is stable for 2 months at $2\text{--}8\text{ }^{\circ}\text{C}$.
2. Leibovitz's L15 liquid media (1X) with L-glutamine and phenol red (Invitrogen).

2.3 Anesthesia

1. Ethyl 3-aminobenzoate methanesulfonate salt (MS-222, Sigma) is dissolved at 2% into chloride-free water and stored at around $4\text{ }^{\circ}\text{C}$ up to 3 months.

2. Ethyl 3-aminobenzoate methanesulfonate salt (MS-222, Sigma) is dissolved at 0.06% into FETAX medium and stored at around 4 °C up to 3 months.

2.4 FETAX Culture and Treatment

1. FETAX medium: 10.7 mM NaCl, 1.14 mM NaHCO₃, 0.4 mM KCl, 0.1 mM CaCl₂, 0.35 mM CaSO₄, 2H₂O, and 0.3 mM MgSO₄ in deionized water. Adjust pH to 7.6–7.9. FETAX medium can be purchased as a custom preparation (Invitrogen from Thermo Fisher Scientific).
2. Dimethyl sulfoxide Hybri-Max™ (DMSO, Sigma).
3. Thin forceps straight MORIA MC40 (11 cm) or MORIA 9980 (13 cm) (Fine Science Tools ref 11370-40 and 11399-80) and thin forceps curved MORIA MC40/B (11 cm) or MORIA 9987 (13 cm) (Fine Science Tools ref 11370-42 and 11399-87).
4. Binocular stereomicroscope WILD MZ8 (Leica) or equivalent with a magnification of 15× and a ring light illuminator (optional), optical fibers with a cold light source as Intralux 5000-1 (Volpi, Switzerland) or equivalent (3190/3200°K color temperature, 450,000 fc illumination intensity).

3 Methods

The test method is described in four main stages, starting with *in vitro* egg fertilization, following by egg selection, test article treatment, and then larva observation with the different developmental endpoints to assess. Finally, a section is dedicated to analysis and interpretation of the results. Timelines of FETAX test are shown in Fig. 1. *In vitro* egg fertilization leads to sacrifice of *Xenopus* male to collect the sperm but provides a large amount of synchronized mid-blastula-stage eggs to develop at the same time (*see Note 5*). Fertilization and egg selection are crucial steps to succeed in the test. Furthermore the capability to identify accurately larva malformations needs much of experience acquired after many examinations of a very large number of larvae. This methodology is performed in-house under the approval from local ethical committee.

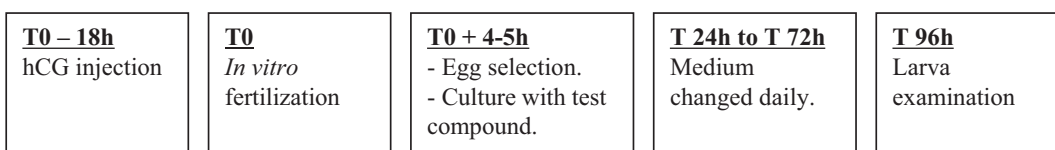


Fig. 1 Timelines of the test

3.1 *In Vitro* Egg Fertilization

1. On the previous evening (T0-15/18 h) maintain the *Xenopus* frog with one hand on a benchkote paper or similar to perform a subcutaneous injection of 700 IU hCG to female and 300 IU hCG to the male from a 1 IU/ μ L hCG solution into the dorso-lymphatic sac (*see Note 6*).
2. At T0, about 15–18 h after hCG injection, anesthetize the *Xenopus* male putting it into the 2% MS-222 solution before lobotomizing it. Make an abdominal incision to remove testes from the abdominal cavity and place them in Leibovitz's L15 medium. Testes can be kept up to 4 days at 4 °C in this medium.
3. *Xenopus* female generally does not release all the eggs. Therefore it is necessary to make them get out from the cloaca. Therefore maintain the *Xenopus* female firmly in one hand with its head placed towards the wrist, keeping its posterior legs folded up next to its body.

With the thumb give an abdominal massage in the rostro-caudal direction carefully not to push too strongly on the *Xenopus* abdomen. Finally, put down the oocytes that are released from the cloaca on a 90-mm dry plastic Petri dish.

4. To fertilize oocytes, first, make multiple thin incisions with scissors and forceps in a piece of testis that is applied on the oocytes. Next, spread well oocytes on the Petri dish to obtain a monolayer, using the testis as a tool to make it. A few minutes later cover the oocytes with FETAX medium.
5. Incubate eggs at 25 °C about 5 h to develop up to the mid-blastula stage. Check them regularly to ensure that development occurs correctly and not to miss the mid-blastula stage (*see Note 7*).

3.2 Egg Culture and Compound Treatment

3.2.1 Concentration Range Selection and Preparation

1. Determine the tested concentration range of the compound. According to the limit of solubility (*see Note 8*), compound is tested up to the limit of solubility or through a standard range of five concentrations 1, 4, 16, 32, and 62.5 mg/L with a 0.5% DMSO maximum concentration when this vehicle is used to dissolve the compound. When no effects are observed on *Xenopus* embryos with the standard dose range a second assay is performed up to a maximum of 400 mg/L even if the solubility is higher than 400 mg/L in FETAX medium. Upper concentration is generally toxic whatever the compound from experience.
2. At T0, dissolve compound in DMSO or in FETAX medium according to the solubility, under a laminar flow microbiological safety cabinet. The volume of this stock solution has to be sufficient for the entire assay.
3. Distribute the stock solution in identified dark flasks such as the minimum volume of each final concentration is 32 mL

Table 1
Example of standard range preparation

Concentration identification	Final concentration in FETAX medium (mg/L)	Compound stock solution 10 g/L (μ L)	DMSO (μ L)	Complete with FETAX medium to (mL)
1	0	0	160	32
2	1	4	196	40
3	5	16	144	32
4	10	32	128	32
5	25	80	80	32
6	50	160	0	32

FETAX medium (*see Note 9*). Add DMSO, as needed, to get 0.5% in each final concentration and complete with FETAX medium to the appropriate volume.

An example of a concentration range preparation is shown in Table 1.

- Concentration range is kept at around 4 °C during the 96-h test period. But stock solution prepared in DMSO is kept at room temperature to avoid freezing.

3.2.2 Egg Seeding and Treatment (T0 + 4–5 h)

- Distribute 8 mL of each concentration in a 50 mm sterile vented Petri dish previously labeled (concentration and compound name) under a laminar flow microbiological safety cabinet. If compound range has been refrigerated, maintain the Petri dishes filled with the test compound solutions at least 1 h 30 min at room temperature before adding the eggs. Low temperature is toxic for egg development and induces malformations. In case of a FETAX test conducted with a metabolic activation system (MAS), it should be added simultaneously with the compound (*see Note 10*).
- Fill a 50 mm sterile vented Petri dish with 8 mL of culture medium without test compound as control culture.
- Using MORIA thin forceps, pick over the eggs which have their pigmented pole up (animal pole), a regular spherical shape, and a homogeneous cellular division (Fig. 2) under a binocular stereomicroscope placed under the laminar flow microbiological safety cabinet (*see Note 11*). Unfertilized eggs are totally white without pigmentation. Add 20 mid-blastula-stage selected eggs in each Petri dish previously filled with test compound or control solution ensuring that they are at room temperature.

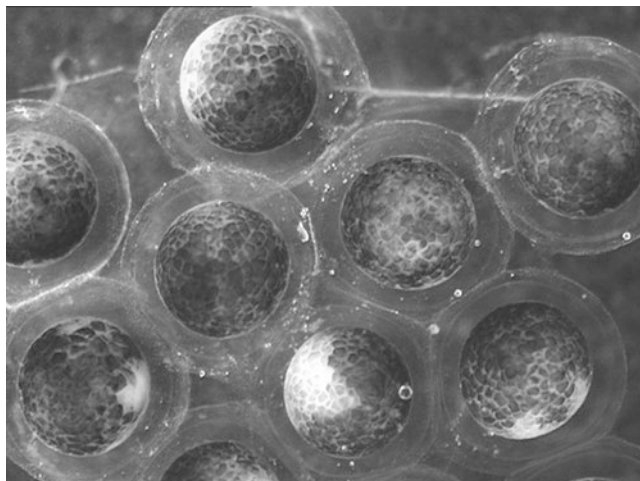


Fig. 2 Mid-blastula-stage eggs

4. Maintain egg cultures in Petri dishes with the cover on and keep them at room temperature (around 20 °C) in dark light under the laminar flow microbiological safety cabinet for 96 h.

3.2.3 Culture Monitoring (T 24 h to T 72 h)

FETAX medium with or without tested compound is changed daily under the laminar flow microbiological safety cabinet. Light can be switched on during this operation.

1. Add 8 mL of each compound final concentration prepared at T0 or culture medium in new 50 mm sterile vented Petri dishes previously labeled.
2. Keep those Petri dishes at least 1 h 30 min at room temperature to ensure that FETAX medium is at room temperature (around 20 °C) before adding eggs.
3. Transfer the living larvae in the new Petri dishes under a binocular stereomicroscope, at T 24 h using MORIA thin forceps, as the eggs are a little sticky and at T 48 h and T 72 h, with a transfer polyethylene 2 mL Pasteur pipette with the thin end cut, as larvae have swimming capability.
4. Switch the light off and keep the culture in dark light under the laminar flow microbiological safety cabinet.
5. Report daily on an observation sheet the number of dead larvae and compound's precipitates for each culture (*see Note 12*).

3.2.4 Culture End (T 96 h): Larva Examination

Follow the different steps described below for each concentration and each larva:

1. Check that all larvae swim and if not report it on a developmental parameter sheet where malformations will be recorded too.
2. Write down the precipitates, if any, and the number of dead larvae on the observation sheet, and then remove them from the Petri dishes.

3. Euthanize larvae by putting them into 0.06% MS-222 solution (lethal dose) in a 50 mm Petri dish.
4. Measure only each straight larva from the head to the tail end with a measurement system (cell^A image acquisition software by Olympus or equivalent) and report the value on the developmental parameter sheet. Do not measure larvae with axis malformations as it would not be relevant.
5. Examine each larva under a binocular stereomicroscope equipped, if possible, with a ring light illuminator to identify developmental malformation described in Table 2 and by leaning on the *Atlas of abnormalities* [7].

Figures 3 and 4 show examples of normal and abnormal larvae.

Table 2
Malformation types

General malformations		Specific malformations	
–	No swimming	Blisters	Ventral fin
Pigmentation	No pigmentation		Dorsal fin
	Abnormal pigmentation	Cranium	Acephaly
Axis	Stunted larvae		Macrocephaly
	Skeletal kinking		Microcephaly
	Wavy tail	Face	Abnormally flattened
–	Hemorrhage	Nares	Malpositioned
Edema	Cardiac	Mouth	Small
	Abdominal		Incomplete development
	Facial	Eyes	Absent
	Cephalic		Malpositioned
Gut	Optic		Irregular shape
	Miscoiling		Cyclopia
Other(s)			Incomplete separation
			Abnormal pigmentation
			Failure of the choroid
			Abn pigmented optic nerves
		Heart	Enlarged
			Malpositioned
		Underdeveloped	

Specific malformations are considered more severe than general ones. *Abn* abnormally, *sl* slight, *mo* moderate, *se* severe, *uni* unilateral, *bi* bilateral



Fig. 3 Normal larva

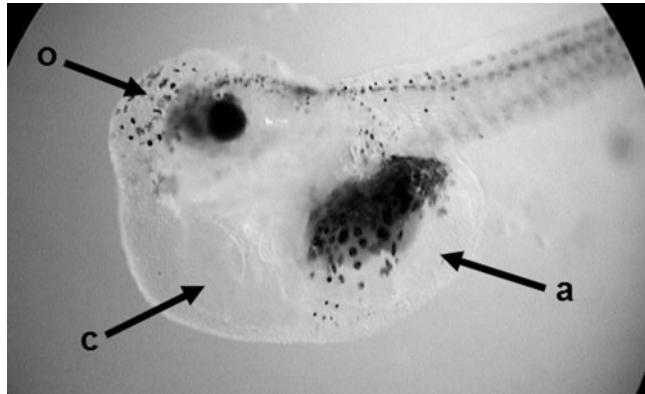


Fig. 4 Abnormal larva. *a* Abdominal edema; *c* cardiac edema; *o* optic edema

6. After examination eliminate larvae according to your internal rules concerning biological samples.

3.3 Result Analysis

Once FETAX technical part is completed, a teratogenic index based on mortality and number of abnormal embryos is calculated, larva length is analyzed with statistical tools, and finally malformation type ratio is determined. FETAX test is then concluded positive or negative which means that the compound presents or not a teratogenic potential according to this result analysis.

3.3.1 Statistical Analysis of Larva Length

Larva length is a parameter that gives information about the embryotoxic effect of the compound. A statistical analysis is applied to ensure that length differences observed between treated larvae and control ones are significant.

1. Using statistical software, enter concentration and individual length values to perform a normality test.

2. First case: If the test is normal, make a Bartlett test followed by a Dunnett test if the Bartlett test is accepted; otherwise if the Bartlett test is not accepted, perform a Kruskal-Wallis test.
Second case: If the test is “not normal” perform a Kruskal-Wallis test.
3. A compound is considered embryotoxic if a significant length difference is concluded according to the statistical tests. But it is important to check if this statistical difference is biologically relevant based on the dose-length effect relationship observed.
4. Determine the minimum concentration inhibiting growth (MCIG) which is the concentration that reduces significantly the larva length.

3.3.2 Calculation of the Teratogenic Index (TI)

The conclusion of the test is based on the value of the TI calculated as the ratio of the 50% embryo lethal concentration (EmLC50) versus the concentration inducing 50% of malformed larvae (EmMC50) among the living ones.

1. Calculate the percentage of mortality and of malformed embryos for each concentration tested.
2. Enter these data in graph-pad Prism[®] software or similar.
3. Apply a nonregression linear model to establish two curves: (1) mortality percentage as a function of concentration and (2) malformation percentage as a function of concentration.
4. Choose the appropriate function to determine the EmLC50 (x -value) that induces 50% of mortality on the curve [mortality = f (concentration)] and EmMC50 (x -value) that induces 50% of malformed embryos on the curve [malformed embryo = f (concentration)]. If the software does not give exactly the 50% value select the closest one.
5. Determine the TI = (EmLC50)/(EmMC50).

3.3.3 Malformation Parameters

1. Create a table to gather for each concentration the number of malformed embryos, the percentage of malformed embryos among the living larvae, and the percentage of malformed embryos among the living larvae for each malformation type.
2. Create a histogram where malformation percentage is a function of malformation type to visualize the compound effect.
3. Evaluate the malformation severity taking into account that axis, pigmentation, hemorrhage, edema, and gut malformations are general malformations whereas blisters, cranium, face, nares, mouth, eyes, and heart malformations are specific ones. Specific malformations are considered more severe than general ones.

3.4 Interpretation

1. Prior to the interpretation, FETAX assay has to be validated according to acceptance quality criteria based on control results (*see Note 13*).
2. The interpretation is done first with the TI. According to laboratory historical data obtained with reference and in-house compounds we have stated that a FETAX test is concluded positive when the TI value is higher or equal to 1.2 and negative whether the TI value is lower or equal to 1.0. When the TI value is between 1.0 and 1.2 the length parameter, mortality, and types of malformations have to be considered to conclude the test positive or negative based on the decision tree (Fig. 5).
 In some cases the TI cannot be calculated because EmLC50 and/or EmMC50 are not reached. However a conclusion is generally possible according to the decision tree (Fig. 6). If not, a second assay is recommended with concentration range modifications.
 An example of interpretation is shown in Table 3 with nicotine tested as a reference compound. It was concluded positive due to a TI value of 3.51, thus meaning that nicotine presented a teratogenic potential under the experimental conditions used.
3. Apart from FETAX interpretation, the no observable effect concentration (NOEC) can be determined to provide complementary information regarding the minimum concentration that is safe to *Xenopus* eggs (*see Note 14*).

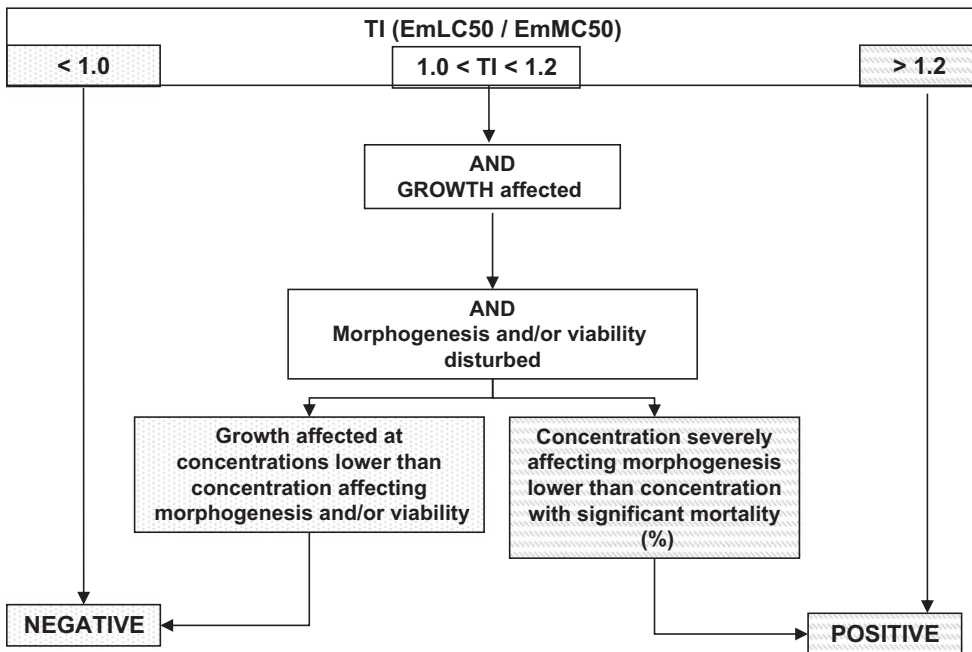


Fig. 5 Decision tree with teratogenic index (TI). Modified growth is evaluated based on larva length measurement

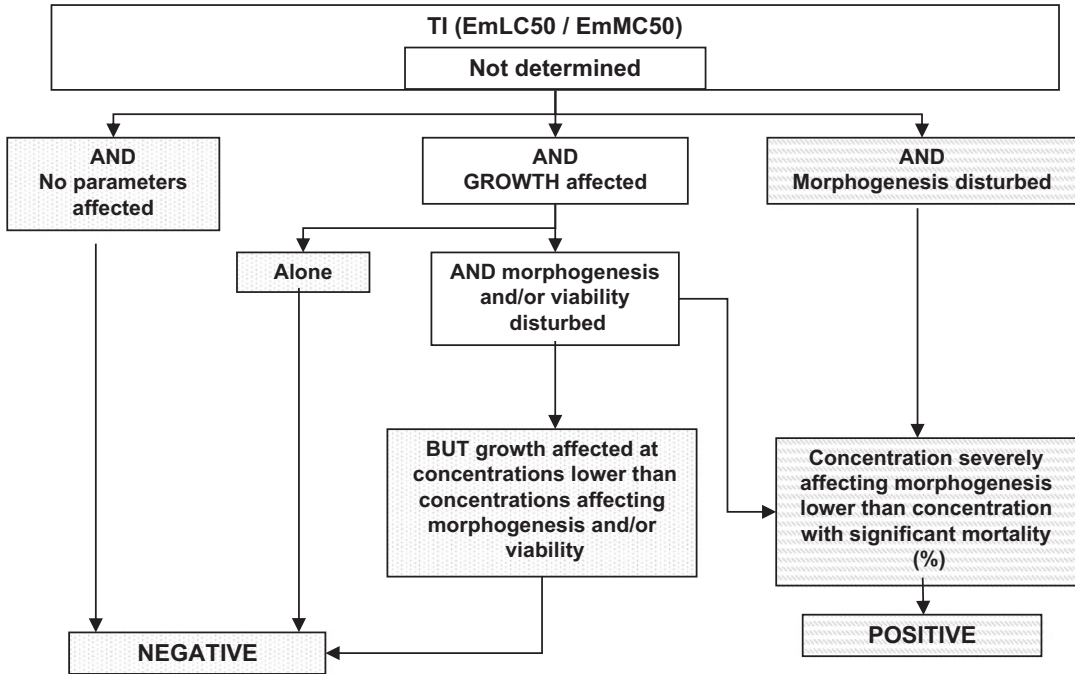


Fig. 6 Decision tree without teratogenic index (TI). Modified growth is evaluated based on larva length measurement

4 Notes

1. Each *Xenopus* can be injected with hCG once every 3 months up to 10 of age. It is recommended to have in-house 40 females and 16 males to ensure a good turnover.
2. The main pathology of *Xenopus laevis* can suffer from is the red leg disease which is a bacteria septicemia.

The major concern is that when the clinical signs are observed the disease is at an advanced stage and then only a few frogs will survive. An antibiotic treatment exists but its effects can interfere with FETAX results. The only efficient solution to get rid of the red leg disease is to euthanize contaminated frogs.

When a *Xenopus* frog is found dead due to the red leg disease, the tank is placed in quarantine to observe the other *Xenopus* during 1 month. If no red leg disease symptoms appear over this period, frogs can be used to perform FETAX test.

However, parasites could also cause this kind of reddening. In that case an anthelmintic treatment (levamisole) can be considered out of study period to avoid interferences with results.

Table 3
Example of nicotine tested in FETAX test

Dose		Number of eggs in culture	Mortality	Number of malformed embryos	Length \pm SD	Number of embryos measured
(mg/L)	(μ M)		Number (%)	Number (%)	(mm)	
0	0	20	0 (0)	0	9.5 \pm 0.24	20
2.5	12	20	1 (5)	0	9.4 \pm 0.16*	20
10	47	20	0 (0)	2 (10.0)	9.3 \pm 0.15*	18
40	189	20	2 (10)	7 (38.9)	9.2 \pm 0.18**	12
160	757	20	8 (40)	12 (100.0)	9.0 \pm 0.12**	7
320	1514	20	20 (100)	–	–	–
EmLC50 (mg/L)		210.1		MCIG (mg/L)	2.5	
EmMC50 (mg/L)		59.8		NOEC (mg/L)	ND	
TI		3.51				

EmLC50 embryo lethal concentration 50%, EmMC50 concentration inducing 50% of malformed embryos, TI teratogenic index (EmLC50/EmMC50), MCIG minimum concentration inhibiting growth, NOEC no observable effect concentration

ND not determined, – not done. A Dunnett test was applied to length parameter

* $p < 0.05$

** $p < 0.001$

After the levamisole treatment procedure, spawning from treated females has to be induced by an injection of 700 UI hCG to remove eggs that were potentially exposed to levamisole.

- Xenopus aquatic housing system uses a four-stage filtration system to provide a recirculating clean water. However, different kinds of tanks can be used under several conditions such as 3–4 L of water at room temperature per *Xenopus*, an air circulation system into water, a turnover of the tank water at least once every 2 weeks or a recirculating filtered water system, and environmental enrichment devices as plastic pipes to provide hiding places.
- Xenopus* are very sensitive to chloride ions that are toxic for them and for egg development. Therefore a key point is to use chloride ion-free water in the tank to get the best conditions for FETAX test success.
- Another method to obtain fertilized eggs is to perform a natural mating. On the previous evening (T0-18 h), once hCG

injection has been performed, one male and two females are left together in a tank overnight. At T0, eggs are collected to be selected at the mid-blastula stage to perform the test. However, the main limit of the natural fertilization is that eggs are not fertilized at the same time depending on how the sperm is spread by the male in the tank. So it is difficult to obtain a large amount of eggs at a mid-blastula stage at the same time to perform an assay. On the other hand, the advantage of the natural fertilization is that the male is not sacrificed. Therefore it can be used once every 3 months up to 10 years of age.

6. The hCG injection is recommended but not mandatory for *Xenopus* male.
7. Development stage series is available on www.xenbase.org in the chapter “Anatomy and Development.”
8. If not known, determine compound solubility in DMSO and FETAX since compounds are more often dissolved in DMSO and diluted at 1/200 in FETAX medium (final DMSO percent is 0.5% maximum) or directly dissolved in FETAX medium. Other vehicles or buffers can be used but they have to be tested to verify that they are free of toxic effect on *Xenopus* egg development. In any case avoid vehicles with chloride ions that are toxic for *Xenopus* embryos.
9. Do not make a cascade range to avoid dilution errors.
10. In the lab, metabolic activation system (MAS) is not included in the method as the results obtained without MAS were satisfying so far even if it is known that *Xenopus laevis* eggs have a poor metabolic potential. However information can be found in an interlaboratory validation [8, 9] and in optimization studies [10, 11]. This validation and MAS model improvement studies showed that several parameters have to be well controlled to reduce variability between assays in order to obtain relevant data.
11. Eggs attributed to a compound have to be selected from a same female laying.
12. Sometimes precipitates appear throughout the study even if at first the compound was soluble. It could be due to the refrigeration storage and/or if the compound is not stable in solution.
13. FETAX assay is accepted when control larva mortality and malformed control embryos rate are equal or lower than 10%, and control larva length is in accordance with historical data.
14. The no observable effect concentration (NOEC) is the tested concentration that induces neither mortality nor malformation or lower than 10% and does not involve larva length modification compared to historical data range.

References

1. ASTM (1998) Standard guide for conducting the frog embryo teratogenesis assay – *Xenopus*. Designation E 1439-98, Annual book of ASTM standards, vol 11.5. American Society for Testing and Materials, Philadelphia, pp 825–836
2. Bantle JA, Finch RA, Burton DT, Fort DJ, Dawson DA, Linder G, Rayburn JR, Hull M, Kumsher-King M, Gaudet-Hull AM, Turley SD (1996) FETAX interlaboratory validation study: Phase III – Part I testing. *J Appl Toxicol* 16(6):517–528
3. Leconte I, Mouche I (2013) Frog embryo teratogenesis assay on *Xenopus* and predictivity compared with in vivo mammalian studies. *Methods Mol Biol* 947:403–421
4. ASTM (2012) Standard guide for conducting the frog embryo teratogenesis assay – *Xenopus* Designation E 1439-12, ASTM book of standards, vol 11.6. American Society for Testing and Materials, Philadelphia
5. Sipe CW, Saha MS (2007) The use of microarray technology in non mammalian vertebrate systems. In: Rampal JB (ed) *Microarrays: volume II: applications and data analysis*, *Methods in Molecular Biology*, vol 382. Humana, Totowa, NJ, pp 1–16
6. Vallée M, Aiba K, Piao Y, Palin MF, Ko MS, Sirard MA (2008) Comparative analysis of oocyte transcript profiles reveals a high degree of conservation among species. *Reproduction* 135(4):439–448
7. Bantle JA, Dumont JN, Finch RA, Linder G, Fort DJ (1998) Atlas of abnormalities, a guide for the performance of FETAX, 2nd edn. Oklahoma State University, Stillwater, OK
8. Fort DJ, Stover EL, Bantle JA, Rayburn JR, Hull MA, Finch RA, Burton DT, Turley SD, Dawson DA, Linder G, Buchwalter D, Dumont JN, Kumsher-King M, Gaudet-Hull AM (1998) Phase III interlaboratory study of FETAX, Part 2: interlaboratory validation of an exogenous metabolic activation system for frog embryo teratogenesis assay-*Xenopus* (FETAX). *Drug Chem Toxicol* 21(1):1–14
9. Bantle JA, Finch RA, Fort DJ, Stover EL, Hull M, Kumsher-King M, Gaudet-Hull AM (1999) Phase III interlaboratory study of FETAX, Part 3: FETAX validation using 12 compounds with and without an exogenous metabolic activation system. *J Appl Toxicol* 19:447–472
10. Fort DJ, Rogers RL, Stover EL, Finch RA (2001) Optimization of an exogenous metabolic activation system for FETAX. I. Post-isolation rat liver microsome mixtures. *Drug Chem Toxicol* 24(2):103–115
11. Fort DJ, Rogers RL, Paul RR, Stover EL, Finch RA (2001) Optimization of an exogenous metabolic activation system for FETAX. II. Preliminary evaluation. *Drug Chem Toxicol* 24(2):117–127

Chapter 18

Evaluation of Embryotoxicity Using the Zebrafish Model

Lisa Truong and Robert L. Tanguay

Abstract

The embryonic zebrafish model offers the power of whole-animal investigations (e.g., intact organism, functional homeostatic feedback mechanisms, and intercellular signaling) with the convenience of cell culture (e.g., cost- and time-efficient, minimal infrastructure, small quantities of solutions required). The model system overcomes many of the current limitations in rapid to high-throughput screening of drugs/compounds and casts a broad net to rapidly evaluate integrated system effects. Additionally, it is an ideal platform to follow up with targeted studies aimed at the mechanisms of toxic action. Exposures are carried out in multi-well plates so minimal solution volumes are required for the assessments. Numerous morphological, developmental, and behavioral endpoints can be evaluated noninvasively due to the transparent nature of the embryos.

Key words Zebrafish, Development, Embryos, In vivo, Vertebrate, Rapid screening, High-throughput screening

1 Introduction

Numerous biological models can be employed for toxicity evaluations. In vitro techniques, such as cell culture systems, are often preferred because they are both cost- and time-efficient. While these studies are useful, direct translation to whole organisms and human health is often difficult to infer. In vivo studies can provide improved prediction of biological response in intact systems but often require extensive facilities and infrastructure [1–3]. Zebrafish (*Danio rerio*) offer a number of practical advantages as a model organism that overcome these limitations, making these vertebrates highly amenable for toxicologically relevant research. Zebrafish can be employed as a powerful in vivo model system to assess biological interactions and are an outstanding platform to detail the mechanisms by which substances elicit specific biological responses. A remarkable similarity in cellular structure, signaling processes, anatomy, and physiology exists among zebrafish and other high-order vertebrates, particularly early in development [4–8]. Current estimates indicate that over the zebrafish and

human genomes 79% are similar and over 80% of the genes associated with human diseases are present in zebrafish [9]. Thus, investigations using this model system can reveal chemical and genome interactions that are likely to be conserved across species.

Features of the zebrafish's biology are favorable for adapting this model system to high-throughput assays. Female zebrafish are able to produce hundreds of eggs weekly, so large sample sizes are easily achieved, allowing for statistically powerful dose-response studies. This abundant supply of embryos also makes it possible to simultaneously assess the toxicity of a large number of substances in a short period. The vertebrate's rapid developmental progression compared to other mammals makes it an ideal model for high-throughput screening [10]. For example, neuronal plate formation occurs at 10 hours post fertilization (hpf), followed by organogenesis at 24 hpf, which compared to a rat occurs at 9.5 days and 5–6 days respectively. The first heartbeat occurs at 30 hpf for the zebrafish and 10.2 days for rats [11].

Zebrafish embryos can be individually exposed in wells of a multi-well plate so the required volume needed for the model is small; thus, only limited amounts of materials are needed to assess an entire suite of biological interactions and responses. Early developmental life stages are often uniquely sensitive to environmental insult, due in part to the enormous changes in cellular differentiation, proliferation, and migration required to form multiple cell types, tissues, and organs [4, 7, 8, 12]. Since development is highly coordinated requiring specific cell-to-cell communications, if exposure to a substance during that critical period perturbed these interactions, development would be expected to be disrupted. Embryos are waterborne-exposed to a chemical using a continuous method in which 24 embryos are exposed per concentration in individual wells of a multi-well plate from 8 to 120 hpf. Exposure until 120 hpf is the ideal duration for a developmental toxicity testing; primarily due to the vertebrate model's ability to obtain its nutrients from its yolk sac until 5 days, which will not introduce additional external confounding factors. Perturbed development can manifest as morphological malformations, behavioral abnormalities, or death of the embryos. Zebrafish embryos develop externally and are optically transparent so it is possible to resolve individual cells in vivo throughout the duration of an exposure using simple microscopic techniques and numerous effects can be assessed noninvasively over the course of development.

2 Materials

2.1 Zebrafish Husbandry

1. Fish water: 0.3 g/L Instant Ocean salts (Aquatic Ecosystems, Apopka, FL) in reverse osmosis (RO) water.
2. Incubator set at 28 ± 0.1 °C.
3. Fish food: Gemma Micro (Skretting Inc, Tooele France).

2.2 Dechorination

1. Compound stereo microscope for viewing embryos.
2. 60 mm glass petri dish.
3. 22.24 U/mL of total activity pronase per 100 μ L aliquot (Roche, Catalog No: 10165921001) in ultra pure water. Assuming the activity level of the powder pronase is ≥ 7 U/mg, weigh 317.77 mg of pronase into 50 mL glass beaker and fill it with 5 mL of ultra pure water. Gently vortex the 50 mL pronase: ultra pure water mixture with stir bar in refrigerator for 30 min. Remove beaker and keep on ice. Aliquot 100 μ L into 1.5 mL microcentrifuge tube and place them into a freezer box, then immediately place into the box into the freezer. This will make 50 1.5 mL microcentrifuge tubes that can be stored for up to 4 months. Aliquots can be thawed just prior to use.
4. Timer.

2.3 Exposure

1. Multi-well plates.
2. 8 or 12 multichannel pipette.
3. 50 mL reagent reservoir.
4. Wide-bore Pasteur pipette.

2.4 Assessment

1. Anesthesia: 4 mg/mL of 3-aminobenzoate ethyl ester methanesulfonate salt (tricaine, Sigma-Aldrich) in RO water, pH adjusted to 7.0 with 0.1 M Tris-HCl, pH 9.0.
2. Methyl cellulose: 10 mg/mL of methyl cellulose (Sigma-Aldrich, *see Note 1*).

3 Methods

3.1 Zebrafish Husbandry

1. Rear adult zebrafish *Danio rerio* in standard laboratory conditions of 28 °C with a pH of 7 ± 0.2 on a 14 h light/10 h dark photoperiod [13].
2. House zebrafish in 2.0-L polycarbonate tanks with recirculating water system. Keep adult zebrafish in groups to allow for large quantities of embryos to be collected. Group spawning also helps to increase genetic diversity.
3. Feed the fish twice daily with Gemma Micro feed.
4. Spawning: place male and female zebrafish into spawning baskets in polycarbonate tanks the afternoon before the embryos are needed. Zebrafish will typically spawn when the lights come on after the 10 h dark period.
5. The following morning, newly fertilized eggs are collected, rinsed several times in system water, and placed into fresh fish water in a 150 mm plastic petri dish.

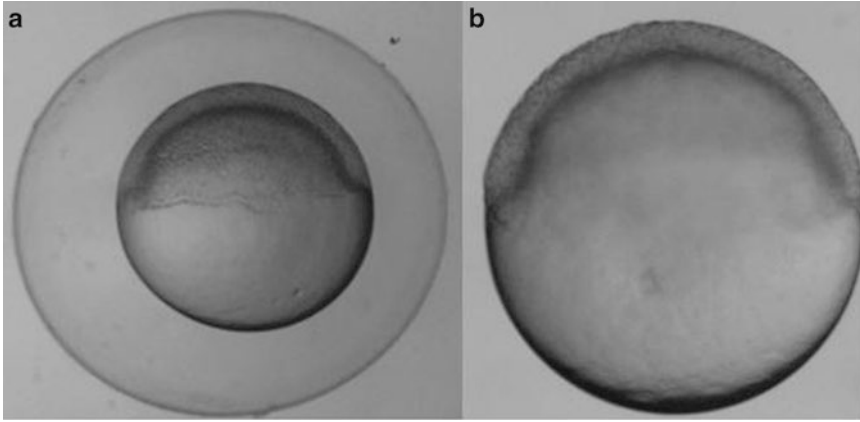


Fig. 1 Six hours post fertilization embryos. (a) Six hpf embryo with its chorion. (b) Six hpf embryo after using pronase to enzymatically remove its chorion

6. Remove embryos that are unfertilized or necrotic prior to placing the petri dish into the incubator to keep warm until the embryos reach 6 hours post fertilization (hpf) (Fig. 1) [10].
7. Remove embryos that are not the same stage as the majority prior to experimental use (*see Note 2*).

3.2 Dechorination

1. To avoid barrier effects potentially posed by the chorion, all embryos should be dechorinated at 6 hours post fertilization (hpf) using a protocol for pronase enzyme degradation [14–16].
2. Place 6 hpf embryos into a 60 mm glass petri dish with 25 mL fish water (*see Note 3*). Up to 1000 embryos can be processed in a single dish using this method [17].
3. Add 83 μL of 31.77 mg/mL pronase (with ≥ 7 U/mg pronase activity level) to the center of the dish and continuously swirl gently to mix the solution.
4. Set a timer for 6 min, and continuously swirl the embryos while occasionally observing the petri dish under the microscope to check for embryos without chorions, chorion pieces in the solution, and “deflated” chorions.
5. When 7 min have passed, or when the above are observed, remove the pronase solution by diluting the solution with fresh fish water, slowly decanting over the edge of the petri dish continuously for 1 min, then repeat this procedure for a total of 10 min (*see Note 4*).
6. After the rinse, allow the embryos to recover in the petri dish in an incubator (or a room at 28 °C) for 30 min (*see Note 5*).

3.3 Exposure

3.3.1 Waterborne Exposure

1. Chemicals should be dissolved in ultra pure water if possible (*see Note 6*). In the case that this is not possible, the solvent of choice for exposure utilizing the embryonic zebrafish is dimethyl sulfoxide (DMSO) (*see Note 7*).
2. Pour each test solution into a 50 mL reagent reservoir, which will fit a multichannel pipette.
3. For each exposure concentration tested, use a multichannel pipette to fill 16 individual wells in a multi-well plate with 100 μ L of chemical solution. Five concentrations and one control group can be tested using two 96-well plates.
4. At 8 hpf, transfer viable, appropriately developing embryos into individual wells of a multi-well plate using a wide-bore glass pipette (*see Note 8*).
5. Incubate at 28 °C until 24 hpf, then perform assessments.

3.3.2 Microinjection Exposure

1. If direct delivery of a chemical is necessary to ensure accurate dose delivery, embryos should be microinjected at 8 hpf (*see Note 9*).
2. Align 8 hpf embryos in troughs embedded in a 1% agarose plate filled with fish water as described by *The Zebrafish Book* [11, 13].
3. Inject each embryo with 2.3 nL of the desired chemical concentration or the appropriate vehicle control directly into the yolk.
4. Place each embryo into individual wells of a 96-well plate, each filled with 100 μ L of fish water. When directly delivering a chemical into the yolk sac, any concentration above 0.1% DMSO caused developmental defects not attributed to the chemical. If a chemical requires a solvent, two sets of serial dilutions should be made. The first serial dilution should be 100 times higher than the final concentration desired made with 100% DMSO (*see Note 10*) For the second set of serial dilutions, from the 100% DMSO serial dilution, make a 1:10 dilution from the first serial dilution. Make sure to have an appropriate control for each chemical, which includes the correct percentage of solvent used in each solution.
5. Incubate at 28 °C until first assessments at 24 hpf.

3.4 Assessment

1. At 24 hpf, embryos are assessed for viability, developmental progression, and spontaneous movements (earliest behavior in zebrafish). Developmental progression is considered perturbed if zebrafish are more than 12 h delayed compared to control animals. Spontaneous movements are assessed over a 2 min period and are considered perturbed if there is a lack of embryonic contractions and/or movement.

2. At 120 hpf, larval morphology (body axis, eye, snout, jaw, otic vesicle, notochord, heart, brain, somite, fin, yolk sac, trunk, circulation, pigment, swim bladder; Fig. 2) is evaluated and recorded and behavioral endpoints (motility, tactile response)



1. **120 hr mortality** – dies between 24 and 120 hours post fertilization (hpf)

2. **24 hr mortality** – dies before 24 hpf



3. **24 hr sp. Mov** – no spontaneous movement at 24 hpf

4. **24 hr dev prog** - delayed development



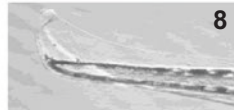
5. **24 hr notochord** – notochord malformation (wavy notochord)

6. **axis** – curved or bent axis in either direction



7. **brain** - brain malformations or necrosis

8. **caudal fin** – malformed or missing



9. **circulation** – no circulation or blood flow

10. **eye** – eyes malformed, missing or smaller/larger than normal

11. **heart** – heart malformation, pericardial edema (fluid around the heart)

11, 12, 15, 16, 17, 18, 20, 21

12. **jaw** – malformed



13. **otic** – malformed or missing

14. **pectoral fin** – malformed or missing

15. **pigmentation** – lack of pigmentation, overpigmentation

16. **snout** – shortened or malformed

17. **somite** – malformed or disorganized, missing somites

18. **swim bladder inflate** – failure of swim bladder to inflate



19. **touch response** – not responsive to touch at 120 hpf

20. **trunk** – short trunk, malformed or missing

21. **YSE** – yolk sac edema, swelling around the yolk sac

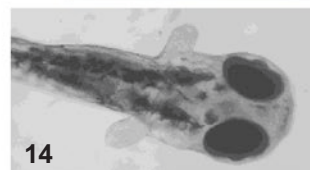


Fig. 2 Visual assessment of zebrafish morphology. Images are given as examples of typical chemical-induced malformations observed in the zebrafish

are thoroughly evaluated *in vivo*. Test for behavioral endpoints and then anesthetize animals for thorough morphological analysis. At the end of the assessments, zebrafish are euthanized with tricaine.

3. Evaluations are completed in a binary notation (present or not present) (*see Note 11*). Control and chemical-exposed groups are statistically compared using Fisher's Exact test at $p < 0.05$ with R software for each endpoint evaluated (Fig. 2).

4 Notes

1. Methyl cellulose is unique in that it “melts” when cold and solidifies when hot. It dissolves best in cold water; however, it is best to disperse the powder form in warm water and then continue to mix while chilling. An alternate to the methyl cellulose is Protoslo® (Carolina Biological Supply Company, Burlington, NC).
2. Eggs can sometimes be laid and fertilized at different times in a group spawns; therefore always remove embryos that are developing more rapidly or significantly slower prior to using them for an experiment. As an alternate, male and female pairs can be set up in several divided tanks, and the dividers can be removed at the same time. The resulting stage matched embryos can then be pooled, prior to random embryo selection.
3. Do not bleach embryos if their chorions are to be removed by pronase digestion. Bleaching modifies the chorion and pronase treatment is completely ineffective. In addition, when dechorinating embryos it is essential to use glass petri dishes. Dechorinated embryos will stick to the bottom of plastic dishes and will be severely damaged during the procedure.
4. The newly dechorinated embryos are very delicate. Water should be administered with a gentle flow and not directly onto the embryos. Some of the embryos will not be out of their chorion even once the 10 min rinsing period is done. More will emerge during the recovery period.
5. Once an embryo is dechorinated, do not bleach the embryos.
6. Chemicals or drugs that are thought to be inactive until metabolized to an active form may be pre-exposed to induce and active conformation prior to waterborne exposures.
7. The Sinnhuber Aquatic Research Laboratory at Oregon State University has demonstrated that an embryo elicited no developmental deformities at 1% DMSO when waterborne-exposed [3, 18–20].

8. Be sure to allow the embryo to fall to the bottom of the wide-bore Pasteur pipette prior to touching the solution in the wells. If an embryo disintegrates when it reaches the solution, make sure to replace the solution and place a new embryo in the well.
9. All methods discussed are continuous waterborne exposure, but if no analytical method is available to determine biological uptake, an alternative is to directly deliver the chemical into the animal through microinjection. Because embryos are transparent, tissue dose and distribution can also be determined using fluorescently labeled materials and laser scanning confocal microscopy.
10. Make sure to vortex each microcentrifuge tube prior to the next dilution to ensure it is a homogenous solution.
11. If more than 20% of the animals in the control group are adversely affected (any endpoint, including mortality), then the experiment is not valid and will need to be repeated. Test chemicals may have specific targets in humans, but this target may not be completely conserved structurally in other vertebrate models. The structural differences between vertebrates and humans can result in either false negatives or false positives. For example, if a drug is designed to target a human specific structure that is not well conserved in zebrafish, upon exposure, the drug would not influence the zebrafish target. The effects observed when this occurs are considered false negatives. Vice versa, a false positive can also occur when effects observed due to a drug impacting a specific target expressed only in zebrafish, but this target is not structurally conserved in humans. Another consideration is that chemical toxicity may be dependent on metabolic activity. False negatives and false positives may also occur if the metabolic activity in the zebrafish embryo is distinct from human metabolic activity. It is possible to use exogenous mammalian metabolic activation system to reduce false positive and false negatives [21].

Acknowledgments

The authors would like to thank the Sinnhuber Aquatic Research Laboratory and the Environmental Health Sciences Center at Oregon State University where much of the protocols were developed. This work was supported by NIEHS grants P30 ES000210.

References

1. Harper SL et al (2008) Proactively designing nanomaterials to enhance performance and minimise hazard. *Int J Nanotechnol* 5(1):124–142
2. Reif DM et al (2016) High-throughput characterization of chemical-associated embryonic behavioral changes predicts teratogenic outcomes. *Arch Toxicol* 90(6):1459–1470
3. Truong L et al (2014) Multidimensional in vivo hazard assessment using zebrafish. *Toxicol Sci* 137(1):212–233
4. Levin ED et al (2004) Developmental chlorpyrifos effects on hatchling zebrafish swimming behavior. *Neurotoxicol Teratol* 26(6):719–723
5. Blechinger SR et al (2002) Developmental toxicology of cadmium in living embryos of a stable transgenic zebrafish line. *Environ Health Perspect* 110(10):1041–1046
6. Rasooly RS et al (2003) Genetic and genomic tools for zebrafish research: the NIH zebrafish initiative. *Dev Dyn* 228(3):490–496
7. Rubinstein AL (2003) Zebrafish: from disease modeling to drug discovery. *Curr Opin Drug Discov Devel* 6(2):218–223
8. Spitsbergen J, Kent M (2003) The state of the art of the zebrafish model for toxicology and toxicologic pathology research—advantages and current limitations. *Toxicol Pathol* 31:62–87
9. Howe K et al (2013) The zebrafish reference genome sequence and its relationship to the human genome. *Nature* 496(7446):498–503
10. Kimmel CB et al (1995) Stages of embryonic development of the zebrafish. *Dev Dyn* 203(3):253–310
11. Westerfield M (1995) *The Zebrafish Book*. University of Oregon Press, Eugene
12. Henken DB et al (2003) Recent papers on Zebrafish and other aquarium fish models. *Zebrafish* 1:305–311
13. Akimenko MA et al (1995) Differential induction of four *msx* homeobox genes during fin development and regeneration in zebrafish. *Development* 121(2):347–357
14. Martinez-Sales M, Garcia-Ximenez F, Espinos FJ (2015) Zebrafish (*Danio rerio*) as a possible bioindicator of epigenetic factors present in drinking water that may affect reproductive function: is chorion an issue? *Zygote* 23(3):447–452
15. Henn K, Braunbeck T (2011) Dechoriation as a tool to improve the fish embryo toxicity test (FET) with the zebrafish (*Danio rerio*). *Comp Biochem Physiol C Toxicol Pharmacol* 153(1):91–98
16. Kim KT, Tanguay RL (2014) The role of chorion on toxicity of silver nanoparticles in the embryonic zebrafish assay. *Environ Health Toxicol* 29:e2014021
17. Mandrell D et al (2012) Automated zebrafish chorion removal and single embryo placement: optimizing throughput of zebrafish developmental toxicity screens. *J Lab Autom* 17(1):66–74
18. Harper S et al (2008) In vivo biodistribution and toxicity depends on nanomaterial composition, size, surface functionalisation and route of exposure. *J Exp Nanosci* 3(3):195–206
19. Olivares CI et al (2016) Arsenic (III, V), indium (III), and gallium (III) toxicity to zebrafish embryos using a high-throughput multi-endpoint in vivo developmental and behavioral assay. *Chemosphere* 148:361–368
20. Noyes PD et al (2015) Advanced morphological—behavioral test platform reveals neurodevelopmental defects in embryonic zebrafish exposed to comprehensive suite of halogenated and organophosphate flame retardants. *Toxicol Sci* 145(1):177–195
21. Busquet F et al (2008) Development of a new screening assay to identify proteratogenic substances using zebrafish *Danio rerio* embryo combined with an exogenous mammalian metabolic activation system (mDarT). *Toxicol Sci* 104(1):177–188

Part VII

Safety Biomarkers

Absolute Quantification of Toxicological Biomarkers via Mass Spectrometry

Thomas Y.K. Lau, Ben C. Collins, Peter Stone, Ning Tang, William M. Gallagher, and Stephen R. Pennington

Abstract

With the advent of “-omics” technologies there has been an explosion of data generation in the field of toxicology, as well as many others. As new candidate biomarkers of toxicity are being regularly discovered, the next challenge is to validate these observations in a targeted manner. Traditionally, these validation experiments have been conducted using antibody-based technologies such as Western blotting, ELISA, and immunohistochemistry. However, this often produces a significant bottleneck as the time, cost, and development of successful antibodies are often far outpaced by the generation of targets of interest. In response to this, there recently have been several developments in the use of triple quadrupole (QQQ) mass spectrometry (MS) as a platform to provide quantification of proteins. This technology does not require antibodies; it is typically less expensive and quicker to develop assays and has the opportunity for more accessible multiplexing. The speed of these experiments combined with their flexibility and ability to multiplex assays makes the technique a valuable strategy to validate biomarker discovery.

Key words Catalase, Mass spectrometry, Quantification, Proteomics, Biomarkers

1 Introduction

Mass spectrometry-based quantification approaches have grown rapidly over the last 10 years. A plethora of acquisition paradigms, quantitative labels, and standards can be used and combined to quantify proteins and peptides [1–4]. However, the gold standard for the most robust, fast, and sensitive approaches remains multiple reaction monitoring of a proteotypic peptide with stable isotope standard. A proteotypic peptide is a (typically tryptic) peptide with a sequence unique to that protein [5]. Labeled standards consist of biologically or chemically produced peptides that have mass shifts produced by the incorporation of isotopically labeled amino acids. These mass shifts allow the standard to be differentiated from the native peptide while maintaining its chromatographic properties. Here, we describe a workflow for the absolute

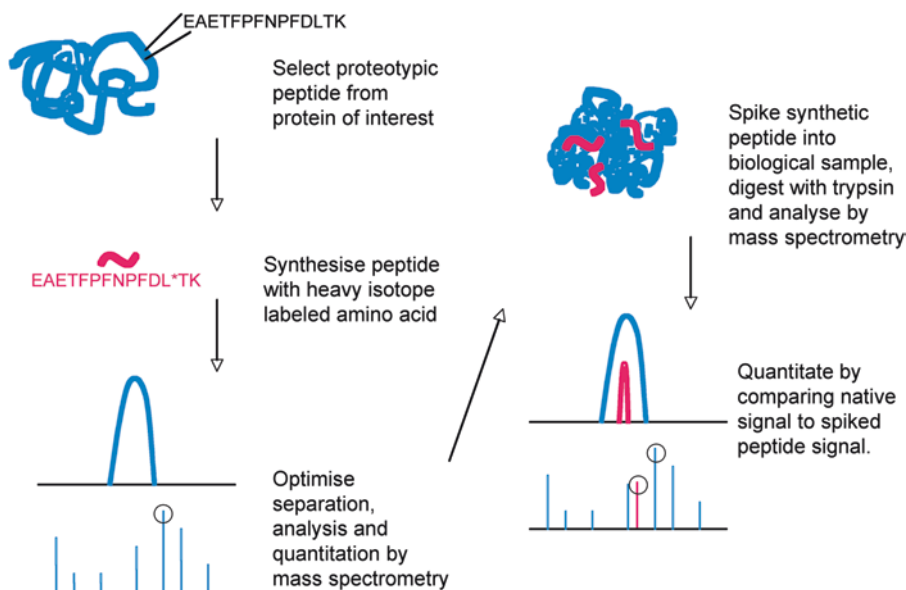


Fig. 1 Workflow for absolute quantification using spiked labeled synthetic peptides. Proteotypic peptides are chosen and then synthesized with an isotope label to differentiate them from endogenous peptides. Quantification is made possible by comparing ratio of known standard to the unknown endogenous

quantification of catalase by peptide multiple reaction monitoring (MRM). In MRM mode, the mass spectrometer filters for a specific precursor mass in the first quadrupole and then another specific fragment ion in the second. This allows for high selectivity even in complex samples matrices. Catalase is an enzyme with a well-established background in removal of reactive oxygen species (ROS) and thus is important to the study of ROS-induced toxicology. Catalase was selected for this proof-of-principle experiment due to its toxicological relevance. The ability to quantify increases in the expression of catalase may indicate oxidative stress and associated toxicological responses. Specifically, we describe in this chapter the selection and design of appropriate stable isotope labeled synthetic peptide standards, protein extraction from rat liver tissue followed by tryptic digestion, sample spiking with synthetic peptide standards, acquisition of data using reverse phase liquid chromatography coupled online to a triple quadrupole mass spectrometer, and processing and interpretation of data. The different steps of the workflow are illustrated in Fig. 1.

2 Materials

Unless otherwise stated all reagents are purchased from Sigma-Aldrich and are of the highest grade available. All solvents were Chromasolv HPLC grade solvents from Sigma-Aldrich. All solutions should be made up in HPLC grade water or solvents.

2.1 Sample Preparation

1. Mortar and pestle.
2. Liquid nitrogen.
3. Tissue Lysis Buffer: 9.8 M urea, 4% CHAPS, 5 $\mu\text{L}/\text{mL}$ protease inhibitor cocktail set III, final conc. 500 μM AEBSF HCl, 0.4 μM Aprotinin, 25 μM Bestatin, 7.5 μM E-64, 10 μM Leupeptin Hemisulfate, 5 μM Pepstatin A (Merck).
4. Reagents for Bradford method.
5. TCEP (tris-2-carboxyethyl-phosphine) is used for denaturing.
6. Iodoacetamide (IAA) for alkylation.
7. Acetone.
8. Ammonium bicarbonate 100 mM.
9. Rapigest 0.1% (w/v) (Waters), an acid labile surfactant, aids solubilization of proteins and increases digestion efficiency.
10. Trypsin (sequencing grade modified porcine) (Promega) for tryptic digestion.
11. Formic acid 2% (v/v).

2.2 Liquid Chromatography and Mass Spectrometry

1. Gradient Buffer A: H_2O with 0.1% formic acid.
2. Gradient Buffer B: 90% acetonitrile with 0.1% formic acid.
3. Column HPLC-Chip 150 mm \times 75 μm , Zorbax 300SB-C18 5 μm , 160 nL trap (Agilent).
4. LC-MS systems: 1200 series nanoLC connected online to a 6510 Q-TOF equipped with a Chip Cube source (Agilent).
5. 1200 series nano LC connected online to a 6410 Triple Quadrupole equipped with a Chip Cube source (Agilent).
6. Mass spectrometer calibrant: ESI-Tuning Mix (Agilent).
7. Synthetic peptides synthesized with C13 and N15 leucine, thus creating a 7 dalton mass shift with respect to the endogenous peptide. Synthetic peptides were synthesized at Peptide Protein Research UK.

2.3 Software

1. Spectrum Mill peptide selector (Agilent).
2. Masshunter qualitative and quantitative analysis software (Agilent).

3 Methods

3.1 Choice and Design of Proteotypic Peptides

As described earlier, a proteotypic peptide is a (typically tryptic) peptide that is unique to a particular protein. Typically a protein will have several proteotypic peptides. However, not all of these peptides will be equally amenable for MS-based quantification, as their abundance and chemical properties may make them

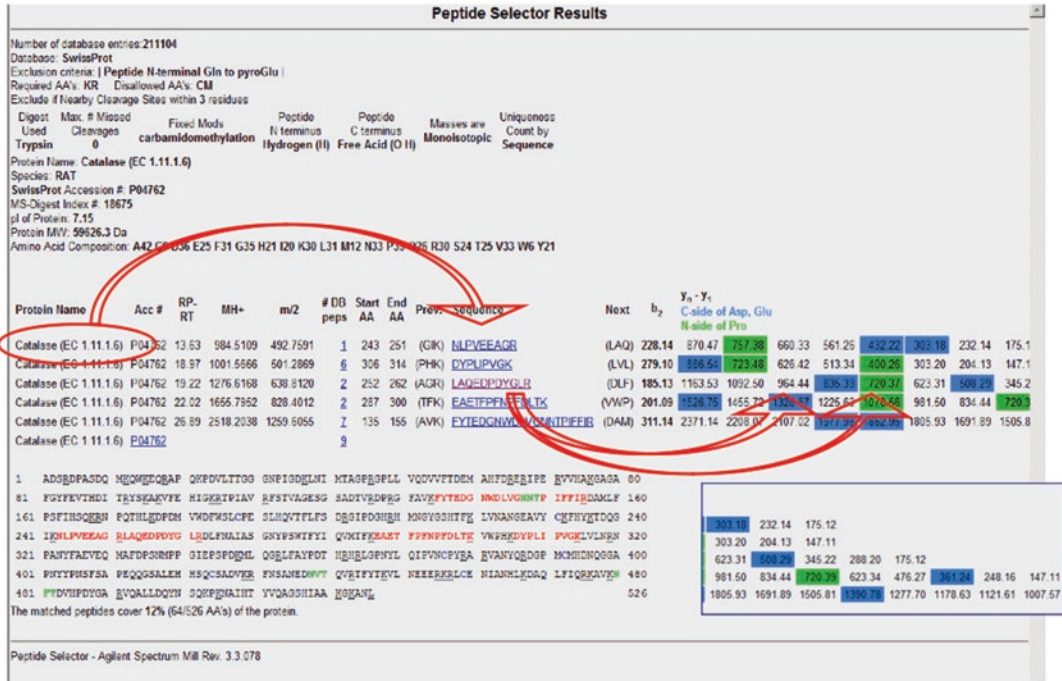


Fig. 2 Search result with Peptide Selector. Peptide Selector performs an in silico tryptic digest and suggests proteotypic peptides and the corresponding fragment ions. It predicts the mass of the ions and which will give the best signal and therefore be good choices to perform MRM quantification on

unsuitable for detection using traditional liquid chromatography and MS. In our experiments, we first used a bioinformatic approach to select peptides that were both unique to catalase and likely to be detected by a mass spectrometer by using the software Peptide Selector as illustrated in Fig. 2.

1. The SwissProt accession number for catalase (*Rattus Norvegicus*) is found at <http://www.expasy.org>.
2. This SwissProt number (P04762) is entered in Spectrum Mill Peptide Selector (Agilent Technologies).
3. The results suggest proteotypic peptides and their likely fragmentation ions in MS/MS.
4. Choose proteotypic peptides that have good predicted ionization and strong predicted fragment ions. In general, it is best to choose peptides that do not contain residues such as cysteine and methionine which are prone to modification during the sample preparation and digestion procedure. Even a substoichiometric modification would cause a portion of the endogenous peptide to be unobservable by this type of targeted approach and could lead to a significant bias in results. See **Notes 1** and **6** for more information on peptide selection.

3.2 Sample Preparation

In this study we analyzed liver tissue from rats that have drug-induced toxicity. Parallel studies have indicated that catalase is upregulated in high doses of the drug.

1. Pulverize 50–100 mg of frozen tissue using a pestle and mortar and liquid nitrogen.
2. Dissolve powdered tissue in 1000 μL tissue lysis buffer.
3. Vortex for 30 s and pipette up and down 30 times.
4. Put the samples on an orbital shaker (~ 1000 rpm) for 60 min at RT.
5. Centrifuge at 13,000 g for 5 min.
6. Determine protein concentration (using Bradford method).
7. Dilute 100 μg of proteins from each sample to 20 μL with tissue lysis buffer and vortex briefly.
8. Reduce disulfide bonds with 5 mM (final conc.) TCEP (tris 2 carboxyethyl phosphine), i.e., add 2 μL of 50 mM TCEP and incubate for 60 min.
9. Alkylate reduced thiols with 10 mM (final conc.) IAA, i.e., add 1 μL of 200 mM IAA and incubate at RT in the dark for 30 min.
10. Precipitate proteins using 6 volumes of acetone (stored at -20 $^{\circ}\text{C}$) for 3 h.
11. Pellet the precipitate by centrifugation for 10 min at 5000 g at 4 $^{\circ}\text{C}$ (pre-cool centrifuge) and aspirate acetone.
12. Resuspend the pellet in 20 μL 100 mM ammonium bicarbonate, 0.1% (w/v) Rapigest. It may be necessary to increase the volume of this solution or the concentration of Rapigest to achieve complete solubilization of proteins.
13. Add 5 μg trypsin and incubate for 18–24 h at 37 $^{\circ}\text{C}$.
14. Add formic acid to a concentration of 2% (v/v) and incubate for 4 h at 37 $^{\circ}\text{C}$ to degrade the Rapigest surfactant. The surfactant hydrolysis products are insoluble and are pelleted by centrifugation at 13,000 g for 30 min. The supernatant is then removed and stored at -80 $^{\circ}\text{C}$ until further analysis. *See Notes 3–5* for more information on tryptic digestion.

3.3 Test Run of Tissue Lysate Sample

To ensure presence of the catalase proteotypic peptide and correct digestion of the sample, the digested tissue lysate sample was run on full scan mode on an Agilent QQQ.

1. Calibrate the mass spectrometer using an ESI-Tuning Mix and purge the liquid chromatography (LC) lines. Set the nano pump to run at 0.3 $\mu\text{L}/\text{min}$ and the capillary pump to run at 3 $\mu\text{L}/\text{min}$. Check that the source is receiving a good stable electrospray.
2. Set the gradient timetable for the LC indicated in Table 1.

Table 1
LC gradient timetable for lysate test run

Minutes	Percentage B
0	2
40	42
45	90
48	90
48.1	3

3. Set the mass spectrometer to run in full scan mode.
4. Run a blank sample of HPLC H₂O to clear and check the system.
5. Assuming the blank sample ran without issues (*see Note 2*), inject a 5 μ L sample.
6. Open the data results in Spectrum Mill. Using an “Easy MS/MS” search, one should be able to detect the catalase proteotypic peptide and also see which fragment ions are the strongest as illustrated in Fig. 3.

3.4 External Calibration of Synthetic Peptides

Before performing the relative quantification typically used in these experiments, we must first optimize the experiment by creating a calibration curve and selecting the best collision energy and fragmentor values for each MRM transition.

1. Purge the LC system and calibrate the instrument using the ESI-Tuning mix.
2. Resuspend the lyophilized synthetic peptides in 3% acetonitrile with 0.1% formic acid and make dilutions to correspond to 100 fg, 1 pg, 10 pg, 100 pg, 1 ng, 10 ng in a pool of the tissue lysate digests.
3. Set the mass spectrometer to detect the MRM transitions under different collision energies and fragmentation values.
4. Run a test sample of tissue with a spike of 1 ng synthetic peptide using the LC gradient indicated in Table 2.
5. Using Masshunter Qualitative Analysis software, assess which collision energy and fragmentation values give the strongest MRM signal for the spiked peptide.
6. Once the collision energy has been optimized, run the tissue lysate with spiked peptides (using the same method as previously) with at least triplicate injections and in order of increasing concentrations of spiked synthetic peptides.



Fig. 3 Detailed information on the fragmentation pattern of the peptide helps select the optimal MRM transitions. Spectrum Mill Peptide Selector can provide in-depth detail of the fragmentation pattern of a peptide. A side-by-side comparison highlights that the in silico predictions can be reasonably accurate when compared to data acquired from the mass spectrometer. The ions detected on the mass spectrometer are matched with predicted masses with arrows, including the precursor, which is marked with an *asterisk*

Table 2
LC gradient timetable for MRM run

Minutes	Percentage B
0	0
35	35
40	90
50	90
54	3

External quantitation curve of catalase peptide EAETFPNPFDL*TK from 60 amol to 6000 fmol

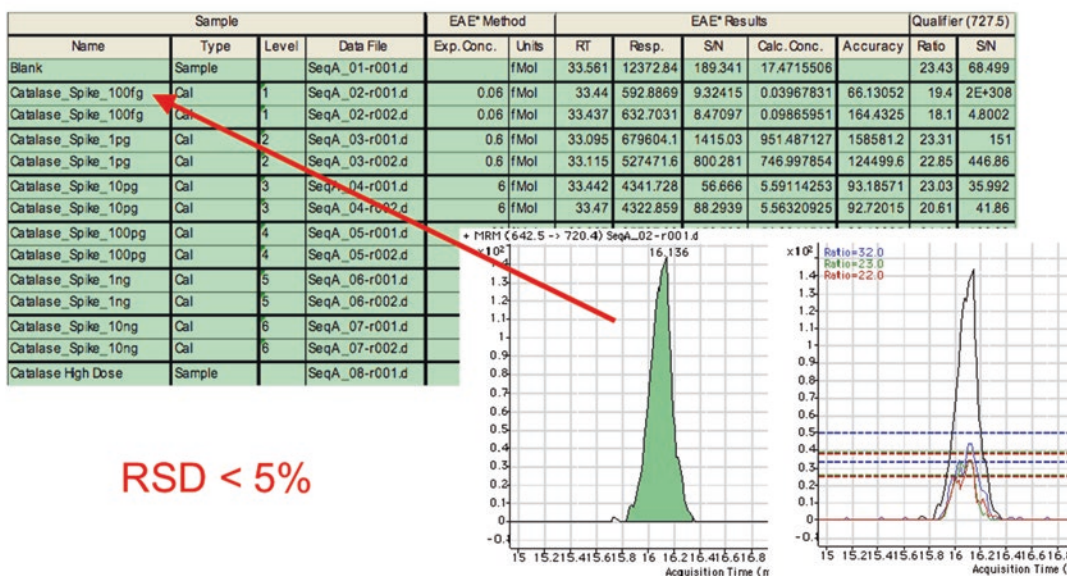


Fig. 4 Quantification of MRM peaks. This figure shows the output following peak integration using the Masshunter quantitative analysis software, which automatically calculates the response of the peptide in the mass spectrometer. The table gives us information such as signal to noise (S/N), response, and accuracy for the different concentrations of our standard. The *arrow* indicates that we can detect and integrate a well-defined peak at low concentrations such as 60 amol. The adjoining image has overlaid the peaks from different concentrations. The quantification is reliable with a relative standard deviation (RSD) of less than 5%

- Using Masshunter Quantitative Analysis software, import the data generated and assign the appropriate concentration values and MRM transitions for peak integration and generation of a calibration curve as illustrated in Figs. 4 and 5.
- The calibration curve should have an R-squared value close to 1.

**External quantitation curve
of catalase peptide
EAETFPFNPFDL*TK from 60
amol to 6000 fmol**

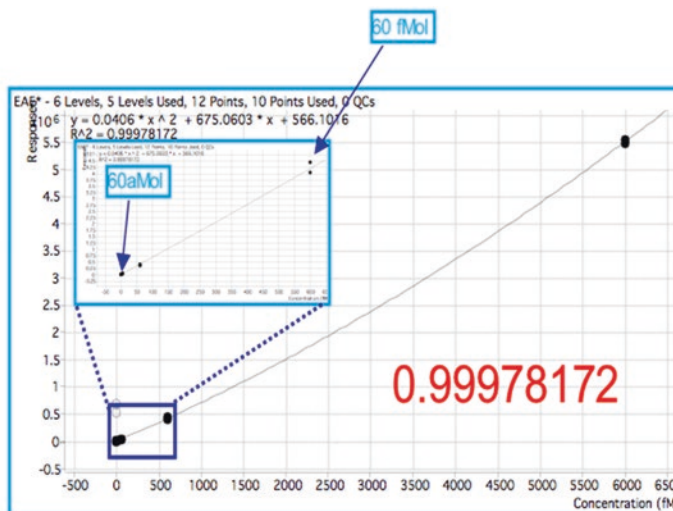


Fig. 5 External calibration curve. The calibration curve shows good linear response over 6 orders of magnitude and sensitivity reaching the amol range. This is important where one might be quantifying biomarkers with very low abundance and/or large dynamic changes in quantity. The coefficient of correlation is indicated in the *bottom right* and is approximately 1

3.5 Relative Quantification

1. Prepare the mass spectrometer and LC systems as described for the External calibration curve (*see* Subheading 3.4). Set the mass spectrometer to monitor the MRM transitions of both the synthetic peptide and the native proteotypic peptide.
2. Run the tissue lysate sample as before but with the addition of a single 1 ng spike of the synthetic peptide.
3. Import the data into the Masshunter Quantitative Analysis software. Assign the synthetic peptide as an internal standard. Integrate the MRM peaks and the software will provide calculated concentrations as illustrated in Table 3.

4 Notes

1. When selecting proteotypic peptides, as well choosing peptides that do not have methionine and cysteines, it may also be necessary to exclude peptides next to multiple cleavage sites and peptides with chemically reactive residues (such as D-G, N-G and end terminal N and E).

To further validate the quantification it is suggested that at least three or four peptides are used so that the calculated concentrations can be compared between different peptides.

For each peptide, several (at least two) MRM transitions should be used for the same reason of comparing consistency of quantification. In addition, the ratio of these qualifier transitions to the primary MRM can be used as a quality control measure

Table 3
The results table gives information on the retention time (RT), Response (Resp) and Signal to Noise ratio (S/N)

Sample	Results			Qualifier 1		Qualifier 2		ISTD		
	RT	Resp	S/N	Calc conc	Ratio	S/N	Ratio	S/N	RT	Resp
Lysate Replicate 1	33.394	11,551	296.85	3063.939	20.65	113.38	25.73	20.79	33.436	3770
Lysate Replicate 2	33.446	12,059	249.95	4599.204	19.16	216.6	23.03	17.85	33.42	2622

A ratio is calculated from the known spiked synthetic peptides (internal standard, ISTD). This is compared to two MRM responses for the native peptide (qualifiers 1 and 2) to produce a calculated concentration

to detect a potential interfering MRM. This ratio, within an acceptable error, as determined with the standard peptides should be consistent for the endogenous peptide and this will be flagged in the Quantitative Analysis software if this is not the case.

- Standard LC-MS practices to minimize carryover should be utilized, i.e., running blanks, run samples in increasing concentrations, etc.
- All samples should be kept at 4 °C while being used. Otherwise, samples should be stored at –20 °C.
- The premise of using a tryptic peptide as a surrogate measure of the concentration of a protein is completely dependent on effective digestion of the parent protein by trypsin. Particular attention should be paid to following the digestion protocol. If modification of the protocol is required a recent article details a number of tryptic digestion protocols and associated issues [6].
- The efficiency of the tryptic digestion tends to decrease with increasing volume. It is recommended to keep the volume below 50 µL where possible.
- It is worth noting that large depositories of empirical mass spectrometry data are now publically available. This can give greater confidence and supplement in silico predictions. Commonly used databases include Proteomicsdb [7], PeptideAtlas [8], and GPM [9]. In addition, a computational tool for predicting observable peptides from physicochemical properties based on empirical data is available [10].

Absolute quantification experiments via MRM are very amenable to multiplexing (naturally this will require the synthesis of additional synthetic peptides). The limit of the multiplex capability is related to the duty cycle of the mass spectrometer.

As additional MRMs are added, the duty cycle will increase and the number of points for each MRM across the chromatographic peak will be reduced (at least 10–12 data points are required for each MRM). As the dwell time for each MRM is decreased, a loss of sensitivity and signal to noise ratio will be observed.

It can be useful to integrate data from multiple steps in assay development and experiments, especially for larger data sets with high numbers of samples and analytes. Software such as Skyline can provide a powerful interface for combining spectral libraries, different data sources, and experiments across the assay pipeline [11].

Acknowledgments

The authors would like to thank Agilent Technologies, Santa Clara, for generating much of the data and figures used in this example. We would like to also thank all members of the PredTox Consortium. Funding is acknowledged under the FP6 Integrated Project, InnoMed. The UCD Conway Institute and the Proteome Research Centre is funded by the Programme for Research in Third Level Institutions (PRTL), as administered by the Higher Education Authority (HEA) of Ireland.

References

1. Gerber SA, Rush J, Stemman O, Kirschner MW, Gygi SP (2003) Absolute quantification of proteins and phosphoproteins from cell lysates by tandem MS. *Proc Natl Acad Sci U S A* 100:6940–6945
2. Anderson L, Hunter CL (2005) Quantitative mass spectrometric multiple reaction monitoring assays for major plasma proteins. *Mol Cell Proteomics* 5:573–588
3. Abbatiello SE, Mani DR, Schilling B, MacLean B, Zimmerman LJ, Feng X, Cusack MP, Sedransk N, Hall SC, Addona T, Allen S, Dodder NG, Ghosh M, Held JM, Hedrick V, Inerowicz HD, Jackson A, Keshishian H, Kim JW, Lyssand JS, Riley CP, Rudnick P, Sadowski P, Shaddox K, Smith D, Tomazela D, Wahlander A, Waldemarson S, Whitwell CA, You J, Zhang S, Kinsinger CR, Mesri M, Rodriguez H, Borchers CH, Buck C, Fisher SJ, Gibson BW, Liebler D, MacCoss M, Neubert TA, Paulovich A, Regnier F, Skates SJ, Tempst P, Wang M, Carr SA (2013) Design, implementation and multisite evaluation of a system suitability protocol for the quantitative assessment of instrument performance in Liquid Chromatography-Multiple Reaction Monitoring-MS (LC-MRM-MS). *Mol Cell Proteomics* 12(9):2623–2639. doi:10.1074/mcp.M112.027078
4. Egertson JD, MacLean B, Johnson R, Xuan Y, MacCoss MJ (2015) Multiplexed peptide analysis using data-independent acquisition and Skyline. *Nat Protoc* 10(6):887–903. doi:10.1038/nprot.2015.055
5. Kuster B, Schirle M, Mallick P, Aebersold R (2005) Scoring proteomes with proteotypic peptide probes. *Nat Rev Mol Cell Biol* 6(7):577–583
6. Chen EI, Cociorva D, Norris JL, Yates JR 3rd (2007) Optimization of mass spectrometry-compatible surfactants for shotgun proteomics. *J Proteome Res* 6(7):2529–2538
7. Wilhelm M, Schlegl J, Hahne H, Moghadda Gholami A, Lieberenz M, Savitski MM, Ziegler E, Butzmann L, Gessulat S, Marx H, Mathieson T, Lemeer S, Schnatbaum K, Reimer U, Wenschuh H, Mollenhauer M, Slotta-Huspenina J, Boese JH, Bantscheff M,

- Gerstmair A, Faerber F, Kuster B (2014) Mass-spectrometry-based draft of the human proteome. *Nature* 509(7502):582–587. doi:[10.1038/nature13319](https://doi.org/10.1038/nature13319)
8. Desiere F, Deutsch EW, King NL, Nesvizhskii AI, Mallick P, Eng J, Chen S, Eddes J, Loevenich SN, Aebersold R (2006) The PeptideAtlas project. *Nucleic Acids Res* 34(Database issue):D655–D658
9. Craig R, Cortens JP, Beavis RC (2004) Open source system for analyzing, validating, and storing protein identification data. *J Proteome Res* 3(6):1234–1242
10. Mallick P, Schirle M, Chen SS, Flory MR, Lee H, Martin D, Ranish J, Raught B, Schmitt R, Werner T, Kuster B, Aebersold R (2007) Computational prediction of proteotypic peptides for quantitative proteomics. *Nat Biotechnol* 25(1):125–131
11. MacLean B, Tomazela DM, Shulman N, Chambers M, Finney GL, Frewen B, Kern R, Tabb DL, Liebler DC, MacCoss MJ (2010) Skyline: an open source document editor for creating and analyzing targeted proteomics experiments. *Bioinformatics* 26(7):966–968. doi:[10.1093/bioinformatics/btq054](https://doi.org/10.1093/bioinformatics/btq054)

Next-Generation Sequencing to Investigate Urinary microRNAs from *Macaca fascicularis* (Cynomolgus Monkey)

Yaligara Veeranagouda, Jean-François Léonard, Jean-Charles Gautier, and Eric Boitier

Abstract

Advanced sequencing technologies like next-generation sequencing (NGS) not only detect microRNAs (miRNAs) in biological samples but also facilitate de novo identification of miRNAs. Using an Ion Torrent's Ion Proton System, here we described miRNAs sequencing of urine samples collected from *Macaca fascicularis* (Cynomolgus monkey) to investigate miRNAs as potential novel biomarkers of nephrotoxicity in this species. Urinary miRNA sequencing methodologies described here include (a) urinary exosomal RNA isolation, (b) sequencing library preparation, (c) sequencing template preparation, and (d) template library sequencing using Ion Proton System. The sequencing method presented in this study serves as a valuable resource in the identification of novel urinary miRNAs in *M. fascicularis*.

Key words Next-Generation Sequencing, microRNAs, Ion Torrent, Cynomolgus monkey, Urine, Biomarkers, Kidney

1 Introduction

Recent evolution in sequencing technologies has enabled the massively parallel and high-throughput sequencing of DNA/RNA [1, 2]. Next-generation sequencing (NGS) is a hypothesis-free approach which allows sequencing of all existing DNA/RNA present in a given sample. Several platforms can be used to perform NGS experiments. Among these platforms the Ion Torrent's Ion Proton System is a benchtop sequencing system capable of human-scale genome, exome, or transcriptome sequencing in a few hours—with DNA-to-variants called in a single day. Unlike other sequencing platforms such as Illumina which rely on fluorescent-labeled nucleotides and the detection of a fluorescent signal, the Ion Proton System is based on the detection of protons that are released during the polymerization of a template-directed DNA

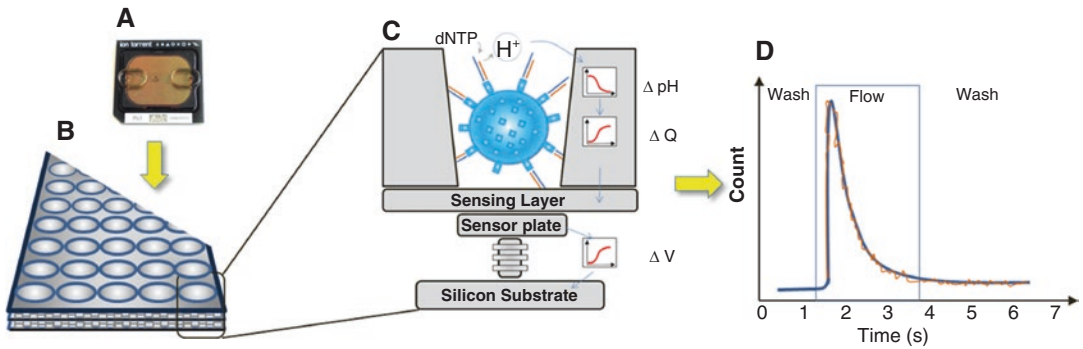


Fig. 1 Principle involved in ion proton sequencing. (A) Ion PI chip, (B) enlarged view of PI chip, (C) schematic view of a single sequencing well, a Ion Sphere Particles (ISPs) containing DNA template and transistor-based sensor, and (D) 1-nucleotide incorporation signal. Protons (H^+) are released when DNA polymerase incorporates nucleotide to the growing DNA. Each well in Ion PI chip contains ion-sensitive, field-effect transistor-based sensors in perfect register with 148 million wells, which provide confinement and allow parallel, simultaneous detection of independent sequencing reactions. Ion Proton sequencer uses the most widely used technology for constructing integrated circuits, the complementary metal-oxide semiconductor (CMOS) process. The Ion PI Chip provides 80 million usable reads/sequencing run (figures were adapted from Life Technology, Ion Proton sequencing presentations)

sequence made of unmodified natural nucleotides by using a massively parallel semiconductor-sensing device on Ion PI chip [3, 4]. It combines complementary metal-oxide semiconductor (CMOS) based sequencing technology with biochemistry to directly translate chemical information into digital data [3] (Fig. 1).

MicroRNAs (miRNAs) are small (18–24 nucleotide long) non-coding RNAs and play a vital role in the regulation of gene expression [5]. They are involved in almost all biological processes and hence their dysregulation is associated with diseases such as cancer and autoimmune disorders [6, 7]. MiRNAs expressed in tissue are transported to different location through biofluids [8]. In biofluids, miRNAs are packed in exosomes and/or associated with proteins/lipoproteins and hence they are protected from nucleases [9]. Several studies in the past decade indicated that miRNAs in biofluids could reveal physiological status/pathological condition of tissue/organ. Thus there is a growing interest in exploring miRNAs as potential biomarkers in biofluids [10–12]. Recently, urinary miRNAs have been identified as candidate kidney safety biomarkers in rats by the HESI Biomarkers of Nephrotoxicity Committee [13, 14]. However, there is a knowledge gap on urinary miRNAs in other preclinical species like *Macaca fascicularis* (*Cynomolgus monkeys*) which can be used in the safety evaluation of new biopharmaceuticals.

The NGS approach allows identification/sequencing of known miRNAs and also potentially identifies novel miRNAs in a given biological sample. We used the Ion Torrent's Ion Proton System to extensively investigate urinary miRNAs in *M. fascicularis* [15, 16]. In this chapter, we describe the various steps involved in urine miRNA sequencing.

2 Materials

2.1 RNA Isolation from *M. fascicularis* Urine and Determination of RNA Concentration

2.1.1 Urine Exosome Precipitation

1. Urine from *Macaca fascicularis* (see **Note 1**).
2. miRCURY Exosome Isolation Kit—Cells, Urine and CSF.
3. Benchtop centrifuge (or swing bucket centrifuge) and microcentrifuge ($\geq 13,000 \times g$).
4. 1.5 mL and 2 mL nuclease-free Microfuge tubes.
5. Pipette and nuclease free tips.
6. Vortexer/multi-vial vortex shaker.
7. Ethanol (96–99.9%, v/v).
8. Ice bucket and ice.

2.1.2 RNA Isolation from Exosomes and RNA Concentration

1. miRCURY RNA Isolation Kit—Cell & Plant.
2. Benchtop microcentrifuge.
3. Ethanol (96–100%, v/v).
4. Pipette and nuclease free tips.
5. Vacuum concentrator.

2.2 Accessing miRNA Quality and Quantity

1. Agilent 2100 Bioanalyzer system (Agilent Technologies).
2. Agilent 2100 Chip priming station.
3. IKA vortex mixer.
4. Agilent Small RNA kit.
5. RNaseZAP for electrode decontamination (Ambion, Inc.).
6. RNase-free water.
7. Pipette and nuclease free tips.
8. Heating block or water bath for ladder/sample preparation.
9. Pipette and nuclease free tips.

2.3 Sequencing Library Preparation

2.3.1 Adapter Ligation to RNA and Reverse Transcription

1. Ion Total RNA-Seq Core Kit v2 and Ion RNA-Seq Primer Set v2 (Part of Ion Total RNA-Seq Kit v2).
2. Thermocycler.
3. PCR Tubes with Caps, RNase-free, 0.2 mL.
4. Ice bucket and ice.

2.3.2 Purification and Size Selection of cDNA

1. Magnetic bead cleanup module (part of Ion Total RNA-Seq Kit v2).
2. Magnetic Stand-96.
3. Ethanol (100%, v/v).

4. MicroAmp optical adhesive film.
5. Scalpel.
6. PCR Tubes with caps, RNase-free, 0.2 mL.
7. Ice bucket and ice.

2.3.3 Amplification of cDNA

1. Ion Total RNA-Seq Core Kit v2 and Ion RNA-Seq Primer Set v2 (Part of Ion Total RNA-Seq Kit v2).
2. Ion Xpress RNA 3' Barcode Primer: 5' -CCGCTTTCCTCTCTATGGGCAGTCGGTGAT -3'.
3. Ion Xpress RNA RNA-seq 5' Barcode primer: Used in the study
 IonXpress_RNA_17:5'CCATCTCATCCCTGCGTGTCTCC
 GACTCAGTCTATTTCGTTCGGCCAAGGCG-3'
 IonXpress_RNA_18:5'CCATCTCATCCCTGCGTGTCTCC
 GACTCAGAGGCAATTGCGGCCAAGGCG-3'
 IonXpress_RNA_20:5'CCATCTCATCCCTGCGTGTCTCC
 GACTCAGCAGATCCATTCGGCCAAGGCG-3'
4. Thermocycler.
5. PCR Tubes with caps, RNase-free, 0.2 mL.
6. Ice bucket and ice.

2.3.4 Purification and Size Selection of Amplified cDNA

1. Magnetic bead cleanup module (part of Ion Total RNA-Seq Kit v2).
2. Magnetic Stand-96.
3. Ethanol 100%.
4. Amp optical adhesive film.
5. Scalpel.
6. PCR tubes with caps, RNase-free, 0.2 mL.
7. Ice bucket and ice.

2.3.5 Assessing the cDNA Size Distribution and Yield, and Pooling Barcoded cDNA Libraries

1. Agilent 2100 Bioanalyzer system (Agilent Technologies).
2. Agilent 2100 chip priming station.
3. IKA vortex mixer.
4. Agilent high sensitivity DNA kit.
5. RNaseZAP for electrode decontamination (Ambion, Inc.).
6. RNase-free water.
7. Pipette and nuclease free tips.
8. Heating block or water bath for ladder/sample preparation.
9. Pipette and nuclease free tips.

2.4 Sequencing Template Preparation

2.4.1 Preparation of Template-Positive Ion PI Ion Sphere Particles Using Ion OneTouch 2 Instrument

1. Ion OneTouch 2 instrument (Part of Ion OneTouch 2 system, Thermo Fisher Scientific).
2. Ion PI Hi-Q OT2 200 Kit (Thermo Fisher Scientific).
3. Thermocycler.
4. 1.5-mL Eppendorf LoBind tubes.
5. PCR tubes with caps, RNase-free, 0.2 mL.
6. Pipettes and nuclease free tips.
7. Vortexer with a rubber platform.
8. Tube rack to fit 15-mL conical tube.

2.4.2 Washing the Template-Positive ISPs

1. Ion PI Hi-Q OT2 200 kit (Thermo Fisher Scientific).
2. 1.5-mL Eppendorf LoBind tubes (Eppendorf).
3. PCR Tubes with Caps, RNase-free, 0.2 mL.
4. Pipettes and nuclease free tips.
5. Microcentrifuge.
6. Vortexer with a rubber platform.

2.4.3 Enriching the Template-Positive ISPs with the Ion OneTouch ES

1. Ion OneTouch ES (Part of Ion OneTouch 2 system, Thermo Fisher Scientific).
2. Ion PI Hi-Q OT2 200 Kit (Thermo Fisher Scientific).
3. Dynabeads MyOne Streptavidin C1 magnetic beads (Thermo Fisher Scientific).
4. DynaMag-2 magnet (Thermo Fisher Scientific).
5. Microcentrifuge.
6. Vortexer with a rubber platform.
7. 1 M NaOH.

2.5 Sequencing

2.5.1 Creating “Planned Run”

1. Torrent Browser for the Torrent Server.

2.5.2 Cleaning Ion Proton

1. Ion Torrent’s Ion Proton System from Thermo Fisher Scientific consisting of an Ion Proton Sequencer connected to an Ion Proton Torrent Server (Dell T620).
2. Ion PI Hi-Q Sequencing 200 Kit (Thermo Fisher Scientific).
3. Used Ion PI chip.
4. Tank of compressed nitrogen (grade 4.5, 99.995% pure or better).
5. Multistage (dual-stage) gas regulator (0–50 psi, 2–3 bar output).
6. Uninterruptable power supply (UPS).

7. ELGA PURELAB Flex 2 water purification system (Thermo Fisher Scientific) or Equivalent 18 M Ω water system.
8. Nuclease-free water molecular biology grade.
9. Glass bottles (1 L).
10. 0.22- μ m or 0.45- μ m vacuum filtration system and filters.
11. Standard laboratory vacuum line.

2.5.3 Initialization of Ion Proton

1. Ion PI Hi-Q Sequencing 200 Kit (Thermo Fisher Scientific).
2. 10 M NaOH molecular biology grade.
3. 1 N HCL.
4. Nuclease-free water molecular biology grade.
5. Pipettes and nuclease free tips.
6. Ice buckets and ice.

2.5.4 Loading the Chip and Starting Sequencing Run

1. Ion PI Hi-Q Sequencing 200 Kit (Thermo Fisher Scientific).
2. Ion PI Chip Kit v3 (Thermo Fisher Scientific).
3. Ion PI Controls 200 Kit (Thermo Fisher Scientific).
4. Isopropanol (100%, v/v).
5. Microcentrifuge.
6. Thermocycler.
7. 1.5-mL Eppendorf LoBind tubes.
8. PCR Tubes with Caps, RNase-free, 0.2 mL.
9. Pipettes and nuclease free tips.
10. Ion chip minifuge.

2.6 Data Analysis

1. Array studio (OmicSoft Corp V.8.0.3.67 or later). Open source or any commercial software dedicated to NGS data analysis may be used alternatively.
2. *Macaca fascicularis* miRNA list [17].

3 Methods

3.1 RNA Isolation from *M. fascicularis* Urine and RNA Concentration

3.1.1 Urine Exosome Precipitation

1. Before getting started, ensure that the centrifuge run is at 4 °C. Thaw urine samples on ice or at 4 °C. Vortex precipitation buffer B prior to use.
2. Spin 1.05 mL urine sample for 5 min at 3200 g in a 2 mL tube to remove cell debris/precipitate (*see* **Notes 2–6**).
3. Transfer 1.0 mL of supernatant into a new 2 mL tube/vial.
4. Add 400 μ L precipitation buffer B, invert tubes several times, and vortex for 5 s to mix thoroughly.

5. Incubate for 60 min at 4 °C.
6. Spin for 30 min at 10,000 *g* at 20 °C.
7. Remove supernatant completely and discard it. Respin the tubes (pellet may not be visible) for 5 s and remove residual supernatant. Continue directly with Subheading 3.1.2 for RNA isolation.

3.1.2 RNA Isolation from Exosomes and RNA Concentration

1. Add 350 μL of lysis solution to tubes containing exosomes (prepared from Subheading 3.1.1). Lyse exosomes by vortexing for 15 s. Ensure that the mixture becomes transparent before proceeding to the next step.
2. Add 200 μL of 95–100% ethanol to the lysate. Mix by vortexing for 10 s.
3. Assemble a column with one of the provided collection tubes. Apply the lysate with the ethanol onto the column and centrifuge for 1 min at 14,000 $\times g$. Discard the flowthrough and reassemble the spin column with its collection tube.
4. Apply 400 μL of wash solution to the column and centrifuge for 1 min at 14,000 $\times g$. Discard the flowthrough and reassemble the spin column with its collection tube.
5. Repeat the above step two more times.
6. Spin the column for 2 min at 14,000 $\times g$ in order to thoroughly dry the resin. Discard the collection tube.
7. Place the column into a fresh 1.5 mL Elution tube provided with the kit. Add 100 μL of elution buffer to the column. Centrifuge for 2 min at 200 $\times g$, followed by 1 min at 14,000 $\times g$.
8. Concentrate the purified RNA sample to 10 μL using vacuum concentrator and use 1 μL for accessing the miRNA/RNA quality/quantity using the Bioanalyzer. Concentrate the remaining 9 μL of RNA to 3 μL and use it for sequencing library preparation (*see* **Note 6**).
9. Alternatively purified sample can be stored at -20 °C for a few days. It is recommended that samples be placed at -70 °C for long-term storage.

3.2 Assessing miRNA Quality and Quantity

1. Denature the ladder for 2 min at 70 °C. Immediately cool the vial on ice. Prepare 3.5 μL aliquots in 0.2 mL RNase-free vials. Before use, thaw ladder aliquots and keep them on ice.
2. Allow dye, gel matrix, and RNA marker reagents to equilibrate to room temperature for 30 min.
3. Pipette the complete volume (approx. 650 μL) of the gel matrix (red) into a spin filter.
4. Centrifuge at 10,000 $\times g \pm 20\%$ for 15 min at room temperature. Use filtered gel within 4 weeks. Store at 4 °C.

5. Allow all reagents to equilibrate to room temperature for 30 min.
6. Vortex dye concentrate (blue) for 10 s and spin down.
7. Pipette 2 μL of dye into 0.5 mL RNase-free microtubes (provided with the kit).
8. Add 40 μL of filtered gel (gel is very viscous, careful pipetting is required).
9. Mix using pipetting, or by flipping over and flicking the vial several times until the dye is distributed equally. Visually inspect that the mix is homogeneous.
10. Spin tube at $13,000 \times g$ for 10 min at room temperature.
11. Put a new Small RNA chip on the chip priming station.
12. Pipette 9 μL of gel-dye mix in “white G in block circle.”
13. Make sure that the plunger is positioned at 1 mL and then close the chip priming station.
14. Press plunger until it is held by the clip.
15. Wait for exactly 60 s then release clip.
16. Visually inspect that the plunger moves back at least to the 0.3 mL mark.
17. Wait for 5 s, then slowly pull back the plunger to the 1 mL position.
18. Open the chip priming station and pipette 9 μL of gel-dye mix in the wells marked “G.”
19. Discard the remaining gel-dye mix.
20. Pipette 9 μL of the RNA conditioning solution (white) into the well marked “CS.”
21. Pipette 5 μL of RNA marker (green) in all 11 sample wells and in the well marked with a ladder.
22. Pipette 1 μL of prepared ladder in the well marked with a ladder.
23. Pipette 1 μL of RNA (prepared in Subheading 3.1.2) in each of the 11 sample wells. Pipette 1 μL of RNA Marker (green) in each unused sample well.
24. Put the chip horizontally in the IKA vortexer and vortex for 1 min at $2400 \times g$.
25. Run the chip in the Agilent 2100 Bioanalyzer instrument within 5 min. A typical chromatogram of urine RNA was shown in Fig. 2.

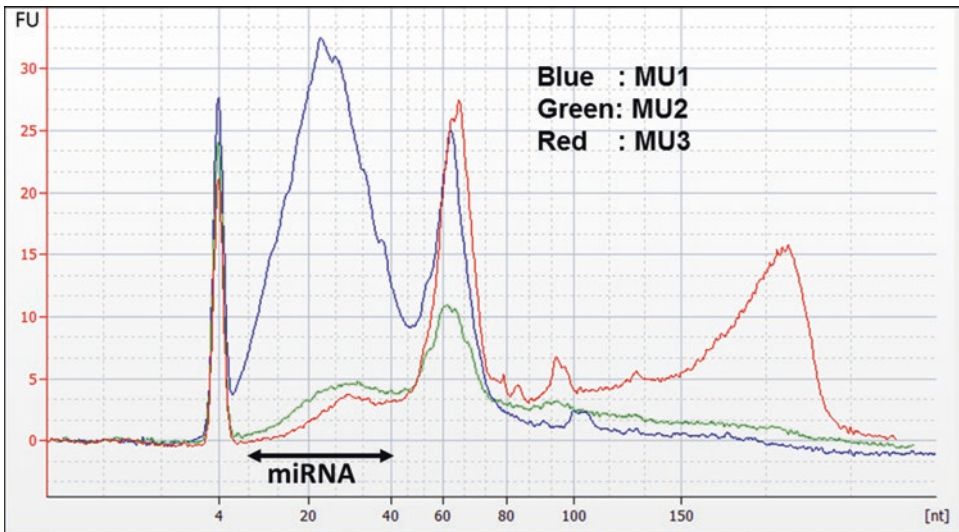


Fig. 2 *M. fascicularis* urine small RNA Bioanalyzer profile. Following exosome isolation from 1 mL urine, RNA was isolated, concentrated to 10 μ L, and 1 μ L was analyzed using Agilent 2100 Bioanalyzer and Agilent Small RNA kit. MU1, MU2, and MU3 represent urinary RNA samples from three *M. fascicularis*

3.3 Sequencing Library Preparation

3.3.1 Adapter Ligation to RNA and Reverse Transcription

1. On ice, prepare the hybridization master mix using 2 μ L Ion adaptor mix v2 and 3 μ L hybridization solution. Include 5–10% excess volume to compensate for pipetting error when preparing the master mix.
2. Add 5 μ L of hybridization master mix to 3 μ L of concentrated RNA (prepared at Subheading 3.1.2) (1–100 ng of miRNA in \leq 1 μ g of small RNA). Mix the reaction mixture by pipetting up and down 5 times (*see* **Note 7**).
3. Run the hybridization reaction in a thermal cycler: 10 min at 65 $^{\circ}$ C followed by 5 min at 16 $^{\circ}$ C.
4. On ice, prepare the ligation master mix consisting of 10 μ L of 2 \times ligation buffer and 2 μ L of ligation enzyme mix. Include 5–10% excess volume to compensate for pipetting error when preparing the master mix. Gently vortex to mix, then centrifuge briefly.
5. Add 12 μ L of ligation master mix to each 8- μ L hybridization reaction, for a total of 20 μ L per reaction. Flick the tube or pipet up and down 5 times to mix, then centrifuge briefly.
6. Incubate the 20- μ L ligation reactions in a thermal cycler at 16 $^{\circ}$ C for 16 h.
7. On ice, prepare the RT master mix: 2 μ L nuclease-free water, 4 μ L 10 \times RT Buffer, 2 μ L of 2.5 mM dNTP Mix, and 8 μ L Ion RT Primer v2. Include 5–10% excess volume to compensate for pipetting error when preparing the master mix.

8. Add 16 μL of RT master mix to each 20- μL ligation reaction (**step 6**). Pipet up and down 5 times to mix and then centrifuge briefly.
9. Incubate in a thermal cycler with a heated lid at 70 °C for 10 min, then snap-cool on ice.
10. Add 4 μL of 10X SuperScript® III enzyme mix to each ligated RNA sample. Gently vortex to mix thoroughly, then centrifuge briefly.
11. Incubate in a thermal cycler with a heated lid at 42 °C for 30 min. At this step, the cDNA can be stored at -30 to -10 °C for a few weeks, or stored at -86 to -68 °C for long-term storage, or used immediately.

3.3.2 Purification and Size Selection of cDNA

1. Bring the nucleic acid binding beads to room temperature (usually stored at 4 °C).
2. If you have not done so already, add 44 mL of 100% (v/v) ethanol to the wash solution concentrate and mix well. Mark the label on the bottle to indicate that you added ethanol. Store the solution at room temperature (15–30 °C).
3. If you see a white precipitate in the binding solution concentrate, warm the solution at 37 °C, then shake the solution to dissolve any precipitate before use.
4. Incubate the nuclease-free water at 37 °C for ≥ 5 min.
5. Open 96-well (1.2 ml deep well) processing plates and seal it with optical adhesive film. With scalpel open the required number of wells for cDNA purification.
6. Gently vortex the nucleic acid binding beads tube to completely resuspend the magnetic beads. Add 7 μL beads to wells on the 96-well Processing Plate.
7. Add 140 μL of binding solution concentrate to each well, and then mix thoroughly by pipetting up and down 10 times.
8. Transfer each 40- μL RT reaction (from Subheading 3.3.1) to a well with beads of the processing plate.
9. Set a P200 pipettor at 120 μL . Attach a new 200- μL tip to the pipettor, then pre-wet the new 200- μL tip with 100% ethanol by pipetting up and down 3 times. Without changing tips, add 120 μL of 100% ethanol to each well.
10. Set a single or multi-channel P200 pipettor at 150 μL . Attach new 200- μL tips to the pipettor, then mix the suspension in each well thoroughly by pipetting the wells up and down 10 times.
11. Incubate the samples for 5 min at room temperature off the magnetic stand.

12. Place the processing plate on a magnetic stand for 5–6 min to separate the beads from the solution. Wait for the solution to clear before proceeding to the next step.
13. Leave the processing plate on the magnetic stand, then transfer the supernatant to a new well on the plate or to a well on a new plate.
14. Remove the processing plate from the magnetic stand. Add 72 μL of nuclease-free water to the supernatant in the new sample well.
15. Set a P100 or P200 pipettor at 78 μL . Attach a new 100- μL or 200- μL tip to the pipettor, then pre-wet the new 100- or 200- μL tip with 100% ethanol by pipetting up and down 3 times.
16. Without changing tips, add 78 μL of 100% ethanol to each well (*see Note 8*).
17. Gently vortex the Nucleic Acid binding beads tube to completely resuspend the magnetic beads. Add 7 μL beads to the wells of the Processing Plate.
18. Set a single or multi-channel P200 pipettor at 150 μL . Attach new 200- μL tips to the pipettor, then mix the suspension in each well thoroughly by pipetting the wells up and down 10 times.
19. Incubate the samples for 5 min at room temperature off the magnetic stand.
20. Place the processing plate on a magnetic stand for 5 min to separate the beads from the solution. Wait for the solution to clear before proceeding to the next step.
21. Leave the processing plate on the magnetic stand, then carefully aspirate and discard the supernatant from the plate.
22. Leave the processing plate on the magnetic stand, and then add 150 μL of wash solution concentrate with ethanol to each sample. Incubate the samples for 1 min.
23. Aspirate and discard the supernatant from the plate. Use a P10 or P20 pipettor to remove residual ethanol.
24. Air-dry the beads at room temperature for 1–2 min to remove all traces of ethanol.
25. Remove the processing plate from the magnetic stand. Add 12 μL of prewarmed (37 °C) nuclease-free water to each sample.
26. Mix thoroughly by pipetting up and down 10 times.
27. Place the processing plate on the magnetic stand for 1–2 min to separate the beads from the solution. Wait for the solution to clear before proceeding to the next step.
28. For each sample, collect 12 μL of the eluent without disturbing the beads (*see Note 9*).

Table 1
cDNA amplification conditions

Stage	Temp (°C)	Time
Hold	94	2 min
Cycle (2 cycles)	94	30 s
	50	30 s
	68	30 s
Cycle (16 cycles)	94	30 s
	62	30 s
	68	30 s
Final extension	68	5 min
Hold	4	–

3.3.3 Amplification of cDNA

1. For each cDNA sample, prepare the PCR mix: 45 μ L Platinum PCR SuperMix High Fidelity and 1 μ L Ion Xpress RNA 3' barcode primer. Include 5–10% excess volume to compensate for pipetting error when preparing master mix.
2. Add 6 μ L of cDNA sample (from Subheading 3.3.2) to 46 μ L PCR master mix.
3. Add 1 μ L of the selected Ion Xpress RNA-Seq 5' barcode primer to each PCR tube. In the present study we prepared RNA from three monkey urine samples (MU1, MU2, and MU3). Hence we used IonXpress_RNA_17, 18, and 20 primers for MU1, MU2, and MU3 respectively.
4. Flick the tube or slowly pipet the solution up and down 5 times to mix well, then centrifuge briefly.
5. Run the PCRs in a thermal cycler using the setting described in Table 1.

3.3.4 Purification and Size Selection of Amplified cDNA

1. Bring the nucleic acid binding beads to room temperature (usually stored at 4 °C).
2. If you see a white precipitate in the binding solution concentrate, warm the solution at 37 °C, then shake the solution to dissolve any precipitate before use.
3. Incubate the nuclease-free water at 37 °C for \geq 5 min.
4. Open 96-well (1.2 ml deep well) processing plates and seal it with optical adhesive film. With scalpel open the required number of wells in 96-well processing plate.
5. Gently vortex the nucleic acid binding beads tube to completely resuspend the magnetic beads. Add 7 μ L beads to wells on the 96-well processing plate.

6. Add 140 μL binding solution concentrate to each well, then mix the binding solution concentrate and beads by pipetting up and down 10 times.
7. Transfer each 53 μL of amplified cDNA (from Subheading 3.3.3) to a well with beads of the processing plate.
8. Set a P200 pipettor at 110 μL . Attach a new 200- μL tip to the pipettor, then pre-wet the new 200- μL tip with 100% ethanol by pipetting the ethanol up and down 3 times. Without changing tips, add 110 μL of 100% ethanol to each well (*see Note 8*).
9. Set a single or multi-channel P200 pipettor at 150 μL . Attach new 200- μL tips to the pipettor, then mix the suspension in each well thoroughly by pipetting the wells up and down 10 times.
10. Incubate the samples for 5 min at room temperature off the magnetic stand.
11. Place the processing plate on a magnetic stand for 5–6 min to separate the beads from the solution. Wait for the solution to clear before proceeding to the next step.
12. Leave the processing plate on the magnetic stand and then transfer the supernatant to a new well on the plate or to a well on a new plate.
13. Remove the processing plate from the magnetic stand. Add 35 μL of nuclease-free water to the supernatant in the new sample well.
14. Set a P100 or P200 pipettor at 35 μL . Attach a new 100- μL or 200- μL tip to the pipettor, then pre-wet the new 100- or 200- μL tip with 100% ethanol by pipetting the ethanol up and down 3 times.
15. Without changing tips, add 35 μL of 100% ethanol to each well (*see Note 8*).
16. Gently vortex the nucleic acid binding beads tube to completely resuspend the magnetic beads. Add 7 μL beads to the wells of the processing plate.
17. Set a single or multi-channel P200 pipettor at 150 μL . Attach new 200- μL tips to the pipettor, then mix the suspension in each well thoroughly by pipetting the wells up and down 10 times.
18. Incubate the samples for 5 min at room temperature off the magnetic stand.
19. Place the processing plate on a magnetic stand for 5 min to separate the beads from the solution. Wait for the solution to clear before proceeding to the next step.

20. Leave the processing plate on the magnetic stand, then carefully aspirate and discard the supernatant from the plate.
21. Leave the processing plate on the magnetic stand, and then add 150 μL of Wash Solution Concentrate with ethanol to each sample. Incubate the samples for 1 min.
22. Aspirate and discard the supernatant from the plate. Use a P10 or P20 pipettor to remove residual ethanol.
23. Air-dry the beads at room temperature for 1–2 min to remove all traces of ethanol.
24. Remove the Processing Plate from the magnetic stand. Add 15 μL of pre-warmed (37 °C) nuclease-free water to each sample.
25. Mix thoroughly by pipetting up and down 10 times.
26. Place the processing plate on the magnetic stand for 1–2 min to separate the beads from the solution. Wait for the solution to clear before proceeding to the next step.
27. For each sample, collect 15 μL of the eluent without disturbing the beads (*see Note 9*). Store the prepared cDNA at $-20\text{ }^{\circ}\text{C}$ for 6 months or at $-80\text{ }^{\circ}\text{C}$ for long-term use.

*3.3.5 Assessing
the cDNA Size Distribution
and Yield, and Pooling
Barcoded cDNA Libraries*

1. Allow High Sensitivity DNA dye concentrate (blue) and high sensitivity DNA gel matrix (red) to equilibrate to room temperature for 30 min.
2. Add 15 μL of High Sensitivity DNA dye concentrate (blue) to a High Sensitivity DNA gel matrix vial (red).
3. Vortex solution well and spin down. Transfer to spin filter.
4. Centrifuge at $2240\text{ }g \pm 20\%$ for 10 min. Protect solution from light. Store at 4 °C.
5. Allow the gel-dye mix equilibrate to room temperature for 30 min before use.
6. Put a new High Sensitivity DNA chip on the chip priming station.
7. Pipette 9.0 μL of gel-dye mix in “white G in block circle.”
8. Make sure that the plunger is positioned at 1 mL and then close the chip priming station.
9. Press plunger until it is held by the clip.
10. Wait for exactly 60 s then release clip.
11. Wait for 5 s, then slowly pull back the plunger to the 1 mL position.
12. Open the chip priming station and pipette 9.0 μL of gel-dye mix in the wells marked “G.”

13. Pipette 5 μL of marker (green) in all 11 sample wells and in the well which is marked with a ladder.
14. Pipette 1 μL of high sensitivity DNA ladder (yellow) in the well which is marked with a ladder.
15. Pipette 1 μL of appropriately diluted cDNA (usually 100 \times diluted) in each of the 11 sample wells (pipette each cDNA sample in at least three well). Pipette 1 μL of Marker (green) in each unused sample well.
16. Put the chip horizontally in the IKA vortexer and vortex for 1 min at 2400 rpm.
17. Run the chip in the Agilent 2100 Bioanalyzer instrument within 5 min. Results are shown in Fig. 3 (*see* **Notes 9** and **10**).
18. Using the 2100 expert software, perform a smear analysis to determine size distribution of the amplified DNA:
 - (a) Measure the area for the DNA that is:
 - 50–300 bp (the size range for all of the ligation products)

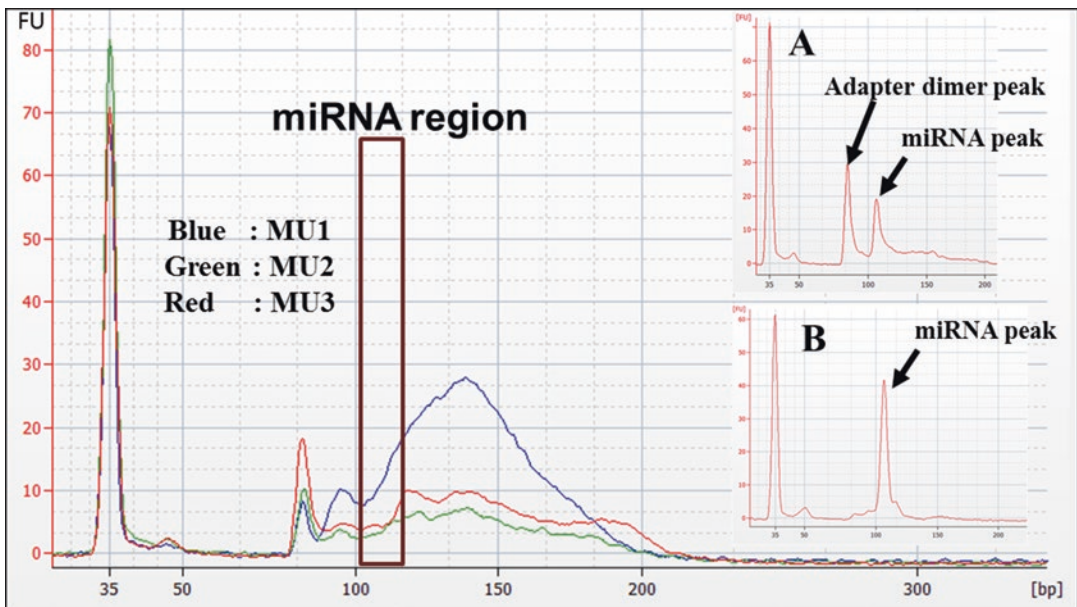


Fig. 3 Bioanalyzer profile of *M. fascicularis* urine small RNA-seq library. Sequencing libraries were prepared using Ion Total RNA-Seq Kit v2. MU1, MU2, and MU3 represent urine Small RNA-seq libraries from three *M. fascicularis*. Three libraries were barcoded using barcode primers (IonXpress_RNA_17, 18, and 20 barcodes MU1, MU2, and MU3 respectively) and analyzed using Agilent 2100 Bioanalyzer and Agilent High Sensitivity DNA Kit. Region between 103 and 110 bp corresponds to miRNA (18–25 nt)

Note that urine small RNA-seq libraries prepared from three *M. fascicularis* did not have peak at miRNA region. The miRNA peak was clearly seen in small RNA-seq library prepared using urine from drug treated *M. fascicularis* (inset A) and kidney cortex tissues (inset B)

- 94–114 bp for barcoded libraries (the size range for the desired miRNA ligation products)
 - (b) Calculate the ratio of miRNA ligation products in total RNA ligation product using the formula: Ratio = [Area (94–114 bp)] ÷ [Area (50–300 bp)]*100
 - (c) If the ratio is (*see Note 11*):
 - ≥50% proceed to pooling barcoded cDNA library.
 - <50% proceed to pooling barcoded cDNA library but expect to see an increase in the number of filtered reads (no insert, tRNA or rRNA reads).
 - (d) Determine the molar concentration of cDNA libraries using size range 50–300 bp. Use this concentration for “Pool barcoded small RNA libraries” and “Determine the library dilution required for template preparation”.
19. Dilute each barcoded cDNA library to the same molar concentration (pM). For example, if you have three different barcoded libraries that are 4432, 1698, and 2297 pM (which is the case in the present study), choose a concentration that is equal to or lower than the lowest concentration of the three libraries, such as 1000 nM or 500 pM. Dilute part of the library to 1000 pM (in 20 μL).
 20. Mix an equal volume (20 μL of 1000 pM or 500 pM) of each diluted library to prepare a pool of the barcoded libraries.
 21. The final molar concentration of the pooled library is the same for each diluted library. For example, if you dilute each library to 1000 pM, the concentration of the pooled library is 1000 pM.
 22. Prepare 100 μL of 100pM pooled barcoded library mix and use appropriate volume for sequencing. Do not store the diluted (either 1000 pM or 100 pM), pooled barcoded library for sequencing (always prepare fresh).

3.4 Sequencing Template Preparation

3.4.1 Preparation of Template-Positive Ion PI Ion Sphere Particles Using Ion OneTouch 2 Instrument

1. Allow Ion PI master mix (2 mL) to come to RT before use (*see Note 12*).
2. Allow Ion PI ion sphere particles to come to room temperature.
3. Before use centrifuge Ion PI enzyme for 2 s.
4. Switch on Ion OneTouch 2 instrument. On the instrument display, touch Open Lid, wait until the lid clicks open, then lift and hold the side of the centrifuge lid.
5. Dispense 150 μL Ion OneTouch breaking solution into each of two Ion OneTouch recovery tubes. Insert a recovery tube containing Ion OneTouch™ breaking solution into each slot of the centrifuge.

6. Slide the recovery router in position around each recovery tube extension. Pinch the sides of the recovery router and push it down into the center slot of the centrifuge. Close the lid of the centrifuge.
7. If there is a used Ion OneTouch cleaning adapter on the instrument, remove and appropriately discard it. Push the handle back to open the heat block.
8. Obtain an Ion OneTouch 2 amplification plate. Hold the disposable injector in one hand and the amplification plate in the other hand. Pull the handle of heat block and insert the amplification plate into the heat block so that the single plate port aligns with the left hole of the Ion OneTouch 2 Instrument.
9. Pull the handle of the heat block to close the block. Make sure that disposable tubing is under the handle. Thread the disposable tubing through the Ion OneTouch DL tubing catch.
10. Align the disposable tubing with the slot that runs along the bottom of the pinch valve. Gently pull the disposable tubing upwards on both sides of the pinch valve until the disposable tubing is in the slot and secured in the round notch on each side of the pinch valve.
11. Place one hand on the centrifuge lid. Place the other hand at the top of the disposable injector, and insert the disposable injector straight into the port of the Ion OneTouch DL injector hub.
12. Keep your hand on the centrifuge lid, and then push the disposable injector through the port until the disposable injector just stops at the base of the router.
13. Invert the Ion OneTouch™ oil bottle (450-mL size) 3 times to mix, then fill the Reagent Tube half full with Oil. Minimize bubbles. Insert the Ion OneTouch oil on the left front port and screw the reagent tube firmly into place, one-quarter turn on the instrument.
14. Invert the Recovery Solution 3 times to mix, and then fill the reagent tube one-third-full with recovery solution. Minimize bubbles. Insert the filled reagent tube into the right front, and screw the reagent tube firmly into place, one-quarter turn on the instrument.
15. Pull the external tubing from the port of the waste container. Empty the waste container into the appropriate receptacle. Push the tubing onto the port of the empty waste container.
16. Dilute 8–10 μL of 100 pM library (from Subheading 3.3.5) with nuclease-free water in a 1.5-mL Eppendorf LoBind tube to give a total volume of 100 μL . Vortex the diluted library for 5 s, centrifuge for 2 s, then place the diluted library on ice.

17. Vortex the Ion PI ISPs at maximum speed for 1 min, centrifuge for 2 s, pipet the ISPs up and down to mix; then immediately proceed to the next step.
18. Take 3 mL tube and add 2 mL Master Mix, 80 μ L nuclease-free water, 120 μ L Ion PI Enzyme Mix, 100 μ L Ion PI ISPs, and 100 μ L diluted library (total 2400 μ L). Vortex the amplification solution at maximum speed for 5 s, then centrifuge the solution for 2 s. Proceed immediately to “Fill the Ion OneTouch reaction filter.”
19. Take Ion OneTouch™ reaction filter and place it on a tube rack so that the 3 ports of the Ion OneTouch™ reaction filter face up.
20. Slowly pipet 800 μ L the 2.4 mL amplification solution through the sample port. Keep the plunger of the pipette depressed to avoid aspirating solution from the Ion OneTouch™ reaction filter. With the plunger still depressed, remove the tip from the sample port, then appropriately discard the tip.
21. Repeat **step 20** two more times (for a total of 3 times) to load the entire amplification solution volume into the Ion OneTouch™ reaction filter.
22. Invert the Ion OneTouch Reaction Filter. Insert the 3 ports of the reaction filter into the three holes on the top stage of the Ion OneTouch 2 Instrument so that the Ion OneTouch reaction filter is firmly seated on the instrument.
23. Ensure that the centrifuge lid of the Ion OneTouch 2 Instrument is closed. On the home screen, touch Run and select “Proton: Ion PI™ Hi-Q™ OT2 200 Kit” from the drop-down menu. Touch **Next**. Touch Assisted and complete each task. After you touch “Next” on the last task, you see a progress bar, and the run begins.
24. At the end of the run, follow the screen prompts to centrifuge the sample. On the home screen, touch **Options**, touch **Final Spin**, and then follow any screen prompts to centrifuge the sample.
25. Immediately after the centrifuge has stopped, on the instrument display, touch **Open Lid**, wait until the lid clicks open, then remove and discard the Ion OneTouch Recovery Router.
26. Carefully remove both Ion OneTouch Recovery Tubes from the instrument and put the two recovery tubes in a tube rack. You may see some cloudiness in the tube, which is normal.

3.4.2 Washing the Template-Positive ISPs

1. Label a new 1.5-mL Eppendorf LoBind tube for the template-positive ISPs.
2. Use a pipette to remove all but ~100 μ L of Ion OneTouch Recovery Solution from each Ion OneTouch™ Recovery

Tube. Withdraw the supernatant from the surface and on the opposite side from the pellet. Do not disturb the pellet of template-positive ISP (*see* **Note 13**).

3. Resuspend the template-positive ISPs in the remaining recovery solution in each tube by pipetting the suspension up and down.
4. Transfer the suspension from each Recovery Tube to a new labeled 1.5-mL Eppendorf LoBind tube.
5. Add 100 μ L of nuclease-free water to each of the recovery tubes, then pipette each aliquot in the tube up and down to mix and recover residual beads.
6. Transfer the 100- μ L aliquot from each recovery tube to the new labeled 1.5-mL Eppendorf LoBind tube to combine the aliquots.
7. Bring the combined suspensions in the new labeled 1.5-mL Eppendorf LoBind tube to 1 mL with nuclease-free water (*see* **Note 14**).
8. Vortex for 30 s to completely resuspend the template-positive ISPs, then centrifuge the tube for 2 s.
9. Centrifuge the template-positive ISP suspension for 8 min at $15,500 \times g$ and gently remove the tube from centrifuge.
10. Remove all but 20 μ L of supernatant (*see* **Note 15**). Add 80 μ L of ISP Resuspension Solution. Vortex the pellet for 30 s to completely resuspend the template-positive ISPs, then centrifuge the tube for 2 s. Proceed to “Enrich the template-positive ISPs with the Ion OneTouch ES”.

3.4.3 Enriching the Template-Positive ISPs with the Ion OneTouch ES

1. Before you begin, thaw Dynabeads MyOne Streptavidin C1 Beads and bring it to room temperature.
2. Vortex the tube containing the Dynabeads MyOne Streptavidin C1 Beads for 30 s to thoroughly resuspend the beads, then immediately proceed to the next step.
3. Transfer 100 μ L of Dynabeads MyOne Streptavidin C1 Beads to a new 1.5-mL Eppendorf LoBind tube.
4. Place the tube on a magnet such as a DynaMag-2 magnet for 2 min, then remove and discard the supernatant without disturbing the pellet of Dynabeads MyOne streptavidin C1 beads.
5. Add 1 mL of Ion OneTouch Wash Solution to the aliquot of Dynabeads MyOne streptavidin C1 beads.
6. Remove the tube from the magnet, vortex the tube for 30 s, and centrifuge the tube for 2 s.
7. Place the tube on a magnet such as a DynaMag-2 magnet for 2 min, then remove and discard the supernatant.

8. Add 130 μL of MyOne Beads Capture Solution to the Dynabeads MyOne streptavidin C1 beads. Remove the tube from the magnet, vortex the tube for 30 s, and centrifuge the tube for 2 s.
9. Place 8-well strip on lab bench and ensure that square-shaped tab of the 8-well strip on the left. Pipet the ISPs up and down 10 times to mix, then transfer the entire volume (100 μL) of template-positive ISP (Subheading 3.4.2) sample into well 1.
10. Pipette 130 μL of Dynabeads MyOne Streptavidin C1 Beads resuspended in MyOne Beads capture solution (from **step 7**) into well 2.
11. Pipette 300 μL of Ion OneTouch ES wash solution in well 3, 4, and 5.
12. Prepare Melt-Off solution by mixing 280 μL of Tween solution and 40 μL 1 M NaOH. Pipette 300 μL of this melt-off solution in well 7.
13. Leave the well 6 and 8 empty.
14. Confirm that the square-shaped tab is on the left, and then insert the filled 8-well strip with the 8-well strip pushed all the way to the right end of the slot of the tray in OneTouch ES.
15. Load a new tip in the Tip Arm of OneTouch ES. Ensure that the back/bottom end of the Tip Arm is not resting on top of the thumb screw, causing the Tip Arm to tilt forward.
16. Insert a new opened 0.2-mL PCR tube into the hole in the base of the Tip Loader.
17. Turn ON the Ion OneTouch ES and wait for the instrument to initialize. The screen displays “**rdy.**” The Tip Arm performs a series of initialization movements and returns to the home position (~5 s).
18. Press **Start/Stop**. The screen displays “**run**” during the run. The run takes 35 min approximately.
19. Immediately after the run, securely close and remove the PCR tube containing the enriched ISPs (ensure that tube has a minimum solution volume of 200 μL). Remove the used tip and the 8-well strip. Press Start/Stop and turn off Ion OneTouch ES.
20. Centrifuge the 0.2-mL PCR tube containing the enriched ISPs at $15,500 \times g$ for 5 min.
21. Remove all but ~10 μL of supernatant without disturbing the pellet, then add 200 μL of nuclease-free water.
22. Pipet the solution up and down 10 times to resuspend the pellet. The pellet may be difficult to see.
23. Centrifuge the 0.2-mL PCR tube at $15,500 \times g$ for 5 min.

24. Check for absence of brown tinted pellet at the bottom of tube (containing Dynabeads MyOne Streptavidin C1 Beads). Remove all but ~10 μ L of supernatant without disturbing the pellet. Add sufficient nuclease-free water for a final volume of 100 μ L. Pipet up and down 10 times to resuspend the pellet.
25. Proceed to sequence the template-positive ISPs using Ion Proton sequencer (*see* **Note 16**).

3.5 Sequencing

3.5.1 Creating "Planned Run"

1. Open Torrent Browser for the Torrent Server connected to your sequencer.
2. Select the **Plan** tab, select **Templates**, and locate the application **Small RNA-seq**, then select **Plan New Run** to plan a new run using the generic template for the selected application.
3. In the wizard, enter a name for the run (Ex, *M. fascicularis* Urine miRNA seq), select correct kits, select correct barcodes, and enter respective sample name (in the present study IonXpress_RNA_17, 18, and 20 barcodes were assigned to MU1, MU2, and MU3 respectively). Selecting the reference sequence is optional.
4. When you have completed your selections, click **Plan Run** to save your selections. The run is listed on the **Planned Runs** page under the name you specified.

3.5.2 Cleaning Ion Proton

1. To avoid possible damage to the chip due to electrostatic discharge, ground yourself before picking up a chip or placing a chip on a surface such as a lab bench. For example, touch the metal trim on the chip compartment before inserting or removing a chip from the chip clamp.
2. Fill a glass bottle with 1 L of 18 M Ω water and add a chlorite cleaning tablet. When the tablet has dissolved, add 1 mL of 1 M NaOH and filter the solution using a 0.22 μ m or 0.45 μ m filter. Use the chlorite solution within 2–3 h and discard any unused solution after this time.
3. Turn on Ion Proton sequencer and select **Clean** on the Ion Proton Sequencer touchscreen Main Menu, and then follow the instructions on the touchscreen to perform the cleaning procedure.
4. When prompted, secure a cleaning chip in the chip clamp.
5. When prompted, remove all of the Reagent Tubes and the Wash 2 Bottle:
 - (a) Remove and save the C1 and C2 Reagent Tubes for use with chlorite solution. (Label these tubes for chlorite cleaning only and discard after the chlorite cleaning cycle is completed; do not use these tubes for 18 M Ω water cleaning.)
 - (b) Remove and discard all other 140 mL Reagent Tubes.

- (c) Remove the Wash 2 bottle, discard the liquid, and save the bottle for reuse in initialization.
- (d) Remove the old Sippers from the C1 and C2 positions. Put on fresh gloves and install new short blue sippers in those positions.
6. Remove the waste container, empty the waste, replace the container on the instrument, and then press **Next**.
7. Add 100 mL of filtered chlorite solution to each of the two reagent tubes. On the Ion Proton™ Sequencer, install the tubes containing chlorite solution in the C1 and C2 positions.
8. Place the collection tray on the instrument, then direct all sippers into the collection tray. Press **Next** to begin cleaning.
9. When cleaning is finished press **Next** to return to the Main menu. Remove and discard the reagent tubes and sippers used for chlorite solution from the C1 and C2 positions.
10. Put on fresh gloves and install new short blue Sippers in the C1 and C2 positions.
11. Fill the two new Reagent Tubes with 100 mL of 18 MΩ water, then install the tubes in C1 and C2 positions.
12. Select **Clean** on the touchscreen Main Menu, and then press **Next** to advance through the instrument prompts until the cleaning procedure begins.
13. When the post-chlorite water rinse is complete, press **Next** to return to the Main Menu. Now the Ion Proton sequencer is ready for initialization.

3.5.3 Initialization of Ion Proton

1. Remove the dNTP stock solutions from the freezer and begin thawing on ice.
2. Check the tank pressure for the nitrogen gas. When the tank pressure drops below 500 psi, change the tank.
3. Thaw deoxyribonucleotide (dNTP) stock solution, vortex to mix, and briefly centrifuge to collect the contents. Keep dNTP stock solutions on ice.
4. Remove the Sippers from the W1, W2, and W3 positions. Do not remove the used sippers from the dNTP ports until instructed to do so.
5. Select **Initialize** on the touchscreen Main Menu.
6. When prompted, select the Ion PI Hi-Q sequencing 200 Kit from the drop-down list.
7. Secure a used chip from an old sequencing run in the chip clamp (do not use a cleaning chip).
8. Press **Next** to begin the initialization.

9. With fresh gloves, install new short Sippers in the W1 and W3 positions. Do not let the new sippers touch other sippers on the instrument or any other surfaces.
10. Add 32 μL of 1 M NaOH solution to the Wash 1 reagent tube. Install the W1 Reagent tube into the W1 positions of the Ion Proton Sequencer.
11. Add 40–50 mL of the 1X W3 Solution from the kit to the Wash 3 Reagent Tube. Install the W3 reagent tube into the W3 positions of the Ion Proton Sequencer.
12. Place the collection tray beneath the dNTP sippers, then press **Next**.
13. Rinse the Wash 2 Bottle three times with 200 mL of 18 M Ω water, directly from the water purification system. Do not use water stored in other containers.
14. Extend the spigot from the water purification system into the neck of the Wash 2 bottle, then add 18 M Ω water up to the groove on the bottle.
15. Add the entire bottle of Ion PI Hi-Q W2 Solution to the Wash 2 bottle. Immediately cap the bottle securely and invert five times to mix.
16. With fresh gloves to install a new long Sipper in the cap for the Wash 2 bottle. Do not let the Sipper touch any surfaces. Immediately attach the prepared Wash 2 bottle in W2 position and tighten the cap. Ensure that the cap is screwed on tightly, then place the Wash 2 bottle in the reagent compartment before you continue.
17. Direct sippers to the collection tray, then press **Next** to continue initialization. The instrument will test the tubes for leaks, fill the Wash 1 reagent tube, adjust the pH of the Wash 2 solution, and then dilute the Wash 1 reagent tube solution to the optimal concentration for the sequencing run. This procedure takes 40 min, approximately.
18. After the wash solutions have initialized, follow the on-screen prompts to remove the used dNTP sippers and the collection tray.
19. Using new gloves, attach a new short Sipper to each dNTP port.
20. Attach the four dNTP stickers (dGTP, dCTP, dATP, and dTTP) to four new 140-mL reagent tubes. Using a new filtered pipette tip, carefully transfer 70 μL of each dNTP stock solution into the bottom of the appropriate reagent tube, then attach the dNTP reagent tube to the Ion Proton Sequencer in the correct position (front left row) and firmly tighten.

21. Confirm that all reagent tubes and Wash 2 bottle are tightly secured, then press **Next**.
 - The Ion Proton™ Sequencer checks the pressure of the reagent tubes and Wash 2 bottle, then adds W2 solution to each dNTP reagent tube.
 - If a tube or bottle leaks, you will be prompted to check that it is tightly attached to the instrument. If it continues to leak, replace it. If you replace the tube or bottle but the instrument does not pass the leak check, contact Technical Support.
22. At the end of initialization, the Ion Proton Sequencer measures the pH of the reagents. If every reagent is in the target pH range, a Passed screen is displayed. Press **Next** to return to the Main Menu. Proceed to “**Loading the chip and starting sequencing run**”.

3.5.4 Loading the Chip and Starting Sequencing Run

1. Thaw the sequencing primer. Keep primer tube on ice
2. Thaw the Ion PI Control ion sphere particles and keep it on ice.
3. Prepare the following stock solutions fresh weekly or more frequently as needed:
 - (a) 50% Annealing Buffer: In a 1.5 mL tube, combine 0.5 mL of Ion PI™ annealing buffer with 0.5 mL of nuclease-free water (you need 360 µL of 50% annealing buffer for each run).
 - (b) Flushing solution: In a 1.5-mL tube, combine 0.5 mL of 100% isopropanol with 0.5 mL of Ion PI™ annealing buffer.
4. Vortex the Ion PI Control IS Ps for 5 s, then centrifuge for 2 s before taking aliquots.
5. Add 5 µL of control ISPs directly to the entire volume of enriched, template-positive ISPs in a 0.2-mL PCR tube (from Subheading 3.5.3), then pipet up and down to mix.
6. Centrifuge the enriched, template-positive ISPs for 5 min at $15,500 \times g$.
7. Carefully remove the supernatant without disturbing the pellet, leaving 10 µL of supernatant in the tube (visually compare to 10 µL of liquid in a separate tube).
8. Add 15 µL of Ion PI annealing buffer for a total volume of 25 µL.
9. Add 20 µL of Ion PI™ sequencing primer and confirm that the total volume is 45 µL. Add Ion PI Annealing Buffer if necessary to bring the total volume to 45 µL. Briefly vortex to mix, then centrifuge briefly to collect the contents at the bottom of the tube.

10. Program a thermal cycler for 95 °C for 2 min and then 37 °C for 2 min, using the heated lid option. Place the tube in the thermal cycler and run the program.
11. After cycling, add 10 μL of Ion PI Loading Buffer, briefly vortex to mix, then centrifuge briefly to collect the contents at the bottom of the tube.
12. Place the new Ion PI Chip v3 chip in the Ion Chip minifuge bucket with the chip notch pointing out. Place a used chip in the opposite bucket with the chip notch pointing out. Dispense the entire prepared sample (55 μL from **step 8**) into the chip loading well (not the chip loading port) of the calibrated chip.
13. Centrifuge for 10 min.
14. In a 1.5-mL tube, combine 49 μL of 50% annealing buffer with 1 μL of foaming solution (10% Triton X-100). Create foam by injecting air into the solution using a pipette set to dispense 100 μL . Next, break the large bubbles into smaller bubbles by rapidly pipetting for ~5 s. (Do not over-inject the air; the final volume of foam should be approximately 250 μL .)
15. After 10 min, take out chip and place the chip on a stable surface such as a benchtop, then inject 100 μL of foam into the chip loading port. Remove the expelled liquid from the opposite port.
16. Dispense 55 μL of 50% annealing buffer into the chip loading well (not the chip loading port).
17. Place the chip back in the minifuge with the chip notch pointing out, and centrifuge for 30 s.
18. Place the chip on a stable surface such as a benchtop. Remove the liquid that has accumulated in both of the chip loading wells. Briefly “re-foam” the foam sample by pipetting rapidly for ~5 s, then inject 100 μL of foam into the chip loading port. Remove the expelled liquid from the opposite port.
19. Dispense 55 μL of 50% annealing buffer into the chip loading well (not the chip loading port).
20. Place the chip back in the minifuge with the chip notch pointing out, and centrifuge for 30 s.
21. Inject 100 μL of the flushing solution into the chip loading port two times. After each injection, discard the solution that is expelled from the opposite port.
22. Inject 100 μL of 50% annealing buffer into the chip loading port three times. Do not introduce air bubbles. After each injection, remove the expelled liquid from the opposite port.
23. Combine 6 μL of Ion PI™ Hi-Q™ Sequencing Polymerase with 60 μL of 50% annealing buffer. Inject 65 μL of the polymerase solution into the chip loading port and remove the

- expelled liquid from the exit port. Be careful to avoid introducing air bubbles.
24. Allow the chip to incubate for 5 min, then immediately proceed to the next steps.
 25. With the used chip from initialization still in the chip clamp, press **Run** on the Main Menu, then press **Next** and confirm that “Cleaning fluid lines” displays on the instrument touchscreen. Observe the chip for leaks.
 26. After line cleaning, press **Next**.
 27. In the drop-down list, select a Planned Run that you created (from Subheading 3.5.1, *M. fascicularis* Urine miRNA seq) in the Torrent Suite Software, then press **Next**. Confirm that the run settings are correct, or make changes using the buttons and drop-down lists if necessary.
 28. Remove the used chip from the chip clamp and secure the chip loaded with template-positive Ion PI ISPs (from **step 21**). Close the chip compartment lid, then press **Next** to begin the sequencing run. The system calibrates the chip for 1 min, then begins the sequencing run.
 29. When the run is complete, the touchscreen returns to the Main Menu. Clean and initialize the instrument before beginning a new run.
 30. Use the Torrent Browser software to review your results. The Torrent Server trims (removes sequencing key, barcode and adaptor sequences, lower-quality -3p ends with low quality scores) and filters (reads with <8 nucleotides, adaptor dimers, reads lacking key, polyclonal reads, reads with low signal) the sequencing reads and generates FASTQ files for downstream analysis. Download FASTQ files corresponding to your samples/barcode primers (IonXpress_RNA_17, 18, and 20 barcodes MU1, MU2, and MU3 respectively) from Torrent Browser and use it in data analysis.

3.6 Data Analysis

1. Generated FASTQ files were uploaded to server and analyzed using Array studio (OmicSoft Corp V.8.0.3.67 or later, *see Note 17*) or any open-source/commercially available software dedicated to NGS data analysis (*see Note 17*).
2. As shown in Table 1, each urine sample had at least seven million sequencing reads.
3. In the preprocessing step, reads with a length below 18 nucleotides (which may not be miRNA) and average quality score below 20 were removed from FASTQ files. Only 25–50% of sequencing reads passed set filtering criteria. Interestingly, one can note that three urine samples had different percentage of passed RNA reads (Table 1).

4. Then, filtered FASTQ files were mapped against *M. fascicularis* miRNA reference sequences and resulting BAM files were used for read quantitation. Although we used same volume of urine (1 mL) in all three animals, MU3 had relatively high number miRNA sequencing reads which in turn yielded higher number of miRNAs (Table 1).
5. Comparison of miRNAs indicated that at least 92 miRNAs were present in all three monkey urine samples (Fig. 4a).
6. Generated miRNA reads were normalized by DESeq method. Top 30 miRNAs present in *M. fascicularis* urine samples were shown in Fig.4b. Interestingly, highly expressed miRNA had same trend across the three animals.
7. We also mapped the urinary RNA sequencing reads to *M. fascicularis* genome. In our tested conditions, only 9–20% of sequencing reads were able to map to *M. fascicularis* genome (Table 2) (see Note 18).

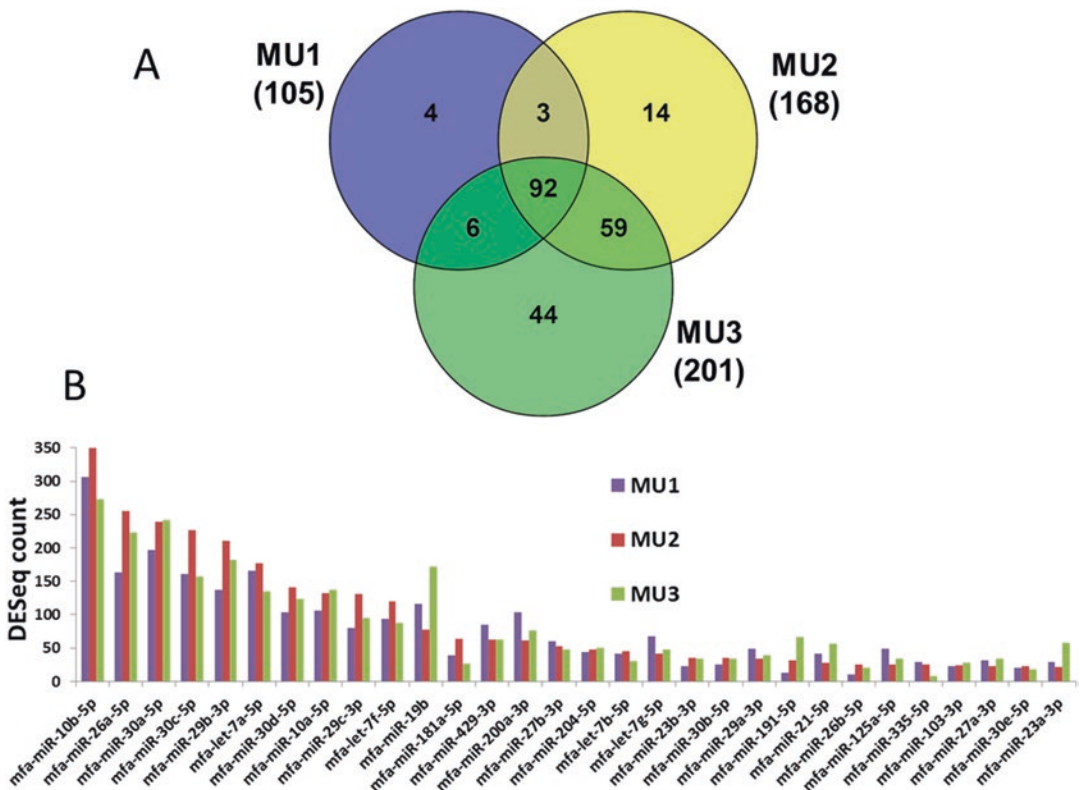


Fig. 4 (a) Comparison of urinary miRNAs detected in three *M. fascicularis* urine samples. Numbers of miRNAs (having at least 1 read) detected in three *M. fascicularis* (MU1, MU2, and MU3) were shown in parenthesis. (b) Top 30 miRNAs detected in *M. fascicularis* urine

Table 2
Mapping sequencing reads to *M. fascicularis* miRNA and genome

	MU1	MU2	MU3
Sequencing reads	8,717,297	7,182,192	8,085,730
<i>Mapping sequencing reads to M. fascicularis miRNA</i>			
Reads after filtering <18 nucleotides	2,027,195	2,672,916	4,179,991
Reads mapped to miRNA	1132	4579	10,854
miRNAs detected (≥ 1 read)	105	168	201
<i>Mapping sequencing reads to M. fascicularis genome</i>			
Reads after filtering <16 nucleotides	2,684,483	3,106,725	4,646,663
Reads mapped to genome	537,811	421,039	423,996
% of reads mapped to genome	20	14	9

4 Notes

1. In this study, we used urine samples collected overnight on ice from three naive monkeys (one male and two female). In order to get rid of cells/cell debris, it is essential to centrifuge the urine samples at $3000 \times g$, at 4°C for 10 min. Store the collected urine samples in 5 or 10 mL aliquots at -80°C . Avoid repeated freeze-thaw cycles.
2. Ensure that sample (urine) acquisition conditions and pretreatment conditions (centrifugation steps) are same for all samples.
3. Compared to RNA extracted from crude urine, use of RNA isolated from urine exosomes provides better results in sequencing. So it is recommended, first, to isolate exosomes from urine and then to extract the RNA.
4. Considering very low quantity of miRNAs in urine, a minimum volume of 1 mL urine was recommended for exosome isolation.
5. Exiqon-miRCURY Exosome Isolation-Cells, Urine and CSF—kit allows RNA isolation from 1 to 10 mL of urine. For urine volumes higher than 1 mL, maintain the appropriate reagents ratio.
6. When working with concentrated RNA, avoid repeated pipetting and changing tips. Stop the drying process before volume reaches 1–2 μL . If RNA dries, add 5 μL of water and leave it

on ice for 10 min, then pipette the solution thoroughly. Do not over dry the RNA.

7. 1 mL urine usually contains very small amount of miRNAs. For miRNA sequencing, it is recommended to use entire eluted RNA (prepared from 1 mL urine).
8. While dispensing the ethanol, do not force out the last drops. Remove the last drop by touching the drop to the well wall. Accurate pipetting of 100% ethanol is critical for best results.
9. Do not disturb the magnetic beads. If any beads are aspirated, leave 2–3 μ L of supernatant behind.
10. Peak at 103–110 bp (equivalent to miRNA size of 18–25 nt) corresponds to miRNA. Due to low urinary miRNA content, this peak is rarely seen in sequencing library prepared from urine sample.
11. Peak corresponding to primer-dimer is usually found at 85 bp (no RNA insert). If the ratio of 82–87 bp to 50–300 bp is above 25%, avoid such samples from sequencing (due to their short size, primer-dimer reads are selectively enriched in clonal amplification step and thereby reduces total number of usable sequencing reads). This type of peak is typically seen in libraries prepared from urine samples which had very low small RNA content.
12. Setting OneTouch 2 Instrument for the template preparation takes 30–40 min and run will complete in 6 h. User has an option to prolong the run up to 20 h. So plan the experiment at 4 pm and chose to finish the run the next day by 9–10 am.
13. Pellet may not be visible sometimes. Do not touch the pipette tip to walls of tube. Remove the supernatant as gently as possible.
14. Upon resuspension of ISPs in water, it can be stored at 2–8 °C for up to 3 days. If stored at 2–8 °C, bring the template-positive ISPs to room temperature and proceed to the washing ISPs.
15. ISP pellet cannot be seen. Without touching the walls of tube gently remove supernatant as gently as possible.
16. Enriched ISPs can be stored at 2–8 °C for up to 3 days.
17. Analysis of FASTQ files requires high computing power and efficient NGS data analysis software. Various open-source and commercially available NGS data analysis software can also be used. Although online servers such as <https://oasis.dzne.de/index.php> and <http://tools.genxpro.net/omiras/> are freely available for miRNA NGS data analysis, they do not contain *M. fascicularis* genome and/or miRNA reference in their database. Nevertheless, these URLs provide simple solutions to

miRNA NGS data analysis and one may anticipate *M. fascicularis* genome inclusion in future.

18. Sequencing library prepared from rat urine also displayed similar characteristics; large proportion (20–60%) of urinary RNA sequencing reads could not be aligned to rat genome.

References

1. Mardis ER (2013) Next-generation sequencing platforms. *Annu Rev Anal Chem (Palo Alto, Calif)* 6:287–303. doi:[10.1146/annurev-anchem-062012-092628](https://doi.org/10.1146/annurev-anchem-062012-092628)
2. Ansorge WJ (2009) Next-generation DNA sequencing techniques. *New Biotechnol* 25:195–203. doi:[10.1016/j.nbt.2008.12.009](https://doi.org/10.1016/j.nbt.2008.12.009)
3. Rothberg JM, Hinz W, Rearick TM et al (2011) An integrated semiconductor device enabling non-optical genome sequencing. *Nature* 475:348–352. doi:[10.1038/nature10242](https://doi.org/10.1038/nature10242)
4. Merriman B, Torrent I, Rothberg JM (2012) Progress in ion torrent semiconductor chip based sequencing. *Electrophoresis* 33:3397–3417. doi:[10.1002/elps.201200424](https://doi.org/10.1002/elps.201200424)
5. Ha M, Kim VN (2014) Regulation of microRNA biogenesis. *Nat Rev Mol Cell Biol* 15:509–524. doi:[10.1038/nrm3838](https://doi.org/10.1038/nrm3838)
6. He L, Hannon GJ (2004) MicroRNAs: small RNAs with a big role in gene regulation. *Nat Rev Genet* 5:522–531. doi:[10.1038/nrg1415](https://doi.org/10.1038/nrg1415)
7. Iorio MV, Croce CM (2012) MicroRNA dysregulation in cancer: diagnostics, monitoring and therapeutics. A comprehensive review. *EMBO Mol Med* 4:143–159. doi:[10.1002/emmm.201100209](https://doi.org/10.1002/emmm.201100209)
8. Sun Y, Koo S, White N et al (2004) Development of a micro-array to detect human and mouse microRNAs and characterization of expression in human organs. *Nucleic Acids Res* 32:e188. doi:[10.1093/nar/gnh186](https://doi.org/10.1093/nar/gnh186)
9. Weber JA, Baxter DH, Zhang S et al (2010) The microRNA spectrum in 12 body fluids. *Clin Chem* 56:1733–1741. doi:[10.1373/clinchem.2010.147405](https://doi.org/10.1373/clinchem.2010.147405)
10. Hayes J, Peruzzi PP, Lawler S (2014) MicroRNAs in cancer: biomarkers, functions and therapy. *Trends Mol Med* 20:460–469. doi:[10.1016/j.molmed.2014.06.005](https://doi.org/10.1016/j.molmed.2014.06.005)
11. D'Alessandra Y, Devanna P, Limana F et al (2010) Circulating microRNAs are new and sensitive biomarkers of myocardial infarction. *Eur Heart J* 31:2765–2773. doi:[10.1093/eurheartj/ehq167](https://doi.org/10.1093/eurheartj/ehq167)
12. Zeng L, Cui J, Wu H, Lu Q (2014) The emerging role of circulating microRNAs as biomarkers in autoimmune diseases. *Autoimmunity* 47:419–429. doi:[10.3109/08916934.2014.929667](https://doi.org/10.3109/08916934.2014.929667)
13. Kanki M, Moriguchi A, Sasaki D et al (2014) Identification of urinary miRNA biomarkers for detecting cisplatin-induced proximal tubular injury in rats. *Toxicology* 324:158–168. doi:[10.1016/j.tox.2014.05.004](https://doi.org/10.1016/j.tox.2014.05.004)
14. Nassirpour R, Mathur S, Gosink MM et al (2014) Identification of tubular injury microRNA biomarkers in urine: comparison of next-generation sequencing and qPCR-based profiling platforms. *BMC Genomics* 15:485. doi:[10.1186/1471-2164-15-485](https://doi.org/10.1186/1471-2164-15-485)
15. Pritchard CC, Cheng HH, Tewari M (2012) MicroRNA profiling: approaches and considerations. *Nat Rev Genet* 13:358–369. doi:[10.1038/nrg3198](https://doi.org/10.1038/nrg3198)
16. Li N, You X, Chen T et al (2013) Global profiling of miRNAs and the hairpin precursors: insights into miRNA processing and novel miRNA discovery. *Nucleic Acids Res* 41:3619–3634. doi:[10.1093/nar/gkt072](https://doi.org/10.1093/nar/gkt072)
17. Veeranagouda Y, Rival P, Prades C et al (2015) Identification of microRNAs in *Macaca fascicularis* (Cynomolgus monkey) by homology search and experimental validation by small RNA-Seq and RT-qPCR using kidney cortex tissues. *PLoS One* 10:e0142708. doi:[10.1371/journal.pone.0142708](https://doi.org/10.1371/journal.pone.0142708)

Chapter 21

Quantitative RT-PCR for MicroRNAs in Biofluids

Michael Thorsen, Thorarinn Blondal, and Peter Mouritzen

Abstract

MicroRNAs in biofluids hold great promise as minimally invasive diagnostic biomarkers for a wide range of diseases and biological processes. One of the most sensitive technologies for detection and measuring expression levels of microRNA is quantitative RT-PCR. However, quantification of microRNA in biofluid samples is challenging in many ways. Biofluids contain low levels of RNA and high levels of inhibitors of enzymatic processes like reverse transcription and PCR. Furthermore, biofluids are susceptible to many preanalytical variables. Here we describe procedures developed to address these challenges, which include highly sensitive and accurate microRNA detection methods, combined with optimized protocols for sample handling and preparation, and extensive quality control (QC) procedures.

Key words Biofluids, RNA isolation, microRNA, RT-qPCR, Expression analysis

1 Introduction

MicroRNAs in biofluids hold great promise as minimally invasive biomarkers in toxicology, to indicate drug-induced toxicity, or altered biological processes, as well as diagnostic biomarkers for a wide range of diseases. These short regulators of mRNA translation have wide-ranging biological potential, and are very stable in clinical samples such as serum/plasma, urine, and other biofluids, and the number of different microRNAs identified (around 2000 in humans) is amenable for screening projects. However, microRNA profiling in biofluid samples is challenging in many ways. Biofluids contain low levels of RNA and high levels of inhibitors and are susceptible to many preanalytical variables. To address these challenges, we have focused on developing highly sensitive and accurate microRNA detection methods, combined with optimized protocols for sample handling and preparation, and extensive quality control procedures.

The techniques we have developed are based on many years' experience with both microRNA profiling and biomarker discovery and validation in biofluid samples.

Various approaches exist to perform microRNA RT-qPCR [1] which are beyond the scope of this chapter. Here we focus on the main advantages of Locked Nucleic Acid (LNATM)-enhanced qPCR assays for microRNA detection compared to other available systems. LNATM is a RNA analogue with higher affinity to RNA and DNA than these two nucleic acids themselves and may be incorporated into oligonucleotides like PCR primers to increase sensitivity and specificity of the PCR reaction. In the LNATM-enhanced microRNA RT-qPCR system we have developed, the reverse transcription is truly universal due to the use of poly(A) polymerase extension of RNA targets prior to reverse transcription. The following very efficient cDNA synthesis reaction results in unbiased conversion of microRNA to cDNA by applying a universal RT primer. The subsequent qPCR is performed with two microRNA-specific primers which have equal performance across microRNA in the miRNome irrespectively of microRNA GC content, both features that are enabled by applying LNATM to normalize the T_m and shorten the PCR primers. The high processivity of cDNA synthesis and PCR results in a very sensitive PCR which does not require preamplification, even when applied to very RNA dilute samples like biofluids. The rigorously validated LNATM-enhanced qPCR assays were developed to offer sensitive and specific analysis of both known and novel microRNAs. We have performed linear dilution series of synthetic microRNA templates for all assays over 6 log10s down to an equivalent of 10 copies per PCR reaction, and we have checked microRNA assay specificity by analyzing cross-reactivity within microRNA families using more than 800 synthetic microRNAs.

In addition to a very sensitive and specific RT-qPCR platform for identifying microRNA biomarkers in biofluids, there are several steps prior to the RT-qPCR which are crucial for robust results. First of all, protocols for collection of biofluids must be optimized and implemented to ensure person- and site-independent concordance in sample microRNA content. For example if the goal is to analyze the extracellular microRNA (cell free) profile of biofluids, it is important to set up procedures which avoid cellular contamination and hemolysis (lysis of red blood cells in the case of serum/plasma samples or other biofluids contaminated by blood). For urine and depending on the clinical indication it may be of importance when the urine is collected during the day, whether it is first volume of stream, and how urine is processed after collection such as spinning and subsequent storage.

Since biofluids contain very low amounts of RNA, normal RNA quality control using Bioanalyzer or spectrophotometric absorbance measurements is not suitable. Furthermore, biofluids contain inhibitors of the reverse transcriptase and polymerase enzymes that can inhibit the enzymatic reactions in RT-qPCR.

To circumvent and deal with these obstacles, we have developed RT-qPCR-based RNA quality control procedures which also enable consistent assessment of the RNA yields, level of hemolysis, and presence of carryover of inhibitors into the RNA sample.

Once the RT-qPCR has been performed, important decisions must be made on data filtering taking individual assay background into account, followed by normalization, and finally which microRNA has been detected sufficiently frequently to be considered in biomarker discovery. Particularly the normalization is often a subject for considerable discussion as some researchers use longer small-RNA species such as U6 snRNA, despite the fact that this RNA has a different cellular location, has a different biogenesis, and purifies differently during RNA isolation as a consequence of its size. Other more recommendable procedures for normalization involve application of global mean or stably expressed normalizer microRNAs. The latter can be identified using algorithms such as geNorm or NormFinder. In the below sections we will share our hands-on experience in RNA isolation, RT-qPCR technique using LNA™, and data analysis.

2 Materials

To conduct microRNA expression profiling in biofluids using RT-qPCR, a laboratory is required which is equipped with general molecular biology equipment. It is important to work in an RNase-free environment, and standard protective clothing is to be worn during all steps from RNA isolation to the conduct of PCR. If biofluids are clinical samples and can potentially be contaminated with contagious microorganisms and viruses, all necessary standard precautions must be taken to eliminate infection risks. Hazardous reagents in some RNA isolation kits may require work to be carried out in fume hoods. Precautions should also be taken to ensure that equipment and surfaces are clean with ideally no RNases present; furthermore, all plastic vials and pipette tips must be RNase free and of low RNA/DNA binding quality.

2.1 Sample Collection

1. Sample tubes: BD Vacutainer® tubes for blood collection with anticoagulants such as EDTA or citrate when preparing plasma, or RNase-free Cryo tubes for urine and cerebrospinal fluid (CSF) collection (*see Note 1*).
2. Centrifuge.
3. Nanodrop for assessment of hemolysis.
4. RNase-free Cryo tubes for storage.
5. Freezer ($-80\text{ }^{\circ}\text{C}$).

2.2 Exosome Isolation

Exosome isolation is recommended to concentrate biofluids like urine, CSF, and cell culture media which have an especially low RNA content, but it may also be used for serum/plasma if specifically the membrane-bound population of microRNAs is of interest. Further, exosome isolation from biofluids can be a means of circumventing the problems with co-purification of inhibitors from large volumes of biofluids.

1. miRCURY™ Exosome kit (Exiqon) (*see Note 2*).
2. Benchtop microcentrifuge.
3. Swing-bucket centrifuge.
4. Standard pipettes 2 to 1000 μL (+ RNase-free tips).
5. Vortex mixer.
6. 15 mL Conical tube.
7. Refrigerator.

2.3 RNA Isolation

1. miRCURY™ RNA Isolation Kits (Exiqon) (*see Note 3*).
2. Vacuum manifold (*see Note 4*).
3. Benchtop microcentrifuge.
4. Standard pipettes 2 to 1000 μL .
5. Nuclease-free, aerosol barrier pipette tips.
6. Vortex mixer.
7. MS2 RNA (Roche, cat. no. 10165948001) (*see Note 5*).
8. RNA Spike-In Kit (UniSp2, UniSp4 and UniSp5, Exiqon, Prod. No. 203203) (*see Note 6*).
9. Freezer ($-80\text{ }^{\circ}\text{C}$).

2.4 RNA Quality Assessment and RT-qPCR

1. miRCURY LNA™ Universal RT microRNA PCR System (Exiqon) (*see Note 7*).
2. RNA quality assessment—Individual primer sets for the various RNA Spike-in templates or the dedicated microRNA QC PCR Panel (*see Note 8*).
3. Individual primer sets or ready-to-use panels, e.g., miRNome panels.
4. Universal cDNA synthesis kit II.
5. ExiLENT SYBR® Green master mix.
6. Nuclease-free PCR tubes or plates for use with individual assays.
7. Nuclease-free, aerosol barrier pipette tips.
8. Nuclease-free, low-nucleic-acid-binding microcentrifuge tubes, e.g., Eppendorf DNA LoBind tubes, and original 50 mL NUNC vials.

9. Clear, adhesive sealing foils for PCR plates.
10. Microcentrifuge and plate centrifuge.
11. Heating block, thermal cycler, or other incubators.
12. Real-time PCR instrument.
13. ROX or other passive reference dye (required on some PCR cyclers).
14. Real-time PCR instrument (384-well for full miRNome panels, or 96-well for smaller panels).

2.5 Data Analysis and Normalization

Different approaches exist for normalization and data analysis. Some steps are perfectly handled in Excel sheets whereas others are difficult without software dedicated for normalization and downstream analysis. Identification of microRNA stably expressed across the sample set is required to find the microRNAs best suited for normalization. Several free tools have been developed for this purpose, e.g., geNorm or NormFinder. For larger studies where many samples and microRNA are involved, data analysis quickly becomes complex and a software solution dedicated to handle qPCR data will be a great help. The Bioconductor Package for R contains some tools for qPCR data analysis [2]. We generally use the GenEx 6 software (Exiqon AS/MultiD Analyses) for analysis of RT-qPCR data for microRNA, lncRNA, and mRNA.

3 Methods

3.1 Study Setup

There are several important parameters to consider when setting up a RT-qPCR study to ensure that correct data is obtained. In this section some of the most important parameters will be discussed, such as Panel format, sample size versus sampling method, number of replicates, and types of controls (*see Note 9*).

3.1.1 Determine the Optimal Sample Size of Your Study

The sample size needed to get a statistically relevant answer from the study depends on the intragroup variance, introduced technical variation, and magnitude of differential expression between the sample groups the study is expected to show. To obtain knowledge of the expected biological and technical variation, performing a power analysis in a smaller pilot study can be very helpful to determine the number of samples needed. We perform pilot studies using a nested design, where three replicates are performed at each potential level of variation and the results are analyzed using a nested ANOVA [3], e.g., in a data analysis software such as GenEx 6 qPCR analysis software, or one of many free online tools (*see Note 10*).

3.1.2 Determine the Number of Replicates or Samples in Each Step of the Study

The purpose of performing technical replicates of any test is to evaluate and remove noise caused by technical variance within the experimental system including RNA purification, cDNA synthesis, and qPCR reactions. The term biological replicates often causes confusion. Biological replicates can be as simple as cell cultures grown from the same batch of cells under the same conditions, or a group of mice derived from specific mouse line raised and treated in the same manner. However, biological replicates can also be diverse group of humans (including multidimensional biological variance) that share some phenotypic or genetic identifier(s), for example lung cancer patients that are positive for the ALK fusion gene. Biological replicates should capture a major part of the biological variation within the system or organ to be interrogated. A minimum of three replicates is required for many statistical analyses; however with only three biological replicates per group statistical analysis will be weak at best since most parametric and nonparametric statistical methods favor comparison between larger groups. When performing a screening study, we would always choose to include a higher number of biological replicates in preference to technical replicates (profiling the same sample twice), provided that the profiling platform being used has been demonstrated to introduce minimal technical variation. The false discovery rate (FDR) or type I errors in null hypothesis when conducting [multiple comparisons](#) is a problem when performing microRNA profiling on hundreds of assays simultaneously but can be controlled by various methods. Commonly used methods to control FDR include the Benjamini-Hochberg FDR correction method [4] or the Bonferroni FDR correction method [5].

3.1.3 Selection and Use of Controls for Optimal Data Validation

In order to ensure that experiments have performed well, and enable troubleshooting if they have not, it is always a good idea to include a number of negative and positive controls. Which controls to include depends on the type of study and the main risks inherent to the study. Negative controls are important for two purposes of equal importance: one is to reveal potential contamination in the experiment, and the other is to determine background levels for each assay. Background may arise from contamination or primer-dimer formation. Positive controls verify that all reagents including template were added and that procedures were followed correctly.

1. A no-template control (NTC) in the PCR reaction or in the RT reaction (adding water instead of cDNA or RNA, respectively) will reveal if any of the reagents used have been contaminated. Each NTC will address possible contamination of a specific subset of reagents, or if primer-dimers are an issue (*see Note 11*).
2. A no-enzyme control (NEC) is an RT reaction performed without enzyme, but with RNA template. It will reveal if there is any amplifiable genomic DNA contamination in the RNA

sample or amplicon from a previous PCR experiment. The level of primer-dimer (if any) in the NEC is likely to better resemble the level of primer dimer formation in a biological sample than the NTC because RNA in the NEC will act as a “carrier,” helping to prevent primer-dimer formation.

3. If using a carrier during RNA isolation such as Bacteriophage MS2 RNA (see below), glycogen, or bovine serum albumin (BSA), it is important to test that this carrier does not contain microRNA or homologous sequences. The MS2 RNA is free of potential contaminants, but other carriers should be checked by performing an RT reaction with carrier RNA only.
4. The use of positive controls allows the performance of the RNA extractions, sample quality, and performance of enzymatic reactions to be monitored. Positive controls also aid in troubleshooting if the results look suboptimal. We recommend adding synthetic spike-in RNAs to the lysis buffer during the RNA isolation step, and to the RT reaction. The RNA spike-ins are then monitored by qPCR. We also measure endogenous microRNAs which are expected to be expressed in the given sample type. Further details are described in the RNA QC section below.

3.2 Sample Collection

1. We recommend the NCI’s Early Detection Research Network (EDRN) standard operating procedures [6] for the collection and preparation of serum and plasma (*see Note 1*).
2. It is important to remove cells and cell debris as soon as possible after biofluid collection. All cell removal should take place before freezing of samples since the freeze/thaw process often causes lysis of cells (*see Note 12*). Storage at 4 °C as stated in the EDRN standard operating procedures may result in lysis or activation of thrombocytes and contamination of the cell-free microRNA profile. Once prepared, serum and plasma samples should be centrifuged for 5 min at 3000 × *g* to remove cells (prior to freezing), and then stored in RNase-free tubes (e.g., cryo-tubes) at −80 °C. Plasma samples can have very different platelet loads which can affect the microRNA profiles obtained from corresponding samples. To obtain plasma which is as free from cells and platelets as possible, it is recommended to spin once at 1300–1800 × *g* for 5–10 min to remove cells after collecting plasma (without disturbing the buffy coat), followed by spinning twice at 16,000 × *g* for 20 min, and discard cell pellets each time. It is important to handle all samples consistently to avoid introducing any technical variation. Urine: Centrifugation before freezing is also important in urine since cells are known to be found in urine.
3. MicroRNAs show high stability in cell-free urine samples but nevertheless we recommend to standardize sample handling

and storage protocols. Whether analyzing cell-free urine or exosomes, the fresh urine samples should be centrifuged at $3200 \times g$ for 5 min to remove cell debris and subsequently stored at $-80\text{ }^{\circ}\text{C}$. We have successfully analyzed urine samples collected in RNase-free cryo tubes with and without stabilizer; however other tube types may also be applicable. If cell debris cannot be removed immediately, samples should be stored at $4\text{ }^{\circ}\text{C}$ for maximum 24 h until centrifugation.

4. When collecting urine from animals (such as in preclinical studies), urine is typically collected over several hours and here we recommend continuous cooling of the urine during the collection period.

3.3 Isolation of Exosomes with Low-Speed Centrifugation Protocol

Exosome isolation enables the analysis of those microRNAs which are selectively and actively incorporated into these membrane-bound vesicles and secreted by cells into a range of biofluids. In addition, exosome isolation allows RNA isolation from larger volumes than would be possible directly, which will enhance the signals from very dilute biofluid samples such as urine and CSF, enabling more microRNAs to be detected. This is in part enabled by allowing microRNA extraction while avoiding the co-purification of inhibitors of RT and PCR enzymes. The procedure for exosome isolation depends to some extent on the type of biofluid. Here we describe the procedure for isolation of exosomes from cell-free urine using the miRCURY™ Exosome Isolation Kit—Cells, Urine, and CSF (*see Note 13*).

1. Before getting started ensure that the centrifuge is operating at room temperature.
2. Thaw samples on ice or at $4\text{ }^{\circ}\text{C}$.
3. Prior to use, vortex precipitation buffer B (part of the miRCURY™ Exosome Isolation Kit).
4. Spin 10 mL urine sample for 5 min at $3200 \times g$ in a 15 mL conical tube to remove cell debris and transfer supernatant into a new 15 mL conical tube (*see Note 14*).
5. Add 4 mL precipitation buffer B and vortex for 5 s to mix.
6. Incubate for 60 min at $4\text{ }^{\circ}\text{C}$ (*see Note 15*).
7. Spin for 30 min at $3200 \times g$ at $20\text{ }^{\circ}\text{C}$ and remove supernatant completely and discard (or save for separate analysis).
8. Respin the pellet for 5 s and remove residual supernatant. The resulting pellet—which may be barely visible for low volumes of biofluid—consists of exosomes. The pellet may be stored at $-80\text{ }^{\circ}\text{C}$, or RNA isolation may be performed right away.

3.4 Isolation of RNA

1. Efficient preparation of microRNA from biofluids where RNA concentration is very low is critical for successful microRNA expression profiling. Therefore, the method used for RNA

isolation is crucial to the success of the experiment. Our routine procedure applies the miRCURY™ RNA Isolation Kit—Biofluids for serum/plasma, urine, CSF, and serum/plasma-derived exosomes, whereas the miRCURY™ RNA Isolation Kit—Cell & Plant works best for exosomes derived from urine, CSF, and cell culture media.

2. Irrespectively of the kit used for RNA isolation, RNA carrier MS2 should be added to the lysis buffer (*see* **Note 16**) together with RNA spike-ins to assess RNA isolation efficiency and presence of inhibitors or nucleases. Carrier or spike-ins should never be added directly to the biofluid sample itself, as the RNA spike-ins are unprotected and may be degraded by RNases. Therefore prior to starting the RNA isolation protocol, lysis buffer, carrier, and RNA spike-ins are premixed in a volume sufficient for all samples.
3. Before proceeding to RNA isolation of plasma and serum samples, two different checks are recommended to assess the degree of sample hemolysis. The first check is simply a visual inspection of the serum or plasma tubes by holding tubes up against a well-lit white background. Tubes where the sample appears pink or orange should be disregarded for further microRNA analysis. The second check consists of a Nanodrop™ absorbance scan at wavelengths from 220 to 700 nm to identify samples affected by hemolysis, which will display an absorbance peak at 414 nm (oxyhemoglobin). We would always include “borderline” samples for further analysis on the RT-qPCR-based RNA quality control panel (*see* below and **Note 17**).
4. The amount of lysis buffer varies depending on whether the starting material is biofluid (60 µL lysis solution BF to 200 µL biofluid) or exosome pellets (350 µL lysis solution).
5. Add 1 µg MS2 RNA and 1 µL RNA spike-in mix (UniSp2, UniSp4, and UniSp5, Exiqon product number #203203) per sample to the lysis solution.
6. Vortex/mix to ensure homogenous distribution.

3.5 RNA Quality Assessment

1. Standard methods for measurement of the RNA yield and quality are inappropriate for use with biofluid samples. The RNA concentration in the eluate is too low for reliable OD260 quantification or RNA quality assessments at OD230/280 on a NanoDrop™ or other spectrophotometers, and the presence of contaminants that absorb at different wavelengths may also confound the readings. In addition, the presence of carrier RNA in samples makes measuring the low levels of endogenous RNA by OD260 impossible. Here we describe procedures for how to operate despite the lack of information on

sample RNA concentrations, and how to assess RNA quality by RT-qPCR to monitor RNA isolation efficiency or presence of nucleases, hemolysis, cellular contamination, and presence of inhibitors.

2. With no assessment of RNA concentrations, input amounts are standardized based on starting volume rather than RNA quantity (starting with the same volume of biofluid in each RNA isolation, and using the same volume of purified RNA for all samples). The amount of RNA to be added to cDNA synthesis reaction is described in the next section.
3. RT-qPCR can be used to assess RNA isolation efficiency, hemolysis, cellular contamination, and presence of inhibitors, by using assays which monitor RNA spike-ins added during RNA isolation, and RNA spike-ins which are added during cDNA synthesis, as well as assays that measure levels of a selected number of endogenous microRNAs in the samples. For simplicity we have designed a microRNA QC PCR panel in which primers have been predispensed and dried down (miRCURY™ microRNA QC PCR Panel) so that only cDNA and mastermix have to be added. For an overview of applied RNA spike-ins and assays *see* Table 1.

Table 1
Overview of miRNA and spike-ins for RNA quality assessment

Assay name	Applications for biofluid samples
UniSp2, UniSp4, and UniSp5	<ul style="list-style-type: none"> • Three spike-ins added in different concentrations to lysis buffer during RNA purification • Use to monitor RNA isolation efficiency or presence of nucleases
UniSp6 and cel-miR-39-3p	<ul style="list-style-type: none"> • Two spike-ins added in different concentrations to cDNA synthesis reaction • Check for signs of RT and PCR inhibitors
UniSp3	<ul style="list-style-type: none"> • Template and primers present in PCR panels • Independent PCR monitoring • Use as interplate calibrator, IPC
miR-451a and miR-23a-3p	<ul style="list-style-type: none"> • Unique hemolysis indicator • Check ΔCq (miR-23a-3p–miR-451a)
miR-30c-5p, miR-103a-3p, miR-124-3p, and miR-191-5p	<ul style="list-style-type: none"> • Biologically relevant, endogenous microRNAs • Should be present in RNA from serum/plasma, urine or CSF, and some other biofluids • Use for general sample quality check

4. The UniSp2, UniSp4, and UniSp5 are microRNA-sized spike-ins which when added during RNA isolation allow to monitor the uniformity and efficiency of the RNA extraction procedure. Samples which show altered Cq for these three spike-ins may have been purified inefficiently, may contain noninactivated nuclease, or may contain inhibitors co-purified with the RNA, in which case the RNA spike-ins added during cDNA synthesis will also be affected (*see* next point).
5. The UniSp6 and cel-miR-39-3p RNA spike-ins added during cDNA synthesis (*see* Subheading 3.6) monitor the efficiency of the cDNA synthesis and RT-qPCR reaction. Increased Cq values in selected samples may indicate co-purification of inhibitors of either the cDNA synthesis reaction or the RT-qPCR (*see* **Note 18**).
6. When initiating work with a new protocol for biological sample collection or with a new type of biofluid, e.g., urine or CSF, we recommend testing different RNA sample input amounts in the cDNA synthesis reaction (e.g., 1.0 μ L, 2.0 μ L, 4.0 μ L, and 8.0 μ L in a 20 μ L RT reaction). This dilution series is performed using assays for the RNA spike-ins and a few microRNA assays (*see* Table 2) in order to evaluate the linear relationship between sample input and signal, and identify a suitable RNA input amount for further studies. Samples containing PCR inhibitors will show dilution curves without the expected linear relationship between sample input and signal (Fig. 1).
7. UniSp3 is supplied as dried-down primers and DNA template in a well on the PCR plate which can be used for interplate calibration if the microRNA profiling experiment requires more than one PCR plate. Interplate calibration is relevant for some RT-qPCR instruments and the Cq value of the UniSp3 assay will show whether calibration is needed.
8. The RT-qPCR assays for the endogenous microRNAs hsa-miR-451a and hsa-miR-23a-3p compare the level of a microRNA highly expressed in red blood cells (miR-451a), with a microRNA unaffected by hemolysis (miR-23a-3p) [7]. The delta Cq (miR-23a-3p–miR-451a) is a good measure of the degree of hemolysis where values of more than five is an indicator of possible erythrocyte microRNA contamination, and a delta Cq of 7–8 or more indicates a high risk of hemolysis affecting the data obtained in human serum/plasma samples (*see* **Note 19**).
9. The assays for the endogenous microRNA miR-30c-5p, miR-103a-3p, miR-124-3p, and miR-191-5p can indicate not only if the RNA isolation was successful, but also if the biological samples are of similar quality with regard to microRNAs expected to be present in a given sample set. miR-103 and

Table 2
Endogenous microRNAs typically detected or stably expressed in human biofluid samples

microRNA	Serum/plasma	Urine	CSF (exosomes)
hsa-let-7i-5p	X (s)		
hsa-miR-23a-3p	X		X
hsa-miR-23b-3p		X	X
hsa-miR-30c-5p		X	X
hsa-miR-30e-5p	X (s)		
hsa-miR-93-5p	X		X
hsa-miR-103a-3p	X	X	X
hsa-miR-106b-5p	X		
hsa-miR-107		X	X
hsa-miR-141-3p		X	
hsa-miR-148b-3p	X (s)		
hsa-miR-191-5p	X		X
hsa-miR-222-3p	X (s)		
hsa-miR-423-5p/3p	X		
hsa-miR-425-5p	X (s)		X
hsa-miR-484	X (s)		

Often, one or more of these microRNA assays may be good for the normalization of expression data, but the stability of their expression must be verified in any new sample set (*see* section on Normalization). The list of microRNA is based on microRNA profiles analyzed in thousands of serum/plasma samples from individuals with a range of different diseases as well as healthy individuals. “X (S)”: very often stably expressed in serum/plasma or “X”: typically detected but not necessarily stably expressed

miR-191 are well expressed in most tissues, and miR-30c is well expressed in kidney and found in urine samples. Finally miR-124 is well expressed in central nervous system tissues and found in CSF.

3.6 RT-qPCR

1. In case of biofluids it is recommended to perform cDNA synthesis in a larger reaction volume than for other samples, in order to minimize or alleviate the effect of smaller variations in inhibitor content between samples. If the amount of RNA input volume exceeds 20% v/v in the RT reaction, it is very important to monitor the samples for any signs of inhibition as described in Subheading 3.5 on RNA quality assessment.
2. Our standard biofluid protocol for human serum/plasma uses 8 μ L of eluted RNA in a 40 μ L RT reaction (20% v/v) which

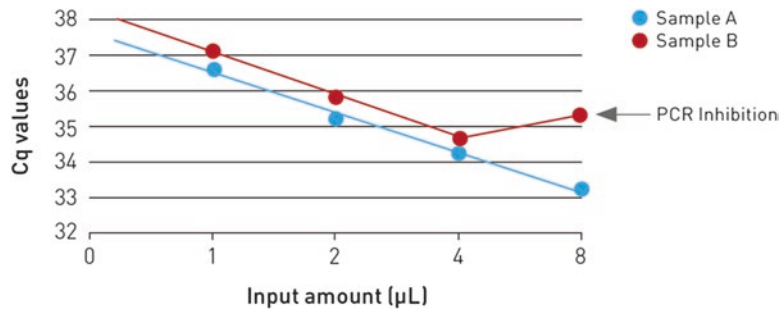


Fig. 1 Assessment of optimal RNA input volume. Performing of an RNA dilution series can be used to determine that input amounts are within the linear range of the system, and to ensure a good level of signal, with no sign of inhibition (e.g., Sample A at 8 µL). Increasing the RNA volume to increase signal levels can have the opposite effect and result in less signal due to carryover of inhibitory compounds into the RT-qPCR reaction (e.g., Sample B at 8 µL). Input amount refers to µL RNA in a 20 µL RT reaction

generally gives a good signal. One 40 µL RT reaction gives enough cDNA for one 384-well plate full of microRNA assays, e.g., Human Panel I (*see Note 20*).

3. As negative control run a mock/blank purification where RNA isolation is conducted with only water and MS2 as input, but if this is not possible we would set up a no-template control (NTC) by adding water to the reverse transcription (RT) instead of RNA. Subsequently qPCR is performed on a full 384-well plate full of the same assays as samples are analyzed on. This will be used to determine assay background levels in the given experimental setting, and enable true signals to be distinguished from background.
4. Due to the large RT reaction volume, the dilution factor of the cDNA is reduced to 50× compared to 100× for standard samples. To avoid low concentrations of cDNA adhering to tube surfaces, the following procedure is recommended: combine and mix gently 2× PCR mastermix and water, then add undiluted cDNA and mix very thoroughly (*see Note 21*).
5. From this point on, all handling and PCR cycling conditions follow procedures described in the Instruction Manual for miRCURY LNA™ Universal RT microRNA PCR for biofluid samples.
6. One of the benefits of using a SYBR Green-based RT-qPCR system is that PCR product(s) can be analyzed after the PCR by dissociation curve analysis. Most real-time PCR instruments are able to incorporate a dissociation curve analysis of the PCR product(s) after the last PCR cycle and this is highly recommended to verify specificity and identity of the amplification reaction (*see Subheading 3.7*).

3.7 Data Handling

1. After completion of the PCR, check the amplicon dissociation curve in all PCR wells to ensure that this always is a single clean peak indicating a unique amplification product. Also ensure that the amplicon melting temperature is consistent for the same assay between samples. Assays should be disregarded if they display more than one peak, “heavy peak shoulders,” or inconsistent melting temperatures.
2. Analyze the amplification efficiency in each PCR well using LinRegPCR or similar algorithm [8] to make sure that there are no signs of PCR inhibition. Because some assays may be more sensitive to inhibition than others, it is a good idea to monitor efficiency on the actual study data, including all data points.
3. Determine the background level for each assay by analyzing the NTC PCR plate. In challenging samples such as biofluids, characterized by low levels of microRNAs combined with the presence of PCR inhibitors, the Cq values obtained will often be at the high end (Cq values in the range of 28 and above). This is acceptable as long as the signal can be easily discerned from any background. Any signals that are less than 5 Cq below the Cq value of the NTC for the specific assay should be disregarded.
4. Evaluate the performance of the RNA spike-ins by comparing the Cq values of the spike-ins between the different samples in the study, in order to identify samples affected by poor RNA isolation efficiency, nucleases, or inhibitors of reverse transcription and/or PCR. Consider disregarding such samples or as a minimum flag these for later consideration after data analysis is complete.
5. Evaluate Cq values for hemolysis indicator assays miR-23a-3p and miR-451a as well as marker assay miR-142 indicative of thrombocyte contamination [9]. It is difficult to provide a cut-off value to indicate excessive contamination of thrombocytes; rather a comparison of miR-142 levels across samples should be in the same range. Samples with significantly altered levels should be considered as outlier samples which may be flagged and/or disregarded in further data analysis. Finally it is also recommended to compare Cq values of assays for microRNA which are often found to be stably expressed in the given biofluid sample type (*see* Table 2 for microRNA very often stably expressed in serum/plasma). If outlier samples are identified, disregard or flag samples, depending on severity.
6. Once assay and sample flagging is completed, start filtering the dataset by removing assays that are flagged in a high number of samples (e.g., 20% or higher) and remove samples that are flagged in a high number of assays.

7. Select a normalization strategy. The purpose of normalization is to remove technical variation in data which is not related to the biological changes under investigation. Proper normalization is critical for the correct analysis and interpretation of results. One commonly used method is to use the mean expression value of all commonly expressed microRNAs in a given sample set as normalization factor [10]. This is usually the best approach when analyzing PCR panels containing a larger number of microRNA assays, where a considerable number of microRNAs are expressed. Another approach is to identify and use stably expressed microRNAs as reference genes. Algorithms such as geNorm or NormFinder software can be used for this approach. The GenEx 6 software supports both approaches. It is recommended to investigate different approaches to identify the method that will provide the best normalization of the data in question (*see* **Notes 22** and **23**).
8. Cellular contamination can affect normalization because cellular contamination or hemolysis may result in release of cellular RNA which may affect the overall microRNA content, thus impacting the mean expression value in affected samples. Therefore it is crucial to monitor RNA samples for signs of cellular contamination or hemolysis (*see* above) and ensure that the microRNAs selected for use as normalizers are not affected by hemolysis [11].
9. When using stably expressed endogenous genes for normalization, it is recommended to test 5–6 candidates (reference genes) before setting up the actual microRNA expression analysis, in order to identify 2–3 stably expressed reference genes for normalization. These candidates should be chosen from a selection of genes that are expected to be stably expressed over the entire range of samples being investigated. When working with serum/plasma, urine, or CSF, the candidates are typically chosen based on the literature or preexisting data (e.g., qPCR panel screening). Several microRNAs are available on Exiqon's PCR Panels as candidate reference genes including the serum/plasma panel (*see* Table 2). These are typically medium to highly expressed and may be stably expressed, but their use as reference genes must *always* be evaluated on a study-to-study basis.
10. Certain treatments can result in dramatic changes in the overall microRNA content of biofluid samples, e.g., drug-induced toxicity. In these situations it may be very challenging to identify stably expressed microRNAs, and the mean expression value of all microRNAs may not be stable either, so alternative strategies such as use of microRNA ratios may need to be considered. Urine samples can pose additional challenges for normalization. There can sometimes be large variation in RNA

concentration between urine samples (depending on the time of day, state of hydration, as well as disease state), so care should be taken when selecting stable reference genes, and it may also be necessary to normalize to urinary volume or creatinine. For other biofluid samples we recommend to empirically determine the best reference microRNAs by doing an initial pilot study and use geNorm or NormFinder algorithms (supplied in the GenEx software or as “stand-alone” tools) to identify the best candidates.

4 Notes

1. In all steps of collection of biofluids, measures should be taken to prevent lysis of cells which can alter the microRNA content of the samples drastically. This is also important for processing of biofluids from other sources like urine or CSF. Failure to do so may lead to contamination of the samples with RNA from intact cells. The RNA from intact cells could mask or prevent the subsequent detection of subtle changes in the microRNA expression profile. The preparation of serum and plasma starts with collection of whole blood where hemolysis can occur at the time of phlebotomy. The choice of blood collection tube has been shown to affect this and therefore it is recommended to use just one type of high-quality collection tube for all samples to be analyzed. We have not analyzed all available tubes on the market; we have good experience with BD Vacutainer® tubes, but other tube types may also be applicable. When preparing plasma, anticoagulants such as EDTA or citrate are normally used. These anticoagulants cause no problems in downstream processing of samples, in contrast to heparin, which is known to inhibit downstream enzymatic steps such as cDNA synthesis and PCR. Currently, there is no reliable way of removing heparin from RNA samples or from the original blood serum/plasma samples. Therefore, do not use heparin in any of the collection tubes or processing steps of whole blood. For urine and CSF the choice of tubes seems to be less critical and although different tube types may be applicable we have successfully used RNase-free cryo tubes with or without stabilizer for storage.
2. Most exosome kits on the market will also isolate other larger microvesicles at the same time as the exosomes, unless they are already size filtered. This is also the case for the miRCURY™ Exosome Kit which has been optimized together with miRCURY™ RNA Isolation Kits to produce the highest and most robust yield of exosomes and RNA.
3. For isolation of microRNA we use the miRCURY™ RNA Isolation Kits. The biofluid kit is optimized to work well for

isolation of microRNA directly from biofluids as well as exosomes isolated from serum/plasma using the miRCURY™ Exosome Isolation Kit—Serum and Plasma.

The miRCURY™ RNA Isolation Kit - Cell & Plant, works best with exosomes isolated from urine and CSF using the miRCURY™ Exosome Isolation Kit—Cells, Urine, and CSF.

4. The vacuum system should enable a vacuum of between -800 and -900 mbar. In some cases additional extension tubes or adaptors may be necessary.
5. MS2 RNA is added as a carrier to prevent adsorption of the very minute amounts of RNA to plastic surfaces of tubes and pipette tips. It's highly recommended as it increases RNA yield and improves reproducibility.
6. RNA spike-in kit is recommended for quality control of extraction efficiency. The spike-ins should be added to the lysis buffer right before use and not added directly to the sample as they will be degraded by RNases in the sample.
7. Several RT-qPCR providers and systems exist. To identify the platform that offers both high sensitivity and high specificity, consult the largest study (miRQC) comparing microRNA profiling platforms, published in *Nature Methods* [10]. We have the most extensive experience with the miRCURY LNA™ Universal RT microRNA PCR System which we developed ourselves. The three main challenges about microRNA detection are the following: (1) microRNA are short approximately 22 nucleotides long which makes it impossible to carry out a regular reverse transcription and PCR, (2) microRNAs vary considerably in their GC content which affects the melting temperature of primers, and (3) microRNA families exist where individual family members differ by only a single nucleotide and this makes discrimination difficult. We exploited the characteristics of Locked Nucleic Acid (LNA™) for making short T_m -normalized primers which all have the 3'-end anchored within microRNA sequence ensuring the maximum specificity and an independency of microRNA GC content, hereby addressing the three main challenges about microRNA detection.

The high affinity of LNA™ for RNA and DNA allows very short PCR primers to be functional because T_m is adjustable to the temperature required in PCR. This strategy is applied to handle the variable GC content of microRNA so they can all be interrogated by qPCR under the same PCR protocol and buffer composition. The reverse transcription step for the miRCURY LNA™ Universal RT microRNA PCR System is universal, unbiased, and efficient which means that preamplification is not needed.

8. It is recommended to use spike-ins to monitor RNA isolation yields from biofluids. miRCURY LNA™ Universal RT microRNA PCR, RNA spike-in kit, and QC Panel is a complete solution with both RNA spike-ins and RT-qPCR assays for validation of the spike-ins as well as selected microRNAs, hemolysis indicator, and cDNA synthesis inhibitors.
9. The revised MIQE guidelines state that you should provide, as a minimum, the sequence of each qPCR amplicon when publishing. For microRNA analysis, the sequence of the microRNA targeted is considered sufficient. However, do note that miR-Base updates may involve changing the microRNA sequence and/or name while keeping the accession number constant. For this reason, it is important to provide the actual microRNA sequence the assay was designed for as well as the microRNA name or miRBase accession number.
10. An overview of tools can be found at <http://statpages.org>.
11. To monitor possible contamination throughout the entire process from RNA isolation to qPCR, implementation of a purification negative control may also be beneficial. For the purification negative control biofluids would be replaced with an equal volume of RNase-free water.
12. If whole blood is not centrifuged immediately after collection (or after the clotting time, in the case of serum), the samples should be stored at room temperature for no longer than 4 h.
13. Other isolation kits may be appropriate for other biofluids; for example for isolation of exosomes from serum or plasma samples we use the miRCURY™ Exosome Isolation Kit—Serum and Plasma, followed by RNA isolation using the miRCURY™ RNA Isolation Kit—Biofluids.
14. The procedure is scalable from 500 µL to 10 mL urine.
15. Precipitation time can be extended, e.g., overnight, to accommodate a more optimal workflow if needed.
16. Because biofluid samples contain only small amounts of RNA, there is a high risk that a significant proportion of the RNA is lost during extraction. For this reason, we recommend using low-nucleic-acid-binding tubes and addition of carrier RNA during the purification procedure. MS2 RNA is an excellent carrier which we routinely use. It is guaranteed to be free from microRNAs and sequences homologous to microRNA. The use of a carrier ensures the highest and most consistent yield from serum and plasma samples and other low-yield biofluids [12], and may also minimize selective loss of structured low GC content microRNA which can be observed in samples with low RNA content isolated by Trizol [13].
17. Samples affected by hemolysis will have a microRNA profile which is distorted by the microRNA content of red blood cells.

However, if all samples in a given study are affected by a similar and relatively low degree of hemolysis, they may still qualify for microRNA expression profiling in particular if the microRNAs of interest are not present at high concentrations in red blood cells.

18. Not all assays are equally sensitive to different inhibitors which means that the presence of some inhibitors may not be revealed by the spike-ins. Therefore, it is also recommended to monitor the amplification efficiency of all assays, as described in the RT-qPCR and Data Handling sections.
19. The values are different in mouse and rat samples, or biofluids other than serum/plasma.
20. The use of 8 μ L RNA per 384-well PCR plate equates to the use of 32 μ L original serum/plasma per 384-well PCR plate, assuming that RNA isolation was performed from 200 μ L biofluid and the RNA was eluted in 50 μ L. For urinary exosomes obtained using the miRCURY™ Exosome Isolation Kits, we typically start with 3 mL of urine, so here the 8 μ L RNA per 384-well PCR plate equates to the use of 480 μ L original cell-free urine, again assuming that RNA was eluted in 50 μ L.
21. If the cDNA is not mixed into the mastermix-water mixture, reproducibility will be affected in particular for microRNAs that are only present in low copy numbers.
22. Normalization using spike-in RNAs is not recommended as this approach does not correct for many aspects of technical variation, e.g., variation in endogenous RNA content or sub-optimal conditions during sample collection until RNA isolation possibly resulting in RNA degradation.
23. When using endogenous RNAs for normalization, we recommend to use stably expressed microRNAs as reference genes, rather than larger small RNA species, e.g., 5S, U6, and snoRNAs, which are sometimes used for normalization in other sample types. The main reason for this is that the larger RNAs have a different biogenesis pathway and may not be secreted or protected in biofluids in the same way as microRNAs. Larger RNAs may also behave differently than short microRNA during RNA purification.

References

1. Jacobsen N, Andreasen D, Mouritzen P (2011) Profiling MicroRNAs by real-time PCR. MicroRNAs in development volume 732 of the series. *Methods Mol Biol* 732:39–54
2. Gentleman RC, Carey VJ, Bates DM, Bolstad B, Dettling M, Dudoit S, Ellis B, Gautier L, Ge Y, Gentry J, Hornik K, Hothorn T, Huber W, Iacus S, Irizarry R, Leisch F, Li C, Maechler M, Rossini AJ, Sawitzki G, Smith C, Smyth G, Tierney L, Yang JY, Zhang J (2004) Bioconductor: open software development for computational biology and bioinformatics. *Genome Biol* 5(10):R80
3. Tichopad A, Kitchen R, Riedmaier I, Becker C, Stählberg A, Kubista M (2009) Design and optimization of reverse-transcription

- quantitative PCR experiments. *Clin Chem* 55(10):1816–1823
4. Benjamini Y, Hochberg Y (1995) Controlling the false discovery rate: a practical and powerful approach to multiple testing. *J R Stat Soc Ser B* 57:289–300
 5. Dunn OJ (1959) Estimation of the medians for dependent variables. *Ann Math Stat* 30(1): 192–197
 6. EDRN standard operating procedures. <http://edrn.nci.nih.gov/resources/standard-operating-procedures/standard-operating-procedures>
 7. Blondal T, Jensby Nielsen S, Baker A, Andreasen D, Mouritzen P, Wrang Teilum M, Dahlsveen IK (2013) Assessing sample and miRNA profile quality in serum and plasma or other biofluids. *Methods* 59(1):S1–S6
 8. Merkerova M, Belickova M, Bruchova H (2008) Differential expression of microRNAs in hematopoietic cell lineages. *Eur J Haematol* 81(4):304–310
 9. Ruijter JM, Pfaffl MW, Zhao S, Spiess AN, Boggy G, Blom J, Rutledge RG, Sisti D, Lievens A, De Preter K, Derveaux S, Hellemans J, Vandesompele J (2013) Evaluation of qPCR curve analysis methods for reliable biomarker discovery: Bias, resolution, precision, and implications. *Methods* 59(1):32–46
 10. Mestdagh P, Van Vlierberghe P, De Weer A, Muth D, Westermann F, Speleman F, Vandesompele J (2009) A novel and universal method for microRNA RT-qPCR data normalization. *Genome Biol* 10(6):R64
 11. Pritchard CC, Cheng HH, Tewari M (2012) MicroRNA profiling: approaches and considerations. *Nat Rev Genet* 13(5):358–369
 12. Andreasen D, Fog JU, Biggs W, Salomon J, Dahlsveen IK, Baker A, Mouritzen P (2010) Improved microRNA quantification in total RNA from clinical samples. *Methods* 50(4): S6–S9
 13. Kim YK, Yeo J, Kim B, Ha M, Kim VN (2012) Short structured RNAs with low GC content are selectively lost during extraction from a small number of cells. *Mol Cell* 46(6): 893–895

Chromogenic In Situ Hybridization Methods for microRNA Biomarker Monitoring of Drug Safety and Efficacy

Barbara R. Gould, Tina Damgaard, and Boye Schnack Nielsen

Abstract

Disease research and treatment development have turned to the impact and utility of microRNA. The dynamic and highly specific expression of these molecular regulators can be used to predict and monitor disease progression as well as therapeutic treatment efficacy and safety, thus aiding decisions in patient care. In situ hybridization (ISH) of biopsy material has become a routine clinical pathology procedure for monitoring gene structure, expression, and sample characterization. For ribonucleic acid (RNA), determining cell source and level of expression of these biomarkers gives insight into the cellular function and physiopathology. Identification and monitoring of microRNA biomarkers are made possible through locked nucleic acid (LNA)TM-based detection probes. LNATM enhances the sensitivity and specificity of target binding, most profoundly so for the short, highly similar, microRNA sequences. We present a robust 1-day ISH protocol for formalin-fixed, paraffin-embedded (FFPE) tissue sections based on microRNA-specific LNATM detection probes which can be labeled with digoxigenin (DIG) or 6-carboxyfluorescein (FAM) and detected through enzyme-linked specific antibodies that catalyze substrates into deposited chromogen products at the target RNA site. The variety of haptens and detection reagents in combination with LNATM chemistry offer flexibility and ease to multiple target assessment of therapeutic response.

Key words microRNA, Biomarker, Locked nucleic acid, Detection probe, Formalin-fixed paraffin-embedded tissue

1 Introduction

In the past decade, interest in small noncoding RNA has exploded, particularly so for the smallest, 19–23 nucleotides (nt) in length, microRNA. The most frequently described function of microRNA is the repression of protein synthesis from their target messenger RNA (mRNA). microRNA, in complex with the RNA-induced silencing complex (RISC) of proteins, most often associate with specific sequences within mRNA 3' untranslated regions, effectively blocking the procession of translating ribosomes from completing their journey towards peptide synthesis and protein production [1, 2]. High-throughput microRNA screening methods such as microarray hybridization, reverse-transcription quantitative

polymerase chain reaction (qPCR) panels, and more recently next-generation sequencing (NGS) have taken a broad view to identify microRNA expression patterns within various biological contexts [3–10]. With these approaches, it is apparent that microRNA exhibit dynamic changes in expression levels and a high degree of tissue and temporal specificity, thus playing important roles in molecular pathway regulation and tissue differentiation in normal development and homeostasis. When these molecules divert from this pattern, disease often ensues.

Regulating protein expression can also affect or reflect responses to toxins or therapy. Recent studies present microRNA as biomarkers for drug safety and efficacy, tissue injury, and as therapeutic targets [11, 12]. microRNA (miR)-122, for example, is a liver-specific microRNA which is proving itself as tissue and bio-fluid biomarker for liver injury [13]. In a knockout mouse model, loss of miR-122 levels was shown to be associated with liver disease and cancer [14]. Currently, LNATM-enhanced anti-miR-122 oligonucleotide therapy is in phase II clinical trials as antiviral Miravirsen (SPC3649) preventing hepatitis C virus miR-122-mediated liver damage [15]. In the brain, miR-124 is highly abundant and associated with normal age-related neurodegeneration. Resveratrol treatment reduced miR-124, having a positive effect on miR-124 target gene expression levels, improving cognitive function in mice [16]. Endothelial-specific, angiogenesis-related miR-126 is implicated as a prognostic biomarker of hypertension [17]. Intraplacental injection of miR-126 mimic in pre-eclamptic mid-gestation rats improved blood pressure and pup survival [18]. miR-145 was determined to be the most abundant of its kind in vascular smooth muscle cells and important for vascular contractility and neointima formation through microRNA microarray studies followed by confirmation with *in situ* hybridization (ISH) staining, [19, 20]. Studies of mice with a deleted miR-143/145 cluster showed that smooth muscle miR-143/145 is essential for normal healing after intestinal injury [21].

Interpreting the patterns of microRNA biomarker expression in tissues and cells can be achieved through ISH. The technique has become a mainstay for microRNA studies since 2005, when the highly sensitive and specific LNATM/DNA chimeric detection probes were first used in zebrafish embryos and proven an essential component to microRNA ISH success [22]. The LNATM is a bicyclic RNA analog where a methylene bridge links the 2' oxygen to the 4' carbon, restricting the natural flexibility of a DNA sequence. This increases the binding energy and stability of the detection probe hybridization to its target by 2–8 °C per nucleotide substitution [23]. This is ideal for increasing the sensitivity and specificity of target detection, exceptionally so for short and highly homologous sequences as seen for microRNA. Also ideal, a non-formamide hybridization buffer is available which, in

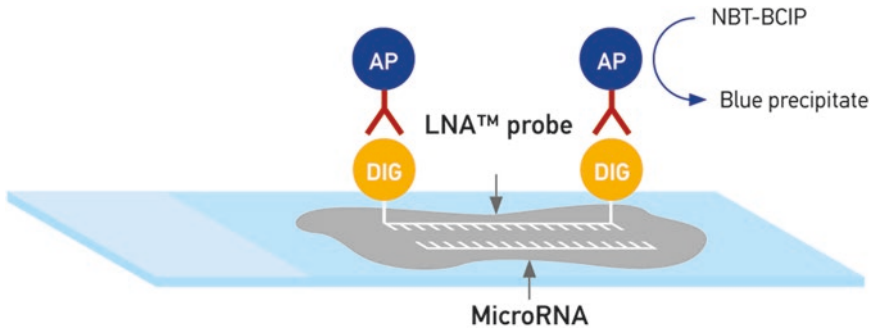


Fig. 1 Overview of the detection approach using hapten-labeled LNA™ microRNA detection probes. The non-mammalian hapten digoxigenin (DIG) is conjugated to LNA™ microRNA detection probes. During the protocol, the microRNA are demasked using proteinase K, which allows access of labeled LNA™ probes to hybridize to the microRNA sequence. The labeled LNA™ probes can then be recognized by a specific anti-DIG antibody that is directly conjugated with the enzyme alkaline phosphatase (AP). AP converts the soluble substrates 4-nitro blue tetrazolium (NBT) and 5-bromo-4-chloro-3-indolyl-phosphate (BCIP) into a water- and alcohol-insoluble dark blue NBT-BCIP precipitate [33]

addition to being non-toxic, affords improved rates of probe: target hybridization and reduced background signal from LNA™ detection probes. This formulation allowed for the development of a 1-day ISH protocol for FFPE tissues [24, 25] and with minor adaptations, to frozen tissues [26]. Adding antibody-binding haptens such as digoxigenin (DIG) or 6-carboxyfluorescein (FAM) or other labels to LNA™ detection probes allows flexibility in experimental design and ability to co-localize multiple microRNA species [27], co-localize microRNA to putative target mRNA [28], detect multiple mRNA sequences [29], or combine ISH with immunohistochemical mapping of protein expression [30, 31]. Figure 1 depicts the antibody-binding hapten detection approach followed by signal generation through antibody-linked enzymatic substrate reactions. Deciding to label one end or the other of an oligonucleotide detection probe (5' end or 3' end) is a matter of choice; however it has been demonstrated that labeling both ends and creating a dual-labeled probe affords a synergistic effect on the detection signal [32].

The intersection of LNA™ probe sensitivity and specificity, probe labeling alternatives, a safe, optimized hybridization buffer, and ease of application to microRNA biomarker detection alone or in combination through ISH are described in the following protocol.

2 Materials

2.1 Reagents

1. RNaseZap® (Ambion).
2. RNase-free Milli-Q water (Millipore).

3. Formalin-fixed and paraffin-embedded (FFPE) tissue samples: For best results use FFPE tissue samples that have been fixed in neutral-buffered formalin 24–48 h at room temperature and then processed for paraffin embedding.
4. Dual-labeled LNA[™] probes (Exiqon): Examples shown in this chapter are the miRCURY LNA[™] microRNA Detection Probes labeled at the 5' and 3' with FAM, henceforth referred to as double-FAM and 5' and 3' DIG-labeled probes, referred to as double DIG. Probes are specific for miR-126-3p and miR-145-5p and a scramble negative control sequence. The performance of these labeled probes and alternate label choices is found in **Note 1**.
5. Xylene.
6. Ethanol.
7. Nuclear Fast Red[™] (Vector Laboratories).
8. Eukitt[®] mounting medium (VWR).

2.2 Equipment

1. Superfrost[®]Plus microscope slides (Thermo Fisher Scientific).
2. Non-stick RNase-free microfuge tubes.
3. Sterile filter tips.
4. Slide rack(s) and several glass jars.
5. Hybridizer (Dako).
6. Glass cover slips.
7. Dako Pen (or equivalent hydrophobic PAP pen).
8. Humidifying chamber or equivalent for immunohistochemical detection.
9. Whatman 1.001–125 filter papers.
10. Bright-field microscope.

2.3 Buffers and Solutions

1. Proteinase K stock: Reconstitute the 12 mg lyophilized proteinase K (microRNA ISH buffer set, Exiqon) to 20 mg/mL by adding 600 μ L of 10 mM Tris–HCl pH 7.4.
2. Proteinase K buffer: To 900 mL RNase-free water add 5 mL of 1 M Tris–HCl pH 7.4, 2 mL of 0.5 M EDTA, and 0.2 mL of 5 M NaCl. Adjust volume to 1000 mL. Autoclave.
3. Proteinase K reagent: Prepare immediately before use. For a proteinase K concentration of 15 μ g/mL, add 7.5 μ L proteinase K stock to 10 mL proteinase K buffer.
4. microRNA ISH buffer (2 \times) (microRNA ISH buffer set, Exiqon).
5. 20 \times SSC pH 7.0: If purchased as RNase-free then leave as it is. SSC solutions: 5 \times SSC (1 L = 250 mL 20 \times SSC + 750 mL

- water); 1 × SSC (1 L = 50 mL 20 × SSC + 950 mL water); 0.2 × SSC (1 L = 10 mL 20 × SSC + 990 mL water). Autoclave.
6. PBS 1×, sterile.
 7. PBS-T (0.1%), pH 7.4: Add 1 mL of Tween-20 to 1 L of PBS. Autoclave.
 8. Antibody blocking and dilutant solutions: To make 10 mL blocking and 10 mL dilutant solutions start with 15 mL PBS-T and add 300 μL sheep serum (Jackson Immunoresearch) (2% final concentration). Label the tube “Blocking solution.” Remove 5 mL from this tube, place in a new tube, and label “Dilutant solution.” To the tube labeled Blocking solution, add 330 μL 30% BSA to give a final concentration of 1%. The blocking solution is now ready to use. To the tube labeled Dilutant solution, add 5 mL PBS (to give 0.05% Tween and 1% sheep serum final concentration) and 330 μL 30% BSA to give 1% final concentration. The Dilutant solution is now ready for use.
 9. Anti-DIG and anti-FAM reagents: Dilute sheep-anti-DIG-AP antibody (Roche) 1:800 in antibody dilutant solution (see above, range 1:500–1:2000). For FAM-labeled probes, apply sheep-anti-FAM-AP antibody (Roche) (range 1:500–1:2000).
 10. Nitro blue tetrazolium (NBT)-5-bromo-4-chloro-3-indolyl-phosphate (BCIP) substrate for alkaline phosphatase (AP): Immediately prior to use, dissolve a NBT-BCIP ready-to-use tablet (Roche) in Milli-Q water according to the manufacturer’s instructions. Add levamisole to a final concentration of 0.2 mM. Example: If 10 mL AP substrate is prepared, then add 20 μL levamisole stock. Protect from light before and during incubation.
 11. Levamisole stock: Prepare 100 mM stock by adding 10 mL Milli-Q water to 250 mg levamisole (Fluka).
 12. KTBT (AP stop solution): To 900 mL RNase-free water add 7.9 g Tris-HCl (50 mM), 8.7 g, NaCl (150 mM), and 0.75 g KCl (10 mM). Adjust volume to 1000 mL. Do not adjust pH. Autoclave.

3 Methods

3.1 Instrument and Glassware Preparation

To reduce potential RNase contamination of instruments and glassware, it is recommended to use an RNase removal solution such as RNaseZap[®], autoclave, or heat-treat aluminum-wrapped glassware for 8 h at 180 °C. This includes appropriate stacks of cover slips. Keep separate from untreated glassware.

3.2 FFPE Tissue Preparation

1. Prepare two water baths with RNase-free water, one at room temperature and the other at 40–50 °C (depending on the paraffin type).
2. Cut 5–6 µm thick paraffin sections and place them in the room-temperature RNase-free water, where folding can be reversed. For uniformity in sectioning please *see* **Note 2**. Transfer the sections to the heated water bath to allow expansion.
3. Mount sections immediately on electrostatic treated microscope slides obtained from a new RNase-free package.
4. Dry the sections for 1–2 h at room temperature and store at 4 °C for up to 1 week prior to use. Avoid melting the paraffin until the day prior to the ISH analysis.
5. Melt paraffin in an oven at 60 °C for 45 min on the day before conducting the ISH experiment.
6. Store slides overnight at 4 °C in an RNase-free environment.

3.3 Probe Preparation

1. Dilute the 2× Exiqon ISH buffer 1:1 with RNase-free water.
2. For each LNA™ probe to be used in the experiment, place the appropriate amount in a 2 mL non-stick RNase-free tube.
3. Denature the probes at 90 °C for 4 min and spin down briefly in a table-top microfuge.
4. Immediately add the 1× microRNA ISH buffer to each of the tubes with the different LNA™ probes.

3.4 In Situ Hybridization Steps

The following 1-day ISH protocol is summarized in Fig. 2 and can be used as reference for those familiar with the protocol. The protocol can be adapted to cryo sections [26] (*see* **Note 3**).

1. Deparaffinize slides in xylene and ethanol solutions at room temperature by placing slides in a slide rack, and then move from solution to solution in glass jars. Submerge sections in xylene for a 5 min soak and transfer to a new jar of xylene for three rounds total. Follow with ten dips into a jar with 100% ethanol, move to a fresh jar of 100% ethanol, and repeat before transferring to a new 100% ethanol solution for a 5 min soak. Move the slides to a glass jar containing 96% ethanol and plunge gently ten times before submersing for 5 min. Repeat this last with 70% ethanol before transferring the slides to a PBS solution for 2–5 min.
2. Immediately before use, add proteinase K to proteinase K buffer to the optimized concentration. *See* **Note 4** for guidance on optimizing proteinase K treatment of tissue. Place slides on a flat surface and apply approximately 300 µL/slide to fully cover the section and incubate slides for the optimized duration at 37 °C. If a hybridizer such as a Dako hybridizer is used, be sure to remove the humidifying strip inserts.

Process*	Step	Equipment	Time	Temperature
Deparaffination	1	Slide rack and Jars	40 min.	Room Temperature
Proteinase-K	2	Hybridizer	10 min.	37°C
<i>In situ</i> hybridization	4	Hybridizer	60 min.	50-60°C
Stringent washes	6	Water bath	30 min.	50-60°C
Blocking	8	IHC staining racks	15 min.	Room Temperature
Anti-DIG/AP	9		60 min.	
AP reaction	11	IHC staining racks in Oven	120 min.	30°C
Counter stain	14	IHC staining racks	10 min.	Room Temperature
Dehydration	16	Slide rack and Jars	10 min.	
Mounting	17		5 min.	

* PBS washing steps are excluded from the overview. Total time required is 7 hours.

Fig. 2 Overview of the 1-day microRNA in situ hybridization protocol for FFPE tissue sections [33]

3. Place slides into a slide rack inside a jar of PBS and wash twice in PBS (*see Note 5*).
4. Place slides on a flat surface and apply 50 μ L probe hybridization mix as prepared in Subheading 3.3. Optimization of probe concentration must be performed (*see Note 6*). Avoid touching the tissue sections with the pipette tip. When applying the sterile cover slip onto each section, be careful to avoid air bubbles. Leftover hybridization mix can be used in later experiments (*see Note 7*). Place the slides in the hybridizer (equipped with humidifying strips humidified with Milli-Q water) and start a program hybridizing for 1 h at the determined hybridization temperature (typical range is 52–57 °C). *See Note 8* for recommendations when using alternate hybridization systems.
5. Prepare a jar with 5 \times SSC at room temperature. One by one, carefully remove the cover slip and immediately place the slide into a slide rack in the 5 \times SSC buffer (*see Note 9*). If the cover slips do not easily detach, place the slides directly into the 5 \times SSC buffer. After a few minutes the cover slips will detach and the slides are transferred into the jar containing 5 \times SSC.

6. Wash slides in glass jars placed in a water bath set to the hybridization temperature to ensure sufficient stringency. Proceed as follows: $5 \times$ SSC 5 min, $1 \times$ SSC 5 min, $1 \times$ SSC 5 min, $0.2 \times$ SSC 5 min, and $0.2 \times$ SSC 5 min. Transfer to a final jar containing $0.2 \times$ SSC at room temperature for 5 additional minutes.
7. Transfer slides to glass jars with PBS. Apply a hydrophobic barrier around tissue sections using a Dako-Pen following the manufacturer's instructions. Tissue sections are not allowed to dry out during this and the subsequent immunohistochemistry steps. Alternatively, if Shandon Slide Racks are employed, then assemble slides on cover plates using PBS-T.
8. Place the slides in a humidifying chamber and incubate with blocking solution for 15 min at room temperature. Important: **Steps 8–15** are carried out in the humidifying chamber or in Shandon Slide Racks.
9. Remove blocking solution, apply anti-DIG or anti-FAM reagent, and incubate for 60 min at room temperature.
10. Wash the slides 3×3 min with PBS-T.
11. Apply freshly prepared NBT-BCIP substrate for AP to the sections and incubate slides for 2 h at 30 °C in the humidifying chamber. Protect from light during development.
12. Incubate slides in KTBT buffer 2×5 min to stop the reaction and then wash with water, 2×1 min.
13. Depending on the size of the tissue, apply 200–300 μ L Nuclear Fast Red™ for 1 min for nuclear counterstaining. Right before application, it is recommended to pass the Nuclear Fast Red™ solution through a paper filter to remove undissolved precipitates.
14. Remove slides from the humidifying chamber to a slide rack placed within a glass jar containing tap water. Carefully rinse the slides with running tap water for about 10 min.
15. Dehydrate slides in ethanol solutions with a quick ten dip wash followed by a 1-min submersion wash. The ethanol solutions become progressively higher in %. Start with 70%, then 96, and finally with 100% ethanol washes. Place the slides on clean paper towels.
16. Mount slides directly with 1–2 drops of Eukitt® mounting medium. Avoid air-drying sections at this step.
17. Allow the dark blue diformazan precipitate to settle overnight and analyze results by light microscopy the subsequent day. Assess the specificity of the signals through the use of appropriate assays (*see Note 10*) and interpret the results.

The above-described protocol using chromogenic detection can be modified into fluorescence detection (*see Note 11*), which would allow co-localization with other RNA molecules (*see Note 12*) or proteins (*see Note 13*).

4 Notes

1. *Alternative labels.* The original microRNA ISH protocol was developed using DIG-labeled miRCURY LNA™ microRNA Detection probes [25]. Figure 3 shows examples of the performance of double-DIG- and double-FAM-labeled probes, and indicates that similar sensitivity can be obtained with the two different probe labels. Other labels, including biotin detected with streptavidin, can also be used. The concentration of the miRCURY LNA™ microRNA Detection probe and the detecting antibodies should be optimized for best performance regardless of the choice of label type.
2. *FFPE tissue preparation.* FFPE blocks are placed on a cooling plate to cool down to approximately -15°C before cutting. Trim the block in order to avoid the first few sections.
3. *Fresh frozen tissue.* Additional guidelines for fresh frozen samples can be found at <http://www.exiqon.com/Is/Documents/Scientific/FrFr-ISH-supplementary-protocol.pdf>. After tissue sectioning and washing with PBS, resume the protocol described above at the probe hybridization, **step 4**. The protocol will require optimization for individual sample types and microRNA targets.
4. *Proteinase K treatment.* The degree of proteinase K treatment depends on fixation and tissue of origin. In general terms, the harder the fixation, the more proteinase K is needed; however there are lower and upper limits. As a starting point we recommend working with 5–20 $\mu\text{g}/\text{mL}$ at 37°C for 10 min for human FFPE material and 0.5–5.0 $\mu\text{g}/\text{mL}$ for 10 min for mouse paraformaldehyde-fixed FFPE samples. Optimizing duration of treatment may also be needed. In the case of co-localization with protein (*see Note 13*), protease treatment may be contraindicated and the use of fresh frozen tissue is the recommended sample preparation [26].
5. *Breaks in the protocol.* The individual steps in this protocol have been optimized for completion in 1 day; however it is possible to prolong the PBS steps but it is not recommended.
6. *Optimization of probe conditions.* The optimization range of LNA™-enhanced microRNA detection probes is 20–80 nM. Various probe concentrations should be tested in combination with hybridization temperature ranges. Optimal perfor-

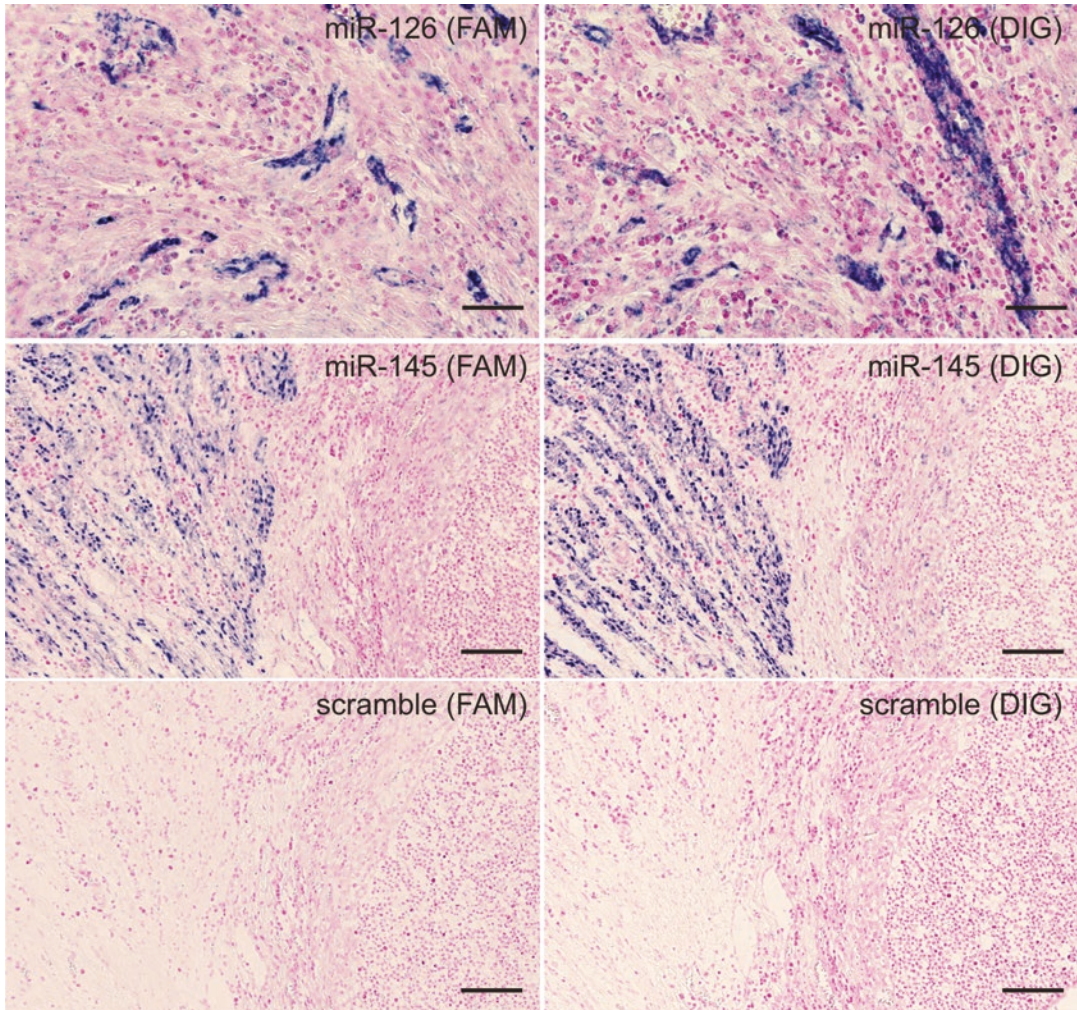


Fig. 3 In situ hybridization using FAM- and DIG-labeled LNATM probes in FFPE samples. The examples show double-FAM-labeled probes and double-DIG-labeled probes for miR-126 and miR-145 and the scramble negative control on serial sections from a human colon cancer sample. The miR-145 and scramble probes show the same area. Probes were incubated at 30 nM probe concentration and hybridized at 57 °C. The double-FAM-labeled LNATM probes show the same signal-to-noise as the double-DIG-labeled LNATM probes and can be used independently or in combination to co-localize microRNAs detected with different hapten-labeled probes or antibodies, in the case of protein co-detection by immunohistochemistry. Bars: miR-126: 50 μ m, miR-145 and scramble: 200 μ m

mance of an ISH probe is related to its signal-to-noise ratio. Oligonucleotide probes, and especially LNATM-containing probes, can potentially hybridize to highly similar sequences if the hybridization temperature is too low. Conversely, working at too high a temperature will reduce the specific binding efficiency. As a rule of thumb, hybridization should be performed at 25–30 °C (+/– a few degrees) below the given RNA T_m (or 20 °C below DNA T_m).

7. *Hybridization mix.* Leftover hybridization mix can be stored at -20°C and will be stable for up to 6 months. It is important to avoid multiple freeze-thaw cycles. With Exiqon's Optimization kit hybridization buffer, used here, it is important not to denature the probe after it has been added to the hybridization mix. It is sufficient and preferred that the probe hybridization mix simply be warmed back to the hybridization temperature early in the hybridization step.
8. *Hybridization equipment.* ISH does not require any specific hybridization equipment and simple hybridization ovens, plate hybridizers such as those from Dako, Invitrogen, and Vysis, and automated systems such as Ventana's Discovery System and Tecan's Genepaint systems are very successful. When using a hybridization oven without a humidified environment during the hybridization step, it is advisable to seal the cover slips using Fixogum or other rubber cement to prevent evaporation of the probe hybridization mix which would increase the effective probe concentration and prevent easy detachment of the cover slip. When using an automated system, additional volumes and quantities of probe are needed. As well, due to the transfer of solutions through tubing, higher temperature settings are recommended starting points.
9. *Tissue hydration.* Sections should be maintained in buffered solutions after the hybridization step to prevent protein denaturation. This may be particularly harmful to the detecting antibody and its conjugated alkaline phosphatase, lowering the sensitivity and specificity of staining. Drying out of tissue sections may also reduce the quality of the tissue morphology.
10. *Specificity of signal.* An important aspect of microRNA ISH is the verification of specificity of target identification and localization. As microRNAs are 19–23 nucleotides in length, designing probes to alternative regions of the microRNA and demonstrating reproducible results are not possible. Instead we rely more on alternative designs of the microRNA probe, altering length and LNATM pattern [34]. Some microRNAs are expressed from the same primary transcript and are part of a "cluster." Probes to other microRNAs within the same cluster can be used as positive controls since they specifically hybridize to different sequences on the same transcript. Examples include the miR-143/145 cluster [25] and the miR-17 ~ 92 cluster [35]. The use of a probe designed with no sequence recognition within the species (scramble negative control) or a mismatch of 3 of DNA nucleotides within the sequence of the tested probe, each with the same choice of label, demonstrates any confounding background due to the presence of a labeled oligo in general. Background fluorescent signal derived from natural autofluorescence or signal from the detection reagents

reacting to endogenous phosphatase (for AP-based detection) or peroxidase (e.g., HRP-based detection) can be assessed with experiments which exclude the specific probe or specific antibody from the protocol [34]. An additional approach to validating the specificity of the signal is through laser capture microdissection of the various regions across un-probed tissue sections. RNA isolation followed by real-time qPCR for the microRNA confirms visualized localization of the probe [34]. The use of Exiqon's miRCURY LNA™ Universal RT microRNA PCR, superior in specificity and sensitivity, ensures the most reliable results [36].

11. *Alternate detection methods.* The miRCURY LNA™ microRNA Detection Probes can be detected using alternative methods such as tyramide signal amplification (TSA)-based systems. The FAM-labeled LNA™ probes can also be detected directly with fluorescent microscopy when detecting a highly expressed or highly localized target. The use of alternative systems may necessitate additional steps to be added at various stages of the protocol and requires optimization.
12. *Co-localization.* Two microRNAs can be detected in the same FFPE section by double-fluorescence analysis [31]. It may also be possible using double-chromogen detection; however, this has not been documented. Fluorescence detection of the two RNAs is performed using peroxidase-conjugated sheep antibodies and tyramine substrates (TSA), such as TSA-Cy3 (red fluorophore) and TSA-FITC (green fluorophore). ISH can be performed by mixing the two probes. However, if different hybridization temperatures are required for optimal hybridization, or if the two probes interact, hybridization should be performed consecutively. All steps need optimization and should be evaluated against negative control sections in order to adjust for background staining and auto-fluorescence. The slides can be mounted with DAPI mounting medium.
13. *Co-localization with a protein.* A microRNA can be detected together with a protein in tissue sections by combined ISH and immunohistochemistry double-fluorescence staining. The main limitation in such an assay is the compatibility of pretreatment procedures required for the microRNA probe and the primary antibody. MicroRNA ISH on FFPE material is limited to protease-dependent pretreatment, and therefore identifying an appropriate primary antibody that works well with proteolytic pretreatment is necessary. Alternative strategies may involve frozen sections, in which microRNA ISH can be performed [26], and most primary antibodies can be applied without pretreatment.

Acknowledgments

The authors would like to thank Trine Møller at Bioneer for technical expertise as well as Marie-Louise Lunn at Exiqon for her support in the preparation of this manuscript. Exiqon is a QIAGEN company.

References

1. Bartel DP (2004) MicroRNAs: genomics, biogenesis, mechanism, and function. *Cell* 116(2):281–297
2. Wienholds E, Plasterk RH (2005) MicroRNA function in animal development. *FEBS Lett* 579(26):5911–5922
3. Li L, Chen HZ, Chen FF et al (2013) Global microRNA expression profiling reveals differential expression of target genes in 6-hydroxydopamine-injured MN9D cells. *NeuroMolecular Med* 15(3):593–604
4. Huang M, Lou D, Cai Q et al (2014) Characterization of paraquat-induced miRNA profiling response to hNPCs undergoing proliferation. *Int J Mol Sci* 15(10):18422–18436
5. Su YW, Chen X, Jiang ZZ et al (2012) A panel of serum microRNAs as specific biomarkers for diagnosis of compound- and herb-induced liver injury in rats. *PLoS One* 7(5):e37395. doi:[10.1371/journal.pone.0037395](https://doi.org/10.1371/journal.pone.0037395)
6. Wu X, Zhang Y, Xu H et al (2015) Identification of differentially expressed microRNAs involved in non-traumatic osteonecrosis through microRNA expression profiling. *Gene* 565(1):22–29
7. Gandhi R, Healy B, Gholipour T et al (2013) Circulating microRNAs as biomarkers for disease staging in multiple sclerosis. *Ann Neurol* 73(6):729–740
8. Anderson AL, Stanger SJ, Mihalas BP et al (2015) Assessment of microRNA expression in mouse epididymal epithelial cells and spermatozoa by next generation sequencing. *Genom Data* 18(6):208–211
9. Ma L, Li P, Wang R et al (2015) Analysis of novel microRNA targets in drug-sensitive and—insensitive small cell lung cancer cell lines. *Oncol Rep* 35(3):1611–1621
10. Pellegrini KL, Gerlach CV, Craciun FL et al (2015) Application of small RNA sequencing to identify microRNAs in acute kidney injury and fibrosis. *Toxicol Appl Pharmacol* 312:42–52. doi:[10.1016/j.taap.2015.12.002](https://doi.org/10.1016/j.taap.2015.12.002)
11. Koturbash I, Tolleson WH, Guo L et al (2015) microRNAs as pharmacogenomics biomarkers for drug efficacy and drug safety assessment. *Biomark Med* 9(11):1153–1176
12. Marrone AK, Beland FA, Pogribny IP (2015) The role for microRNAs in drug toxicity and in safety assessment. *Expert Opin Drug Metab Toxicol* 11(4):601–611
13. Thrakral S, Ghoshal K (2015) miR-122 is a unique molecule with great potential in diagnosis, prognosis of liver disease, and therapy both as a miRNA mimic and antimir. *Curr Gene Ther* 15(2):142–150
14. Hsu J, Xu Y, Hao J et al (2012) Essential metabolic, anti-inflammatory, and anti-tumorigenic functions of miR-122 in liver. *J Clin Invest* 122(8):2871–2883
15. Gebert LFR, Rebhan MAE, Crivelli SEM et al (2014) Miravirsin (SPC3649) can inhibit the biogenesis of miR-122. *Nucleic Acids Res* 42(1):609–621
16. Zhao Y-N, Li W-F, Zhang Z et al (2013) Resveratrol improves learning and memory in normally aged mice through microRNA-CREB pathway. *Biochem Biophys Res Commun* 435(4):597–602
17. Kontaraki JE, Marketou ME, Zacharis EA et al (2014) MicroRNA-9 and microRNA-126 expression levels in patients with essential hypertension: potential markers of target-organ damage. *J Am Soc Hypertens* 8(6):368–375
18. Yan T, Cui K, Huang X et al (2014) Assessment of therapeutic efficacy of miR-126 with contrast-enhanced ultrasound in preeclampsia rats. *Placenta* 35(1):23–29
19. Cheng Y, Liu X, Yang J et al (2009) MicroRNA-145, a novel smooth muscle cell phenotypic marker and modulator, controls vascular neoinimal lesion formation. *Circ Res* 105(2):158–166
20. Boettger T, Beetz N, Kostin S et al (2009) Acquisition of the contractile phenotype by murine arterial smooth muscle cells depends on the Mir143/145 gene cluster. *J Clin Invest* 119(9):2634–2647

21. Chivukula RR, Shi G, Acharya A et al (2014) An essential mesenchymal function for miR-143/145 in intestinal epithelial regeneration. *Cell* 157(5):1104–1116
22. Wienholds E, Kloosterman WP, Miska E et al (2005) MicroRNA expression in zebrafish embryonic development. *Science* 309(5732):310–311
23. Vester B, Wengel J (2004) LNA (locked nucleic acid): high-affinity targeting of complementary RNA and DNA. *Biochemistry* 43(42):13233–13241
24. Jorgensen S, Baker A, Møller S et al (2010) Robust one-day in situ hybridization protocol for detection of microRNAs in paraffin samples using LNA probes. *Methods* 52(4):375–381
25. Nielsen BS (2012) MicroRNA in situ hybridization. *Methods Mol Biol* 822:67–84
26. Nielsen BS, Møller T, Holmstrøm K (2014) Chromogen detection of microRNA in frozen clinical tissue samples using LNA™ probe technology. *Methods Mol Biol* 1211:77–84
27. Singh U, Keirstead N, Wolujczyk A et al (2013) General principles and methods for routine automated microRNA in situ hybridization and double labeling with immunohistochemistry. *Biotech Histochem* 89(4):259–266
28. Toledano H, D'Alterio C, Loza-Coll M et al (2012) Dual fluorescence detection of protein and RNA in *Drosophila* tissues. *Nat Protoc* 7(10):1808–1817
29. Keeney JG, Davis JM, Siegenthaler J et al (2015) DUF1220 protein domains drive proliferation in human neural stem cells and are associated with increased cortical volume in anthropoid primates. *Brain Struct Funct* 220(5):3053–3060
30. Nielsen BS, Holmstrøm K (2013) Combined microRNA in situ hybridization and immunohistochemical detection of protein markers. *Methods Mol Biol* 986:353–365
31. Sempere LF, Peris M, Yezefski T et al (2010) Fluorescence-based co-detection with protein markers reveals distinct cellular compartments for altered MicroRNA expression in solid tumors. *Clin Cancer Res* 16(16):4246–4255
32. Darnell DK, Stanislaw S, Kaur S et al (2010) Whole mount in situ hybridization detection of mRNAs using short LNA containing DNA oligonucleotide probes. *RNA* 16:632–637
33. Exiqon (2016) miRCURY LNA™ microRNA ISH Optimization Kit (FFPE) manual. V.3 <http://www.exiqon.com/ls/Documents/Scientific/miRCURY-LNA-microRNA-ISH-Optimization-Kit-manual.pdf>
34. Nielsen BS, Jørgensen S, Fog JU et al (2011) High levels of microRNA-21 in the stroma of colorectal cancers predict short disease-free survival in stage II colon cancer patients. *Clin Exp Metastasis* 28:27–38
35. Knudsen KN, Nielsen BS, Lindebjerg J et al (2015) microRNA-17 is the most up-regulated member of the miR-17-92 cluster during early colon cancer evolution. *PLoS One* 10(10):e0140503. doi:10.1371/journal.pone.0140503
36. Mestdagh P, Hartmann N, Baeriswyl L et al (2014) Evaluation of quantitative miRNA expression platforms in the microRNA quality control (miRQC) study. *Nat Methods* 11(8):809–815

Urine Exosome Isolation and Characterization

Jonathan M. Street, Erik H. Koritzinsky, Deonna M. Glispie,
and Peter S.T. Yuen

Abstract

Exosomes are nanometer-scale, membrane-enclosed vesicles that can potentially be used to detect nephrotoxicity, and reveal the subsequent response of the kidney. Epithelial cells of every nephron segment can contribute to the urinary exosome population, which is rich in potential biomarkers, including membrane proteins such as transporters and receptors, transcription factors, and microRNAs. These exosomal biomarkers may be up- or downregulated upon nephrotoxicant exposure. Exosome isolation is an area of ongoing research. Although faster and simpler methods have been developed, ultracentrifugation remains a mainstay for purification. A single ultracentrifugation step provides an enriched preparation suitable for biomarker discovery, and a second ultracentrifugation on a sucrose/D₂O cushion provides the purest exosome preparation currently available and may be preferred for bioactivity assays. The concentration of exosomes can be determined using Nanosight Nanoparticle Tracking Analysis and their contents studied with a variety of approaches including western blots for proteins and RT-qPCR for microRNAs.

Key words Exosomes, Biomarker, Urine, TSG101, Ultracentrifugation, Nanosight, Nephrotoxicity

1 Introduction

Urinary exosomes are extracellular vesicles that originate from glomerular podocytes, epithelial cells lining the renal tubules, and the rest of the epithelial lining of the genitourinary tract, including the bladder and prostate [1]. Exosomes are formed from the endocytic pathway, a process that involves two sequential membrane invaginations. First, plasma membrane-derived endocytosis forms endocytic vesicles with an inside-out orientation that contain extracellular fluid. The fusion of multiple endocytic vesicles results in the formation of an early endosome, which matures into a multivesicular body (MVB). Then, the MVB outer membrane can generate intraluminal vesicles by a subsequent invagination, resulting in a right-side-out orientation with cytoplasm trapped inside. The MVB can then follow one of the two alternate paths. Either it fuses with a lysosome to degrade and recycle its contents or it is routed to the cell surface. When the MVB fuses with the plasma membrane of a

renal/genitourinary tract epithelial cell, the right-side-out intraluminal vesicles are released into the urinary lumen as exosomes. Exosomes are distinct from microvesicles/microparticles/ectosomes, which are right-side-out extracellular vesicles that are released directly from plasma membrane outpouching, and are typically not found in urine. Proteins that were identified through the proteomic analysis of human urinary exosomes [2] and are known to be involved in the biogenesis of MVB, such as TSG101, can be used to estimate exosomal mass by western blot, which may be useful as a denominator for exosomal biomarker normalization.

Exosome isolation is a straightforward enrichment strategy of potential nephrotoxicant biomarkers by reducing the complexity of urine composition, with minimal loss of yield. By isolating exosomes, high-abundance constituents may be removed in nonexosomal urine fractions, while low-abundance constituents that may have toxicological significance may be simultaneously enriched.

Collection, storage, and handling methods can greatly affect the quality and quantity of urinary exosomal protein biomarkers [3]. Protease inhibitors are needed to preserve some proteins exposed to exosome exteriors such as NCC or NKCC2. On the other hand, exosomal miRNA or mRNA do not need protection from RNases found in urine. When shipping and/or storage of urine is necessary, it is recommended to freeze fresh urine samples at $-80\text{ }^{\circ}\text{C}$ instead of $-20\text{ }^{\circ}\text{C}$. During the final stages of thawing, samples should be vortexed extensively to maximize the yield of exosomes from frozen urine [3].

We describe an ultracentrifugation protocol for isolation of urinary exosomes, and comment on alternatives. Methods for exosomal RNA isolation, exosome characterization by Nansight Nanoparticle Tracking Analysis, and preparation of exosome samples for western blot are described. Electron microscopy and proteomics were described previously [4] and will not be covered here.

2 Materials

2.1 Purification of Urinary Exosomes

1. Urine collection additive cOmplete, Mini Protease Inhibitor Cocktail (Roche): Add 1 Roche cOmplete Mini tablet (stored at $4\text{ }^{\circ}\text{C}$) per $\leq 50\text{ mL}$ of fresh urine. When dissolving the tablet, swirl the sample until no longer visible (*see Note 1*).
2. Sterile $1\times$ phosphate-buffered saline (PBS).
3. 15 or 50 mL conical centrifuge tubes.
4. Centrifuge with swinging bucket rotor.
5. Clean Crystalgen 23–2589 (or equivalent) tube(s).
6. Ultracentrifuge.

7. Clean ultracentrifuge tubes.
8. 30% Sucrose/D₂O for density cushion: Volume for 50 mL solution: mix 15 g of ultrapure sucrose with D₂O to 50 mL (*see Note 2*).

2.2 Preparation of Exosomes for Western Blot

1. 2× SDS-Laemmli-DTT sample buffer: 2× Laemmli Sample Buffer (Bio-Rad) supplemented with 200 mM dithiothreitol (30.86 mg/mL) and stored at −20 °C.
2. Heat block.
3. 1.5 mL Microfuge tube.

2.3 Nanosight Nanoparticle Tracking Analysis (NTA)

1. Nanosight LM-10 instrument (Malvern Instruments Ltd.) with NTA version 3.1 software.
2. Syringe pump.

2.4 RNA Extraction Materials

1. TRIzol Reagent (Invitrogen).
2. Chloroform.
3. 100% Ethanol.
4. Phase-Lock Gel Heavy 1.5 mL Tubes (5 Prime).
5. miRNeasy Mini Kit (Qiagen): Contains sufficient quantities of the following reagents for 50 samples: RNeasy Mini Spin Columns, 1.5 mL and 2 mL collection tubes, QIAzol lysis reagent, concentrated stock RWT and RPE buffers, RNase-free water.
6. Ultrapure water.

3 Methods

Exosomes were originally purified by ultracentrifugation, which enabled their initial characterization, and this technique remains the most common approach for their isolation. The high capital costs and time-consuming nature of ultracentrifugation are recognized as impediments to the widespread study of exosomes, beginning with preclinical toxicology studies, translation to clinical trials, and perhaps postapproval monitoring. As such, there is significant interest in alternative isolation methods. Although our previously described nanomembrane concentrator method is a viable option [5], we eventually concluded that ultracentrifugation is preferable when available. We have limited experience with other newer techniques now available, and the increasing availability of commercial kits will allow higher throughput screening of large sample sets; biomarkers identified from this process should be validated as exosomal by using the best available methods for purification and validation. For this chapter we focus on ultracentrifugation, as it enables the

greatest breadth of postpurification analyses. A single ultracentrifugation step is usually sufficient for biomarker discovery studies, and greater purity for bioactivity assays can be achieved with an additional ultracentrifugation step using a sucrose/D₂O cushion [6, 7].

Analysis of purified exosomes falls into four main categories: size, number, purity, and content. For size and purity, transmission electron microscopy remains the standard, but it is a very-low-throughput method to perform and analyze data [4]. More recently the Nanosight system [8] has been used to determine size and number. A promising approach to assessing purity uses Nanosight combined with protein assay to determine a value analogous to specific activity [9], but would require that standards be determined for each biofluid source of exosomes. Content can be surveyed by -omics methods such as proteomics, transcriptomics (miRNA or mRNA), lipidomics, or glycomics (glycoproteins), or analyzed by more focused methods such as western blot, RT-qPCR, or GC-MS.

3.1 Purification of Urinary Exosomes (Fig. 1)

3.1.1 Ultracentrifugation

1. Add protease inhibitors to a fresh urine sample if detecting proteins.
2. Process whole urine immediately or store at $-80\text{ }^{\circ}\text{C}$ for future processing.
3. If thawing frozen samples, vigorous vortexing should be used prior to complete melting of sample to maximize exosome recovery.
4. Centrifuge urine sample in a 15 or 50 mL conical centrifuge tube at $1000 \times g$ for 10 min at $4\text{ }^{\circ}\text{C}$ (*see Note 3*).
5. Transfer the $1000 \times g$ supernatant to a clean Crystalgen 23–2589 (or equivalent) tube(s).
6. Centrifuge $1000 \times g$ supernatant at $17,000 \times g$ for 15 min at $4\text{ }^{\circ}\text{C}$ (*see Note 4*).
7. Transfer the $17,000 \times g$ supernatant into a clean ultracentrifuge tube(s) (*see Note 5*).
8. Ultracentrifuge $17,000 \times g$ supernatant at $200,000 \times g$ for 1 h at $4\text{ }^{\circ}\text{C}$.
9. Discard the $200,000 \times g$ supernatant. If more $17,000 \times g$ supernatant is available, add additional $17,000 \times g$ supernatant to tubes used for **step 8** and then repeat **step 8** (*see Notes 6 and 7*).
10. Add 100 μL sterile 1X PBS to each ultracentrifuge tube and vigorously vortex until pellet has been resuspended.

3.1.2 Ultracentrifugation with Sucrose/D₂O Cushion

1. Process urine as per **steps 1** through **10** of the ultracentrifugation protocol.
2. Add 1 mL of 30% sucrose/D₂O to clean ultracentrifuge tube(s) before transferring the resuspended $200,000 \times g$ pellet.

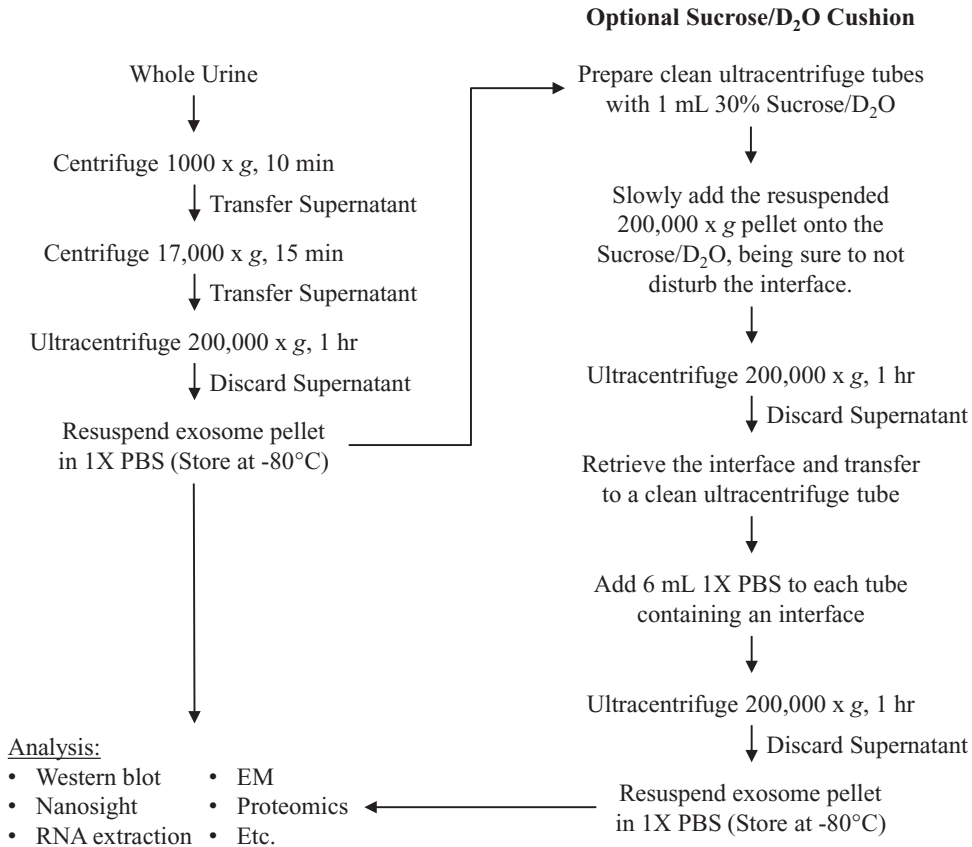


Fig. 1 Flowchart outlining the ultracentrifugation protocol for urinary exosome isolation. A single ultracentrifugation is typical for biomarker discovery studies (*left*). If a higher level of purity is required, such as for bioactivity assays, an additional ultracentrifugation step using a sucrose/D₂O cushion may be added (*right*)

3. Slowly pipette the resuspended 200,000 × *g* pellet onto the sucrose/D₂O cushion in order not to disturb the interface.
4. Ultracentrifuge at 200,000 × *g* for 1 h at 4 °C.
5. Remove the supernatant. Retrieve the interface and transfer to a clean ultracentrifuge tube.
6. Add 6 mL sterile 1X PBS to each ultracentrifuge tube containing a retrieved interface sample.
7. Ultracentrifuge the diluted interface at 200,000 × *g* for 1 h at 4 °C.
8. Discard the supernatant from the 200,000 × *g* wash step (*see Note 7*).
9. Add 100 μL sterile 1X PBS to each ultracentrifuge tube and vigorously vortex until pellet has been resuspended.

3.2 Preparation of Exosomes for Western Blot

1. Add an equal volume of 2X SDS-Laemmli-DTT sample buffer to the resuspended exosomes, vortex thoroughly, and spin briefly in microfuge to remove bubbles.
2. Heat samples on heat block at 95 °C for 5 min, and spin briefly in microfuge to consolidate condensation on the lid of the microfuge tube.
3. Store at -80 °C.

3.3 Nanosight Nanoparticle Tracking Analysis (NTA) (See Note 8)

1. Dilute exosome preparation with sterile 1X PBS, so that particle concentration is within the instrument's linear dynamic range ($\sim 10^7$ - 10^9 particles/mL). Load a sample into the Nanosight chamber using a syringe, taking care not to introduce bubbles. If possible, use a syringe pump (~ 0.2 mL/h) to allow for the acquisition of more accurate data.
2. Turn on the camera, adjust the x-y position to center the laser beam, set the camera level using the software, focus the instrument if necessary, and confirm on the monitor that there are approximately 20-100 particles in view at any given time (Fig. 2). Note the temperature of the chamber.
3. Under the Standard Operating Procedure (SOP) tab create and run a new script for five acquisitions of 60 s each.
4. Withdraw or push through the rest of the sample and thoroughly rinse with ultrapure water to ensure that there is no contamination between samples. Contamination can be assessed by looking at the screen when the chamber is filled with water to see if there are particles still present.

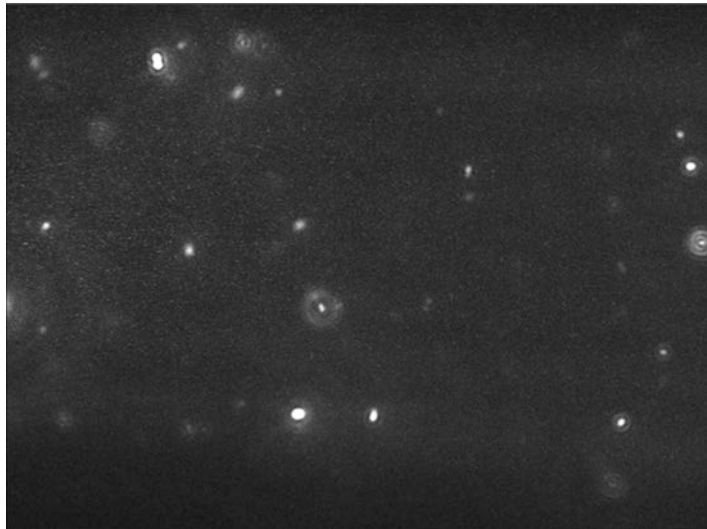
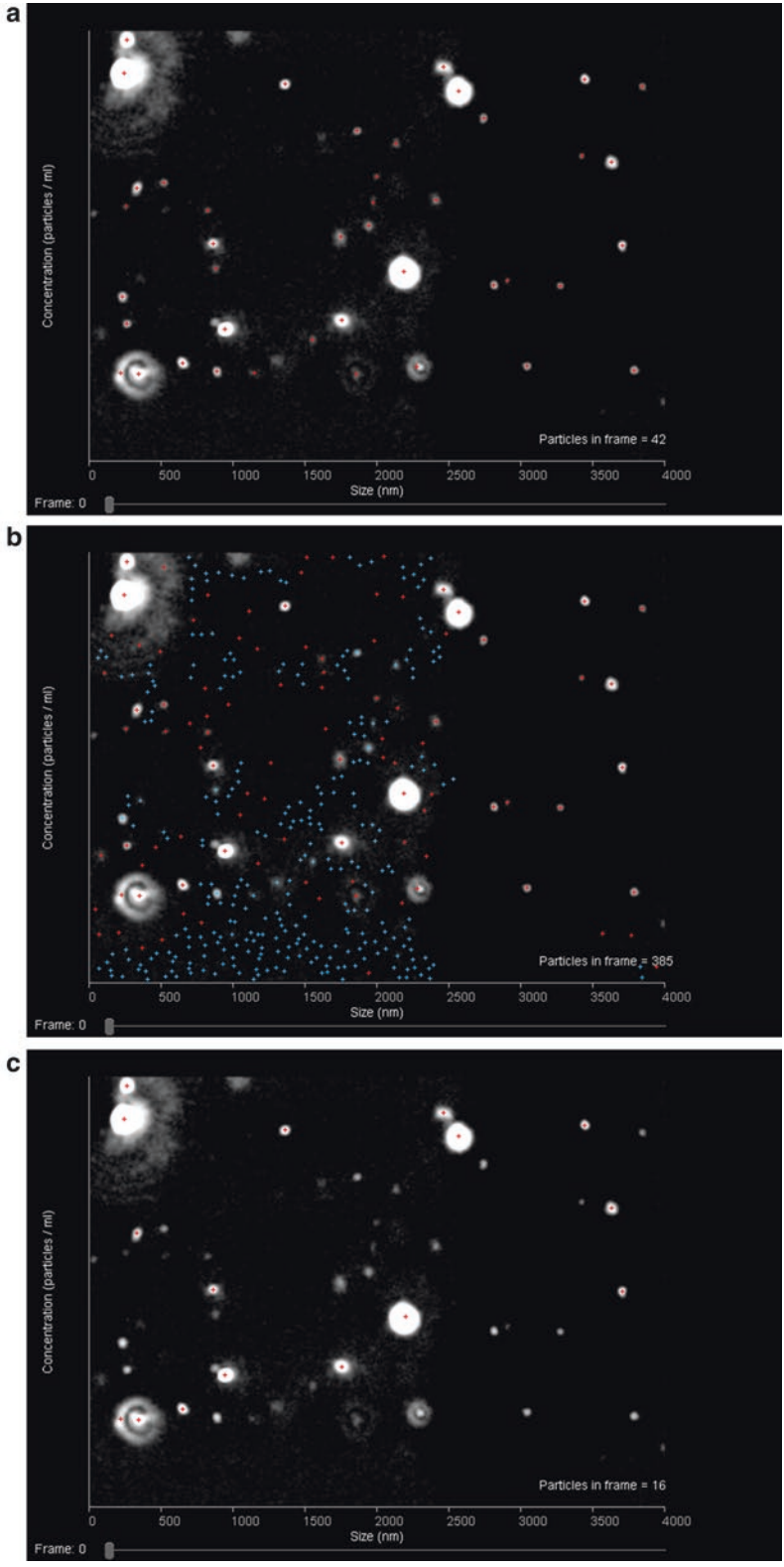


Fig. 2 Sample image from NTA 3.1 illustrating a proper concentration of particles present in the field of view (20-100 particles)

5. Repeat **step 1** and load the next sample until finished (*see Note 9*).
6. For data analysis the detection threshold should be set such that the number of visible particles with red crosses is maximized while the number of blue crosses on the screen is minimized (less than five). If the detection threshold is too low, nonparticle background noise will be tracked. If the threshold is too high, some particles will be excluded (Fig. 3).
7. Raw data can be exported to .csv files for further analysis (*see Fig. 4* for example).

3.4 RNA Extraction Using miRNeasy Kit (See Notes 10 and 11)

1. Add a 10- (preferable) to 3- (minimum) fold excess (by volume) of TRIzol to the exosome preparation (~50 μ L). Vortex and incubate at room temperature (RT) for 5 min.
2. Add one-fifth volume of chloroform, shake tube vigorously, and incubate at RT for 2 min.
3. Centrifuge sample at $12,000 \times g$ for 15 min at 4 $^{\circ}$ C.
4. Transfer aqueous phase to a phase-lock tube and add 700 μ L QIAzol. Vortex and incubate at RT for 5 min.
5. Add 140 μ L chloroform, shake tube vigorously, and incubate at RT for 2 min.
6. Centrifuge sample at $12,000 \times g$ for 15 min at 4 $^{\circ}$ C.
7. Transfer aqueous phase to a 2 mL tube and add 1.5 volumes 100% ethanol.
8. Transfer 700 μ L sample, including any precipitate, into an RNeasy mini spin column in a 2 mL collection tube. Centrifuge at $>8000 \times g$ for 15 s at RT and discard flow-through.
9. Repeat **step 8** until the entire sample has been loaded on the column.
10. Add 700 μ L RWT buffer and centrifuge at $>8000 \times g$ for 15 s at RT. Discard flow-through.
11. Add 500 μ L RPE buffer and centrifuge at $>8000 \times g$ for 15 s at RT. Discard flow-through.
12. Repeat **step 11** but centrifuge for 2 min.
13. Transfer mini column to a fresh 2 mL tube and centrifuge for 1 min at $>8000 \times g$.
14. Transfer mini column to a 1.5 mL tube. Add 30 μ L ultrapure water and centrifuge for 1 min at $>8000 \times g$ to elute RNA.
15. Transfer flow-through back to mini column and centrifuge for 1 min at $>8000 \times g$.
16. Store flow-through at -80° C.



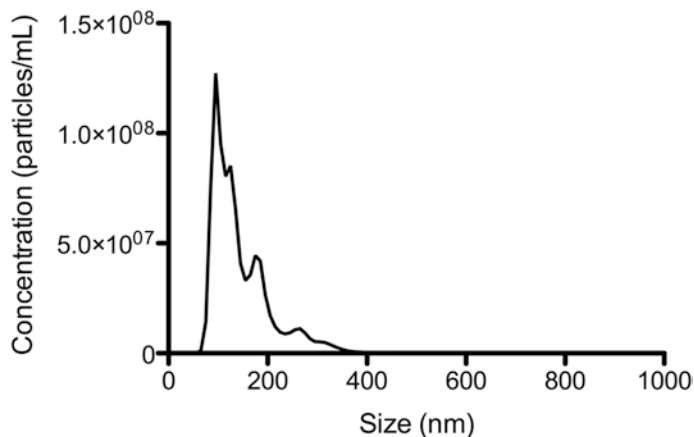


Fig. 4 Sample size-concentration distribution of urine exosomes isolated from a healthy patient obtained using Nanosight NTA. Exosomes were resuspended in 1X PBS. The sample was diluted in order for the measured concentration to fall within the dynamic range of the instrument

4 Notes

1. Alternatively, homemade protease inhibitors can be used. For a volume per ≤ 50 mL of urine mix 1.67 mL 100 mM NaN_3 , 2.5 mL PMSF (2.5 mg/mL in ethanol, store at -20°C) or 5 mL AEBSF (2.75 mg/mL in dd- H_2O , store at -20°C) (as an alternative to PMSF, AEBSF offers lower toxicity and improved stability in aqueous solutions), and 50 μL leupeptin (1 mg/mL in dd- H_2O , stable at 4°C for 1 week).
2. The sucrose/ D_2O solution should be filtered twice before use in ultracentrifugation. First, filter the solution through a 0.22 μm filter followed by a 0.1 μm filter. This should remove almost all nanoparticle impurities originating from raw materials from the solution.
3. This step removes whole cells, large aggregates, and other debris. We use the Sorvall RT7Plus centrifuge with a RTH750 swinging bucket rotor.

Fig. 3 Sample images from NTA 3.1 illustrating how to choose a proper detection threshold setting for analysis. When the detection threshold is set properly (**a**), there should be *red* crosses on each particle in the field of view and no crosses on other parts of the field. The number of *blue* crosses present should also be minimized (less than five). When the detection threshold is set too low (**b**), there will be crosses on nonparticle background as well as an abundance of *blue* crosses visible. When the detection threshold is set too high (**c**), there will be particles visible but without red crosses on them

4. This step removes organelles, cell fragments, and some Tamm Horsfall protein fibrils. We use the Sorvall RC-6+ refrigerated centrifuge and a SA-600 rotor and Crystalgen 23–2589 tubes.
5. We use the Beckman Coulter Optima MAX ultracentrifuge with the MLA-55 rotor. The high-speed tube we use is the thick-walled, polycarbonate tube #355630 from Beckman, with a practical capacity of ~7.5 mL.
6. Minimizing the number of tubes used for ultracentrifugation increases the yield of exosomes because resuspension and pooling are more labor intensive and less reliable when more tubes are used. However, using fewer tubes results in more spins, and this trade-off needs to be considered. For example, a single spin with five tubes would be faster, but would result in lower yield. On the other end of the spectrum, five consecutive spins with a single tube would maximize recovery, but would be much more time consuming. Three spins in two tubes or two spins in three tubes would be rational approaches.
7. To remove the last traces of $200,000 \times g$ supernatant, the nearly empty tube can be recentrifuged for 10 min using the same orientation within the rotor, and then using a pipette to remove the remaining supernatant, or ultracentrifuge tubes can be tipped upside-down for ~15–30 s (to avoid a dry pellet) and aspirated inside the tube opening.
8. This procedure may vary slightly if other instruments than the Nanosight LM-10 and if other versions of the NTA software than the 3.1 version are used.
9. Lower temperature and increased viscosity will artificially increase the size of particles during Nanosight Tracking Analysis. Monitoring temperature during data acquisition and ensuring that all sucrose is removed during preparation are essential for accurate sizing data.
10. This protocol follows the manufacturer's recommendations with the addition of a second-phase extraction step and the use of phase-lock tubes to minimize contamination.
11. To prevent degradation of the sample the extraction should proceed as quickly as possible. Extraction is performed on batches of up to 12 samples. This number can be processed simultaneously using one standard centrifuge.

Acknowledgments

This study was supported by the Intramural Research Program of the NIH, the National Institute of Diabetes, and Digestive and Kidney Diseases (NIDDK).

References

1. Pisitkun T, Johnstone R, Knepper MA (2006) Discovery of urinary biomarkers. *Mol Cell Proteomics* 5(10):1760–1771. doi:[10.1074/mcp.R600004-MCP200](https://doi.org/10.1074/mcp.R600004-MCP200)
2. Pisitkun T, Shen RF, Knepper MA (2004) Identification and proteomic profiling of exosomes in human urine. *Proc Natl Acad Sci U S A* 101(36):13368–13373. doi:[10.1073/pnas.0403453101](https://doi.org/10.1073/pnas.0403453101)
3. Zhou H, Yuen PS, Pisitkun T, Gonzales PA, Yasuda H, Dear JW, Gross P, Knepper MA, Star RA (2006) Collection, storage, preservation, and normalization of human urinary exosomes for biomarker discovery. *Kidney Int* 69(8):1471–1476. doi:[10.1038/sj.ki.5000273](https://doi.org/10.1038/sj.ki.5000273)
4. Gonzales PA, Zhou H, Pisitkun T, Wang NS, Star RA, Knepper MA, Yuen PS (2010) Isolation and purification of exosomes in urine. *Methods Mol Biol* 641:89–99. doi:[10.1007/978-1-60761-711-2_6](https://doi.org/10.1007/978-1-60761-711-2_6)
5. Cheruvanky A, Zhou H, Pisitkun T, Kopp JB, Knepper MA, Yuen PS, Star RA (2007) Rapid isolation of urinary exosomal biomarkers using a nanomembrane ultrafiltration concentrator. *Am J Physiol Renal Physiol* 292(5):F1657–F1661. doi:[10.1152/ajprenal.00434.2006](https://doi.org/10.1152/ajprenal.00434.2006)
6. Raj DA, Fiume I, Capasso G, Pocsfalvi G (2012) A multiplex quantitative proteomics strategy for protein biomarker studies in urinary exosomes. *Kidney Int* 81(12):1263–1272. doi:[10.1038/ki.2012.25](https://doi.org/10.1038/ki.2012.25)
7. They C, Amigorena S, Raposo G, Clayton A (2006) Unit 3.22: Isolation and characterization of exosomes from cell culture supernatants and biological fluids. *Curr Protoc Cell Biol*. doi:[10.1002/0471143030.cb0322s30](https://doi.org/10.1002/0471143030.cb0322s30)
8. Gardiner C, Ferreira YJ, Dragovic RA, Redman CW, Sargent IL (2013) Extracellular vesicle sizing and enumeration by nanoparticle tracking analysis. *J Extracell Vesicles* 2. doi:[10.3402/jev.v2i0.19671](https://doi.org/10.3402/jev.v2i0.19671)
9. Webber J, Clayton A (2013) How pure are your vesicles? *J Extracell Vesicles* 2. doi:[10.3402/jev.v2i0.19861](https://doi.org/10.3402/jev.v2i0.19861)

INDEX

A

Absolute quantification 237, 281, 337
 Amplification efficiency 284–290, 392, 397
 Antigen retrieval (AR)..... 116, 117, 119, 120, 122–127
 Arrhythmia..... 187
 ATP..... 207, 262, 271, 298, 303, 307
 Automatization..... 188

B

Biofluids 230, 231, 234, 237, 238, 240, 241, 245, 246, 250, 350, 379–382, 385–397, 400, 416
 Biomarkers 12, 130, 222, 232, 238, 260, 337, 350, 379–381, 399–410, 414–417

C

Carbon 13 NMR..... 259–277
 Cardiomyocytes 201–209
 Catalase 338, 340–342
 Cell culture 162, 173, 180, 189, 192, 202–204, 231, 233–234, 247, 299, 301, 303, 325, 382, 384
 Cell preparation..... 189, 193–194, 299–301
 CellTiter-Glo® 299, 302, 303
 Cellular metabolomics..... 231, 259–277
 Clark electrodes 299, 304
 Combination drugs..... 3–22, 39–40
 Comet assay..... 173–183
 Contractility measurement 202
 Cytotoxicity study..... 299, 301–303, 307

D

Developmental toxicity..... 21, 22, 28, 48, 52, 54, 55, 62, 311–323, 326
 DNA damage 174, 175, 180, 181
 Dose selection..... 8, 10, 18–19, 36, 48, 50–51
 Drug development..... 7, 15, 26, 30, 31, 39, 40, 61, 201, 231, 311
 Drug metabolism..... 34, 260

E

Egg culture 314–318
 Egg fertilization..... 312–314, 322, 323, 327, 331
 Electrophoresis 164, 170, 173–179, 181
 Electrophysiology..... 188, 190, 191, 195, 201

Embedding..... 77, 87, 95, 96, 102, 103, 105–109, 113, 117, 123, 130, 137, 173, 176, 178, 183, 329, 401
 Embryos 58, 318, 319, 323, 326–329, 331, 332, 400
 Embryotoxicity..... 312, 318, 319, 325–332
 Exosome 350, 351, 354–355, 357, 376, 382, 386, 387, 390, 394–397, 413–422

F

Fixation 72, 73, 77, 85–88, 90–97, 102, 104–105, 112, 116–118, 123, 127, 130, 137, 138, 407
 Flow cytometry..... 144–146, 151, 154, 156, 162, 166–167, 171
 Frog embryo teratogenesis assay Xenopus (FETAX) 311

G

Gas chromatography-mass spectrometry (GC-MS) 231, 246, 247, 251, 416
 Genetic toxicology..... 11, 173
 Genomics 230

H

High performance liquid chromatography (HPLC)..... 130, 131, 245, 246, 338, 342
 Histological slide 72, 104
 Histology..... 72, 77, 101–103, 105, 113, 115, 116, 129
 Histopathological procedures 102
 Human *ether-a-go-go* (hERG)..... 187–199, 201

I

Immunohistochemistry (IHC)..... 102–104, 110, 115–127, 135, 406, 408, 410
 Impedance measurement 201–207
 Induced pluripotent stem cells (iPSCs) 201–209
 In silico 33, 241, 340, 343, 346
In situ hybridization (ISH) 102, 399, 405, 408
 Investigative toxicology 54

J

Juvenile toxicity 39, 47–49

K

Kidneys..... 32, 34, 44, 45, 72, 76, 83, 87, 90, 244, 261, 264, 265, 267, 268, 273, 277, 298, 390

L

Lactate dehydrogenase (LDH) release 262, 273, 301
 Liquid chromatography-mass spectrometry
 (LC-MS) 130, 231, 232, 234, 235, 245–247,
 339, 340, 346
 Liver 32, 35, 39, 45, 72, 76, 83–86, 95, 96,
 261, 264–268, 271, 272, 297, 298, 300, 338, 400

M

Macroscopy 71, 75, 77, 85
 Malformations 313, 315–320,
 323, 326, 330
 Mass spectrometry (MS) 130, 133, 138, 229–254, 260,
 337–345
 Mass spectrometry imaging (MSI) 129–139
 Matrix assisted laser desorption/ionization (MALDI)
 imaging 129, 130, 133–135, 138
 Metabolic profiling 229, 235, 236, 247,
 250, 252–253
 Metabolomics 229–254
 MicroRNA 349–378, 399
 Microtomes 103, 107–109, 117
 Mitochondrial respiration 297–307
 Monkey 42, 43, 45–47, 49, 57, 227, 349
 Mouse 19, 43, 45, 48, 49, 53, 62, 73, 76, 81,
 85–87, 94, 96, 124, 132, 136, 146, 148, 161–171, 219,
 221, 224, 232, 233, 312, 384, 397, 400, 407
 Multiple reaction monitoring (MRM) 246, 338, 340,
 342–347

N

Necropsy 45, 59
 Next-generation sequencing (NGS) 349, 400
 Normalization 195, 242–245, 282–283, 286,
 381, 383, 390, 393, 397, 414
 Nuclear magnetic resonance (NMR)
 spectroscopy 229–254, 260

O

Oxygen consumption 304, 306, 307

P

Patch-clamp 187–199, 201
 Pathology 45, 57–59, 62,
 233, 312
 Pediatric 25–62
Pig-a assay 143–159, 162–167
 Potassium channel 187–199
 Precision-cut tissue slices 259–277
 Preclinical studies 18, 20–22, 39, 298
 Protein extraction 176, 338
 Proteomics 230, 414, 416

Q

QT interval 8
 Quality control (QC) 132–134, 180–181,
 230, 379–382, 385, 387, 395, 396
 Quantitative RT-PCR 281

R

Rat 19, 25, 35–40, 42, 44–49, 51, 53, 54, 56,
 61, 62, 73, 76, 81, 85–89, 91, 94, 96, 132, 143–159,
 162, 219, 221, 232, 233, 238, 261, 264–272, 274, 300,
 326, 338, 341, 350, 378, 397, 400
 Rat hepatocytes 267, 297
 Regulatory guidelines 7–15, 27, 38, 51
 Relative quantification 281–286, 292, 342, 345
 Repair endonucleases 173–183
 Respirometer 299, 306, 307
 Reverse transcription-polymerase chain reaction
 (RT-PCR) 163, 167, 281–295, 392, 395
 RNA extraction 156, 376, 385, 389, 396, 415, 419
 Rodents 8, 19, 38, 39, 42, 45–48, 51–59, 62,
 72, 75, 76, 80, 84, 85, 87, 91, 93, 96, 144, 201, 232

S

Safety biomarkers 48, 225
 Safety pharmacology 8, 9, 11, 14, 16–18, 27, 47, 58
 Safety testing 49, 62
 Sampling
 blood 57, 96, 231, 233
 GC-MS 247
 LC-MS 231
 NMR 232, 235
 urine 87, 231, 232, 380, 386
 Sampling procedures 72, 86
 Screening assay 312
 Sectioning 102–105, 107–110, 112, 130,
 132–133, 137, 138, 404, 407
 Staining 102, 104, 110–113, 118, 119,
 122–125, 127, 129, 131, 134–135, 139, 163–165, 175,
 178, 179, 400, 409, 410
 Standardization 102, 115, 123
 Statistical analysis 52, 247, 263, 281, 318, 384
 Strand breaks (SBs) 173–175, 179–182
 Study design 29, 31, 43, 44, 49–50, 59

T

Target safety assessment 213–228
 Teratogen 311, 318, 320
 Teratogenic index (TI) 318–322
 Tissue sampling 233–234
Torsades de Pointes (TdP) 188
 Toxicology 11, 15, 18, 38, 41, 43, 47–49, 51,
 61, 76, 85, 220, 226, 260, 379, 415

Transcriptomics 312, 416
 Trimming 72, 73, 77, 86, 87, 96, 97, 102–103,
 105, 109, 117, 149, 369, 374
 Trypsinization..... 300, 303,
 306, 307

U

Ultra Performance Liquid Chromatography-Mass
 Spectrometry (UPLC-MS) 231, 249

W

Western blot..... 123, 414–416, 418

X

Xenopus laevis..... 312–314, 321–323

Z

Zebrafish 325, 330, 400